Kazan Golovkinsky Stratigraphic Meeting

2020

Kazan Federal University
Institute of Geology and Petroleum Technologies

1804

Kazan Golovkinsky Young Scientists' Stratigraphic Meeting 2020

Sedimentary Earth Systems: Stratigraphy, Geochronology, Petroleum Resources

October 26-30, 2020, Kazan, Russia

PROCEEDINGS

filo diritto editore DAL 2008

PROCEEDINGS
4th Kazan Golovkinsky Stratigraphic Meeting 2020

Sedimentary Earth Systems: Stratigraphy, Geochronology, Petroleum Resources

(Kazan, Russian Federation, 26-30 October 2020)

Editor-in-Chief:
Danis K. Nurgaliev
Scientific editors:
Max Barclay, Svetlana Nikolaeva, Vladimir Silantiev
Technical editor:
Milyausha N. Urazaeva

FILODIRITTO
INTERNATIONAL PROCEEDINGS

Proceedings of International Young Scietists' Stratigraphic Meeting are dedicated to all aspects of stratigraphy, biotic and abiotic events and the evolution of sedimentary basins at that time, and their resources.
The volume of the Conference Proceedings is prepared according to the Russian Government Program of Competitive Growth of Kazan Federal University.
On the cover: sketch by Roderick I. Murchison 'The Gurmaya Hills, South Urals, approaching from the Steppes' (Murchison *et al*., 1845)

Log in to find out all the titles of our catalogue
Follow Filodiritto Publisher on Facebook to learn about our new products

ISBN 979-12-80225-03-0
DOI: 10.26352/E922_KAZAN2020

First Edition November 2020

filodirittoeditore.com
inFOROmatica srl, Via Castiglione, 81, 40124 Bologna (Italy)
inforomatica.it
tel. 051 9843125 - Fax 051 9843529 - commerciale@filodiritto.com

INDEX

FOREWORD

This volume of Conference Proceedings brings together written versions of most of the contributions presented during the Golovkinsky Young Scientists Stratigraphic Meeting, which took place at Kazan Federal University, Kazan, Russia, October 26-30, 2020.

The conference aimed to create a forum for further discussion on the integration of a range of geological information on the Precambrian and Phanerozoic. The call for papers was addressed to scholars in the fields of paleontology, stratigraphy, geochemistry, mineralogy, geophysics, and mineral resources.

The conference provided a setting to discuss recent developments in a wide variety of topics concerning the Precambrian and Phanerozoic, including Biostratigraphy, Chemostratigraphy, Biogeography, Paleoclimate, Facies, Mineralogy, Lithology, Geophysical methods and Resources. Furthermore, the contributions focused on issues of facies and paleogeographical interpretations were also welcomed along with papers, regarding climate, biota and changes in the sedimentary environment during the Precambrian and Phanerozoic. Various aspects of sedimentary successions and rock composition and properties were developed by high-precision methods and presented in contributions discussing bedding patterns, grain size changing, coal seams, carbonate deposition, incised valley formation, and conventional and unconventional mineral resources prospects in Europe and Asia. The general topics and spirit of the Golovkinsky meetings are in full agreement with the high priority stratigraphic tasks of the International Commission on Stratigraphy and cover such important aspects of its work as GSSP selection, and developing high-precision regional stratigraphic schemes and interregional correlations.

This conference volume is addressed jointly to academics and applied geologists, and provides a forum for a number of perspectives, based on either theoretical analyses or empirical case studies that foster dialogue and the exchange of ideas.

Professor Danis Nurgaliev,
Vice-rector for scientific activities,
Director of the Institute of Geology and Petroleum Technologies,
Kazan Federal University (RUSSIA)

Late Viséan Foraminiferal Assemblages of the 106 Oktyabrskaya Borehole, South-East of the East European Platform

BASHLYKOVA Elena[1], KULAGINA Elena[1,2]

[1] *Institute of Geology of the Ufa Federal Research Centre of the Russian Academy of Sciences (IG UFRC RAS), Ufa (RUSSIA)*
[2] *Kazan Federal University, Kazan (RUSSIA)*
Email: duss_06@mail.ru

Abstract

Zonal foraminiferal assemblages from the Upper Viséan deposits of the 106 Oktyabrskaya Borehole in the south-east of the East European Platform are discussed. The Upper Viséan is represented by bioclastic, foraminiferal-algae limestones and dolomites. The taxonomic composition of the *Endothyranopsis compressa – Paraarchaediscus koktjubensis, Ikensieformis proikensis, Ikensiformis ikensis*, and *Ikensiformis tenebrosa* zones is discussed.

Keywords: Viséan, West European Platform, foraminiferal zones

Introduction

Carboniferous deposits of the southeastern regions of the East European Platform were studied in a series of oil and gas exploration boreholes. The 106 Oktyabrskaya Borehole is at the junction of the East European Platform and the western side of the Uralian Foredeep (Orenburg region). The borehole uncovered Devonian, Carboniferous and Permian deposits.

The lower Viséan deposits of the section (29 m thick) are characterized by assemblages of foraminifers, ostracodes, conodonts, spores and pollen [1]. About 240 m-thick series of foraminiferal-algae limestones and dolomites is assigned to the Upper Viséan (Fig. 1). The upper Viséan of the southeastern regions of the East European Platform contains the *Endothyranopsis compressa – Paraarchaediscus koktjubensis*, *Ikensieformis proikensis*, *Ikensiformis ikensis*, and *Ikensiformis tenebrosa* zones [2]. These zones correspond to the *Endothyranopsis compressa – Paraarchaediscus koktjubensis*, *Ikensieformis proikensis – Archaediscus gigas, Eostaffella ikensis*, and *Eostaffella tenebrosa – Endothyranopsis sphaerica* zones, respectively, of the Moscow Basin, coinciding with regional substages (horizons): Tulian, Aleksinian, Mikhailovian and Venevian [3].

Foraminiferal zonal assemblages

The assemblages of the following zones characterize Viséan deposits of the 106 Oktyabrskaya Borehole section.

The *Endothyranopsis compressa – Paraarchaediscus koktjubensis* Zone is set in the range of 3253-3286 m (samples 101-104). According to geophysical and paleontological data, the thickness of the Tulian is about 50 m. The strata are composed of finely bioclastic wackestones and packstones in the lower part, and foraminiferal limestones in the upper part. The foraminiferal assemblage includes: *Paraarchaediscus koktjubensis* (Rauser-Chernousova), *P. convexus* (Grozdilova and Lebedeva in Grozdilova, 1953), *Planoarchaediscus eospirillinoides* Brazhnikova, *Endothyranopsis* cf. *compressa* (Rauser-Chernousova et Reitlinger), *Omphalotis* spp., *Endothyra* spp., Palaeotextulariida, *Eoparastaffella* spp. (Fig. 2).

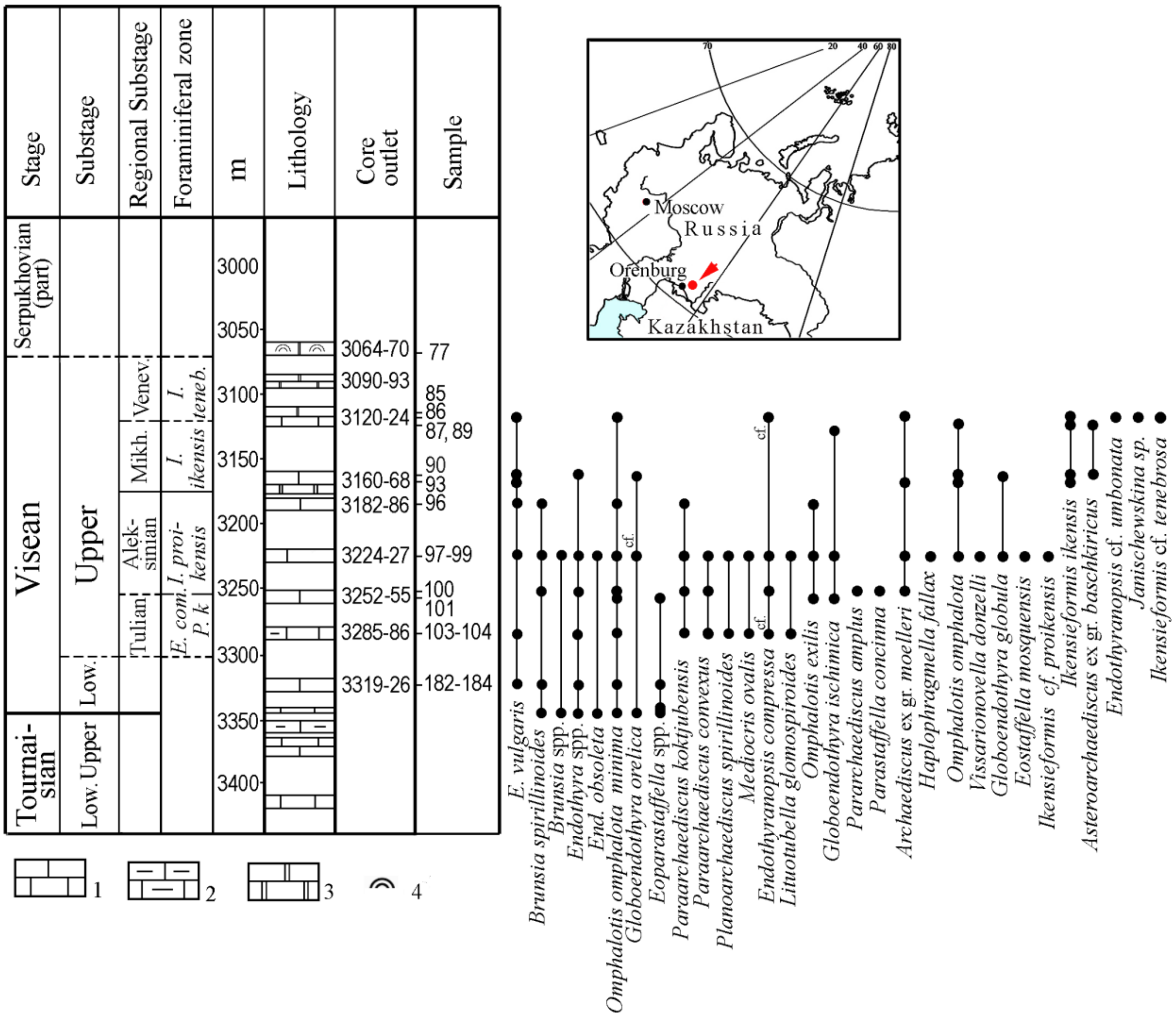

Fig. 1. Distribution of selected foraminifers in the Upper Viséan deposits of the 106 Oktyabrskaya Borehole. (1) Limestone; (2) argillaceous limestone; (3) dolomite; (4) stromatolites; *E. com. P. k. – Endothyranopsis compressa – Paraarchaediscus koktjubensis. I. – Ikensieformis*

The *Ikensieformis proikensis* Zone is recognized in the range of 3186-3252 m. It is composed of bioclastic grainstones, bioclastic wackestones, and algal and sometimes crinoidal packstone.

The foraminiferal assemblage includes *Endothyra obsoleta* Rauser-Chernousova, *Omphalotis omphalota* (Rauser-Chernousova et Reitlinger), *Cribrospira panderi* Moeller, *Endothyranopsis and compressa* (Rauser-Chernousova et Reitlinger), *Eostaffella mosquensis* Vissarionova, *Ikensieformis* cf. *proikensis* (Rauser-Chernousova).

The *Ikensiformis ikensis* zone is recognized in the range of 3121-3168 m (samples 93. 90, 87-89) where it is represented by bioclastic algal-bioclastic and lithoclastic grainstones with a bed of dolomite. The foraminiferal assemblage is supplemented with *Archaediscus* ex gr. *moelleri* Rauser-Chernousova, *Asteroarchaediscus* spp., *Spinothyra pauciseptata* (Rauser-Chernousova), *Endothyranopsis crassa* (Brady). Numerous algae *Koninckopora* spp. are present. This assemblage characterizes the Mikhailovian, its thickness is 47 m.

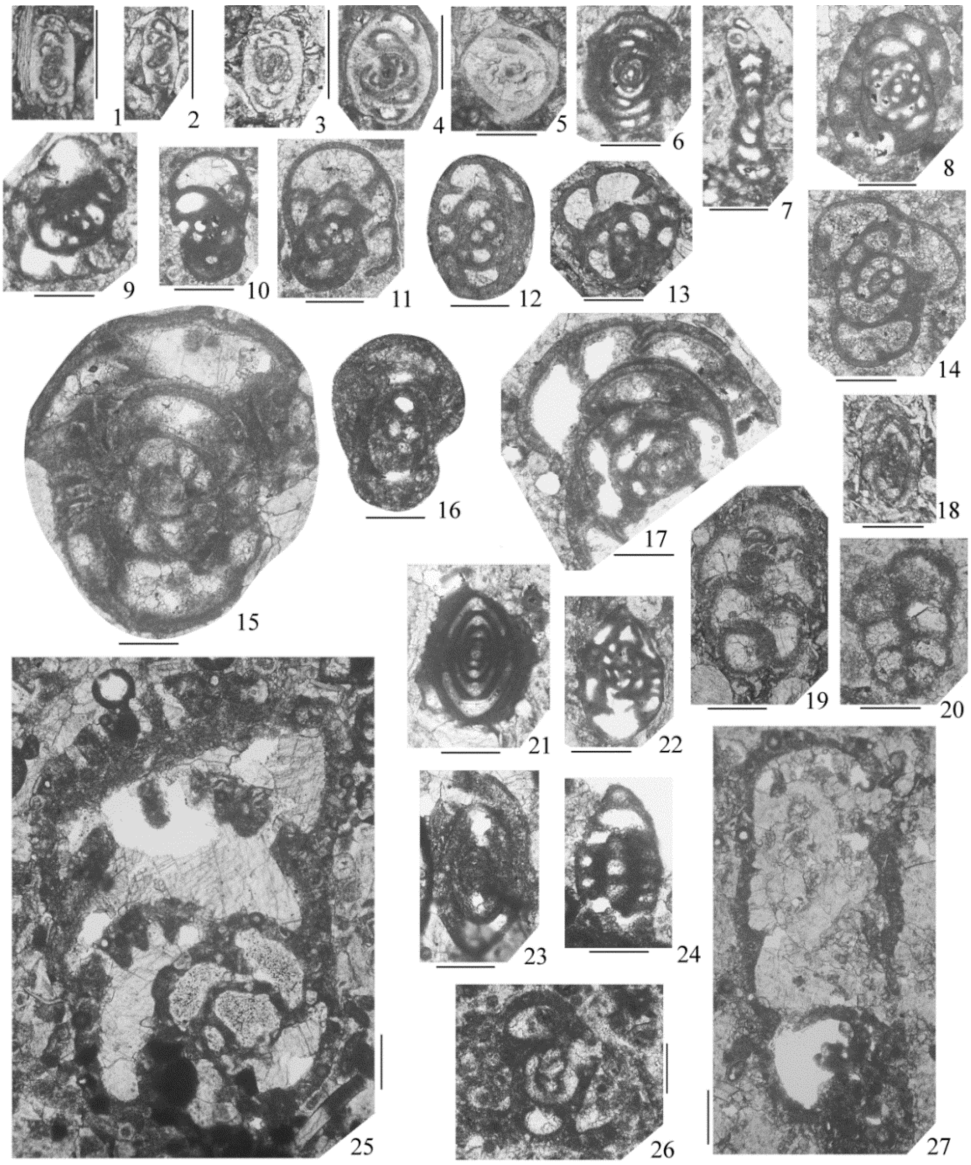

Fig. 2. Foraminifers from the upper Viséan Substage of the 106 Oktyabrskaya Borehole. Scale bar = 0.2 mm. (1, 2) *Paraarchaediscus koktjubensis* (Rauser-Chernousova, 1948), axial sections, both from Sample 101(5); 3) *Paraarchaediscus amplus* (Conil *et* Lys, 1964), Sample 101(1); (4) *Paraarchaediscus convexus* (Grozdilova et Lebedeva in Grozdilova, 1953), Sample 97(2); (5) *Asteroarchaediscus* ex gr. *baschkiricus* (Krestovnikov *et* Theodorovich, 1936), Sample 90(1); (6) median section, *Brunsia spirillinoides* (Grozdilova *et* Glebovskaya, 1948), Sample 98(2); (7) *Brunsia* sp., near axial section, Sample 98(1); (8) *Vissarionovella donzelli* Cózar and Vachard, 2001, Sample 97(2); (9) *Endothyra devexa* Rauser-Chernousova, 1948, Sample 98(1); (10) *Endothyra prisca* Rauser-Chernousova et Reitlinger in Rauser-Chernousova *et al*., 1936, Sample 98(1); (11) *Endothyra* cf. *apposita* Ganelina, 1956, Sample 104(2); (12, 13) *Omphalotis exilis* (Rauser-Chernousova, 1948), oblique sections, both from Sample 101(1); (14) *Endothyra expressa* Ganelina, 1956, Sample 104(2); (15) *Endothyranopsis* cf. *umbonata* (Ganelina, 1956); (16) *Endothyranopsis compressa* (Rauser-Chernousova et Reitlinger in Rauser-Chernousova *et al*., 1936), Sample 98(1); (17) *Globoendothyra globula* (d'Eichwald, 1860), broken test, oblique section, Sample 99(3); (18) *Eoparastaffella* sp., axial section, Sample 101; (19) *Palaeotextularia* sp., Sample 101(1); *Consobrinellopsis consobrina* (Lipina, 1948), longitudinal section, Sample 99(3); 21, 22 *Ikensieformis ikensis* (Vissarionova, 1948): 21 – axial section, Sample 90(4); 22 – tangential section, Sample 93(1); (23) *Eostaffella mosquensis Vissarionova*, 1948, axial section, Sample 98(2); (24) *Ikensieformis* cf. *tenebrosa* (Vissarionova, 1948), tangential section; (25) *Haplophragmella fallax* Rauser-Chernousova et Reitlinger in Rauser-Chernousova *et al*., 1936, median section, Sample 98(2); (26, 27) *Lituotubella glomospiroides* Rauser-Chernousova, 1948: 26 – axial section, Sample103(1), 27 – longitudinal section, Sample 99(4)

The assemblage of *Ikensieformis tenebrosa* Zone is provisionally identified in Sample 86 of coral-algal boundstone at a depth of 3120 m. The foraminifers *Endothyranopsis umbonata* (Ganelina), *Janischewskina* sp., *Ikensieformis* cf. *tenebrosa* Vissarionova are found in this limestone. The overlying beds (3118-3119 m) are composed of highly recrystallized limestone with rare foraminifers *Globoendothyra* sp. and *Omphalotis* sp. of poor state of preservation.

The overlying interval of 3070-3117 m is composed of dolomites may also be referred to the Venevian. The Viséan-Serpukhovian boundary is lithological and is defined at the base of the stromatolite limestones.

Conclusions

The upper Viséan foraminiferal assemblages of the 106 Oktyabrskaya Borehole includes species preliminary described by Vissarionova [4], [5] from the deposits of the western slope of the South Urals, boreholes of the eastern regions of the East European Platform, from east-western regions of the Moscow Basin [6], Belgium [7], and Montagne Noire (France) [8], [9].

The zonal assemblages correlate with the assemblages of the Upper Viséan of the Moscow Basin [3], the South Urals [10], [11], and Kazakhstan [12].

***Acknowledgment*s**

This work was supported by State Programs 0246-2019-0118 IG UFRC RAS. This study was partly funded by a subsidy of the Russian Government to support the Program of Competitive Growth of Kazan Federal University among the world's leading academic centers.

REFERENCES

1. Kulagina, E. I., Kochetkova, N. N., Byvsheva, T. V. (1988). The paleontological characteristics of the Lower–Middle Visean deposits of the Orenburg Region. Biostratigrafiya devona i karbona Urala. Ufa: Bashkir. Fil. Akad. Nauk SSSR, pp. 42-58.
2. Kulagina, E. I., Gorozhanina, E. N., Gorozhanin, V. M., Filimonova, T. V. (2019). Upper Viséan and Serpukhovian Biostratigraphy and Lithofacies of the Southeast of the East European Platform. Stratigraphy and Geological Correlation 27 (6), pp. 613-637.
3. Makhlina, M. Kh., Vdovenko, M. V., Alekseev, A. S., Byvsheva, T. V., Donakova, L. M., Zhulitova, V. E., Kononova, L. I., Umnova, N. I., Shik, E. M. (1993). Nizhniy karbon Moskovskoi Sineklizy I Voronezhskoi Anteklizy (Carboniferous of the Moscow Syneclise and Voronezh Anteclise). Nauka, Moscow, 221.
4. Vissarionova, A. I. (1948). Foraminifers of the Endothyra globulus Eichwald group from the Viséan of the Lower Carboniferous of the European part of the Union. Trudy Instituta Geologicheskikh Nauk 62 Geologicheskaya Seriya (19), pp. 182-185.
5. Vissarionova, A. I., (1948). Primitive fusulinids from the Lower Carboniferous of the European part of the Union. Trudy Instituta Geologicheskikh Nauk 62 Geologicheskaya Seriya (19), pp. 216-226.
6. Ganelina, R. A. (1956). Viséan foraminifers from the northwestern region of the Moscow Basin. Microfauna SSSR 8, pp. 61-184.
7. Conil, R., Lys, M. (1964). Matériaux pour l'étude micropaléontologique du Dinantien de la Belgique et de la France (Avesnois). Partie 1, algues et foraminifères. Mémoires de l'Institut de Géologie de l'Université de Louvain 23.
8. Cózar, P., Vachard, D. (2001). Dainellinae subfam. nov. (Foraminiferida du Carbonifère inférieur), révision et nouveaux taxons. Geobios 34 (5), pp. 505-526.
9. Vachard D., Cózar P., Aretz M., Izart, A. (2016). Late Viséan-Serpukhovian foraminifers in the Montagne Noire (France): biostratigraphic revision and correlation with the Russian substages. Geobios 49 (6), pp. 469-498.
10. Kulagina, E. I., Klimenko, T. V. (2014). Upper Viséan foraminiferal assemblages of the Sikaza River on the Western Slope of the Southern Urals. Geologicheskiy sbornik 11, pp. 48-57.
11. Stepanova, T. I., Kucheva, N. A. (2006). The «Khudolaz» section as a stratotype of horizons of the Subregion Scheme of the Urals Eastern Slope of the Lower Carboniferous Deposits. Litosfera 1, pp. 45-75.

12. Rauser-Chernousova, D. M. (1948). Materials on the foraminiferal fauna of the Carboniferous deposits of central Kazakhstan. Trudy Instituta Geologicheskikh Nauk, Geologicheskaya Seriya 21 (66), pp. 1-28.

Permian Biota in Back-Arc Basins of the Okhotsk-Taigonos Volcanic Arc (Northeast Asia)

BIAKOV Alexander[1]

[1] *North-East Interdisciplinary Scientific Research Institute n.a. N.A. Shilo, Far East Branch, Russian Academy of Sciences, Magadan (RUSSIA)*
Kazan Federal University Kazan (RUSSIA)
North-Eastern State University Magadan (RUSSIA)
Email: abiakov@mail.ru

Abstract

The characteristics of Permian biota in back-arc basins (Okhotsk, Ayan-Yuryakh, Balygychan, Nyavlenga, and Taigonos) of the Okhotsk-Taigonos volcanic arc (OTVA) are considered. The taxonomic composition of faunistic communities is in many respects similar and includes mainly representatives of *Inoceramus* – like bivalves – kolymiids, some nuculids, and gastropods. The most numerous and diverse Permian communities are from the Okhotsk basin, where almost all groups of organisms known in the Permian of Northeast Asia are found.

The relative diversity of the faunistic communities of the Okhotsk basin is probably due not only to the shallower conditions for the existence of the fauna, but also to the more “open” nature of this basin, which can be explained by the existence of a nearby strait within the OTVA.

The taxonomic composition of communities in other basins of the OTVA is much poorer, evidently largely due to their deep water and predominantly clayey nature of the bottom with a relatively low diversity of biotopes. During most of the Permian, the OTVA apparently represented a high land and played the role of a large biogeographic barrier separating the basins of Northeast Asia from the Paleo-Pacific. At the end of the Permian, this barrier was largely eliminated, as evidence by the invasion of the Southern Verkhoyansk basin by Tethyan bivalves (*Claraioides, Eumorphotis, Myalina, Pteria*), ammonoids (*Otoceras*), and conodonts (*Hindeodus* and *Clarkina*).

Keywords: Biota, faunal community, back-arc basin, Okhotsk-Taigonos volcanic arc, Northeast Asia, Permian

Introduction

In the Permian, Northeast Asia was a system of sea basins of varying geodynamics, belonging to the eastern part of the Boreal Superrealm [1], [2] (Fig. 1).

Of particular interest are the back-arc basins of the Okhotsk-Taigonos volcanic arc (OTVA), which separated the entire system of Northeast Asian basins from the Paleo-Pacific Ocean – Okhotsk (connected with the Okhotsk massif), Ayan-Yuryakh, Balygychan, Nyavlenga, and Taigonos. These basins are characterized mainly by deep-water conditions and an avalanche, predominantly clayey, character of sedimentation, which was largely determined by the connection with the volcanic arc.

Characteristics of biota in Permian basins of the Okhotsk-Taigonos volcanic arc

The Permian fauna communities of the back-arc basins of the OTVA are largely similar and consist mainly of *Inoceramus* – like bivalves – kolymiids, some nuculids and gastropods-euomphalids. To a large extent, such a taxonomic composition of the fauna is determined by deep-sea environments and mainly clayey composition of sediments. Kolymiids are a fairly euryfacial group [4], occurring in both shallow-water carbonate and deep-water sandy-clayey facies. Nuculids, being detritus-gatherers, also prefer deep-water clayey facies. Euomphalid gastropods are found almost exclusively in deep-water clayey sediments, and not known in shallow-water communities.

At the same time, the systematic composition, taxonomic diversity and frequency of occurrence of the fauna in the considered basins (especially in the Okhotsk one) have a number of differences.

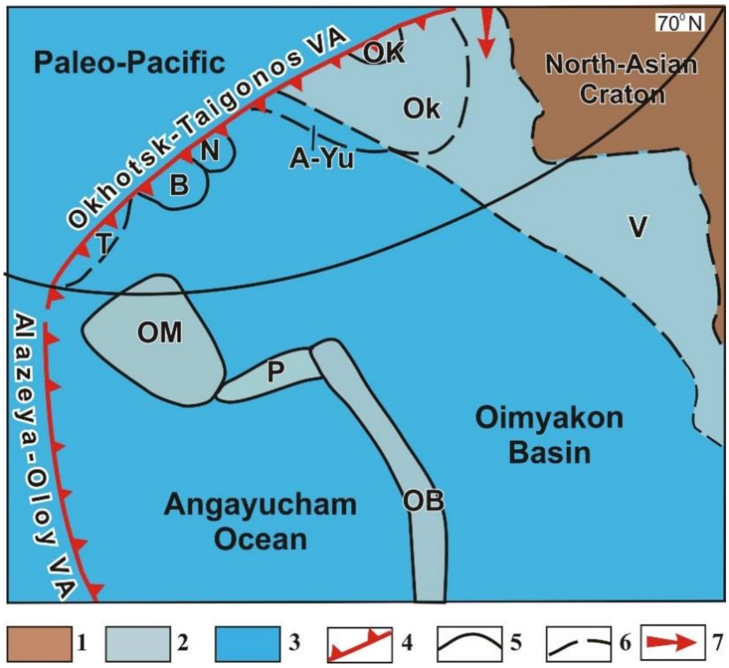

Fig. 1. Paleogeography of Northeast Asia and back-arc sedimentary basins of the Okhotsk-Taigonos volcanic arc in the Permian (Capitanian) (after [1], added and amended).
1 – land, 2 – shallow sea, 3 – deep sea, 4 – volcanic arc, 5 – tectonic structure boundaries, 6 – sedimentation basin boundaries, 7 – probable direction of the fauna migration from the Paleo-Pacific. Tectonic blocks and massifs: OK – Okhotsk, OB – Omulyovka, OM – Omolon, P – Prikolyma; sedimentary basins: A-Yu – Ayan-Yuryakh, B – Balygychan, N – Nyavlenga, Ok – Okhotsk, T – Taigonos; V – Verkhoyansk margin-epicontinental sea. Paleolatitude after [3]

The most numerous and diverse are the Permian communities of **the Okhotsk basin**. They are represented by almost all groups of organisms known in Northeast Asia, with a sharp predominance of *Inoceramus*-like bivalves [5]. However, in the Asselian-Middle Artinskian benthonic communities, brachiopod is dominant, primarily to productids, representatives of the genera *Verchojania* and *Jakutoproductus* [6].

Coral remains are very rare and are found only in the Upper Permian (tabulatomorphs *Cladochonus* and indeterminable single rugoses). The remains of bryozoans are also sporadic and are represented by indeterminable reticulated colonies. Brachiopods are sporadically found throughout the section. Representatives of almost all orders of articulate brachiopods are known: productids (*Cancrinelloides, Strophalosia*), rhynchonellids (*Rhynchopora*), spiriferids (*Tumarinia, Olgerdia, Neospirifer,* and *Crassispirifer*), athyridids (*Bajkuria, Cleiothyridina,* and *Bajtugania*). However, in some places there are known quite dense populations of the productids, which form the “brachiopod banks” consisting of representatives of the genus *Mongolosia*.

The most widespread are bivalves, primarily *Inoceramus*-like (genera *Maitaia, Intomodesma, Aphanaia, Kolymia,* less often *Cyrtokolymia, Okhotodesma*, and *Cigarella*).

They are found in both relatively shallow and deep-water environments. In shallow marine facies, kolymiids often formed limestones-coquina. Other bivalve groups include vacunellines (*Pachymyonia*), undulomiines (*Praeundulomya*), nuculids (*Nuculopsis, Phestia*), and aviculopectinoids (*Kolymopecten, Streblopteria, Guizhoupecten*).

Ammonoids are found in the Okhotsk basin, at least at three stratigraphic levels: Sakmarian – a representative of the genus *Uraloceras* (possibly *U.* ex gr. *omolonense* Bogoslovskaya et Boiko), Kungurian – the *Paragastrioceras* and *Baraioceras*, and Roadian – *Sverdrupites* and *Pseudosverdrupites* [7], [8]. Gastropods are rare throughout the section and include species of the genera *Mourlonia, Glabrocingulum, Ptychomphalina, Peruvispira,* and rare bellerophontids.

The remains of echinoderms are often found almost throughout the entire section. Crinoids are represented by fragments of stems of the pelagic (*Neocamptocrinus*) and benthic (*Uniformicrinus*) genera. Blastoid *Deltoblastus* sp. and a starfish were found at the eastern periphery of the Okhotsk basin [5]. In the lower part of the Permian, R.B. Umitbaev [9] mentions finds of sea urchins, typical representatives of the Tethyan communities, uncharacteristic for the Boreal Superrealm.

The diversity and abundance of the biota of **the Ayan-Yuryakh basin** are significantly impoverished compared to the Okhotsk basin. This is largely due to the deep-water habitat of the fauna, which for most of Permian history corresponded to the foot of the continental slope [10]. Here, as well as in the Okhotsk basin, *Inoceramus*-like bivalves dominate, but their shell rock accumulations are usually absent. Only occasionally they form deep-sea “bioherms”, the emergence of which may have been due to the influx of underwater fluids or methane seeps. A certain confirmation of the hydrothermal nature of these “bioherms” can be their very large size: the length up to a few tens of meters, the thickness – up to several meters and their association with deep-sea sediments. These “bioherms” consist of clusters of *Inoceramus*-like bivalves without signs of redeposition of the latter. Byssus-attached *Maitaia* and *Trabeculatia*, to a lesser extent *Intomodesma*, and very rarely *Kolymia* and *Aphanaia* (the latter belong mainly to semi-infaunal and free-lying benthos) predominate. Also, single nuculids (*Glyptoleda, Phestia*, rarely *Nuculopsis* and *Palaeoneilo*) occur, which are mobile benthos. Representatives of other bivalve groups are extremely rare.

Gastropods are quite common for the Ayan-Yuryakh basin, among which the genus *Straparolus* dominates; *Mourlonia, Glabrocingulum, Ptychomphalina, Peruvispira*, and bellerophontids are less common. It should be noted that all the Permian gastropods of northeastern Asia require monographic study. The fragments of stems and cirri of crinoids, both benthic (*Uniformicrinus*) and pelagic (Neocamptocrinus), are also quite common.

The role of other fauna groups in the Ayan-Yuryakh basin is very insignificant. Single small foraminifers (*Frondina, Rectoglandulina,* Saccamminidae) are known here. As well as in the Okhotsk basin, there are rare corals represented by the same taxa. Single remains of indeterminable nautiloids and scaphopods (?) are known. Ammonoids are found at two stratigraphic levels: Late Artinskian (*Neopronorites*) and Roadian (*Sverdrupites*) [8]. Colonies of reticulated bryozoans are very rare. Brachiopods are also rare and are represented by single productids (*Cancrinelloides*) and spiriferids (*Crassispirifer* and *Neospirifer*).

The Permian communities of **the Balygychan basin**, where environmental conditions were largely similar to the Ayan-Yuryakh basin, are characterized by an even poorer taxonomic composition compared to the Okhotsk and Ayan-Yuryakh basin [11]. It is also dominated by kolymiids, mainly byssus-attached *Kolymia*, *Maitaia*, and large free-lying *Intomodesma*, as well as gastropods-euomphalids (*Straparolus*). The nuculid bivalves *Phestia*, gastropods *Glabrocingulum* and *Peruvispira* are occasionally found. The single representative of Tethyan pectinoids *Claraioides* was found in the west of the basin, and in the east, small peculiar “*Streblopteria*” sp. In the eastern part of the basin, there are also rare brachiopods:

Rhynchopora, spiriferids (*Attenuatella* and *Neospirifer*), athyridids (*Cleiothyridina*), productids (*Stepanoviella*) and chonetids (*Lissochonetes* and *Tornquistia*). Colonies of reticulated bryozoans are very rare. We should also mention rare finds of small foraminifera (*Nodosaria*) and indeterminable radiolarians. A distinctive feature of the communities in the Balygychan basin is the complete absence of cephalopods and echinoderms (an exception is a single find of a starfish from the Upper Permian).

The Permian biota of **the Nyavlenga and Taigonos basins** has been much less-studied well than the three considered above. As in other basins, kolymiids are strikingly dominant here. In the Nyavlenga basin, which includes shallower facies, there are many byssus-attached *Kolymia* that form shell rock; free-lying *Cigarella* are less common [12]. Finds of corals *Cladochonus* and *Tamnopora*, brachiopods *Spiriferella*, aviculopectinoid bivalves, and bryozoans are known in the lower part of the section [13]. In the Taigonos Basin, in addition to the kolymiid bivalves, which are especially numerous in the Upper Permian, where they are represented by *Maitaia* and large *Intomodesma*, very rare brachiopods are known in the middle part of the section: *Rhynchopora, Neospirifer,* and *Magadania.*

For both basins, as well as for the Balygychan, the complete absence of cephalopods and echinoderms is characteristic, but there are known finds of indeterminable spherical radiolarians [14], [15], [13].

Possible causes of differences in communities of different basins

In our opinion, the above noted relative diversity of fauna communities in the Okhotsk basin is due not only to shallower conditions of the fauna's existence, but also to its greater "openness" compared to other back-arc basins. The presence of such faunal groups as corals, cephalopods, pelagic crinoids, blastoids, and starfish indicates the normal salinity of the basin.

Of particular interest is the presence of pelagic crinoids *Neocamptocrinus*, first described from the Permian of Eastern Australia. Its representatives were also found in Indonesia (Timor Island), Eastern Transbaikalia, Western Primorye, Mongolia, Omolon, Ayan-Yuryakh, and the southern part of the Verkhoyansk basin [16]. Blastoids of the genus *Deltoblastus* are so far known only from the Permian of Timor [17]; their rare remains are also found in Oman [18].

Such "openness" of the Okhotsk basin can be explained by the existence of a strait within the OTVA, which served as a natural biogeographic barrier between the eastern Boreal and Tethyan (Panthalassic) basins [19]. During most of the Permian, this arc was, apparently, a high land (perhaps, to some extent, the Kamchatka Peninsula and Kuril Islands can serve as a modern analogue of the OTVA). At the end of the Changhsingian, it seems, that almost complete disappearance of the arc considered (at least of its Okhotsk part) occurred, as evidence by the invasion of the ammonoids *Otoceras*, bivalves *Claraioides*, *Eumorphotis, Myalina, Pteria*, and conodonts *Hindeodus typicalis* (Sweet) and *Clarkina* cf. *changxingensis* (Wang et Wang) into the southern part of the Verkhoyansk basin [20], [21], [22].

The extreme taxonomic impoverishment of the communities in the Balygychan, Nyavlenga, and Taigonos basins is obviously largely due to their deep-water environments and predominantly clayey character of the bottom with a relatively low diversity of biotopes.

However, the absence in them of such a nektonic faunal group as ammonoids, as well as crinoids, which characterize the normal salinity of the basin, suggests they were to some extent isolated from the main water area of the World Ocean. At the same time, the radiolarians are known in the Balygychan and Taigonos basins, represented by indeterminable spherical forms, which could not exist under conditions of significant isolation from oceanic sea areas.

Acknowledgments

This work was supported by the Russian Foundation for Basic Research (project no. 20-05-00604) and by the State Russian Government Program for competitive growth of the Kazan Federal University among World’s leading scientific and education centers.

REFERENCES

1. Biakov, A. S., Prokopiev, A. V., Kutygin, R. V., Vedernikov, I. L., Budnikov, I. V. (2005). Geodinamicheskiye Obstanovki Formirovaniya Permskikh Sedimentatsionnykh Basseynov Verkhoyano-Kolymskoy Skladchatoy Oblasti. Otechestvennaya geologiya 5, pp. 81-85.
2. Biakov, A. S. (2010). Zonal Stratigraphy, Event Correlation, and Paleobiogeography of the Permian of Northeastern Asia (Based on Bivalves). SVKNII DVO RAN, Magadan, pp. 1-262.
3. Lawver, L. A., Dalziel, I. W. D., Gahagan, L. M., Kygar, R., Herber, B. (2004). The Plates 2004. Atlas of Plate Reconstructions (750 Ma to Present Day). Plates Progress Report no. 290-0804. Report N 191 University of Texas, pp. 1-88.
4. Biakov, A. S. (2006). Permian Bivalve Mollusks of Northeast Asia. Journal of Asian Earth Sciences 26(3-4), pp. 235-242.
5. Biakov, A. S. (2007). Permian Biostratigraphy of the Northern Okhotsk Region (Northeast Asia). Stratigraphy and Geological Correlation 15 (2), pp. 161-184.
6. Klets, A. G. (2005). Verkhnii Paleozoi Okrainnykh Morei Angaridy. Geo, Novosibirsk, pp. 1-240.
7. Andrianov, V. N. (1985). Permskie i Nekotorye Kamennougolnye Ammonoidei Severo-Vostoka Azii. Nauka, Novosibirsk, pp. 1-181.
8. Kutygin, R. V., Biakov, A. S. (2015). Permian Ammonoids of the Okhotsk Region, Northeast Asia. Paleontological Journal 49 (12), pp. 1275-1281.
9. Umitbaev, R. B. (1963). Stratigraphiya Verchnepaleozoiskih Otlozhenyi Tsentralnoi Chasti Okhotskogo Massiva. Uchenyie zapiski NIIGA, Seriya Paleontologiya i Biostratigrafiya 2, pp. 5-15.
10. Biakov, A. S., Vedernikov, I. L. (1990). Stratigraphiya Permskih Otlozhenii Severo-Vostochnogo Obramleniya Okhotskogo Massiva, Tsentralnoi i Yugo-vostochnoi chastei Ayan-Yuryakhskogo Antiklinoriya. SVKNII DVO AN USSR, SVPGO, Magadan, pp. 1-69.
11. Biakov, A. S. (2004). Permian Deposits of the Balygychan Uplift. NEISRI FEB RAS, Magadan, pp. 1-87.
12. Biakov, A. S., Vedernikov, I. L., Ivanov, Y. Y., Kolesov, E. V. (2018) New Data on Permian Bivalves and the Age of Volcanogenic Beds of the Arman-Viliga Folded Zone, Northeastern Asia. Paleontological Journal 7, pp. 65-71.
13. Skibin, Y. P. (1977). Gosudarstvennaya Geologicheskaya Karta SSSR Mashtaba 1:200000. Seriya Magadanskaya. List P-55-XXXIV. Mingeo SSSR, Moskva, pp. 1-84.
14. Zhulanova, I. L., Petrov, A. N., Byalobzhesky, S. G., Likman, V. B. (1997) K stratigraphii i Genezisu Verhnepermskih Otlozhenii Poluostrova Taigonos. Magmatizm i Orudenenie Severo-Vostoka Rossii. NEISRI FEB RAS, Magadan, pp. 135-154.
15. Kuznetsov, V. M. (1989). Gosudarstvennaya Geologicheskaya Karta SSSR Mashtaba 1:200000. Seriya Verhnekolymskaya. List P-56-XVI. Soyuzgeolfond, Moskva, pp. 1-106.
16. Stukalina, G. A. (1990). Harakteristika Pelagicheskih Krinoidei *Neocamptocrinus* iz Permskih Otlozhenii Severo-Vostoka SSSR. Opornyi Razrez Permi Omolonskogo Massiva. Nauka, Leningrad, pp. 134-142.
17. Charlton, T. R., Barber, A. J., Harris, R. A., Barkham, S. T., Bird, P. R., Archbold, N. W., Morris, N. J., Nicoll, R. S., Owen, R. M., Sorauf, J. E., Taylor, P. D., Webster, G. D., Whittaker, J. E. (2002). The Permian of Timor. Journal of Asian Earth Sciences 20, pp. 719-774.
18. Webster, G. D., Sevastopulo, G. D. (2007) Paleogeographic Significance of Early Permian Crinoids and Blastoids from Oman. Palaeontologische Zeitschrift 81 (4), pp. 399-405.
19. Biakov, A. S, Shi, G. R. (2010). Palaeobiogeography and Palaeogeographical Implications of Permian Marine Bivalve Faunas in Northeast Asia (Kolyma-Omolon and Verkhoyansk-Okhotsk Regions, Northeastern Russia). Palaeogeography, Palaeoclimatology, Palaeoecology 298, pp. 42-53.
20. Kozur, H. W., Ramovs, A., Zakharov, Y. D., Wang, C. (1995). The Importance of *Hindeodus parvus* (Conodonta) for the Definition of the Permian-Triassic Boundary and Evaluation of the Proposed Sections for a Global Stratotype Section and Point (GSSP) for the Base of the Triassic. Geologija 37, 38, pp. 173-213.
21. Zakharov, Y. D. (2002). Ammonoid Succession of Setorym River (Verkhoyansk Area) and Problem of Permian-Triassic Boundary in Boreal Realm. Journal of China University of Geosciences 13 (2), pp. 107-123.

22. Biakov, A. S., Kutygin, R. V., Goryachev, N. A., Burnatny, S. S., Naumov, A. N., Yadrenkin, A. V., Vedernikov, I. L., Tretyakov, A. V., Brynko, I. V. (2018). Discovery of the Late Changhsingian Bivalve Complex and Two Fauna Extinction Episodes in Northeastern Asia at the End of the Permian. Doklady Biological Sciences 480, pp. 78-81.

Lithochemical Features of Shungites from Shunga Deposit (Onega Basin, Russia)

DEINES Yulia[1]

[1] Institute of Geology, Karelian Research Centre, Russian Academy of Science (RUSSIA)
Email: deines@krc.karelia.ru

Abstract

Shungites of the Shunga deposit of the Onega structure were studied. Shungite rocks were classified into two groups by the composition of their mineral component, namely, miosilites and siallites. Some basic lithochemical features of shungites within the Shunga deposit were revealed, and they have been compared with shungite-bearing rocks of the Melnichnaya deposit of the Onega structure.

Keywords: shungite, petrochemical modules, stratigraphy

Introduction

Onega basin, Russian Fennoscandia, is stratotypical for shungite-bearing rocks of Precambrian (Fig. 1) [1]. The c. 2000 Ma, 900-m-thick, Zaonega Formation in the Onega basin contains one of the greatest accumulations of organic matter (OM) in the early Precambrian during the period known as the worldwide Shunga Event [2]. Zaonega Formation rocks are greenschist-facies volcaniclastic greywackes, dolostones, limestones, shungite-bearing rocks, mafic tuffs and lavas intruded by numerous mafic sills. Several sedimentary beds are enriched in OM with the overall content of total organic carbon (TOC) ranging from 0.1 to 16 wt.%. The shungite-bearing rocks occur in nine stratigraphic levels [3]. We consider the formation of shungite-bearing rocks within the framework of the diapir model. Depending on the rheological properties of the system (layer and overburden), the development of diapirs can be suspended either at the stage of formation of domes, stocks, or go to completion, when the diapir «hat» is formed. The development of the diapir fold into the hat occurs when the stock-like body that forms from the dome either comes to the surface or reaches a strong impermeable layer or horizon with a lower density. In the extreme case, complete separation of the hat from the stock and transformation into a local subconforming body is possible. Maksovites ((shungite-bearing rocks containing from 10 to 45% of mixed OM) are confined to dome deposits, and shungites (shungite-bearing rocks containing from 45 to 80% of mixed organic matter with a predominance of migratory matter) – to sublayer deposits [4].

The chemical composition of shungites of the Shunga deposit has been studied by many researchers. It was noted that variations in the composition of shungites are quite large even within the same stratified bed both vertically and laterally. With an average carbon content of about 50%, in individual parts (“interlayers”), it rises to 80%. At the same time, it is difficult to draw clear boundaries between shungites with different carbon contents. The current work attempts to reveal some major lithochemical features of the shungites within Shunga deposit.

Due to a high content of OM, the maksovites appear to be opaque under transmitted-light, thus traditional optical petrography has a limited use for their detailed study and classification.

Hence, a geochemical approach has been employed for classifying the rocks and for revealing their major geochemical features.

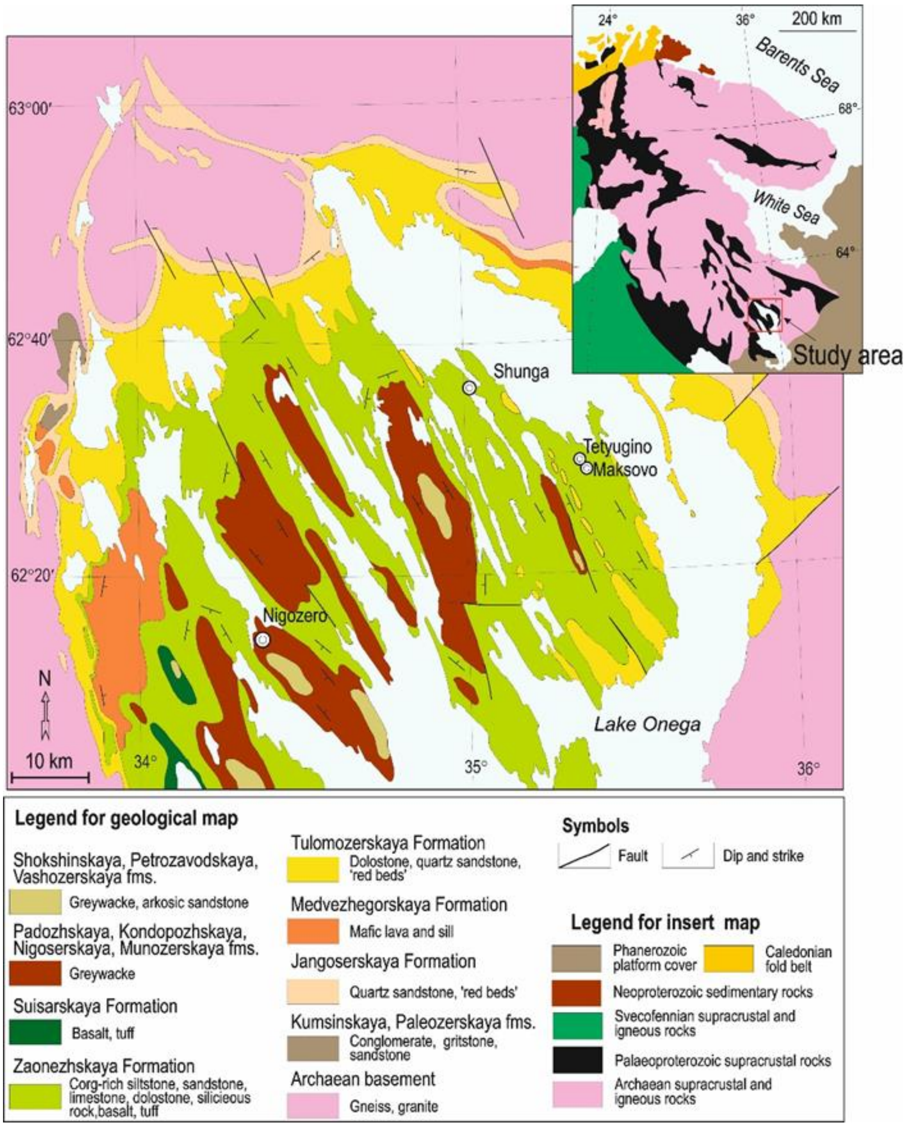

Fig. 1. Geological map of the Palaeoproterozoic Onega basin [1]

Methodology

The shungite chemical composition has been calculated on a TOC-free basis, and the rock-classification of Yudovich and Ketris [5] has been used to categories the TOC-free chemical composition of shungites.

Determination of the content of petrogenic (i.e., rock-forming) elements in the samples was carried out by the methods of chemical analysis [6]. The work was carried out in the Analytical laboratories of the Institute of Geology, KarRC RAS (Petrozavodsk).

Result and discussion

15 samples were taken from the geological section through the Shunga deposit (Fig. 2) and 18 samples from the geological section through the Melnichnaya deposit (see Tetyugino on fig. 1).

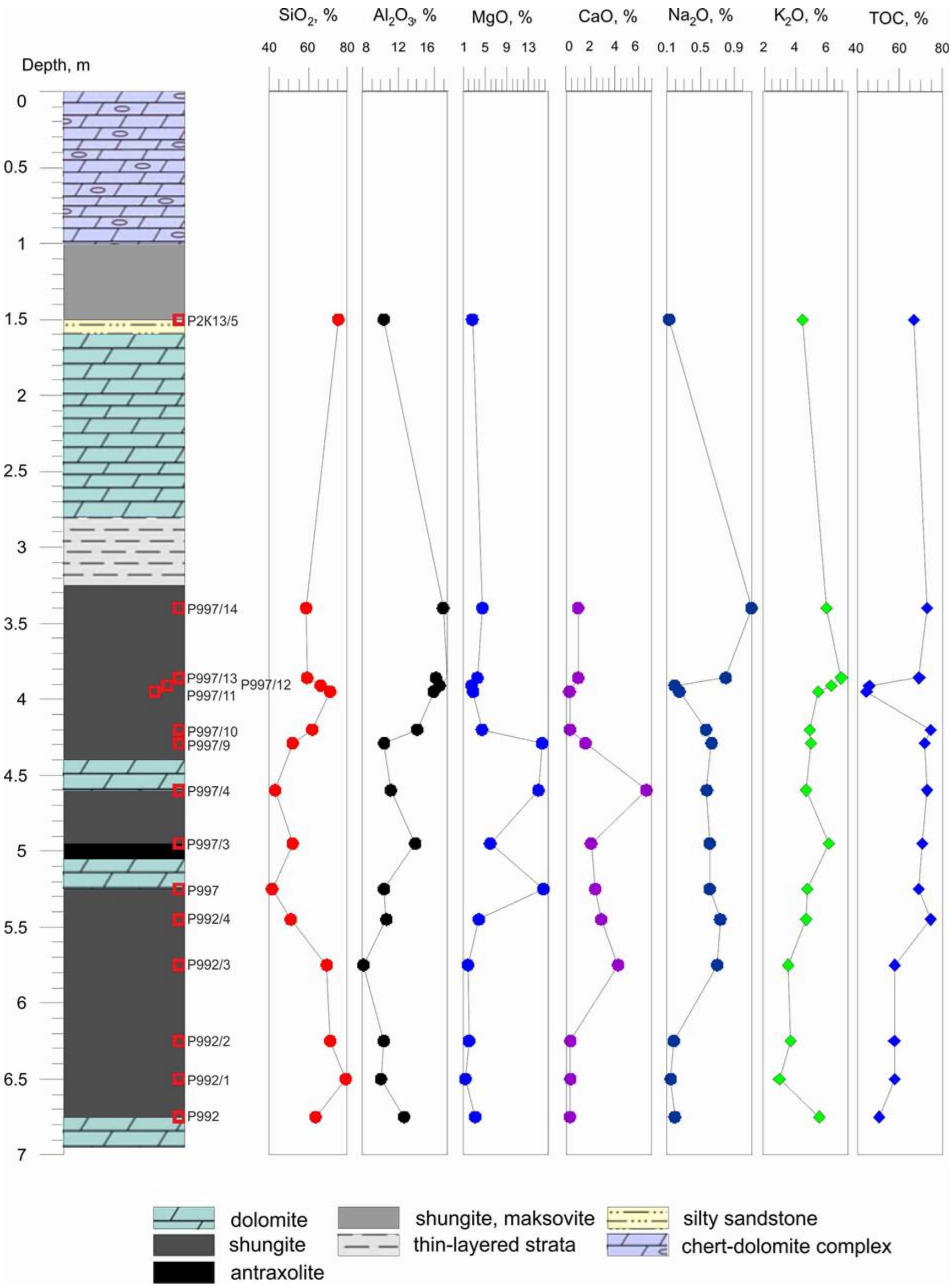

Fig. 2. Lithostratigraphic column of the Shunga deposit and chemical composition of shungites. Sampling was by A. E. Romashkin

The petrochemical modules were calculated to reveal the differences in the chemical composition of shungites, namely, hydrolysate – GM=(TiO_2+Al_2O_3+Fe_2O_3+FeO+MnO)/SiO_2; titanium – TM=TiO_2/Al_2O; iron – ZhM=(Fe_2O_3+FeO+MnO)/(TiO_2+Al_2O_3); femic – FM=(Fe_2O_3+FeO+MnO+MgO)/SiO_2; normalized alkalinity module – NKM=(Na_2O+K_2O)/Al_2O_3; aluminum-silicon – AM=Al_2O_3/SiO_2; alkaline – SCHM=Na_2O/K_2O, long-term practice of using which has shown their effectiveness in the study of sedimentary rocks [6]. The average chemical composition of shungites presented on Fig. 2 and petrochemical modules are presented in Table 1. Based on a GM, the classification revealed two groups, namely, miosilites (GM=0.21-0.30) and siallites (GM=0.31-0.55).

Table 1. Petrochemical modules of shungites

	Na_2O+K_2O, %	GM	ZhM	FM	AM	TM	NKM	SCHM
P992	5.51	0.36	0.53	0.17	0.21	0.12	0.43	0.03
P992/1	3.10	0.20	0.34	0.07	0.13	0.09	0.31	0.05
P992/2	3.78	0.25	0.54	0.12	0.15	0.08	0.36	0.05
P992/3	4.14	0.22	0.64	0.11	0.12	0.11	0.51	0.18
P992/4	5.19	0.37	0.57	0.21	0.21	0.10	0.48	0.15
P997	5.14	0.46	0.63	0.54	0.25	0.12	0.49	0.12
P997/3	6.45	0.42	0.36	0.22	0.27	0.12	0.46	0.09
P997/4	5.05	0.41	0.41	0.45	0.26	0.10	0.45	0.12
P997/9	5.38	0.32	0.37	0.38	0.21	0.13	0.51	0.12
P997/10	5.26	0.32	0.24	0.13	0.24	0.10	0.37	0.11
P997/11	5.47	0.30	0.20	0.09	0.23	0.07	0.34	0.04
P997/12	6.18	0.36	0.28	0.12	0.26	0.09	0.37	0.03
P997/13	7.33	0.39	0.19	0.12	0.30	0.08	0.42	0.11
P997/14	6.75	0.38	0.17	0.13	0.30	0.10	0.40	0.17
P2K13/5	4.42	0.21	0.25	0.08	0.15	0.14	0.42	0.03

Inhomogeneities in the composition of the shungite mineral matter are due to the presence of various micas. Three groups are distinguished, corresponding to samples from the bottom of the lower layer (5.7-6.5 m), the roof of the upper layer (3.3-3.9 m), and rocks occupying an intermediate position (fig. 3). The rocks of the bottom of the lower layer are similar to shungite-bearing rocks of the eighth shungite horizon of the Zaonega Formation; the remaining samples are similar to fluidolites of the Melnichnaya deposit. It can be assumed that the lower layer is the eighth shungite-bearing horizon, and the overlying shungites are fluidolites that have risen from the dome-like body developed along the sixth shungite-bearing horizon.

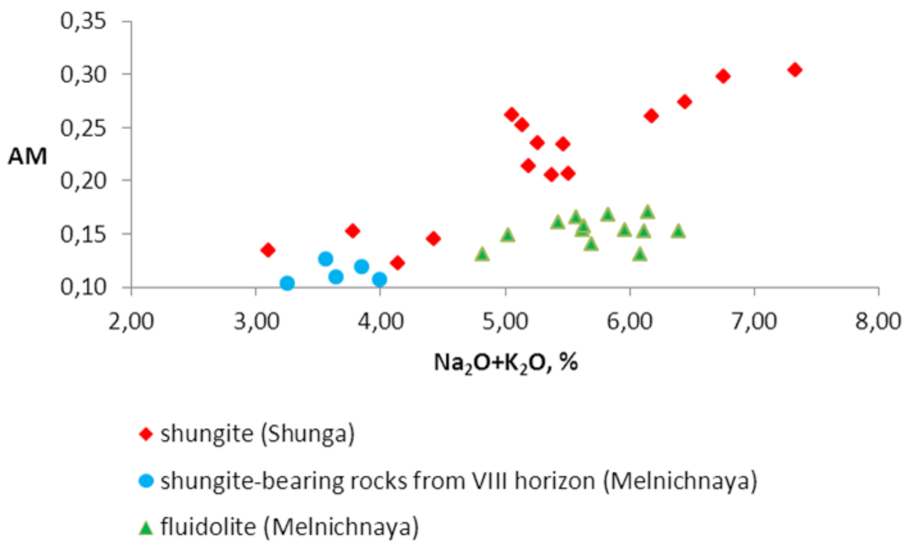

Fig. 3. Correlation between AM and (Na_2O+K_2O) in shungites

Conclusions

The free groups of shungites from Shunga deposit exhibit the following geochemical features:

1. A positive correlation between (Na_2O+K_2O) and (Al_2O_3/SiO_2).
2. There is no negative correlation between Al_2O_3 and SiO_2, which is typical for maksovites [7].
3. No distinct boundaries between shungites with different content of carbon.
4. Shungites differ from maksovites in all lithochemical parameters, excluding the iron module.

The established geochemical regularities have a potential to assist in correlation of distant exposures, as well as, drilled section within Onega basin.

Acknowledgements

The study was conducted as part of a state project accomplished by Institute of Geology of the Karelian Research Centre of the Russian Academy of Sciences. I would like to express my gratitude to Dr. A. E. Fallick (University of Glasgow) for his help in preparing this article and correcting it in English.

REFERENCES

1. Melezhik, V. A., Fallick, A. E., Filippov, M. M., Larsen, O. (1999). Karelian shungite – an indication of 2.0-Ga-old metamorphosed oil-shale and generation of petroleum: geology, lithology and geochemistry. Earth-Science Reviews 47, pp. 1-40.
2. Melezhik, V. A., Fallick, A. E., Rychanchik, D. V., Kuznetsov, A. B. (2005). Palaeoproterozoic evaporites in Fennoscandia: implications for seawater sulphate, the rise of atmospheric oxygen and local amplification of the $\delta^{13}C$ excursion. Terra Nova 17 (2), pp. 141-148.
3. Kupryakov, S. V. (1988). Report on the results of prospecting works conducted in the Onega structure in 1985-1988. Petrozavodsk, 148.
4. Filippov, M. M. (2002). Shungite-bearing rocks of the Onega structure. KarRC RAS, Petrozavodsk, p. 280.
5. Yudovich, Ya. E., Ketris, M. P. (2000). Fundamentals of Lithochemistry. Nauka, St. Petersburg, p. 479.
6. Ponomarev, A. I. (1961). Methods of Chemical Analysis of Silicate and Carbonate Rocks. AN SSSR, Moscow, 414.
7. Deines, Yu. E. (2018). Lithochemical features of shungite rock horizons in the Onega structure. Trans. KarRC RAS 11, pp. 111-115. doi: 10.17076/geo846.

Correlation of Geophysical Search Features of Shungite-Bearing Rock Deposits with Geological Prerequisites for Prospecting (Onega Basin, Russia)

DEINES Yulia[1]

[1] *Institute of Geology, Karelian Research Centre, Russian Academy of Science (RUSSIA)*
Email: deines@krc.karelia.ru

Abstract

The stratigraphic and structural prerequisites for prospecting shungite-bearing rock deposits were studied. This work shows how the geological features of shungite-bearing rock deposits manifest themselves in geophysical fields. The median gradient method and natural electric field method as well as gamma spectrometric survey were used.

Keywords: maksovite, structure features, stratigraphic features, geophysical methods

Introduction

The Onega basin represents one of the largest fragments of continental margin preserved on the eastern part of the Fennoscandian Shield. It consists of a system of parallel, second order synclinal structures trending NW-SE (Tolvuiskaya (Fig. 1), Khmeleozerskaya, and others). The c. 2000 Ma, 900-m-thick, Zaonega Formation in the Onega basin contains one of the greatest accumulations of organic matter (OM) in the early Precambrian during the period known as the worldwide Shunga Event [2].

The Zaonega Formation was subdivided into Lower and Upper sub-suites [3].

The Lower sub-suite is a c. 200-m-thick succession composed mainly of clastic, horizontally bedded, cross-bedded and laminated rocks [3]. Member A of the sub-suite comprises 100-130 m of rhythmically interbedded feldspar-quartz sandstones and siltstones with a variable content of carbonate and mica. Member B has a thickness of 60-90 m and consists of fine-grained sandstone, siltstone and shale.

The Upper sub-suite is 600-650 m thick and differs from the Lower sub-suite in that it contains several intervals of C_{org}-rich sedimentary rocks interbedded with abundant lava flows and intruded by gabbro sills. Member A is a c. 200-m-thick unit [4] and consists mostly of cyclically interbedded greywackes and mudstones with subordinate calcareous greywackes, sandy limestones, and minor intraformational, matrix-supported conglomerates and breccias.

Member B is c. 300 m thick [4] and composed of greywacke, black C_{org}-bearing siltstone and mudstone. The member contains six intervals of C_{org}-rich rocks (shungite-bearing horizons) ranging in thickness from 5 to 120 m. Maksovites are shungite-bearing rocks containing from 10 to 45% of mixed OM, and shungites are shungite-bearing rocks containing from 45 to 80% of mixed organic matter with a predominance of migratory matter [5]. The association of dolomite-chert-shungite of Member B can potentially be used as a marker horizon for correlation of Zaonega sections elsewhere in the Onega Basin [6]. Member C is a 200- to 300-m-thick unit. Member C comprises siltstones, tuffite, quartz-biotite-chlorite and biotite-albite-quartz schists with beds of black, C_{org}-bearing dolostones. The member contains three shungite-bearing horizons. The formation of shungite-bearing rocks is within the framework of the diapir model. Depending on the rheological properties of the system (layer and overburden), the development of diapirs can be suspended either at the stage of formation of domes, stocks, or go to completion, when the diapir "hat" is formed. The development of the diapir fold into the hat occurs when the stock-like body that forms from the dome either comes to the surface or reaches a strong impermeable layer or horizon with a lower density. In extreme cases, complete separation of the hat from the stock and transformation into a local subconforming body is possible. Maksovites are confined to dome deposits, and shungites – to sublayer deposits [5].

Building upon the known geological features of the Zaonega Formation, the main stratigraphic objectives of the study are: (i) identification of the formation controls of dome deposits on to the sixth shungite-bearing horizon, and (ii) assessment of increased radioactivity of the rocks of the seventh shungite-bearing horizon within the shungite-chert-dolomite association. The structural objectives include: (i) assessment of the shape of shungite-bearing horizons (dome structures), (ii) their confinement to third-order anticlines within the synclinal structures of the second order (Tolvuiskaya, Khmelozerskaya and other synclines of the Onega basin), and (iii) assembly of a system of domes located on the same wavelength.

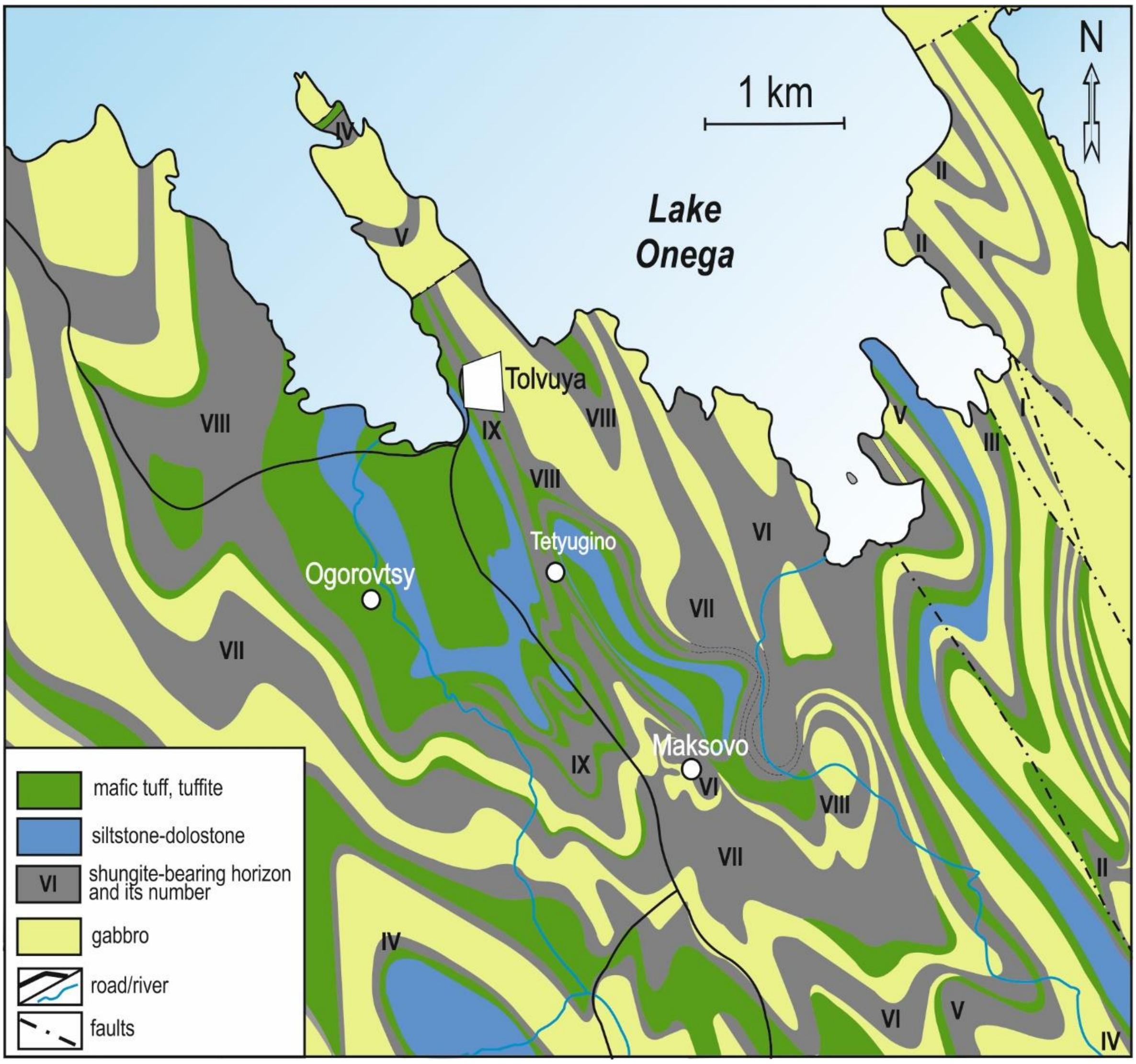

Fig. 1. Geological scheme of the North part of Tolvuiskaya syncline of Onega basin [1]

Methodology

Geophysical methods including the median gradient method and natural electric field method as well as gamma spectrometric survey were used on two areas within the Tolvuiskaya syncline (Ogorovtsy and Tetugino, Fig. 1) to identify geological and structural features of maksovite deposits. Contour maps and sections were made using Surfer and Profiler software.

Result and discussion

The main geological features can be identified within the Maksovo deposit (Fig. 2); namely, the symmetric shape of dome-like body, and the presence of a marginal syncline.

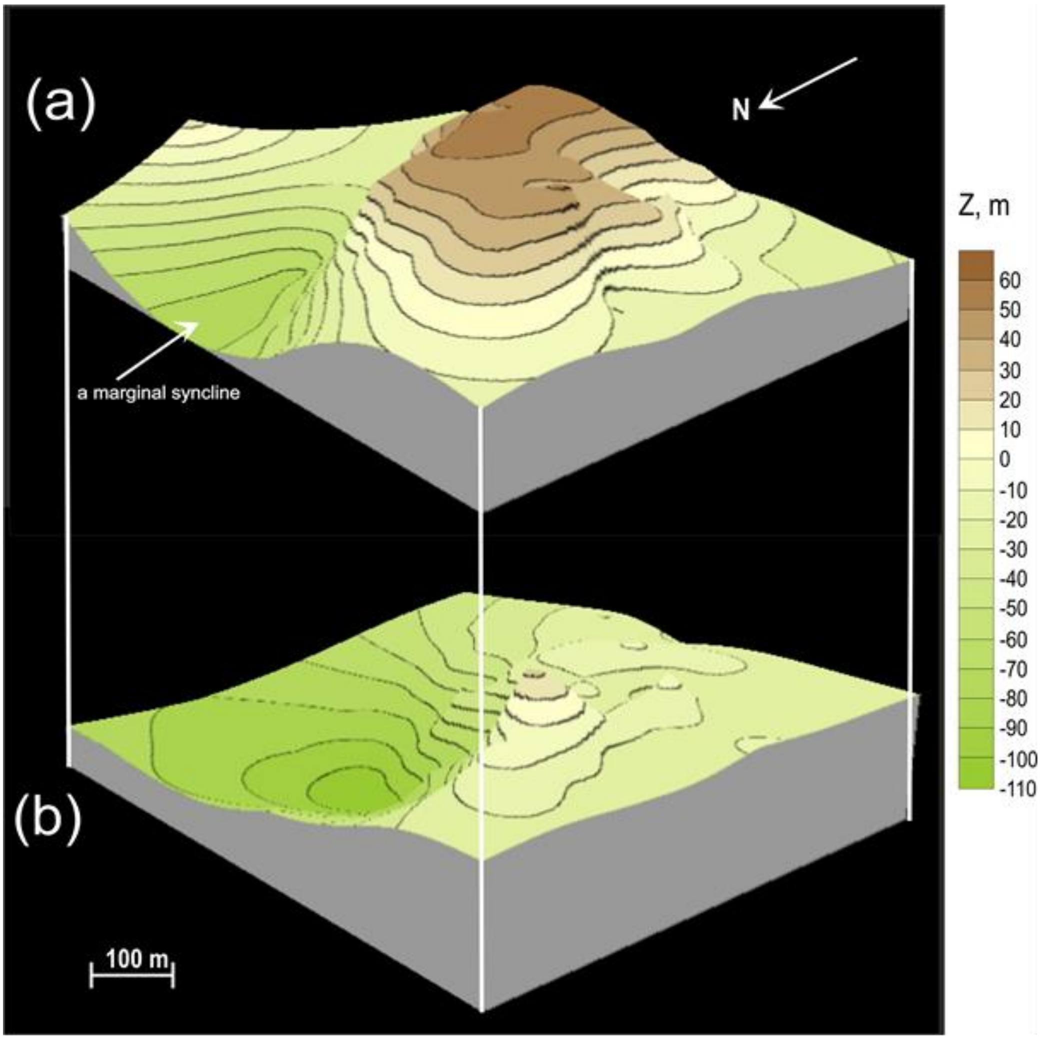

Fig. 2. 3-D model of the maksovite body at Maksovo (Fig. 1): morphology of the upper (a) and lower (b) surfaces

A complex of geophysical methods was selected based on the physical properties of the maksovites and host rocks. Two areas of the Tolvuiskaya syncline were selected for investigation. Ogorovtsy is located 2 km southeast of the village of Tolvuya (Fig. 1) where the rocks consist mostly of siltstone and of shungite-chert-dolomite association. Exposing shungite-bearing rocks of seventh-eighth horizons are overlain by a thin Quaternary cover. An intense negative anomaly of self-potential was discovered, presumably caused by the shungite-bearing rocks of the eighth horizon (Fig. 3a). The isometric anomalous zone is distinguished on the contour maps of the exposure dose of gamma radiation, apparently corresponding to the rocks of the seventh shungite horizon, the so-called gamma-reference (Fig. 3b). Local faults were identified by the median gradient method. The body of maksovite in Ogorovtsy was formed along the sixth shungite-bearing horizon and has a transitional contact to the overlying rocks.

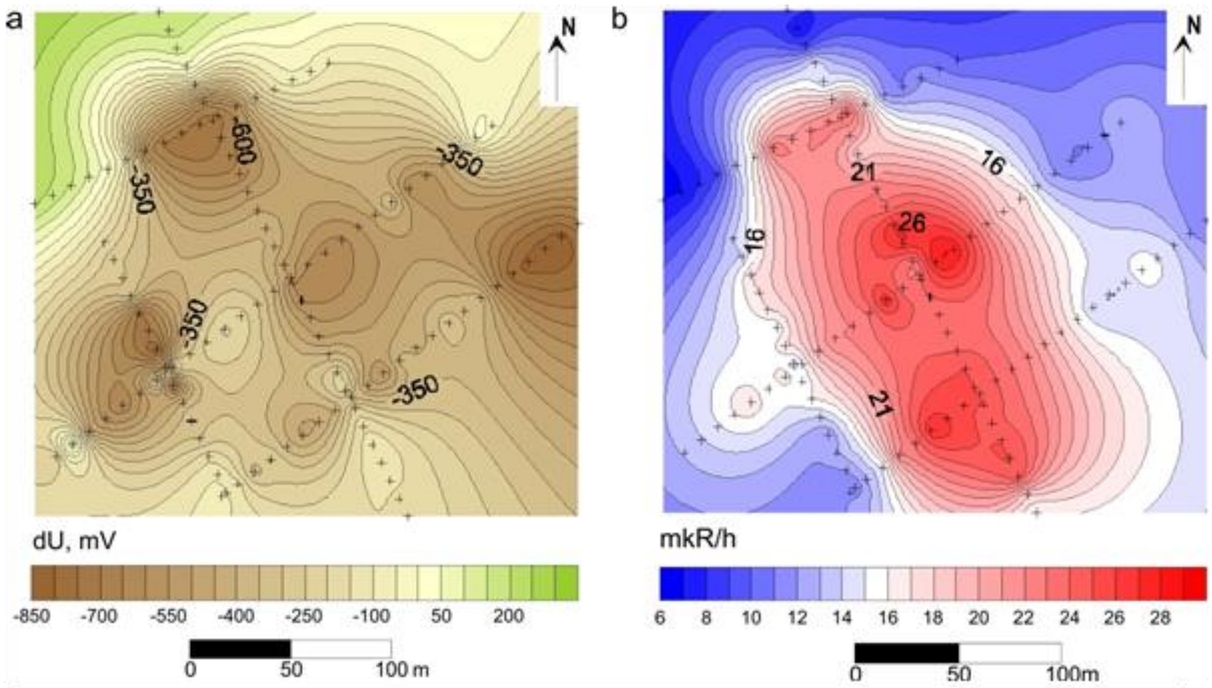

Fig. 3. Contour maps of: a – difference of potential of the natural electric field; b – exposure dose of gamma radiation

Tetyugino is located 2 km southwest of the village of Tolvuya (Fig. 1). In the cross-section several reference strata are identified, throughout the Tolvuiskaya syncline, including lithological-geochemical regional reference – shungite-chert-dolomite association. In the northwest, siltstones and shungite-bearing rocks of the ninth horizon appear in the section.

Combining the information from the contour map of the difference of potential of the natural electric field with the known geological context of the area, it is possible to distinguish the seventh, eighth and ninth shungite-bearing horizons. In the southwestern part of the area, a linear boundary is well recorded, which characterizes the transition between the anticline and syncline. The central part of the diapir structure is recognized by the median gradient method.

Regional and local faults are traced across the entire area, most likely formed as a result of the development of the diapir structure.

Conclusion

Thus, using geophysical methods, it is possible to determine the shape and size of shungite-bearing rocks deposits (the median gradient method, gamma-spectrometric survey), their confinement to third-order anticlines, and the presence of a marginal syncline (the natural electric field method), as well as the presence of local block tectonics (the median gradient method).

Acknowledgements

The study was conducted as part of a state project accomplished by Institute of Geology of the Karelian Research Centre of the Russian Academy of Sciences. I would like to express my gratitude to A. Lepland (Geological Survey of Norway) for his help in preparing this article and correcting it in English.

REFERENCES

1. Kupryakov, S. V. (1988). Report on the results of prospecting works conducted in the Onega structure in 1985-1988, Petrozavodsk, 148.
2. Melezhik, V. A., Fallick, A. E., Rychanchik, D. V., Kuznetsov, A. B. (2005) Palaeoproterozoic evaporites in Fennoscandia: implications for seawater sulphate, the rise of atmospheric oxygen and local amplification of the $\delta^{13}C$ excursion. Terra Nova 17 (2), pp. 141-148.
3. Rychanchik, D. V. (2011). The Zaonega Horizon. The Onega Palaeoproterozoic structure (Geology, tectonics, deep structure and minerageny). Glushanin, L.V., Sharov, N.V., Shchiptsov, V.V. (eds). Institute of Geology, Karelian Research Centre of RAS, Petrozavodsk, pp. 67-69.
4. Galdobina, L. P. (1987). The Ludicovian Super-Horizon. Geology of Karelia. Sokolov, V.A. (ed). Nauka, Leningrad, pp. 56-67.
5. Filippov, M. M. (2002). Shungite-bearing rocks of the Onega structure. KarRC RAS, Petrozavodsk, 280.
6. Melezhik, V. A., Medvedev, P. V., Svetov, S. A. (2013). The Onega Basin. Reading the Archive of Earth's Oxygenation. Volume 1: The Palaeoproterozoic of Fennoscandia as Context for the Fennoscandian Artic Russia – Drilling Early Earth Project. Series: Frontiers in Earth Sciences. Melezhik V.A. *et al*., eds. Springer, Heidelberg, pp. 387-490.

The Garnet-Biotite Temperature Indicator for the Kozhim Massif (Subpolar Urals)

DENISOVA Yulia[1]

[1] Institute of Geology named after academician N. P. Yuskin of Komi SC RAS, Syktyvkar (RUSSIA)
Email: yulden777@yandex.ru

Abstract

The first attempts to use individual minerals or mineral pairs as geothermometers were made by G. Ramberg and T. Barth in the 1950s. Perchuk [1], [2] made a great contribution to geothermobarometry by developing a theory of phase correspondence based on the ideas of G. Ramberg and V. S. Sobolev. He calibrated several coordinated geothermometers: garnet-biotite, garnet-cordierite, garnet-amphibole, amphibole-plagioclase, amphibole-clinopyroxene, etc. The garnet-biotite exchange equilibrium is one of the most common parageneses. To date, there are more than twenty calibration options. Nikitina's [3] thermometry is one of the latest developments of the garnet-biotite geothermometer. The formation temperatures of the Kozhim Massif granites were calculated based on Nikitina's thermometry in the course of the study [3]. The data obtained show that the Kozhim granites are high-temperature formations. The temperature regime of crystallization of these rocks is from 713 °C to 815 °C according to the garnet-biotite geothermometer.

Keywords: biotite, garnet, granite, geothermometer, Kozhim Massif, Subpolar Urals, Nikitina

Introduction

The Kozhim Massif is located in the northeastern Subpolar Urals on the banks of the Ponyu, Oseyu and Epkoshor rivers (Kozhim basin) (Fig. 1). This group of granite bodies forms one of the interstratal intrusion cutting through the deposits of the Puvinskii Group (middle Riphean).

The rocks of the massif are strongly cataclazed shale and in places became sericite dynamometamorphic shales [4]. The Kozhim granites with the maximum preservation of the primary structure and appearance are dense gneiss-like rocks of pink color (an indicator of the increased content of alkaline feldspar in the rock) with a well-defined greenish-gray hue (a characteristic sign of the presence of sericite and muscovite, small grains of quartz in the granite). The structure of the studied rocks varies from granular hypidiomorphic (large subidiomorphic grains of feldspars immersed in a medium-fine-grained mass consisting of quartz grains, feldspars and mica flakes) to medium-grained allotriomorphic [5], [6]. The mineral composition of the granites is represented by potassium-sodium feldspar (40%), plagioclase (13%), quartz (35%), biotite (5%), muscovite (7%). The rocks of the studied massif belong to the A – type according to Chappel's classification.

Biotite is represented mainly by greenish-brown, small (up to 0.1 mm) scales in the main mass of the rock, sometimes marked as inclusions in feldspar inclusions. According to its chemical composition, the mineral is iron-rich biotite biotite. Zircon, apatite, garnet, orthite, titanite, etc. are the most common accessory minerals of the Kozhim Massif rocks [7]. The Kozhim Massif garnet is represented by translucent and transparent pink crystals of rhombododecahedral habitus. The size of the mineral grains is 0.1-0.50 mm. Often garnet grains contain inclusions of biotite, apatite and titanite. According to the results of microprobe analysis, the mineral is almandine garnet. The average garnet content in Kozhim granites is 20 g/t according to Fishman *et al*. [5].

Methodology

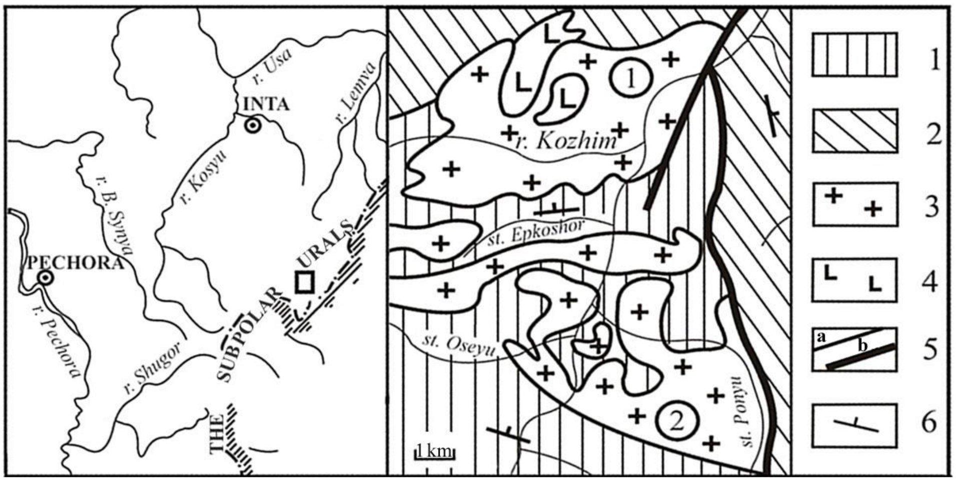

Fig. 1. a) Overview map of the area of the Subpolar Urals (rectangle shows area of study). b) Layout of granite massifs (according to L. V. Makhlaev [8]).
1 – isinglass-quartz shales, green orthoshales, quartzite; 2 – isinglass-quartz shales, porphyries, porphyrites, interlayers of marbles and quartzites; 3 – granites; 4 – gabbro; 5 – geological boundaries: stratigraphic and igneous, b – tectonic; 6 – planar structures of bedding elements. Massifs (numerals in circles): 1 – Kuzpuayu Massif; 2 – Kozhim Massif

There are many variants of geothermometers based on the reactions of ion exchange of elements in different media. The garnet-biotite equilibrium is the most popular due to the wide prevalence of this paragenesis (in alumina rocks and granites, Grt associated with Bt is mainly represented by a solid solution of Alm-1) and increased sensitivity to changes in the temperature of the distribution of Mg and Fe between biotite and garnet. Currently, more than 10 calibration options are used (see Thompson, Holdaway and Lee, Goldman and Albee, Lavrentieva and Perchuk, Perchuk, Nikitina, Blundy and Holland, etc.). In some variants, only the Fe/Mg ratio in biotite and garnet is taken into account, while others consider the influence of CA, Mg impurities, the assumed range of temperatures and pressures, etc. One of the latest developments is a garnet – biotite thermometer, developed by Nikitina [3]. This temperature indicator is based on the temperature correlation of the distribution coefficient of iron and magnesium between garnet and biotite. The applied parameter does not depend on the content of calcium or manganese in garnets, titanium or aluminum in biotites, or the pressure, in comparison with many other garnet – biotite geothermometers [9].

Nikitina's geothermometer is represented by the following formula:

$$T = (-14811{,}25A + 60034{,}08A^2 - 97177A^3 + 46500A^4) / (\mathrm{Ln}K^{Fe+Mn} - 10{,}95A + 48{,}24A^2 - 81{,}78A^3 + 43{,}80A^4 + C + D + E),$$

где $A = 1 - X_{Gr}^{Fe+Mg}$,

$C = -2{,}55(X_{Gr}^{Ca} - 0{,}100) - 2{,}70(X_{Gr}^{Ca} - 0{,}100)^2 + 3{,}54(X_{Gr}^{Ca} - 0{,}100)^3$,

$D = -4{,}08(X_{Bt}^{Al} - 0{,}15) - 21{,}6(X_{Bt}^{Al} - 0{,}15)^2 - 634{,}5(X_{Bt}^{Al} - 0{,}15)^3 + 3628{,}8(X_{Bt}^{Al} - 0{,}15)$,

$E = 1{,}8(X_{Bt}^{Ti} - 0{,}033) - 1{,}8(X_{Bt}^{Ti} - 0{,}033)^2$,

где K^{Fe} – the distribution coefficient of iron between biotite and garnet,
X_{Gr}^{Fe+Mg} – the content of iron and magnesium in garnet, mass. weight,
X_{Gr}^{Ca} – calcium content in garnet, mass. weight,
X_{Bt}^{Al} – the aluminum content in biotite, mass. weight,
X_{Bt}^{Ti} – the content of titanite in biotite, mass. weight.

Results and Discussion

Testing of the Kozhim granite Massif was carried out by the point method with the selection of several samples of 10 units. Pieces of unaltered rock with an average weight of 10-15 kg were selected for each sample. Biotite and garnet were taken from each sample to apply Nikitina’s method. The contents of iron, magnesium, calcium, aluminum, garnet, titanite and biotite were obtained using a Vega3 energy dispersive spectrometer in NBI “Science” Institute of Geology, Komi science center URD RAS (Syktyvkar, analyst A. S. Shujskij). The data obtained allowed us to calculate the thermal parameter for each sample (Table 1).

Table 1. Temperature of formation of the Kozhim Massif granites according to Nikitina’s geothermometer

The number of samples	Temperature, ºC
1	713
2	800
3	778
4	742
5	800
6	809
7	798
8	795
9	815
10	802
Average	785

The research showed that the temperature of formation of granites of the Kozhim Massif according to the Nikitina garnet-biotite geothermometer lies in a range from 713 °C to 815 °C, on average 785 °C.

Conclusions

According to the Nikitina garnet – biotite geothermometer, the author calculated the temperature regime for the garnet of the Kozhim Massif as from 713 °C to 815 °C. The rocks of the massif under consideration are high temperature formations. The author’s earlier conclusions are confirmed. The formation of the Kozhim Massif occurred at a temperature of 700 °C to 900 °C based on the study of the Kozhim zircon morphology using the J. Pupin and G. Turco analysis [11].The studied granites were crystallized at temperatures from 722 °C to 856 °C according to a complex study of accessory minerals (zircon, apatite, monazite) [12] of the massif using saturation thermometry of Watson [13], Bea [14] and Montel [15]. However, the results obtained refute the data of Fishman *et al*., [16] who claimed that the Kozhim massif granites are lower-temperature rocks with a formation temperature not exceeding 720 °C

REFERENCES

1. Perchuk, L. L. (1973). Termodinamicheskij rezhim glubinnogo petrogeneza. Nauka, 318.
2. Perchuk, L. L., Ryabchikov, I. D. (1976). Fazovoe sootvetstvie v mineral’nyh sistemah. Nedra, 287.
3. Nikitina, L. P. (2005). Mezhfazovye geotermometry, geobarometry i geooksobarometry. SPb, pp. 17-23.
4. Pystin, A. M., Pystina, Ju. I. (2008). Metamorfizm i granitoobrazovanie v proterozojsko-rannepaleozojskoj istorii formirovanija Pripoljarnoural'skogo segmenta zemnoj kory. Litosfera 11, pp. 25-38.

5. Fishman, M. V., Jushkin, N. P., Goldin, B. A., Kalinin, E. P. (1968). Mineralogija, tipomorfizm i genezis akcessornyh mineralov izverzhennyh porod severa Urala i Timana. Nauka, 251.
6. Udoratina, O. V., Shujskij, A. S., Kapitanova, V. A. (2020). Granitoidy kozhimskogo massiva (pripolyarnyj ural): U-Pb, Lu-Hf dannye. Izvestiya Komi nauchnogo centra UrO RAN 41, pp. 96-105. doi 10.19110/1994-5655-2020-1-96-105.
7. Denisova, Ju. V. (2014). Tipomorficheskie i tipohimicheskie osobennosti akcessornyh cirkonov granitoidov pripoljarnogo Urala. Vestnik Instituta geologii Komi NC UrO RAN 5, pp. 9-16.
8. Mahlaev, L. V. (1996). Granitoidy severa Central'no- Ural'skogo podnjatija (Poljarnyj i Pripoljarnyj Ural). UrO RAN, Ekaterinburg, 189.
9. Denisova, Yu. V. (2020). Akcessornye geotermometry granitov. Tendencii razvitiya nauki i obrazovaniya 61, pp. 12-15. doi: 10.18411/lj-05-2020-22.
10. Pupin, J.-P. (1980). Zircon and granite petrology. Contrib. Miner. Petrol. 73, pp. 207-220.
11. Denisova, Ju. V. (2016). Termometrija cirkona iz granitoidov Pripoljarnogo Urala. Vestnik Instituta geologii Komi NC UrO RAN 12, pp. 11-22.
12. Denisova, Yu. V. (2019). Termometriya nasyshcheniya cirkona, apatita, monacita (Kozhimskij massiv, Pripolyarnyj Ural). Izvestiya Komi nauchnogo centra UrO RAN 39, pp. 25-30. doi 10.19110/1994-5655-2019-3-47-52.
13. Watson, E. B., Harrison, T. M. (1983). Zircon saturation revisited: Temperature and composition effects in a variety of crustal magma types. Earth and Planetary Science Letters 64, pp. 295-304.
14. Bea, F., Fershtater, G. B., Corretgé, L. G. (1992). The geochemistry of phosphorus in granite rocks and the effects of aluminium. Lithos 48, pp. 43-56.
15. Montel, J. M. (1993). A model for monazite/melt equilibrium and application to the generation of granitic magmas. Chem. Geol. 110, pp. 127-146.
16. Fishman, M. V., Goldin, B. A. (1963). Granitoidy central'noj chasti Pripolyarnogo Urala. AN SSSR, 105.

Changes in the Cladocera Community Within the Bottom Sediments of a Small Tundra Lake (The Yamal Peninsula, Erkuta River Basin)

IBRAGIMOVA Aisylu[1], FROLOVA Larisa[1], GAREEV Bulat[1], FROLOVA Anastasia[1], FEDOROV Grigory[2], TUMANOV Oleg[1]

[1] *Kazan Federal University, Kazan (RUSSIA)*
[2] *Saint Petersburg State University, Saint Petersburg (RUSSIA)*
Email: AGIbragimova@kpfu.ru

Abstract

Climate change and technogenic impacts, mainly on the territories of oil and gas extraction, are particularly noticeable in the pristine territories of the Arctic. Results of the Cladocera analysis from the bottom sediments of a small tundra lake referred to as K1 (within the Yamal Peninsula, Erkuta River Basin) are presented in the current paper. The Cladocera community is characterized by low taxonomic diversity, consisting of typical northern species. In total 13 taxa of Cladocera belonging to 3 families (*Chydoridae*, *Bosminidae*, *Daphniidae*) were identified in 30 cm of bottom sediments. The Cladocera community of K1 was dominated by *Chydorus* cf. *sphaericus*, when *Bosmina* (*Eubosmina*) cf. *longispina* was subdominant in the sediment. At the depth of 13-16 cm an increased proportion of *B.* (*E.*) cf. *longispina* was observed along with a decrease of *C.* cf. *sphaericus*, indicating climate change may have an impact on Cladocera. According to the values of the Shannon-Weaver index K1 has initial signs of eutrophication.

Keywords: Cladocera, bottom sediments, Holocene, Yamal Peninsula, thawing of permafrost

Introduction

The Arctic region is one of the four regions of the world identified by the intergovernmental panel on climate change as the most sensitive and vulnerable to environmental change [1].

Important changes occurred in the Arctic climates during the 20th century [2]. Recent decades have been characterized by noticeable climate change occurring in the Arctic faster and on a larger scale than in the rest of the world [1]. According to the data of the Hydrometeorological Center of Russia the average annual temperature in the Arctic in 2011 reached a record maximum observed over the last 130 years [3]. Warming occurs synchronously for the Western Arctic region with short-term fluctuations, with both increasing and decreasing average annual temperatures observed. Climate warming is accompanied by an increase in annual precipitation [4]. Studies of lakes bottom sediments are of particular importance for reconstructing the ecological and climatic conditions of the past, whilst also assessing the current state of lakes [5]. In the absence of long-term climatic and environmental monitoring data, proxy data from lakes bottom sediments can be used to obtain a longitudinal perspective of environmental change. Siliceous algal and chitinous invertebrate remains (Chironomidae, Diptera and Cladocera, Crustacea) are among the most common paleo indicators in lake sediments that provide reliable records of changes in water quality, habitat and catchment processes [5], [6]. Complex studies of lake bottom sediments in Canada, Arctic, Scandinavia and Fennoscandia have shown that changes in their ecosystems are mostly associated with climate warming over the past 150-200 years [7]. However, only a single study has been conducted in the territory of the Polar Ural [7], [8], [9]. The aim of this study is to explore the Cladocera community from the bottom sediments of lake K1 (an unnamed lake on the

Erkuta River Basin) whilst attempt to reconstruct the ecological and climatic conditions for the Yamal Peninsula.

Research region

The Yamal Peninsula is located in the north of the world's largest West Siberian plain in the tundra zone, beyond the Arctic Circle. The peninsula is a relatively flat a low-lying accumulative plain (heights of 0-70 m, with the highest point of 90 m) composed of sand and clay deposits.

Factors such as a high-latitude location, small influxes of solar radiation, significant distance from the warm air of the Atlantic and Pacific oceans; moreover, flat terrain open to the invasion of air from the Arctic in summer and super cooled continental air in winter determines the continentality and severity of the peninsula [10]. Annual precipitation is 230-400 mm. High humidity, fog and cloud cover are typical for the region. The average annual temperature in the south of the peninsula is – 6.6 °C and in the north – 10.2 °C. The duration of the polar days from north to south varies from 92 to 47 days and the duration of polar nights from 75 to 21 days.

Continuous distribution of permafrost on the lands surface determine the widespread development of cryogenic and thermokarst landforms [11].

Methodology

In 2014 during an expedition to the Yamal Peninsula 13 Arctic lakes located along the temperature gradient of the Erkuta River Basin were sampled for hydrobiological analysis.

Moreover, columns of bottom sediment were collected from the lakes to allow complex study.

The object of the research was the thermokarst lake K1 (68°09'12.0"N, 69°04'36.0"E), located in the Erkuta River Basin (Fig. 1). The lake covers an area of 0.43 km^2, with a maximum depth reaching 6.5 m. In the sampling period (31.07.2014) the transparency and pH of the water was assessed using a Secchi disk, transparency was 3 m and pH 6.93.

A 30-cm column of the bottom sediments was sampled from a depth of 6.1 m. For Cladocera analysis 15 samples of the bottom sediments were selected using a method of sample preparation improved by Korhola and Rautio [12]. Sample preparation and identification of Cladocera remains were analysed in the laboratory of “Paleoclimatology, paleoecology, paleomagnetism” of the Kazan (Volga Region) Federal University. In each sample 100 specimens were identified at minimum. The maximum number of headshields, carapaces or postabdomens of a single taxon was used to calculate the total number of specimens in the sample. Two samples of bottom sediments (27-30 cm) were excluded from the statistical analysis due to an insufficient amount of Cladocera remains. Identification of Cladocera remains was carried out using an Axiostar Plus Carl Zeiss (magnification x100-400) light microscope along with a specialized key for identification subfossil [13] and modern Cladocera [14]. Changes in the diversity of biotic groups were analysed using Shannon-Weaver index and uniformity of each of ecological groups by using the Pielou index, consequently, determining the degree of species richness, diversity and dominance of Cladocera communities. Statistical and stratigraphic analyses were performed in the program C2 version 1.5. Statistically significant stratigraphic zones were identified using CONISS cluster analysis of the Tilia/TiliaGraph software.

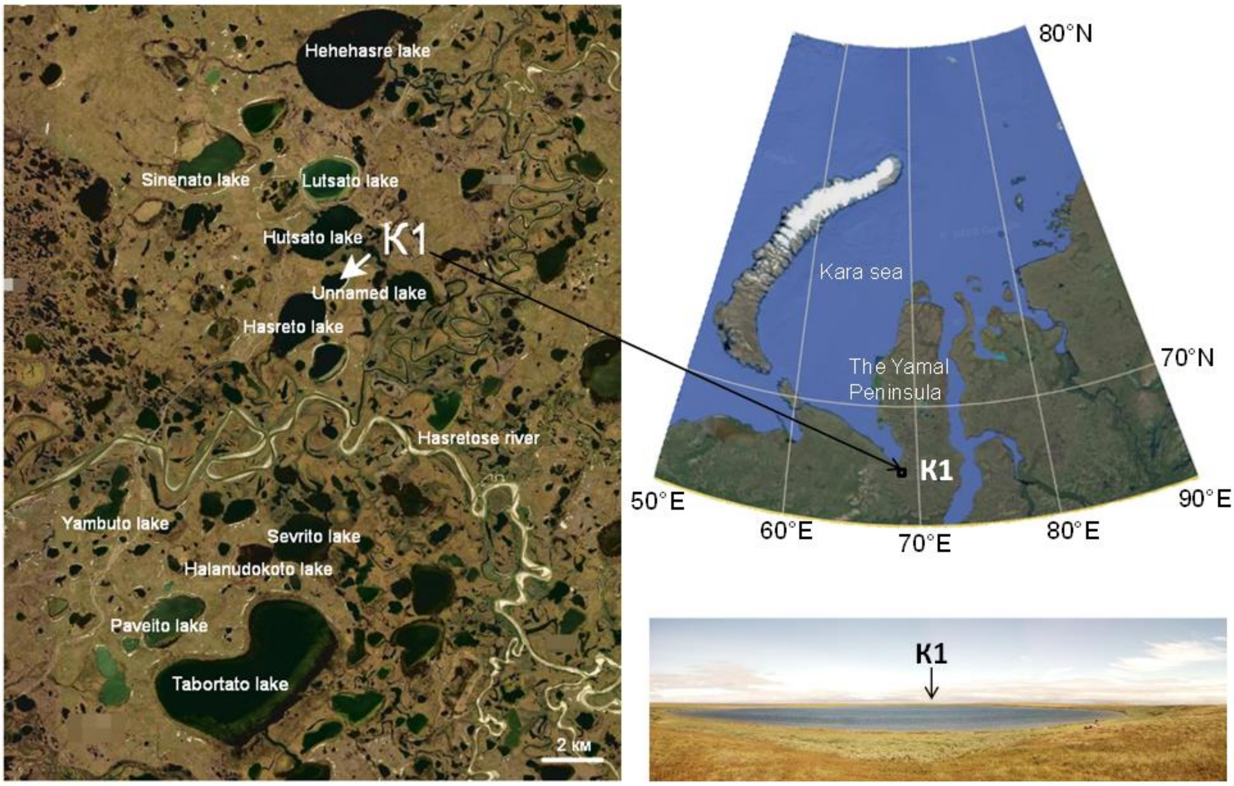

Fig. 1. Location of the small tundra lake K1

Results and discussion

The Cladocera communities are characterized by low taxonomic diversity, consisting of typical northern species. In total 13 taxa of Cladocera belonging to 3 families (*Chydoridae*, *Bosminidae*, *Daphniidae*) were identified in the column of bottom sediments of K1. According to the Lubarsky scale Cladocera community of the K1 was dominated by *Chydorus* cf. *sphaericus* (71.34%) with *Bosmina* (*Eubosmina*) cf. *longispina* being subdominant (24.43%). According to Bogdanov *et al*., [15] plankton of different ecological groups are noted in all reservoirs of the Yamal Peninsula, but pelagic species are the most diverse and numerous. However, inhabitants of the thicket zones have not received sufficient development [15].

The stratigraphic diagram was divided into 2 faunal zones (Fig. 2). The remains of 11 Cladocera taxa were identified in Zone I. Both *B.* (*E.*) cf. *longispina* (50.47%) and *C.* cf. *sphaericus* (41.12%) were dominant in the lowest layers of the bottom sediments at a depth of 25-26 cm: a sufficient quantity of Cladocera specimens were found at this depth to allow for statistical analysis. Moving up the column of bottom sediments (depth <25 cm) a significant increase in the proportion of *C.* cf. *sphaericus* (80-99.12%) and a decrease in the proportion of *B.* (*E.*) cf. *longispina* (0.84-11%) was revealed. The dominance of *C.* cf. *sphaericus* is common in northern lakes and is often the first to colonise such lakes [16], [17], [18]. Moreover, this taxon can successfully develop in both eutrophic and oligotrophic reservoirs [18] as its adaptations for living in littoral, allow it to develop on mass as a plankton species in the presence of suspended algae or other organic particles [19].

An increase of *C.* cf. *sphaericus* can be regarded as evidence of eutrophication [18].

Acroperus harpae and *Alonella exigua* remains were identified in small quantities in Zone I, with complete absence in Zone II. *A. harpae* is considered an Arctic species due to its frequent occurrence in Arctic lakes. However, this taxon is sensitive to hydrological changes and eutrophication [18]. *Alonella exigua* is widely distributed in Europe, recorded in ponds, rivers, bogs and temporary water bodies. This taxon prefers to reside between vegetation and prefers waters with pH 3.8-9.0 with a higher concentration of calcium [18], [21].

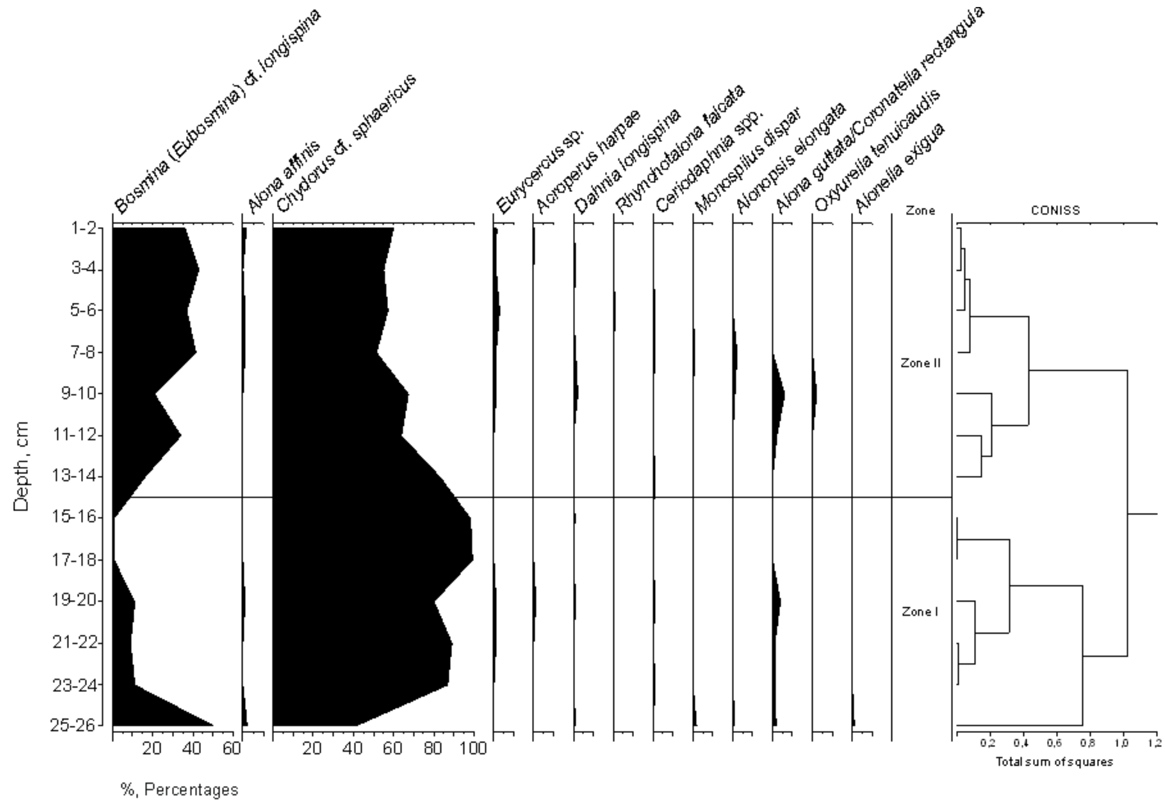

Fig. 2. Cladocera community of the bottom sediments of K1

In Zone II, an increase in the proportion of *B.* (*E.*) cf. *longispina* (15.84-43%) and the decrease of *C.* cf. *sphaericus* (51.49-83.17%) was observed. *B.* (*E.*) cf. *longispina* is a typical representative of species found in the open pelagic areas of reservoirs, of northern and central latitudes. The optimum temperature for this species ranges from 4 to 12 °C, which is typical for oligotrophic and moderately eutrophic reservoirs [18]. Changing the ratio of taxa in favor of increasing pelagic *B.* (*E.*) cf. *longispina* is often associated with an increase in areas of open water in a lake due to thawing permafrost. Furthermore, similar changes were noted while studying subfossil Cladocera communities in the bottom sediments of the unnamed lake, located on the catchment of the Pyasedayakha river (the Yamal Peninsula) and the Harbey lakes system (Bolshezemelskaya tundra) [17]. An increase in the effective moisture consequently has resulted in higher water level of lakes aiding the development of pelagic fauna which have been observed in the last 100 years within Russia [22], [23]. Similar changes (Cladocera, Chironomidae, Diatoms) have been observed according to biological indicators in the last 100-150 years in Finland [12], [24], Norway [25] and Canada [26]. An increase in the proportion of pelagic species in Arctic regions is often associated with climate warming. For example, a study of the diatom's communities of the bottom sediments in Finnish Lapland lakes indicated increases in temperature [5].

In Zone II remains of *Rhynchotalona falcata* and *Oxyurella tenuicaudis* were identified. *R. falcata* – which are Palearctic benthic species widely distributed in Europe, Kazakhstan, Siberia and Mongolia [27]. Furthermore, these taxa are often reported in both lowland and highland. Moreover, with preference for shallow stagnant areas of oligotrophic and mesotrophic lakes with sandy substrate without vegetation. Ideal pH for these taxa is acidic >4.2 and calcium (Ca^{2+}) [19], [27]. Also *R. falcata* has been reported in shallow marshes of Malozemelskaya tundra [28].

O. tenuicaudis – a salt water tolerant taxa are widely distributed in Europe and has been recorded in oligotrophic-eutrophic lake littoral, ponds and shallow marshes with a preference to inhabit areas between vascular plants, marginal vegetation and water with a pH>4.8 [20].

The Cladocera community of K1 is characterized by low taxonomic diversity, consisting of typical tundra lake species. Similarly, to those observed in previous investigations in other tundra lakes within Russia [6], [17], [29]. The values of the Shannon index ranged from 0.07-1.3, averaging at 0.88. While the Pielou index values ranged from 0.07-0.66 averaging at 0.38. In accordance with the obtained index values K1 indicates initial signs of eutrophication with the community structure of Cladocera not sufficiently aligned with these conditions.

Conclusion

According to the analysis of the Cladocera community from the bottom sediments of K1 an increase in the proportion of the pelagic taxon *Bosmina* (*Eubosmina*) cf. *longispina* was observed.

These observed shifts in community may be associated with an increase in the pelagic section of the lake due to the thawing of permafrost. Similar changes were also observed while studying other lakes of the Yamal Peninsula and Bolshezemelskaya tundra. Moreover, according to other studies of bottom sediments using different biological indicators, an increase in the proportion of pelagic taxa has similarly been observed in the last 100-150 years in the Arctic lakes of Europe and Canada.

Acknowledgments

The part of this study concerning paleolimnological work was supported by the grant of Russian Science Foundation (project 20-17-00135). Ibragimova A. research was supported by the subsidy allocated to Kazan Federal University for the state assignment #671-2020-0049 in the sphere of scientific activities. The text of the article was checked by a native English speaker Doctor of Philosophy (PhD) in Biology Robyn Geldard (Imperial College London, Beijing Forestry University).

REFERENCES

1. Katcov, V. M., Porfir'ev, B. N. (2012). Klimaticheskie izmeneniya v Arktike: posledstviya dlya okruzhayushchej sredy i ekonomiki. Arktika: ekologiya i ekonomika 2 (6), pp. 66-79.
2. Moritz, E., Bitz, C. M., Steig, E. J. (2002). Dynamics of Recent Climate Change in the Arctic. Science 297 (5586), pp. 1497-1502. DOI: 10.1126/science.1076522.
3. Birman, B. A., Berezhnaya, T. V. (2012). Osnovnye pogodno-klimaticheskie osobennosti Severnogo polushariya Zemli. 2011 god. Analiticheskij obzor, Gidrometcentr Rossii, 56.
4. Shirokov, R. S., Vasiliev, A. A. (2019). Bathymetric and Bottom Temperatures GIS of the Barents and Kara Seas. Natural Resource Management, GIS & Remote Sensing, Iran 1 (1), pp. 21-27.
5. Smol, J. P., Wolfe, A. P., Birks, J., Douglas, M., Jones, V. *et al*., (2005). Climate-driven regime shifts in the biological communities of arctic lakes. Proceedings of the National Academy of Sciences 102 (12), pp. 4397-4402. https://doi.org/10.1073/pnas.0500245102.
6. Frolova, L., Ibragimova, A., Fedorova, I. (2016). Stratigraphy of Cladocera in a core from A Yamal Peninsula lake (Arctic Russia). Proceedings of 16th International Multidisciplinary Scientific GeoConference, SGEM 4 (2), STEF92 Technology Ltd., Bulgaria, pp. 579-587.
7. Brooks, S. J. (2003). Chironomid analysis to interpret and quantify Holocene climate change (Mackay A.W., Battarbee R.W., Birks H.J.B. and Oldfield F., Eds). Global Change in the Holocene, Arnold, London, pp. 328-341.
8. Solovieva, N., Jones, V. J., Nazarova, L., Brooks, S. J., Birks, H. J. B., Grytnes, J. A., Appleby, P. G., Kauppila, T., Kondratenok, B., Renberg, I., Ponomarev, V. (2005). Palaeolimnological evidence for recent change in lakes from the northern Urals, arctic Russia. Journal of Paleolimnology 33, pp. 463-482.
9. Solovieva, N., Jones, V., Birks, J. H. B., Appleby, P., Nazarova, L. (2008). Diatom responses to 20th century climate warming in lakes from the northern Urals, Russia. Palaeogeography, Palaeoclimatology, Palaeoecology 259, pp. 96-106.

10. Kalinin, V. M., Kozin, V. V., Larin, S. I. (2001). Geografiya YANAO. Priroda, naselenie, hozyajstvo, ekologiya. Uchebnoe posobie dlya obshcheobrazovatel'nyh uchrezhdenij (Larina S.I., Eds), TGU, 327.
11. Morozova L. M., Magomedova M. A. (2004). Struktura rastitel'nogo pokrova i rastitel'nye resursy poluostrova YAmal. Izd-vo Ural. un-ta, Ekaterinburg, 63.
12. Korhola, A., Rautio, M. (2001). Cladocera and other branchiopod crustaceans. Tracking environmental change using lake sediments 4, Zoological indicators, Dordrecht, Kluwer Academic Publishers, pp. 125-165.
13. Szeroczyńska, K., Sarmaja-Korjonen, K. (2007). Atlas of Subfossil Cladocera from Central and Northern Europe, Świecie: Friends of the Lower Vistula Society, 84.
14. Kotov, A., Forró, L., Korovchinsky, N. M., Petrusek, A. (2013). World checklist of freshwater Cladocera species. World Wide Web electronic publication. Available online at http://fada.biodiversity.be/group/show/17.
15. Bogdanov, V. D., Bogdanova, E. N., Gos'kova, O. A., Mel'nichenko, I. P. (2000). Retrospektiva ihtiologicheskih i gidrobiologicheskih issledovanij. na YAmale. Izd-vo «Ekaterinburg», Ekaterinburg, 88.
16. Smirnov, N. N. (2010). Istoricheskaya ekologiya presnovodnyh zoocenozov. T-vo nauchnyh izdanij KMK, Moscow, 225.
17. Frolova L. A., Ibragimova A. G. (2015). Karcinologicheskij analiz donnyh otlozhenij ozer Kilometrovoe i Kotovo Harbejskoj sistemy (Bol'shezemel'skaya tundra). Trudy Karel'skogo nauchnogo centra Rossijskoj Akademii Nauk, Seriya Limnologiya (5), pp. 5-17.
18. Flössner D. (2000). Die Haplopoda und Cladocera (ohne Bosminidae) Mitteleuropas. Backhuys Publishers, Leiden, p. 428.
19. Fryer, G. (1968). Evolution and adaptive radiation in the Chydoridae (Crustacea: Cladocera): a study in comparative functional morphology and ecology. Philosophical Transactions of the Royal Society of London 254 (795), pp. 221-385.
20. Błędzki, L. A., Rybak, J. I. (2016). Freshwater Crustacean Zooplankton of Europe, Cladocera and Copepoda (Calanoida, Cyclopoida). Key to species identification, with notes on ecology, distribution, methods and introduction to data analysis. Springer, Germany, 918.
21. Alonso, M. (1996). Crustacea Branchiopoda Fauna Iberica. Madrid, Museo Nacional de Ciencias Naturales CSIC 7. 486.
22. Ibragimova, A., Frolova, L., Subetto, D. (2017). Subfossil Cladocera from boreal lake Gahkozero (The Republic of Karelia, Russia) as paleoenvironmental proxies. Proceedings of 17th International Multidisciplinary Scientific GeoConference, SGEM (17). STEF92 Technology Ltd., Bulgaria, pp. 589-597.
23. Ibragimova, A. G., Frolova, L. A., Subetto, D. A., Belkina, N. A., Potakhin, M. S. (2017). The changes in the composition of Cladocera community in bottom sediments of Lake Maloye Shibrozero (Zaonezhsky Peninsula) as a consequence of shifts of environmental and climatic conditions. IOP Conference Series: Earth and Environmental Science 107 (012029), pp. 1-8.
24. Nevalainen, L., Luoto, T., Sarmaja-Korjonen, K. (2008). Late Holocene water-level changes in Lake Iso Lehmälampi, southern Finland, reflected in subfossil cladocerans and chironomids. Studia Quaternaria 25, pp. 33-42.
25. Jensen, T. C., Zawiska, I., Oksman, M., Słowiński, M., Woszczyk, M., Luoto, T. P., Tylmann, W., Nevalainen, L., Obremska, M., Schartau A. K., Walseng B. (2019). Historical human impact on productivity and biodiversity in a subalpine oligotrophic lake in Scandinavia. Journal of Paleolimnology 63, pp. 1-20.
26. Sweetman, J. N, LaFace, E., Rühland, K. M., Smol, J. P. (2008). Evaluating the response of Cladocera to recent environmental changes in lakes from the central Canadian Arctic treeline region. Arctic, Antarctic, and Alpine Research 40 (3), pp. 584-591.
27. Sinev, A. Y., Kotov, A. A. (2014). Revision of the Holarctic genus *Rhynchotalona* Norman, 1903 (Anomopoda: Chydoridae). Zootaxa 3841 (2), pp. 188-210. DOI: 10.11646/zootaxa.3841.2.
28. Cherevichko, A. V. (2017). Zooplankton in water bodies of coastal marshes in Malozemelskaya tundra. Inland Water Biology 10 (2), pp. 203-208. DOI: 10.1134/S1995082917010047
29. Nigmatullin, N., Frolova, L. (2019). Zooplankton community structure and environmental conditions of tundra lakes in the Pechora River Delta (Northern Russia). 19th International multidisciplinary scientific geoconference, SGEM 19 (5.1), pp. 817-824. https://doi.org/10.5593/sgem2019/5.1 doi: 10.5593/sgem2019/5.1/S20.101

Late Paleozoic Odonata Assemblages of the East European Platform

FELKER Anastasiya[1]

Borissiak Paleontological Institute of RAS, Moscow (RUSSIA)
Moscow State University, Moscow (RUSSIA)
Email: felkafelka95@gmail.com

Abstract

Odonata are known from several Carboniferous and Permian localities of the East European Platform, from famous Lagerstätten and from relatively new localities where small numbers of fossils have been found. Apparently, the paleoenvironment of these localities, as well as taphonomic factors and the incompleteness of the fossil record, influenced the composition of their insect fauna. In this paper, we discuss the most significant Late Paleozoic localities for fossil Odonata and the features of their odonate assemblages.

Keywords: Odonata, Permian, Carboniferous, East European Platform

Introduction

The Late Paleozoic history of Odonata is quite interesting. First, it covers the origins and the earliest stages of evolution of the order Odonata. Second, Late Paleozoic Odonata, in contrast to the Mesozoic taxa, differ from modern ones at the systematic (suborder) and partly paleoecological level [1]. In their morphology, the wings of Late Paleozoic Odonata, like modern ones, have two main types. One of them is the wing with a wide base, as in modern dragonflies (suborder Anisoptera), and another is the petiolate wing similar to modern damselflies (suborder Zygoptera). However, the great variety in venation and size doubles the number of Late Paleozoic ecological types of Odonata. Thus, despite the similar shape of the wing base, it is impossible to attribute to the same ecological type permagrionids and kennedyids, or meganeurids and ditaxineurids, such as *Meganeuropsis permiana* Carpenter, 1939 and the relatively small ditaxineurid *Permaeschna dolloi* Martynov, 1931 with wingspans up to 71 cm and 14 cm, respectively [2], [3]. Both of these odonates are Paleozoic equivalents of modern dragonflies of the suborder Anisoptera, however, the cardinal differences in wing size and venation do not allow them to be classified together ecologically. Below we discuss the main ecological types of Late Paleozoic Odonata and their distribution in the insect assemblages of the East European Platform.

Ecological types of Late Paleozoic Odonata

The first odonatopteran insects, *Kirchnerala treintamil* Petrulevičius & Gutiérrez, 2016 and *Argentinala cristinae* Petrulevičius & Gutiérrez, 2016 are known from the Serpukhovian of Guandakol in Argentina [4]. In fact, they have few similarities with true Odonata and represent a "transitional form" from Ephemeroptera to Protodonata. In Pennsylvanian, odonatopteran insects are found in many Lagerstätten of Germany, Great Britain, China and Argentina [4], [5], [6]. Most of them are represented by large-sized meganeurids, which have unspecialized wing venation without nodus, arculus, or pterostigma. In modern odonates, these wing structures are responsible for the wing bending during flapping and pronation by reducing the aerodynamic load on wing sections potentially at risk of ‘kinking’, and are necessary for active flapping flight [7]. In meganeurids, damping of dangerous aerodynamic effects and creating lift on the underside of the wing were apparently achieved through the sharp bending of most branches of the anal, cubital and median veins towards the posterior wing margin [7], [8].

However, such a design could hardly be compared with the wings of modern Odonata, and the predominant type of flight in meganeurids was apparently gliding [9]. This type of flight is directly related to the habitat and accordingly, to the paleoecological reconstructions of meganeurid fossil sites. According to the latter, meganeurids lived in open spaces, above large rivers and lakes, and were ecological equivalents of modern hawker predators, Aeschnidae [8].

Rare representatives of the second ecological type of Odonata appeared in the same time interval (late Middle Pennsylvanian). These are medium-sized petiolate-winged damselflies of the suborder Protozygoptera, *Bechlya ericrobinsoni* Jarzembowski *et al*., 2002 and *Jacquesoudardia magnifica* Prokop *et al*., 2014 from Great Britain and France, respectively [10], [11]. Their venation characters, such as the wing petiole, nodus and arculus, indicate that the type of flight in these damselflies has changed from gliding, characteristic of meganeurids, to a more active flapping. Their reconstructed habitats were dense lycopsid forests or overgrown banks of swampy river deltas. Damselflies of this ecological type (mainly relatively large protozygopterans of the family Permagrionidae) are known from many Permian localities of the world. The best known of them are Chekarda (Perm Region, Russia), Lodeve (France), Soyana (Arkhangelsk Region, Russia) Kargala (Orenburg Region, Russia), Tikhie Gory (Tatarstan, Russia), Isady (Vologda Region, Russia), Balgovan (KwaZulu-Natal, South Africa), Bodie Creek Head (Falkland Islands) etc. [12], [13], [14], [15], [16], [17], [18].

Two more specialized derivatives of both the above ecological types appear in the Permian: broad-winged ditaxineuroids (Ditaxineuridae and Permaeshnidae) and small petiolate-winged Kennedyidae [19]. Small and medium-sized ditaxineuroids with wide, non-petiolate wings have a complete “true” nodus about 2/3 wing length and an enlarged pterostigma, in contrast to meganeurids, but, like the latter, lack an arculus, having a convergence of the radial, median and cubital branches instead [7]. Apparently, modern equivalents of this ecological type are small dragonflies of the families Libellulidae and Corduliidae [7]. Most fossil ditaxineuroids are confined to marginal lagoonal facies.

The fourth ecological type is represented by the family Kennedyidae, small damselflies with petiolate wings having sparse venation (some longitudinal veins reduced), arculus, pterostigma, an incomplete nodus, and a pronounced long main vein stem at least 1/3 wing length. The distally widened wings of kennedyids are best suited for active, maneuverable but slow flight.

Modern ecological equivalents of this type are small zygopteran damselflies of the endemic Australian family Hemiphlebiidae, the South American family Protoneuridae, and the widespread family Coenagrionidae [19].

Late Paleozoic localities of the East European Platform

Fossils of Odonata are quite rare and account for about 1-4% of total insects in most Late Paleozoic localities [19]. This is due to both the peculiarities of the habitat and the setting of the burial of odonates. Odonata are usually buried in sediments of small stagnant, or weak-flowing and marginal water bodies, geologically interpreted as lacustrine or more rarely lagoonal and marginal-marine facies. Nine Late Paleozoic localities of fossil Odonata are known from the East European platform. There are Kamensk-Shakhtinsky (Bashkirian; Rostov Region), Chekarda (Kungurian, Perm Region), Tyulkino (Ufimian, Perm Region), Soyana (Kazanian, Arkhangelsk Region), Tikhie Gory (Kazanian, Tatarstan), Kityak (Kazanian, Kirov Region), Isady (Severodvinian, Vologda Region), Kargala and Vyazovka (Severodvinian, Orenburg Region). The odonate assemblages of large localities such as Chekarda (more than 6,500 total insects and 62 odonate specimens), Soyana (about 5,000 total insects and 65 odonate specimens) and Isady (more than 7,000 total insects and 40 odonate specimens) are quite rich and diverse. In the remaining localities, with fewer than 1,000 total insects collected, the number of odonate specimens varies greatly (from 1 to 30 specimens). In the localities of Kargala, Tyulkino and Kityak, Odonata are few in number, and representatives of only one ecological type prevail. Only single specimens of Odonata are known from Vyazovka, Tikhie Gory, and Kamensk-Shakhtinsky.

Among the above localities, we distinguished several varieties, showing the relationship between the ecological types of Odonata found in them [19] and the assumed conditions of their formation. A similar distribution of Odonata is observed in the Soyana and Tyulkino localities, though about 5000 total insects were collected in Soyana and only about 550 in Tyulkino. Thus, large inhabitants of open spaces (meganeurids), prevail in both of these localities (28 specimens in Soyana and 29 specimens in Tyulkino) (Fig. 1). Other types have fewer specimens, in approximately equal numbers. In addition, almost the same number of both protozygopteran types of Odonata was recorded in Soyana locality. These types include both medium-sized permagrionids (11 specimens) and small kennedyids (10 specimens). Odonata, other than that of the dominant type, are differently represented in Tyulkino. Only one incomplete specimen of kennedyid damselfly, *Kennedya tyulkinensis* Felker, 2020 is known [18]. That distribution is quite consistent with the resemblance of the proposed paleoreconstructions of the above localities. Deposits of these localities are interpreted as marginal parts of brackish lagoons [20], [21]. Hence, the primary ecotopes were located within open wide areas suitable for large-sized meganeurids.

The famous Permian Lagerstätte of Chekarda shows another kind of Odonata assemblage.

The most productive fossil insect layers of Chekarda are reconstructed as deposits of branches of a paleo-river delta, gradually transformed into a brackish lagoon [22]. The Odonata fossils (62 specimens) make up less than one percent of the total insects (more than 6500 specimens). Most of them (28 specimens) belong to the second ecological type [19], represented by broad-winged medium-sized ditaxineuroids (Ditaxineuridae and Permaeschnidae). Small kennedyids are less numerous (17 specimens) and quite diverse (presumably 3 undescribed genera and 5 species). Long-winged Odonata of the two other ecological types, represented by large-sized meganeurids and petiolate-winged medium-sized permagrionids, are rarer (11 and 6 specimens, respectively) (Fig. 1). The predominance of medium-sized and small Odonata with wide and petiolate wing bases indicates that the banks of the Chekarda paleo-delta were covered with dense vegetation. The modern equivalents of these ecological types of Permian Odonata, small Libellulidae, Hemiphlebiidae, and Protoneuridae, inhabit similar ecotopes in Australia and Argentina [23], [24].

Isady and Kityak localities represent the third group. These localities exclusively contain fossils of protozygopteran damselflies (Fig. 1). The richest (40 specimens) and most interesting assemblage is found in the Isady locality. Its peculiarity concludes in the noticeable predominance (19 specimens) of the smallest petiolate-winged damselflies of the family Kennedyidae (similar to the genus *Progoneura*) [19]. At the same time, 5 specimens of ordinary representatives of the genus *Kennedya* are known from this locality. In addition, two fossils of damselflies formally referable to the same ecological type as kennedyids, but systematically different from them were found here. They are similar to typical representatives of Triassic protomyrmeleontoids of genus *Terskeja* Pritykina, 1981 [25]. Apparently, they represent undescribed ancestral forms of these Triassic damselflies, possibly belonging to the family Voltzialestidae [26]. The other fossils (13 specimens) belong to the second medium-sized protozygopteran type represented by the families Permagrionidae and Permepallagidae. Paleozoic equivalents of modern Anisopterous dragonflies, are not known from this locality.

Despite the general similarity of composition, the odonate assemblage of Kityak differs from the previous in the number of damselflies (7 specimens) and the proportion of ecological types.

Most of the odonates (6 specimens) belong to the family Permagrionidae, medium-sized damselflies with long wings. The small protozygopteran damselfly type includes only one specimen, described as *Progoneura kityakensis* Felker, 2020 (Kennedyidae) [18]. The prevalence of petiolate-winged protozygopteran damselflies suggests that localities of this type were formed by small, possibly slow-flowing rivers surrounded by dense vegetation. This is confirmed by paleoreconstructions, whereby these localities were formed in the marginal parts of small riverbeds or their cut-off meanders [19], [27], [28].

Odonata are known from very few specimens in the remaining localities of Tikhie Gory, Kargala, Vyazovka, and Kamensk-Shakhtinsky, so it is difficult to link their ecology and the paleoenvironment. In the Tikhie Gory locality, odonates are represented by three specimens belonging to two ecological types. The first type is represented by an undescribed specimen of the ditaxineuroid family Permaeschidae.

The second type includes two specimens of protozygopteran damselflies of the genus *Sushkinia* Martynov, 1930 (Fig. 1). Martynov originally assigned *Sushkinia elongata* Martynov, 1930 and *S. parvula* Martynov, 1930 to the family Kennedyidae, but later transferred them to Permolestidae [29], [30]. According to the latest revision of Late Paleozoic damselflies, the genus *Sushkinia* was treated as a protozygopteran of an uncertain systematic position [17].

However, the rather large size and some venation characters (“true” nodus, shape of pterostigma, length of the anal vein) suggest that this genus belongs to Permagrionidae (=Permolestidae), that is, to the ecological type of medium-sized protozygopteran damselflies.

Five odonate specimens of two ecological types are known from Kargala. The first type is represented by meganeurids family Kargalotypidae (2 specimens) [31].

The second type includes medium-sized damselflies of the family Permagrionidae (3 specimens) [32] (Fig. 1). Only one small protozygopteran of the family Kennedyidae is known from Vyazovka [18].

Two undescribed dragonflies are known from the Lower Pennsylvanian of Kamensk-Shakhtinsky. In their wing shape and venation, they are close to the earliest Argentinian Protodonata *Kirchnerala* and *Argentinala* and, accordingly, are referred to the ecological type of large meganeurids (Fig. 1).

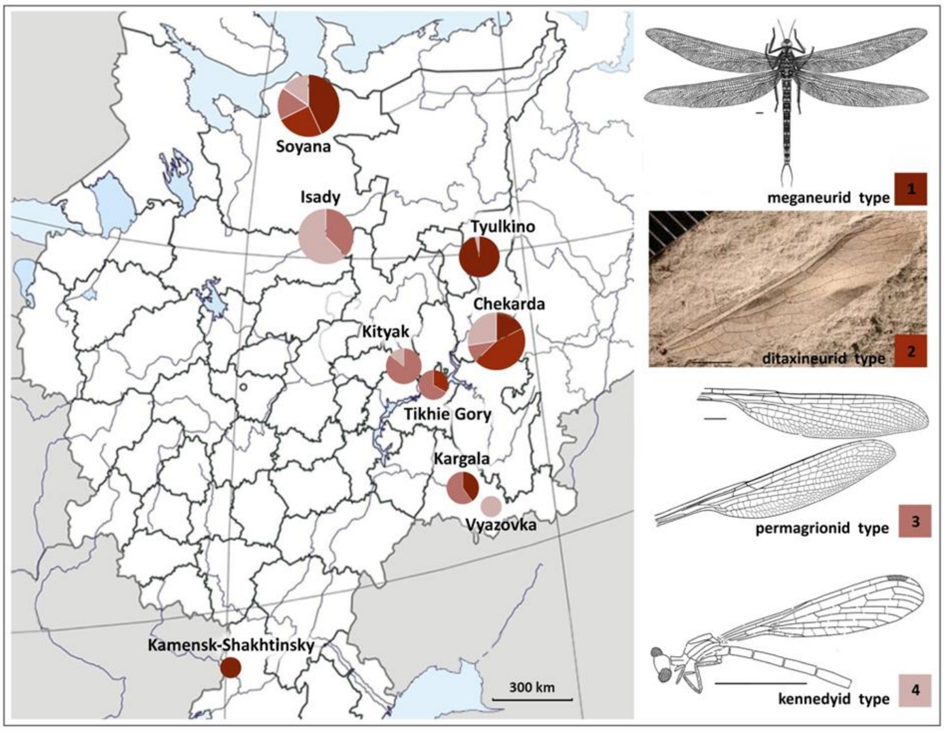

Fig. 1. Distribution of ecological types of Late Paleozoic Odonata in the localities of the East European Platform (the size of the circle graphs represents the abundance of the Odonata assemblages; scale bar 5 mm) [13], [15], [18], [20], [26], [29], [30], [31], [32].

Conclusions

The paleoenvironment of fossil localities often significantly affects the composition of their insect assemblages. In the Permian of the East European Platform, there are three main groups of odonate assemblages, distinguished according to the predominant ecological type of Odonata. (1) The assemblages of Soyana and Tyulkino preserved in lagoonal deposits show a marked predominance of large-sized, long-winged Meganeuridae. (2) The assemblage of Chekarda, formed in the zone transitional between the river delta and brackish lagoon, shows dominance of relatively small and medium-sized odonates with different wing shape, from broad-winged Ditaxineuridae to petiolate-winged Kennedyidae. (3) The assemblages of Isady and Kityak deposited in fluvial facies contain only Paleozoic equivalents of modern damselflies: small to medium-sized petiolate-winged protozygopterans Kennedyidae and Permagrionidae.

Acknowledgments

The author is deeply grateful to Dr. Dmitry E. Shcherbakov, Dr. Svetlana V. Nikolaeva and Dr. Maxwell V.L. Barclay for constructive revision of the English version of the text, and Prof. Alexander S. Alekseev for corrections of the text and useful suggestions.

REFERENCES

1. Pritykina, L. N. (1989). Paleontologiya i evoluciya strekoz. In Fauna i ekologiya strekoz (Mordkovich, V. G. Ed). Nauka, Sibirskoe otdelenie, Novosibirsk, pp. 43-59.
2. Carpenter, F. M. (1939). The Lower Permian insects of Kansas. Part 8. Additional Megasecoptera, Protodonata, Odonata, Homoptera, Psocoptera, Protelytroptera, Plectoptera, and Protoperlaria. Proceedings of the American Academy of Arts and Sciences 73 (3), pp. 29-70.
3. Huguet, A., Nel, A., Martinez-Delclos, X., Bechly, G., Martins-Neto, R. (2002). Preliminary phylogenetic analysis of the Protanisoptera (Insecta: Odonatoptera). Geobios 35 (5), pp. 537-560.

4. Petrulevicius, J. F., Gutierrez, P. R. (2016). New basal Odonatoptera (Insecta) from the lower Carboniferous (Serpukhovian) of Argentina. Arquivos Entomoloxicos 16, pp. 341-358.
5. Nel, A., Fleck, G., Garrouste, R., Gand, G., Lapeyrie, J., Bybee, S. M., Prokop, J. (2009). Revision of Permo-Carboniferous grifenfies (Insecta: Odonatoptera: Meganisoptera) based upon new species and redescription of selected poorly known taxa from Eurasia. Palaeontographica (A) 289, pp. 89-121.
6. Zhang, Z. J., Hong, Y. C., Lu, L. W., Fang, X. S., Jin, Y. G. (2006). *Shenzhousia qilianshanensis* gen. et sp. nov., Protodonata, Meganeuridae, a giant dragonfly from the Upper Carboniferous of China. Progress in Natural Science 16 (3), pp. 328-330.
7. Wootton, R. J., Kukalova-Peck, J. (2007). Flight adaptations in Palaeozoic Palaeoptera (Insecta). Biological Reviews 75 (1), pp. 129-167.
8. Nel, A., Prokop, J., Pecharova, M., Engel, M. S., Garrouste, R. (2018). Palaeozoic giant dragonflies were hawker predators. Scientific Reports 8, 12141.
9. Brauckmann, C., Zessin, W. (2008). Neue Meganeuridae aus dem Namurium von Hagen-Vorhalle (BRD) und die Phylogenie der Meganisoptera (Insecta, Odonata). Deutsche Entomologische Zeitschrift. 36(1-3), pp. 177-215.
10. Jarzembowski, E. A. Nel, A. (2002). The earliest damselfly-like insect and the origin of modern dragonflies (Insecta: Odonatoptera: Protozygoptera). Proceedings of the Geologists’ Association 113 (2), pp. 165-169.
11. Prokop, J., Roques, P., Nel, A. (2014). New non-holometabolous insects from the Pennsylvanian of the Avion locality in Pas-de-Calais, France (Insecta: “Exopterygota”). Alcheringa 38 (2), pp. 155-169.
12. Tillyard, R. J. (1928). A Permian fossil damselfly wing from the Falkland Island. Transactions of the Entomological Society of London 76 (1), pp. 55-63.
13. Martynov, A. (1932). New Permian Paleoptera with the discussion of some problems of their evolution. Trudy Paleontologicheskogo Instituta Akademii Nauk SSSR 1, pp. 1-44.
14. Nel, A., Gand, G., Garric, J., Jarzembowski, E. A., Lapeyrie, J. (1999). The first recorded protozygopteran insects from the upper Permian of France. Palaeontology 42 (1), pp. 83-97.
15. Nel, A., Bechly, G., Prokop, J., Bethoux, O, Fleck, G. (2012). Systematics and evolution of Paleozoic and Mesozoic damselfly like Odonatoptera of the Protozygopteran grade. Journal of Paleontology 86 (1), pp. 81-104.
16. Geertsema, B., van Dijk, D. E., van den Beever, J. A. (2002). Palaeozoic insects of Southern Africa: a review. Palaeontologica Africana 38, pp. 19-25.
17. Fate, C., Lapeyrie, J., Nel, A. (2013). A new Permagrionidae from the Middle Permian of the South of France (Odonatoptera: Protozygoptera). Zootaxa 3702 (4), pp. 397-400.
18. Felker, A. S. (2020). New damselflies of the family Kennedyidae from Permian deposits of European Russia. Paleontological Journal (in print).
19. Vasilenko, D. V. (2013). Dragonflies of the family Kennedyidae Tillyard, 1925 (Insecta: Odonata) in Permian odonatofaunas. Hydroentomology in Russia and adjacent countries: Materials of the Fifth All-Russia Symposium on Amphibiotic and Aquatic Insects. Papanin Institute for Biology of Inland Waters, Russian Academy of Sciences, Filigran, Yaroslavl, pp. 32-35.
20. Zekkel, Ya. D. (1940). Mestonahozhdeniya ostatkov permskih nasekomyh v basseyne r. Kuloya. Trudy Paleontologicheskogo Instituta Akademii Nauk SSSR 11 (2), pp. 81-94.
21. Vodolazskaya, V. P., Teterin, I. P., Kirillov, V. A., Lukianova, L. I., Petrov, G. A., Stefanovskiy, V. V., Morozov, G. G., Zhdanov, A. V., Stryapunina, E. V., Es’kin, A. G., Petrova, T. A., Verbitskiy, I. V., Verbitskaya, N. V. (2015). Gosudarstvennaya geologicheskaya karta Rossiyskoi Federacii. Mashtab 1:1 000 000 (tretie pokolenie). Seriya Uralskaya. List O-40 – Perm. Objasnitel’naya zapiska. Kartograficheskaya fabrika VSEGEI, Sankt-Peterburg, 497.
22. Ponomareva, G. Y. (2015). The geological structure of the section Checkarda. In Chekarda is a location of fossil insects and plants from the Permian period (Zhuzhgova, L. V., Ponomareva, G. Y., Aristov, D. S., Naugolnykh, S. V., Eds.). Izdatelstvo Permskogo universiteta, Perm, pp. 26-57.
23. Trueman, J. W. H. (1999). The enigmatic Australian endemic species Hemiphlebia mirabilis Selys (Zygoptera: Hemiphlebioidea): four short observations and a new record. International Journal of Odonatology 2 (1), pp. 115-121.
24. Muzon, J., Lozano, F., del Palacio, A., Ramos, L. S., Lutz, A. (2015). Odonata from the Lower Delta of the Parana River, Argentina. Agrion 20 (2), pp. 68-72.
25. Pritykina, L. N. (1981). Novye triasovye strekozy srednej Azii. In Novye iskopaemye nasekomye s territorii SSSR (Vishniakova V. N., Dlussky G. M., Pritykina L. N. Eds.). Trudy Paleontologicheskovo Instituta Akademii Nauk SSSR 183, pp. 5-42.
26. Felker, A. S. (2021). New Damselflies of the Family Kennedyidae (Odonata: Protozygoptera) from the Upper Permian Deposits of the Vologda Region. Paleontological Journal (in print).
27. Efremov, I. A. (1954). Fauna nazemnyh pozvonochnyh v permskih medistyh peschanikah Zapadnogo Priuralia. Izdatelstvo Akademii Nauk, Moscow, 453.

28. Golubev, V. K. (2013). Locality of Late Permian animals and plants Mutovino (=Isady) on the Sukhona River in Vologda Region: Historical geology. In Fossil Insects of the Middle and Upper Permian of European Russia (Aristov, D. S. Ed). Paleontological Journal 47 (7), pp. 651-658.
29. Martynov, A. V. (1930). New Permian insects from Tikhie Gory, Kazan province. 1. Palaeoptera. Trudy Geologicheskogo Muzeya Akademii Nauk SSSR 6, pp. 69-86.
30. Martynov, A. V. (1938). Ocherki geologicheskoi istorii i filogenii otryadov nasekomykh (Pterygota). 1. Palaeoptera i Neoptera-Polyneoptera. Trudy Paleontologicheskogo Instituta Akademii Nauk SSSR 7, pp. 1-149.
31. Nel, A., Bethoux, O., Bechly, G., Martinez-Delclos, X., Papier, F. (2001). The Permo-Triassic Odonatoptera of the ‘Protodonate’ grade (Insecta: Odonatoptera). Annales-Societe Entomologique de France 37(4), pp. 501-525.
32. Martynov, A.V. (1937). Permian fossil insects from Kargala and their relationships. Trudy Paleontologicheskogo Instituta Akademii Nauk SSSR 7, pp. 8-92.

The New NMR Relaxometry Method for Identifying Organic Matter Contained in the Rocks of the Boca De Jaruco Oilfield in Cuba

GALEEV Ranel[1], SAKHAROV Boris[1], KHASANOVA Nailia[1]

[1] Kazan Federal University, Kazan (RUSSIA)
Email: Ranel.galeev@mail.ru

Abstract

This article describes a new method for determining the content of organic matter (OM) by NMR (Nuclear magnetic resonance) relaxometry in the rocks of the productive formation (601-708m) of the Boca de Jaruco oilfield. A hypothesis was created about the time of formation of the object under study, the composition of the heterogeneity of the productive section and its genesis, as well as about the problem associated with the extraction of organic matter from rocks.

Keywords: NMR relaxation, Carr-Parcel-Meibum-Gill, organic matter, thermogravimetry, EPR spectrometry

Introduction

The main parameters affecting profitability during the exploitation of oilfields are the distribution of organic matter along the reservoir section of the productive well, the oil recovery factor, and heterogeneity.

Currently, there are thermal methods that have proven themselves in determining the above parameters [1]. Thermogravimetry (TGA) is one of the main methods for determining the organic matter in rocks. The quality of the reservoir depends on the amount of organic matter, its transformation, and the thermal stability of minerals in the rocks. The quality is diagnosed simultaneously by thermogravimetry methods based on weight loss during the combustion of the sample. The choice of methods for extracting and using combustion in the reservoir depends on information about the thermal properties of the heavy oil and bitumen [2, 3] along with the host rock's minerals [4, 5].

This article proposes a new complex method for determining the organic matter in rocks, based on NMR relaxometry. The new NMR relaxometry method, including the simultaneous registration of the decay of free induction (FID) and the decay of the transverse magnetization of the Carr-Purcell-Mayboom-Gill (CPMG) sequence, with the subsequent determination of their amplitude-relaxation characteristics (deconvaluation), has demonstrated a high efficiency at determining the group and phase composition of heavy oils [6, 7]. In this work, this method was first used to estimate the content of total OM, and OM typing, in rock samples taken along the section of the productive formation of the Boca de Jaruco oilfield.

In addition, the heterogeneity of the section, which consists of organogenic limestones interlayered with clay rocks, was studied by determining the manganese ion in the rocks by the EPR method, and the thermal parameters of the rock, which were used to determine the content of light fractions of organic matter and clay material (TGA) as the sum of rock mass losses (% wt.) in the temperature range Δ 40-200 ^{0}C. A hypothesis has been put forward about the formation time of the studied object, the lithological composition of heterogeneities and problems associated with oil recovery in these rocks.

Material and Methodology

Low-field (LF) NMR measurements. LF NMR measurements were conducted by a Proton 20M NMR analyzer, manufactured by the joint-stock company “SKB Chromatec”, Russia.

Rock samples were placed in an ampoule with a diameter of 10 mm and sealed with rubber stoppers. The resonance frequency for protons was 20 MHz. The dead-time of the NMR receiver was no more than 10 microseconds. The phase of the high-frequency pulses was set independently on the 4 channels to 00, 900, 1800 and 2700. Signals of free induction decay (FID) and echo in the modified Carr-Purcell-Meiboom-Gill (CPMG) series were obtained in phase-sensitive mode. Subsequent quadrature detection provided an increase in the signal-to-noise ratio by a factor of √2 and the independence of the result from the possible drift of the high-frequency phase. Moreover, to reduce the influence of inhomogeneities of constant B_0 and high-frequency B_1 magnetic fields on the accuracy of setting 180° pulses in the detectable volume, the sensor was placed in the most homogeneous part of the magnetic gap (the half-life time of the glycerol FID was t1/2≥1.6 ms) of the glycerin and filled the ampoule no more than 80% (≤1,1 cm) from the height of the high-frequency coil. The effectiveness of these measures was evaluated by checking the differences between the amplitudes of the first odd and even echo signals in the CPMG series [6].

Thermostabilization of the magnet at 40 °C provided the instability of a constant magnetic field no worse than 5.10-6 per hour. The device automatically adjusts resonant conditions based on the phase detection of the free-induction signal of the standard sample, usually glycerin, or the FID of the analyzed substance if it has a sufficiently intense slow component. All the rock samples in this study met this requirement. Thus, the resonant conditions in the process of measuring and accumulating NMR signals (FID and echo) were maintained with accuracy not much different from the accuracy of the stabilization of spectrometers equipped with separate NMR magnetic field stabilizers [6].

Thermogravimetric method. Analysis of the oil content of rock samples along the section of an oil reservoir was performed on a TG209F1 Librec precision thermogravimeter combined with an IR-Fourier Alpha attachment.

EPR-spectroscopy. The analysis of the Mn^{2+} ion content was performed by electron paramagnetic resonance (EPR) on a CMS8400 spectrometer (ADANI, 9.4 MHz) at room temperature.

Results and discussions

Geology. Primary production in Cuba has been performed for more than 30 years from large overthrusted carbonate structures along the north coast of Cuba between Havana and Varadero.

Within the Veloz Group, the Ronda and Cifuentes Formations are the most important reservoirs. These reservoirs are also the principal hydrocarbon producing horizons in the Boca de Jaruco oilfield (Fig. 1).

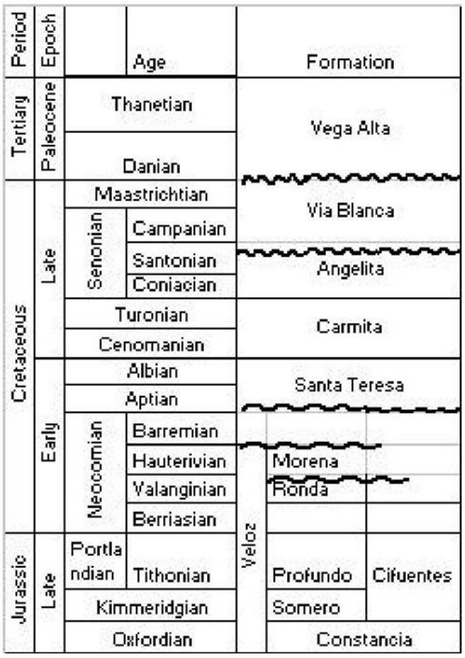

Fig. 1. Cuban Stratigraphic Column [8]

The Ronda-Cifuentes section is composed mainly of carbonate, cherts, and minor amounts of shale that were deposited in both deep water and shallow water environments. The carbonates that form the reservoir in the Ronda-Cifuentes are mainly light to medium-brown fine-grained, micritic to chalky limestones, bioclastic wackestones with bitumen laminations, and some dolomite. Primary porosity is poor but secondary porosity has been developed through fracturing, dolomitization and pressure solution. Vugs are frequently visible along with fractures and cavernous porosity may also be present. The cherts are mainly medium-brown, gray, or white, translucent, and are fragmental or interlaminated with limestones [8].

Hydrocarbons within the Ronda-Cifuentes are trapped structurally due to a compressional event during the Tertiary that created duplexes and anticlinal stacks as a result of thrust faulting within the Mesozoic and Cenozoic Strata (Fig. 2).

These structural traps are sealed by shales, cherts, limestones, and fine-grained sediments of the thick Tertiary (Paleogene) Vega Alta formation that unconformably overlies the Veloz Group. The unit of the Vega Alta that immediately overlies the Veloz is informally known as the “Seal Unit” and is mainly composed of claystones, cherts, and bituminous black shales with loose silicified radiolarians and minor serpentine fragments [8].

Thermogravimetric exploration. The TGA method in this work was used to determine the content of clay materials in the section’s rocks (section heterogeneity).

The TGA technique for the determination of light fractions and clay materials is based on the determination of the mass loss of a substance during heating in the range of T=40-200 ^{0}C.

It is possible to directly correlate the loss of mass and clay matter only if the organic matter throughout the studied section has the same component composition (the content of light and heavy fractions). That is why the determination of clay matter along the section was simultaneously determined by the EPR method (Ch. 3.3). The results of TGA exploration are presented in Fig. 7.

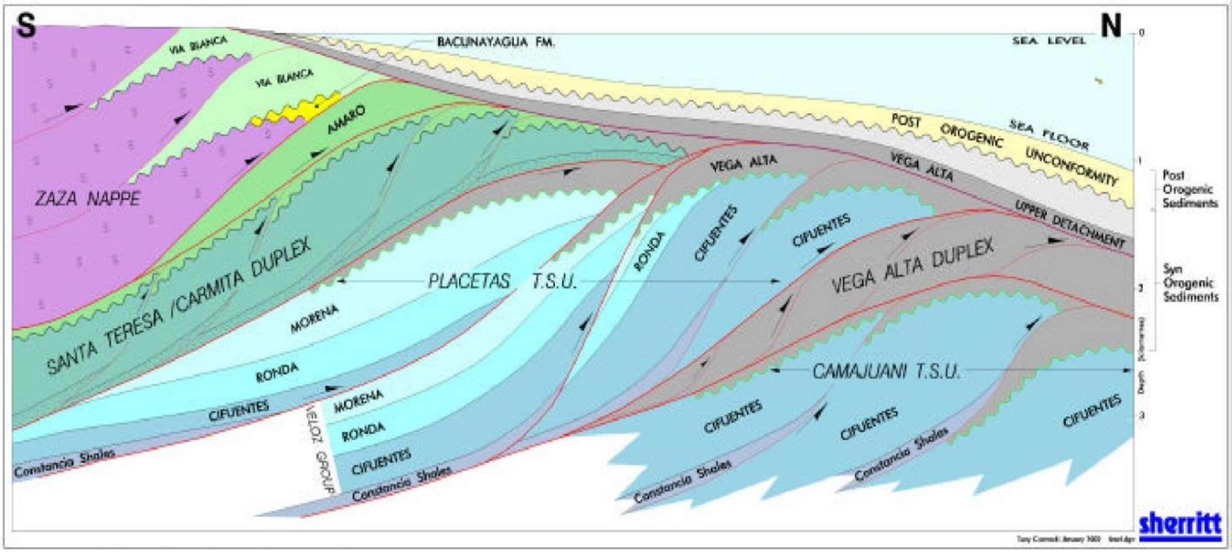

Fig. 2. Cuban Overthrust Schematic [8]

EPR-spectroscopy exploration. EPR spectroscopy is a method of non-destructive monitoring of the state of a mineral and organic collector under thermochemical influences without the use of chemical solvents, without burning a sample.

During testing, the EPR technique was used to study carbonate sediments by the amplitude of the weak-field EPR line of the Mn^{2+} ion [8, 9]. The results of EPR exploration are presented in Fig. 7.

LF NMR exploration. The NMR relaxometry method is based on the fact that the initial amplitude of relaxation decays is strictly proportional to the number of protons in the sample and, consequently, to the OM content in the sample. The total initial NMR decay amplitude (A_0) is determined as the sum of the amplitudes of the liquid-phase (A_{0L}) and solid-phase (A_{0S}) decay components, which in turn are calculated from the fitting using the Voight and Abraham model functions, respectively.

For each of 10 rock samples taken from the depth interval 601-708 m, the OM content was determined by the formula OB (NMR) = $(A_{0S} + A_{0L})$ *k/m, where k is the conversion factor, and m is the mass of the rock sample. The results of EPR exploration are presented in Fig. 7.

A study was carried out to determine the residual organic matter after extraction with deuterated chloroform for samples #676 and #708 (Fig. 3, 4). The results showed that extraction from the rock recovered 86.14% and 52.82% for samples 676 and 708, respectively.

When examining rock samples (#627-#708), two of them (#644, #708) had a long-term component, which indicates the oil content in large pores (Fig. 5).

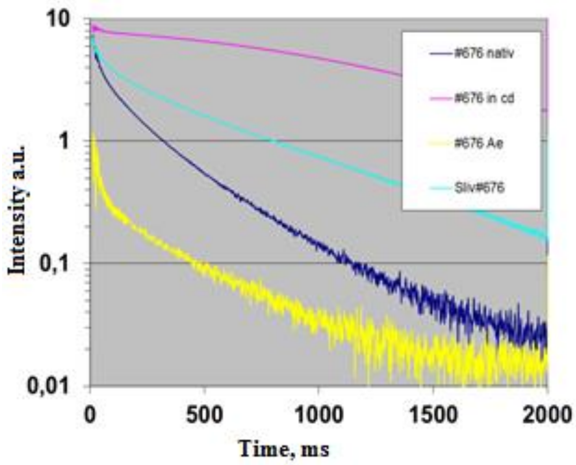

Fig. 3. Experimental KPMG decay curves from native (nativ) and deuterated chloroform-filled (in cd) rock #676, extract from rock (Sliv) and rock after extraction (Ae)

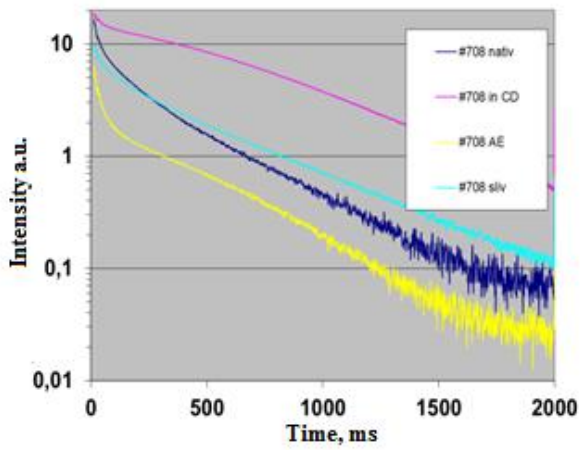

Fig. 4. Experimental KPMG decay curves from native (nativ) and deuterated chloroform-filled (in cd) rock #708, extract from rock (Sliv) and rock after extraction (Ae)

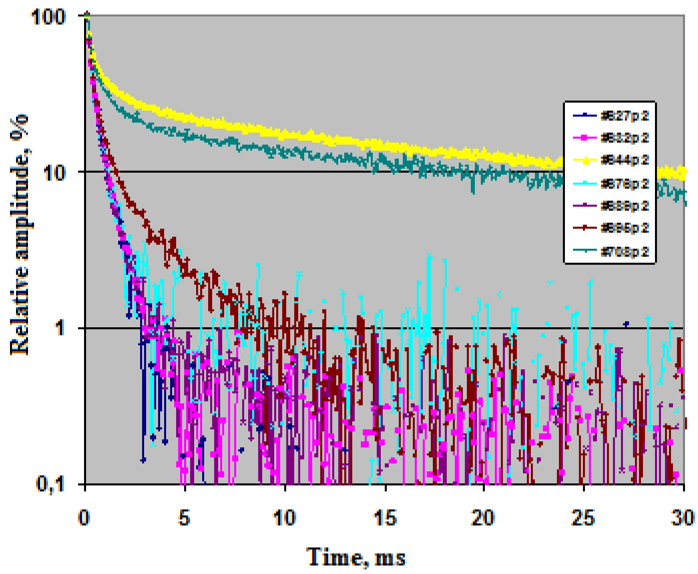

Fig. 5. KPMG decays of samples (#627-#708), normalized to the maximum amplitude, were taken as 100% for each sample

Interpretation of geological information

According to the data of the geological setting of the Boca de Jaruco oilfield [10, 11], it can be assumed that the studied object belongs to the upper part of the Jurassic system, which is represented by an interlayer of oil-saturated organogenic limestones and shales, with heterogeneity (interlaying) being represented by the Vega Alta duplex. Thus, using the EPR and TGA methods, a lithostratigraphic column of the Jurassic deposits of the Boca de Jaruco oilfield was constructed (Fig. 6), in which the presence of the Vega Alta duplex is observed in the form of oil-saturated shales with the presence of clay material.

The long relaxation time of the samples from depths of 644m and 708m indicates that the rock contains a system of large pores with a small surface-to-volume ratio. As a result, the surface of the walls has little effect on the mobility of molecules and the relaxation of protons in them. These layers are surrounded by rocks with thin pores, in which there is hard-to-extract organic matter in solid and highly viscous states.

The data on the distribution of the Mn^{2+} ion shows that the organic matter contained in the large pores is in the shale. It is possible that the OM in smectites, which have large systems, is ported, which is observed by a decrease in NMR relaxation.

According to the data on the extraction of organic matter, it can be assumed that the Vega Alta duplex rocks have a low oil recovery coefficient due to a decrease in the content of smectites in their composition, seeing as OM does not dissolve during extraction.

This assumption can be used for further planning of oilfield development (provided that enhanced oil recovery is applied) for more efficient oil recovery.

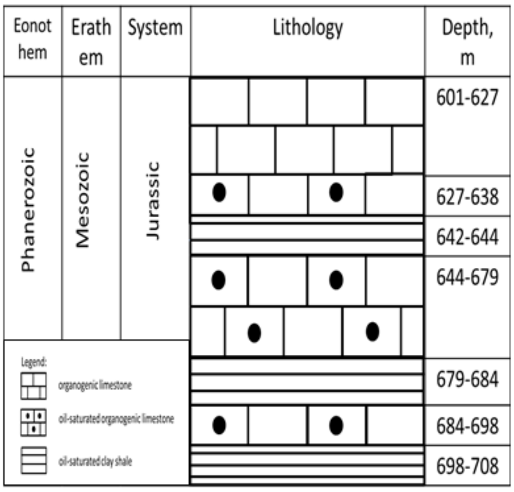

Fig. 6. Lithostratigraphic column of oil-bearing rocks of Boca de Jaruco oilfield

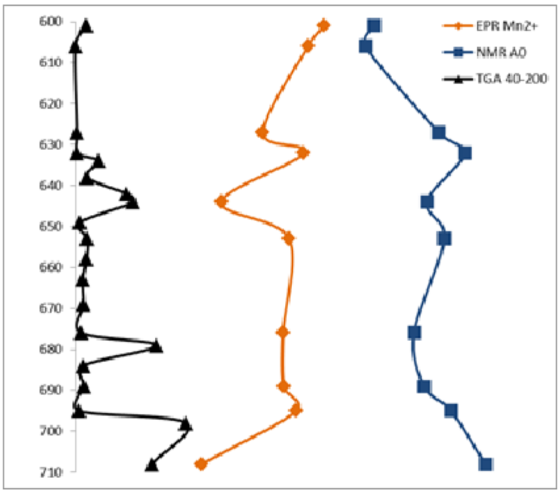

Fig. 7. Distribution curves for organic matter (NMR), manganese ion (EPR), and the presence of clay material (TGA)

Conclusion

In this article, the content of organic matter in the rocks was determined along the section (601-708 m) of the Boca de Jaruco deposit using a new non-invasive NMR relaxometry method.

A hypothesis was put forward for the problem of oil recovery, which is based on the content of residual organic matter in large pores of smectite material, which does not allow dissolving oil for its further extraction. Based on the TGA and EPR methods, a study of the heterogeneity of the section and its genesis was carried out, which showed the presence of clay material at depths (#642-#644, #679-#684 and #698-#708 m), which belongs to the Vega Alta duplex, a lithological column was built, it was determined, that the rocks belong to the upper Jurassic system.

Acknowledgments

This work was performed according to the Russian Government Program of Competitive Growth of Kazan Federal University.

REFERENCE

1. Jihui, N., Hu, J., Wanfen, P., Hang, J., Jianjun, Y., Qiang, R. (2014). Thermal kinetics study of light oil oxidation using TG/DTG techniques. Journal of Thermal Analysis and Calorimetry 117 (3), pp. 1349-1355.
2. Ganeeva, Y. M., Yusupova, T. N., Okhotnikova, E. S. (2019). Thermal analysis methods to study reservoir bitumens. Journal of Thermal Analysis and Calorimetry 139 (6/н), pp. 273-278.

3. Yusupova, T. N., Ganeeva, Y. M., Okhotnikova, E. S., Romanov, G. V. (2018). The use of thermal analysis methods for monitoring the development of bitumen reservoirs using thermal recovery technologies. Journal of Thermal Analysis and Calorimetry 131 (2), pp. 1405-1411.
4. Ariskina, K. A., Abaas M., Chengdong, Y., Emelianov, D. A., Varfolomeev, M. A. (2020). Effect of calcite and dolomite on crude oil combustion characterized by TG-FTIR. Journal of Petroleum Science and Engineering 37 (6), pp. 1-7.
5. Ariskina, K. A., Abaas M., Chengdong, Y., Emelianov, D. A., Rodionov, N., Varfolomeev, M. A. (2020). The catalytic effect of clay rocks as natural catalysts on the combustion of heavy oil. Applied Clay Science 193, 105662.
6. Volkov, V. Ya., Sakharov, B. V., Khasanova, N. M., Nurgaliev, D. K. (2018). Analysis of the composition and properties of heavy oils in situ by low field NMR relaxation method. Georesources 20 (4), pp. 308-323.
7. Volkov, V. Ya. (2013). Restore FID using a modified CPMG pulse sequence. Nuclear Magnetic Resonance in Condensed Matter. NMRCM 2013, 10th meeting "NMR in Life Sciences", 119.
8. Nurgalieva, N. G., Anikina, E. A., Khasanova, N. M. (2017). The structure of the Tournaisian oil-bearing limestones of the South rock of the South Tatar arch according to petrophysical and geochemical studies. Oil industry 2, pp. 46-48.
9. Nurgalieva, N. G., Anikina, E. A., Khasanova, N. M. (2017). Characteristics of the Famennian oil-bearing limestones of the southern slope of the South Tatar arch according to petrophysical and geochemical data. Oil industry 12, pp. 90-93.
10. Smith, G. E., Hurlburt, G., Li, V. P. (2002). Heavy Oil Carbonate: Primary Production in Cuba. SPE/PS-CIM/CHOA International Thermal Operations and Heavy Oil Symposium and International Horizontal Well Technology Conference 89 (12), pp. 1955-1959.
11. Ananev, V. V., Verzhbutskiy, V. E., Obukhov, A. N., Borisov, D. V. (2014). Geology and Petroleum Potential of the Gulf of Mexico, Cuba. SPE Rissian Oil and Gas Exploration and Exhibition 1, pp. 574-579.

The Use of Extraterrestrial Microspherules to Facilitate Correlation of Permian Evaporites

GLUKHOV Mikhail[1], KADYROV Rail[1], SUNGATULLIN Rafael[1], GAREEV Bulat[1], GALIULLIN Bulat[1], NIZAMOVA Aigul[1], IBRAGIMOV Rafail[1]

[1] *Kazan Federal University, Kazan (RUSSIA)*
Email: gluhov.mixail2015@yandex.ru

Abstract

This paper addresses the morphology and mineral and chemical composition of magnetic microspherules found in the Roadian gypsum deposits (Guadalupian Series of the Permian) of the Baymatskoye and Kamsko-Ustinskoye fields. Microspherules of both fields have similar dendritic (wrinkly, lattice) and platy (feathery, scaly, fractured) structure and consist primarily of magnetite with admixtures of Al, Si, Mn, Ni, and Cu. We analyzed the distribution of microspherules in gypsum beds and demonstrated that they originated from cosmic dust and were formed due to meteoroid ablation. We also suggest that magnetite microspherules in sedimentary rocks can be used as an additional tool for stratigraphic correlation.

Keywords: Permian, Roadian, evaporites, magnetite microspherules, dendritic structure, correlation

Introduction

Biostratigraphic, lithological and geochemical methods, as well as absolute dating of sedimentary rocks often do not provide enough data for correlation of productive zones within a field [1]. As we have shown previously [2], [3], [4], extraterrestrial magnetic microspherules (less than 1 mm in diameter) can be used as an additional tool for stratification and correlation of coeval sedimentary rocks. Microspherules are well preserved for a long time (hundreds of millions of years) [5] in marine and continental deposits, so they can also be useful for correlation of multi-facies deposits. In the future, this can be applied to prospecting for stratified extractable resources (gas, oil, etc.).

The objective of this study is to correlate the gypsum beds of the Kamsko-Ustyinskoye and Baymatskoye fields (Roadian deposits, Guadalupian series of the Permian). Kamsko-Ustyinskoye and Baymatskoye gypsum fields are located 66-84 km south of the city of Kazan (on the right bank of the Volga River, European Russia). The fields belong to the southern part of the Kazan-Kirov Depression of the Volga-Ural Anteclise. We suggest that the correlation can be based on magnetite microspheres sometimes found in evaporites. The project tasks included detection of microspherules in the rocks (gypsum, anhydrite and dolomite) of the fields mentioned above and their morphological, mineralogical and chemical analysis. Previously, we have studied gypsum samples taken from both fields [6], [7], [8], [9]. X-ray computed tomography revealed X-ray-dense particles in the samples, including magnetic microspherules.

This excluded anthropogenic sources from the list of possible origins of microspherules in the evaporites under study.

Methodology

In Baymatskoye field, we took 12 samples from the lower gypsum bed and 10 samples from the upper one. 16 and 10 samples (respectively) were taken from the same layers in the Kamsko-Ustinskoye field. All the samples were powdered in an agate mortar. Then, magnetic minerals were extracted from each sample (the average weight of the samples was ~80g) with a neodymium magnet. Microspherules were separated under a microscope. More than 70 microspherules and 5 drop-shaped particles (4 in the lower bed and 1 the upper bed of Baymatskoye field) were found. A Phillips XL-30 scanning electron microscope (equipped with an energy-dispersive spectrometer) was used to photograph the surface of the microspherules and perform the chemical analysis (accelerating voltage was 20 kV; measuring section was 8.9-15 mm; probing depth was 1.0–1.5 microns; measurement accuracy was 0.1% (KFU, analyst B.M. Galiullin). In the end, 15 EDS analysis results were obtained for the studied microspherules: 7 for those found in Kamsko-Ustinskoye field, and 8 for the ones from Baymatskoye field. The mineral composition of the microspherules was studied using the confocal Raman spectrometer inViaQontor (Renishaw) equipped with the Leica dm2700m microscope. The spectra were excited by a double-pulsed Nd: YAG laser (532 nm), 50× lens.

The accumulation time was 25 sec; spectral wavelength range was 100-2000 cm^{-1}.

Calibration was performed based on spectral lines and the position of the laser beam on the silicon standard. The mineral phases were identified using the Renishaw spectrometer, the «CrystalSleuth» software and the RRUFF.INFO database (KFU, analyst A.V. Nizamova). Two microspherules from each field were studied using this method (4 microspherules in total).

Results and Discussions

We found that microspherules had a size distribution of 5-150 microns and different surface types: A – wrinkled (Fig. 1a, e), B – lattice (Fig. 1b, f), C – feathery (Fig. 1g), D – scaly (Fig. 1h), E – fractured (Fig. 1j), and implicit (Fig. 1d). Inside some of the microspherules, voids were found (Fig. 1b). Implicit texture (Fig. 1d) was found to be scaly under a strong magnification of the microscope.

Types A and B were the most common among the studied microspherules. Two transition types were also observed: C-D (Fig. 1g) and D-E (Fig. 1c, i). The presence of A-E, B-E and A-C transition types was not recorded.

According to other researchers [10], type A forms under the highest temperature. Type E corresponds to the lowest temperature [10].

The EDS results (Table 1) showed that all the microspherules consist of iron oxides with an admixture of Si, Al, Ca, Ni, Cu, Mg, Mn (both on the surface and inside of them).

Raman spectroscopy (Fig. 2) showed asymmetrical Fe-O bending (T2g) vibrations (~298 and 540 cm^{-1}), symmetrical bending (Eg) vibrations and valence (A1g) vibrations (~319 and 668 cm^{-1}) indicating that the microspherules consist primarily of magnetite [11].

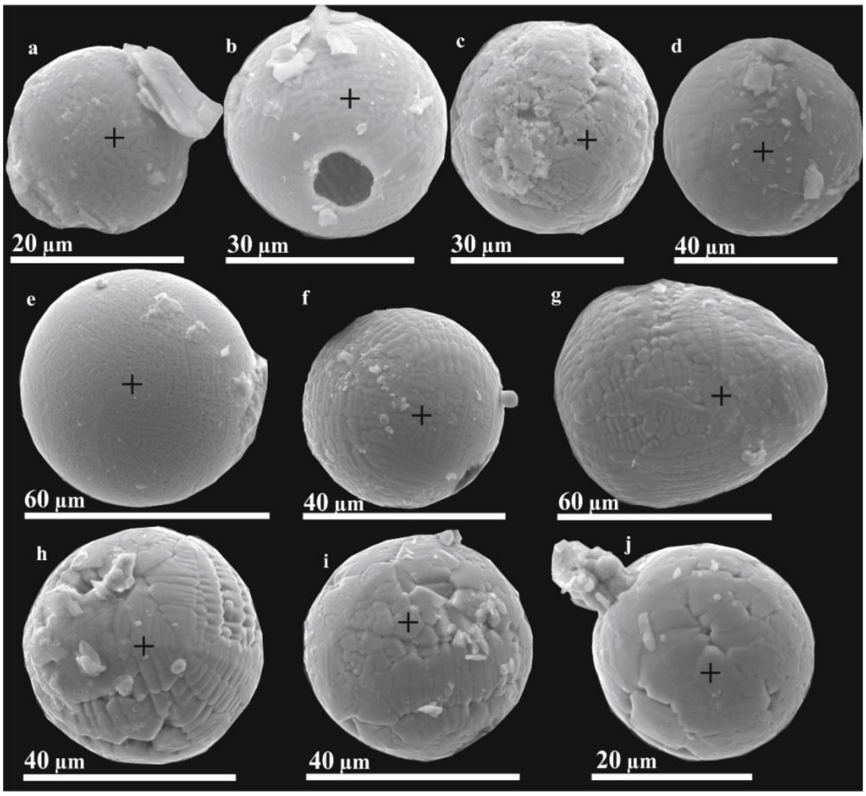

Fig. 1. Electron microscopic images of microspherules from Roadian deposits of Kamsko-Ustinskoye field (a-d) and Baymatskoye field (e-j)

Table 1. Surface chemical composition of microspherules from Permian evaporates

Sample	Elements, wt %										
	SiO_2	Al_2O_3	Cr_2O_3	FeO	NiO	CuO	MnO	MgO	CaO	SO	Total
Kamsko-Ustinskoye field											
1(Fig. 1, a)	1.19	1.02	*	94.03	2.53	*	0.76	*	0.47	*	100
2(Fig. 1, b)	2.19	*	*	92.86	*	1.56	1.62	*	1.32	0.45	100
3(Fig. 1, c)	1.32	*	*	96.38	*	1.29	1.01	*	*	*	100
4(Fig. 1, d)	0.94	*	*	96.52	*	1.60	0.94	*	*	*	100
5	0.79	*	*	97.33	*	1.88	*	*	*	*	100
6	*	*	*	100	*	*	*	*	*	*	100
7	1.32	0.87	*	97.81	*	*	*	*	*	*	100
Baymatskoye field											
8(Fig. 1, e)	2.17	*	*	93.68	2.11	*	2.04	*	*	*	100
9(Fig. 1, f)	*	*	*	97.73	1.62	*	0.65	*	*	*	100
10(Fig. 1, g)	1.32	*	*	96.51	2.18	*	*	*	*	*	100
11(Fig. 1, h)	2.60	*	*	94.44	1.72	*	1.24	*	*	*	100
12(Fig. 1, i)	1.36	*	*	88.52	0.97	*	0.77	5.77	2.61	*	100
13	1.06	*	*	97.47	1.47	*	*	*	*	*	100
14	2.30	1.17	*	94.13	0.89	*	1.51	*	*	*	100
15	*	*	*	100	*	*	*	*	*	*	100

**- not detected*

Quantitative distribution of microspherules in the beds are shown in Fig. 3 and Fig. 4. Microspherules are quite numerous and evenly distributed within the upper and lower gypsum bed of Baymatskoye and Kamsko-Ustinskoye fields. The number of microspherules is greater in the lower bed of Baymatskoye field than in the upper bed. Often there are more than 5 microspherules found in one sample.

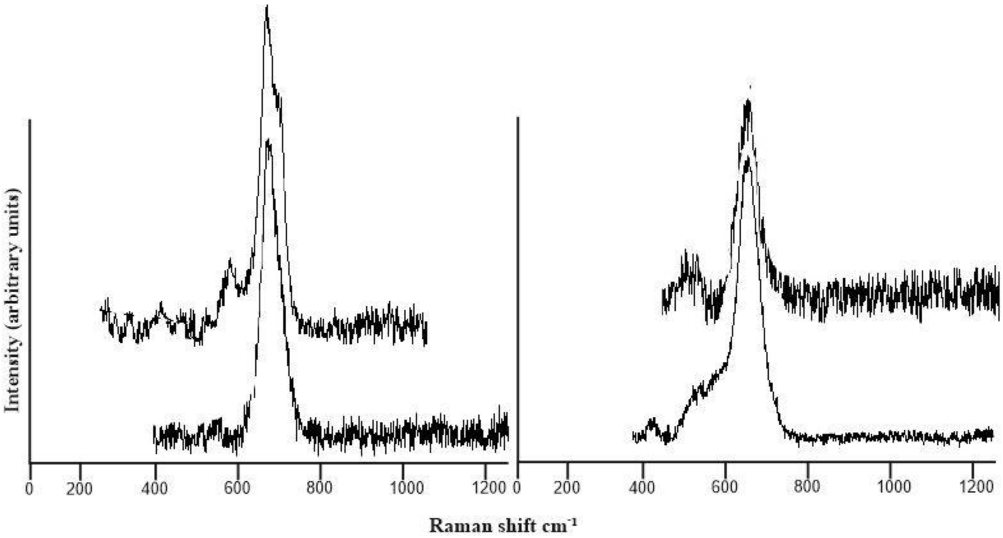

Fig. 2. Raman spectra of the microspherules: a – Kamsko-Ustinskoye field, b– Baymatskoye field

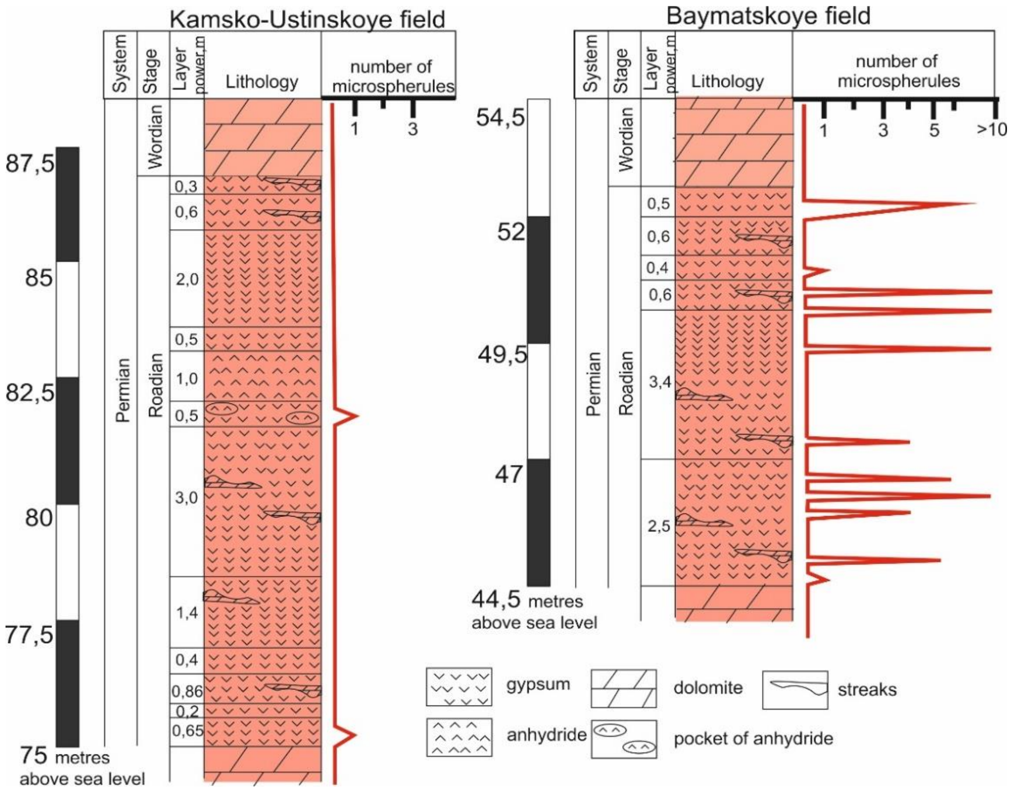

Fig. 3. Distribution of microspherules in the lower gypsum layer

The similarities in the structure and composition of magnetic microspherules from both the upper and lower gypsum layers of two different fields indicate that the microspherules share a common origin. Spherical and drop-shape form, size, dendrite texture and composition indicate a high-temperature environment [10]. All of the above suggests that the microspherules originated from cosmic dust and were formed due to meteoroid ablation [12], [13], [14]. Si, Mg and S found on the surface of the microsperules suggest that the meteoroid was probably a chondrite [15], [12].

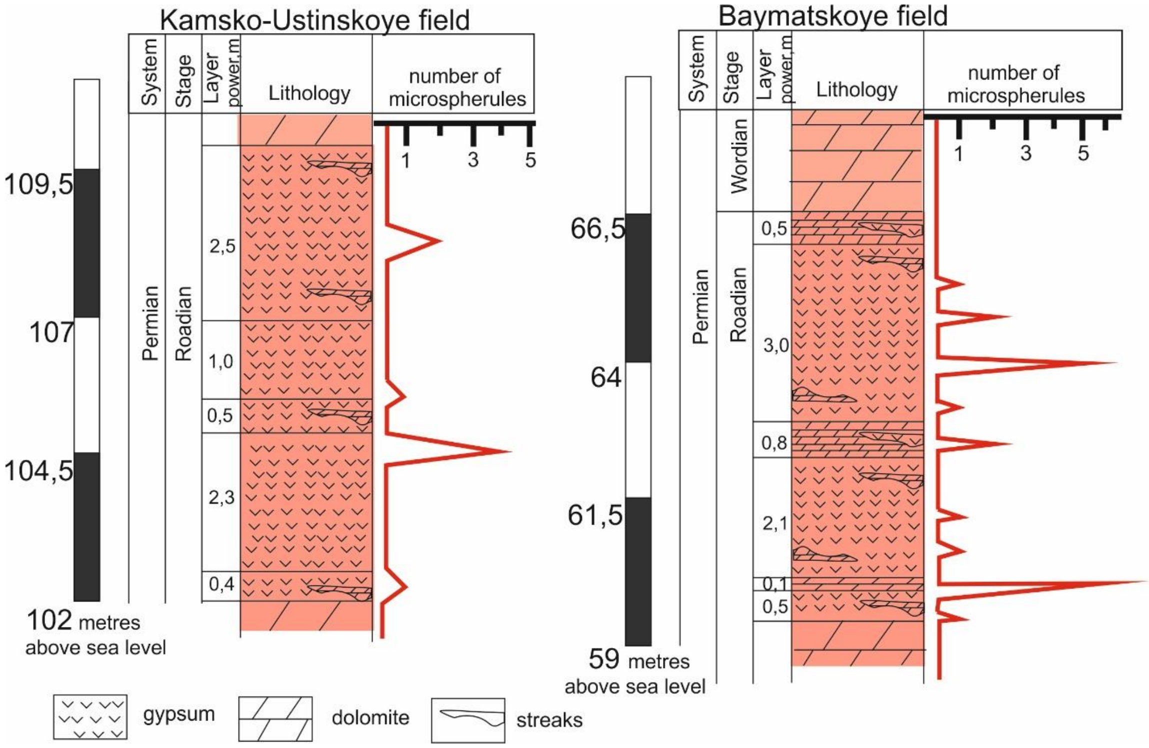

Fig. 4. Distribution of microspherules in the upper gypsum bed

Conclusions

The microspherules discovered in the course of this study may be the product of the fall of space objects (meteoroids) to the Earth during the Roadian Age. Quantitative distribution of magnetic microspherules can serve as an indicator of the intensity of space events that occurred simultaneously with the formation of the evaporite basin. Other researchers [16], [14], [17] have previously proposed an extraterrestrial hypothesis for the formation of microspherules similar to those described above.

The microspherules studied in this paper were numerous, clearly recognizable and well-preserved objects. This allows them to be used as an additional tool for stratigraphic correlation and also yields information on the intensity of space events in the geological past.

Acknowledgements

This work was funded by the subsidy allocated to Kazan Federal University for the state assignment in the sphere of scientific activities (Project № 0671-2020-0048 of State Assignment № 075-00216-20-05 of 04.06.2020 (Part II Section 1)). Also, the work is performed according to the Russian Government Program of Competitive Growth of Kazan Federal University.

REFERENCES

1. Korchagin, O. A. (2013). Fossil micrometeorites, microtektites and microkristites: method of investigations, classification and Impact-Stratigraphy Scale. Stratigraphy of the early XXI century tendencies and new ideas. M: Geokart, GEOS 6, pp. 112-142.
2. Sungatullin, R. Kh *et al*., (2015). The possibility of using space correlation with microspheres petroleum deposits Oil industry 2, pp. 16-19 [inRus.].
3. Sungatullin, R. Kh *et al*., (2017). Cosmic microspheres in the Carboniferous deposits of the Usolka section Russian Geology and Geophysics 58, pp. 59-69.
4. Sungatullin, R. Kh., *et al*., (2017). Cosmic dust in the deposits of the Moscovian and Kasimovian stages, Usolka section, Cisuralian foredeep, Russia Meteoritics & Planetary Science 52, 6121.
5. Suttle, M. D., Genge, M. J. (2017). Diagenetically altered fossil micrometeorites suggest cosmic dust is common the geological record Earth and Planetary Science Letters 476, pp. 132-142.
6. Glukhov, M. S. (2019). Magnitnyemicrospheruly v permskikh evaporitakh / Geologiya v razvivayushchemsya mire: collection of articles based on materials from the XII International scientific and practical conference of students, postgraduates and young scientists. Perm, pp. 69-71.
7. Glukhov, M. S. *et al*., (2019). Magnitnye microspheruly I ikh znachenie dlya korrelatcii evaporitovykh tolshch. Osadochnye planetarnye sistemy pozdnego paleozoya: stratigraphiya, geokhronologiya, uglevodorodnye resursy: collection of articles based on materials from the International stratigraphic conference of Golovkinsky. Kazan, pp. 104-105.
8. Glukhov, M. S. (2019). Morphology and internal structure of natural and technogenic iron oxide microspheres News of the Ural State Mining University 53, pp. 60-66.
9. Kadyrov, R. I. *et al*., (2019). Enigma of Ferruginous Inclusions in Evaporites Proceedings of the 1st Springer Conference of the Arabian Journal of Geosciences (CAJG), Petrogenesis and Exploration of the Earth's Interior. Advances in Science, Technology & Innovation, pp. 97-99.
10. Iwahashi, J. (1991). Shape and Surface Structure of the Magnetic Micro-Spherules from Permian and Triassic Bedded Chert Journal of Geosciences, Osaka City University 2, pp. 55-73.
11. Legodi, M. A., de Waal D. (2007). The preparation of magnetite, goethite, hematite and maghemite of pigment quality from mill scale iron waste Dyes and Pigments 1, pp. 161-168.
12. Genge, M. J. *et al*., (2008). The classification of micrometeorites Meteoritics & Planetary Science 3, pp. 497-515.
13. Genge, M. J., Grady, M. M. (1999). The fusion crusts of stony meteorites: Implications for the atmospheric reprocessing of extraterrestrial materials Meteoritics& Planetary Science 34, pp 341-356.
14. Love, S. G., Brownlee, D. E. (1991). Heating and termal transformation of micrometeoroids entering the Earth's atmosphere Icarus 89, pp. 26-43.
15. Brownlee, D. E. *et al*., (1983). Meteor ablation spherules as chondrule analogs Chondrules and Their Origins: Houston, Texas, Lunar and Planetary Institute 1, pp. 10-25.
16. Ivanov, A. V., Florensky, K. P. (1968). Kosmicheskie shariki v nizhnepermskikh solyanykh otlozheniyakh Geochemisty 4, pp. 483-485.
17. Mutch, T. A. (1964). Extraterrestrial particles in paleozoic salts Annals of the New York Academy of Sciences, pp. 166-185.

Ore Minerals in the Upper Riphean Deposits of the Subpolar Urals

GRAKOVA Oksana[1], POTAPOV Igor[1], PANFILOV Aleksey[1]

[1] N.P. Yushkin Institute of Geology, Komi Science Centre, Ural Branch, RAS, Syktyvkar (RUSSIA)
Email: ovgrakova@geo.komisc.ru

Abstract

Sulfide mineralization has been studied in the Upper Precambrian rocks in the Subpolar Urals. The Puyva Formation, contains pyrrhotite and chalcopyrite, and the Khobeya Formation contains pyrite. In the Puyva Formation, pyrrhotite is produced by breakdown of pyrite during metamorphism. Chalcopyrite formation is most likely associated with late oxidative processes.

In the rocks of the Khobeya suite, pyrite is represented by two generations, the first cubic without admixtures, most likely formed at the stage of metamorphism. The second type of pyrite is represented by scattered fractured grains, which probably formed in near-surface conditions.

Keywords: Sulfide mineralization, Subpolar Urals, pyrite, metamorphism

Introduction

The Timan-Northern Urals region has significant mineral resources: oil, gas, coal, bauxite, titanium, and high-quality vein quartz. The discovery, development, introduction into industrial development of deposits is a very urgent task [1]. Establishing the genesis of ore minerals is of great importance for determining the patterns of ore formation and identifying industrially significant objects in the north of the Urals.

Samples for research were taken from the rocks of the Puyva and Khobeya formations of the Subpolar Urals (Fig. 1). The Puyva Formation unconformably overlies the rocks of the Mankhobeya and Shchokurya formations [3]. The Puyva Formation is composed of mica-albite quartz schists with interlayers of amphibole and calcareous schists and quartzites. The total thickness of the Puyva Formation is 1400-1600 m. The Khobeya Formation unconformably overlies the shale of the Puyva Formation. It is represented by chlorite-muscovite-albite-quartz and muscovite-albite-quartz schists, quartzites and calcareous quartzite sandstones. The thickness is 700-1000 m. The rocks of the Puyva suite underwent at least two stages of metamorphism in the Precambrian, the early stage reached the amphibolite facies, and the later, greenschist. In the rocks of the Khobeya Formation, greenschist metamorphism of moderate pressure occurred [4], [5]. To determine the age of the Puyva Formation, isotopic studies of detrital zircons U – Pb LA – SF – ICP – MS were performed. The authors have shown that the earliest age of the basal deposits of the Puyva Formation does not extend beyond the Late Riphean [6], [7].

Methods

Ore minerals of the Upper Proterozoic deposits of the Subpolar Urals were studied. The study of ore minerals in polished sections was carried out at the Center for Collective Use “Geonauka” of Institute of Geology of Komi Scientific Center Ural Branch of the Russian Academy of Sciences. The chemical compositions and photographs of ore minerals were obtained using a Tescan Vega 3 LMH scanning electron microscope equipped with an Instruments X-Max energy dispersive attachment (analysts S. Shevchuk, E. Tropnikov).

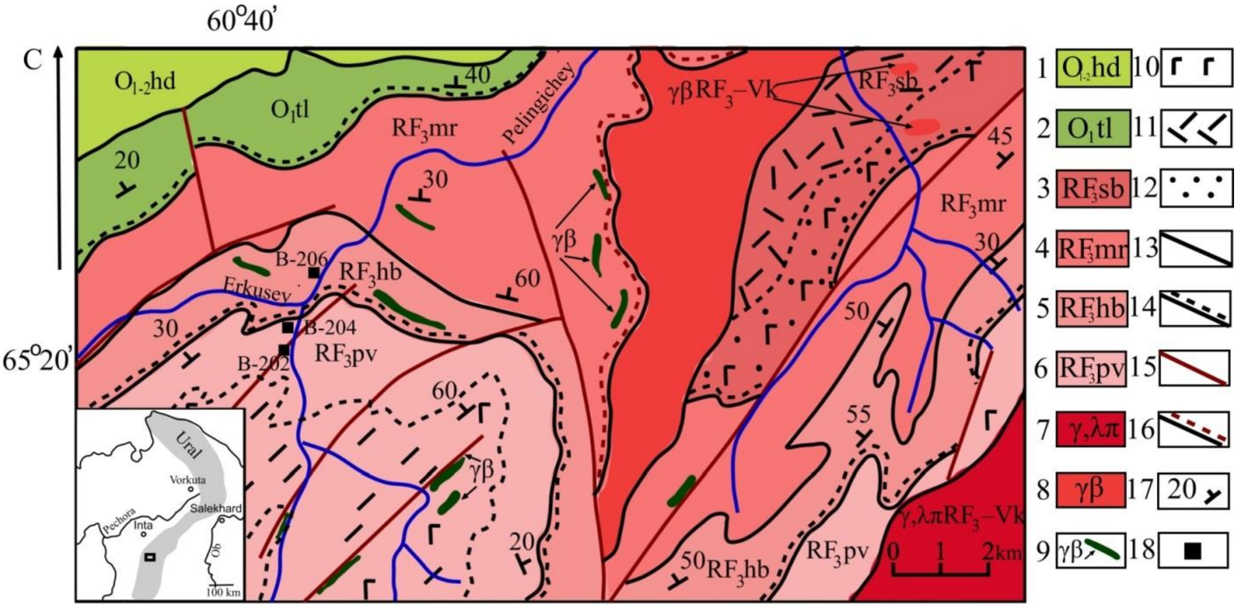

Fig. 1. Schematic geological map of the River Pelingichey (Subpolar Urals) (Based on A. Pystin *et al.*, [2]). *Legend:* 1 – Khidey suite; 2 – Telpos suite; 3 – Sablegor suite; 4 – Moroya suite, 5 – Khobeya Formation; 6 – Puyva Formation; 7 – granite, lipartite porphyry; 8 – granodiorite; 9 – dykes of gabbro, gabbro-diabase, diabase; 10 – dacite porphyry; 11 – quartz porphyry; 12 – tuffs; 13 – boundaries of stratified and intrusive bodies; 14 – boundary of discordant stratigraphic contact; 15 – faults; 16 – contact rocks; 17 – elements of occurrence of crystallization schistosity, lamination; 18 – sampling points

Results and Discussions

Samples for research were collected in the summer of 2019 on the left bank of the Pelingichey River at the mouth of the Erkusey River in the Subpolar Urals from the rocks of the upper part of the Puyva and lower part of the Khobeya formations of the Subpolar Urals (Fig. 1).

We studied sulfides of the Puyva and Khobeya formations. Sulfides in the Puyva Formation (B-202, B-204) are represented by pyrrhotite and chalcopyrite. Pyrrhotite is observed as inclusions in apatite, and individual grains are present. Pyrrhotite is often oxidized (dark gray inclusions against a background of bright, light pyrrhotite, Fig. 2a, b). The composition of pyrrhotite is shown in Table 1 Analyses 1-5. Chalcopyrite is represented by oxidized fractured grains (Fig. 2 c), apparently formed after pyrrhotite. Chalcopyrite formation is most likely associated with late oxidative processes.

Khobeya Formation (B-206, B-206-2) pyrite, galena. Pyrite is presented in the form of clearly defined characteristic cubic crystals (Fig. 2e, f) and broken aggregates of grains (Fig. 2 d). Most often confined to cracks, and inclusions of galena are observed (Fig. 2f). The chemical composition of pyrrhotite is presented in Table 1, analysis nos. 8-11.

Table 1. Chemical composition of sulfide minerals in the rocks of the Puyva and Khobeya suite, atom%

The elements	Puyva Formation								Khobeya Formation			
	pyrrhotite						chalcopyrite		pyrite			
	1	2	3	4	5	6	7	8	9	10	11	12
S	39.62	40.11	40.36	38.61	38.81	39.07	36.7	35.19	53.43	53.9	53.55	53.79
Fe	60.19	60.06	57.21	61.15	60.54	60.83	31.4	30.5	46.19	46.54	46.26	46.53
Cu	-	-	-	-	-		32.82	34.01	-	-	-	-
Ni		0.57										
Total	99.81	100.74	97.57	99.76	99.35	99.89	100.92	99.69	99.62	100.44	99.81	100.32

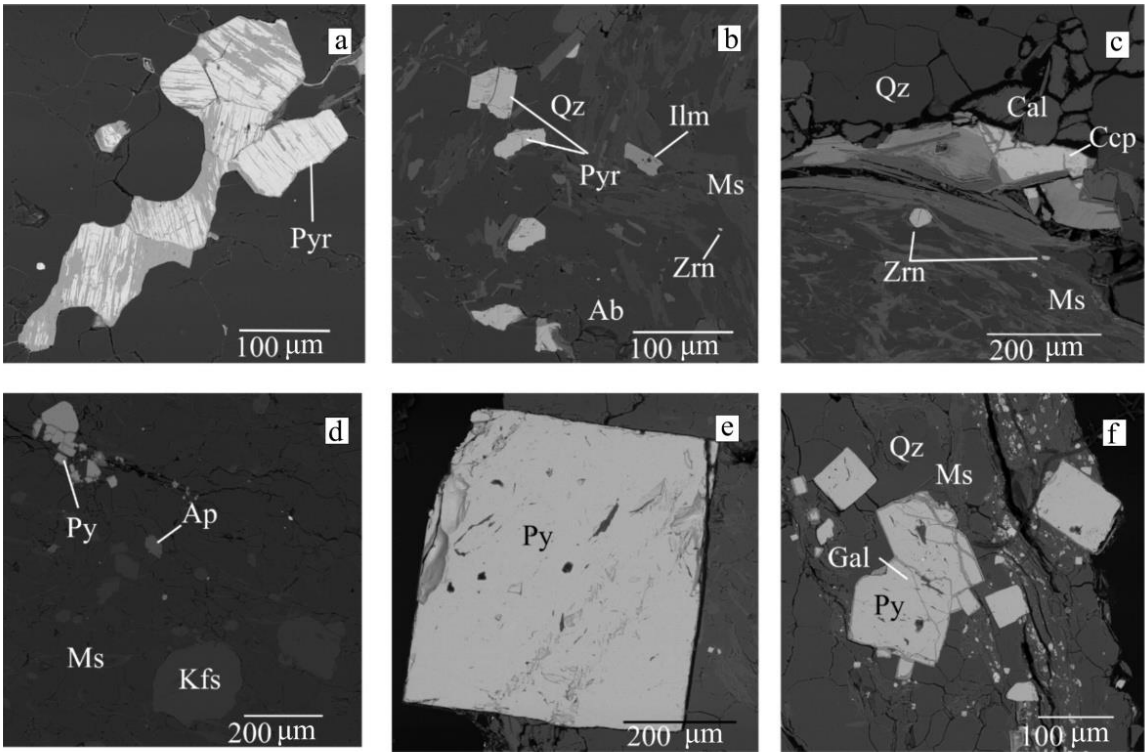

Fig. 2. Sulfide mineralization in the rocks of the Puyva (a, b, c) and Khobeya (d, e, f) formations. Pyr – pyrrhotite, Ccp – chalcopyrite, Py – pyrite, Gal – galena, Ab – albite, Ms – muscovite, Ap – apatite, Zrn – zircon, Qz – quartz, Ab – albite, Cal – calcite, Kfs – potassium feldspar, Ilm – ilmenite

Conclusions

In the deposits of the Puyva Formation, pyrrhotite is associated with the replacement of pyrite under metamorphic conditions; chalcopyrite arose later and its formation is associated with late oxidative processes. Pyrite in the rocks of the Khobeya Formation is represented by two generations, the first is cubic, having clear outlines and a cubic shape, without admixtures, most likely formed at the stages of metamorphism. The second type was found in the form of scattered grains, mainly confined to cracks; probably, it was already formed in near-surface conditions.

Acknowledgments

The study was carried out within a framework of State Program no. AAAA-A17-117121270035-0 FITZ Institute of Geology Komi SC UB RAS.

REFERENCES

1. Askhabov, A. M., Kuznecov, S. K., Tarbaev, M. B., Burcev, I. N., Timonina, N. N., Pystin, A. M. (2015). Mineral'no-syr'evaya baza Timano-Severoural'skogo regiona i perspektivy ee razvitiya. Izvestiya Komi nauchnogo centra UrO RAN 3 (23). pp. 79-90.
2. Pystin, A. M. (1994) Polimetamorficheskie kompleksy zapadnogo sklona Urala [Polymetamorphic complexes of the western slope of the Urals]. Nauka, St. Petersburg, 208.
3. Pystin, A. M., Pystina, Yu. I. (2019). Dokembrij Pripolyarnogo Urala: Khronostratigraficheskij aspect. Trudy Karel'skogo nauchnogo centra Rossijskoj akademii nauk 2. pp. 34-52.
4. Pystina, Yu. I., Pystin, A. M. (2002). Cirkonovaya letopis' ural'skogo dokembriya. UrO RAN, Ekaterinburg, 168.
5. Pystin, A. M., Pystina, Yu. I. (2008). Metamorfizm i granitoobrazovanie v proterozojsko-rannepaleozojskoj istorii formirovaniya Pripolyarno-Ural'skogo segmenta zemnoj kory. Litosfera 6, pp. 25-38.
6. Pystin, A. M., Pystina, Yu. I., Hubanov, V. B. (2019). Pervye rezul'taty U-PB-datirovaniya detritovyh cirkonov iz bazal'nyh otlozhenij verhnego dokembriya Pripolyarnogo Urala. Doklady Akademii nauk 488 (2), pp. 172-175.
7. Pystin, A. M., Pystina, Yu. I., Ulyasheva, N. S., Grakova, O. V. (2019). U-Pb dating of detrital zircons from basal Post Paleoproterozoic metasediments in the Subpolar and Polar Urals: Evidence for a Cryogenian, not Mesoproterozoic Age. International Geology Review. ISSN: 0020-6814 (Print) pp. 1938-2839 (Online) journal homepage: https://www.tandfonline.com/loi/tigr20. DOI: 10.1080/00206814.2019.168533. 3.

Devonian Phoebodontid-Based Zonation

IVANOV Alexander O.[1,2]

[1] *St. Petersburg State University, Institute of Earth Sciences (RUSSIA)*
[2] *Kazan Federal University (RUSSIA)*
Email: IvanovA-Paleo@yandex.ru

Abstract

The six phoebodontid zones proposed for the Middle – Upper Devonian are updated based on new data of index species distribution. The refined *Phoebodus sophiae* Zone corresponds to the Lower *varcus – disparilis* conodont zones (CZ), the *Ph. latus* Zone – the Lower *falsiovalis – jamieae* CZ, the *Ph. typicus* Zone – the Lower – Upper *triangularis* CZ, the *Ph. gothicus* Zone – the Lower *crepida* – Upper *marginifera* CZ, and the *Ph. limpidus* Zone – the Uppermost *marginifera* – Middle *praesulcata* CZ.

Keywords: phoebodontid sharks, Devonian, zonation

Introduction

The phoebodontids are one of most taxonomically diverse and widely distributed group of Devonian chondrichthyans. The family Phoebodontidae of the order Phoebodontiformes includes three genera, *Diademodus* Harris, *Phoebodus* St. John et Worthen and *Thrinacodus* St. John et Worthen [1]. *Phoebodus* is the most species rich genus, presently including 12 species: *Ph. bifurcatus* Ginter et Ivanov; *Ph. depressus* Ginter, Hairapetian et Klug; *Ph. fastigatus* Ginter et Ivanov; *Ph. gothicus* Ginter; *Ph. latus* Ginter et Ivanov; *Ph. limpidus* Ginter; *Ph. politus* Newberry; *Ph. rayi* Ginter et Turner; *Ph. saidselachus* Frey, Coates, Ginter, Hairapetian, Rücklin, Jerjen et Klug; *Ph. sophiae* St. John et Worthen; *Ph. turnerae* Ginter et Ivanov; *Ph. typicus* Ginter et Ivanov.

The six phoebodontid zones were suggested for the Middle – Upper Devonian based on the distribution of *Phoebodus* species in the Givetian – Famennian interval of the Holy Cross Mountains (Poland) and South Urals (Russia) [2]. They corresponded to the Middle *varcus* – Middle *praesulcata* interval of the conodont zonation (CZ). The oldest *Ph. sophiae* phoebodontid Zone was correlated with the Middle *varcus* – Lower *hassi* CZ of the Givetian – Frasnian, the *Ph. latus* Zone was coinciding the Upper *hassi – jamieae* CZ, the *Ph. bifurcatus* Zone – the *rhenana – linguiformis* CZ [2]. The Famennian *Ph. typicus* Zone corresponded to the Upper *triangularis* – Upper *rhomboidea* CZ, the *Ph. gothicus* Zone – to the interval of Lower *marginifera* – Upper *postera* CZ, and the *Ph. limpidus* Zone – the Lower *expansa* – Middle *praesulcata* [2]. There were no records of *Phoebodus* species in the Lower – Middle *triangularis* CZ.

Distribution of *Phoebodus* index species

The oldest index species, *Phoebodus sophiae,* is known mainly from the Givetian interval of the Middle *varcus – disparilis* CZ of Iowa, Indiana (*varcus* CZ) and New York (*varcus – hermanni-cristatus* CZ and probably earliest Frasnian), USA; Aragonian Pyrenees, Spain, Portugal (Middle – Upper *varcus* CZ); Rhenish Slate Mountains, Germany (*hermanni-cristatus* CZ); Holy Cross Mountains, Poland (Middle *varcus-hermanni-cristatus* CZ); Southern

Mauritania (*hermanni-cristatus* CZ); Australia (*varcus* CZ) [1], [3], [4] [5], [6], [7], [8]. But the species occurs in the Lower – Middle *varcus* CZ of Kuznetsk Basin, Western Siberia, Russia [9]. The tooth described as *Ph. sophiae* from the Upper *rhenana – linguiformis* CZ of Iran [10] differs from the teeth of the species in the close placed and more lingually directed lateral cusps, the narrow labial edge of the base and the labio-basal projection, and is similar to the teeth of *Phoebodus* sp. C [11].

Phoebodus latus was previously reported from the Upper *hassi-linguiformis* CZ, Frasnian of Holy Cross Mountains, Poland (*rhenana* CZ); South Urals (Upper *hassi – linguiformis* CZ), South Timan (*rhenana-linguiformis* CZ), Gorniy Altay and Kuznetsk Basin (*rhenana* CZ), Russia; Western Australia (Upper *hassi* Lower *rhenana* CZ) [11], [12], [6], [9], [13]. However, this taxon was recorded in the older interval of the Middle *falsiovalis-hassi* CZ in Iran [14].

Phoebodus bifurcatus occurs in the Lower *rhenana-linguiformis* CZ, Upper Frasnian of Utah, USA; Dinant Synclinorium, Belgium; Holy Cross Mountains, Poland; Moravia, Czech Republic; South Urals, South Timan, Central Devonian Field, Kuznetsk Basin and Gorniy Altay, Russia; Southern Mauritania; eastern Iran; southern China; Western Australia [9], [11], [10], [12], [13], [15], [16], [17], [18], [19].

The first index species *Phoebodus typicus* of the Famennian was previously recorded in the Upper *triangularis*-Lower *marginifera* CZ of the South Urals, Russia (Upper *triangularis*-Lower *marginifera* CZ); Morocco (Uppermost *crepida* or Lower *rhomboidea* CZ); Iran (*crepida* CZ); Queensland, Australia (*marginifera* CZ); probably Armenia (?*crepida* CZ) and Belarus (*triangularis* and *rhomboidea* CZ) [6], [7], [15], [20], [21], [22]. Hairapetian and Ginter [23] mentioned the occurrence of species also in the Middle *triangularis* CZ of central Iran.

Phoebodus gothicus was reported until recently from the Lower *marginifera*-Middle *praesulcata* CZ of Iowa (*marginifera*-Lower *trachytera* CZ) and Utah (Lower *expansa* CZ), USA; Montagne Noire, France (Lower-Middle *expansa*); Germany (Lower-Middle *expansa* CZ); Holy Cross Mountains, Poland (Lower *marginifera*-Middle *praesulcata* CZ); South Urals, Russia (Lower *postera* – Middle *expansa* CZ); Anti-Atlas, Morocco (Uppermost *marginifera*-Lower *expansa* CZ); Algeria (lower or middle Famennian); Iran (*marginifera*-Upper *expansa* CZ); Armenia (possible *crepida* and *expansa* CZ); southern China (*praesulcata* CZ); probably Vietnam (*marginifera* CZ) [1], [10], [11], [15], [17], [20], [21], [24], [25], [26], [27], [28]. Two subspecies *Ph. gothicus gothicus* Ginter and *Ph. gothicus transitans* Ginter, Hairapetian and Klug were established for the species [20]. The stratigraphic range of the first subspecies includes the range of the second one [1].

Phoebodus limpidus was known from the Lower *expansa* – Middle *praesulcata* CZ of Nevada (Upper *expansa* or Lower *praesulcata* CZ), Wyoming (Middle or Upper *expansa* CZ), Utah (Lower *expansa* and Upper *expansa* or Lower *praesulcata* CZ), USA; Mexico (*expansa* CZ); Montagne Noire, France (*expansa* CZ); Thuringian Slate Mountains, Germany (Middle *expansa* – Lower *praesulcata* CZ); Holy Cross Mountains, Poland (Upper *expansa* – Lower *praesulcata* CZ); South Urals, (Lower *expansa* – Lower *praesulcata* CZ) and North Caucasus (Middle *expansa* – *praesulcata* CZ), Russia; Anti-Atlas, Morocco (Upper *expansa* CZ); southern China (Lower *expansa* and *praesulcata* CZ) (Ginter, 1990; [1], [6], [15], [17], [20], [26], [29], [30], [31], [32], [33]. The record of species in the Upper *praesulcata* CZ was not confirmed but the range in some regions probably includes the entire *praesulcata* CZ.

New information on the occurrence of *Phoebodus* index species has appeared lately. Diverse fish microremains were collected recently from the Pokrovskoe section of the Givetian/Frasnian boundary beds in the eastern slope of the Middle Urals, Russia (collecting of A. Z. Bikbaev and M. P. Snigireva, Ekaterinburg). The deposits of this section are referred to the Vysotinka and Brodovskiy regional stages and correlated to the interval of Middle *varcus – norissi* (Lower *falsiovalis*) CZ [34]. The fish microremains are represented by plates of the placoderm Ptyctodontidae; scales of the acanthodian Acanthodiformes; chondrichthyan teeth of the phoebodontids *Phoebodus fastigatus, Ph. latus, Ph. sophiae* and *Ph*. sp. C [11]; various chondrichthyan scales of *Ohiolepis*, *Cladolepis,* protacrodontid and ctenacanthid types; teeth, fragments of jaws and scales of a struniiform sarcopterygian; teeth and scales of actinopterygians resembling *Mimipiscis* and *Moythomasia*. *Phoebodus fastigatus* (Fig. 1 A-C) and *Ph. sophiae* (Fig. 1 D, E) occur in the Middle *varcus – norissi* CZ of that section, but *Ph. latus* (Fig. 1 F, G) is recorded only in the *norissi* CZ. The discovery of *Ph. latus* in the Lower *falsiovalis* CZ is the oldest in the world. *Ph. sophiae* was mentioned in the possibly earliest Frasnian [4] but its definite occurrence in the Lower *falsiovalis* CZ is reported for the first time.

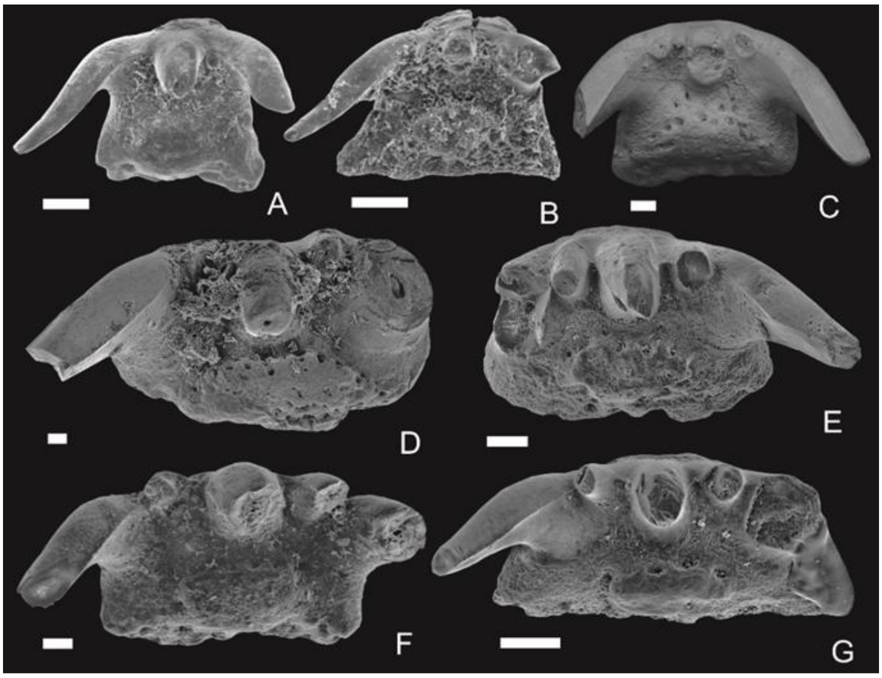

Fig. 1. The teeth of *Phoebodus* species from the Pokrovskoye section. A-C – *Ph. fastigatus* Ginter et Ivanov, 1992; D, E – *Ph. sophiae* St. John et Worthen, 1875; F, G – *Ph. latus* Ginter et Ivanov, 1995. Scale bars – 100 µm

Phoebodus typicus Ginter et Ivanov was found in the Kosoy Ures Beds of Pescherka Regional Stage in the Kuznetsk Basin (Western Siberia, Russia) correlated with the Lower-Upper *triangularis* CZ [9], [35]. The index species is recorded in the interval of the Lower-Middle *triangularis* CZ where the occurrence of *Phoebodus* species was not known previously.

Ph. cf. *typicus* occurs also in the Podonino Regional Stage in the Kuznetsk Basin corresponding to the Lower *trachytera*-Upper *expansa* CZ [36].

Phoebodus gothicus Ginter in Iran and Morocco is known also from the Lower *crepida – rhomboidea* CZ [20], [23], [37].

Phoebodus limpidus Ginter was found in the wide interval of the Uppermost *marginifera* – Lower *praesulcata* CZ in the Carnic Alps, northern Italy [38]. Thus, this occurrence of the index species is oldest in the world and considerably extended the *Ph. limpidus* Zone.

New version of phoebodontid zonation

The phoebodontid-based zonation based on a new data of distribution of *Phoebodus* index species was updated (Fig. 2). The ranges of five zones have been changed.

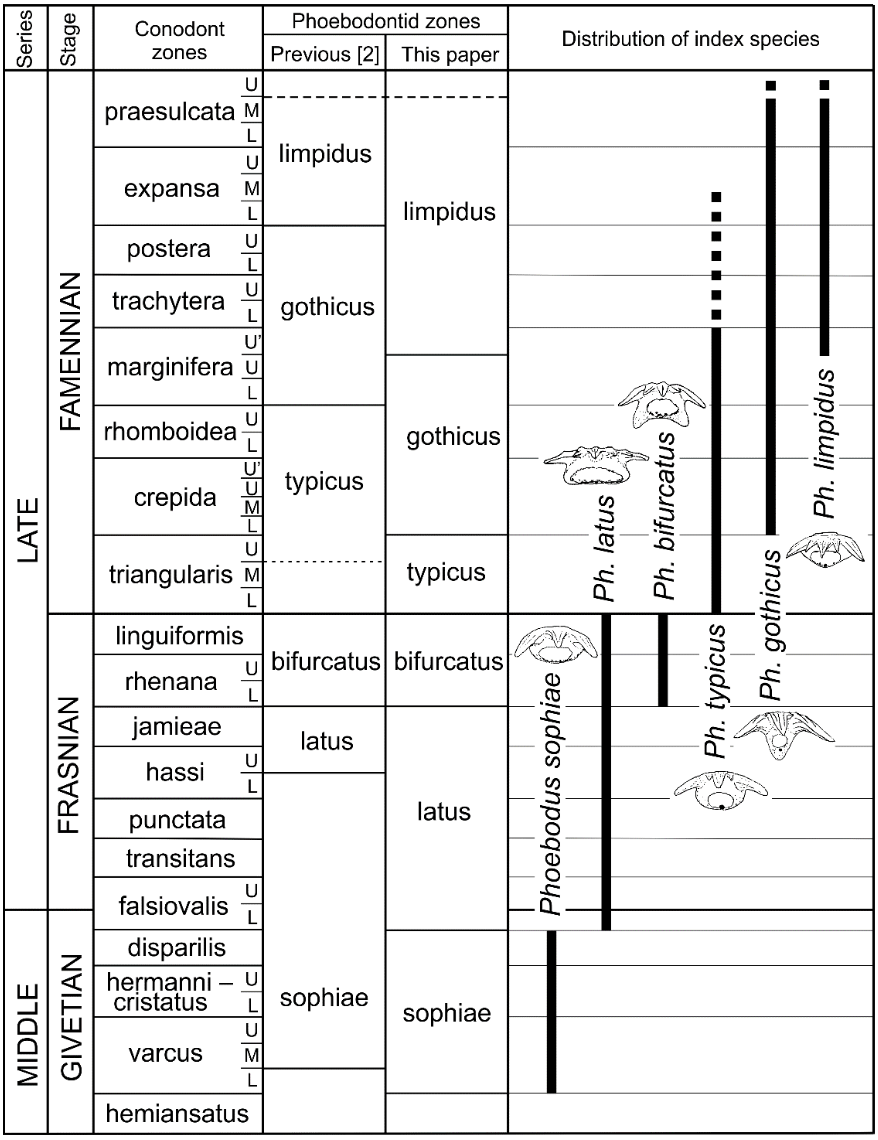

Fig. 2. The phoebodontid-based zonation and distribution of *Phoebodus* index species (dotted line shows the range of *Ph.* cf. *typicus*)

The new assemblage from the Pokrovskoe section allows the boundary between the *Ph. sophiae* and *Ph. latus* zones at the base of the *falsiovalis* CZ to be recognized. The *Ph. typicus* Zone is corresponded with the Lower – Upper *triangularis* CZ due to the record of index species in that interval in the Kuznetsk Basin. The range of the *Ph. gothicus* Zone was changed on the Lower *crepida*-Upper *marginifera* CZ based on occurrence of species in the interval of the Lower *crepida-rhomboidea* CZ in Iran and Morocco. Finally, the *Ph. limpidus* Zone now starts from the Uppermost *marginifera* CZ, based on a record of the species in the Carnic Alps.

Conclusions

Thus, the refined phoebodontid zones are defined as follows: The *Ph. sophiae* Zone is corresponded to the Lower *varcus – disparilis* CZ, the *Ph. latus* Zone – the Lower *falsiovalis – jamieae* CZ, the *Ph. typicus* Zone – the Lower – Upper *triangularis* CZ, the *Ph. gothicus* Zone – the Lower *crepida* – Upper *marginifera* CZ, and the *Ph. limpidus* Zone – the Uppermost *marginifera* – Middle *praesulcata* CZ.

Acknowledgments

The work was performed according to the Russian Government Program of Competitive Growth of Kazan Federal University and was partly supported by the Russian Foundation for Basic Research, project no. 20-05-00445a.

REFERENCES

1. Ginter, M., Hampe, O., Duffin, C. J. (2010). Chondrichthyes Paleozoic Elasmobranchii: Teeth. Handbook of Palaeoichthyology, v. 3D (Schultze, H.-P., Ed.). Verlag Dr. Friedrich Pfeil, München, 168.
2. Ginter, M., Ivanov, A. (1995). Middle/Late Devonian phoebodont-based ichthyolith zonation. Geobios, Mémoire Special 19, pp. 351-355.
3. Gross, W. (1973). Kleinschuppen, Flossenstacheln und Zähne von Fischen aus europäischen und nordamerikanischen Bonebeds des Devons. Palaeontographica Abteilung A 142, pp. 51-155.
4. Turner, S. 1997. "*Dittodus*" species of Eastman 1899 and Hussakof and Bryant 1918 (Mid to Late Devonian). Modern Geology 21, pp. 87-119.
5. Ivanov, A., Derycke, C. (1999). Distribution of the Givetian Omalodus shark assemblage. Ichthyolith Issues, Special Publication 5, pp. 22-24.
6. Ginter, M., Ivanov, A. (2000). Stratigraphic distribution of chondrichthyans in the Devonian on the East European Platform margins. Courier Forschungs-lnstitut Senckenberg 223, pp. 325-339.
7. Turner, S., Basden, A., Burrow, C. J. (2000). Devonian vertebrates of Queensland. Courier Forschungs-lnstitut Senckenberg 223, pp. 487-521.
8. Ginter, M., Liao, J. C., Valenzuela-Rios, J. I. (2008). New data on chondrichthyan microremains from the Givetian of the Renanuer section in the Aragonian Pyrenees (Spain). Acta Geologica Polonica 58, pp. 165-172.
9. Ivanov, A., Rodina, O. (2001). Middle and Late Devonian vertebrate biostratigraphy of SW Siberia, Russia. In Abstracts of the 15th International Senckenberg Conference, Frankfurt am Main, Germany, 50.
10. Hairapetian, V., Ginter, M. (2010). Pelagic chondrichthyan microremains from the Upper Devonian of the Kale Sardar section, eastern Iran. Acta Geologica Polonica 60 (3), pp. 357–371.
11. Ginter, M., Ivanov, A. (1992). Devonian phoebodont shark teeth. Acta Palaeontologica Polonica 37 (1), pp. 55-75.
12. Ivanov, A. (1999). Late Devonian – Early Permian chondrichthyans of the Russian Arctic. Acta Geologica Polonica 49 (3), pp. 267-285.
13. Roelofs, B., Playton, T., Barham, M., Trinajstic, K. (2015). Upper Devonian microvertebrates from the Canning Basin, Western Australia. Acta Geologica Polonica 65 (1), pp. 69-101.
14. Hairapetian, V., Ginter, M., Yazdi, M. (2008). Early Frasnian sharks from central Iran. Acta Geologica Polonica 58 (2), pp. 173-179.
15. Ivanov, A. (1995). Late Devonian vertebrate fauna of the South Urals. Geobios, Mémoire Special 19, pp. 357-359.
16. Turner, S., Youngquist, W. (1995). Late Devonian phoebodont (Pisces: Chondrichthyes) from the Confusion Range, Utah. Geobios, Mémoire Special 19, pp. 389-392.
17. Wang, S.-t., Turner, S. (1995). A re-appraisal of Upper Devonian – Lower Carboniferous vertebrate microfossils in South China. Professional Papers of Stratigraphy and Palaeontology 26, pp. 59-70.
18. Racheboeuf, P.R., Girard, C.; Lethiers, F., Derycke, C., Herrera, Z.A.; Trompette, R. (2001). Evidence for Givetian stage in the Mauritanian Adrar (West Africa): biostratigraphical data and palaeogeographic implications. Newsletters on Stratigraphy, 38 (2-3), pp. 141-162.
19. Ginter, M., Gouwy, S., Goolaerts, S. (2017). A classic Late Frasnian chondrichthyan assemblage from southern Belgium. Acta Geologica Polonica 67 (3), pp. 381-392.
20. Ginter, M., Hairapetian, V., Klug, C. (2002). Famennian chondrichthyans from the shelves of North Gondwana. Acta Geologica Polonica 52 (2), pp. 169-215.

21. Ginter, M., Hairapetian, V., Grigoryan, A. (2011). Chondrichthyan microfossils from the Famennian and Tournaisian of Armenia. Acta Geologica Polonica 61 (2), pp. 153-173.
22. Ivanov, A. O., Plax, D. P. (2018). Chondrichthyans from the Devonian – Early Carboniferous of Belarus. Estonian Journal of Earth Sciences 67 (1), pp. 43-58.
23. Hairapetian, V., Ginter, M. (2009). Famennian chondrichthyan remains from the Chahriseh section, central Iran. Acta Geologica Polonica 59 (2), pp. 173-200.
24. Derycke, C. (1992). Microrestes de sélaciens et autres Vértébres du Dévonien supérieur du Maroc. Bulletin de Musée national d'Histoire naturelle 14, pp. 15–61.
25. Long, J.A. (1993). Palaeozoic vertebrate biostratigraphy of south-east Asia and Japan. Chapter 11. In Palaeozoic Vertebrate Biostratigraphy and Biogeography (Long, J. A., Ed.). Belhaven Press, London, pp. 277-289.
26. Ginter, M. (1999). Famennian - Tournaisian chondrichthyan microremains from the eastern Thuringian Slate Mountain. Abhandlungen und Berichte für Naturkunde 21, pp. 25-47.
27. Hampe, O. (2000). Occurrence of *Phoebodus gothicus* (Chondrichthyes: Elasmobranchii) in the middle Famennian of northwestern Iran (Province East Azerbaijan). Acta Geologica Polonica 50 (3), pp. 355-367.
28. Hampe, O., Schindler, T. (2004). Late Famennian fish remains from the Refrath 1 Borehole (Bergisch Gladbach-Paffrath Syncline; Ardennes-Rhenish Massif, Germany). Courier Forschungsinstitut Senckenberg 251, pp. 267-289.
29. Xia, F.-S. (1997). Marine microfaunas (bryozoans, conodonts and microvertebrate remains) from the Frasnian-Famennian interval in Northwestern Junggar Basin of Xinjiang in China. Beiträge zur Paläontologie 22, pp. 91-207.
30. Ginter, M. (2001). Chondrichthyan biofacies in the late Famennian of Utah and Nevada. Journal of Vertebrate Paleontology 21, pp. 714-729.
31. Ivanov, A. (2003). Vertebrates from the Late Devonian – Carboniferous of North Caucasus (Russia). Ichthyolith Issues, Special Publication 7, pp. 27-28.
32. Gauchey, S., Girard, C., Adnet, S., Renaud, S. (2014). Unsuspected functional disparity in Devonian fishes revealed by tooth morphometrics. Naturwissenschaften 101, pp. 735-743.
33. Martínez-Pérez, C., Navas-Parejo, P., Lara-Peña, R.A., Ferrón, H.G., Palafox-Reyes, J., Botella, H. (2020). Late Devonian (Famennian) Chondrichthyes from Mexico. Journal of Vertebrate Paleontology 39, DOI: 10.1080/02724634.2019.1764008.
34. Bikbaev, A. Z., Snigireva, M. P., Tupitsina, M. A. (2014). Lithological characteristic and conodonts of the Upper Givetian deposits of key section Pokrovskoe. Ezhegodnik-2013, Trudy IGG UrO RAN 161, pp. 4-14.
35. Ivanov, A., Rodina, O. (2002). Change of chondrichthyan assemblages in the Frasnian/Famennian boundary of Kuznetsk Basin. In Geology of the Devonian System (Yushkin, N. P., Tsyganko, V. S., Männik, P., Eds.). Syktyvkar, pp. 84-87.
36. Ivanov, A., Rodina, O. (2004). A new omalodontid-like shark from the Late Devonian (Famennian) of western Siberia, Russia. Fossils and Strata 50, pp. 82-91.
37. Derycke, C. (2017). Paléobiodiversité des gnathostomes (chondrichthyens, acanthodiens et actinoptérygiens) du Dévonien du Maroc (NW Gondwana). Mémoires de la Société Géologique de France 180, pp. 44-77.
38. Randon, C., Derycke, C., Blieck, A., Perri, M. C., Spalletta, C. (2007). Late Devonian-Early Carboniferous vertebrate microremains from the Carnic Alps, northern Italy. Geobios 40 (6), pp. 809-826.

Representative Elementary Volume Definition of A 1 M Long Whole Core Segment of Bashkirian Limestones, Using Porosity Data

KHASSANOV Damir[1], LONSHAKOV Marat[1]

[1] *Kazan Federal University, Kazan (RUSSIA)*
Email: damir.khassanov@mail.ru

Abstract

Practical methods for representative elementary volume calculation of core samples is investigated. Different methodologies of core sampling in petrophysical laboratories in Russia and abroad are analysed. The connected porosity of a 1 m long whole core segment is evaluated in two ways, using porosity data of the 7.3 cm diameter core samples in the first approach and porosity values of the core samples 6 cm long by 3 cm in diameter in the second way. Porosity values from the neutron-gamma log and porosity data of core samples have been compared, to define optimal core sizes for the analysis of the relationship between core and log data.

Keywords: representative elementary volume (REV), buoyancy method, intergranular porosity, fracture porosity, grainstone, scale effect

Introduction

The relevance of the problem is that core porosity values depend largely on sample size.

This phenomenon is known as the scale effect [1]. The scale effect has a great influence estimates of the sizes oil and gas reserves.

The goal of the research work is to analyse changes in connected porosity values depending on the sizes of samples drilled out from the Bashkirian whole core segment 1 m long by 10 cm in diameter.

The tasks of the research work are to compare porosity values of a 1 m long whole core fragment evaluated in two ways, and analyse the relationship between core and log porosity data. Articles focused on core sampling have been analysed.

Object

The whole core segment used is 1 m long by 10 cm in diameter and was recovered from the borehole # 4993 of the Ivinskoye heavy oil field located in the Republic of Tatarstan, Russian Federation. The whole core segment was extracted in a depth interval of 962.0-963.0 m. The extracted rocks appeared to be Bashkirian limestones (grainstones) with porosity varying from 17 to 21.8% according to the data of the neutron-gamma well logging method.

Literature review

The routine core analysis allows geoscientists to evaluate permeability, porosity and lithotype.

It is important to choose the optimal sample size to calculate accurate values of reservoir properties. In American and European petrophysical laboratories, core plugs 2-3 inches long by

1 (1.5) inch in diameter taken at regular intervals from the whole core segments (often every 25 cm) are used to evaluate porosity and permeability of homogeneous rocks [2].

In Russian laboratories homogeneous rocks are investigated using core samples 1.18 inches (3 cm) long by 1.18 inches (3 cm) in diameter [3]. Changes in lithology of heterogeneous rocks have an influence on sampling interval. It should be smaller than 25 cm. Sometimes full-diameter core samples are used to estimate porosity and permeability of carbonate heterogeneous rocks [4], [5]. Investigations of eight-ten full-diameter core samples drilled out of the 1 m long whole core segment take much liquid (chloroform) for fluid extraction, so it is necessary to define minimum sizes of core samples the provide the accurate values of whole core porosity.

The concept of representative elementary volume was discussed by J. Bear and B. Prilous [6], [7]. The representative elementary volume is the minimum volume describing significant physical particularities of the porous media. P. Tomin described a practical technique for representative elementary volume calculation for core samples that is used in this research work [8].

Methodology

In the first step, lithological and mineralogical researches of drilled out core samples using thin sections were used to identify lithotypes of limestones. It was concluded that the 1 m long interval consists of grainstones [9].

In the second step, core samples were cleaned using the Soxhlet distillation extractor.

In the third step core samples were saturated with distilled water to compare the dry weight, suspended weight and saturated weight in air for connected porosity determination.

The six 7.3 cm diameter core samples were drilled out of the whole core segment 1 m long perpendicular to its axis. Then five core samples 6 cm long by 3 cm in diameter were taken at 0.2-0.3 cm intervals (Table 1). Core sample # I was damaged so a 3 cm long core sample was used.

Table 1. Original sizes of core samples drilled-in in the depth interval of 962.0-963.0 m

Core number	Diameter, cm	Length, cm	Volume, cm^3	Depth, m
1	7.34	5.25	221.91	962.12
2	7.35	5.21	220.79	962.22
3	7.34	5.43	229.84	962.34
4	7.34	5.31	224.67	962.49
5	7.34	5.23	221.44	962.64
6	7.34	5.83	247.05	962.8
I	2.96	6.49	44.67	962.03
II	2.96	3.16	21.77	962.19
III	2.97	6.44	44.50	962.42
IV	2.96	6.29	43.40	962.59
V	2.96	4.53	31.19	962.92

The buoyancy method was used for porosity determination with application of the special equipment known as “Napor-RM” according to the approach described in the “Petrophysics MC Course Notes” [10].

Results and Discussion

Results of laboratory measurements are shown in Fig. 1. Average porosity values (calculated for every core volume) change from 24 to 27.2% in the volume range varying from 21.19 to

222.2 cm^3. In the volume range changing from 222.20 to 238.44 cm^3 average porosity values exceed 27%.

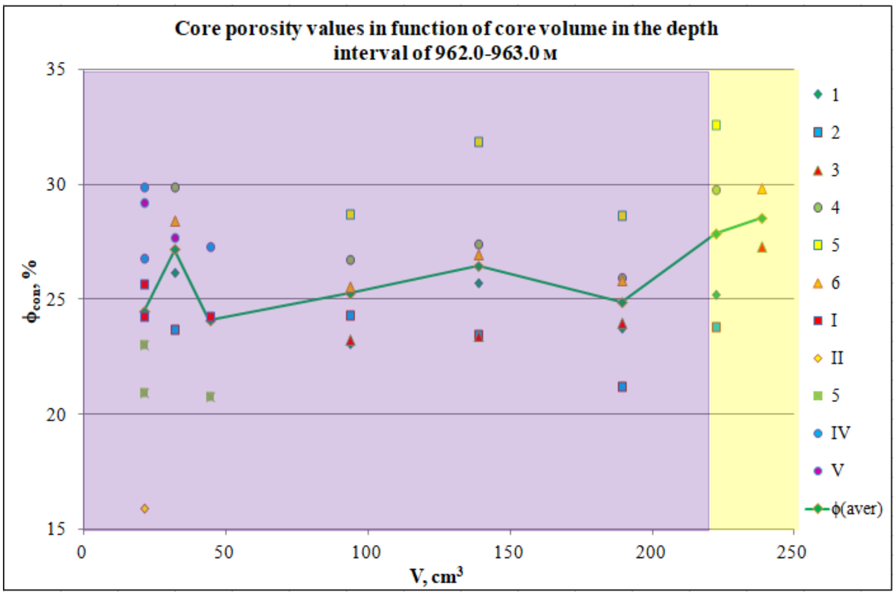

Fig. 1. Core porosity values in function of core volume in the depth interval of 962.2-963.0 m

In Fig. 1, average values are connected with a green polyline. Consequently, intergranular porosity occurs in core samples having volume less than 222.2 cm^3 while the complex of fracture, intergranular and vuggy porosity occurs in big core samples. In Fig. 1 the first volume range 21.19-222.2 cm^3 is highlighted in purple while the second volume range 222.2-238.44 cm^3 is marked in yellow. Porosity values of some whole core segments ϕ_{con} were calculated using porosity data of 7.3 cm diameter core samples.

The representative elementary volume of the 1 m long whole core segment is calculated using values of the maximum deviation of connected porosity from the average value estimated for every core volume. Results of maximum deviations are presented in Fig. 2 and Fig. 3.

Investigation of minimum increments of maximum deviations allow to define values of the representative elementary volume (Table 2). Measurement inaccuracies are 1.25% and 0.33% for core samples having volume less and more than 44 cm^3 respectively.

It was concluded that the analysis of a core sample 6 m by 3 cm in diameter allows investigation of intergranular porosity of the whole core fragment, while analysis of a core sample 44 cm by 10 cm in diameter allows the complex of fracture, intergranular and vuggy porosity in the whole 1 m long core to be investigated.

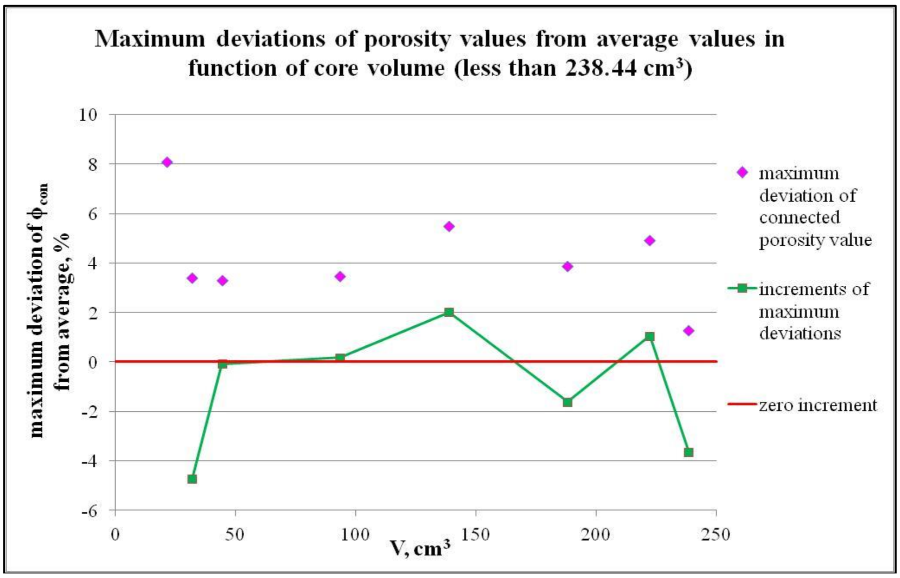

Fig. 2. Maximum deviations of porosity values from average values in function of the core volume (less than 238.44 cm^3)

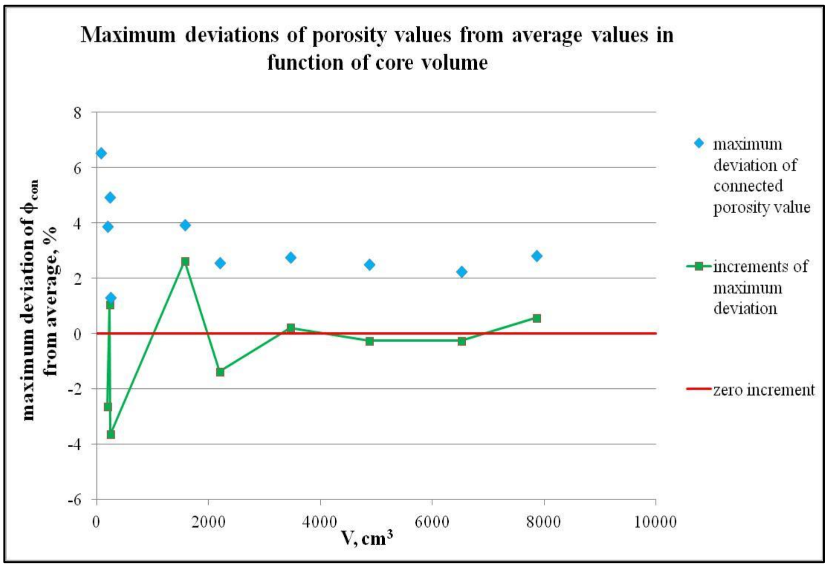

Fig. 3. Maximum deviations of porosity values from average values in function of the core volume

Table 2. Values of representative elementary volume

Type of investigated porosity	REV, cm^3	Length, cm	Diameter, cm	Range of representative volumes, cm^3
Intergranular porosity	44	6	3	44-94
The complex of fracture, intergranular and vuggy porosity	3455	44	10	3455-6518

Data of well-logging methods are demonstrated in Fig. 4. It is obvious that values of the neutron-gamma porosity log are not reliable in the depth interval of 962.0-963.0 m because fluctuations of density are not significant enough. There are three zones in the depth interval:

1. The first zone is in the depth interval of 962.0-962.1 m. Porosity values of core samples 6 cm long by 3cm in diameter and core sample 3 cm long by 3 cm in diameter are similar.
2. The second zone is in the depth interval of 962.1-962.6 m. Porosity values of 7.3 diameter core samples exceed porosity data of 3 cm diameter core samples and constantly increase with depth increment. The maximum difference is equal to 8%. Bigger porosity data of 7.3 diameter core samples are explained by the complex of fracture, intergranular and vuggy porosity occurring in large core samples. The porosity increase of large core samples with depth increment is closely related to the density decrease. Density data were calculated with the use of gamma-gamma logging (GGL) method.
3. The third zone is in the depth interval of 962.6-963.0 m. Porosity values of core samples 6 cm long by 3cm in diameter and core sample 3 cm long by 3 cm in diameter are similar. The porosity decrease of all core samples with depth increment is explained by the density increase.

Lithological and mineralogical investigations of drilled out core samples show that

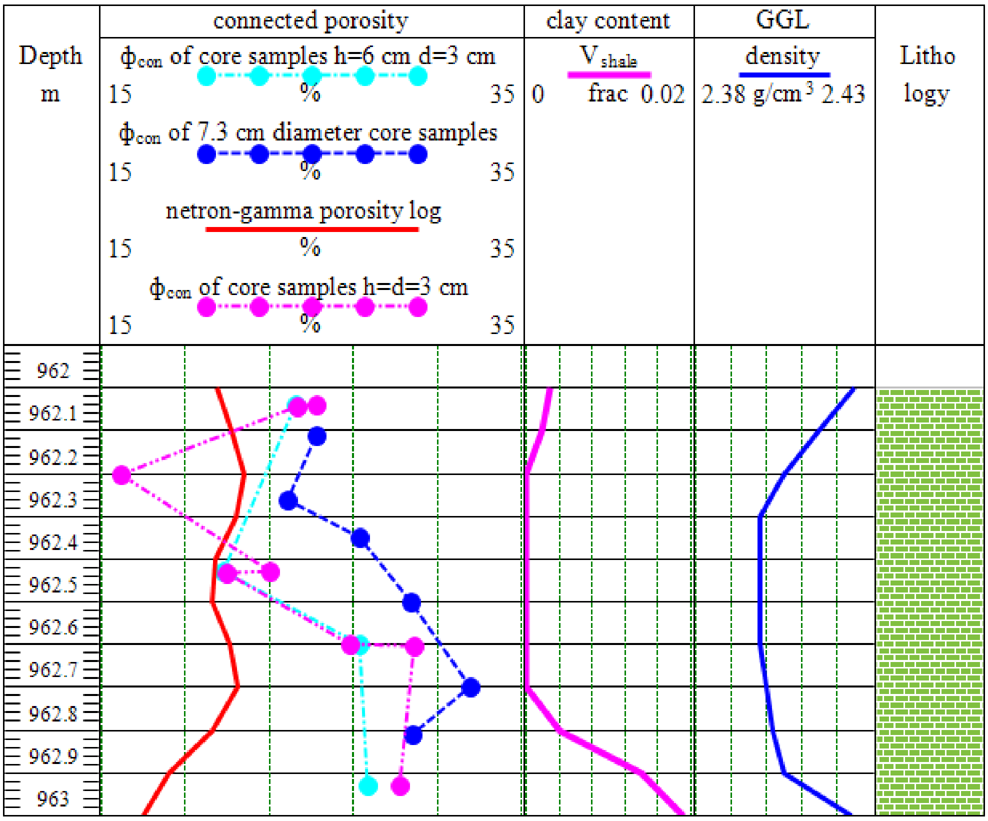

Fig. 4. The comparison of porosity log and porosity values of core samples. In the lithology column grainstones marked in green. Vertical scale is 1:15

limestones in the interval of 962.0-963.0 m are grainstones [9]. The comparison of log and core porosity data is not possible in this interval. It is necessary to analyse additional porosity values calculated with gamma-gamma well-logging method data.

Results of the connected porosity of the 1 m long whole core segment calculated in two ways are presented in Table 3. Dykstra-Parsons coefficients V_k were also defined to choose the best averaging technique (geometric or arithmetic) applying for the evaluation of the whole core porosity.

Table 3. Whole core porosity values calculated in two ways

	Porosity data of 7.3 cm diameter core samples	Porosity data of core samples 6 cm long by 3 cm in diameter
V_k	0.15	0.33
ϕ_{con}, %	28.08	22.73

Conclusions

Results of laboratory porosity measurements demonstrate that the scale effect occurring in Bashkirian limestones in the depth interval of 962.0-963.0 m is explained by fracture and vuggy porosity that is widely spread in big core samples. The investigation of core samples 44 cm by 10 cm in diameter allows a reliable porosity value for the 1 m long whole core segment to be defined.

The whole core segment connected porosity evaluated using porosity data of core samples 6 cm long by 3 cm long is lower than the whole core fragment connected porosity calculated using porosity data of 7.3 cm diameter core samples by 19%.

Values of the neutron-gamma porosity log are shown not to be reliable in the interval investigated. Another method such as a gamma-gamma well logging method should be used to define accurate porosity values.

Acknowledgments

The work was supported by the Ministry of Science and Higher Education of the Russian Federation (Agreement No. 075-11-2019-032 from 11/26/2019).

REFERENCES

1. Shashenko, A. N., Sdvizhkova, E. A., Kuzhel, S. V. (2004). Masshtabnyi effekt v gornykh porodakh. Donetsk, Izd. Nord-Press, p. 126.
2. Glover, P. (2001). Formation Evaluation MSc Course Notes. Aberdeen University, p. 141.
3. State Standard 26450.1-85. (1985). Rocks. Method for determination of open porosity coefficient by fluid saturation. Izd. Standartov, Moscow, 7.
4. Andersen, M. A., Brent, D., McLin, R. (2013). Core Truth in Formation Evaluation. Oilfield Review 25 (2), pp. 16-25.
5. Goroyan V. I. (1978). Metodicheskie rekomendatsii po issledovaniyu porod-kollek torov nefti i gaza fizicheskimi i petrograficheskimi metodami. VNIGNI, Moscow, 395.
6. Bear, J. (1972). Dynamics of Fluids in Porous Media. American Elsevier Publishing Co., New York, 764.
7. Prilous, B. I. (2013). About introduction of concept of the representative volume element in the theory of the structured continuum. The international scientific conference GEO-Sibir. Novosibirsk, pp.115-120.
8. Tomin, P. Yu. (2011). On the Representative elementary volume concept. Preprinty IPM im. M.V. Keldysha 13, pp. 1-13.
9. Dunham, R. J. (1962). Classification of carbonate rocks according to depositional texture. Simp. Amer. Assoc. Petrol. Geol. Mem. 1, pp. 108-121.
10. Glover P. (2009). Petrophysics MSc Course Notes. Aberdeen University, 376.

Potential of Geophysical Methods for Studying the Cryogenic State of the Upper Part of the Permafrost Section During Mine Development in the Central Kolyma Region

KHASANOV Ibragim[1,3], VOLKOV Vasiliy[2], BIAKOV Alexander[1,3,4]

[1] *North-East Interdisciplinary Scientific Research Institute n.a. N.A. Shilo, Far East Branch, Russian Academy of Sciences, Magadan, (RUSSIA)*
[2] *Southern Federal University, Rostov-on-don (RUSSIA)*
[3] *North-Eastern State University, Magadan (RUSSIA)*
[4] *Kazan Federal University, Kazan (RUSSIA)*
Email: aumaglan@yandex.ru

Abstract

The results of geophysical studies performed to assess the effectiveness and resolution of electric exploration methods in the search for different-rank thawed zones and areas in frozen sediments are presented and discussed. The changes are considered and values of the electrical resistivity and induced polarization of soils are given depending on the nature and degree of freezing. The working procedure is proposed, objects of exploration are localized.

Keywords: permafrost, thawed zones, geophysical methods, electrical tomography, electrical resistivity, induced polarization, Northeast Russia

Introduction

The complexity of hydrogeological conditions of permafrost development areas causes significant problems in the exploration and development of placer deposits. To obtain information about the geocryological state of rocks, it is necessary to drill a significant number of wells with sampling and logging studies. The use of geophysical methods based on measuring the properties of physical fields created by geological bodies can significantly reduce the amount of drilling and the cost of work.

Methods of ground geophysics in the hydrogeological study of ore and placer deposits of metals are effective in delineating different-rank thawed zones, studying their morphology in plan and section, identifying areas of permafrost, searching for areas of increased fracturing in bedrock (and, as a result, of their water encroachment rate).

The paper presents the results of the cryogenic state study for a rock mass of a placer gold deposit located in the middle reaches of river Debin in the Central Kolyma area of the Magadan region, Northeast Russia (Fig. 1).

Materials and methods of research

The study of the cryogenic state of the upper part of section of permafrost rocks (0-20 m) in the territory was carried out on the basis of the authors' materials obtained in the course of field operations in 2015-2018 (LCC Gold Mining Corporation) and published data.

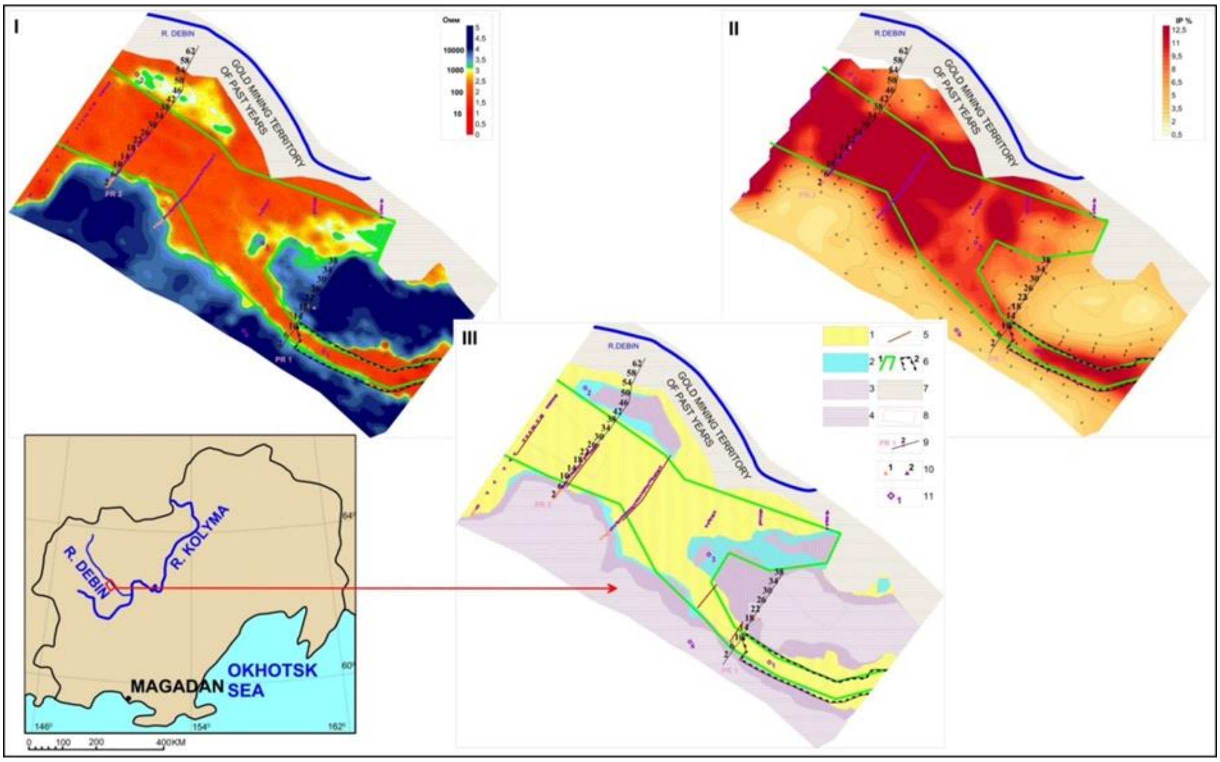

Fig. 1. Overview of the research area. Schemes for isolines of SER (I), IP (II) and the interpretation scheme (III) 1 – Thawed zones in the depth range of 1-20 meters; 2 – Seasonally frozen rocks; 3 – Rocks of patchy permafrost; 4 – Permafrost; 5 – Confirmatory gutters; 6 – Site proposed due to geologic-geophysical data (1) and measured dredging site (2); 7 – Development of the past years; 8 – Sites with concentrations of gold higher than 0.5 g/m^3; 9 – Profiles of VES-IP (electrotomography), their numbers and pickets; 10 – Temperature measurement points (1, 2) positive (1) negative (2); 11 – Observation points for symmetric VES-IP (Schlumberger), their numbers. Explanation: SER – Specific electric resistivity; IP – induced polarization; VES – Vertical electrical sounding

To address these tasks, a range of geophysical techniques were used, including: electrical profiling (subsurface symmetrical induced polarization electrical profiling) and electrical sounding using IP-VES methods. A hardware system was used, consisting of IPPM (IP pulse method) measuring devices, MESM-24 (multifunctional electrical survey meter) and an ASTRA-100 ge

To address these tasks, a range of geophysical techniques were used, including: electrical profiling (subsurface symmetrical induced polarization electrical profiling) and electrical sounding using IP-VES methods. A hardware system was used, consisting of IPPM (IP pulse method) measuring devices, MESM-24 (multifunctional electrical survey meter) and an ASTRA-100 generator. RES2DINV and IPI2win2 programs were used for interpretation of the sounding materials. In order to control the geophysical data obtained, several confirmatory trenches were examined.

The temperature of rocks in their natural occurrence was measured in the confirmatory trenches with an industrial thermometer TGZ-MG4 (small-sized digital thermohygrometer) using a contact method with a probe.

Results and Discussion

The geological structure of the area includes Jurassic terrigenous deposits, represented mainly by coal-clay shales, less often siltstones, sandstones and tuffites. Poorly consolidated alluvial deposits are divided by age into upper quaternary and recent ones. The lithological composition of alluvium for the floodplain and high floodplain terrace is presented by (from top to bottom): topsoil, silt and peat (0.0-0.4 m); silt and clay with pebbles and stones of different composition and size (up to 0.4-2.0 m); loose sediment pebbles of various size with sand and clay, small granite stones (10-20%), ice lenses, gravel (2.0-14.0 m); pebbles of various sizes, and consolidated by clay, and gravel from destroyed sandy-and-clay slates (14.0-15.0 m).

The thickness of alluvial deposits is 8.0-15.0 m. In general, these formations are characterized by a fairly high ice content.

According to hydrogeological conditions, the physical state of loose sediments is mostly permafrost. In the core of the watercourse channel part, the presence of suprapermafrost and subjacent thawed zones has been established. According to the degree of mineralization, the waters are fresh – 30-100 mg/dm^3. Their composition is mainly hydrocarbonate-and-calcium and sulfate-and-sodium, acidic and slightly alkaline (pH varies from 4.2 to 7.8). In relation to the cryolithic zone, supra- and intrapermafrost waters are distinguished among the subterranean waters of the area. Seasonally thawed waters are ubiquitous and circulate in alluvial sediments and fractured bedrock. The water-resistant horizon for them is the permafrost layer.

Based on the comparative analysis of geophysical studies in plan and section, the following geoelectric elements of the cryogenic structure of the geological terrain in the depth range of 1–20 meters were established:

The search objects – thawed zones – are registered due to specific electrical resistance (resistivity) of less than 500 Ohm×m and values of the induced polarization parameter (IP) of 9 to 12 %.

Seasonally thawed rocks have a distribution in the near-surface layer up to a depth of 3-4 meters and have a resistance of 500-1000 Ohm×m and an induced polarization of 7-9%.

Locally frozen rocks or focal (insular) permafrost, which is alternate in the section of thawed and frozen rocks. As a rule, this is due to the presence of near-surface thawed rocks within the active layer, lensed frozen rocks among the thawed ones, or, more rarely, the presence of subpermafrost thawed zones on the border of loose rocks and bedrock. The complex nature of the interaction of unfrozen water with the mineral skeleton and ice causes a wide range of changes in the resistance from 3000 to 10000 Ohm×m and an IP of 5-8% for frozen soils.

Permafrost rocks have a specific electrical resistance of more than 10,000 Ohm×m and the IP of less than 5% (Figs. 1-3).

The results of electrical sounding by the electrotomography method are presented in the form of geoelectric sections (Fig. 2). They reflect the distribution of various degrees of frozen and thawed rocks in the section. The presented data of symmetrical four-electrode electric sounding record the most characteristic cryo-hydrogeological conditions of the state of rocks from thawed and seasonally frozen to focal and permafrost ones (Fig. 3).

The given electrical characteristics of rocks obtained with different installations are comparable to each other, which indicates the objectivity of the selected gradations of the cryogenic state of the upper part of the section.

The close correlation between the geocryological parameters of rocks and their specific electrical resistance and IP allows us to create a clear picture of the structure of the geological terrain laterally and to the depths determined by the linear dimensions of the measuring lines (spacings).

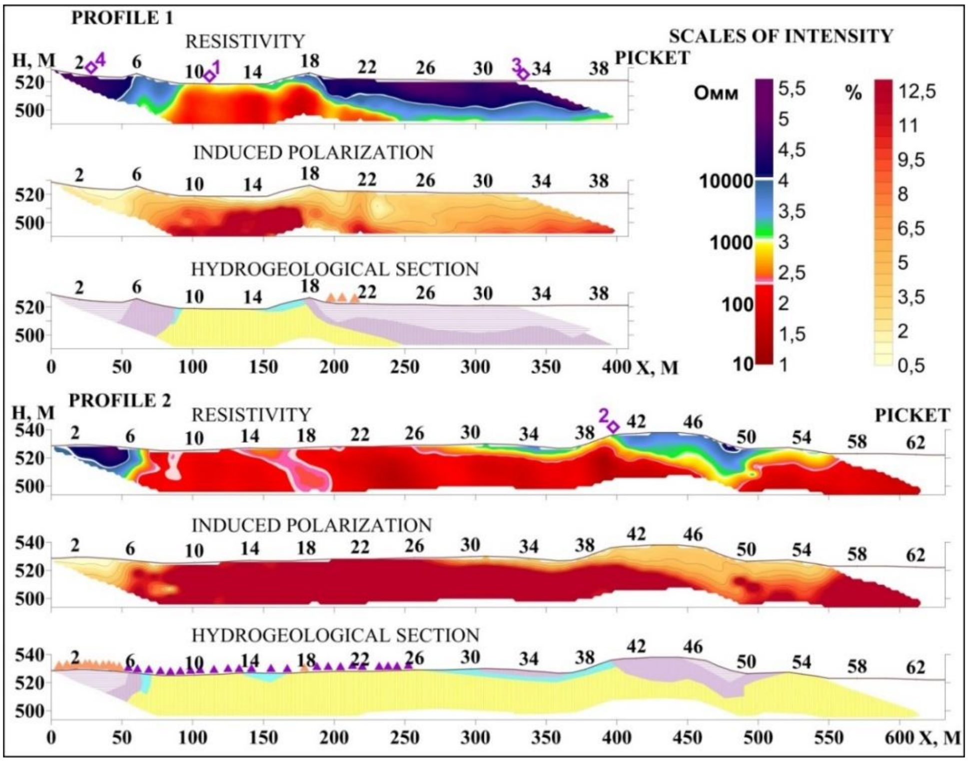

Fig. 2. Geoelectric sections of VES-IP (electrical tomography) and their interpretation. Symbols in Fig. 1

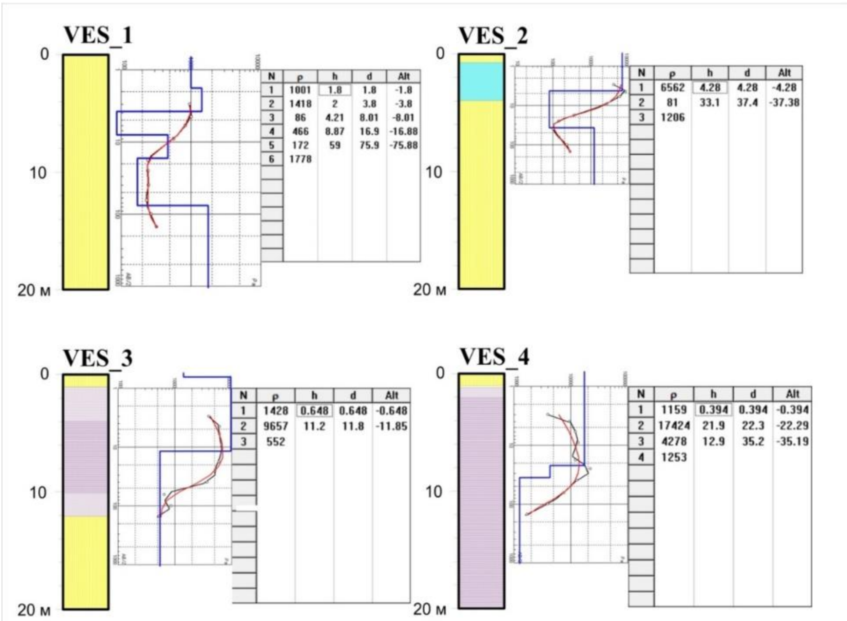

Fig. 3. Results of symmetrical VES-IP (Schlumberger installation). Symbols in Fig. 1

As a result of the works, subjacent and subpermafrost thawed zones have been identified and tests sites for dragging operations are planned for them (Fig. 1). Within the boundaries of the dragging site, several verification trenches with a depth of 3 to 6 meters were passed, which fully confirmed the results of geophysical research in the absence of frozen rocks. Along the trench bed and across the entire area, measurements were made of the soil temperature in the natural occurrence. Their results are also consistent with the geophysical diagnostics on the presence of thawed and frozen rocks (Figs. 1, 2).

A sharp increase in the specific electrical resistance of watered soils in the zone of negative temperatures is naturally associated with the formation of ice in the pores and cracks, which has a high (more than 10,000 Ohm×m) resistivity [1], [3], [4], [6], [7], [8].

The increase in the IP of thawed rocks in comparison with frozen ones is associated with a number of mechanisms of natural electrochemical processes. The first one is the content of clay material. Rocks containing fine clay substance have a noticeable polarization and may have an increased induced polarization comparable to that characteristic of ore inclusions [5]. The second one is related to the existence of a functional relationship between permeability and polarization.

In this case, it means the movement of liquid in the pores of the rock under the influence of the superimposed field. In the aeration zone, polarization is supplemented by phenomena related to free water transport, when the relationship of the IP with the filtration properties of the geological terrain is preserved.

When the soil is frozen, with medium and coarse sand fractions present (0.315-1.25 mm), there is a sharp decrease in the values of polarization capacity (by two or more times), which is due to processes occurring in all three types of water (free, loose and consolidated), simultaneously existing in comparable quantities at a given temperature [2].

The obtained results of geophysical research have demonstrated the high efficiency of the applied complex of electrical methods for the purpose of separating thawed rocks in the permafrost massif. These research methods can be recommended for studying the cryogenic state of soils, as well as engineering and geocryological processes.

Conclusions

Thus, within the research area, pronounced patterns of the cryohydrogeological state of rocks with different values of specific electric resistance and IP have been established, i.e., thawed, seasonally thawed, locally frozen and permafrost states. On the basis of the obtained geophysical materials, thawed zones and zones suitable for dredging and mining of commercial blocks, as well as areas of permafrost distribution, have been identified.

Acknowledgments

This work was is performed according the State Russian Government Program for competitive growth of Kazan Federal University among the World’s leading scientific and education centers.

REFERENCES

1. Zykov, Yu. D. (2007). Geofizicheskiye Metody Issledovaniya. Moscow State University, Moscow, 272.
2. Kormiltsev, V. V. (1980). Perekhodnye Protsessy pri Vyzvannoy Polyarizatsii. Nauka, Moscow, 111.
3. Melnikov, V. P., Skvortsov, A. G., Malkova, G. V. *et al*., (2010). Resultaty Izucheniya Geokriologicheskikh Usloviy Arkticheskikh Territoriy s Pomoshchyu Geofizicheskikh Metodov. Geologiya i Geofizika 51 (1), pp. 171-180.
4. Neradovsky, L. G. (2013). Opyt Izucheniya Vliyaniya Temperatury na Udel’noye Elektricheskoye Soprotivleniye Merlykh Porod. Geofizika 1, pp. 67-70.
5. Olenchenko, V. V., 2002. Izucheniye Informativnosti Metoda Ranney Stadii Vyzvannoy Polyarizatsii (RSVP) pri Reshenii Zadach Geokriologii. PhD thesis in Geological and Mineralogical Sciences. Tomsk, 211.

6. Khasanov, I. M., Sharafutdinov, V. M., Koshurnikov, A.V. (2011). Otsenka Vliyaniya Kriolitozony pri Geofizicheskikh Issledovaniyakh Zolotorudnykh Mestorozhdeniy na Poiskovoy Stadii, Raspolozhennykh vo Vmeshchayushchey Srede, Sosotoyshchey iz Tonkodispersnykh Osadochnykh Porod. Proceedings of the 4th Conference of Geocryologists of Russia, Universitetskaya kniga, Moscow, pp. 257-262.
7. Khasanov, I. M., Alevskaya, N. L., Koshurnikov, A.V. (2011). Effectivnost Geofizicheskikh Metodov pri Izuchenii Kriolitozony v Protsesse Drazhnoy Obrabotki Rossypnykh Mestorozhdeniy. Ibid., pp. 253-257.
8. Yakupov, V. S. (2008). Geofizika Kriolitozony. Yakutsk State University, Yakutsk, 342.

Carbonaceous Matter in Black-Shale Deposits of the Bredy Formation (Southern Urals)

KOLOMOETS Alexandra[1], SNACHEV Alexander[2], SMOLEVA Irina[3]

[1] *Orenburg State University (RUSSIA)*
[2] *Institute of Geology, Subdivision of the Ufa Federal Research Centre of the Russian Academy of Sciences (RUSSIA)*
[3] *Institute of Geology, Federal Research Center, Komi Scientific Center, Ural Branch of the Russian Academy of Sciences (RUSSIA)*
Email: kolomoyets56@mail.ru

Abstract

This paper addresses the geological structure of the Kumakskoye ore field located within the Anikhovsky Graben (Southern Urals). Special attention is given to the carbonaceous shales of the Bredinskaya Formation, which are widespread in this area. The carbonaceous matter, and its distribution within the shales are studied. Thermal and isotopic analyses showed that the carbonaceous matter was of biogenic nature and underwent metamorphism under conditions of high-temperature subfacies of greenschist facies.

Keywords: Southern Urals, carbonaceous shale, black shale, Bredy Formation

Introduction

Black-shale deposits are widely distributed globally. They form a very favorable geochemical environment for the sorption of noble and rare metals. They can also be a source of such metals while undergoing metamorphic transformations [1], [2], [3], [4], [5], [6], [7]. In the Southern Urals, black shales can be found in the Bredy Formation (C_1bd) along with gold and quartz ore bodies [8], [9]. The stratigraphic section is dominated by carbonaceous terrigenous sedimentary rocks: siltstone, carbonaceous clay shale and sandstone, and rare beds of limestone and coal. At the base of the section, there are subdominant effusive rocks (dacite and andesite porphyrites and tuffs).

The Kumakskoe gold deposit is one of the most promising objects within the Bredy Formation

Geological Setting

The Kumakskoe ore field is located in the Anikhovsky Graben, which stretches in the meridional direction. It is filled with carbonaceous terrigenous-carbonate sediments; its side parts are composed of volcanic sedimentary rocks. The graben's geometry is complicated by the Kumak-Kotansunskaya shear zone – part of a large tectonic fault (Chelyabinsk Deep Fault), which can be traced along the East Ural Uplift. In the adjacent zones of the Anikhovsky Graben, there is a pronounced near-fault longitudinal compression folding. Intense shearing masks the layering of the folds, creating the appearance of monoclinal bedding. In the central part of the shear zone, at 10 km along its strike, there are a number of gold occurrences (Kumak, Kumak-Yuzhny, Zabaikalskoye, Tsentralnoye fields) (Fig. 1).

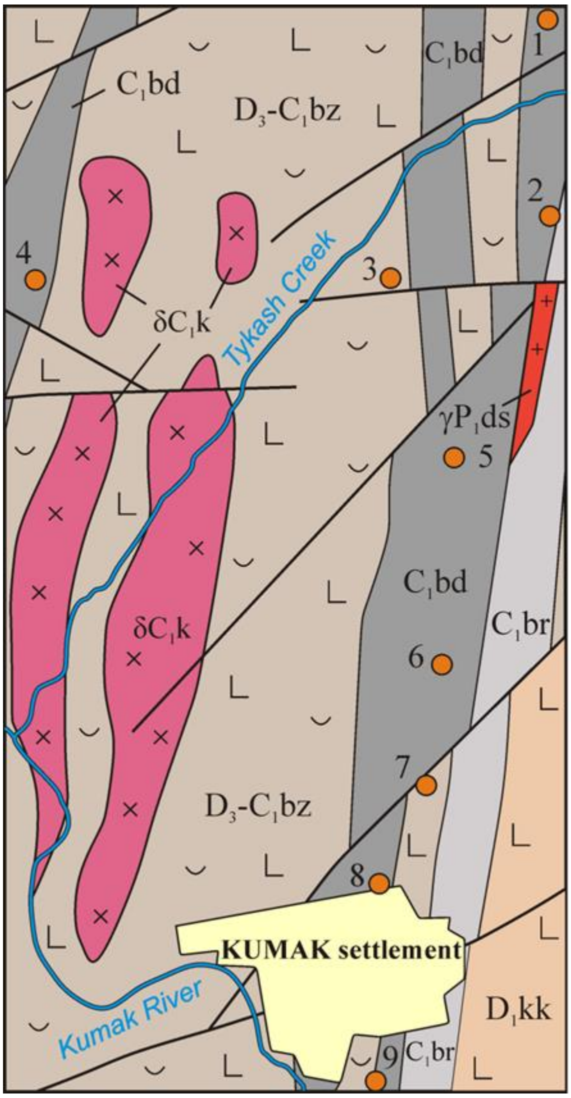

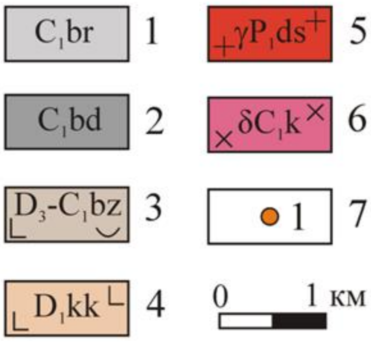

Fig. 1. Geological map of the Kumakskoe ore field (Southern Urals) (modified after [10]).
Legend: 1 – Birgilda Series (conglomerates, sandstones, limestones, carbonaceous shales), 2 – Bredy Formation (carbonaceous shales, sandstones, siltstones, conglomerates), 3 – Bereznyaki Series (basic and acidic tuffs, lavas, layers of siltstone and carbonaceous shale), 4 – Kokpeky Series (basaltic lavas and tuffs, subvolcanic gabbro-dolerites, rhyolites), 5 – Dzhabyk-Sanarka Series (granite, leucogranite), 6 – Kumak Series (diorite, plagiogranite), 7 – gold occurrences and fields: 1 – Vostochno-Tykashinskoe, 2 - Kommercheskoe, 3 – Milya, 4 – Tamara, 5 – Zabaikalskoe, 6 – Baikal, 7 – Tsentralnoe, 8 – Kumak, 9 – Kumak-Yuzhny

The ore bodies gravitate towards a set of carbonaceous shales, 70-120 m thick and stretching for several tens of kilometers. Carbonaceous shales are widespread in the Bredy Formation (C_1bd), which overlays the Bereznyaki Series (D_3-C_1bz) and is overlain by the Birgilda Series (C_1br). It is 350-700 m thick [10]. The black shales of this region can be subdivided into several groups depending on their composition: (1) sericitic-quartz-carbonaceous; (2) quartz-carbonaceous-tourmaline; (3) ottrelite-carbonaceous; and (4) quartz-carbonaceous-ottrelite.

The first ones are the most widespread. They are grayish-black (sometimes black) fine-grained rocks with poor schistosity, easily splitting along cleavage planes. In the western part of the field, there are mostly rocks with a significant ottrelite content.

Carboniferous shales have microlepidoblastic, lepidogranoblastic or heterogranoblastic structure and mostly shale texture. The structure is conditioned on the presence of quartz and tourmaline grains, and also scales, laths and scaly mica aggregates. The texture is characterized by layers of quartz-carbon-sericite, thin layers and elongated lenses of quartz, and fine-to-coarse-grained quartz alteration. The thickness of these layers varies widely. The banded texture is complicated by a series of asymmetrical sub-parallel cleavage folds (Fig. 2). The average mineral composition of black shale rocks is: quartz (up to 40%), sericite (5-10%), carbonaceous matter (up to 50%), carbonates (5-10%), sulfides (up to 5%).

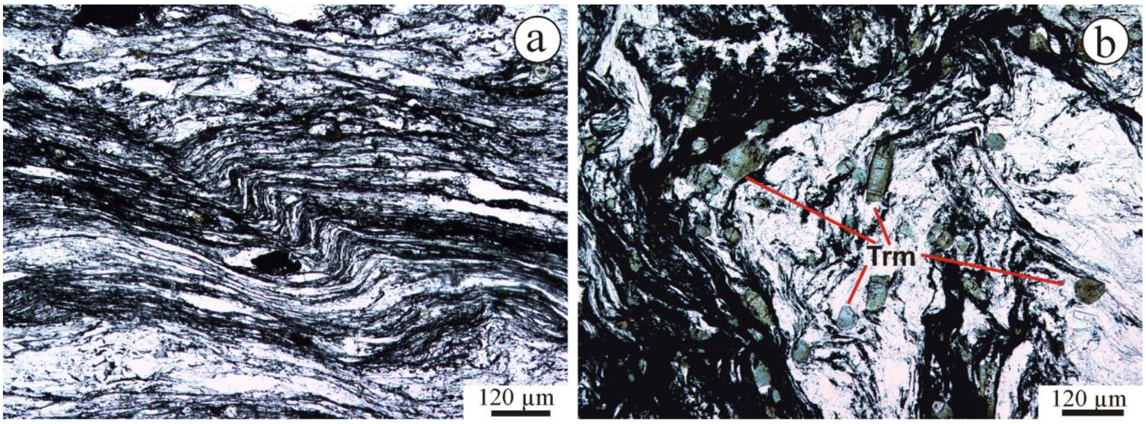

Fig. 2. Banded texture of the rock complicated by cleavage folds (**a**), and quartz-mica-tourmaline veins in carbonaceous shale (**b**) (without analyzer, 200x)

Results and Discussion

The carbonaceous matter is in a finely dispersed state or in the form of a mass that cements the rest of the minerals. It is dominated by sapropel in the form of irregularly shaped fragments; however, in metamorphic parts, it is represented by large flaky graphite veins. The amount of carbonaceous matter is often quite significant (Fig. 2a). Hydrothermal metamorphism is expressed in layers of sericite, recrystallized quartz, and carbonate, cementing (and sometimes consuming) the quartz. Tourmaline is also constantly present in the shales. It forms prismatic crystals 0.1-0.3 mm in size along the long axis, clearly pleochroic, changing its color from dark green to light green (Fig. 2b). Small particles of carbonaceous matter are constantly present in the central parts of tourmaline grains (sealed inside during growth). Its content ranges from single grains to 15-20% near tourmaline-sericite shales. The sulfide content does not exceed a few tenths of a percent, reaching 2-3% in the richest areas.

It is known that C_{org} content in typical black shales is 1% or above, and the rocks can be classified into three groups [11]: 1) low-carbon, 1-3%; 2) carbonaceous, 3-10%; 3) high-carbon, >10%. Thermal and gravimetric analysis showed that the shales of the Kumakskoe field have on average a C_{org} content of 6.4% (with a maximum of 11.1%), and this allocates them to the carbonaceous group.

A Delta V Advantage mass spectrometer, together with a Flash Elemental Analyzer, was used to study the carbon isotope composition and identify the genesis of the carbonaceous matter. The measurements were carried out at the "Geonauka" CCU (analyst I.V. Smoleva, Institute of Geology, Komi Scientific Center, Ural Branch of the Russian Academy of Sciences, Syktyvkar).

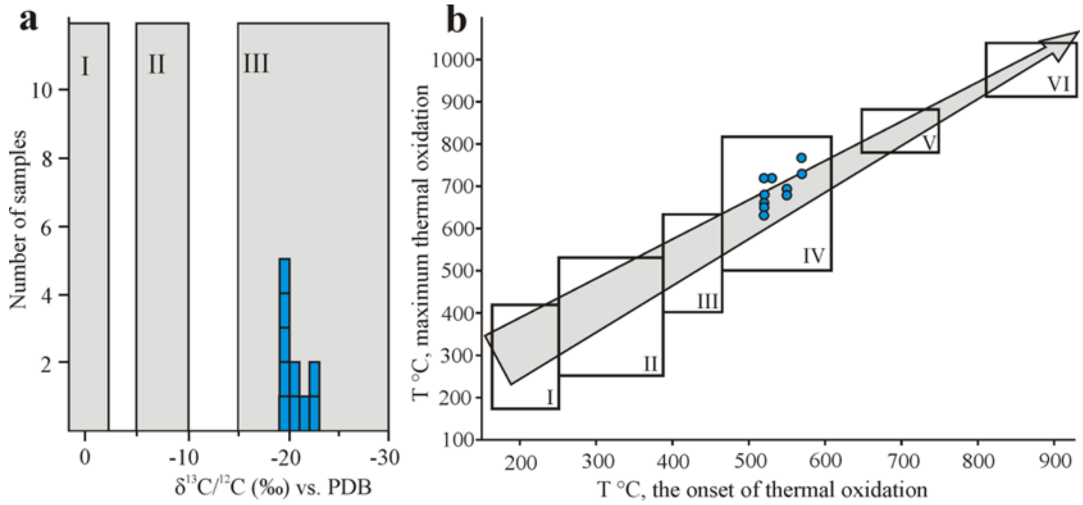

Fig. 3. Carbon isotope composition (**a**) and the black shales of the Bredy Formation (blue points) on the diagram of thermal stability of carbonaceous materials (**b**).
a: typical values of carbon isotopes in marine carbonates (I), mantle carbon (II) and biogenic carbon (III) according to Javoy *et al*. [12].
b: burn-off stages according to Silayev et al. [16]: I – modern plants, organic matter in unmetamorphosed sedimentary rocks, coprolite; II – asphalt, low kerite; III – asphaltite, kerite; IV – high kerite, anthraxolite, shungite; V – graphite, carbon diamond; VI – diamond

The accuracy was ±0.15‰. $\delta^{13}C$ (vs. PDB) values fall within the range of (-19.07) – (-22.80) (Fig. 3), which indicates the biogenic nature of carbon. The minor variations are most probably associated with varying intensity of metamorphism [12], [13], [14], [15].

Black shales are convenient for determining the degree of metamorphism [17], [18]. This is because carbon reacts to metamorphic transformations only by changing its structure and aggregate state. The temperature at which the exothermic effect corresponding to the graphite burn-off is observed changes abruptly by about 100 °C in the rocks of each subsequent facies as metamorphism intensifies. It is also assumed that graphitization is an irreversible process [19]. The least altered samples of carbonaceous rocks were selected for the analysis, allowing for determination of the degree of regional metamorphism. Thermal and gravimetric analysis was performed on the Q-1500 derivatograph (Hungary) (analyst T.I. Chernikova, Institute of Geology, Ufa Federal Research Center of the Russian Academy of Sciences, Ufa). Heating was carried out in air, from 20 to 1000 °C at a rate of 10 °C/min. The ratio between the initial temperature of the exothermic effect and its maximum value on the thermal stability diagram shows that organic carbon underwent high-grade metamorphism, comparable to that of high kerite, anthraxolite and shungite [16]. The maximum temperature of the exothermic effect falls within the range of 630-770 °C (during metamorphism, temperature was around 560-700 °C), which corresponds to the epidote-amphibolite subfacies of the greenschist facies [20].

Conclusions

The study of the Kumakskoe ore field showed that the rocks of the Bredy Formation are of the carbonaceous type. The carbonaceous matter is represented by little- metamorphosed sapropel diagenetic and metamorphic graphite, is of biogenic origin and underwent metamorphism under conditions of high-temperature subfacies of the greenschist facies.

Acknowledgements

The authors thank T.I. Chernikova and S.A. Yagudina for their contribution to the analysis reported in this paper, as well as E.O. Kalistratova for her help in describing the thin sections.

Fieldwork was supported by a regional grant in the field of scientific and technical activities for 2019 (Agreement No. 23 dtd 08/14/2019). Analytical work was carried out within the framework of the state assignment No. 0246-2019-0078.

REFERENCES

1. Arifulov Ch. Kh. (2005). Chernoslantsevyye mestorozhdeniya zolota razlichnykh geologicheskikh usloviyakh. Rudy i metally 2, pp. 9-19.
2. Snachev, A. V., Puchkov, V. N. (2010). First findings of palladium-gold-REE ore mineralization in Precambrian carbonaceous shales on the western slope of the Southern Urals. Doklady Earth Sciences 433 (1), pp. 866-869.
3. Large, R. R., Bull, S. W., Maslennikov, V. V. (2011). A Carbonaceous Sedimentary Source-Rock Model for Carlin Type and Orogenic Gold Deposits. Economic Geology 106 (3), pp. 331-358.
4. Snachev, A. V., Rykus, M. V., Snachev, M. V., Romanovskaya, M. A. (2013). A model for the genesis of gold mineralization in carbonaceous schists of the Southern Urals. Moscow University Geology Bulletin 68 (2), pp. 108-117.
5. Snachev V. I., Snachev A. V. (2014). Zakonomernosti razmeshcheniya zolotorudnykh proyavleniy v uglerodistykh otlozheniyakh Beloretskogo metamorficheskogo kompleksa (Yuzhnyy Ural). Vestnik Voronezhskogo gosudarstvennogo universiteta. Seriya: Geologiya 2, pp. 79-87.
6. Shumilova, T. G., Shevchuk, S. S., Isayenko, S. I. (2016). Metal concentrations and carbonaceous matter in the black shale type rocks of the Urals. Doklady Earth Sciences 469 (1), pp. 695-698.
7. Snachev A. V., Nugumanova J. N., Saveliev D. E. (2019). Ore prospects of carbonaceous deposits of the Maksyutovo complex (Uraltau zone). Geologicheskii vestnik 1, pp. 55-67. DOI: 10.31084/2619-0087/2019-1-4.
8. Loshchinin V. P., Pankrat'yev P. V. (2006). Zolotonosnost' nizhne-srednepaleozoyskikh chernoslantsevykh formatsiy Vostochnogo Orenburzh'ya. Strategiya i protsessy osvoyeniya georesursov. Perm, pp. 79-82.
9. Sazonov V. N., Koroteyev V. A., Ogorodnikov V. N., Polenov Yu. A., Velikanov A. Ya. (2011). Zoloto v "chernykh slantsakh" Urala. Litosfera 4, pp. 70-92.
10. Lyadskiy P. V., Chen-Len-Son B. I., Alekseyeva G. A., Olenitsa T. V., Kvasnyuk L. N., Manuylov N. V. (2018). Gosudarstvennaya geologicheskaya karta Rossiyskoy Federatsii. Masshtab 1:200000. List M-41-I. Anikhovka. Objasnitel'naya zapiska. VSEGEI, Moscow, 100.
11. Yudovich, Ya. E., Ketris, M. P. (1988). Geokhimiya chornykh slantsev. Nauka, Leningrad, 271.
12. Javoy M., Pineau F., Delorme H. (1986). Carbon and nitrogen isotopes in the mantle. Chemical Geology 57, pp. 41-62.
13. Des Marais D. J. (1997). Isotopic evolution of the biogeochemical carbon cycle during the Proterozoic Eon. Organic Geochemistry 27 (5), pp. 185-193.
14. Van Kaam-Peters H. M. E., Schouten S., Koster J., Sinninghe Damste J. S. (1998). Controls on the molecular and carbon isotopic composition of organic matter deposited in a Kimmeridgian euxinic shelf sea: Evidence for preservation of carbohydrates through sulfurisation. Geochimica et Cosmochimica Acta 62, pp 3259-3284.
15. Bushnev D. A., Smoleva I. V. (2011). Carbon isotopes of organic matter from the upper Jurassic oil shales from the Volgian-Pechora shale province and its accumulation mechanisms. Doklady Earth Sciences 441 (1), pp. 1543-1545.
16. Silayev V. I., Smoleva I. V., Antoshkina A. I., Chaykovskiy I. I. (2012). Opyt sopryazhennogo analiza izotopnogo sostava ugleroda i azota v uglerodistykh veshchestvakh raznogo proiskhozhdeniya. Problemy mineralogii, petrografii i metallogenii: materialy nauchnykh chteniy pamyati P. N. Chirvinskiy. PGU, Perm, pp. 342-366.
17. Blyuman B. A. D'yakonov Yu. S., Krasavina T. N., Pavlov M. G. (1974). Ispol'zovaniye termo- i rentgenograficheskikh kharakteristik grafita dlya opredeleniya urovnya i tipa metamorfizma. Zapiski Vsesoyuznogo Mineralogicheskogo obshchestva 103 (1), pp. 95-103.
18. Snachev A. V. (2015). Ispol'zovaniye termicheskogo analiza uglerodistykh slantsev pri prognozirovanii zolotogo orudeniya. Vestnik Akademii nauk RB 20 (3), pp. 28-36.
19. Buseck P. R., Beyssac O. (2014). From organic matter to graphite: graphitization. Elements 10, pp. 421-426.
20. Ivanova V. P., Kasatov B. K., Krasavina T. N., Rozinova Ye. L. (1974). Termicheskiy analiz mineralov i gornykh porod. Nedra, Leningrad, 399.

Reconstruction of the Depositional Environment of Paleoproterozoic Stromatolitic Dolostones Based on Geochemical Data

KONDRASHOVA Natalia, MEDVEDEV Pavel

Institute of Geology, Karelian Research Centre of RAS, Petrozavodsk (RUSSIA)
Petrozavodsk State University, Petrozavodsk (RUSSIA)
Emails: kondr@krc.karelia.ru, pmedved@krc.karelia.ru

Abstract

Major, trace and rare earth element (REE) analyses were carried out on stromatolitic dolomites collected from drill cores of the project FAR-DEEP International Continental Drilling Program (ICDP) revealed Upper Jatulian carbonate succession of the Onego Paleoproterozoic sedimentary basin (Russian Karelia). We used laser ablation-inductively coupled plasma-mass spectrometry (LA-ICP MS) to measure trace and REE element concentrations in both dark and light stromatolite laminae.

Comparison of the trace element composition of the stromatolites with corresponding clarke values for the carbonate rocks and the values of geochemical markers suggest that the stromatolites were forming in an open system in the Late Jatulian and upon transition to the Ludikovian. The evolution of transgression in the Onega paleobasin by the early Ludikovian, based on analysis of the geochemical characteristics of the stromatolites, is consistent with the conclusion drawn earlier based on facies analysis.

The data based on analysis of the trace element composition of Paleoproterozoic Late Jatulian stromatolites could be used to assess facies settings in the sedimentary basin.

Keywords: Rare earth elements, Paleoproterozoic, stromatolites, dolomites, sedimentary basin, paleoenvironment, geochemical markers

Introduction

More and more attempts to reconstruct the geological evolution of paleobasins are made these days using geochemical criteria based on evidence for the behaviour of chemical elements in the water and sediments of modern water bodies. Various geochemical indicators are widely used to assess a paleogeographic depositional environment, because the trace element composition of carbonate and other rocks can be estimated. As the number of such markers increases, the scholar inevitably faces problems in verification and, consequently, in the validity of conclusions based solely on the use of geochemical indicators.

To assess the data obtained with various geochemical markers for carbonate rocks well-studied by geological methods, we used Paleoproterozoic stromatolites from the various stratigraphic levels of the Jatulian succession of the Onego paleobasin in Karelia (Fig. 1).

The lithofacies of a growing shallow water-marine carbonate platform in the Upper Jatulian sequences of the Onego paleobasin have been shown to be ubiquitous. Several recurring carbonate-evaporite cycles, sediments from sebkha and playa water bodies, dissolution and collapse breccias and surface and submarine karst phenomena have been reported. This evidence is indicative of frequent sea level fluctuations, numerous drainage episodes in an oxidative environment and sedimentation in a shallow epicontinental sea. On the present level of the erosion section, Late Jatulian carbonate rocks, up to 800 m in thickness, have been documented from some local sequences of the Onego paleobasin.

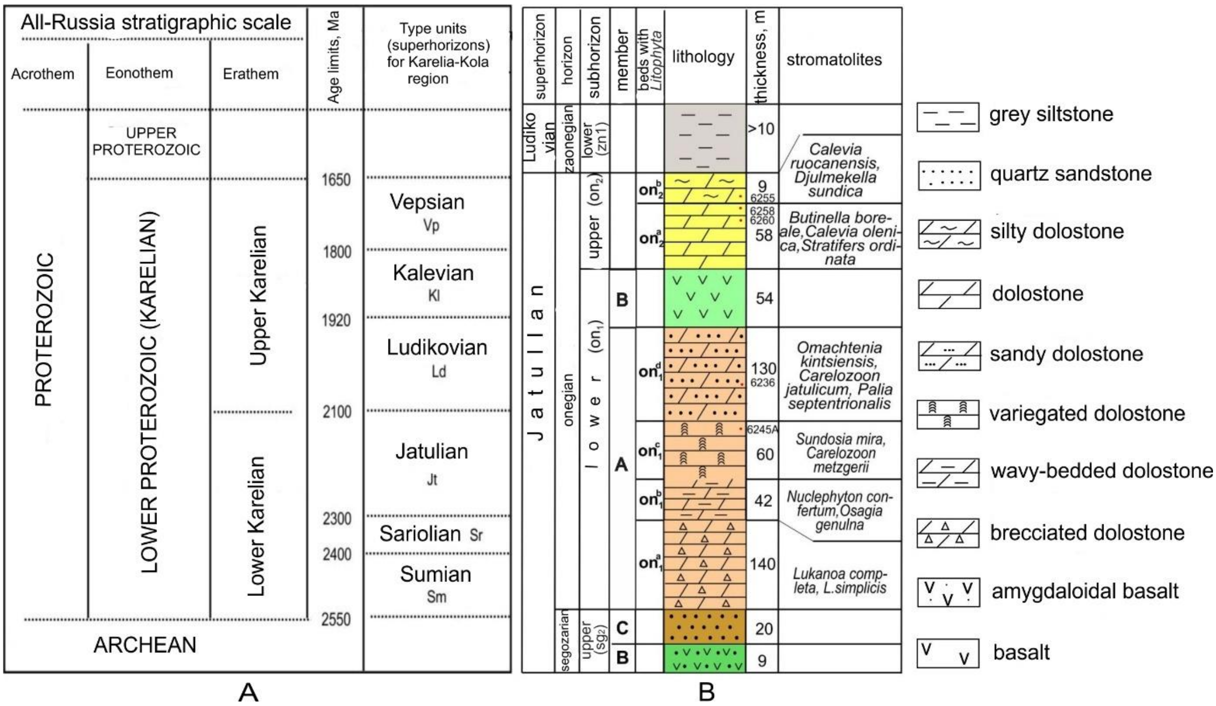

Fig. 1. Stratigraphic position of the stromatolitic dolomite samples analyzed. A fragment of the all-Russia stratigraphic scale for Paleoproterozoic (a) and the Jatulian succession (b) are shown

A collection of stromatolite samples from cores, obtained by drilling under the international project FAR-DEEP International Continental Drilling Program (ICDP) at the northwestern closure of the North Onegian Synclinorium which intersected the carbonate sequence of the Jatulian Onego horizon (Tulomozero formation) [1], was studied.

Methodology

Trace element concentrations in g/t or ppm were measured in each of the samples analyzed in the dark and light laminae of a stromatolitic buildup using the laser ablation inductively coupled plasma mass spectrometry (LA ICP-MS) method in the Collective Analytical Center of KarRC RAS (analyst A. S. Paramonov). Chemical element concentrations were estimated on an X-SERIES 2 quadrupole mass-spectrometer. The laser work energy was 0.133 mJ, the scanning speed was 70 µm/s and the impulse frequency was 10 Hz. Data from three measurements at each point were obtained. As a result, the ablation crater diameter increased to 70 µm and its depth was up to 40 µm. The first values obtained were used for calculation of indicator ratios. Measurements were made using NIST 612 standard. The measurement error did not exceed 25% for K, Mg, Ca, Sr, Nb, Zn, Co, V, Cr, As, Ge and Ga at most of the points of the samples. The measurement error for Na, Fe, Ti, Cu, Ba, Zr, Y and especially U and Th at most of the points was over 25%. The laser sampling parameters (laser wavelength, impulse duration, etc.), affecting analytical results, remain constant for all the points in all the samples analyzed. Therefore, an increase in the measurement error of some element concentrations in some of the points in the same sample could be due to a difference in the physical characteristics of a stromatolite sample at different points (the crystalline structure of carbonate or an impurity mineral, the absorption and reflection coefficient of radiation, etc.). The data obtained can thus be used for qualitative analysis.

The mineral composition of the stromatolite samples was studied on a Tescan VEGA II LSH scanning electron microscope with an INCA Energy 350 energy dispersion microanalyzer (Oxford Instruments).

Results

The macroscopically studied stromatolite samples consist of individual alternating light and dark laminae (Table 1). The laminae differ in either the size of dolomite crystals or the quantity of impurities. The dark laminae also contain abundant sandy-clayey impurities.

Table 1. Characteristics of stromatolite samples from the Upper Jatulian sequence of the Onego paleobasin, Karelia. Dots indicate the sites at which trace element concentrations in a sample were measured

Sample		Depth, m – Drill hole	Stratigraphic unit	Lithological description
6255	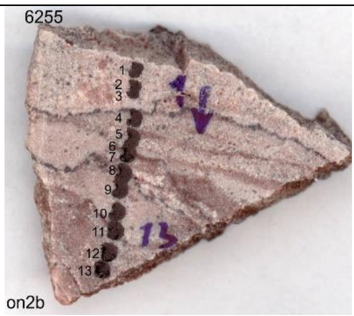	107.49 – DH11A	Beds with *Calevia ruokanensis* (on_2^b)	Pale-pink dolomite with red-brown layers of small dome-shaped and stratiform stromatolites *Stratiferales* with a clotted structure.
6258		115.35 – DH11A	Beds with *Butinella* (on_2^a)	Light-grey, parallel-laminated dolarenite with the mini-columnar stromatolites *Klimetia sp.* and well-defined sedimentary deformations
6260		127.43 – DH11A	Beds with *Butinella* (on_2^a)	Variegated, indistinctly laminated dolomite with the stratiform stromatolites *Stratifera ordinata* Mak., 1983

6236		65.58 – DH10A	Beds with *Omachtenia kintsiensis* (on$_1^d$)	Recrystallized mottled dolomite with the columnar-stratiform stromatolites *Omachtenia sp.*
6245a		328,61 – DH10A	Beds with *Sundosia* (on$_1^c$)	Light-brown dolomite with deformed layers of the stratiform stromatolites *Stratiferales* and flaser layering. Asymmetrical ripple marks, emphasized by dark clay, are occasionally encountered.

The carbonate rocks discussed were recrystallized under low-temperature greenschist-facies conditions. Primary sedimentary textures and structures were partly obliterated during recrystallization, but all the rocks have retained easily identifiable layering and fine stromatolitic lamination. Micritic dolomites are fairly scarce. Most carbonate microstructures display granulated, crystalline and microsparitic dolomite. Late carbonate phases, which fill cavities and veins and support breccia, consist of sparitic dolomite.

Most of the carbonate rocks are contaminated. The main non-carbonate impurity is silica, both chemically precipitated and occurring as clastic quartz grains.

Feldspar grains, represented by microcline and orthoclase, as well as magnetite, goethite, sphene, chalcopyrite, scarce biotite, muscovite and phlogopite grains, are encountered. The mineral composition of stromatolite sample 6245a is most diverse: in addition to dolomite and calcite, it contains large quantities of fluorapatite, phlogopite, K-feldspar, goethite and rutile.

Scarce zircon, barite and sphene grains occur. Quartz, phlogopite and goethite are abundant higher in the sequence (sample 6236). Apatite is occasionally encountered.

The purest dolomite occurs on the stratigraphic level of beds with *Butinella* (on$_2^a$).

The mineral composition of stromatolites from the unit of beds with *Calevia ruokanensis* (on$_2^b$) is represented by dolomite and calcite. Scarce micron-sized quartz, goethite, fluorapatite and K-feldspar grains are observed.

Stromatolites from the various levels of the stratigraphic sequence are similar in the mineral composition of carbonate-silt laminae, suggesting the scour of dominantly granitoid rocks. Consequently, in the Paleoproterozoic terrigenous materials was mainly supplied into the sedimentation basin by Archean basement granitoids. This assumption is supported by the trace element composition of the stromatolites (Table 2).

Table 2. Petrogenic (wt. %) and trace element (ppm) concentrations in stromatolite laminae (median value)

	6236	6245A	6255	6258	6260	*
Li	1.597	16.66	13.02	5.5	1.21	5
Na (%)	0.10	0.28	0.03	0.27	0.09	(0.25)
Mg (%)	5.92	5.81	4.57	8.95	4.83	4.6
K (%)	0.11	0.45	0.13	0.08	0.10	0.28
Ca (%)	30.61	14.37	11.95	46.09	23.89	32.5

Sc	28.54	34.19	16.45	38.09	34.11	1
Ti	38.39	45.08	486.90	36.66	18.21	1200
V	33.44	46.37	14.68	31.82	34.21	20
Cr	33.66	36.90	20.99	29.75	35.70	11
Mn	107.30	73.94	210.60	53.54	80.40	400
Fe	136.20	761.30	6829.00	143.95	48.80	8600
Co	9.72	22.26	6.51	14.57	12.90	0.1
Ni	28.88	40.76	11.83	31.06	26.57	2
Cu	56.07	48.60	89.07	48.26	59.37	4
Zn	71.55	68.17	84.98	39.96	74.13	20
Ga	25.98	39.90	9.71	28.76	28.40	4
Ge	22.67	29.25	10.50	26.84	25.43	0.2
As	26.35	32.21	14.33	28.94	30.44	1
Rb	3.89	38.52	1.83	5.82	4.27	3
Sr	362.40	218.00	84.93	174.00	78.23	610
Y	2.94	8.22	3.25	6.55	4.28	30
Zr	3.52	9.63	9.76	8.18	4.47	20
Nb	5.13	10.02	2.07	8.69	5.44	0.3
Cd	5.07	10.35	2.16	10.69	7.86	0.035
Ba	3.56	70.36	12.10	8.06	4.26	10
Pb	6.95	0.97	1.79	5.20	4.49	9
Th	0.14	0.44	0.60	0.33	0.09	1.7
U	0.08	0.35	0.53	0.58	0.14	2.2

** – average chemical element concentrations in the carbonate rocks (After [2])*

The trace element behaviour (the median value for all determination points in a particular sample is then estimated) in all stratigraphic units of the sequence displays the same type.

In the lower part of the sequence Mg, Ca, K and Na are present in small quantities not exceeding the clarke values of these elements in the carbonate rocks (the clarke values after [2]). Their concentrations decrease upwards, except for a local increase in Na and Ca concentrations to the clarke value in sample 6258.

Mn, Fe, Ti, Sr, Y, Zr, Pb, Th and U concentrations in stromatolites from all levels in the Jatulian sequence are much smaller than their abundance ratios in the carbonate rocks. Fe concentration on the on2b level (sample 6255) increases sharply to 6829 ppm in comparison with Fe in stromatolites from the lower part of the Jatulian sequence, but does not reach the Fe clarke value in the carbonates (8600 ppm).

The clark values are three times as high for Cr, ten times as high for Ni, Sc, Cu, Ge, Ga, As, Nb and Sn and hundreds of times as high for Co.

Rb exceeds clarke values only in the on_1^c unit. Ba concentrations in this unit exceed clark values, decreasing to lower clarke values upwards.

All the stromatolites contain Cs on the clarke value level.

The distribution of some elements in the stromatolite samples estimated in some of the laminae is shown below (Fig. 2).

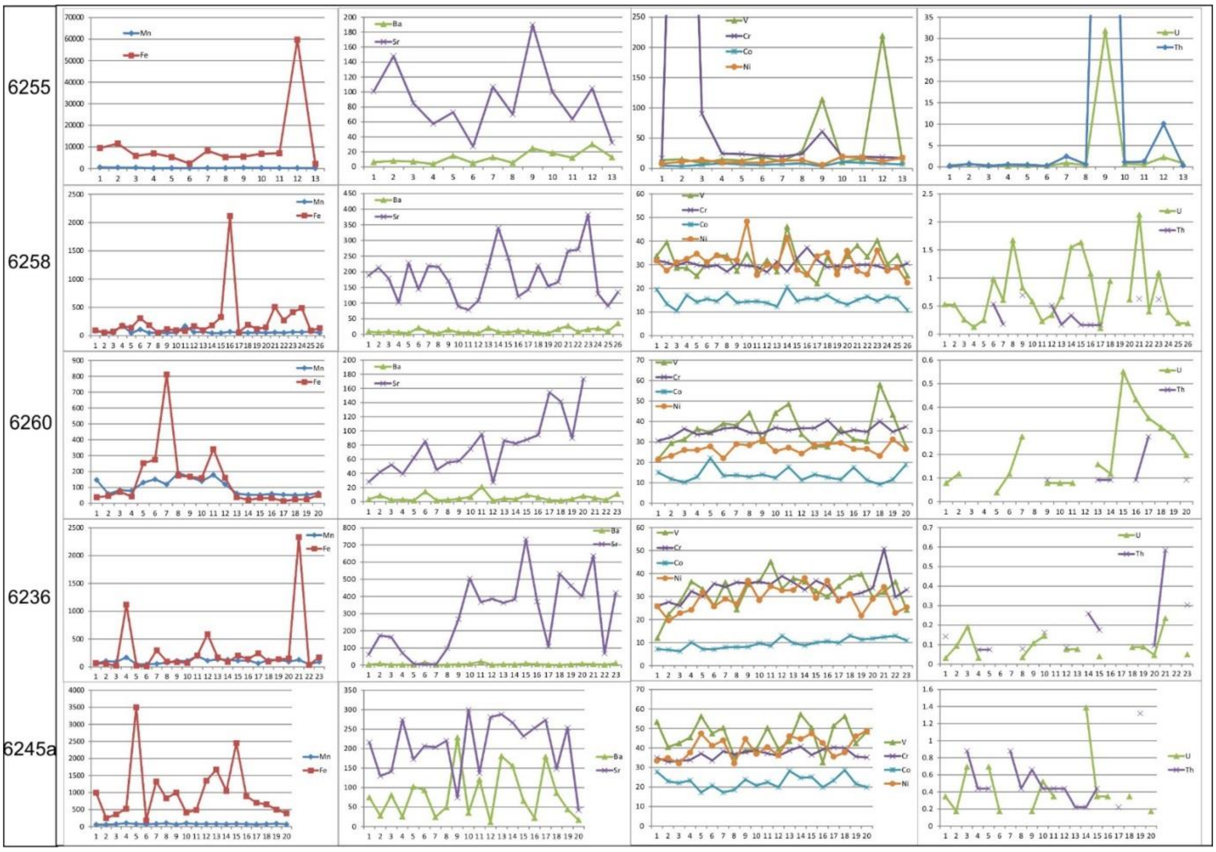

Fig. 2. Trace element distribution in Jatulian stromatolite laminae

There is much in common in Fe and Mn distribution in the stromatolite laminae. Fe concentrations in samples 6245a, 6236, 6260 and 6258 do not reach its clarke value in the carbonates, varying from tens to hundreds g/t (ppm). Fe concentration in some laminae increases, as indicated by the peaks (Fig. 2), but fails to reach its clarke value. Fe concentration increases sharply only in the on_2^b unit, either reaching clarke values or being several times as high.

Mn is present in all the laminae of all the samples in subclarke concentrations, increasing in stromatolites from the stratigraphic level on_2^b but not reaching clarke values.

Ba concentrations in some of the laminae in sample 6245a are 2-3 to tens of times the clarke value. Its concentration drops upwards below the clarke value. Only in the on_2^b unit Ba concentrations in the laminae increase, reaching clarke values and even exceeding them.

Strontium is present in all the samples in subclarke concentrations, in spite of variations in concentration in some of the laminae.

V, Cr, Co and Ni concentrations are several times more the corresponding clarke in carbonate rocks and decrease markedly only in the on_2^b unit, V is below clarke values for most of the stromatolite laminae.

Zn, Cu, Ge, Ga, As and Nb in all the laminae of all the samples from the various levels of the sequence display similar concentrations that markedly exceed the corresponding clarke value. Sc is 2-3 times the crustal abundance, except for sample 6255, where its concentration is close to clarke values.

Rb concentration is high in all the stromatolite laminae from the stratigraphic unit on_1^c (sample 6245a). It decreases upwards but remains 2-3 times the clarke value. In the on_2^a unit Rb concentrations are below clarke values, except for some of the laminae.

Concentrations that exceed clarke values were observed for all the laminae of all Sc, Sn and Sb samples. Absolute Li concentrations in the lower part of the sequence considerably exceed clarke values and drop below subclarke values upwards. Li concentrations increase to clarke values only on the on_2 stratigraphic level in some of the laminae of all the samples.

Zr and Y are present in small quantities throughout the carbonate sequence.

Discussion

The degree of post-sedimentation alterations of the carbonate rocks discussed can be reliably estimated from the Mn/Sr ratio. This index, as well as Mg/Ca, Fe/Sr values, suggest that the stromatolites analyzed have suffered minor diagenetic alterations. Therefore, they can be analyzed using geochemical data. Sample 6255 showed high Mn/Sr and Fe/Sr ratios, and the Fe/Sr value for sample 6245a in many laminae is over three. It is in the mineral composition of these stromatolites that micron-sized goethite and hematite are abundant. We believe that as a result, some of the index values, used to assess post-sedimentation alterations, increase. High Mn/Sr ratios could be provoked by a rise in Mn concentration and a simultaneous decline in Sr concentration, which may occur in an alkaline medium because more fresh water is supplied from land into the basin. Such a situation would arise upon the advance of transgression. This argument is consistent with available geological evidence [3]. It has been assumed earlier that most of Sr in a Late Jatulian basin has derived from the mantle [4], [5]. However, this assumption is not supported by the trace element composition of the stromatolite samples discussed.

An essential index, used to reconstruct a paleogeographic setting, is the oxidation-reduction environment of a sedimentary basin. Several markers, such as V/(V+Ni) [6], [7], U/Th, Ni/Co [8], V/Cr [9] and Mo/Mn [10], are used in the geological literature to describe redox conditions.

Analysis of V/V+Ni and U/Th ratios suggests that the growth of stromatolitic buildups in Jatulian time was paralleled by the alternation of oxic – disoxic – (seldom euxinic) settings.

Conclusions about redox conditions, drawn from the U/Th index, are not always consistent with the results obtained with other geochemical markers. This could be connected with two uranium accumulation mechanisms: accumulation in a reduction medium and the supply of pyroclastics into the basin. Mechanical enrichment in uranium, contributed to by accessories (monazite and zircon) in the carbonate analyzed, is not discussed because there are no such minerals in the stromatolites.

The values of such geochemical indicators as Ni/Co and V/Cr suggest that these stromatolites were formed in an oxic zone under good aquatic aeration conditions. The formation of the stromatolitic buildups under elevated hydrodynamic activity conditions is also indicated by subclark Sr concentrations in all the samples.

To measure the depth of a sedimentary basin, a Fe/Mn value is used [11]. The value of this index for the upper portion of the sequence suggests a deep-water environment and sea transgression.

However, the lower portion of the sequence (stratigraphic unit on_1^c, sample 6245 a) evolved in a shallow-water environment, as indicated by its rare-earth distribution pattern (Fig. 3). Data on rare-earth elements (REE) were obtained for two samples: 6245a and 6236. REE concentrations decrease upwards from 11.21 to 1.59 ppm. This could be due to transgression, which had begun by the accumulation of carbonates of the on_1^d unit, and the reduction of the supply of terrigenous material from land.

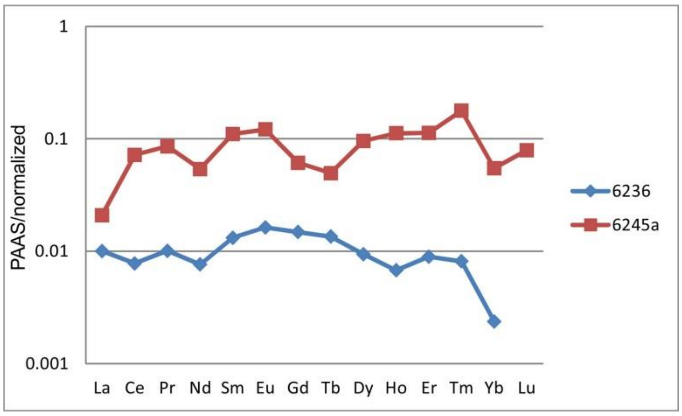

Fig. 3. REE spectra in Jatulian stromatolites

The Ce anomaly sign changes upwards from positive (1.3) to negative (0.7), suggesting the increased contribution of sea water to its formation, i.e. the onset of transgression. Ce anomaly was calculated using the formula $Ce^{*}=2^{*}Ce/Ce^{NASC}/(La/La^{NASC}+Pr/Pr^{NASC})$ [12].

The absence of positive Eu anomaly does not suggest the transport of hydrotherms or volcanogenic pyroclastics into the basin. However, this assumption seems to be inconsistent with above-clark Pb, Zn, Cu and as concentrations in stromatolites on this stratigraphic level.

In addition to the above elements, the hydrotherms are characterized by elevated uranium concentrations, but in the stromatolites discussed, except for some of the laminae in a sample from the upper portion of the sequence, uranium is present in subclarke concentrations and often below detection limits.

The elevated concentrations of the above trace elements, together with Nb, Ga, Ge, Co and No, are associated with the transport of material from the eroded granite-greenstone area of the Karelian Craton.

It should be noted that there is actually no Early Jatulian basalt destruction products formed upon basalt-sea water interaction in the sedimentary basin.

Jatulian basalts are rich in sodium, while underlying Sumian andesite-basalts are rich in magnesium. However, Mg concentrations in stromatolitic dolostones throughout the sequence are below clarke values, as are Na concentrations.

Comparison of the trace element composition of the stromatolites with corresponding clarke values for the carbonate rocks and the values of geochemical markers suggest that the stromatolites were forming in an open system in the Late Jatulian and upon transition to the Ludikovian. This conclusion about the evolution of transgression in the Onega paleobasin by the early Ludikovian, based on analysis of the geochemical characteristics of the stromatolites, is consistent with the conclusion drawn earlier based on facies analysis.

Conclusions

Data on trace element distribution in stromatolitic dolomites are consistent with the results of lithologo-facies analysis and with data obtained using some geochemical markers. This has led the authors to conclude that the data based on analysis of the trace element composition of

Paleoproterozoic Late Jatulian stromatolites could be used to assess facies settings in the sedimentary basin. These conclusions can be verified in reference areas by lithologo-facies analysis that takes more effort.

Acknowledgements

The research was financed from the federal budget for the fulfilment of the state assignment of the KarRC RAS (Institute of Geology).

Prave A.R., Department of Earth and Environmental Sciences, University of St. Andrews, St. Andrews, KY16 9AL Scotland/UK

REFERENCES

1. Melezhik, V. A., Prave, A. R., Fallick, A. E., Hanski, E. J., Lepland, A., Kump, L. R., Strauss, H. (Eds.) (2013). Reading the Archive of Earth's Oxygenation. The Core Archive of the Fennoscandian Arctic Russia – Drilling Early Earth Project. Series: Frontiers in Earth Sciences 2, pp. 769-945.
2. Beus, A. A., Grigoryan, S. V. (1975). Geochemical methods for prospecting and exploration of solid useful mineral deposits. Nedra, Moscow, 280.
3. Paleoproterozoic Onega Structure: geology, tectonics, deep structure and mineralogeny (2011). Executive Editors Glushanin, L. V., Sharov, N. V., Shchiptsov, V. V. Karelian Research Centre, RAS, Petrozavodsk, 431.
4. Gorokhov, I. M., Kuznetsov, A. B., Melezhik, V. A., Konstantinova, G. V., Melnikov, N. N. (1998). Isotope composition of strontium in the Upper Jatulian dolomites of the Tulomozero suite, southeastern Karelia, Early Paleoproterozoic. Proceedings of the Academy of Sciences 360 (4), pp. 533-536.
5. Kuznetsov, A. B., Melezhik, V. A., Gorokhov I. M., Melnikov N. N. *et al*., (2010). Sr isotopic composition of Paleoproterozoic ^{13}C-rich carbonate rocks: The Tulomozero Formation, SE Fennoscandian Shield. Precambrian Research 182, pp. 300-312.
6. Hatch, J. R., Leventhal, J. S. (1992). Relationship between inferred redox potential of the depositional environment and geochemistry of the Upper Pennsylvanian (Missourian) Stark Shale Member of the Dennis Limestone, Wabaunsee County, Kansas, U.S.A. Chemical Geology 99, pp. 65-82.
7. Hatch, J. R, Leventhal, J. S. (1997). Early diagenetic partial oxidation of organic matter and sulfides in the Middle Pennsylvanian (Desmoinesian) Excello Shale member of the Fort Scott Limestone and equivalents, northern midcontinent region, USA. Chemical Geology 134 (4), pp. 215-235.
8. Jones, B., Manning, D. A. C. (1994). Comparison of geochemical indices used for the interpretazion of palaeoredox conditions in ancient mudstones. Chemical Geology 111, pp. 111-129.
9. Ernst, V. (1976). Geochemical facies analysis. Leningrad: Nedra, 127.
10. Kholodov, V. N., Nedumov, R. I. (1991). On the geochemical criteria of the hydrogen sulphide contamination of old water bodies. Izv. AN SSSR. Ser. Geol. 12, pp. 74-82.
11. Yudovich, Ya. E., Ketris, M. P. (2011). Geochemical indicators of lithogenesis. Geoprint, Syktyvkar, 742.
12. Dubinin, A. V. (2004). Geochemistry of rare-earth elements in an ocean. Lithology and Useful Minerals 4, pp. 339-358.

Carbon and Oxygen Isotope Composition of Paleozoic Stromatolites of the Timan-North Ural Region, Russia

MATVEEV Vladimir[1], MATVEEVA Natalya[1]

[1] *N.P. Yushkin Institute of Geology, Komi Scientific Centre, UB, RAS, Syktyvkar (RUSSIA)*
Email: vamatveev@geo.komisc.ru

Abstract

This paper presents the first results for carbon and oxygen isotopic compositions of Ludlow (upper Silurian), as well as the Frasnian and Famennian (Upper Devonian) stromatolite buildups from Timan-North Ural region. A regularity was revealed in the change in the isotopic values of carbon and oxygen in the studied buildups. These changes are possibly associated with different hydrochemical regimes of sea waters, as well as with the processes of sulphate reduction in stromatolites.

Keywords: carbon isotope, oxygen isotope, stromatolites, Silurian, Devonian, Chernov Swell, South Timan, Khoreyver depression

Introduction

Stromatolites are usually considered as biogenic sedimentary formations – products of mechanical capture, binding and sedimentation of particles that were formed by microorganisms, mainly cyanobacteria [1]. They have a wide stratigraphic range, from the Proterozoic to the present.

Thier greatest abundance occurred during the Precambrian, before gradually waning during the Paleozoic. In the geological history of the Phanerozoic Earth, stromatolites are quite often found during periods of geobiological crises and biodiversity reduction associated with climatic changes, as well as sharp fluctuations in the global sea level [2], [3], [4], [5].

Analysis of the isotopic composition of carbon and oxygen is currently widely used to reconstruct the paleoecological conditions of the formation of sedimentary strata. Stromatolites as biogenic-sedimentary formations may contain primary isotopic information about environmental conditions in the past [6].

Currently, the stable isotopic geochemistry of Paleozoic stromatolite buildups in the Timan-North Ural region have not been studied. The purpose of this study is to analyze the first data on the isotopic composition of carbon and oxygen in stromatolites of this region in the Upper Ludlow (Silurian), Frasnian, and Famennian (Upper Devonian), to establish the paleoenvironmental conditions of stromatolite-forming organisms in the sea basin.

Material and methods

The object of the study were the sections of the Upper Silurian and Upper Devonian, which located in the Timan-North Ural region (Fig. 1A). The Silurian stromatolites were studied in outcrop 1 of the Padimeityvis (sample 1/6/2) (Fig. 2A) and Sizim (sample 17/429) (Fig. 2B) Ludlow horizons. This section is located in the central part of the Chernov Swell (Padimeityvis River) (Fig. 1B). Frasnian (Upper Devonian) stromatolites (sample 12/18) (Fig. 2C) were studied in outcrop 12 along the Sedyu River. This section is located within the Ukhta anticlinal fold of the East Timan megaswell of South Timan (Fig. 1D). Famennian (Upper Devonian) stromatolites (sample 19/14) (Fig. 2D) was studied from the borehole 19 in the Oshkotynskaya area (Khoreveyskaya depression) (Fig. 1C). The collection of stromatolites is kept in the Geological Museum of A. A. Chernov in N. P. Yushkin Institute of Geology, Komi Scientific Centre, UB, RAS, Syktyvkar (collection no. 654).

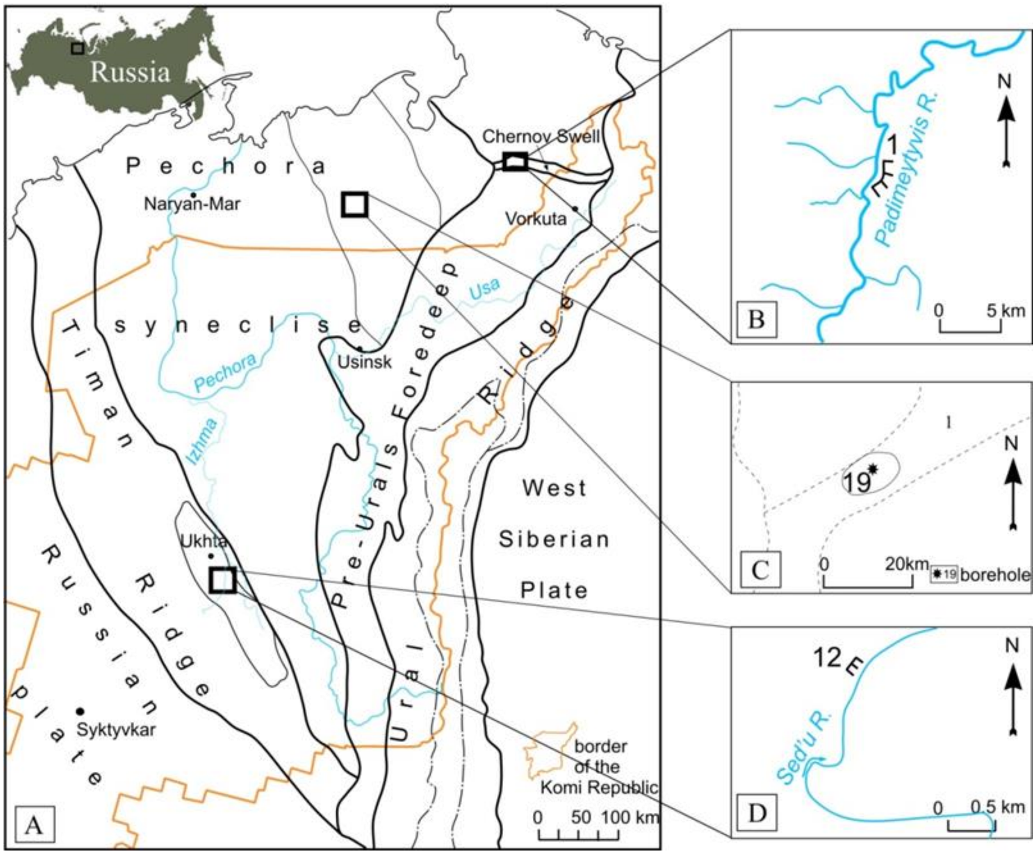

Fig. 1. Map of the studied localities: A – tectonic zones of the Timan-Pechora province (according to: [6] with simplifications and additions), B – outcrop 1, the Padimeityvis River; C – borehole 19 of Oshkotynskaya area; D – outcrop 12, the Sedyu River

The lithological features of the stratigraphic sections, as well as the microscopic and morphological diversity of stromatolite structures were studied by the authors earlier [7], [8], [9], [10], as well as by G. A. Chernov on the Padimeityvis River [11] and E. S. Ponomarenko on the Sedyu River [12].

Powdered samples (up to 1 mg) obtained from polished tiles using a diamond drill 3.5 mm in diameter served as the material for the analysis of the isotopic composition of carbon and oxygen.

Samples were obtained sequentially in layers. In total, 54 samples (15 from specimen 1/6/2, 11 from specimen 17/429, 12 from specimen 12/18 and 16 from specimen 19/14) were collected and prepared for carbon and oxygen isotopic analyses, which was conducted at the CKP «Geonauka» of N.P. Yushkin Institute of Geology, Komi Scientific Centre, UB, RAS, Syktyvkar on a DELTA V Avantage mass spectrometer (analyst I. V. Smoleva). The isotope coefficients were determined in ppm (‰) according to the PDB NBS18 and NBS19 (TS-limestone) standards for carbon. The error in determining both coefficients did not exceed ± 0.1‰.

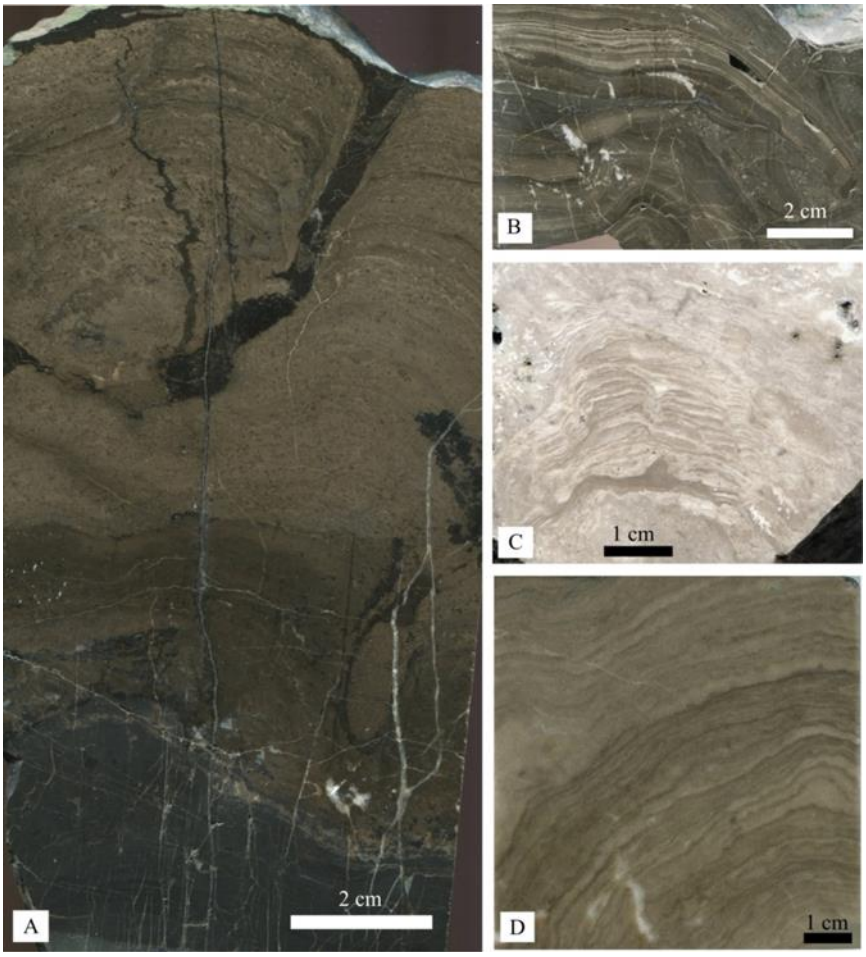

Fig. 2. Silurian and Devonian stromatolite structures. A – sample 1/6/2 (Ludlow, Gorstian/Padimeityvis horizon, the Padimeityvis River); B – sample 17/429 (Ludlow, Ludfordian/Sizim horizon, the Padimeityvis River); C – sample C12/18 (Frasnian, Upper Devonian, outcrop 12, the Sedyu River); D – sample 19/14 (Famennian, Devonian, borehole 19 of Oshkotinskaya area).

Results

The values of the isotopic composition in the Silurian stromatolite of the Padimeityvis horizon range from 0.89 to – 3.77‰ for $\delta^{13}C$ and from 21.85 to 27.29‰ for $\delta^{18}O$ (Fig. 3C). The average values of isotopic coefficients are: $\delta^{13}C$ – 2.02, $\delta^{18}O$ – 25.11‰. The $\delta^{13}C$ and $\delta^{18}O$ values show a slight negative correlation (r = –0.34). At the base of the buildup more weighted values of $\delta^{13}C$ = – 0.45 to 0.89‰ were recorded, compared to the values $\delta^{13}C$ = – 1.61 to – 3.77‰ in the upper part of the structure. Also, the regularity in the distribution of $\delta^{18}O$ values was established for the light and dark layers of the buildup. So, in light layers, the oxygen isotopic composition has more weighted values up to 27.09‰, whereas in dark layers it is up to 21.85‰. Thus, from bottom to top of the stromatolite buildup, we observe a lightening of the isotopic composition of carbon and an increase in the values of oxygen isotopes.

The isotopic composition of the stromatolite of the Sizim horizon differs from the stromatolite of the Padimeityvis horizon by possessing lower $\delta^{13}C$ values of – 6.3 to – 7.54‰ and $\delta^{18}O$ values from 22.87 to 25.07‰ (Fig. 3D). Average values are $\delta^{13}C$ = – 6.57‰, $\delta^{18}O$ = 23.89‰. The $\delta^{13}C$ and $\delta^{18}O$ values also show insignificant correlation (r = -0.66). In the middle part of the buildup, there is a tendency for an insignificant increase in $\delta^{13}C$ values to – 7.54‰ and $\delta^{18}O$ values to 25.07‰. The distribution of $\delta^{13}C$ and $\delta^{18}O$ values within dark and light layers are irregular.

In the Frasnian stromatolite, the content of $\delta^{13}C$ ranges from 0.06 to 0.57 ‰, and $\delta^{18}O$ varies from 22.5 to 23.67‰, which correspond to carbonates of normal marine composition (Fig. 3E). The average $\delta^{13}C$ value is 0.27‰ with a deviation of 0.16‰, and $\delta^{18}O$ is 22.98 ‰ with a deviation of 0.43‰. No correlation was found between carbon and oxygen (r=-0.08). Despite the fact that the scatter of isotope data is insignificant, one can nevertheless observe some regularity in the distribution of $\delta^{18}O$ values throughout the layers. At the base of the buildup, dark layers have slightly more weighted values ($\delta^{18}O$ = 23.37-23.67 ‰) compared to light ones ($\delta^{18}O$ = 22.21-22.5‰). In this case, the $\delta^{18}O$ values tend to decrease upward through the buildup.

According to the results of isotope analysis of the Famennian stromatolite samples, $\delta^{13}C$ values range from 0.8 to 1.5‰, and $\delta^{18}O$ ranges from 23 to 24.4‰. Based on these data, we can say that the studied samples belong to normal-marine carbonates. The average value of $\delta^{13}C$ is 1.18‰ with a deviation of 0.2‰, and the average value of $\delta^{18}O$ is 23.94‰ with a deviation of 0.34‰ (Fig. 3F). It should be noted that a fairly strong direct correlation is revealed between carbon and oxygen (r=0.73). Despite the fact that the data form a compact distribution in the diagram [7] some regularity in the variation in isotope value is present. The lowest values of $\delta^{13}C$ and $\delta^{18}O$ are observed in the lower part of the buildup (0.8-1.2‰; 23.3-23.6‰, respectively). In the middle part of the buildup, the isotopic composition of both $\delta^{13}C$ and $\delta^{18}O$ increase to 1.5‰ and 24.4‰, respectively. In the upper part of the buildup, the values of $\delta^{13}C$ and $\delta^{18}O$ decrease to 1.2‰ and 23.8‰, respectively, compared to the middle part. Thus, in spite of the fact that the entire buildup was formed in a normal marine environment, three stages are clearly distinguished, during which insignificant fluctuations in the hydrochemistry of waters are noted.

Discussion

The results of the studies showed that the character of the change in the isotopic values of carbon and oxygen in stromatolites was influenced by the influx of isotopically light fresh water into the shallow sedimentary basin saturated with dissolved soil carbon dioxide during climatically humid periods and a corresponding increase in terrigenous runoff. The lithological sign of the influx of terrigenous material is clay matter on the surface and between stromatolite buildups, which is well observed in the sections of the upper Silurian. The lighter isotopic composition of carbon and oxygen may also be associated with sulfate reduction processes occurring in microbial buildups, which results in the oxidation of organic matter and the formation of isotopically light CO_2 [13], [14], [15]. The presence of pyrite aggregates in the Ludlow stromatolites [10] indicates the presence of sulfate-reducing bacteria in the anoxygenic development zone, which is part of the cyanobacterial mat and is comparable to the model of their structure [16].

The heavier values of the isotopic composition of carbon in the dark layers can be explained by an increase in the primary biological productivity of the basin [5]. The isotopic composition of stromatolite structures generally confirms the participation of microorganisms in the distribution of carbon isotopes.

The Upper Devonian stromatolites are characterized by $\delta^{13}C$ and $\delta^{18}O$ that are typical of normal marine carbonates of Phanerozoic age [17]. A slight decrease in the $\delta^{18}O$ values up through the buildup in the Frasnian may indicate the inflow of weakly desalinated water during the growth of the stromatolite and an increase in the temperature gradient. This study identified a regularity in the distribution of $\delta^{13}C$ and $\delta^{18}O$ values within the Famennian stromatolite, which made it possible to define the stages of the buildup's growth associated with possible fluctuations in the hydrochemistry of waters [7]. The isotopic composition of carbon and oxygen of the Ludlow Silurian stromatolites is characterized by lighter values than those of the Devonian.

Similar differences in carbon and oxygen isotopic composition between the Silurian and

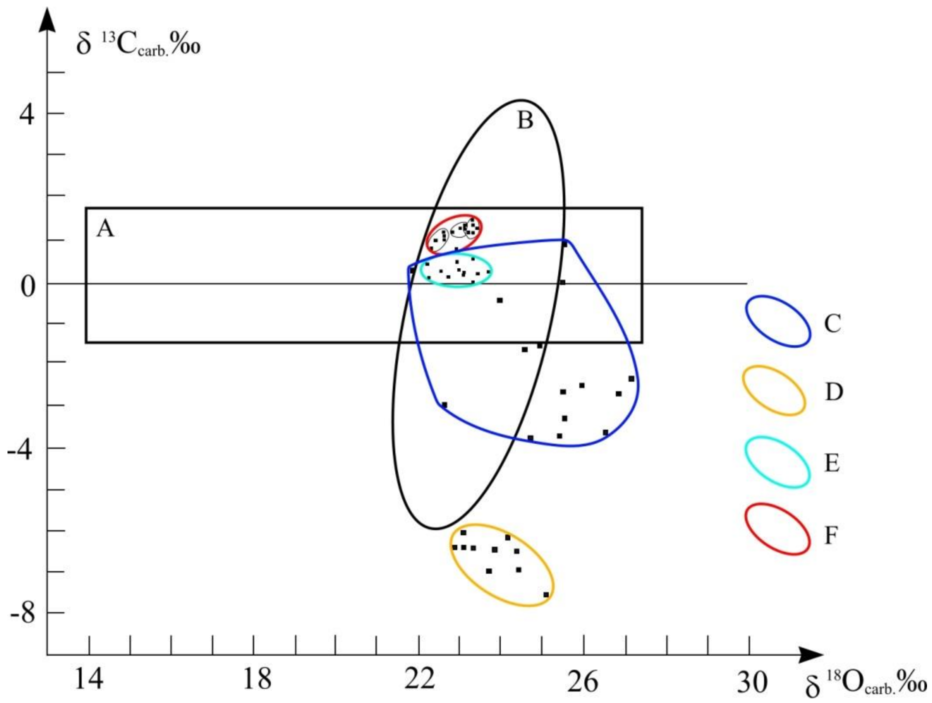

Fig. 3. Distribution of the isotopic composition of carbon and oxygen in the Silurian and Upper Devonian stromatolites. A-B – according to: [17] with simplification: A – statistics for marine carbonate of Paleozoic age; B – sedimentary formations of the Middle Urals; C-F – authors' data: C – sample 1/6/2, stromatolite buildup of the Padimeityvis horizon, Ludlow; D – sample 17/427, stromatolite buildup of the Sizim horizon, Ludlow; E – sample C12/18, Frasnian stromatolite buildup; F – sample 19/14, Famennian stromatolite structure.

Devonian were mentioned for the bulk carbonates [18]. L. A. Anischenko and co-authors concluded that the isotopic composition of carbon and oxygen in the carbonate rocks of the Silurian boreholes of the Timan-Pechora oil and gas province is characterized by the lightest composition of carbon and oxygen, in contrast to the Devonian carbonates. In general, the carbonate rocks of the Timan-Pechora province are similar in isotopic characteristics to the Phanerozoic marine carbonate sediments that did not undergo significant post-diagenetic transformations. This difference is possibly associated with different hydrochemical regimes of sea waters during the Silurian and Devonian times.

Conclusions

As a result of the isotopic analysis of the Silurian and Devonian stromatolite buildups, systematic changes in $\delta^{13}C$ and $\delta^{18}O$ isotope values are recognized both from the bottom upward within the buildup and in their distribution over the dark and light layers. Low values of the isotopic composition of carbon and oxygen in the Silurian stromatolites may indicate the desalination of waters in the sea basin. The lightening of the isotopic composition of $\delta^{13}C$ and $\delta^{18}O$ may also be associated with the processes of sulfate reduction occurring in microbial buildups.

The Upper Devonian stromatolites were formed in normal marine environments. In the Famennian stromatolite structure, an analysis of the distribution of isotope data made it possible to trace the stages of growth.

The study of the isotopic composition of carbon and oxygen in the Silurian and Devonian stromatolites provided additional information on the conditions of their formation in the marine paleobasin and the participation of microorganisms in their formation.

Acknowledgments

The authors thank Dr. M. L. Curtis (CASP, Cambridge, United Kingdom) for linguistic revision and improving the final version of the paper. Acknowledgment is also made Dr. E. S. Ponomarenko (Institute of Geology Komi SC UB RAS, Syktyvkar) for providing material of the Frasnian stromatolite. I. V. Smoleva (Institute of Geology Komi SC UB RAS, Syktyvkar) for stable carbon and oxygen isotopes measurements.

REFERENCES

1. Pratt, B. R. (1982). Stromatolite decline – a reconsideration. Geology 10, pp. 512-515.
2. Schidlowski, M. (2000). Carbon isotopoes and microbial sediments, in Microbial Sediments (Riding, R., and Awramik, S. M., eds.). Berlin, Springer-Verlag, pp. 84-95.
3. Walter, M. R. ed. (1976). Stromatolites. Amsterdam, Elsevier, 790.
4. Riding, R (2006). Microbial carbonate abundance compared with fluctuations in metazoan diversity over geological time. Sedimentology 185, pp. 229-238.
5. Sheehan, P. M., Harris, M. T. (2004). Microbialite resurgence after the late Ordovician extinction. Nature 430, pp. 75-78.
6. Yudin, V. V. (1994). Orogenez Severnogo Urala i Pay-Khoya. Ekaterinburg, Nauka, 285.
7. Kaneva, N. A. (2011). A Middle Famennian organic buildup formation environments in the central part of the Horeyver Depression of the Pechora Syneclise. Proceedings of the Sixth International Conference "Environmental Micropaleontology, Microbiology and Meiobenthology". Moscow, PIN RAS, pp. 122-124.
8. Matveeva, N. A. (2016). Stroenie i usloviya obrazovaniya famenskikh karbonatnykh otlozheniy Tsentral'no-Khoreyverskoy rifogennoy zony: Avtoref.dis....kand. geol.-min. nauk. Syktyvkar, 19.
9. Matveev, V. A. (2018). Osnovnye morfologicheskie tipy stromatolitovykh postroek silura (Timano-Severoural'skiy region). Materialy IX Sibirskoy konferentsii molodykh uchenykh po naukam o zemle. Novosibirsk, pp. 353-355.
10. Matveev, V. A. (2019). Mikrostruktura siluriyskikh stromatolitov. Syktyvkarskiy paleontologicheskiy sbornik № 9. IG FITS Komi NTS UrO RAN, Syktyvkar, pp. 39-44. (Trudy Instituta geologii Komi nauchnogo tsentra UrO RAN, 131).
11. Chernov, G. A. (1966). Siluriyskie stromatolity podnyatiya Chernova (Bol'shezemel'skaya tundra). Stratigrafiya i paleontologiya severo-vostoka Evropeyskoy chasti SSSR. Nauka, Moscow-Leningrad. pp. 90-105.
12. Ponomarenko E. S. (2019). Osobennosti stroeniya mikrobnykh obrazovaniy v sisteme "rif-laguna" (na primere verkhnedevonskogo rifovogo kompleksa Sed'yu, Yuzhnyy Timan). Vestnik IG Komi NTS 8, pp. 14-19.
13. Makhnach A. A. (1996) Izotopy ugleroda i kisloroda v karbonatnykh konkretsiyakh i porodakh verkhnedevonskoy tolshchi Pripyatskogo progiba. Litologiya i poleznye iskopaemye 6, pp. 614-624.
14. Kuleshov V. N. (2001). Evolyutsiya izotopnykh uglekislotno-vodnykh sistem v litogeneze. Soobshcheniye 1. Sedimentogenez i diagenez. Litologiya i poleznye iskopaemye 5, pp. 491-508.
15. Yudovich Ya. E., Ketris M. P. (2008). Mineral'nye indikatory litogeneza. Syktyvkar, Geoprint, 564.
16. Bakterial'naya paleontologiya, Rozanov A. Yu., Ed., Moscow, PIN RAN, 2002. 188.
17. Silaev V. I., Khazov A. F. (2003). Izotopnoe disproportsionirovanie karbonatnogo ugleroda v protsessakh gipergeno-ekzogennoy peregruppirovki veshchestva zemnoy kory. Syktyvkar, Geoprint, 41.
18. Anishchenko L. A., Klimenko S. S., Protsko O. S. Silaev V. I. (2011). Rezul'taty izotopno-geokhimicheskikh issledovaniy karbonatolitov v predelakh neftegazonosnykh Khoreveyskoy i Denisovskoy vpadin. pp. 26-44. Geologiya i geokhimiya goryuchikh iskopaemykh evropeyskogo severa Rossii (Trudy Instituta geologii, 128).

Reflection of Global Events in the History of the Paleoproterozoic Earth in the Stratigraphic Successions of Eastern Fennoscandia

MEDVEDEV Pavel, KONDRASHOVA Natalia

Institute of Geology, Karelian Research Centre of RAS, Petrozavodsk (RUSSIA)
Petrozavodsk State University, Petrozavodsk (RUSSIA)
Email: pmedved@krc.karelia.ru

Abstract

The Paleoproterozoic interval from 2.5 to 2.0 billion years ago was a time of significant changes in the history of the Earth. The expansion of the Kenorland supercontinent, which began about 2.48 billion years ago, coincided with the accumulation of ferruginous formations and bimodal magmatism on the continental margins, which was recorded by the first thick sedimentary successions on cratons. After the accumulation of ferruginous formations, rifting gives way to a compression process, which also manifested itself on other Archean cratons.

Soon the climate changed dramatically, ice sheets emerged, reaching low latitudes and consisting of three glacial epochs. The increase in oxygen content in the atmosphere coincided with this glaciation. Mature sandstones, red beds, and aluminum-rich clay rocks indicate significant chemical weathering on continents following inter-and post-glacial greenhouse conditions. Sedimentary strata with an age of 2.22-2.10 Ga include carbonate rocks with abnormally high positive $\delta^{13}C$ values, indicating a significant deviation in the isotopic composition of seawater. The end of the carbon isotope anomaly in the interval of 2.11-2.06 Ga matches with the accumulation of manganese, phosphorites, ferruginous formations and carbonaceous shales, probably associated with the development of oceanic basins. This time interval coincides with the final split of Kenorland.

Keywords: Paleoproterozoic, Fennoscandian Shield, event-stratigraphy

Introduction

The emergence of the Earth’s aerobic system and a number of interrelated global events in the Paleoproterozoic, which led to irreversible changes in the Earth's surface environments, represent one of the most complex fundamental problems of geology. The causal relationships of these environmental events remain only partially elucidated. By now, it has become possible to recognize these events in the Paleoproterozoic successions of the eastern part of the Fennoscandian Shield.

The main geological events in Paleoproterozoic time

1. <u>Change in fractionation of sulfur isotopes.</u> Several lines of evidence suggest that Earth’s early atmosphere gradually became oxygenated between 2500 and 2000 million years ago. This dramatic change is known as the Great Oxidation Event (GOE). The processes that led to it, as well as their exact dating and duration, remain controversial. The appearance of “red beds” and sulfates in the stratigraphic sequences of the Paleoproterozoic sedimentary rocks is one of the most convincing evidence reflecting the change in oxygen conditions. Additional support for oxygenation was obtained from the study of S isotopes, which showed the presence of mass-

independent fractionation of S-isotopes (MIF) in rocks older than 2360 Ma and the disappearance of such fractionation after this milestone. The disappearance of MIF is usually attributed to atmospheric oxygenation and related changes in photochemical reactions. In Imandra-Varzuga greenstone belt (Kola Peninsula), in the succession of the Seidorechka Formation (ca. 2442 Ma), a transition from MIF to mass-dependent fractionation of sulfur sotopes was recorded [1].

2. Huronian global glaciation. The rapid onset of global glaciation about 2320 million years ago is another important Paleoproterozoic ecological event. The triggers of this global glaciation are still poorly understood. On the Fennoscandian Shield, the Huronian glaciation is traditionally associated with polymictic conglomerates and tillites of the Sarioli group. The hypothesis of the glaciogenic origin of these formations, expressed at the beginning of the 20th century by P. Eskola, was later confirmed by the finds of diamictites and dropstones, indicating the participation of glacial processes in sedimentation. According to drilling data carried out within the framework of the FAR-DEEP project in the Imandra-Varzuga greenstone belt, the Polisarka formation contains Huronian diamictites overlain by spinifex-structured komatiites and underlain by Sr-bearing limestones [2].

3. An unprecedented change in the global carbon cycle. The largest positive $\delta^{13}C$ excursion in the history of the Earth recorded in sedimentary carbonates is known as the Lomagundi-Jatuli event. There is currently no consensus on the reasons for this event. The possible role of local factors in amplifying the global signal remains unclear. Moreover, understanding of the causal relationships of the Lomagundi-Jatuli event with other global paleoecological changes in the Paleoproterozoic remains incomplete [3]. In the east of the Fennoscandian Shield, carbonate rocks enriched in ^{13}C are known in the successions of the Umba formation (Imandra-Varzuga greenstone belt, $\delta^{13}C$ = 3.2±2.1‰), the Kuetsjarvi formation (Pechenga paleobasin, $\delta^{13}C$ = 7.4±0.7‰), and so in the thick carbonate succession of the Tulomozero formation (Onego paleobasin, $\delta^{13}C$ = ca.10 ‰).

4. Oxidized ocean-abundant Ca-sulfates. The progressive oxygenation of the Earth's surface environments has led to an increase in the oxidation of sulfides during continental weathering and a concomitant increase in the concentration of marine sulfate. To date, available estimates of the size of marine sulfate reservoirs indicate that sulfates in the ancient ocean were at least 10 µmol/kg.

This concentration corresponds to 23% of the oxidizing capacity of the modern ocean [4].

The result was obtained after analyzing sulfur isotopes in anhydrite from an 800-m evaporite sequence drilled by a parametric well in the Onego paleobasin. Pseudomorphs after gypsum and anhydrite, with relics of primary minerals, have been described in large numbers in carbonate rocks of the Pechenga paleobasin (Kuetsjarvi and Kolasjoki formations), Imandra-Varzuga greenstone belt (Umba formation) and Onega paleobasin (Tulomozero formation) [5].

Detailed mineralogical and isotopic studies are underway to decipher their ecological significance.

5. Iron-rich volcanic rocks: upper mantle oxidative event. Why, how and when the level of oxygen in the atmosphere increased remains a fundamental problem: was it connected with the appearance of oxygen producing organisms-photosynthetic or with the reduction of volcanic emissions [6]. Volcanic rocks with an age of 2060 Ma have high Fe^{3+}/Fe^{2+} ratios, which indicates a possible change in the redox potential of volcanic gases, which could cause irreversible oxidation of the Earth's atmosphere. In the Jatulian successions of Karelia and the Kola Peninsula, signs of the process of mantle oxidation of basalts are recorded. In the volcanogenic part of the Kuetsjarvin formation in the Pechenga paleobasin wells of the FAR-DEEP project have exposed more than 300 m of intensely oxidized basalts, which can be interpreted as signs of magma oxidation in the upper mantle chambers [7].

6. A revolution in the biological cycle of phosphorus and organic matter. After the Lomagundi-Jatuli isotopic event, about 2 billion years ago, the emergence and then worldwide distribution of diagenetic carbonate nodules, significantly depleted by the heavy carbon isotope ^{13}C, is recorded.

They are associated with other diagenetic products such as phosphorites, which appear to be absent in older rocks. On the Kola Peninsula, in the sedimentary rocks of the Ilmozero formation (Imandra-Varzuga greenstone belt), carbonate and siliceous nodules with a P_2O_5 content of up to 1.2% are noted [8], and in the tuff schists and coarse-grained sandstones of the Pilgujarvi formation (Pechenga paleobasin), the P_2O_5 content reaches 8.2% [9]. In the Onego paleobasin, the sedimentary carbon-bearing rocks of the upper part of the Zaonego formation (ca. 2 Ga) contain phosphorus-rich intervals with abundant apatite (P_2O_5>15%). They contain phosphatized microfossils similar to modern methanotrophic and sulfur-oxidizing archaebacteria living in deep-water environment and upwelling zones with low oxygen content [10].

7. Shunga Black Shale Event. The most significant accumulation of sediments rich in organic matter (OM) and the generation of oil in the Precambrian occurred about 2 billion years ago after the Lomagundi-Jatuli event [11]. Numerous data suggest that the most probable source of OM were planktonic microorganisms, and the reasons for its unprecedented accumulation were high bioproductivity and favorable preservation conditions, under which complete oxidation of OM to CO_2 did not occur. In eastern Fennoscandia, this event is represented by black shale strata accumulated on the continental slope or in the rift basin, and is reflected in the successions of the Ilmozero Formation (Imandra-Varzuga greenstone belt), the Pilgujarvi formation (Pechenga paleobasin), and is maximally developed in the Zaonego formation (Onega paleobasin). Here, several hundred meters of organic-rich source rocks, a petrified oil field with preserved oil migration routes, and several bodies of organic-siliceous rocks containing up to 40 wt. % organic carbon. These rocks were formed under the influence of hydrothermal fluids or under conditions of hydrocarbon seepage simultaneously with basaltic volcanism and contain highly depleted ^{13}C organic matter [12].

Conclusions

The listed events can be considered a starting point for using the event stratigraphic method in the subdivision and correlation of the Paleoproterozoic sequences in the eastern part of the Fennoscandian Shield. Successful application of this method requires accurate dating of the identified events, together with a comprehensive understanding of paleoenvironmental settings and the geochemical characteristics of sedimentary and volcanic rocks on a global scale.

Acknowledgements

The research was financed from the federal budget for the fulfilment of the state assignment of the KarRC RAS (Institute of Geology).

Prave A.R., Department of Earth and Environmental Sciences, University of St. Andrews, St. Andrews, KY16 9AL Scotland/UK

REFERENCES

1. Reuschel, M., Strauss, H., Lepland, A., Melezhik, V.A., Cartigny, P., Kaufman, A. J. (2009). Multiple sulfur isotope measurements from the 2.44 Ga Seidorechka Sedimentary Formation. Geochimica et Cosmochimica Acta 73, p. A1091.
2. Brasier, A. T., Martin, A. P., Melezhik, V. A., Prave, A. R., Condon, D. J., Fallick, A. E. (2013). Earth's earliest global glaciation? Carbonate geochemistry and geochronology of the Polisarka Sedimentary Formation, Kola Peninsula, Russia. Precambrian Research 235, pp. 278-294.

3. Melezhik, V. A, Fallick, A. E., Martin, A. P., Condon, D. J., Kump, L. R., Brasier, A. T., Salminen, P. E. (2013). The paleoproterozoic perturbation of the global carbon cycle: The Lomagundi-Jatuli isotopic event. In Reading the Archive of Earth's Oxygenation: Global Events and the Fennoscandian Arctic Russia - Drilling Early Earth Project (Melezhik, V.A., Kump, L.R., Strauss, H. Hanski, E.J., Prave, A.R., Eds). Springer, Heidelberg, vol. 3, pp. 1111-1150.
4. Blättler, C. L., Claire, M. W., Prave, A. R., Kirsimäe, K., Higgins, J. A., Medvedev, P. V., Romashkin, A. E., Rychanchik, D. V., Zerkle, A. L., Paiste, K., Kreitsmann, T., Millar, I. L., Hayles, J. A., Bao, H., Turchyn, A. V., Warke, M. R., Lepland, A. (2018). Two-billion-year-old evaporites capture Earth's great oxidation. Science 360, pp. 320-323.
5. Strauss, H., Melezhik, V. A., Reuschel, M., Fallick, A. E., Lepland, A., Rychanchik, D. V. (2013). Abundant Marine Calcium Sulphates: Radical Change of Seawater Sulphate Reservoir and Sulphur Cycle. In Reading the Archive of Earth's Oxygenation: Global Events and the Fennoscandian Arctic Russia – Drilling Early Earth Project (Melezhik, V.A., Prave, A.R., Hanski, E.J., Fallick, A.E., Lepland, A., Kump, L.R., Strauss, H., Eds). Springer, Heidelberg, vol. 3, pp. 1169-1194.
6. Kump, L. R., Fallick, A. E., Melezhik, V. A., Strauss, H., Lepland, A. (2013). The Great Oxidation Event. In Reading the Archive of Earth's Oxygenation: Global Events and the Fennoscandian Arctic Russia - Drilling Early Earth Project (Melezhik, V.A., Kump, L.R., Strauss, H. Hanski, E.J., Prave, A.R., Eds). Springer, Heidelberg, vol. 3, pp. 1517-1533.
7. Rybacki, K. S., Kump, L. R., Hanski, E. J., Melezhik, V. A. (2013). An Apparent Oxidation of the Upper Mantle versus Regional Deep Oxidation of Terrestrial Surfaces in the Fennoscandian Shield. In Reading the Archive of Earth's Oxygenation: Global Events and the Fennoscandian Arctic Russia – Drilling Early Earth Project (Melezhik, V.A., Prave, A.R., Hanski, E.J., Fallick, A.E., Lepland, A., Kump, L.R., Strauss, H., Eds). Springer, Heidelberg, vol. 3, pp. 1151-1167.
8. Lepland, A., Melezhik, V. A., Papineau, A. E., Romashkin, A. E., Joosu, L. (2013). The Earliest Phosphorites – Radical Change in the Phosphorus Cycle during the Palaeoproterozoic. In Reading the Archive of Earth's Oxygenation: Volume 3: Global Events and the Fennoscandian Arctic Russia – Drilling Early Earth Project. (Melezhik, V.A., Kump, L.R., Strauss, H. Hanski, E.J., Prave, A.R., Eds.). Springer, Heidelberg, vol. 3, pp. 1275-1296.
9. Joosu, L., Lepland, A., Kreitsmann, T., Üpraus, K., Roberts, N. M. W., Paiste, P., Martin, A. P., Kirsimäe, K. (2016). Petrography and the REE-composition of apatite in the Paleoproterozoic Pilgujarvi Sedimentary Formation, Pechenga Greenstone Belt, Russia. Geochimica et Cosmochimica Acta 186, pp. 135-153.
10. Lepland, A., Joosu, L., Kirsimäe, K., Prave, A.R., Romashkin, A. E., Črne, A. E., Martin, A. P., Fallick, A. E., Somelar, P., Üpraus, K., Mänd, K., Roberts, N. M. W., Van, Z., Wirth, R., Schreiber, A. (2014). Potential influence of sulphur bacteria on Palaeoproterozoic phosphogenesis. Nature Geoscience 7, pp. 20-24.
11. Strauss, H., Melezhik, V. A., Lepland, A., Fallick, A. E., Hanski, E. J., Filippov, M. M., Deines, Y. E., Illing, C.J., Črne, A. E., Brasier, A. T., (2013). Enhanced Accumulation of Organic Matter: The Shunga Event. In Reading the Archive of Earth's Oxygenation: Global Events and the Fennoscandian Arctic Russia – Drilling Early Earth Project (Melezhik, V.A., Prave, A.R., Hanski, E.J., Fallick, A.E., Lepland, A., Kump, L.R., Strauss, H., Eds). Springer, Heidelberg, vol. 3, pp. 1195-1273.
12. Paiste, K., Lepland, A., Zerkle, A. L., Kirsimäe, K., Izon, G., Patel, N. K., McLean, F., Kreitsmann, T., Mänd, K., Bui, T. H., Romashkin, A. E., Rychanchik, D. V., Prave, A. R. (2018). Multiple sulphur isotope records tracking basinal and global processes in the 1.98 Ga Zaonega Formation, NW Russia. Chemical Geology 499, pp. 151-164.

Electrophysical Properties of Shungite Rocks from Different Stratigraphic Levels

MOSHNIKOV Igor[1], KOVALEVSKI Vladimir[1]

[1] Institute of Geology, Karelian Research Center, Russian Academy of Sciences, Petrozavodsk (RUSSIA)
Email: igorm@krc.karelia.ru

Abstract

Electrophysical properties of shungite rocks of various stratigraphic levels of the Zaonega formation have been studied. Electrical conductivity and shielding effectiveness were the electrophysical parameters evaluated. The shielding effectiveness and electrical conductivity of shungite rocks were determined on powder samples by the coaxial transmission line method.

Raman spectroscopy was used to evaluate structural characteristics of carbon in shungite rocks.

The peak metamorphism temperature was used as a criterion for ordering carbonaceous matter associated with its transformation. The results of the study of the electrophysical properties of shungite rocks indicate that there is a general tendency to increase the electrical conductivity and shielding effectiveness of shungite rocks with an increase in the peak temperature of metamorphism. The results obtained will allow us to use the established patterns not only to determine the industrial types of shungite rocks in the context of their most effective use, but also to pay attention to the subtle patterns of their genesis.

Keywords: shungite rocks, stratigraphy, shielding effectiveness, peak temperature of metamorphism, electrical conductivity

Introduction

The shungite rocks of Karelia form a large, diverse group of Precambrian carbon-bearing rocks with poorly-crystallized carbon (shungite). The fundamental problem of searching for the relationship between the structure, properties and genesis of carbonaceous matter has been developed for a long time. Interest in this problem is connected not only with the study of the evolution of the lithosphere, but also with the industrial use of carbon-bearing rocks. There are more than 20 developed methods for the use of shungite rock [1]. Some of these methods relate to the electrophysical properties of shungite rocks, particularly as fillers of composite materials [2].

Shungite fillers give conductive properties to composite materials, also improving their strength and antifriction properties [3].

The electrical conducting properties of shungite rocks are due to the carbon content in their composition. The carbon content of shungite rocks varies from one to 99 wt%. The existing classification of shungite rocks is based on dividing them into groups based on the carbon content in the rock [1]. However, at the moment this classification does not meet production requirements, since the properties of shungite rocks with the same carbon content can differ significantly.

The goal of our work is to develop a more accurate geological-industrial classification of shungite rocks than the existing one. This classification should be based on linking geological data with the physical-chemical properties of shungite rocks. To create this classification, multi-stage studies are required. At this stage, the aim of research is to study the electrophysical properties of shungite rocks of various stratigraphic levels of the Zaonezhskaya formation, which differ in their peak temperature of metamorphism.

Methodology

The objects of research were samples selected from three deposits of shungite rocks of the Onega synclinorium, located on different shungite bearing horizons. Samples were specially selected with a close percentage of carbon to assess the effect of other controlled factors on electrophysical properties.

Raman spectroscopy was used to evaluate structural characteristics of carbon in the shungite rocks. Raman spectra of shungites were obtained using the Nicolet Almega XR dispersion Raman spectrometer (wavelength 532 nm). The quantitative characteristics of the spectra are calculated in the OMNIC program. The peak metamorphism temperatures of the studied samples were estimated from carbon using the equation: $T\ (°C) = 91.4(R2)^2 - 556.3(R2) + 676.3$, which was previously proposed for carbonaceous-material [4]. This equation was optimized for regional metamorphism conditions and tested on metamorphic rocks of Japan [5].

Electrical conductivity and shielding effectiveness were used as the evaluated electrophysical parameters. The shielding effectiveness shows how much the sample under study is able to reduce the intensity of the electromagnetic field by reflecting and absorbing electromagnetic waves. The shielding effectiveness of shungite rocks was determined on powder samples by the coaxial transmission line method of electromagnetic spectral analysis in the frequency range from 100 kHz to 1 GHz (selective microvoltmeters SMV11 and SMV8.5). The electrical conductivity was determined in the coaxial line using a meter L, C, R E7-8 at a frequency of 1 kHz.

Results and discussion

Using Raman studies of shungite rocks of the second and sixth horizons with a close carbon content, peak metamorphism temperatures were determined (Fig. 1). The lowest peak temperature of metamorphism (316-347 °C) is typical for shungite rocks of the sixth horizon, and the highest – for a sample of the second horizon (379 °C). A wide range of values of peak metamorphism temperature for samples of the sixth horizon indicates a significant structural heterogeneity of carbonaceous matter of these shungite rocks and the presence of unaccounted geological factors in the division of shungite rocks by stratigraphic levels.

We have evaluated the electrophysical properties of samples of shungite rocks from the second and sixth horizons with a close percentage of carbon. The results of the study of electrophysical properties of shungite rocks with a close carbon content indicate that there is a general tendency for the electrical conductivity and shielding effectiveness of shungite rocks to increase with an increase in the peak temperature of metamorphism. Rocks of the sixth horizon have the lowest shielding effectiveness and electrical conductivity, and for the sample of the second horizon, they are observed to increase (Fig. 2).

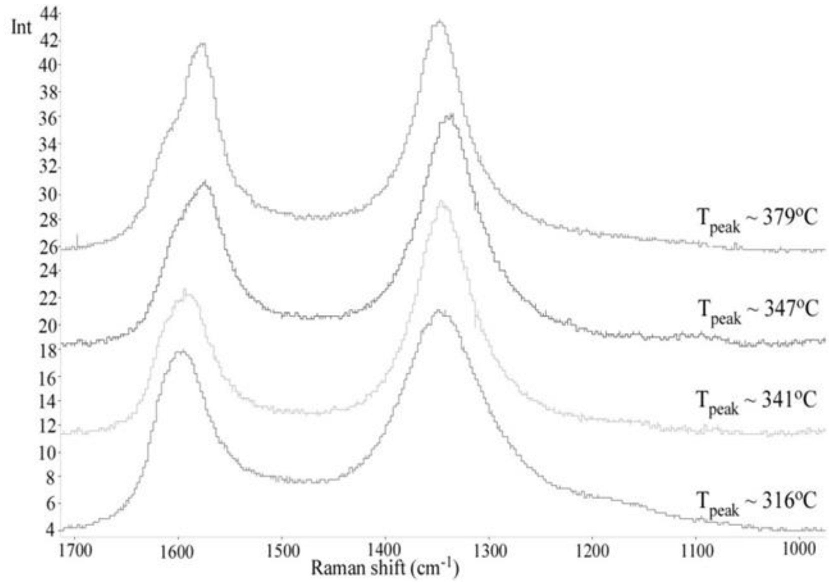

Fig. 1. Raman spectra of shungite rocks of various stratigraphic levels of the Zaonezhskaya formation, differing in the peak metamorphism temperature

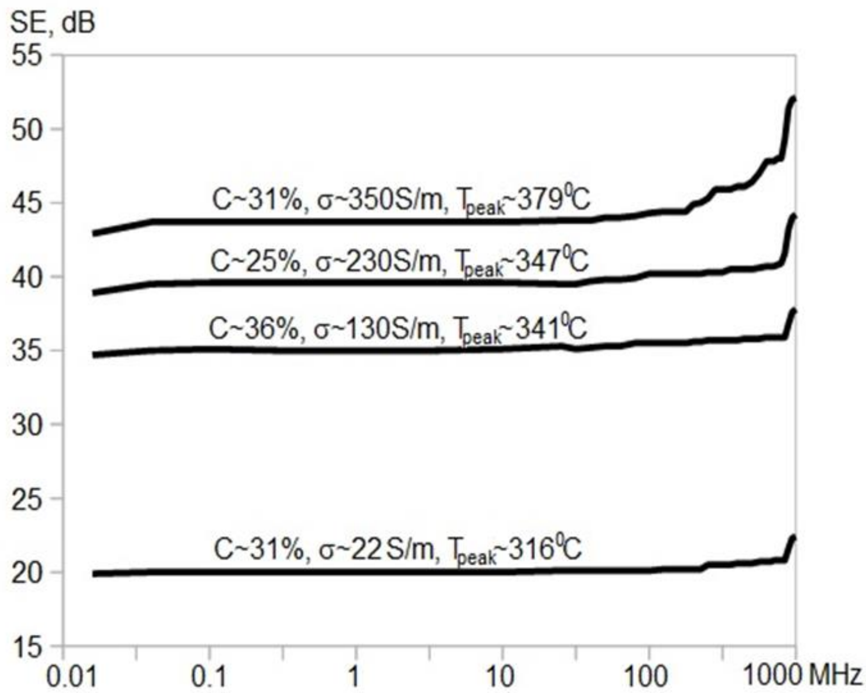

Fig. 2. Dependence of the shielding effectiveness on the frequency of the electromagnetic field for shungite rocks with a close carbon content, but different peak metamorphism temperature

Previously, it was found that the shungite rocks have some differences in chemical composition [6]. Shungite rocks of higher horizons are less alkaline and more siliceous than the lower ones. The predominance of Na_2O over K_2O is remarkable for the samples of the second horizon. Such rocks should be attributed to the rocks of the Na-type. As was shown earlier [7], Na-type rocks are characterized by higher values of shielding effectiveness and electrical conductivity than those of K-type rocks. The use of Na-type rocks allows to obtain composite materials with improved RF shielding [7]. Thus, it can be noted that shungite rocks of the second horizon, the genesis of which is associated with higher metamorphism temperatures, are preferable as raw materials for the manufacture of RF shielding composite materials.

Conclusion

A Raman study and evaluation of the electrophysical properties of samples of shungite rocks of the second and sixth horizons with a similar percentage of carbon was performed. It is shown that the peak metamorphism temperature of the selected samples varies from 316 to 379 °C, while the higher it is, the higher the electrical conductivity and shielding efficiency of the shungite rocks are.

The results obtained allow us to use the established regularities not only to determine the industrial types of shungite rocks for their most effective use, but also to pay attention to the identification of subtle features of their genesis.

Acknowledgments

The work is performed in the framework of the PFNI GAN research of IG KarRC RAS.

For reviewing the English language version of the article, the authors thank Dr Matt Parker (Oxford Brookes University).

REFERENCES

1. Kalinin Yu. K., Kalinin A. I., Skorobogatov (2008). Shungity Karelii - dlya novyh strojmaterialov, v himicheskom sinteze, gazoochistke, vodopodgotovke i medicine. VVM, St-Peterburg, 219.
2. Moshnikov I. A., Kovalevski V. V., Lazareva T. N., Petrov A. V. (2007). Ispol’zovanie shungitovyh porod v sozdanii radioekraniruyushchih kompozicionnyh materialov. Materialy Vserossijskoj konferencii “Geodinamika, magmatizm, sedimentogenez i minerageniya severo-zapada Rossii”, Petrozavodsk, pp. 272-274.
3. Kalashnikov I. E., Kovalevski V. V., Chernyshova T. A., Bolotova L. K. (2010). Aluminum-matrix composite materials with shungite rock fillers. Russian Metallurgy 11, pp. 1063-1071.
4. Aoya M., Kouketsu Y., Endo S., Shimizu H., Mizukami T., Nakamura D., Wallis S. R. (2010). Extending the applicability of the Raman carbonaceous-material geothermometer using data from contact metamorphic rocks. J. Metamorph. Geol. 28 (9), pp. 895-914.
5. Mori Y., Shigeno M., Miyazaki K., Nishiyama T. (2019). Peak metamorphic temperature of the Nishisonogi unit of the Nagasaki Metamorphic Rocks, western Kyushu, Japan. J. Mineral. Petrol. Sci. 114, pp. 170-177.
6. Deines Yu. E., Kovalevski V. V., Kochneva I. V., Moshnikov I. A., Rozhkova V. S. (2020). Physical and chemical properties of shungite rocks from different stratigraphic levels of the zaonega formation. Trudy KarNTs RAN 2, pp. 84-89. (DOI: 10.17076/geo1187)
7. Moshnikov I. A., Kovalevski V. V. (2012). Primenenie iskhodnyh i modificirovannyh shungitovyh porod v radioekraniruyushchih kompozitnyh materialah. Sbornik tezisov dokladov 8-oj Mezhdunarodnoj konferencii “Uglerod: fundamental’nye problemy nauki, materialovedenie, tekhnologiya”, Troick, pp. 304-305.

A Model of Bitumen Reservoir Formation in Permian Sandy Sediments (Sheshmian Horizon), Republic of Tatarstan, Russia

MULLAKAEV Almaz[1], KHASANOV Rinat[1]

[1] *Kazan Federal University, Kazan (RUSSIA)*
Email: almazmullakaev@gmail.com

Abstract

This article describes some aspects of the formation of the Sheshmian sandy bitumen deposits.

The Permian Sheshma Formation (Sheshmian Regional Substage) is recognized in the Ufimian of the East European Platform. The Sheshmian sands on the western slope of the South Tatar arch are reservoirs for bitumen and heavy oil. These sands have features of a very complex depositional environment, with traces of fluvial, marine, and aeolian processes and redeposition, and are tectonically altered. The sand bodies and bitumen deposits are also influenced by the Sheshma River system, which flows directly over the bitumen deposits.

Keywords: bituminous sands, oil sands, tar sands, Sheshmian sands, sedimentary factors, post-sedimental processes, river system, Republic of Tatarstan

Introduction

The purpose of this paper is to study reservoirs of natural bitumens and heavy oils in sand bodies, located in the Republic of Tatarstan in the area between the Volga and Kama rivers and the Ural Mountains. The clastic Ufimian deposits unconformably overlie the Sakmarian sulfate-carbonate sediments [1]. The deposits of natural bitumen are associated with the Sheshmian sands and sandstones of the Shehma Formation (Upper Permian, Ufimian Stage). The bituminous deposits formed as a result of the vertical migration of hydrocarbons from deeper oil horizons of the Earth's crust. The bituminous sand horizon is located in the Sheshma River valley in the southern part of the Republic of Tatarstan (Fig. 1) in an area of approximately 100 x 50 km at shallow depths rarely exceeding a few hundred meters. The clastic material of the Sheshmian horizon was brought from the rocks eroded from the Ural mountain range [2]. It was carried to the platform by various water streams and accumulated there. The sands are predominantly graywacke and are composed of fragments of igneous rocks, quartz, and feldspar. [3]. Tectonic processes associated with the Uralian collision in the Permian time were responsible for vertical migration of hydrocarbons from the underlying Devonian and Carboniferous oil deposits [1]. The accumulation of significant hydrocarbon reserves occurred in the sandy Sheshma Formation, which has high reservoir properties and favorable conditions for the formation of oil deposits (positive structures and impermeable clayey rocks at the top).

These hydrocarbons occur as natural bitumen and heavy oils. The Sheshmian horizon is a stratum consisting of two beds: lower sandy-clayey and upper sandy. The upper bed is rich with bitumen and heavy oil. The exploitation was first organized as a series of adits for bitumen extraction near the village of Shugurovo. For a long time, bitumen-containing rocks were considered only as raw material for the construction industry. However, with new technologies it has become possible to recover natural bitumen and heavy oil.

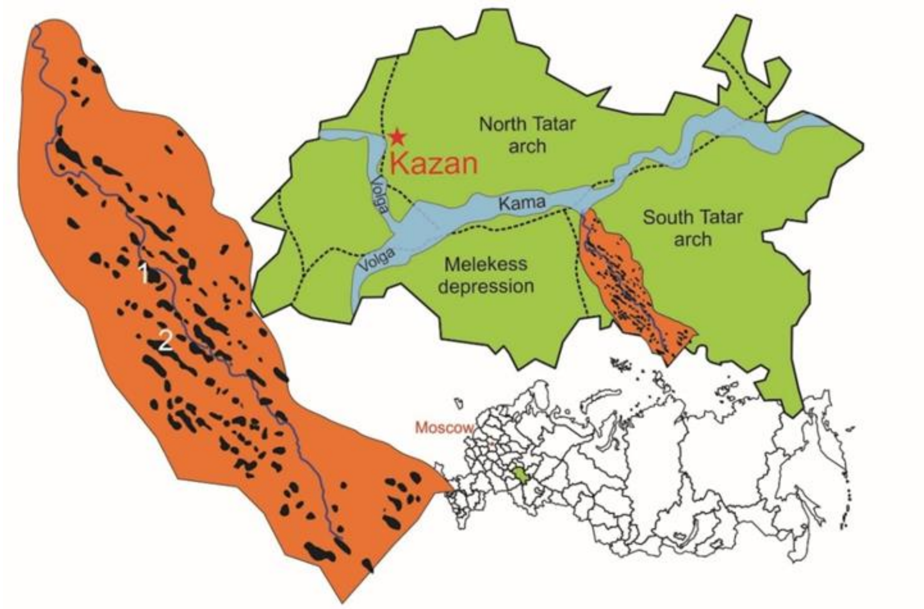

Fig. 1. Bottom right picture: The Republic of Tatarstan (green) on the map of Russia. Right top picture: orange – the area of distribution of the bituminous Sheshma Formation, black – deposits of bitumen in sedimentological structures (1 – Ashalchinskoe Uplift, 2 – Nizhne-Karmalskoe Uplift), dark blue – the Sheshma River

The depositional settings of these beds were extremely complex and difficult to interpret. It can be assumed that initially the entire Sheshma Formation was sandy-clayey in composition like its lower horizon. Formation of these sand bodies is still debatable, with a variety of opinions published. Many authors interpret these sand bodies as terrestrial in origin [4], [5], [6], [7], [8], and some as of deltaic [9], [10], [11] or fluvial [12] origin. The theory of their marine bank origin is very common [13], [14], [15]. The sand bodies could be the product of more than just one process.

A possible aeolian impact on the studied sand strata [16] was also suggested.

Object and methods

The objects of this paper were core samples from a dozen wells drilled within the most studied Ashalchinskoe and Nizhne-Karmalskoe uplifts. The samples were studied microscopically in petrographic thin sections, using granulometric analysis, while morphology of sand bodies was studied using paleogeomorphological analysis. One of the main problems of the paleogeomorphological analysis is that the current morphology of sand bodies has been altered tectonically, which requires using paleotectonic alignment for paleogeomorphological analysis.

The method of paleotectonic alignment is based on the assumption that marine carbonate sediments are initially subhorizontal. This means, that any carbonate bed above the Sheshma Formation can be used as a zero point when modeling the section of wells and the entire uplift [19].

Results and discussions

The Sheshma Formation in the studied region occurs in a series of anticline-like traps located in several parallel series. The sandy bodies are overlain by a layer of Kazanian clay with remains of brachiopods. This shale horizon has become an excellent fluid stop for bottom-up migrating oils.

Basic reservoir properties, such as porosity, are form at the depositional stage. Often the reason for the high porosity of sands is that the debris grains are loosely in contact, leaving communicating voids [17]. However, the reservoir properties are also influenced by various post-depositional processes such as cementation or pore leaching [18]. Clastic material of sandy clay size was transported by water flows from the Paleo-Ural Mountains, which were eroded in the Permian time.

For this reason, sandstones have some of the properties of fluvial deposition. The deposits were accumulated in the western part of the South Tatar arch, which was then still rising, in a basin at the border with the Melekess depression. The Sheshmian horizon combines two units, reflecting the complex history of sand deposition in this area.

The studied region in the Permian was located at 25 °N [1] (which roughly corresponds in modern coordinates to Northern Africa (Sahara) and the Arabian Peninsula), hence the climate was arid [4], [5]. In an arid climate, the coastal Sheshmian desert was formed [16]. The upper part of the Sheshma Formation was affected by winds and formed a relief forms resembling linear (seif) dunes. For the same reason, the clay component is absent in the upper part of the Sheshmian Horizon. The lower sandy-clayey bed was not exposed to wind because it was below the groundwater level, i.e., was saturated with water and the wind could not affect it. The fact that positive landforms were formed at the time of the formation of the Sheshma Formation is confirmed by paleotectonic reconstructions. This reconstruction is based on a 3D model of one such uplift, using core material and geophysical data [19]. It was shown that at the time of clay deposition, positive forms of the Sheshmian paleorelief already existed. This is indicated by the inverse correlation of the thicknesses of clays and sandstones (in places where the thickness of the sand bed increases, the thickness of the clay decreases). The presence of brachiopod shells in the clays indicates marine conditions. Thus, due to a sharp rise of the sea level, the Sheshmian paleorelief was covered by seawater. When the seabed is uneven, sediments primarily fill the relief depressions. This can be seen in the reconstruction from the inverse correlation between the thicknesses of sandstones and clays. Reconstruction of paleofacies shows the existence of various depositional settings. The general conditions of transportation and sedimentation were studied using particle size analysis [20]. Thus, the existing traps for bitumen and heavy oils are sedimentological. It was found that the formation of sediments took place in conditions of coastal marine facies and beaches with coastal dunes [20], such as the Jurassic Norphlet Formation in the deep-water eastern Gulf of Mexico, or the modern environment of the Namib Desert: [16]. The results obtained confirm the proposed model of the formation of the horizon; however, some ratios of the parameters do not show a 100% aeolian impact, but indicate, for example, transportation by water flows. This is because initially the clastic material was transported by water flows, therefore, some statistical indicators are evidence of this. The migration of hydrocarbons also influenced the mineral composition, for example, we associate the formation of pyrite with organic matter and the activity of sulfate-reducing bacteria [21].

However, the mineral composition was influenced not only by oil migration but also by the proximity of deposits to the earth's surface (and in some cases onto the surface). The processes of modern mineral formation (Fig. 2) associated with moving groundwater are widely developed. We recorded extensive processes of calcite and iron oxide formation. The impact of this modern mineral formation could be very considerable during the exploitation of bitumen deposits. Uneven distribution of carbonate zones could have very negative affect to the steam chamber which is created in reservoir system according to SAGD exploitation method.

Fig. 2. Modern processes of mineral formation in the rocks of the Sheshma Formation: left – photograph from an adit, right – photograph of an outcrop

All studied deposits are located in the Sheshma River basin at depths rarely exceeding the first hundred of meters. Sheshma is a large river, it is a left tributary of the Kama. For the most part, it flows over the zone of development of bitumen deposits, and the drainage zone of the river system influences the underlying rock complexes for many meters, up to hundreds of meters [22]. The river divides this zone into two parts: the right bank and the left bank. This division is due to the different composition of the rocks down the section and is of great importance. The river valley has an asymmetrical profile in which the right bank is bedrock and high, composed of dense Middle Permian deposits. The left bank is accumulative, and low, often terraced, composed of easily permeable alluvial sandstones. This is typical for most large rivers [23] and is caused by the Coriolis force and various effects of the river flow on the banks.

The excess of a high steep slope over a gentle low slope can reach up to 100 m [24]. The rivers in the European part of Russia, in particular, in the Republic of Tatarstan, are characterized by the presence of Neogene incisions [25], which are also filled with highly permeable sands. The described circuit is shown in (Fig. 3).

Water exchange is important and can be accompanied by a variety of processes, such as leaching, oxidation, the formation of geochemical barriers, mechanical action on rocks, etc. All these processes can occur both in reservoir systems and in rocks and fluid seals. The integrity of the seal is of particular importance for the Tatneft oil company. Hydrocarbons are developed here by the thermal method, in particular, by the method of steam-gravity drainage. This method involves pumping hot water vapor and creating a steam chamber. The uniformity and permeability within the formation affect the uniformity of the steam chamber, but seals are also of great importance. With a fractured, weak clay cover, steam breakthroughs into the overlying horizons are inevitable. Also due to the shallow bedding, these breakthroughs of the vapor-bitumen mixture can get into drinking water sources and even spill out onto the surface, which can lead to difficult-to-recover environmental consequences. Also, the inconsistency of the fluid stop leads to even greater degradation of bitumen, an increase in the proportion of the heavy component in it, etc.

This directly affects the attractiveness of the field as a development target. Since asymmetrical river valleys and opposite banks of rivers are composed of rocks of different permeability, we conclude that at present the Sheshma river system is one of the most significant factors influencing reservoirs and rocks. This is because the left-bank-deposits could very likely be affected by migrating groundwaters because of high permeability and low thickness of covering rocks, but the right-bank-deposits are covered by strong and thick Permian deposits. This is also confirmed by field data, according to which the deposits of the second (right) group mostly have “gas caps”, which indicates the integrity of the seal rocks. All this imposes difficulties on the process of extracting natural bitumen, but it can be used to select rational development methods and select future industrial development facilities with minimization of environmental and economic risks.

Conclusions

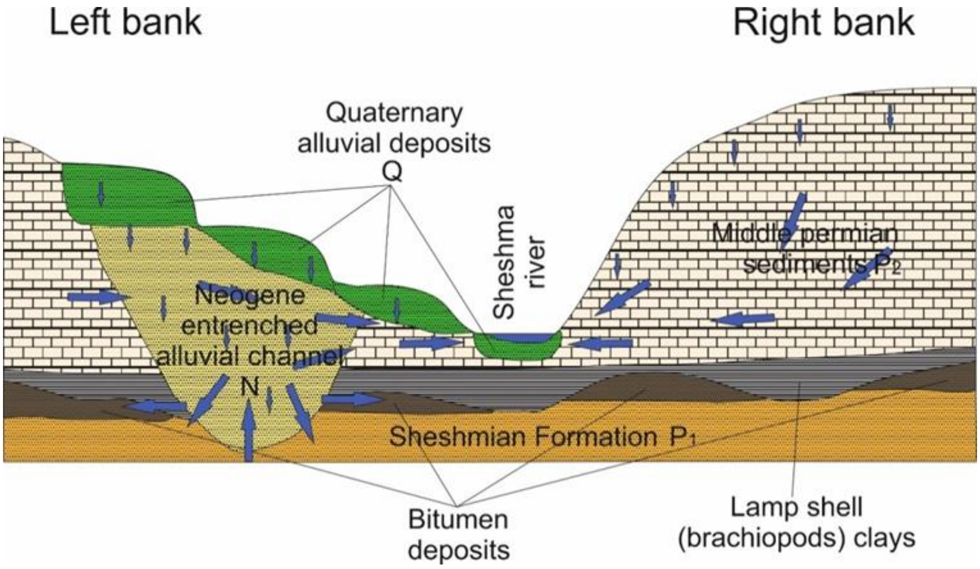

Fig. 3. Schematic image of cross section of Sheshma River valley. Blue arrows show possible directions of movement of groundwater (large arrows) and atmospheric waters (small arrows)

According to the proposed model, aeolian redeposition of sands played a significant role in the formation of the Sheshma Formation relief. The shape of the sandstone bodies is controlled by sedimentological factors. The wind impact factor explains the reason for the division of the Sheshmian Horizon into two layers, and explains the general morphology of sand bodies and their relationships with each other. Sandstones were formed in linear dunes and have formed a series of uplifts almost simultaneously with neighboring ones. The Sheshma River system divides the oil-bearing field into two parts differing in structure and composition. This factor has great geological, economic, and environmental importance in the development of deposits.

Acknowledgments
This work was supported by the research grant of Kazan Federal University and performed according to the Russian Government Program of Competitive Growth of Kazan Federal University.

REFERENCES

1. Burov, B.V. (2003). Geologiya Tatarstana: Stratigrafiya i tektonika. GEOS, Moscow, 402.
2. Khasanov, R. R., Mullakaev, A. I. (2016). Paleogeographic factors of the formation of Permian reservoir rocks of bitumen deposits in the east of the Russian plate (Russia) – International Multidisciplinary Scientific GeoConference Surveying Geology and Mining Ecology Management SGEM 1, pp. 469-474.
3. Khasanov, R. R., Mullakaev, A. I., Dusmanov, E. N. (2017). The structure of sandstones in productive horizons of the Permian bituminous deposits of Tatarstan (Russia). Uchenye Zapiski Kazanskogo Universiteta, Seriya Estestvennye Nauki 159 (1), pp. 164-173.
4. Nechayev, A. V., Zamyatin, A. N. (1913). Geologicheskoye issledovaniye severnoy chasti Samarskoy gubernii. In Tr. Geologicheskogo komiteta, novaya seriya 84, 207.
5. Noinskiy, M. E. (1932). Kratkiy ocherk izucheniya nedr Tatarskoy respubliki in Geologiya i poleznyye iskopayemyye v Tatarskoy respublike, Kazan, pp. 7-25.
6. Tikhvinskaya, E. I. (1941). Ufimskaya svita yevropeyskoy chasti SSSR. In Uch. zap. Kaz. Gos. Univers.101 (1), pp. 213-220.
7. Baturin, V. P. (1947). Petrograficheskiy analiz geologicheskogo proshlogo po terrigennym komponentam. – Izdatelstvo Akademii nauk SSSR, Moscow, 339.

8. Ellern, S. S. (1980). Usloviya obrazovaniya paleogeomorfologicheskikh lovushek nefti i gaza v verkh-nepermskikh otlozheniyakh Volgo-Uralskoy oblasti. In Paleogeomorfologicheskiye metody v neftyanoy geologii, Moskow, pp. 38-44.
9. Ignatyev, V. I. (1976). Formirovaniye Volgo-Uralskoy anteklizy v permskiy period. Izd-vo Kazanskogo universiteta, Kazan, 256.
10. Pustovalov, L. V. (1937). Usloviya osadkonakopleniya v verkhnepermskuyu epokhu. Problemy sov. geol. 12 (11), pp. 963-992.
11. Uspenskiy, B. V., Valeyeva, I. F. (2008). Geologiya mestorozhdeniy prirodnykh bitumov Respubliki Tatarstan. Izdatelstvo OOO “PF Gart”, Kazan, 348.
12. Forsh, N. N. (1955). Ufimskaya svita i kazanskiy yarus. Gostoptekhizdat, Leningrad, 156.
13. Sadreyev, A. M., Sayfullin, Z. G. (1976). Osobennosti stroyeniya i formirovaniya bitumnykh skopleniy i linzovidnykh plastov sheshminskikh peschanikov na zapadnom sklone Yuzhnogo kupola Ta-tarskogo svoda. In RNTS VNIIOENG, seriya «Neftegazovaya geologiya i geofizika» 1, pp. 23-27.
14. Shalin, P. A. (1988). O prirode palegeomorfologicheskikh lovushek nefti i bitumov v sheshminskom gorizonte Yuzhno-Tatarskogo svoda. In Geologiya nefti i gaza 5, pp. 35-38.
15. Goldberg, I. S., Yudin, G. T. (1955). Voprosy klassifikatsii, obrazovaniya i razmeshcheniya skopleniy bitumov. In Geologiya bitumov i bitumovmeshchayushchikh porod, Moskva, pp. 15-20.
16. Mullakaev A. I., Khasanov R. R. (2019). Signs of the aeolian influence on the formation of coastal-marine sand deposits in the Permian (Republic of Tatarstan, Russia). Uchenye Zapiski Kazanskogo Universiteta. Seriya Estestvennye Nauki 161 (1), pp. 128-140.
17. Pettijohn F.J., Potter P., Siever R. (1972). Sand and Sandstone. New York, Springer, 618.
18. Mullakaev, A., Sagirov, R., Khasanov, R. (2018). Post-sidemental changes of bituminous sandstones: Composition and genesis of cementing material – International Multidisciplinary Scientific GeoConference Surveying Geology and Mining Ecology Management, SGEM 18 (1.1), pp. 411-416.
19. Mullakaev A. I, Delev A. N, Usmanov S. A, Sudakov, V. A., Khasanov R. R. (2018). Tectonic causes of uneven cementation zones distribution in the bituminous sandstones productive part of the Sheshminsky horizon of the South Tatar arch. Neftyanoe Khozyaystvo – Oil Industry 2, pp. 23-25.
20. Dudyak, R., Mullakaev, A., Khasanov, R. (2020). Reconstruction of facies conditions of the sedimentation of bitumen-bearing sandstones according to granulometry data (Volga-Ural oil and gas province, Russian Federation) – IOP Conference Series: Earth and Environmental Science 516 (10).
21. Mullakaev, A., Khasanov, R., Bakhtin, A., Galiullin, B. (2019). Thin-dispersed mineral phases of bitumen-saturated deposits of Tatarstan (Russian Federation) under electronic microscopy and energy-dispersive X-ray spectroscopy data – International Multidisciplinary Scientific GeoConference Surveying Geology and Mining Ecology Management, SGEM 19 (1.1), pp.685-690.
22. Perel’man A. I. (1965). Geokhimiya epigeneticheskikh protsessov (zona gipergeneza). Nedra, Moscow.
23. Sementovskiy V. N. (1963). Zakonomernosti morfologii platformennogo rel’yefa. Izd-vo Kazan. un-ta, Kazan, 170.
24. Petrova E. V. (2008). Zakonomernosti razmeshcheniya neogenovykh rechnykh dolin v predelakh territorii Respubliki Tatarstan i ikh sootnosheniye s sovremennoy rechnoy set'yu. Uchen. Zap. Kazan. Un-ta. Ser. Yestestv. Nauki 150 (4), pp. 43-50.

Analysis of Annular Pressure Buildup for the Sustained Annular Pressure Diagnostics

NAGIMOV Vener[1], LONSHAKOV Marat[2]

[1] *TGT Oilfield Services, Technology Centre, Kazan (RUSSIA)*
[2] *Kazan Federal University, Kazan (RUSSIA)*
Email: vener.nagimov@tgtdiagnostics.com

Abstract

The article reviews sustained annular pressure (SAP) buildup reasons and mathematical description of the problem. Main types of contributions to SAP were discussed. The semisteady-state model was used to calculate annular pressure vs annulus temperature changes.

Transient temperature behaviour in annuli using historical temperature modeling are estimated. Annular pressure buildup data in shut-in condition using annular pressure data in flowing condition were extrapolated. The relationship between changes of annular pressure values with time and pressure buildup rate was estimated.

Keywords: annular pressure buildup, process of thermal expansion, spectral noise logging, annular pressure buildup curve, semisteady-state approach, coefficient of isobaric thermal expansion, coefficient of isothermal compressibility, TERMOSIM™

Introduction

Well integrity diagnostics of sustained annulus pressure (SAP) sources is usually performed in the shut-in condition of wells using conventional well logging methods such as thermometry, noise logging or pulsed neutron evaluation [1]. The application of all the methods described is limited by the SAP intensity, which could be understood by analysing annular pressure buildup measured at the wellhead. Since most of the pressure data from pressure gauge attached to evaluated annuli are available on flowing well condition, it is valuable to extrapolate annulus pressure behavior to the shut-in condition, as most of the integrity survey are performed in shut-in mode.

The relevance of this problem is that the estimation of annular pressure buildup curves in shut-in condition for the diagnostics, for instance, use of the noise logging method, takes considerable time resulting in economic losses.

The goal of the research work is to predict annular pressure buildup behaviour in shut-in condition using pressure data of flowing wells.

The brief analysis of scientific articles describing the reasons of annular pressure increase is presented in the research work.

Objects of investigation

Objects of investigations are four production wells (Table 1). Some information is encrypted according to the privacy policy.

Table 1. Well data

Well number	A	B	C	D
Field	Kuyumbinskoe	Korchagina	gas storage	Korchagina
Fluid type	oil	oil	gas	oil
Average rate, m^3/day	55	500	500	700
Perforation interval, m	2600-2615	1912-1980	362-377	4860-4890
Annular liqiud	water-based mud			
Diameter of casing surrounding annulus, mm	178/245	273/406	168/245	273/406
Production time, years	2			

The application of various wells used for semisteady-state modeling [2], [3] allows to estimate the relationship between changes of annular pressure values with time and pressure buildup rate.

Literature review

The annular pressure increase, sometimes occuring in the flowing phases of wells, can lead to barrier failure [4]. It is important to analyse the following reasons of annular pressure buildup:

- poor cement isolation casings;
- production casing leaks;
- leaks of wellhead equipment [5], [6].

There are three mechanisms responsible for annular pressure increase – fluid thermal expansion, annular volume change and annular fluid leakoff. The first component, or the fluid expansion, is the most dominant (80%) in the value of annular pressure increase. The semisteady-state approach used for practical calculations of pressure values focuses on the thermal expansion term in the absence of alterations in annular volume and leakoff.

Consequently, the ratio of annular pressure buildup Δp to temperature changes ΔT is equal to the ratio of the coefficient of thermal expansion α divided by the coefficient of isothermal compressibility κ for the annular fluid [7] (Formula 1).

$$\Delta p = \frac{\alpha * \Delta T}{\kappa} \qquad (1)$$

Methodology

During the first stage results of temperature and noise logging were analysed. To calculate accurate values of temperature fluctuations well schematics and annular pressure data in flowing condition were also investigated.

During the second stage changes of annular temperature with time using TERMOSIM™ software were defined. TERMOSIM™ software numerically solves the problems of flow hydrodynamics and heat exchange between the wellbore fluid, completion components, surrounding anisotropic rocks and reservoirs. Essential data for production and shut-in temperature modeling are fluid production time and rate, well sketches, dates of annular pressure measurements in the flowing phase. Values of the annular pressure increase were calculated at wellhead using the coefficient of thermal expansion α and the coefficient of isothermal compressibility κ for the annular fluid (Formula 1), that are respectively $3*10^{-4}$ k^{-1} and $4.5*10^{-10}$ Pa^{-1} [3].

Results

Annular pressure buildup curves in flowing phases are marked in blue in Fig. 1-4. Changes of annular pressure buildup calculated with the use of Formula 1 were applied to estimate annular pressure increase curves in shut-in phases marked in orange in Fig. 1-4. The maximum relative deviation of pressure was calculated for every well. It is equal to the ratio of the maximum difference between annular pressure values in shut-in and flowing phases divided by the maximum pressure value in the shut-in phase. Values of maximum relative deviations are presented in Table 2. The analysis of Fig. 1-4 allows to prove that the thermal liquid expansion has a significant influence on annular pressure buildup, if pressure buildup rate exceeds 5 bars a day and the production rate is over 50 m^3/d of liquid at standard conditions. The maximum relative deviation can reach 34% under these conditions. In other cases, additional accurate calculations of annular pressure values are required.

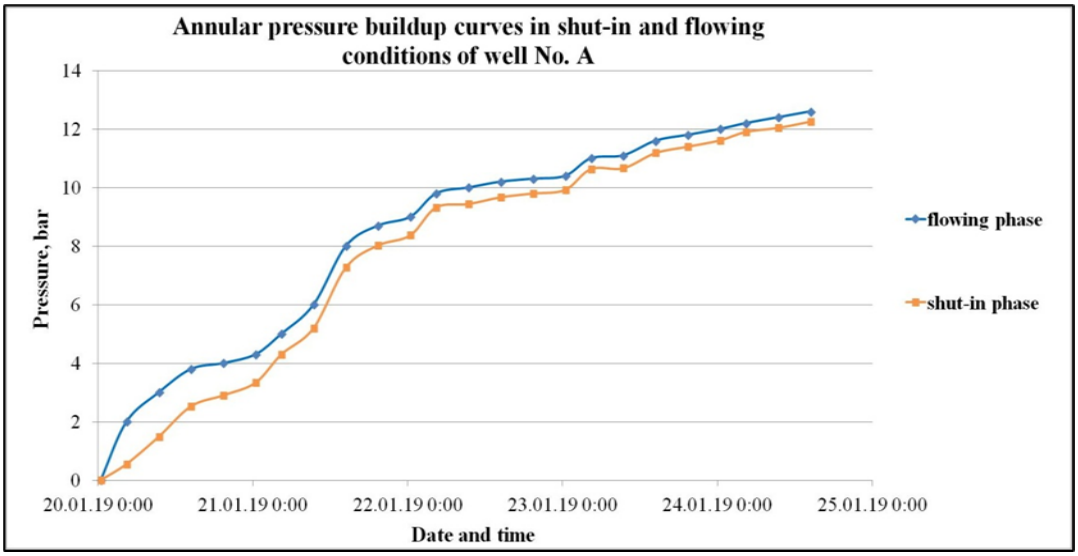

Fig. 1. Annular pressure buildup curves in shut-in and flowing conditions of well No. A

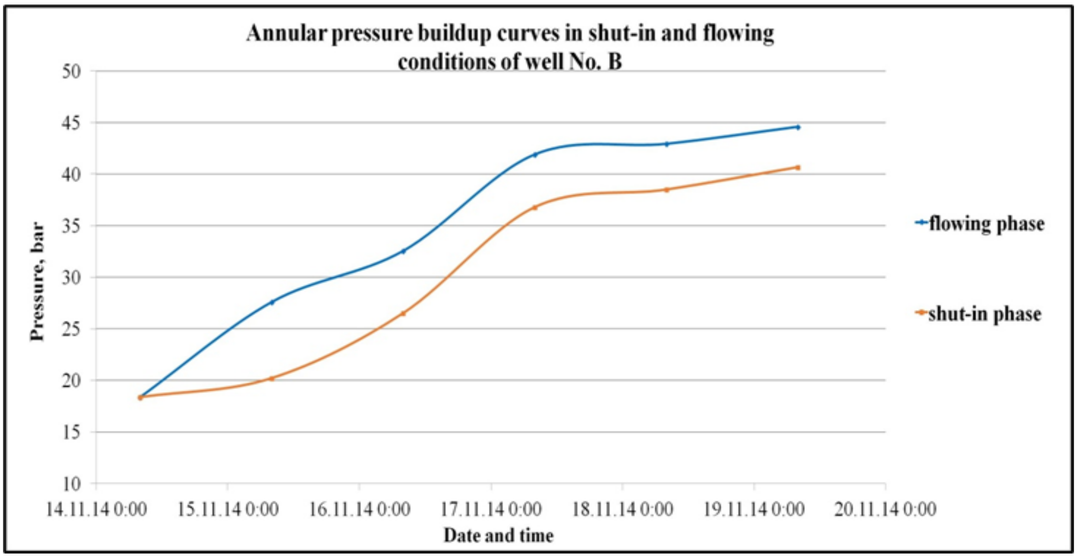

Fig. 2. Annular pressure buildup curves in shut-in and flowing conditions of well No. B

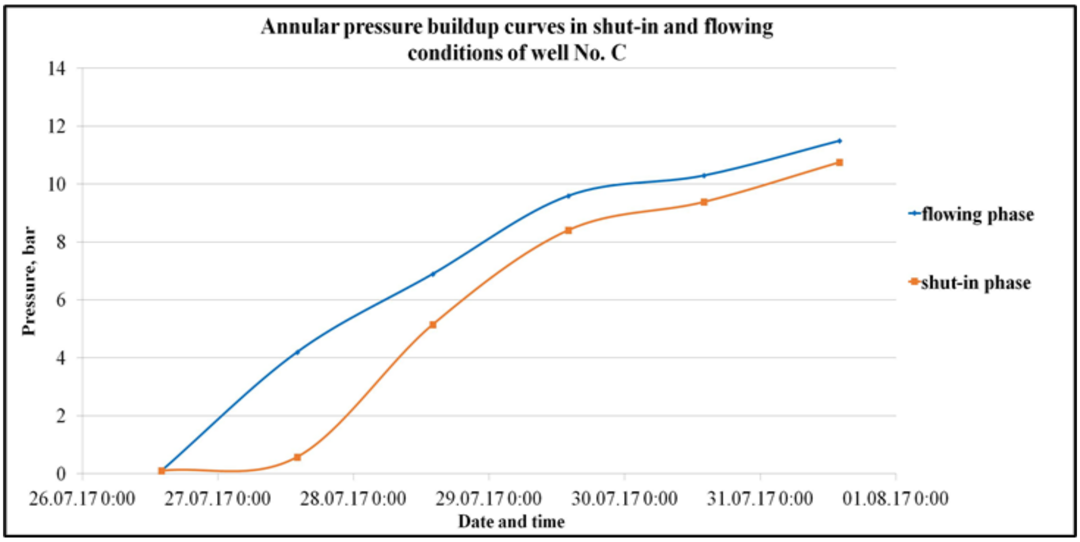

Fig. 3. Annular pressure buildup curves in shut-in and flowing conditions of well No. C

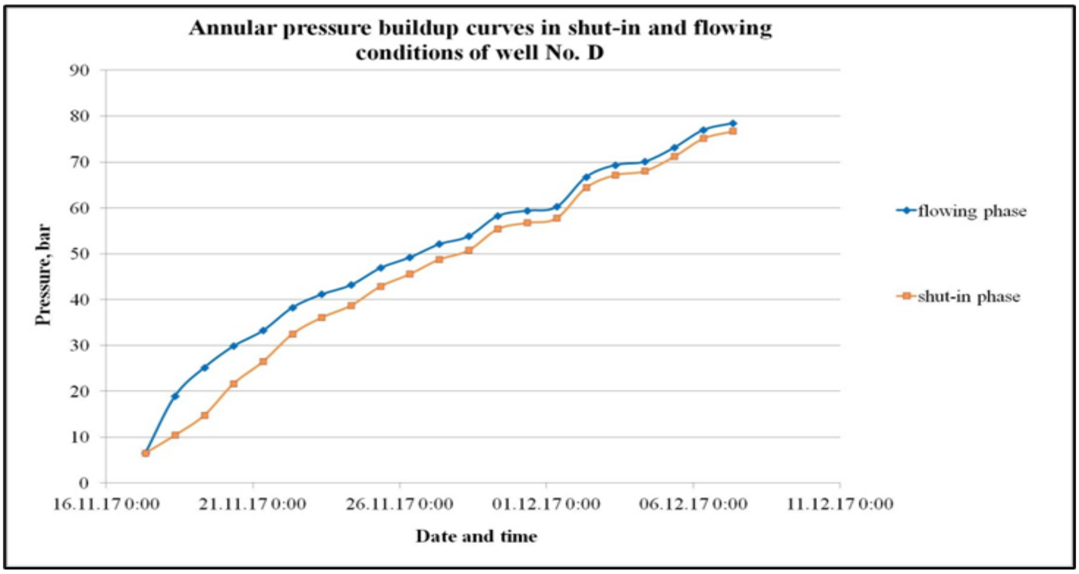

Fig. 4. Annular pressure buildup curves in shut-in and flowing conditions of well No. D

Table 2. Maximum relative deviations of pressure for investigated wells

Well number	Maximum relative deviation of pressure, %
A	14
B	12
C	18
D	34

Conclusions

In the article the main reasons of annular pressure buildup including casing leaks and poor well cement was discussed. Research works on the influence of thermal liquid expansion in sealed annuli of flowing wells on annular pressure have been analysed. The semisteady-state approach allowing to calculate annular pressure buildup was used.

The estimation of the annular pressure buildup data in shut-in condition using pressure data on flowing stage allows to investigate the influence of the mud thermal expansion on pressure data.

The maximum relative deviation of pressure might be significant (as seen from the case D can be as high as 34%) if pressure buildup rate exceeds 5 bars a day and the production rate is over 50 m^3/d of fluid at standard conditions. Consequently, thermal expansion of annular fluid should be taken into account in well integrity diagnostics of sustained annulus pressure (SAP) sources.

Acknowledgements

The authors would like to express their gratitude to Michael Wilson for editing the text of the scientific article, TGT Oilfield Services, Aberdeen, Scotland, UK.

REFERENCES

1. Aslanyan, A. M., Aslanyan, I. Yu., Maslennikova, Yu. S., Minakhmetova, R. N., Soroka, S. V., Nikitin, R.S., Kantyukov, R. R. (2016). Detection of behind-casing gas flows using integrated high-precision temperature logging, spectral noise logging, and pulsed neutron logging toolstring. Oil and Gas territory 6, pp. 52-59.
2. Hasan, A. R., Izgec, B., Rabin, C. S. (2010). Sustaining Production by Managing Annular–Pressure Buildup. SPE Production & Operations 25 (2), pp. 195-203.
3. Oudeman, P., Bacarreza, L. J. (1995). A Field trial results of annular pressure behavior in a high-pressure/high-temperature well. SPE Drilling & Completion 2, pp. 1084-1088.
4. Oganov, S. A., Nadein, V. A. (2014). Some aspects of the problem of annular pressure occurrence in an oil and gas well. Oborudovanie i tekhnologii dlya neftegazovogo kompleksa 5, pp. 29-34.
5. Gorbacheva, O. A. (2012). Control and research of well with intercasing pressure at astrakhan gas condensate field. Problemy sbora, podgotovki i transporta nefti i nefteproduktov 1, pp. 18-26.
6. Pulya, Yu. A., Lukyanov, V. T., Bekukh, I. I. (2009). Operation of wells under casing pressure. Stroitelstvo neftyanykh i gazovykh skvazhin na sushe i na more 8, pp. 28-32.
7. Oudeman, P., Kerem, M. (2005). Transient behavior of annular pressure buildup in HP/HT wells. Journal of Petroleum Technology 57 (3), pp. 58-60.
8. Vasilyev S., Boltunov N. and others. (2019). Determination the Source of Sustained Annulus Pressure in High GOR Oil Wells by Using Acoustic Logging. SPE-198385-MS, SPE Annual Caspian Technical Conference, 16-18 October, Baku, Azerbaijan https://doi.org/10.2118/198385-MS

Permian and Triassic Representatives of the Family Vetlugospermaceae (Peltaspermales, Gymnospermae): First Data on Female Reproductive Organ Architecture

NAUGOLNYKH Serge[1]

[1] Geological Institute, Russian Academy of Sciences, Moscow (RUSSIA)
Kazan Federal University, Kazan, (RUSSIA)
Email: naugolnykh@list.ru

Abstract

The peltasperms (order Peltaspermales), which flourished during the Permian and Triassic periods throughout the world, are a very peculiar group of gymnosperms, which completely vanished, and have no analogs in the modern vegetation. The peltasperms were represented by three families: Peltaspermaceae s.s., Vetlugospermaceae, and Angaropeltaceae. All of them closely related to each other, but distinctly different in details of the morphology of the female reproductive organs.

The family Vetlugospermaceae includes peltasperms with a more or less rhombic shape of the peltate megasporangiate shield, with very specific features, i.e., the protective ridge (belt) concentrically disposed on the adaxial surface of the shield, surrounding the seeds before they became mature. The purpose of the ridge was to protect the ovules/seeds against herbivorous/phytophagous arthropods, mostly insects.

Although the morphology of individual megasporangiate shields of Vetlugospermaceae was studied in detail, there were no exact data on the general architecture of the female reproductive organs. It was assumed that they were organized as loose cones, but this assumption was hypothetical.

A new find of closely aggregated megasporophylls of *Vetlugospermum rombicum* Naug. gives a good basis for the reconstruction of the general architecture of the female reproductive organs of Vetlugospermaceae. Architecture of the female reproductive organ of *Vetlugospermum rombicum* was cone-like, racemose, when the plant was alive, and when the reproductive organ was functional.

Keywords: peltasperms, Vetlugospermaceae, Permian, Triassic

Introduction

The peltasperms (order Peltaspermales), which flourished during the Permian and Triassic periods throughout the world [1-21], are a very peculiar group of gymnosperms, which completely vanished, and have no analogs in the modern vegetation. The peltasperms (order Peltaspermales) were represented by three families: Peltaspermaceae s.s., Vetlugospermaceae, and Angaropeltaceae. They were closely related to each other, but distinctly different in the detailed morphology of the female reproductive organs. The family Vetlugospermaceae was established by the present author [12] for peltasperms with the more or less rhombic shape of the peltate megasporangiate shield possessing very specific features, i.e., a protective ridge (belt) concentrically disposed on the adaxial surface of the shield, surrounding the seeds before they became adult. The purpose of the belt is to protect the seeds against herbivorous/phytophagous arthropods, mostly insects (see Discussion below).

The morphology of the individual megasporangiate shields of Vetlugospermaceae has been studied in the most detail, with the exception of the abaxial surface of the shields of *Navipelta* Karasev [7]. However, here were no exact data on the general architecture of the female reproductive organs. It was assumed that they were organized as loose cones [12, Fig. 9, D], but this assumption was hypothetical.

A new find of closely aggregated megasporophylls of *Vetlugospermum rombicum* Naug. provides a good basis for the reconstruction of general architecture of the female reproductive organs of Vetlugospermaceae.

Material and methods

The specimens under consideration were provided to the present author by the geologist M.P. Arefiev (Geological Institute of Russian Academy of Sciences; GIN RAS), to whom I am sincerely grateful. The most important specimen (Fig. 1) is an imprint (impression) and counter-imprint of cone-like aggregation of several megasporangiate shields, four of which are visible quite clearly and an additional three shields are preserved partly and can hardly be recognized, only in oblique light. There is a thin axis in the middle part of the megasporangiate shield aggregation.

The specimens came from the Spasskoe locality, in the middle part of the Vetluga River Basin, on the left (east) bank of the river near Spasskoe village. All the stratigraphic details and possible correlations were discussed in previous works; for review see: [12]. The plant fossils are accompanied by the shells of Conchostraca, often preserved together with the plant remains (Figs. 1, 2).

The photographs were taken using a combination of direct and oblique light to better show the relief of the fossils. The graphic picture of the specimen studied (Fig. 2, B) was made from the photograph using the line-tracing technique.

The collection is temporarily stored at the Geological Institute of RAS, and will be subsequently transported to the Monographic collections in Department of the State Darwin Museum, Moscow, Russia.

Palaeobotanical observations

The specimen under consideration (an imprint/impression and counter-imprint) shows the general pattern of the megasporophyll attachment in Vetlugospermaceae. The specimen is a representative portion of the cone-like structure bearing at least five megasporophylls arranged in a way supporting their natural position on the fertile axis (Figs. 1, 2). Length of the portion is 30 mm.

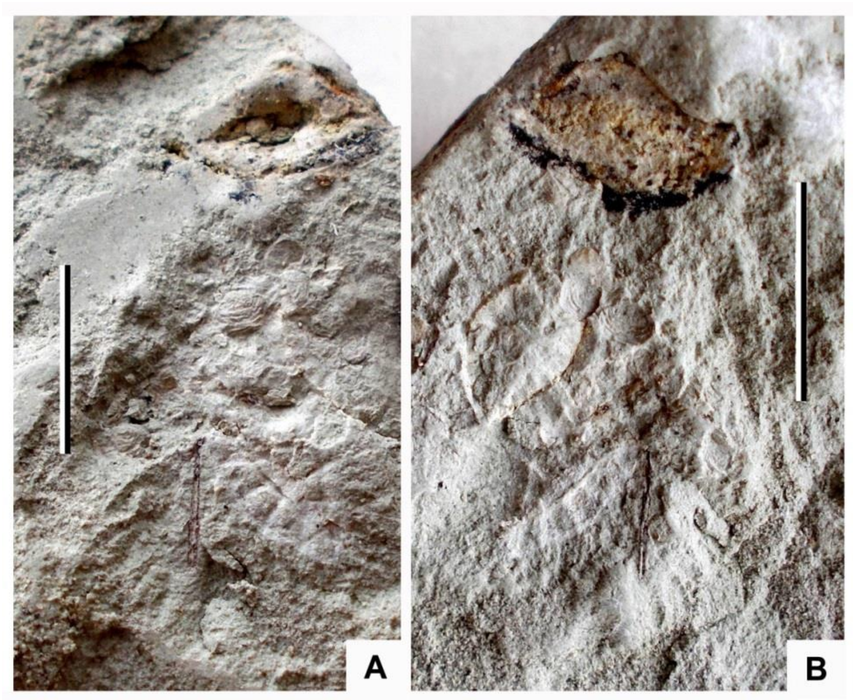

Fig. 1. *Vetlugospermum rombicum* Naug., aggregation of megasporophyll shields. Spasskoe locality, Vetluga River; Lower Triassic, Induan. A – spec. GIN No 4851/358; B – GIN No 4851/359. Scale bar: 1 cm

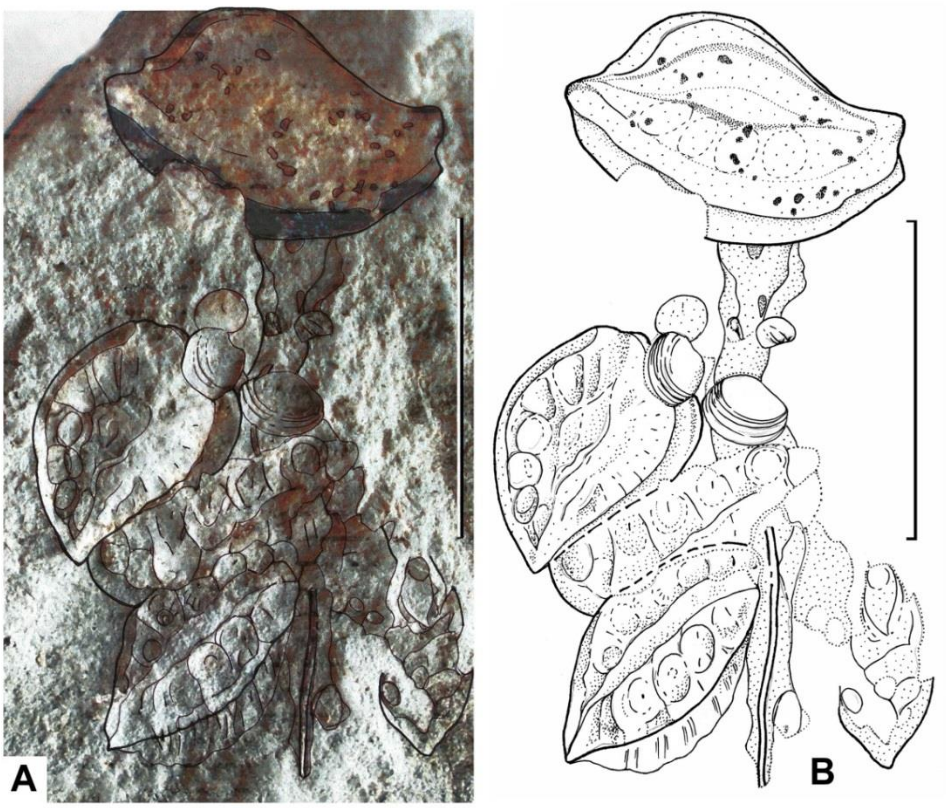

Fig. 2. *Vetlugospermum rombicum* Naug., aggregation of the shields; line tracing sketch of spec. GIN No 4851/359. Spasskoe locality, Vetluga River; Lower Triassic, Induan. Scale bar: 1 cm

One megasporophyll shield is orientated across the cone axis and is observed in front, perhaps somewhat moved aside during pre-diagenetic transformation of the reproductive organ.

Three megasporophyll shields are orientated subparallel to each other and at an average angle of about 45° (40° to 50°) to the fertile axis. There are clearly visible seed scars of round to ovoid shape on the upper and lower (in relation to the position on the fertile axis) megasporophyllous shields on the left side of the cone (Fig. 1, B; Fig. 2, B, C). The third (middle) shield is not well-observed, but it has in general the same shape and size as the shields below and above. The general shape of the megasporophyllous shields closely fits the diagnosis of *Vetlugospermum rombicum* (Fig. 3, A).

There is one more megasporophyllous shield on the right side (in relation to its position on Fig. 1, B; Fig. 2, A, C). Despite its poor preservation, it can be suggested that it is the same shape, size and structure as other shields on this specimen.

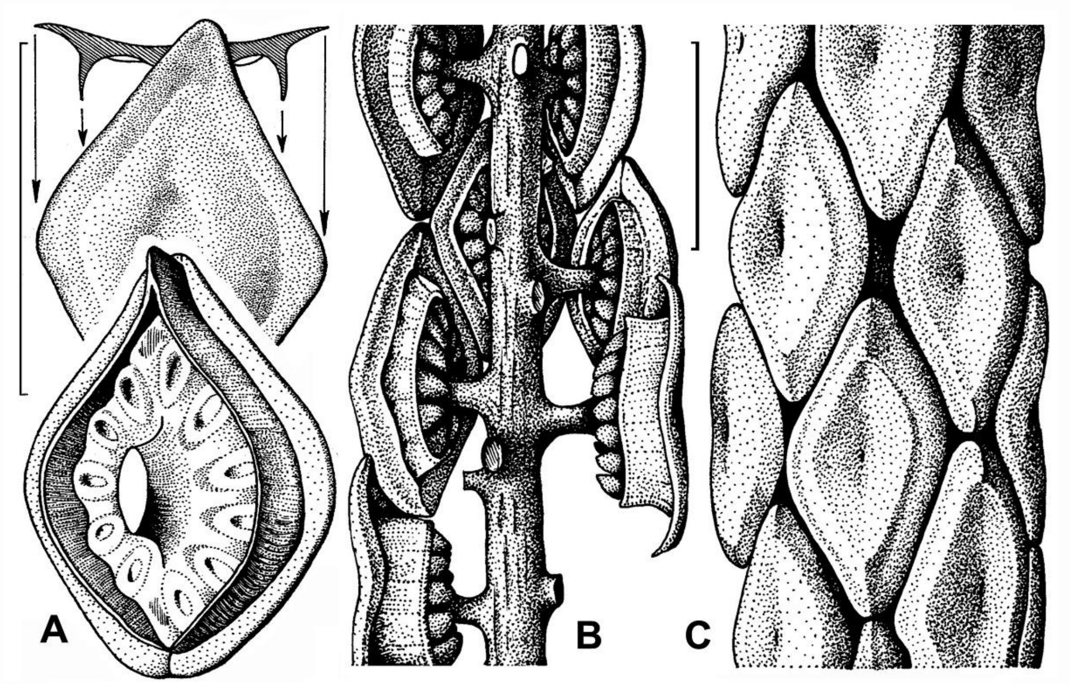

Fig. 3. *Vetlugospermum rombicum* Naug., A – individual megasporophyllous peltate shield; B, C – a reconstruction of aggregation of megasporophyll shields. Spasskoe locality, Vetluga River; Lower Triassic, Induan. Scale bar is 1 cm

The cone axis is relatively thin, perhaps somewhat slender and flexible, with a clearly visible conductive strand disposed in the medial part of the axis. The maximal observed width of the axis is about 2 mm. Architecture of the female reproductive organ of *Vetlugospermum rombicum* was cone-like, racemose (Fig. 3, B, C), when the plant was alive, and when the organ was functional. Most probably the same architecture was typical of some closely related taxa, such as *Navipelta* Karasev.

The same gross morphology of the female cones is typical of many different representatives of the order Peltaspermales s.l. reported from Permian and Triassic deposits around the world, for instance: [1, Fig. 11], *Dejerseia lobata* (Jones et de Jersey) Herbst emend Bombleur *et al.*, from Upper Triassic of Antarctica; [18; Fig. 5, A, D; Fig. 6, A, B], megasporophyllous discs *Peltaspermum townrovii* Retallack, associated with the fronds *Lepidopteris callipteroides* (Carpentier) Retallack and polliniferous organs *Permotheca helbyi* Retallack from Lower Triassic of Sydney Basin, southeastern Australia, and many others. The head-like aggregations of megasporophyllous discs of the species *Peltaspermum buevichiae* Gomankov et S. Meyen [6, Fig. 22] were most probably misinterpreted as a result of inaccurate observation of poorly preserved, fragmentary material.

Discussion

As mentioned above, one of the most particular morphological features of the peltasperms belonging to the family Vetlugospermaceae is the presence of a protective ridge (belt). The functional purpose of the protective ridge became even more obvious after considering the general architecture of the female reproductive organ.

The megasporophyllous peltate shields were closely attached to the cone axis in the life position.

Thus, the unfertilized ovules disposed on the adaxial surface of the megasporophyllous shields, concentrically around the shield stalk, were doubly protected by the protective ridge (belt) and the strong connection between the megasporophyll margins of neighboring peltate shields. Taking in account the reduction of the trophic bases of many herbivorous terrestrial organisms in the latest Permian and early Triassic, such double protection seems more than appropriate. After the ovules became adult and ready for fertilization, the cone axis grew up further, the shield margins of neighboring shields moved aside from each other, the protective ridge (belt) became weaker and then opened to allow access for pollen to the ovule micropyle, and after fertilization the seeds were released and disseminated in an authochtonous/barochorous manner. The process of ovule fertilization was most probably influenced by herbivorous insects [14, 15].

Acknowledgements

This work was funded by the subsidy of the Russian Government to support the Program of Competitive Growth of Kazan Federal University among the World's Leading Academic Centers. M. Naumcheva (Paleontological Institute of RAS, Moscow) and V. Zharinova (Kazan Federal University, Kazan, Tatarstan, Russia) are gratefully acknowledged for discussion of the Conchostraca fossils from the Spasskoe locality. The work was fulfilled in a framework of the State program 0135-2016-0001 of the Geological Institute of RAS and was supported by the RFBR project 18-04-00322. The author expresses his sincere gratitude to M.P. Arefiev (Geological Institute of Russian Academy of Sciences, Moscow), who provided specimens for the present study.

REFERENCES

1. Bomfleur, B., Taylor, E. L., Taylor, T. N., Serbet, R., Krings, M., Kerp, H. (2011). Systematics and paleoecology of a new peltaspermalean seed fern from the Triassic polar vegetation of Gondwana. – International Journal of Plant Sciences 172 (6), pp. 807-835.
2. Chaney, D. S., Mamay, S. H., DiMichele, W. A., Kerp, H. (2009). *Auritifolia* gen. nov., probable seed plant foliage with comioid affinities from the Early Permian of Texas, USA. International Journal of Plant Sciences 170 (2), pp. 247-266.
3. DiMichele, W. A., Kerp, H., Krings, M., Chaney, D. S. (2005). The Permian peltasperm radiation: evidence from the Southwestern United States. The Nonmarine Permian. Albuquerque: New Mexico Museum of Natural History and Science Bulletin 30, pp. 226-242.
4. Dobruskina, I. A. (1975). A role of the peltaspermalean pteridosperms in Permian and Triassic floras. Paleontological journal 4, pp. 120-132.
5. Galtier, J., Broutin, J. (2008). Floras from red beds of the Permian Basin of Lodève (Southern France). Journal of Iberian Geology 34 (1), pp. 57-72.
6. Gomankov, A. V., Meyen, S. V. (1986). Tatarina flora. Composition and distribution in the Late Permian of Eurasia. Nauka, Moscow. Transactions of the Geological Institute of Russian Academy of Sciences 401, p. 175.
7. Karasev, E. V. (2009). A new genus *Navipelta* (Peltaspermales, Pteridospermae) from the Permian/Triassic Boundary Deposits of the Moscow Syneclise. Paleontological Journal 43, pp. 1262-1271.

8. Kerp, H., Broutin, J., Lausberg, S., Aassoumi, H. (2001). Discovery of latest Carboniferous – early Permian radially symmetrical peltaspermaceous megasporophylls from Europe and North Africa. C.R. Acad. Sci. Paris. Sciences de la Terre et des planets 332, pp. 513-519.
9. Mamay, S. H., Chaney, D. S., DiMichele, W. A. (2009). *Comia*, a seed plant possibly of peltaspermous affinity: a brief review of the genus and description of two new species from the Early Permian (Artinskian) of Texas, *C. greggii* sp. nov. and *C. craddockii* sp. nov. International Journal of Plant Sciences 170 (2), pp. 267-282.
10. Naugolnykh, S.V. (2001). A new peltaspermaceous pteridosperm from the Upper Permian of the Russian platform. The Palaeobotanist 50, pp. 189-205.
11. Naugolnykh, S. V. (2008). A new gymnosperm *Sylvocarpus armatus* gen. et sp. nov. from the Lower Permian of the Ural Mountains. Paleontological Journal 42, pp. 431-439.
12. Naugolnykh, S. V. (2012). *Vetlugospermum* and Vetlugospermaceae: a new genus and family of peltasperms from the Lower Triassic of Moscow syneclise (Russia). Geobios 45, pp. 451-462.
13. Naugolnykh, S. V. (2014). *Permocallipteris*, a new genus from the Permian of Angaraland. Wulfenia, Mitteilungen des Karntner Botanikzentrums Klagenfurt 21, pp. 1-20.
14. Naugolnykh, S. V. (2018). A new concept and a newly emended diagnosis of the advanced peltasperm *Kuvakospermum pedatum* Naug. et Sidorov, emend. nov. from the Kazanian (Middle Permian) deposits of Russia. Wulfenia 25, pp. 1-14.
15. Naugolnykh, S. V. (2019). *Quasistrobus* Vladimirovich, 1986, emend. nov., a new interpretation of an advanced angaropeltian gymnosperm from the Middle Permian (Wordian) deposits of the Volga river basin, Russia. Wulfenia 26, pp. 37-52.
16. Naugolnykh, S. V., Kerp, H. (1996). Aspects of Permian Palaeobotany and Palynology. XV. On the oldest known peltasperms with radially symmetrical ovuliferous discs from the Kungurian (uppermost Lower Permian) of the Fore-Urals (Russia). Review of Palaeobotany and Palynology 91, pp. 35-62.
17. Naugolnykh, S. V., Oskolski, A. A. (2010). An advanced peltasperm *Permoxylocarpus trojanus* Naug. from the Lower Permian of the Urals (Russia): an ancient case of entomophily in gymnosperms. Wulfenia 17, pp. 29-43.
18. Retallack, G. J. (2002). *Lepidopteris callipteroides*, an earliest Triassic seed fern of the Sydney Basin, southeastern Australia. Alcheringa 26, pp. 475-500.
19. Taylor, E. L., Taylor, T. N. (2009). Seed ferns from the Late Paleozoic and Mesozoic: any angiosperm ancestors lurking there. American Journal of Botany 96, pp. 237-251.
20. Wang, Z.-Q. (1997). Permian *Supaia* fronds and an associated *Autunia* fructification from Shanxi, China. Palaeontology 40, pp. 245-277.
21. Zhang, Y., Zheng, S., Naugolnykh, S. V. (2012). A new species of *Lepidopteris* discovered from the Upper Permian of China, with its stratigraphic and biologic implications. – Chinese Science Bulletin 57 (27), pp. 3603-3609.

New Data on Morphology of the Early Carboniferous Lagenostomalean Pteridosperm *Serpentocarpus serpentae* Naug. from the Visean of the Urals, Russia

NAUGOLNYKH Serge[1,2], KOKINA Olga

[1] *Geological Institute, Russian Academy of Sciences, Moscow (RUSSIA)*
[2] *Kazan Federal University, Kazan (RUSSIA)*
Email: naugolnykh@list.ru

Abstract

Morphology of sterile fronds and seed-bearing cupules of the Early Carboniferous lagenostomalean pteridosperm *Serpentocarpus serpentae* Naug. is discussed. The plant has dichotomizing fronds with bilobate to pinnate pinnules with deeply dissected margins. The marginal lobes are linear, with acute apices. Young pinnules of bilobate shape ontogenetically transform into pinnate pinnules through overtoping of acroscopical segment of initially bilobate pinnule during development of the frond. The cupules are abaxially open, cup-like, with acute spine-like lobes and solitary ovule disposed in the middle part of the cupule.

Keywords: lagenostomalean pteridosperm, Serpentocarpus, Early Carboniferous

Introduction

Scientific attention to the pteridosperms, a very important Paleozoic and Mesozoic group of gymnosperms, intensively grows during the last decades, mostly because the hypothesis that these plants can be considered as a predecessor of angiosperms. Systematics and morphology of pteridosperms are often discussed in a broad framework of paleoecological studies or in analyses of the history of geology and paleontology [1], [2], [3], [4], [5], [6], [7], [8], [9], [10], [11], [12], [13], [14], [16], [17], [18], [19], [20], [21], [22], [23], [24].

The present paper focuses on morphology and paleoecology of the Early Carboniferous lagenostomalean peridosperm *Serpentocarpus serpentae* Naug. from the Visean deposits of the Eastern slope of the Urals. New material allows to make morphological characteristics of this plant more precise, and to estimate modes of diversity of the sterile leaves probably belonging to the same parent plant.

Material and methods

The basic material for the present study was collected by famous Uralian amateur-paleontologist G.T. Mauer [2], who worked during first half of twentieth century in a number of museums and state geological companies of the cities of Perm and Sverdlovsk (now Ekaterinburg). This part of collection in hands originated from the Lower Carboniferous (Visean) deposits of the Bredy locality, Cheljabinsk region and was discussed in the previous work [5].

Highly informative specimens (Fig. 1) were provided to the present authors by D.V. Solodjankin, an amateur paleontologist from Ekaterinburg. This material originated from the Lower Carboniferous (Visean) deposits, outcropped in Artemovsky Mine (near road to the Kluchi village), Sverdlovsk region. These specimens demonstrate closely disposed representative fragments of sterile fronds, which can be comparable according to formal systematics with the form-genus *Sphenopteridium* Schimper, but they are also identical to the sterile fronds of *Serpentocapus serpentae* Naug. (see the descriptive part and discussion below).

Fig. 1. *Serpentocarpus serpentae* Naug. Sterile leaves. The Artemovsky Mine locality; Lower Carboniferous, Visean; Eastern Urals. Scale bar is 1 cm (A, C); 1 mm (B)

Palaeobotanical observations

The collection studied includes both fertile and sterile leaves, which belonged to one and the same parent plant and thus were attributed to one and the same natural (botanical) species *Serpentocapus serpentae* Naug. This attribution is based both on close co-occurrence of sterile and fertile organs in the Bredy locality, and on typological extrapolation with the closely related taxa of lagenostomalean pteridosperms, such as *Elkinsia polymorpha* Rothwell *et al*. [17], [18].

Sterile leaves

The sterile leaves of *Serpentocarpus serpentae* were organized as fronds with dichotomizing rachis and bilobate to pinnate pinnules (Fig. 1). The pinnules were attached to the pinna rachises branching from the dichotomizing basis of the frond [5; Fig. 5, Plate II, figs. 1-8]. Judging from the most completely preserved specimens, size of the frond could reach 25 cm length and 15 cm width.

Width of the rachis in the point of dichotomy is about 4-6 mm. The frond and pinna rachises are smooth. Branching/dichotomy of the frond rachis can be both isotomizing and non-isotomizing ("anisotomizing"). Angle of dichotomy varies from 60° to 110°. The pinnules are attached to the pinna rachis in 20 mm above the point of the frond rachis dichotomy [5; Fig. 5, a; Plate II, Figs. 1, 5]. The collection studied includes several isolated pinnae showing pinnules preserved in connection to the pinna rachis (Fig. 1, A, B). The young undeveloped pinnules are of more or less isometric shape, 3 to 8 mm long and 2 to 7 mm wide. The pinnules are sphenopteroid, with well-defined pinnule stalk. Normally the pinnules are dissected by medial sinus into two more or less equal parts giving the young pinnule the bilobate shape. Pinnule margins are dissected by smaller sinuses into linear lobes. After growing up, shape of the pinulles changes from bilobate to pinnate, because acroscopical segment of the pinnule develops faster and becomes an axial/medial part of the pinnule. The basiscopical branch generally left same size and shape and thus transformed into basiscopical lobe of the pinnately dissected pinnule (Fig. 1, B, C). Nonetheless, marginal lobes of such pinnately dissected pinnule still kept their more or less bilobate shape (Fig. 1, C). Venation of the pinnules is weakly visible.

The veins are thin, a single vein comes into each pinnule lobe.

The most well-developed pinnules are 9 mm long and 7 mm wide.

The material in hands allowed to propose an integrative reconstruction of the frond architecture of *Serpentocapus serpentae* [5, Fig. 6, a]. Growth form of this plant can be reconstructed as herbaceous or shrubby plant with thin monopodial slender stem, perhaps with climbing adaptations.

The similar growth form was reconstructed for closely related lagenostomalean pteridosperm *Elkinsia polymorpha* Rothwell *et al*. [17], [18].

Reproductive organs

The seed-bearing organs of *Serpentocarpus serpentae* are cupules, each of which contains solitary ovule disposed in central part of the cupule (Fig. 2, A, B). The margins of the cupules bear lobe-like extensions with the pointed spine-like apices. Basal part of the cupules gradually transforms downwards into terminal part of the stem. Upper part of the cupule is cup-like widened.

Average length of the cupule without marginal lobes is about 5 mm; maximal width of the cupule is 4 mm. Lobe length varies from 2 to 3 mm. The ovules are visible in at least four cupules.

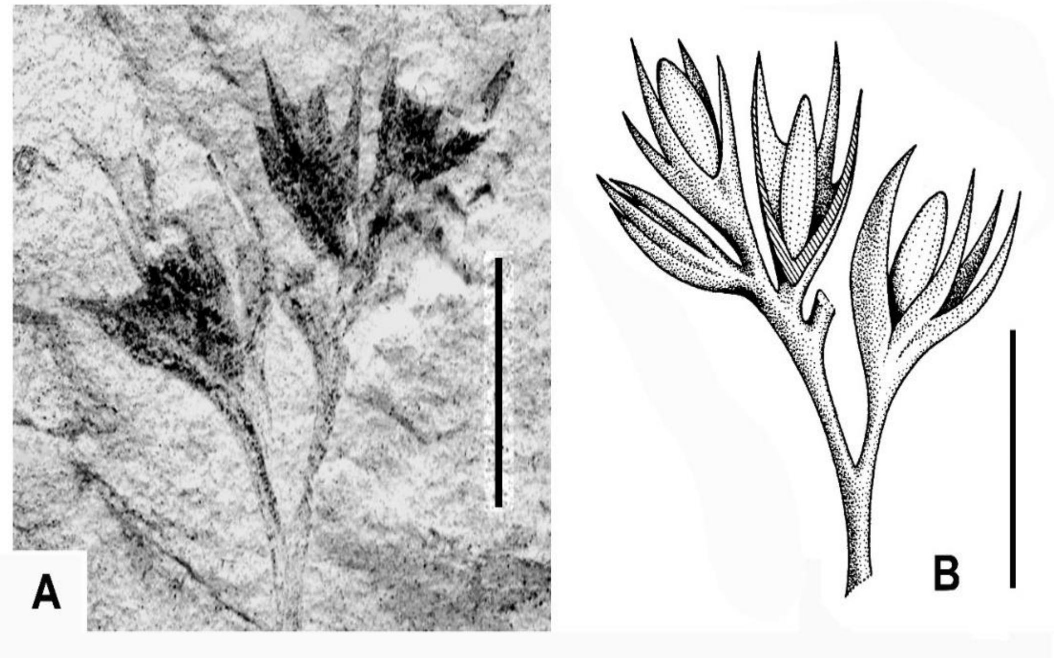

Fig. 2. *Serpentocarpus serpentae* Naug. Reproductive ovuliferous organs.
The specimen (A) and a reconstruction (B). The Bredy locality. Lower Carboniferous, Visean; Eastern Urals.
Scale bar is 1 cm

The most definitive ovule is observed in partly damaged cupule (Fig. 2, A, middle area of the picture). The ovules are long ovoid, with somewhat acute apical part. Spermoderm is smooth, sometimes with weakly developed prolonged folds. Length of the ovule is about 5.5 mm, maximal width is 2 mm.

The cupule is disposed terminally on the fertile stems. The stems are aggregated into clusters consisting of three to four fertile stems. It is possible that one of the fertile stems could have undeveloped or aborted cupule. Average length of the fertile stems varies from 5 to 6 mm. The fertile stems were located on the long axes of previous order, but exact size of these axes is unknown yet. The fertile organs of *Serpentocapus serpentae* most probably were disposed in apical part of the whole plant, above the monopodially branching stem with plagiotropic sterile fronds.

Discussion

Serpentocarpus serpentae has many features in common with other Late Palaeozoic lagenostomalean pteridosperms, although a number of morphological peculiarities makes *Serpentocarpus* different from related plants.

Some of the well-known pteridosperms were reconstructed on the basis of whole-plant methodological concept [16]. Among the taxa discussed in details by G. Retallack and D. Dilcher [16] the most similar to *Serpentocarpus serpentae* is *Lagenostoma lomaxii* Williamson ex Oliver et Scott [13], [14]. This species was an archetypical basis for establishing Pteridospermae or = Lyginopteridophyta as a completely extinct gymnosperm group.

The species *Lagenostoma lomaxii* was studied on the basis of the material from the lower part of the Upper Carboniferous (lower Westfalian) deposits of England. In contrast to *Serpentocarpus serpentae*, the English taxon belongs to a new phase in pteridosperm evolution, when the relatively primitive herbaceous lagenostomalean pteridosperms with weak specialization of reproductive and vegetative organs evolved towards morphologically advanced lyginopterids, often arborescent, with clear diversification of reproductive and vegetative structures. Nonetheless, *Lagenostoma lomaxii* has the same morphological architecture of the seed-bearing capsules as *Serpentocarpus serpentae*, with solitary ovules inside the cupules surrounded by spine-like marginal lobes. But the ovules of *Lagenostoma lomaxii* are larger and wider, and the lobes covered by glands extracted biologically active chemicals, most probably, pheromones responsible for attracting arthropods for pollination or other kind of interactions with the plant (discussion see in: [16]). The leaves and reproductive organs of *Serpentocarpus serpentae* lack any secretory organs, what indirectly points to the absence of active interactions between *Serpentocarpus serpentae* and arthropods. This plant could be anemophilic. Gradual decreasing of length of the marginal lobes could be a result of adaption for more effective anemophily [12].

The sterile fronds of *Serpentocarpus serpentae* and *Lagenostoma lomaxii* (the sterile leaves of latter species belong to the formal species *Sphenopteris hoeninghausii* Brongniart) are basically similar. They are dichotomizing, with sphenopteroid lobed pinnules. But the pinna rachises of *Serpentocarpus serpentae*, in contrast to *Lagenostoma lomaxii*, never bear additional pinnae disposed below the point of dichotomy of the frond rachis, meanwhile the rachises of *Sphenopteris hoeninghausii* always have at least two or three pairs of sterile pinnae beneath the point of the frond rachis dichotomy. The pinnules of *Sphenopteris hoeninghausii* always have distinct midvein coming into the terminal lobe of the pinnule. The venation of *Serpentocarpus serpentae* is not well-pronounced, and the pinnules often are bilobate, without distinct terminal lobe. The sterile leaves of *Serpentocarpus serpentae* superficially similar to the leaves of Early Carboniferous pteridosperm *Sphenopteridium pachyrrachys* (Goeppert) Potonie. The dichotomizing rachis of the latter species does not either have any additional segment below the point of dichotomy. The pinnules of *Sphenopteridium pachyrrachys* are dissected into lobes and thus are similar to the pinnules of *Serpentocarpus serpentae*. Moreover, there are some bilobate modifications among the pinnules of *Sphenopteridium pachyrrachys*.

But in contrast to *Serpentocarpus serpentae*, the penultimate pinnae of *Sphenopteridium pachyrrachys* sometimes can be branched again, having at least one or even two additional orders of branching. And, at last, parent plant with the leaves *Sphenopteridium pachyrrachys* produced the ovules *Lyrasperma scotica* (Calder) Long [12], which are quite different from the ovules of *Serpentocarpus serpentae*.

Palaeoecology

If we take into account the type of associated plant megafossils and type of deposits containing remains of *Serpentocarpus serpentae*, we can suggest that this species grew in large swampy lowlands or swampy forests, perhaps with the soils (histosoles) almost completely covered by water, with active peat accumulating. The dominant plants of these habitats were represented by arborescent lepidodendrids of the species *Lepidodendron acuminatum* (Goeppert) Zeiller [21, Fig. 15]. The pteridosperms *Serpentocarpus serpentae* could be well-adapted for growing in the canopy of the lepidodendrids. Similar type of landscapes was indicated as “Landscape B” by O.P. Fisunenko [1; p. 95, Fig. 3].

Acknowledgements

This work was funded by the subsidy of the Russian Government to support the Program of Competitive Growth of Kazan Federal University among World’s Leading Academic Centers.

The work was fulfilled in a framework of the State program 0135-2016-0001 of the Geological Institute of RAS and was supported by the RFBR project 18-04-00322. The authors express their sincere gratitude to D.V. Solodjiankin (the City of Sverdlovsk), who provided specimens for the present study.

REFERENCES

1. Fisunenko, O. P. (1987). Landscapes of the Middle Carboniferous of the Donetsk Basin. Paleontology and reconstruction of geological history of paleobassins. Leningrad, Nauka, pp. 92-99.
2. Glazyrina, Ju. V. (2010). Preliminary technical report of the paleontological team of G.T. Mauer after collecting in 1934 (from collection of the Perm regional museum). Paleontology and stratigraphy of Permian system in the museum expositions and private collections. Collection of scientific articles. Kungur, Perm: Polygraph City, pp. 53-56.
3. Lele, K. M., Walton, J. (1962). Fossil flora of the Drybrook sandstone in the forest of Dean, Gloucestershire. Bulletin of the British Museum (Natural History), Geology 7 (4), pp. 137-152.
4. Naugolnykh, S. V. (2012a). A new Carboniferous pteridosperm of Angaraland: *Angaranthus victorii* Naugolnykh, gen. et sp. nov. (Angaranthaceae, fam. nov., Callistophytales). Wulfenia. Mitteilungen des Kaerntner Botanikzentrums Klagenfurt 19, pp. 39-55.
5. Naugolnykh, S. V. (2012b). A new lagenostomalean pteridosperm *Serpentocarpus serpentae*, gen. et sp. nov. from the Lower Carboniferous deposits of the Urals. Geology and geophysics. News on paleontology and stratigraphy 18, pp. 69-81.
6. Naugolnykh, S. V. (2014). *Permocallipteris*, a new genus from the Permian of Angaraland. Wulfenia, Mitteilungen des Karntner Botanikzentrums Klagenfurt 21, pp. 1-20.
7. Naugolnykh, S. V. (2017). *Kizelopteris*, a new genus of climbing pteridosperms from the Lower Carboniferous of the Urals, Russia. Wulfenia. Mitteilungen des Kaerntner Botanikzentrums Klagenfurt 24, pp. 241-257.
8. Naugolnykh, S. V. (2018). A new concept and a newly emended diagnosis of the advanced peltasperm *Kuvakospermum pedatum* Naug. et Sidorov, emend. nov. from the Kazanian (Middle Permian) deposits of Russia. Wulfenia. Mitteilungen des Kaerntner Botanikzentrums Klagenfurt 25, pp. 1-14.
9. Naugolnykh, S. V. (2019). *Quasistrobus* Vladimirovich, 1986, emend. nov., a new interpretation of an advanced angaropeltian gymnosperm from the Middle Permian (Wordian) deposits of the Volga river basin, Russia. Wulfenia. Mitteilungen des Kaerntner Botanikzentrums Klagenfurt 26, pp. 37-52.
10. Naugolnykh, S. V., Jin, J. (2014). An Early Carboniferous flora of the Huadu locality from South China: its taxonomic composition, paleophytogeographical position and paleoecological interpretation. Acta Geologica Sinica 88 (5), pp. 1341-1351.
11. Naugolnykh, S. V., Oskolski, A. A. (2010). An advanced peltasperm *Permoxylocarpus trojanus* Naug. from the Lower Permian of the Urals (Russia): an ancient case of entomophily in gymnosperms. Wulfenia. Mitteilungen des Kaerntner Botanikzentrums Klagenfurt 17, pp. 29-43.
12. Niklas, K. J. (1981). Simulated wind pollination and airflow around ovules of some early seed plants. Science 11, pp. 275-277.
13. Oliver, F. W., Scott, D. H. (1903). On *Lagenostoma lomaxi,* the seed of *Lyginodendron.* Proceedings of Royal Society of London B 71, pp. 77-481.
14. Oliver, F. W., Scott, D. H. (1904). On the structure of the Palaeozoic seed *Lagenostoma lomaxi*, with a statement of the evidence upon which it is referred to *Lyginodendron.* Philosophical Transactions B 197, pp. 193-247.
15. Retallack, G. J. (2002). *Lepidopteris callipteroides*, an earliest Triassic seed fern of the Sydney Basin, southeastern Australia. Alcheringa 26, pp. 475-500.
16. Retallack, G. J., Dilcher, D. L. (1988). Reconstructions of selected seed ferns. Annals of Missouri Botanical Garden 75, pp. 1010-1057.
17. Rothwell, G. W., Scheckler, S. E., Gillespie, W. H. (1989). *Elkinsia* gen. nov., a Late Devonian gymnosperm with cupulate ovules. Botanical Gazette 150 (2), pp. 10-189.
18. Serbet, R., Rothwell, G. W. (1992). Characterizing the most primitive seed ferns. I. A reconstruction of *Elkinsia polymorpha.* International Journal of Plant Sciences 153 (4), pp. 602-621.
19. Taylor, E. L., Taylor, T. N. (2009). Seed ferns from the late Paleozoic and Mesozoic: any angiosperm ancestors lurking there? American Journal of Botany 96, pp. 237-251.
20. Tchirkova, H. Th. (1933). Végétaux houillers inférieurs du versant oriental de l'Oural. Bulletin de la Société Géologique de France 5 (3), pp. 521-529.
21. Tchirkova, H. Th. (1937). Contribution nouvelle à le flore Carbonifère inférieure du versant oriental de l'Oural. Problems of Paleontology 2-3, pp. 235-247.
22. Vasilieva, G. N. (1988). Morphology and systematics of Eastern Urals Lower Carboniferous cardiopterids. Paleontological journal 2, pp. 97-108.
23. Wang, Z.-Q. (1997). Permian *Supaia* fronds and an associated *Autunia* fructification from Shanxi, China. Palaeontology 40, pp. 245-277.
24. Zhang, Y. Zheng, S., Naugolnykh, S. V. (2012). A new species of *Lepidopteris* discovered from the Upper Permian of China, with its stratigraphic and biologic implications. Chinese Science Bulletin 57 (27), pp. 3603-3609.

Microborings in Upper Permian Ostracod Shells, East European Platform

NAUMCHEVA Maria[1]

[1] Borissiak Paleontological Institute, Russian Academy of Science (RUSSIA)
Kazan Federal University (RUSSIA)
Email: m.zhokina@gmail.com

Abstract

Borings of endolithic microorganisms in Permian freshwater ostracod shells are found for the first time in the East European platform. Three types of microboring are described. One is attributed to Actinomycetes. The producers of the other two microboring types remain unknown.

Keywords: microborings, endoliths, ostracods, Permian, East European Platform

Introduction

Microorganisms that settle on carbonate substrates are quite widespread in the aquatic environment. Endoliths are organisms which actively penetrate the substrate using chemical or mechanical drilling [1]. Endolithic microorganisms leave traces called microborings. Algae, fungi, cyanobacteria and bacteria often act as endoliths [2]. Diameter of microborings ranges from a fraction of a micron up to about 100 µm [3]. Microborers are widespread, and diversified mostly in marine environments, but are also known from fresh water and air-exposed rocks. [4]

Endoliths often select as a substrate calcite shells of various molluscs [5], [6], fish teeth [7], [8], bryozoans, foraminifera [5] and ostracod shells [5], [9], [10], [11], [12], [13]. In the geological record, such ichnofossils are known since the Precambrian [2]. In Permian continental basins, microborings in ostracod shells were previously found in Uruguay [13], but they were not described. This phenomenon is described for the first time from Permian ostracods of the East European Platform (EEP).

Material and methods

The material studied comes from seven sections and one well located in the central regions of the EEP (Fig. 1): Sundyr, Staroe Slukino, Schekino, Chizhi, well 1 Lyubim, Aristovo, Yaikovo and Eleonora [14], [15], [16]. In total, the sections cover the stratigraphic interval from the Late Severodivinian (≈Wuchiapingian) to the latest Permian.

The author’s collection contains 114 specimens of ostracod shells and valves with microborings.

Specimens belong to different species of the suborders Darwinulocopina (genera *Suchonellina*, *Wjatkellina*, *Suchonella*, *Prasuchonella*, *Dvinella*, *Mishevia* and *Darwinuloides*), Cytherocopina (genus *Sinusuella*) and the genus *Volganella* (suborder Incertae sedis). The collection is housed at the Borissiak Paleontological Institute RAS, no. 5519.

The material was photographed using Cambridge CamScan-4, TESCAN VEGA-II XMU and TESCAN VEGA-III scanning electron microscopes in the Borissiak Paleontological Institute RAS.

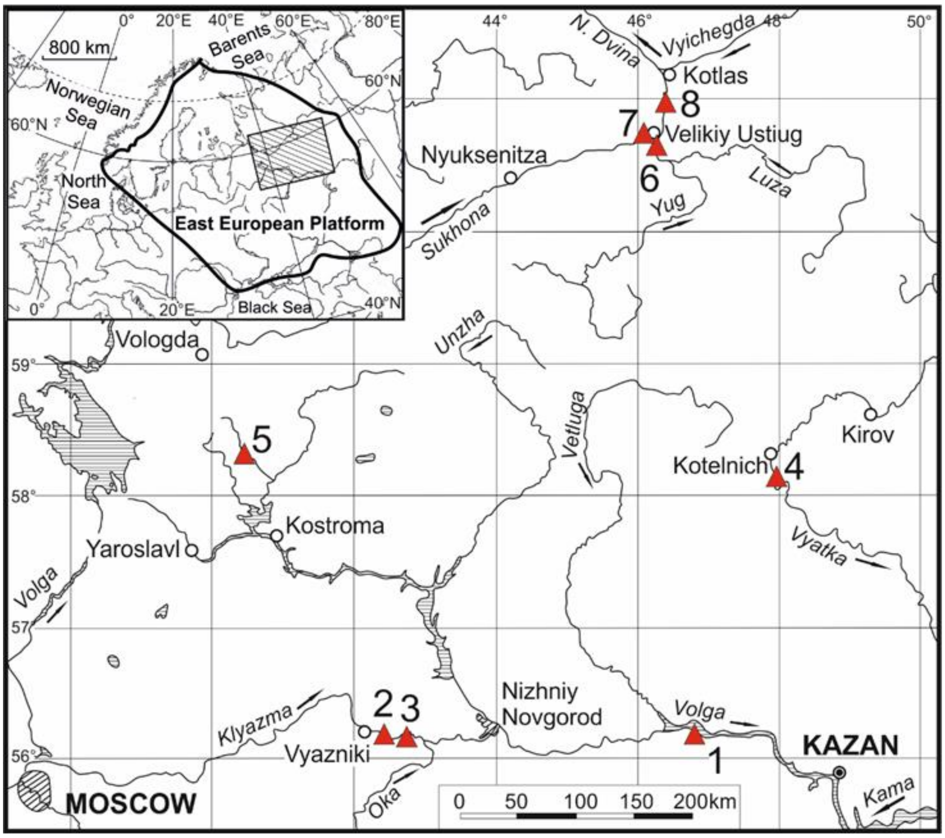

Fig. 1. Microboring location map: 1 – Sundyr, 2 – Schekino, 3 – Staroe Slukino, 4 – Chizhi, 5 – well 1 Lyubim, 6 – Aristovo, 7 – Yaikovo, 8 - Eleonora

Results

The detected microborings are represented by thin channels no more than 4 μm in diameter. There are three types of microborings which differ in branching.

Type A: Channels of uniform diameter, 1-1.5 μm. The channels are very sinuous, meandering and disordered (Fig. 2A-C). They bifurcate and cross one another. The channels are located on the surfaces of valves and penetrate into the valves.

Type B: Radial network of channels (Fig. 2D, E). Channel diameter decreases from center to periphery from 4 to 0.2 μm. The network is only located on the shell surface.

Type C: Dense radial network (Fig. 2F-H). Channel diameter ranges from 0.1 to 2 μm. The channels are sinuous, branching is very frequent. The network is only located on the surface.

Discussion and Conclusions

Microborings in ostracod shells were found across the vast territory of the central regions of the East European Platform and across a wide time range: from the Late Severodvinian (≈Wuchiapingian) to the latest Permian. Bored shells mainly came from gray clay, less often from brown clay or siltstones. This indicates a limited environment in which traces may have formed.

No connection was found between specific microboring types and deposits. Microboring types are not associated with particular ostracod taxa.

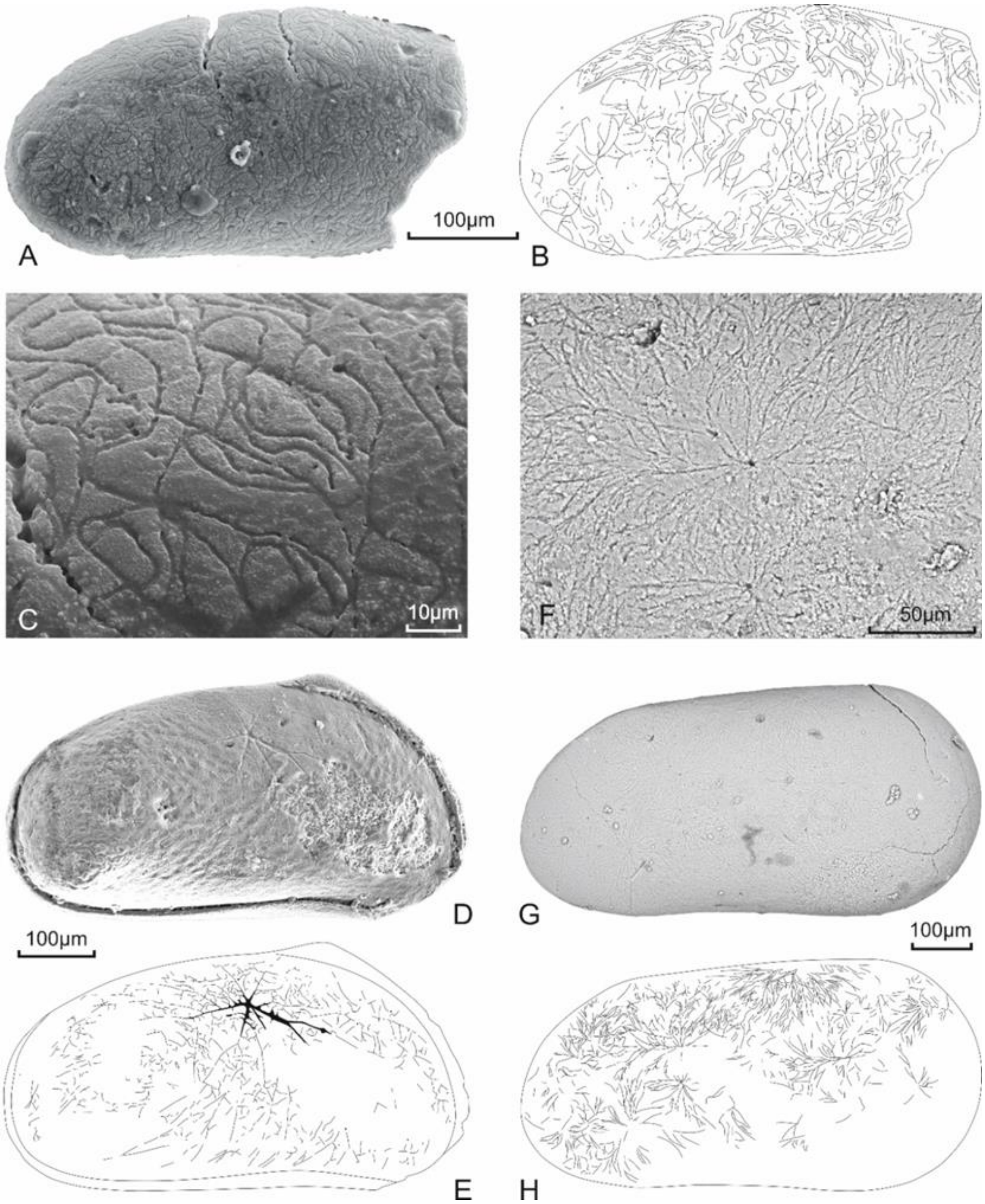

Fig. 2. Microboring types. A-C – Type A, *Suchonellina* sp. (Sundyr outcrop, Upper Severodvinian), left valve: A – general view, outer side; B – drawing of channels; C – details of microborings; D, E – Type B, *Suchonella typica* Spizharski, 1939 (Aristovo outcrop, Upper Vyatkian), carapace, right view: D – general view, outer side; E – drawing of channels; F-H – Type C, *Suchonellina inornata* Spizharski, 1939 (Aristovo outcrop, Upper Vyatkian), carapace, left view: F – details of microborings; G – general view, outer side; H – drawing of channels

The endolithic microorganisms that produce filamentous microborings include bacteria, cyanobacteria, chlorophytes, rhodophytes, and fungi [1], [17]. Microborings similar to type B have been found in recent ostracod shells [10], [11]. The authors of the papers reporting these microborings attribute them to Actinomycetes.

Types A and C have a unique morphology, which could not be found in the literature.

Microborings of fungi and cyanobacteria are known in this size class. They could also exist in freshwater conditions. However, they have another morphology [1], [3], [12], [17], [18], [19], [20], [21], [22].

This article is the first in a series of papers on microborings in the shells of Permian non-marine ostracods. Microborings are interesting and promising for paleoecological reconstructions. They are used as indicators of paleo-depths, salinity, temperature [17], and the rate of sedimentation [10, 11]. Ichnofossils of this kind are reported for the first time from the continental Permian deposits of the EEP. Their further study could provide a new tool for reconstruction of the environmental conditions of freshwater basins.

Acknowledgements

I thank Dr. S. Golubic, Dr. A.S. Alekseev, V.K. Golubev, and R.A. Rakitov for advice and help with preparing the article. This work was funded by a subsidy allocated to Kazan Federal University for the state assignment #671-2020-0049 in the sphere of scientific activities.

REFERENCES

1. Golubic, S., Perkins, R. D., Lukas, K. J. (1975). Boring microorganisms and microborings in carbonate substrates. In: The Study of Trace Fossils (Frey, R. W., Ed.). Springer, Berlin, Heidelberg, pp. 229-259.
2. Glaub, I., Golubic, S., Gektidis, M., Radtke, G., Vogel, K. (2011). Microborings and microbial endoliths: geological implications. In: Trace fossils: Concepts, Problems, Prospects (Miller, W., Ed.). Elsevier, pp. 368-381.
3. Edwards, B. D., Perkins, R. D. (1974). Distribution of microborings within continental margin sediments of the South-Eastern United States. Journal of Sedimentary Petrology 44 (4), pp. 1122-1135.
4. Radtke, G., Schafer, P., Blasher, H., Golubic, S. (2011). Microborings from shallow marine habitats on both sides of the Panama Isthmus. Annalen des Naturhistorischen Museums in Wien, Serie A 113, pp. 245-265.
5. Wisshak, M, Tapanila, L., Eds. (2008). Current developments in bioerosion. Springer, 501.
6. Naidin, D. P. (1969). Morphologia verkhnemelovykh belemnitov. MSU, Moscow, 305.
7. Underwood, C., Schlogl, J. (2013). Deep water chondrichthyans from the Early Miocene of the Vienna Basin (Central Paratethys, Slovakia). Acta Palaeontologica Polonica 58 (3), pp. 487-509. doi: 10.4202/app.2011.0101
8. Underwood, C. J., Mitchell, S. F., Veltkamp, K. J. (1999). Microborings in mid Cretaceous fish teeth. Proceedings of the Yorkshire Geological Society 52, pp. 269-274.
9. Boucot, A. J., Ed. (1990). Evolutionary paleobiology of behavior and coevolution. Elsevier Science, 699.
10. Danielopol, D. L., Casale, L. M., Olteanu, R. (1986). On the preservation of carapace of some limnic ostracods: An exercise in actupalaeontology. Hydrobiologia 143, pp. 143-157.
11. Namiotko, T., Danielopol, D. L., Grafenstein, U., Lauterbach, S., Brauer, A., Andersen, N., Hüls, M. (2015). Palaeoecology of Late Glacial and Holocene profundal Ostracoda of pre-Alpine lake Mondsee (Austria) – A base for further (palaeo-) biological research. Palaeogeography, Palaeoclimatology, Palaeoecology 419, pp. 23-36. doi: 10.1016/j.palaeo.2014.09.009
12. Olempska, E. (1986). Endolithic microorganisms in Ordovician ostracod. Acta Palaeontologica Polonica 31 (3-4), pp. 229-236.
13. Saravia, P. D., Herbst, R. (2001). Ostrácodos dulceacuícolas de la Formación Yaguarí, Pérmico Superior, R.O. dell'Uruguay. AMEGHINIANA (Rev. Asoc. Paleontol. Argent.) 38 (2), pp. 213-218.
14. Arefiev, M. P., Golubev, V. K., Balabanov, Y. P., Karasev, E. V., Minikh, A. V., Minikh, M. G., Molostovskaya, I. I., Yaroshenko, O. P., Zhokina-Naumcheva, M. A. (2015). Type and reference sections of the Permian-Triassic continental sequences of the East European Platform: main isotope, magnetic, and biotic events: XVIII International Congress on the Carboniferous and Permian Sukhona and Severnaya Dvina Rivers fild trip. PIN RAS, Moscow, 104.
15. Naumcheva, M. A. (2019). To the revision of freshwater Permian and Triassic ostracods of the genus Gerdalia Belousova, 1961. Paleontological Journal 53 (12), pp. 1346-1358. doi: 10.1134/S0031030119120037
16. Naumcheva, M. A., Golubev, V. K. (2020). Nonmarine ostracodes at the Permian-Triassic boundary of the central part of the East European Platform. Palaeoworld 29 (2), pp. 353-367. doi: 10.1016/j.palwor.2019.02.001
17. Wisshak, M. (2012). Microbioerosion. In: Trace Fossils as Indicators of Sedimentary Environments 64 (Knaust, D., Bromley, R. G., Eds.). Elsevier, pp. 213-243.

18. Boekschoten, G. J. (1996). Shell borings of sessile epibiontic organisms as palaeoecological guides (with examples from the Dutch coast). Palaeogeography, Palaeoclimatology, Palaeoecology 2, pp. 333-379.
19. Perkins, R. D., Halsey, S. D. (1971). Geologic significance of microboring fungi and algae in Carolina shelf sediments: notes. Journal of Sedimentary Petrology 41, pp. 843-853.
20. Rooney, W. S., Perkins, R. D. (1972). Distribution and geologic significance of microboring organisms within sediments of the Arlington Reef Complex, Australia. Geological Society of America Bulletin 83, pp. 1139-1150.
21. Schneider, J. (1977). Carbonate construction and decomposition by epilithic and endolithic microorganisms in salt- and freshwater. In: Fossil Algae: Recent Results and Developments (Flügel, E., Ed.). Springer, Berlin, Heidelberg, pp. 248-260.
22. Bystrov, A. P. (1956). O razrushenii skeletnykh elementov gribami. Vestnik Leningradskogo universiteta 6, pp. 30-46.

Pollen Records from Lake Lebedinoe (Northern Part of West Siberian Plain)

NIGAMATZYANOVA Gulnara[1], FROLOVA Larisa[1], FEDOROV Grigory[2], NIGMATULLIN Niyaz[1]

[1] *Kazan Federal University, Kazan, (RUSSIA)*
[2] *St. Petersburg State University, St. Petersburg, (RUSSIA)*
Email: gulnaraniga@mail.ru

Abstract

Pollen records from a 36 cm long sediment core of Lebedinoe Lake (64°17.135', 78°07.449') on the northern part of the West Siberian plain (Yamalo-Nenets Autonomous Okrug, Russia) are the evidence of environmental and vegetation history. Relatively low pollen concentrations, high presence of *Betula* and *Pinus* pollen, Cyperaceae pollen, and *Sphagnum* spores characterize the sediments. The vegetation is of a mixed type due to the location of the lake in the forest-tundra zone. *Betula sect. Nana* pollen and *Sphagnum* spores indicate~~s~~ the development of tundra-like vegetation. The presence of pollen of arboreal species (*Pinus*, *Picea*, *Larix*, and *Abies)* indicates the proximity of taiga-like vegetation. The core of the bottom sediment was deposited in a cold and humid climate. Short-term increases in climate humidity were observed during precipitation.

Keywords: Yamal, palynology, lake deposits, Holocene, the Western Siberian Plain

Introduction

Arctic regions are considered to be highly ecologically sensitive. Climatic changes impact on Arctic ecosystems and potentially induce dramatic shifts of community composition. High-latitude lakes, being features of most Arctic landscapes, are extremely sensitive to environmental change [1-2]. Lake sediments provide information about the environmental conditions of the past on a regional and global scale [3]. Their study provides a long-term prediction of environmental change [1]. The paleoindicators in lake sediments (diatoms, chitinous invertebrate remains (Cladocera, Chironomidae), pollen and spores), which are used for reconstruction local and regional palaeoenvironmental conditions, are especially valuable [4-8]. Palynological analysis of lake-sediments provides valuable information on the dynamics of the vegetation cover, linking geomorphology, soils, vegetation, air streams and climate [9].

Study Area

The West Siberian plain is one of the largest accumulative lowland plains. It is characterized by a regular relief without large fluctuations in elevation and is clearly defined by zonal landscapes – from tundra in the North to steppe in the South [10]. The geographical position of the West Siberian plain determines the transitional nature of its climate between the moderate continental Russian plain and the sharply continental climate of Central Siberia. The average January temperature decreases from -15 °C from the South-West to -30°C in the North-East of Western Siberia. The average temperature in July increases from +5 °C in the North to +20 °C in the South. Annual precipitation ranges from 390 to 600 mm. Permafrost covers a third of the

Northern part of the region [11]. The North-East of Western Siberia is the most continental, where the average temperature differences in January and July reach 45° [12].

The waterbody under study – Lebedinoe Lake - is located in the catchment area of the Pur River in the northern part of the West Siberian Plain (Yamalo-Nenets Autonomous Okrug, Russia).

According to Tarasov *et al*. [13], cold deciduous forest and tundra dominate in the northern part of Western Siberia. This zone is a mosaic combination of woodlands, swamps, and thickets of *Betula sect. Nanae*, *Pinus*, *Rhododendron subsect. Ledum*, *Rubus chamaemorus*, Ericaceae [14].

The lake is small and shallow (generally to 1.5 m deep). The bottom of the lake is covered with peat. Macrophytes grow abundantly in the lake.

Data and methods

In August 2017, a 36 cm long sediment core (17-Ya-02A) was extracted from 1.3 m depth in the central part of Lebedinoe Lake (64°17.135', 78°07.449'). The core was retrieved with a Uwitec gravity corer (60 cm diameter). A total of 18 samples, each consisting of 0.9 g of dry sediment that took 2-cm intervals from the core 17-Ya-02A, were treated for spore-pollen analysis using Faegri and Iversen method [15] but without the procedure of acetalization.

Lycopodium spore tablets were added to each sample to calculate the total pollen and spore concentrations as a marker [16].

Determination of pollen and spores was performed using identification guides and atlases [17-21]. For each sample, 330-350 pollen and spores were counted at 400 × magnification. All taxa percentages were calculated based on the sum of all pollen taxa taken as 100% (excluding spores and non-pollen palynomorphs). Tilia/TiliaGraph software [22] has been used for a visualization of the results. The definition of local pollen zones is supported by CONISS [23].

Results and interpretation

The results of spore-pollen analysis provide information for regional vegetation reconstruction.

The pollen assemblage is characterized by the dominance of arboreal pollen taxa (*Betula sect. Nana, Betula sect. Albae, Pinus*) and non-arboreal pollen of Cyperaceae (Fig. 1). Other arboreal pollen has a relatively low abundance and is represented mostly by *Picea*. *Sphagnum* spores have constant percentages throughout the core and are supposedly related to coastal aquatic vegetation.

The pollen percentages diagram is zoned to 6 pollen zones (PZ I – PZ VI) by visual inspection.

Pollen zone I (PZ I) at the 36-30 cm level is characterized by predominance of *Betula sect. Nana* (up to 40%), *Betula sect. Albae* (up to 27%), and *Pinus* (up to 23%). *Picea, Larix, Alnaster,* and *Salix* pollen have low percentages. Cyperaceae pollen (up to 17%) predominate in the herbaceous taxa. The *Sphagnum* spores' content is 15%. The pollen concentration is 100 grains/g.

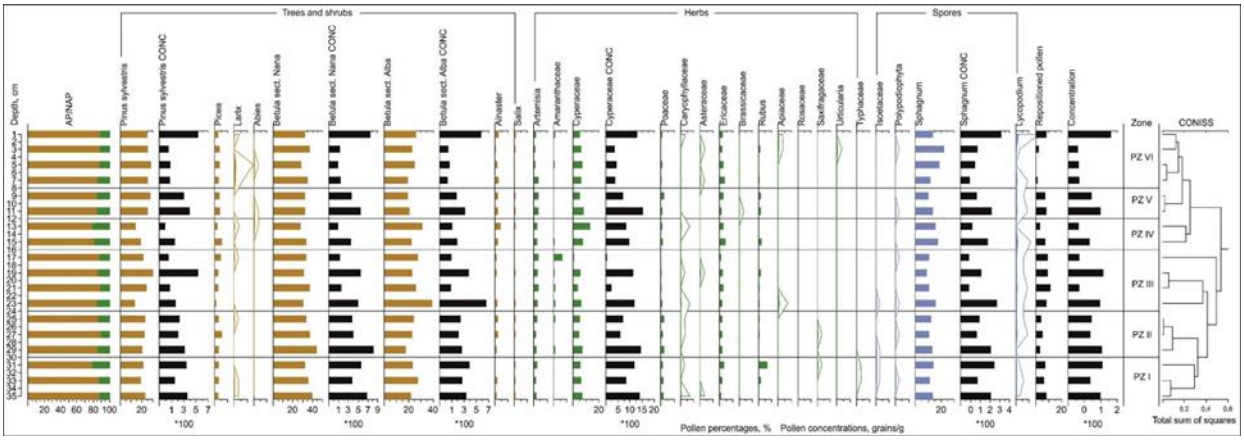

Fig. 1. Palynological analysis of Lake Lebedinoe core, produced with the Tilia/TiliaGraph software [22]. The visual definition of the pollen zones is supported by CONISS [23]

The pollen spectra from zone II (PZ II) (30-24 cm) were relatively stable. The amount of the *Betula sect. Nana* pollen (up to 45%) reaches its maximum. *Picea* pollen percentages slightly increase. The pollen concentration does not change in comparison with the previous zone.

Betula sect. Albae pollen (up to 40%) reaches its maximum in the pollen spectra of the zone III (PZ III) (24-16 cm). The concentrations of *Betula sect. Nana, Pinus, Picea* pollen fluctuate in a small range. The Cyperaceae pollen content does not change significantly throughout the pollen zone III. However, the Cyperaceae pollen concentration varies in a large range: from 5 to 15 grains/g. The minimum value of Cyperaceae pollen content and concentration has been observed at the end of the zone. The percentage of Amaranthaceae pollen increases. Ericaceae pollen content decreases. A sharp increase at the beginning of zone III (up to 260 grains/g) and a decrease by the end of the zone (up to 50 grains/g) have observed in the *Sphagnum* spore's concentration. Similar changes have been observed in the total pollen concentration in this zone: from 100 to 30 grains/g.

In the pollen zone IV (PZ IV, 16-12 cm) *Pinus* pollen content decreases up to 15%. *Abies* pollen was first marked at this zone. The Cyperaceae pollen percentage reaches its maximum – 14%. The percentage of Ericaceae pollen increases. The Amaranthaceae pollen content decreases. The *Sphagnum* spore content increases up to 18%. The pollen concentration in the zone IV is 25-60 grains/g. An increase of *Pinus* pollen content (up to 27%) and a decrease of *Betula sect. Albae* pollen content (up to 20%) was observed in the zone V (PZ V, 12-8 cm). The Cyperaceae pollen percentage decreased slightly. At the same time, its concentration reached the maximum value.

Sphagnum spore content decreased up to 15%, but its concentration did not change. In contrast to zone 4, the pollen concentration in the zone 5 increases to 100 grains/g. Sharp increase of pollen concentration up to 160 grains/g (its value) was observed at the end zone VI (PZ VI, 8-1 cm) which is the upper part of the core. However, there was no significant change in the content of pollen and spores.

Conclusions

Pollen records from Lebedinoe Lake reflect a mixed type of vegetation in the catchment area.

The predominance of *Betula sect. Nana* pollen indicates the proximity of tundra-like vegetation.

The stable content of *Sphagnum* spores throughout the core indicates the presence of swamps and the process of peat accumulation. The presence of *Alnaster* and *Salix* pollen with *Betula* pollen reflect limited presence of shrub communities. The presence of pollen of *Pinus*, *Picea*, *Larix*, and *Abies* indicates taiga-like vegetation. The climate is characterized as relatively cold and humid according to the laying of bottom sediments. An increase in climate humidity is observed at depths of 30-29, 24-23, 12-11, 2-1 cm of the core, evidenced by an increase in the percentage and concentration of pollen of *Betula*, Cyperaceae, and *Sphagnum* spores. However, generally the pollen records show that severe environmental conditions prevailed on the northern part of the West Siberian plain. Our results are consistent with the data available for the study area. Thus, Lapshina *et al*., [14] suggested harsh tundra environments that prevailed on the Yamal Peninsula.

Area were occupied by moss-lichen pine forests and areas with sparse growth of pine and larch trees, peatlands include lichen-dwarf shrubs or lichen-*Sphagnum*-dwarf shrubs, moss-herb-dwarf shrub communities in the lowlands, and *Sphagnum* and brown mosses.

Acknowledgements

The fieldwork for this study funded by the subsidy altocated to Kazan Federal University for the state assignment (project #671-2020-0049). The laboratory work and the pollen microscopy were supported by the Russian Science Foundation (project 16-17-10118). LF was supported by Russian Foundation for Basic Research (research project № 18-45-140053).

REFERENCES

1. Smol, J. P., Wolfe, A. P., Birks, H. J. B., Douglas, M. S. V., Jones, V. J., Korhola, A., Pienitz, R., Ruhland, K., Sorvari, S., Antoniades, D., Brooks, S. J., Fallu, M.-A., Hughes, M., Keatley, B. E., Laing, T. E., Michelutti, N., Nazarova, L., Nyman, M., Paterson, A. M., Perren, B., Quinlan, R., Rautio, M., Saulnier-Talbot, E., Siitonen, S., Solovieva, N., Weckstrom, J. (2005). Climate-driven regime shifts in the biological communities of arctic lakes. Proceedings of the National Academy of Sciences 102 (12), pp. 4397-4402. DOI: 10.1073/pnas.0500245102.
2. Frolova, L. A. (2017). Cladocera from bottom deposits as an indicator of changes in climate and ecological conditions. IOP Conf. Series: Earth and Environmental Science 107, 012084. Doi :10.1088/1755-1315/107/1/012084.
3. Wetterich, S., Rudaya N., Tumskoy V., Andreev A. A., Opel T., Schirrmeister L., Meyer H. (2011). Last Glacial Maximum records in permafrost of the East Siberian Arctic. Quaternary Science Reviews 30, pp. 3139-3151. Doi: 10.1016/j.quascirev.2011.07.020
4. Zinnatova, E., Frolova, L., Nurgaliev, D. (2019). Diatom complexes in the bottom sediments of big Miassovo lake (South Ural, Russia). International Multidisciplinary Scientific GeoConference Surveying Geology and Mining Ecology Management, SGEM, 19 (5.1), pp. 181-188.
5. Palagushkina, O. V., Frolova L. A., Nazarova, L. B. (2020). Diatoms from modern lake sediments of the Lake Lebedinoe (Yamalo-Nenets Autonomous District, West Siberian Arctic, Russia). Golovkinskie chtenia, in this volume.
6. Frolova, L., Nigmatullin, N., Frolova, A. (2018). Paleolimnological studies of tundra lakes in the pechora delta (Nenets autonomous region, Russia). International Multidisciplinary Scientific GeoConference Surveying Geology and Mining Ecology Management, SGEM 18 (5.1), pp. 621-628.
7. Nigmatullin, N., Frolova, L., Gareev B. (2020). Subfossil cladoceran remains from the bottom sediments of Lake Lebedinoe (Yamalo-Nenets Autonomous Okrug, Arctic Russia). Golovkinskie chtenia, in this volume.
8. Nigamatzyanova, G.R., Frolova, L.A., Kadirov, A.G., Nurgaliev, D.K. (2019). Vegetation Changes during the Holocene Inferred from Pollen Study of Lake Rubskoe Bottom Sediments (European Russia). Paleontological Journal 53 (8), pp. 787-789.
9. Blyakharchuk, T. A., Kurina, I. V., Pologova, N. N. (2019). Late-Holocene dynamics of vegetation cover and humidity of climate in the southeastern sector of the West Siberian Plain according to the data of palynological and rhizopod research of peat deposits. Tomsk State University Journal of Biology 45, pp. 164-189. DOI: 10.17223/19988591/45/9
10. Gvozdetskiy, N. A., Mikhaylov, N. I. (1978). Fizicheskaya geografiya SSSR. Aziatskaya chast': Srednyaya Aziya i Kazakhstan, Sibir', Dal'niy Vostok. Izd. 3-e, ispr. i dop. Uchebnik dlya studentov geogr. fak. un-tov. Mysl', Moscow, 512.
11. Solomeshch, A. I. (2005). The West Siberian Lowland. In L. Fraser & P. Keddy (Eds.), The World's Largest Wetlands: Ecology and Conservation, pp. 11-62. doi:10.1017/CBO9780511542091.003.

12. Filandysheva, L. B., Evseeva, N. S., Zhilina, T. N. (2015). Zonal Features of Climate Regime of the West Siberian Plain and Its Influence on Geosystems. Geography and Natural Resources 36 (4), pp. 341-349.
13. Tarasov, P. E., Guiot, J., Cheddadi, R., Andreev, A. A., Bezusko, L. G., Blyakharchuk, T. A., Dorofeyuk, N. I., Filimonova, L. V., Volkova, V. S., Zernitskaya, V. P. (1999). Climate in northern Eurasia 6000 years ago reconstructed from pollen data. Earth and Planetary Science Letters 171, pp. 635-645.
14. Lapshina, E. D., Kirpotin, S. N. (2003). Natural dynamics of sub-arctic landscapes in the West Siberian plain as indicator of global changes of climate. Proceedings – KORUS 2003: 7th Korea-Russia International Symposium on Science and Technology 4, 1222889, pp. 39-45.
15. Faegri, K., Iversen, J. (1989). Textbook of pollen anlysis. P. 328.
16. Stokmarr, J. (1972) Detervinatio of spore concentration with in electronic particlecounter. Geological, pp. 87-89.
17. Kupriyanova, L. A., Alyoshina, L. A. (1978). Pollen and Spores of Plants from the Flora of European Part of USSR, II, 183.
18. Kupriyanova, L. A., Alyoshina, L. A. (1972). Pollen and Spores of Plants from the Flora of European Part of USSR I, 171.
19. Reille, M. (1995). Pollen et spores d'Europe et d'Afrique du nord Supplement 1. Laboratoire de botanique historique et palynologie, URA CNRS, Marseille, France, 520.
20. Reille, M. (1998). Pollen et spores d'Europe et d'Afrique du nord Supplement 2. Laboratoire de botanique historique et palynology. URA CNRS, Marseille, France, 530.
21. Reille, M. (1992). Pollen et spores d'Europe et d'Afrique du nord. Laboratoire de botanique historique et palynologie. URA CNRS, Marseille, France, 520.
22. Grimm, E. (2004). Tilia software 2.0.2. Illinois State Museum Research and Collection Center, Springfield.
23. Grimm, E. (1987). CONISS: a FORTRAN 77 program for stratigraphically constrained cluster analysis by the methods of incremental sum of squares, Computer and geoscience 13, pp. 13-15.

Subfossil Cladoceran from the Bottom Sediments of Lake Lebedinoe (Yamalo-Nenets Autonomous Okrug, Russia)

NIGMATULLIN Niyaz[1], FROLOVA Larisa[1], GAREEV Bulat[1]

[1] *Kazan Federal University, Kazan (RUSSIA)*
Email: NiMNigmatullin@kpfu.ru

Abstract

Bottom sediments are the natural archives shedding light on the development and changes of the environmental and climatic conditions. Cladocerans are widely used as an indicator group in paleoecological studies: their exoskeleton remains accumulate in bottom sediments and can be helpful in inferring the history of a water body. In this work, an attempt is made to reconstruct the past climatic and ecological conditions of Lake Lebedinoe located in the Yamalo-Nenets Autonomous Okrug. The paleoecology of this region has been poorly studied and, therefore, is of great interest, especially due to the ongoing anthropogenic disturbances of the territory and global climate change. Paleolimnological analysis of the sediment core with a length of 36 cm collected from the studied lake is performed. A total of 28 taxa are registered in the cladoceran assemblage of the lake, with *Bosmina (Eubosmina) longispina* dominant throughout the core.

The obtained data show that Palearctic and Holarctic taxa prevail in the lake, while cosmopolitans account for only 17%. According to the Shannon-Wiener diversity index and the Pantle-Buck saprobity index, the lake is β-mesotrophic and oligosaprobic. Using the results of the cluster analysis, four statistically significant ecological zones are singled out. The results of the statistical and stratigraphic analyses are presented.

Keywords: paleoecology, paleolimnology, Lake Lebedinoe, subfossil cladocerans

Introduction

The Yamalo-Nenets Autonomous Okrug (AO) is located in the north of Tyumen oblast and lies entirely within the low Arctic tundra. Ice-rich permafrost is common here, and the landscapes range from moderately to highly unstable. The area is characterized by relatively homogeneous surficial materials (Pleistocene sands underlain by marine clays) and a pronounced lack of relief [1]. During the summer period, temperatures rise and the top permafrost layer melts, thereby leaving the ground very wet, which results in the formation of marshes and lakes in the tundra. The Yamal Peninsula with its rivers, lakes, and permafrost only 180 m above the sea level is highly vulnerable to future climate change [2]. The average monthly minimum air temperature, in January and February, is about -39 °C. The maximum air temperature, in July, is about 20 °C. Due to weak warming and the polar day and night, the daily variation in the air temperature is almost absent in winter and does not exceed an average of 3 °C in summer. The humidity level is low as well, especially in winter [3].

Along with climate change, petroleum development and land use add significantly to environmental disturbance of the Yamal ecosystems. In this regard, our research is of great interest and importance for solving the problems of sustainable nature management, as well as for reconstructing both climate and environmental change in the past. In this work, a paleoecological study of Lake Lebedinoe was performed using subfossil cladoceran remains.

Methodology

Two sediment cores were sampled during the summer expedition organized in August 2017 to the Yamalo-Nenets AO. The cores were taken from Lake Lebedinoe (64°17.135′ N, 078°07.449′ E) located in the forest-tundra zone and size (2000 x 1000 m). Sampling for paleolimnological analysis followed the recommended procedure: cladocerans must be collected from surface sediments or short and long cores of bottom deposits in the middle or deepest parts of water bodies [4-5]. During the field work, we measured the following parameters of the lake with the help of a WTW 340i hand-held multiprobe: mineralization (TDS), pH, water temperature, dissolved oxygen concentration, and electrical conductivity.

For paleoecological study, one sediment core (17-Ya-02 A) was used. The total length of the core was 36 cm. The core was sliced on site in 1-cm sections that were freeze-dried. The sample preparation method used for cladoceran analysis in our study was an adaptation of the subfossil preparation technique described by A. Korhola and M. Rautio [6]. The samples (0.2-0.5 g of dry sediments) were heated for about 30 min in 10% KOH at 75 °C. The resulting mixture was filtered through a 50-µm sieve. A few drops of ethanol and safranin-glycerin solution were added to prevent fungal growth and to stain the cladoceran remains [7]. All samples were analyzed using a light microscope at 100x/200x/400x magnification. At least 200 individuals were counted per sample.

All individuals were identified to the lowest taxonomic level possible [8]. The chitinous remains of cladocerans were identified with specialized identification keys for subfossil [9] and modern cladocerans [10], [11], [12].

Results and Discussion

The water temperature averaged 15.6 °C. The mineralization degree was low (TDS 8 mg/L).

Based on the hydrogen index value (pH= 6.2), the lake water was characterized as slightly acidic and close to neutral. The electrical conductivity equaled 7.7 µs/cm. The dissolved oxygen concentration was high – 9.9 mg/L (101.7%), thus indicating that the lake is very clean (>95% oxygen concentration).

The cladoceran assemblages of Lake Lebedinoe were quite rich and diverse in terms of their species composition. A total of 4027 cladoceran specimens were registered in sediment core 17-Ya-02 A. The average number of cladoceran specimens per sample was 223.7±3.8, with a minimum of 203 specimens and a maximum of 260 specimens, respectively. A total of 28 cladoceran taxa belonging to 6 families – Dapniidae, Bosminidae, Chydorydae, Cercopagidae, Macrothricidae, and Sididae – were identified, with Bosminidae (51.7%) and Chydoridae (47.6%) occurring most frequently throughout the core. Considering the number of taxa encountered in the studied lake, littoral organisms were numerous, and littoral and pelagic species were found in approximately equal proportions. Species typical of the Palearctic (48%) and Holarctic (35%) zones prevailed, and cosmopolitans accounted for only 17%

According to the Lubarsky scale [13], the pelagic *Bosmina (Eubosmina) longispina* (51.7%), inhabiting small and large water bodies in the north [14], is the dominant species of the lake.

Subdominants were not identified. The following species turned out to be secondary in the lake: *Alonella nana* (12.0%), *Chydorus cf. sphaericus* (11.4%), *Alona affinis* (5.1%), and *Eurycercus sp.* (4.2%). The taxonomic diversity and percentage of littoral and phytophilous species remains indicate that different littoral zones can be distinguished in the lake. Notably, crustacean remains were distributed evenly throughout the core. Of particular interest is that we found *Rhynchotalona latens* (0.2%) rare glacial relict and *Drepanothrix dentata* that habits among vegetation and prefers bottom sediment.

In other few works on the Yamal subfossil communities, 24 taxa were reported, as well as a less diverse species composition of cladocerans, as compared with Lake Lebedinoe. Differences in the complex of dominant species were also found [15].

Based on the changes identified in the composition of subfossil cladoceran assemblages, four stratigraphic zones were singled out through CONISS cluster analysis performed using Tilia 2.1.1. (Fig. 1).

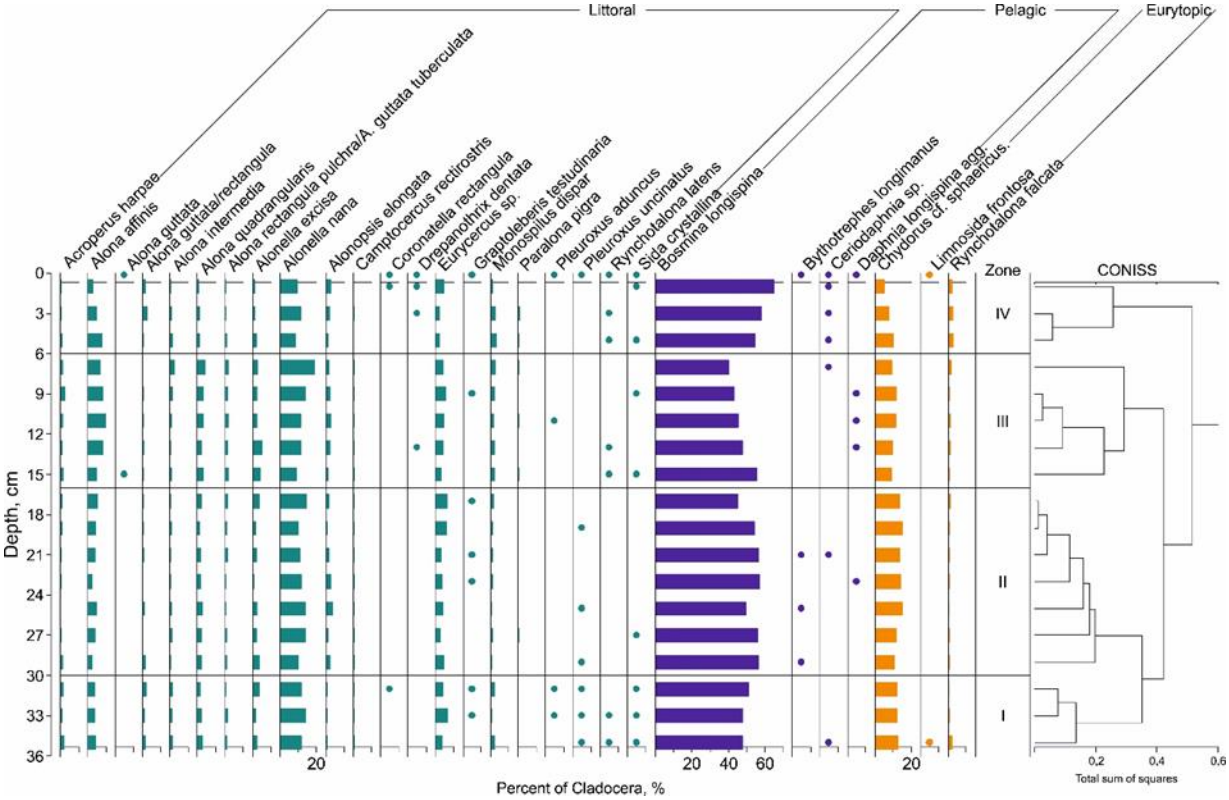

Fig. 1. Stratigraphic distribution of the main cladoceran taxa found in Lake Lebedinoe

The horizon of 36–30 cm was designated as Zone I. In total, 23 cladoceran taxa belonging to 4 families (Dapniidae, Bosminidae, Chydorydae, and Sididae) were present in this zone.

Zone I is characterized by the dominance of *B. (E.) longispina* (307 specimens, 48.9%).

The secondary species were *Alonella nana* (79 specimens, 12.6%), *Chydorus cf. sphaericus.* (78 specimens, 12.4%), and *Eurycercus sp.* (29 specimens, 4.6%). A higher diversity of littoral species during this period may indicate the presence of a large littoral area. The Shannon index varied from 2.37 to 2.52 bit/ind., with the average value of 2.42±0.05 bit/ind. The Pantle-Buck index equaled 1.35±0.00 on average (varying from 1.35 to 1.36), enabling us to characterize the lake as β-mesotrophic and oligosaprobic.

The area with sediment core samples pertaining to the layer of 30-17 cm was considered as Zone II, where 22 cladoceran taxa were found. The average number of cladoceran specimens per sample was 219.86±3.43. *B. (E.) longispina* (824 specimens, 53.5%) was still dominant. Its abundance increased in relation to littoral species, such as *A. nana* (187 specimens, 12.2%) and *Eurycercus sp.* (66 specimens, 4.3%). This may indicate that the trophic status of the lake changed into oligotrophic. The average value of the Shannon index was 2.13±0.06 bit/ind., while the average Pantle-Buck index was 1.34±0.00.

In the horizon of 16-7 cm (Zone III), 24 cladoceran taxa were identified. The species diversity was higher: the number of species varied from 16 to 19. The average number of cladoceran specimens per sample was 238.8±8.7. The dominant *B. (E.) longispina* (555 specimens, 46.5%) gradually became less abundant to the upper part of this horizon. The proportion of such littoral and phytophilic species as *A. nana, A. affinis, A. excise*, and *A. quadrangularis* increased. The growing abundance of *A. affinis*, which prefers stagnant waters, is associated with a change in the trophic status of the lake. The values of the indices change slightly compared to the previous zones: the average value of the Shannon index was 2.48±0.05 bit/ind., while the average Pantle-Buck index was 1.33±0.01.

The sediment core samples of 6-0 cm comprised the stratigraphic Zone IV. Within this zone, 21 cladoceran taxa were found; the average number of cladoceran specimens per sample was 222.0±9.9. *B. (E.) longispina* (395 specimens, 59.3%), which increases to the upper part of the horizon, prevailed. A sharp decrease was noticed in the abundance of littoral and phytophilous species: *A. nana*, *Eurycercus sp.*, and *A. affinis.* A decrease in the number of subfossils remains of the eurytopic *Chydorus cf. sphaericus* was also observed. According to these changes in the composition of subfossil cladocerans, we concluded that the trophic status of the lake changed towards oligotrophy. The average values of the Shannon index (2.05±0.14 bit/ind.) and Pantle-Buck index (1.30±0.01) still characterize the lake as β-mesotrophic and oligosaprobic.

Conclusions

Based on the analysis of the structure of sediment core 17-Ya-02 A taken from Lake Lebedinoe in the Yamalo-Nenets AO, the stages of the lake formation and the changes in the taxonomic composition of subfossil cladocerans were traced. A total of 28 cladoceran taxa were found. *B. (E.) longispina*, a cold-water taxon characteristic of oligotrophic water bodies, was absolutely dominant in all stratigraphic zones. The complex of secondary species included *A. nana*, *Ch. cf. sphaericus*, *A. affinis*, and *Eurycercus sp*. Species typical of the Palearctic and Holarctic zones prevailed.

According to the analysis of the stratigraphic distribution of the main cladoceran taxa, the trophic status of the lake changed throughout the core of bottom sediments. The indices based on the abundance and diversity of subfossil cladocerans characterize the lake as β-mesotrophic and oligosaprobic. Two rare species, *R. latens* and *D. dentata*, were discovered in this region of Russia for the first time, which sparks interest in further research of this region.

Acknowledgements

We thank all colleagues who helped us during the fieldwork. The field work was performed according to the Russian Government Program of Competitive Growth of Kazan Federal University and funded by the subsidy allocated to Kazan Federal University for the state assignment #671-2020-0049. The part of this work concerning the laboratory research and the microscopy of cladocerans was supported by the Russian Science Foundation (project no. 20-17-00135). We thank anonymous reviewers whose constructive comments helped to improve this manuscript. The text of the article was checked by a native English speaker Moses, Isaac Thani (Innopolis University).

REFERENCES

1. Forbes, B. C. (1999). Land use and climate change on the Yamal Peninsula of north-west Siberia: some ecological and socio-economic implications. Polar Research 18 (2), pp. 367-373.
2. Vikhamar-Schuler, D., Hanssen-Bauer I., Forland E. J. (2010). Long-term climate trends of the Yamalo-Nenets AO, Russia. Norwegian Meteorological Institute, 51.
3. Shabanova, N., Channelliere, C. (2013). Climate change on the Yamal Peninsula and its impact on the exogenous processes. SPE Arctic and Extreme Environments Conference, 19.
4. Frolova, L. A. (2018). Cladocera from bottom deposits as an indicator of changes in climate and ecological conditions. IOP Conf. Series: Earth and Environmental Science, Kazan, 4.

5. Lapshina, E. D., Kirpotin, S. N. (2003). Natural dynamics of Sub-Arctic landscapes in the West Siberian plain as indicator of global changes of climate. Proceedings – KORUS 2003: 7th Korea-Russia International Symposium on Science and Technology 4 (1222889), pp. 39-45
6. Korhola, A., Rautio, M. (2001). Cladocera and other branchiopod crustaceans. In: Tracking environmental change using lake sediments (Smol, J. P., Birks, J. B., Last, W. M., Eds.). Kluwer Academic Publishers, Dordrecht, pp 5-41.
7. Frolova, L. A., Nigmatullin, N. M., Frolova, A. A., Nazarova, L. B. (2019). Findings of *Phreatalona protzi* (Hartwig, 1900) (Cladocera: Anomopoda: Chydoridae) in Russia. Invertebrate Zoology 16 (2), pp. 200-210.
8. Frolova, L., Nazarova, L., Pestryakova, L., Herzschuh, U. (2014). Subfossil Cladocera from surface sediment in thermokarst lakes in northeastern Siberia, Russia, in relation to limnological and climatic variables. Journal of Paleolimnology 52 (2), pp. 107-119.
9. Szeroczyńska, K., Sarmaja-Korjonen, K. (2007). Atlas of Subfossil Cladocera from Central and Northern Europe. Friends of the Lower Vistula Society, 84.
10. Kotov, A. A., Sinev, A. Yu., Glagolev, S. M., Smirnov, N. N. (2010). Vetvistousye rakoobraznye (Cladocera). In Opredelitel' zooplanktona i zoobentosa presnykh vod Evropeiskoi Rossii. Tovarishchestvo nauchnykh izdanii KMK, Moscow, pp. 151-276.
11. Flossner, D. (2000). Die Haplopoda und Cladocera (ohne Bosminidae) Mitteleuropas. Backhuys Publishers, Leiden, 428.
12. Smirnov, N. N. (1974). Fauna SSSR, Rakoobraznye. Akademiya Nauk SSSR, Moscow, 268.
13. Lyubarsky, E. L. (1974). K metodike ekspress-kvalifikatsii i sravneniya opisanii fitotsenozov. Kolichestvennye metody analiza rastitel'nosti. Ufa, pp. 123-125.
14. Manuilova, B. F. (1964). Vetvistousye rachki fauny SSSR. Moscow, 526.
15. Frolova, L., Ibragimova, I., Fedorova I. (2016) Stratigraphy of Cladocera in a core from Yamal Peninsula Lake (Arctic Russia). 16th International Multidisciplinary Scientific GeoConference SGEM 2016, 2, pp. 579-586.

Increasing the Republic of Karelia's Sand Resources: Outlook for the Future

NIKIFOROV Alexander[1]

[1] Institute of Geology, Karelian Research Centre, Russian Academy of Science (RUSSIA)
Email: eoaster@yandex.ru

Abstract

Results of the appraisal of Russian Karelia's Quaternary sand deposits, used as building material, are reported. It is shown that sandy moraines, as well as fluvioglacial, fluvial and lacustrine deposits in seventeen study areas could increase Karelia's sand resources for the development of its infrastructure.

Keywords: Holocene, glacial deposits, modulus of sand, lacustrine sediments, Salpausselkä

Introduction

As the development of Arctic Russia and the peri-Arctic regions of the Russian Federation continues, it is important to provide these territories with modern building materials and to increase their mineral potential. Sand-gravel (S-G), boulder-gravel and boulder-pebble deposits, as well as building sand, are commonly used for construction. Coarse and medium-grained sand deposits, as well as sand-gravel-pebble mix deposits, in the southeastern Fennoscandian Shield (Republic of Karelia) are mainly associated with local fluvioglacial sediments in esker ridges and kames [1, 2].

The most accessible sand sources are essential for increasing local resources used for the development of the infrastructure. The data provided were obtained by the author while compiling an engineering-geological zoning map of Karelia [3]. The aim of the present study was to describe accessible and widespread Quaternary deposits with potential for building sand and boulder-pebble-sand mix.

Materials and Methods

Sand samples were obtained using various methods such as core drilling, prospecting pits and extracting. The sands were subjected to a standard set of tests as part of engineering-geological studies (analysis of grain-size composition, organic matter content, the chemical composition of water extract, salinity, carbonate and gypsum content as well as the deformation characteristics of grounds) and classified in accordance with GOST 25100-2011 [4]. A correlation coefficient [5] was used for reducing the grain-size composition indices estimated in accordance with GOST 12536-2014 [6] to a classification consistent with GOST 8726-2014 [7].

Results and Discussion

The study areas were chosen with reference to forthcoming development of the infrastructure and road construction in rapidly growing residential areas (Petrozavodsk, Kondopoga, Kostomuksha, Suojärvi, Medvezhyegorsk, Segezha, Kem and Belomorsk) and developing near-border and peri-Arctic areas (Lahdenpohja, Muezerka, Louhi and Belomorsk districts). Fig. 1 shows that most of the large prospected sand deposits are associated with glacial-stage marginal deposits as well as fluvioglacial and lacustrine strata [1, 8]. Sand samples of various facies from the study areas were taken. These deposits of various facies are often present in one sequence; interestingly, younger strata were produced by the redeposition of older ones.

Holocene alluvial and lacustrine deposits (aQH and lQH) are the youngest; they rest on fluvioglacial (fgQIII), lacustrine-glacial deposits (lgQIII) and moraines (gQIII) associated with glacial activity.

The results of sample analysis were processed statistically and are shown in Table 1. The sand deposits are also described (absolute altitudes, thickness and area).

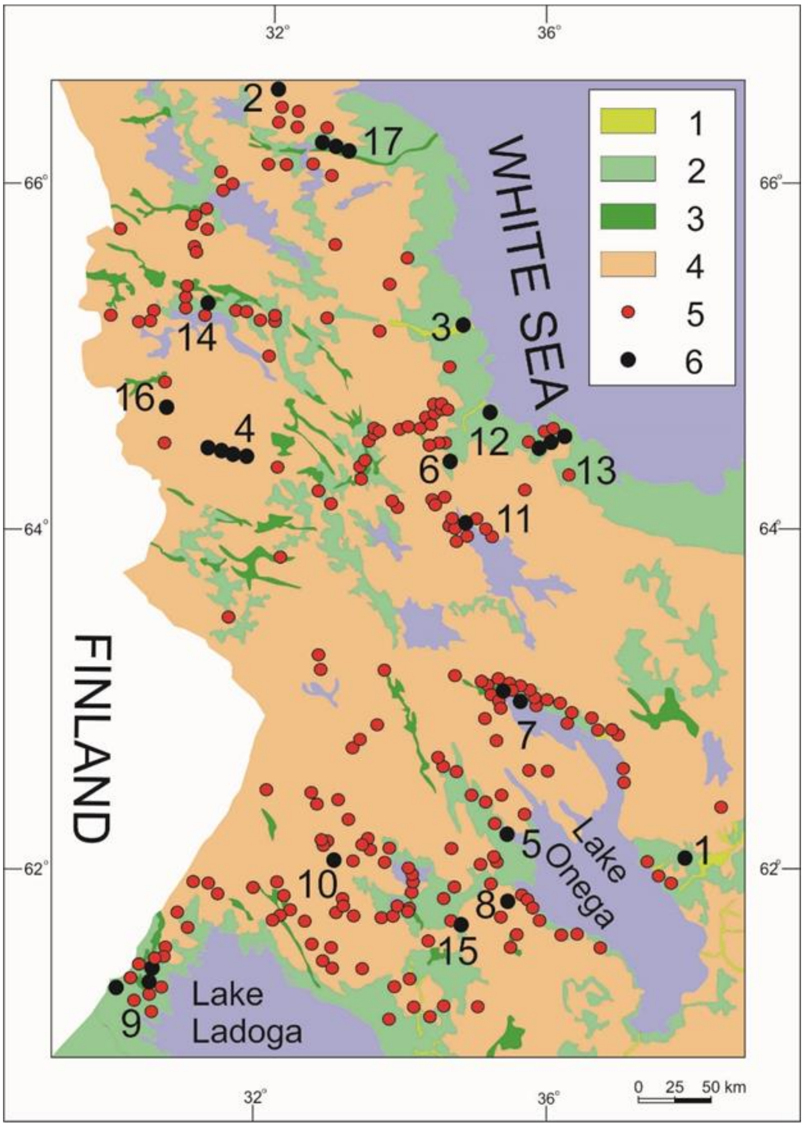

Fig. 1. Summary map based on [1], [9], [10]. 1. Fluvial deposits; 2. lacustrine-glacial and lacustrine deposits; 3. fluvioglacial deposits (esker, delta, sandur, sorted ice-marginal formation, interlobate and till-covered esker); 4. Glacial deposits (gravelly, sandy, silty and clayey moraine), 5. large and medium sand deposits. 6. study areas according to Table 1

Table 1. Geological summary characteristics of promising sequences and the sand coarseness modulus

Study area and its brief description.	Sediment facies.	Absolute altitudes of strata, m.	Sand size modulus range Ms (number of tests).	Average value of the size modulus, Ms.	Sand group and class according [7].	identification of soil according [8].
1, Vodla river bed (fluvial deposits).	aQH	15-25	0,72-1,12 (10)	0,95	very fine and fine, class II	FSa, grFSa.
	lgQIII	28-50	1,5-1,79 (12)	1,62	fine, class II	FSa.
2, main moraine (sandy-gravel).	gQIII	15-46	2,5-3,09 (6)	3,07	coarse and oversized, class I-II	CSa, saGr.
	gQIII	2-30	2,3-2,72 (7)	2,35	medium, class II	boMSa.
3, main moraine and fluvial deposits of the White Sea lowland.	aQH	0-10	2,25-4,64 (8)	2,98	coarse, class II	CSa, grCSa.
	gQIII	0-20	2,8-3,07 (3)	2,94	coarse, class I-II	CSa, boCSa
4, main moraine (sandy-gravel).	gQIII	150-170	1,05-3,3 (16)	2,13	medium, class II	boMSa.
	gQIII	188-212	0,96-1,63 (6)	1,4	very fine, class II	boFSa.
5, main moraine of the N (Neva) stage.	gQIII	51-64	0-3,24 (11)	1,42	very fine, class II	boFSa.
6, main moraine of the N stage.	gQIII	37-43	0,6-4,7 (4)	2,08	medium, class II	boMSa, coMSa.
7, modern lacustrine sediments.	lQH	22-37	0,63-3 (11)	1,46	very fine, class I	FSa.
	lQH	54-88	0,81-1,57 (12)	1,15	very fine, class II	FSa.
	lQH	29-38	1,18-3,6 (13)	1,90	fine, class I	MSa, FSa.
8, fluvial and fluvioglacial sediments in the area of clayey-loam main moraine of the N stage.	fgQIII	57-87	1,7-4,76 (12)	3,55	oversized, class II	Gr, saGr.
	aQH	41-53	0,75-1 (4)	0,84	very fine, class II	siFSa, FSa.
9, fluvioglacial deposits of Salpausselkä stage and lacustrine sediments of the Ladoga basin.	lgQIII	35-57	0,15-1,2 (41)	0,53	very fine, class II	FSa.
	lQH	13-48	0,53-0,99 (8)	0,79	very fine, class II	coFSa.
	lQH	13-48	1,09-2,04 (9)	1,56	fine, class II	coFSa.
	lQH	13-48	2,47-3,57 (7)	2,77	coarse, class II	CSa, grCSa.
	fgQIII	58-102	0,66-1,62 (15)	1,29	very fine, class I	coFSa.
	fgQIII	44-84	1,33-2,27 (7)	1,82	fine, class I	coFSa.
10, lacustrine-glacial and glacial deposits.	gQIII	149-153	0,9-3,3 (14)	1,88	fine, class II	boFSa.
	lgQIII	160-169	0,4-0,72 (4)	0,43	very fine, class II	FSa.

11, modern lacustrine sediments and moraine sands	gQIII	86-97	0,71-2,61 (82)	1,47	very fine and fine, class II	boFSa.
	lQH	79-102	0,2-2,91 (56)	1,57	fine, class I-II	FSa.
12, main moraine of the White Sea lowland.	gQIII	5-13	1,08-1,45 (8)	1,81	fine, class II	boFSa.
13, fluvioglacial sands of the White Sea lowland.	fgQIII	2-16	1,47-3,82 (4)	2,74	coarse, class II	boCSa, CSa.
14, lacustrine-glacial and glacial deposits.	gQIII	105-123	0,1-2,77 (8)	0,934	very fine, class II	boFSa.
	lgQIII	99-117	0-1,33 (25)	0,11	very fine, class II	coFSa, FSa.
15, moraine and fluvioglacial sands of the N (Neva) stage.	fgQIII	80-109	1,05-1,45 (3)	1,26	very fine, class II	coFSa.
	fgQIII	80-109	0,83-1,36 (4)	0,97	very fine, class II	coFSa, FSa.
	gQIII	80-109	0,72-2,41 (4)	1,46	very fine and fine, class II	boFSa.
16, moraine and fluvioglacial sands.	gQIII	213-220	1,22-2 (8)	1,58	fine, class II	boFSa.
	fgQIII	220-223	1,8-2,91 (4)	2,36	medium, class II	MSa, coMSa.
17, moraine and fluvioglacial sands.	fgQIII	83-97	2,3-2,87 (3)	2,51	Medium and coarse, class II	MSa, CSa.
	gQIII	83-97	0,8-1,6 (30)	1,24	very fine, class II	boFSa.

The Table was analyzed and the sand deposits were divided into the following groups:

1. *Glacial deposits proper:*

Basic sandy moraines. occurring to the north-west of Neva glaciations stage marginal deposits, are consistent with fine, medium-grained and coarse sands that can be used after the removal of boulder and silt fractions by dressing.

2. *Fluvioglacial deposits:*

Local intra- and intermorainic deposits of fluvioglacial genesis, up to 10 m in thickness, in thick basic loamy and sandy loamy moraine areas (Neva, Luga and Vepsovian-Krestets glaciations stages) are promising. Often thick (0,6-2 m.) ablation moraine layer rests on a 5-10 m. thick medium-grained sand layer in a hilly area. Such small occurrences have already been quarried for replenishing resources [10]. Sand deposits in NW Karelia and especially Salpausselkä I and II end-moraines are highly homogeneous.

3. *Lacustrine-glacial deposits:*

Almost all of the periglacial lacustrine deposits studied consist of very fine sand; they have the positive property of a high homogeneity, as revealed earlier [2] and supported analytically during our study.

4. *Lacustrine deposits:*

Modern lake deposits are a promising source of well-sorted fine, medium-grained and coarse sand of class I. The thickest sand sequences were studied in the Medvezhyegorsk and Segezha areas.

5. *Fluvial deposits:*

The composition of fluvial deposits depends on the existing hydrographic network and the rocks eroded by rivers. Sand samples of varying grain size from the study areas were analyzed.

They all occur locally and are most commonly identified as river channel or flood plain alluvium.

Conclusions

The results of our studies show that Republic of Karelia's sand resources could be considerably increased by quarrying widespread small local occurrences. Most of them could be located and subjected to engineering-geological study considering regional geological setting. This approach is effective both economically and ecologically, because it utilizes sand resources of areas that are already being developed. None of Karelia's Quaternary sands analyzed contained carbonates, sulfides, oil shale or water-soluble compounds.

Acknowledgements

The work was carried out in the framework of the research program RAS № 210: "Minerageny, technological and ecological-economic assessment of potential mineral resources of the territory of the Republic of Karelia". Registration number: AAAA-A18-118020290175-2.

REFERENCES

1. Demidov, I. N. (1998). Stages of formation and localization pattern of Karelia's useful minerals in the Quaternary Period. Geology and useful minerals of Karelia 1, pp. 137-142.
2. Evzerov V. Ya. (2019). Types of deglaciation and distribution of building material deposits in the Late Pleistocene-Holocene deposits of the Karelian-Kola Region. Vestnik VGU. Geology series 58-63. 10.17308/geology.2019.1/1705.
3. Nikiforov A. (2018). Engineering geological zoning of Karelia (Russia). SGEM2019 GeoConference Proceedings 1.2, pp 177-184.
4. GOST 25100-2011. Grounds. Classification
5. Kozlov A. V. (2011). On the consistence of GOST 25100-95 and GOST 8736-93 classifications for sand based on coarseness. Vestnik MGSU 1997-0935, 3-2 123-127, pp. 123-127.
6. GOST 12536-2014 Grounds. Methods for laboratory analysis of grain-size and microaggregate composition.
7. GOST 8736-2014 Sand for building operations. Technical specifications (Corrected).
8. ISO 14688-2:2017 Geotechnical investigation and testing – Identification and classification of soil – Part 2: Classification principles and quantification of descriptive characteristics
9. Niemelä J., Ekman I. & Lukashov A. (eds.) (1993). Quaternary deposits of Finland and Northwestern part of Russian Federation and their resources. Scale 1:1 000 000. Espoo: Geological Survey of Finland.
10. Mikhailov V. P. *et al*., (2006). Republic of Karelia's mineral potential. Book 2: Nonmetallic useful minerals. Underground water and curable muds. Petrozavodsk, Karelia Publishers. 3554.

On the Genesis of Kem Clays from the White Sea Shore, Republic of Karelia, Russia

NIKIFOROV Alexander[1], SHELEKHOVA Tatiana[1]

[1] *Institute of Geology, Karelian Research Centre, Russian Academy of Science (RUSSIA)*
Email: eoaster@yandex.ru

Abstract

The results of an integrated study of Kem clays are reported. The clays' facies were determined and the various engineering-geological properties of the clays were analyzed. The clays were shown to be less strong than marine deposits. The results obtained can be used for conducting engineering research and for further study of Quaternary rocks from the White Sea Lowland.

Keywords: Karelia, Holocene, diatoms, clay, alluvium, elastic silt, plasticity index

Introduction

Clay formation in the Republic of Karelia is usually associated with periglacial basins that existed on the glacier margin. The study area lies in the City of Kem. The map of Finland's and NW Russia's Quaternary rocks [1] shows homogeneous clay-silt deposits (with no reference to their facies) and peatlands in this area. The lower Kem River area was previously studied by many researchers. The results of their studies were presented by G. S. Biske [2]. She pointed out that the shells of the marine mollusk *Yoldia arctica*, as well as diatom flora, had been found in Kem River clays, "suggesting that the clays formed in a sea supplied with large amounts of fresh water". Clays from Poduzhemye Town were found to contain freshwater diatoms of the genera *Eunotia* spp. and *Pinnularia* spp. characteristic of water bodies with an abundance of humic acids. As early as 1948, N.I Apukhtin [3] assumed that the clays making up the Kem River valley were deposited "in closed lakes discharged later by the Kem River". Scarce finds of *Yoldia arctica* do not prove a Late Glacial age for these deposits. "Neither the age, nor the marine genesis of the clays have been firmly proved" [2]. Although the above studies show that the clays evolved under continental conditions, the authors of special engineering-geological publications argue that clays from the White Sea Lowland are associated with marine deposits.

Marine clays and loams have distinctive physical properties. They are commonly described as poor water-saturated grounds. The engineering-geological zones map of the Murmansk Region and the Karelian ASSR [4] shows that extraglacial Holocene deposits of marine (clay and loam) and continental (peat) genesis are widespread there.

Fig. 1 illustrates the current concept of the structure of Quaternary deposits in the Kem area.

Materials and Methods

Boring was done and core samples were taken in the study area. Boreholes were drilled 10-15 m. apart within and away from the Pueta River channel along a continuous profile throughout the entire Quaternary rock sequence as deep as the top of the bedrock. The cores were described lithologically and samples for integrated study were taken. Geophysical work (georadiolocation survey with an EYE-2 instrument) was performed for the detailed study of the profile. The clay samples were analyzed by the laboratory methods used in engineering geology (analysis of grain-size composition, organic content, chemical analysis of water extract, salinity, carbonate content, gypsum content and the deformation characteristics of the grounds). Lithological, paleontological, X-ray structural (XSA) and X-ray fluorescent (XFA) analyses were done in the Common Use Centre at the Institute of Geology, KarRC, RAS. The aim of our study was to determine the facies of Kem clays and to describe their engineering-geological characteristics.

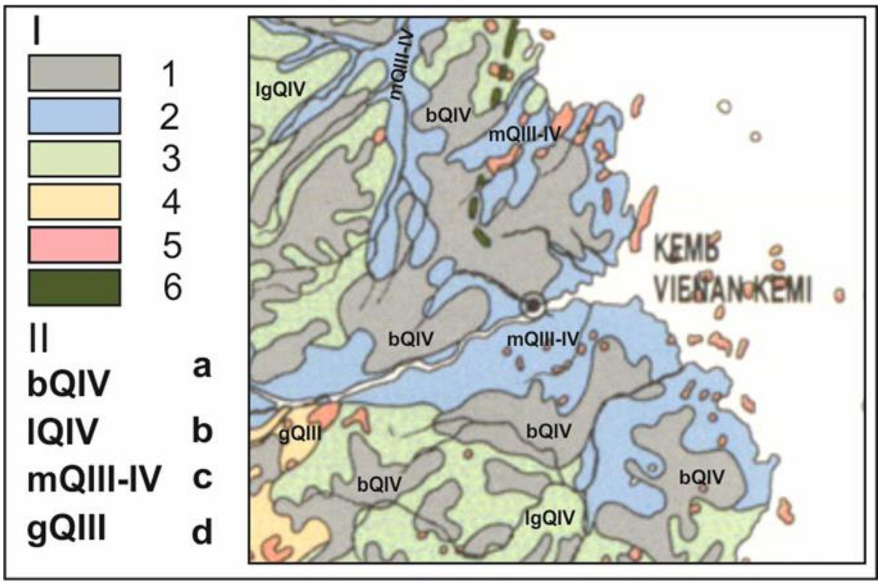

Fig. 1. Summary sketch map based on: [1] I: 1. Peat deposits, 2. Homogeneous clay and silt deposit, 3. Gravel and sand deposit outside eskers, 4. Semigravel and sandy till, 5. Precambrian rocks, 6. Esker, delta, sandur. [2] II: a. peat deposits, b. lake deposits, c. marine deposits, d. glacial deposits

Results and discussion

Well-developed clays overlain by a thin soil layer were revealed in the stratigraphic sequence.

The clays are softly-plastic, quick-plastic and quick. They contain organic matter and look like consolidated gyttja (sediment rich in organic matter deposited at the bottom of a eutrophic lake).

They are underlain by semigravel and coarse sands with pebbles, mostly moist and water-saturated below the groundwater level. The sands were produced by the scour and redeposition of moraines of different ages. They correspond in composition to semigravel sand with up to 5% pebbles and boulders and are described as coarse clastic alluvium ground [5]. The base of the stratigraphic sequence consists of bedrock (gneissose granite). The composite geological profile, made up using geophysical and other methods, is shown in Fig. 2. Grain-size analysis of Kem clays (Table 1) has shown that they consist mainly of clay and silt particles. From the point of view of engineering geology, the grounds are light, as indicated by their plasticity [6].

The low density (ρ), high degree of saturation (Sr) and porosity (n) of the clays indicate the poor ordering of their particles. When used in engineering geology, these clays may display thixotropic properties.

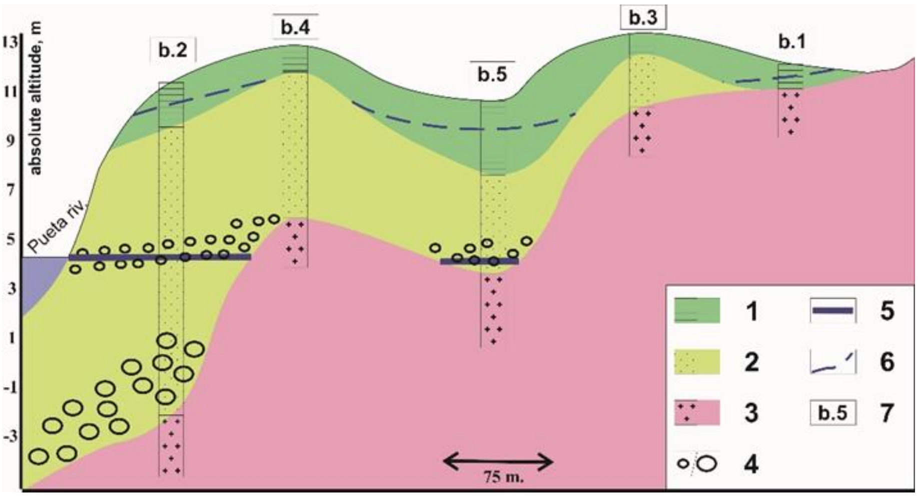

Fig. 2. Geological profile across the Pueta River right bank and the adjacent area. The profile line is perpendicular to the river channel. 1. – firm-stiff, firm and soft clays; 2. –gravel and sand with up to 5% boulders and pebbles to 5%; 3. – slightly fractured gneissose granite; 4. – pebbles and boulders; 5. – constant groundwater level; 6. – top of weak quick clay; 7. – boring point numbers

Table 1. Physico-mechanical characteristics of clays

Borehole number			2	2	3	3	5	5	5	5	5
Sampling depth			1.0	1.5	0.2	0.7	1.1	1.3	2.2	2.4	2.6
Grain-size composition, %	**sand**	**0.5-0.25**		0.02							
		0.25-0.1	0.05	0.05		3.57	0.29				0.30
	silt, mm	**0.1-0.05**	16.04	15.55	16.21	18.18	14.56		2.86		14.9
		0.05-0.01	31.07	23.87	22.87	29.12	32.79		43.44		26.70
		0.01-0.005	16.93	18.02	17.02	13.29	17.89		20.40		21.30
	clay, mm	**0.005-0.002**	14.90	16.47	18.21	15.78	23.20		15.54		
		<0.002	21.00	26.02	25.69	20.06	11.27		17.76		36.80
Liquid limit		**%**	36.21	45.92	35.72	38.26	35.02	47.80	37.92	42.20	61.20
Plastic limit		**%**	17.86	22.81	16.81	19.81	11.12	25.80	16.72	24.50	33.30
Plasticity index		**%**	18.35	23.11	18.91	18.45	23.91	22.00	21.20	17.70	27.90
Water content		**%**	24.22	34.11	22.00	24.20	20.56	36.30	21.77	68.40	95.60
Liquidity index		**u.f.**	0.35	0.49	0.27	0.24	0.39	0.48	0.24	2.48	2.23
Degree of saturation		**%**	70.14	97.35	61.86	67.05	56.13	95.87	60.32	99.66	100.54
Solid particles density		**g/cm^3**	2.71	2.71	2.71	2.71	2.71	2.72	2.71	2.73	2.74
Soil density		**g/cm^3**	1.84	1.85	1.77	1.79	1.80	1.82	1.87	1.60	1.48
Dry soil density		**g/cm^3**	1.40	1.39	1.38	1.37	1.36	1.34	1.37	0.95	0.76
Porosity		**%**	0.48	0.49	0.49	0.49	0.50	0.51	0.49	0.65	0.72
Coefficient of porosity		**-**	0.94	0.95	0.96	0.98	0.99	1.03	0.98	1.87	2.61

The results of XSA and XFA (Table 2) show that the clays consist dominantly of silty particles of quartz, microcline, albite, actinolite and the only layered mineral-muscovite. Such a composition is characteristic of the primary products of weathering of metamorphic complexes in the Belomorian Mobile Belt followed by their transport. The presence of annite, a mineral characteristic of Khibiny mountain range rocks, is indicative of a large watershed area. Clayey minerals such as kaolinite and montmorillonite, the end products of aluminosilicate weathering, are not found. The clays contain organic matter, which stains them black. It is known, however, that sediments accumulating in water bodies located in close proximity to extensive ice sheets are poor in organic matter. The results of diatom analysis show that diatom flora did not evolve during clay accumulation. Its absence in the clays analyzed does not support the assumption that the clays making up the Kem River valley were deposited "in closed lakes discharged later by the Kem River" (according to [3]). Thus, the restriction of the clays to river valleys and their mode of occurrence suggest that clay deposition took place under alluvial rock formation conditions.

Table 2. Summary table showing the results of XFA and XSA (absolute altitudes are shown in parentheses)

Boreholes, [sampling depth] and (absolute altitudes), m.	Borehole 2 [1.15] (10.35)	Borehole 2 [1.25] (10.25)	Borehole 2 [1.7] (9.8)	Borehole 5 [2.0] (8.75)	Borehole 5 [2.4] (8.35)
Constituent	**%**	**%**	**%**	**%**	**%**
SiO_2	69.00	67.90	51.52	55.81	67.62
TiO_2	0.59	0.58	0.88	0.80	0.61
Al_2O_3	13.64	13.84	16.99	16.15	13.64
Total Fe_2O_3	3.85	4.26	9.53	8.21	4.66
MnO	0.06	0.05	0.10	0.10	0.06
CaO	3.14	3.06	2.25	2.57	3.20
MgO	2.14	2.01	4.39	3.92	2.06
K_2O	2.15	2.12	3.59	3.18	1.99
P_2O_5	0.11	0.13	0.15	0.14	0.14
Na_2O	2.85	3.27	2.14	2.37	2.76
S	0.01	0.01	0.01	0.03	0.03
Loss on ignition	2.14	2.60	8.21	6.43	2.88
Total for oxides + loss on ignition	99.68	99.83	99.76	99.71	99.65
Mineral composition	Quartz, Albite, Microcline, Muscovite, Actinolite	Quartz, Albite, Microcline, Muscovite, Actinolite	Quartz, Albite, Microcline, Muscovite, Actinolite, Clinochlore	Quartz, Albite, Microcline, Muscovite, Annite, Actinolite	Quartz, Albite, Microcline, Muscovite, Annite

Paleontological analysis has also revealed no marine fauna in the clays, suggesting continental facies conditions. Organic matter, present in the form of consolidated mud, is abundant (>5%). In accordance with existing regional tables [5], the normative characteristics of modern marine clays and loams at a porosity coefficient (e) of 0.95-1.05 and a liquidity index (I_L) of 0-1 are: φ=16-21, C=15-21 KPa, E=6-9 MPa. The same indices for the clays analyzed, obtained by triaxial compression (φ, C, E) and uniplanar section (φ, C) tests are: φ=9.8-13.5, C=11-25 KPa, E=2.2-2.7 MPa. Thus, the grounds analyzed are not as strong as Holocene marine deposits.

Conclusions

The results of our studies show that the clays analyzed are consolidated mineral-rich flood plain mud deposits of non-glacial and non-marine origin. They cover large areas, not only within the modern Kem River channel and tributaries but also in modern watersheds at an absolute altitude of up to 25 m, resting on sandy alluvium, sand-gravel moraines and

Precambrian rocks. The clays studied are described as weak ground with low strength and density.

Acknowledgements

The work was carried out in the frameworks of the research program RAS № 210 (registration number: AAAA-A18-118020290175-2) and RAS № 214 (registration number: AAAA-A18-118020690231-1).

REFERENCES

1. Niemelä J., Ekman I., Lukashov A. (eds.) (1993). Quaternary deposits of Finland and Northwestern part of Russian Federation and their resources. Scale 1:1 000 000. Espoo: Geological Survey of Finland.
2. Biske G. S. (1959). Quaternary geology and geomorphology of Karelia. Petrozavodsk, Gosizdat KASSR, 307.
3. Apukhtin N. I. (1948). On the stratigraphy of marine and glacial deposits in Trans-Onega Karelia. Izvestiya Karelo-Finsk. Filiala AN SSSR 4.
4. 1: 1500000 scale maps of the engineering-geological zoning of the Murmansk Region and the Karelian ASSR/ Edited by I. K. Zaitsev (1967).
5. Levkin Yu. M., Serba B. I., Samokhvalov V. A., Antonov S. A. (2002). Karelia's grounds. 2nd edition (supplemented); PetrGU, Petrozavodsk, 212.
6. GOST 25100-2011. Soils. Classification.

Identification of Structural Forms, Based on Structural Surfaces and Thickness Map Analysis of Devonian and Lower Carboniferous Deposits of the South Tatar Arch

NOVIKOVA Svetlana[1], SIDOROV Sergey[1], RIZVANOVA Zilia[1]

[1] Kazan Federal University, Kazan (RUSSIA)
Email: novikovaspn@gmail.com

Abstract

This paper presents the results of modern structural surface and thickness map analysis of Devonian and Lower Carboniferous deposits in the North-Almetyevskaya area of Romashkino oilfield (Republic of Tatarstan). We used seismic and well logging data for map construction.

Structural form and thickness of each studied stratigraphic unit were compared based on the constructed maps. The direction of vertical surface movement in different periods, the intensity of uplifts (erosion) or subsidence (deposit accumulation) of some parts of the territory were defined.

This allowed a more accurate determination of the boundaries of the Altunino-Shunaksky and Minibaevsky troughs.

Keywords: Devonian, Carboniferous, tectonics, troughs, paleogeography, sedimentation

Introduction

Devonian troughs have been identified by many scientists [1], [2], [3] in the 1970-1980s, and remain a focus of research in the 21st century [4]. This is because the troughs can work as barriers and can control the oil-bearing capacity of the traps. Common features of the troughs include [5]: linearity, asymmetry of flanks, and conjugation with basement faults. The troughs are identified as regional elements, and in some cases more accurate definition of their boundaries requires detailed study. For example, it has been shown that morphology of troughs may affect development of oil deposits [4].

The purpose of this work is to study the origin and evolution of Altunino-Shunaksky and Minibaevsky troughs using structural and thickness maps. Maps were constructed using well logging and seismic (3D common-midpoint (CMP)) data, which are the most accurate data in the study of deep-seated structural forms.

Identifying troughs in the sedimentary cover section is relevant, because they are applied for more accurate definition of hydrocarbon deposit structure and the morphological features of troughs should be taken into account during oilfield development.

Object and research methodology

The object of investigation is the giant Romashkino oilfield (Fig. 1, I), which is located in the east of the East European Platform (EEP), within the Volga-Kama Anteclise, and belongs to the South Tatar Arch (STA), which is a large structural element of the first order. Within the STA, many oil accumulations have been identified in the rocks deposited during the period from the Eifelian Stage of the Middle Devonian to the Visean Stage of the Lower Carboniferous (Fig. 1, II).

The study area is confined to a platform-type area with stable geodynamic conditions. It includes deep faults and troughs of the platform sedimentary cover. According to the tectonic zoning scheme of the Republic of Tatarstan [6], the studied territory is confined to the top of the STA and its western slope. The boundary between these two zones along the top of the crystalline basement is the submeridional Altunino-Shunaksky fault. The presence of cataclasis and mylonitization in the basement rocks indicates the tectonic origin of the fault.

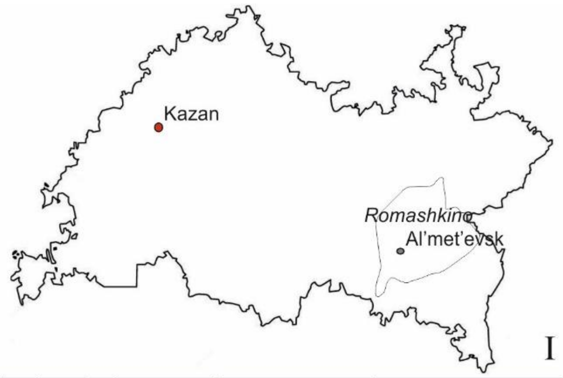

System	Series	Stage	Substage	Suprahorizon	Horizon	
Carboniferous	Lower	Visean	Upper		Venevian	
					Mikhailovian	
					Aleksinian	●
			Middle		Tulian	●
					Bobrikian	●
			Lower		Radaevkian	
					Kosvian	
		Tournaisian	Upper	Shurinovian	Kizelian	●
					Cherepetian	●
			Lower	Khaninian	Upian	
					Malevkian	
Devonian	Upper	Famennian	Upper	Zavolzhian	Ziganian	●
					Khovanshchinian	●
					Ozerkian	
			Middle		Dankovian-	
					Lebedyanian	
			Lower		Eletsian	
					Zadonian	
		Frasnian	Upper		Evlanovian	
					Livenian	
					Voronezhian	
					Rechitsian	
			Middle		Semilukian	
					Sargaevain	
			Lower		Timanian	●
					Pashyian	●
	Middle	Givetian		Starooskolian	Mullinian	
					Ardatovian	●
					Vorobyovian	●
		Eifelian			Biyian	

II

Fig. 1. I – Location of Romashkino field on the territory of the Republic of Tatarstan; II –composite generalized stratigraphic section, ●-oil-bearing stratum

The active period of fault development is the Late Timanian-Sargaevian time [5]. According to the results of seismic surveys and deep drilling, the surface of the crystalline basement has a step-like pitch in the western direction and multidirectional faults. The eroded surface of the Archean basement is overlain by sedimentary rocks.

Riphean and Vendian deposits are absent in the study area [6].

We studied Middle and Upper Devonian and Lower Carboniferous deposits, including the Timanian, Semilukian, Evlanovian, Livenian, Dankovian, Lebedyanian horizons and Zavolzhian suprahorizon of the Upper Devonian and Tournaisian and the Tulian Horizon of the Visean.

We used seismic surveys (3D CMP) and well logging data of 1921 vertical and directional wells.

We constructed structural maps and thickness maps of the studied beds using well tops and seismic maps of reflection horizons.

Petrel (2013) software were applied for map construction. The evolution of the area surfaces was studied using structural analysis [7], [8], which included comparison of modern structural plans and the thickness thicknesses.

Analysis was carried out based on the constructed structural forms, and thicknesses were compared for each stratigraphic unit.

Therefore, the vertical direction of surface movement in different periods, the intensity of uplifts of some parts of the territory (erosion) or subsidence (deposit accumulation) can be established. A method of hiatuses and unconformities was applied [6].

Research and discussion result

Based on geophysical data, structural and thickness maps of the studied layers were constructed.

Structural maps were constructed along the tops of the Timanian, Semilukian, Evlanovian, Livenian, Dankovian, Lebedyanian horizons and Zavolzhian suprahorizon of the Upper Devonian and Tournaisian, Tulian horizon of the Lower Carboniferous. Thickness maps of the Semilukian Horizon, the Upper Frasnian, the Middle-Lower Famennian, Zavolzhian Superhorizon, Tournaisian Stage, the Lower and Middle Visean substages were constructed.

Paleogeography of the Middle and Upper Devonian is mainly associated with a marine transgression [5].

In the *Eifelian time* [9], [10], the transgression began, marine sedimentation was confined to subsided areas (depressions, saddles) resulting in the sandstone and carbonate-argillaceous sequences.

In the *Givetian*, horizontal and vertical tectonic movements occurred [9], [10], which resulted in frequent changes of depositional settings and development of various facies zones.

Sandy, sandy-siltstone and shale-siltstone sediments with limestone interlayers predominate.

Marine sedimentation continued.

In the *Late Pashyian*, the seabed mobility in the northeast of Tatarstan increased, which was the beginning of the STA modern peak bending. The geological section of this time is represented by sandstones, siltstones and clays.

In the *Timanian,* the marine transgression continued. Open sea conditions are established and carbonate sediments are deposited in second part of Timanian time. The structural map of the terrigenous Devonian rocks top has more smoothed forms compared to the crystalline basement.

This surface represents a small slope in the northwest direction with a smooth relief complicated by local uplifts of small amplitude. On the top of the Timanian horizon, the Altunino-Shunaksky fault coincides with the similar graben-like trough, which can be traced in the western part of the territory (Fig. 2. I). In the northern part of the territory, Minnibaevsky trough of the northeastern strike was laid, which in the future would affect the formation of overlying strata.

In the *Middle Frasnian* (Sargaevian, Semilukian, Rechitsian horizons), marine transgression continued. The entire territory was an open shelf area of a shallow sea basin.

In the *Semilukian*, the progressive depression of the marine basin and a stable tectonic regime continued (Fig. 2. II). Carbonate and carbonate-argillaceous sediments accumulated in this time.

The thickness of sediments increases from the east to west, in the center of the site – 50 meters, in the region of the Minnibaevsky depression 45–50 meters, in the Altunino-Shunaksky trough – 60-70 meters (Fig. 3. I). The sediment thickness decreasing in the Minibaevsky trough may be a result of this area's uplift in the Semilukian time. It is possible that a neighboring block was approaching from the northwest. In the Semilukian, global stretching of the EEP eastern margins occurred, which in some areas led to the appearance of systems of faults in the crystalline basement, which influenced further formation the paleorelief. Also, from the Semilukian time to the beginning of the Visean, the Kama-Kinel deflections system (KKDS) developed [11], the Minnibaevsky Trough also continued developing.

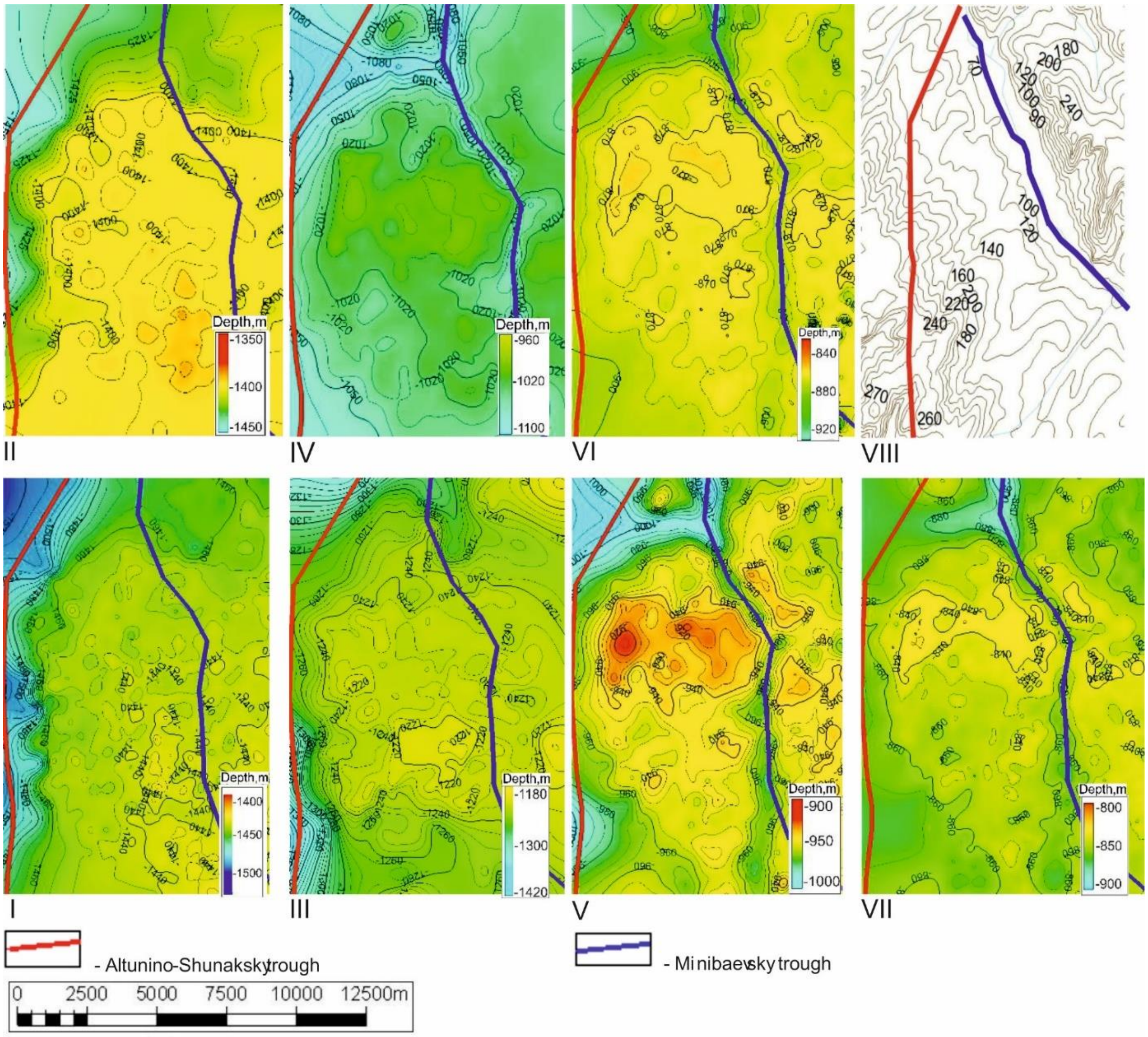

Fig. 2. Structural maps along the tops: I – Timanian; II – Semilukian; III – Evlanovian-Livenian; IV – Dankovian-Lebedyanian; V – Zavolzhian; VI – Tournaisian; VII – Tulian horizon; VIII – surface contour map

A regression in the Devonian basin began in the *Upper Frasnian* (Rechitsian, Voronezhian, Evlanovian, Livenian horizons). Carbonates were deposited in a gradually shallowing basin in relatively stable tectonic settings. The surface of the Upper Frasnian deposits (the surface of the Evlanovian-Livenian Horizon) is an extensive uplift that generally repeats the structural features of the terrigenous Devonian top layers. Several low-amplitude elevations of different shapes are recorded in the study area (Fig. 2. III). The southern part of the area about the hypsometric curve -1220 meters is most likely complicated by a reef buildup, which appeared due to a local elevation of a part in the Devonian time. The shape of the reef buildup is close to isometric with rough contour, the amplitude is about 20 meters from the closing hypsometric curve -1230 meters. Small amplitude elevations (not more than 8 meters) are presented in other parts of the territory. The active zone of the Altunino-Shunaksky trough remained.

At the end of the *Evlanovian-Livenian*, the marine basin shallowed and the deposits were in some places eroded, resulting in a thickness change and complexity of correlations. The thickness of the Upper Frasnian deposits is regular along the section and equal to 160-170 meters (Fig. 3. II), except for Minnibaevsky trough region, where according to well logging

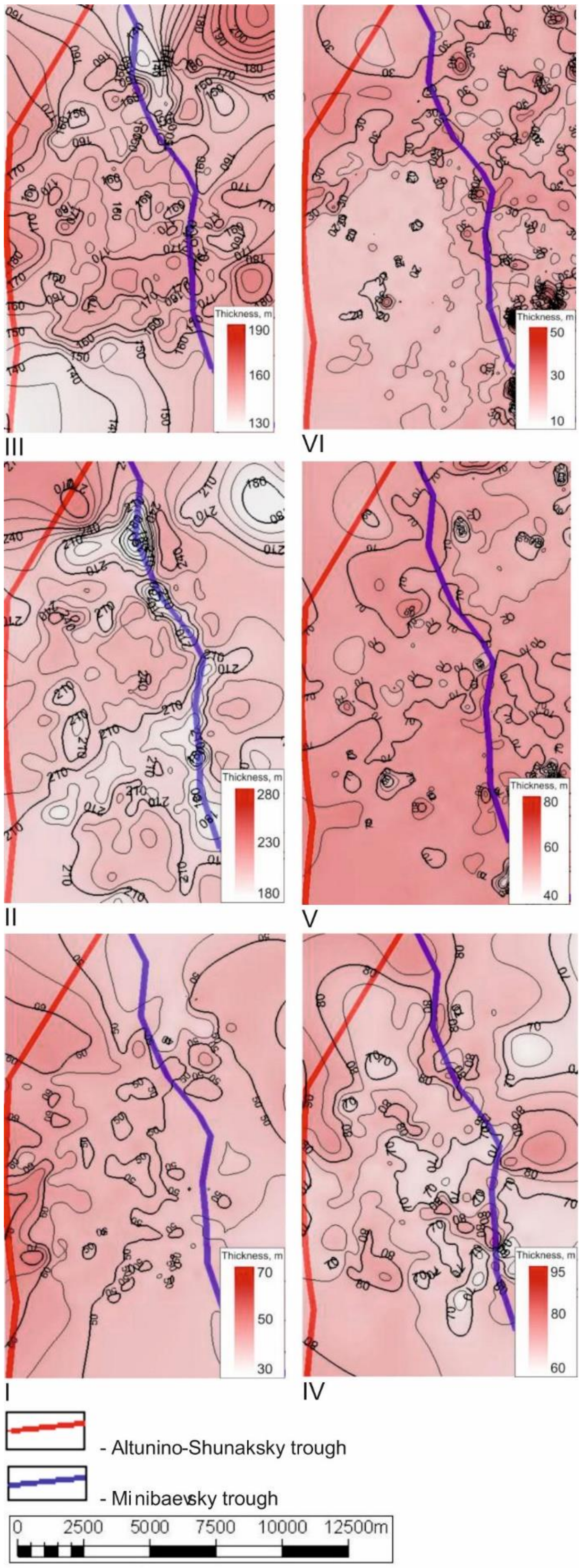

Fig. 3. Thickness map: I – Semilukian horizon; II – Upper Frasnian substage; III – Lower and Middle Famennian substages; IV – Zavolzhian superhorizon; V – Tournaisian horizon; VI –Lower and Middle Visean stage

interpretation, the thickness decreases (150-140 meters) and Altunino-Shunaksky trough with the highest sediment thickness (180 meters).

The decrease in sedimentation thickness in the Minnibaevsky trough may be due to the uplift of the territory in this period of time. It is possible that the neighboring block continued to advance from the northeast. The Altunino-Shunaksky Trough continued to form.

The Famennian (Lower Famennian substage, Eletsian and Zadonian horizons) Regression of the Devonian Sea and the formation of a non-uniform saline basin continued. The STA is a mobile region, on three sides limited by troughs (KKDS from the west and north, Kama-Belsky aulacogen from the east). Carbonate sediments (in sections represented by algal-spherical and algal-clastic limestones) accumulated on the arches and their slopes. Dolomitic sediments accumulated in very shallow areas [9].

The structural plan changed at *the Dankovian-Lebedyanian horizon (Middle Famennian substage)* sediments top (Fig. 2. IV). The dome is observed in its northern part on the Dankovian-Lebedyanian horizon top. During the *Lower and Middle Famennian stage*, a local strip-like positive structure of submeridional strike at the place of the future Minnibaevsky trough was formed, which borders the eastern part of the study area. This is confirmed by the fact that the minimal thicknesses are observed only in the Minnibaevsky trough development zone (170-190 meters) (Fig. 3. III).

From the northeast and east, the neighboring block continued to move towards the studied region [12]. The Altunino-Shunaksky Trough is not so clearly traced, at this time its development is interrupted, in the central part of the area the thicknesses are the same as in the depression -220-230 m [4].

Minimal thicknesses (200 m) are recorded at the place of the dome, formed during the Frasnian in the south of the region, suggesting an uplift.

The *Zavolzhian Superhorizon* (Upper Famennian) top repeats the structural plan of the Dankovian-Lebedyanian (Fig. 2, V). The Minnibaevsky Trough stands as a depression in the Zavolzhian – the total thicknesses increased to 85 m, in the central part of the territory – an average is 75 m. The previously joined blocks in the east and northeast began to diverge, forming a depression. The Altunino-Shunaksky Trough continued to deepen; sediment thickness reached 90 m (Fig. 3, IV).

Carboniferous, Mississippian

The epicontinental sea basin occupied the entire territory of Tatarstan at the beginning of the Tournaisian. The depositional settings in the Tournaisian were inherited from the Devonian and were determined by tectonic and destructive processes of previous periods [13]. The structural plan of the Tournaisian bedding surface repeats that of the Zavolzhian (Fig. 2, VI). The thicknesses of the Tournaisian sediments are stable throughout the entire territory and equal to 60-70 meters (Fig. 3.V). The tectonic setting in the area is stable. Sediments are represented by bioclastic carbonates.

By the beginning of the *Visean*, a change in the tectonic regime occured, which determined the end of regressive stage in development of the Devonian marine basin [14]. During this period, the entire EEP was rising. The process of shallowing of the sedimentary basin continued. KKDS had ceased to exist by the beginning of the Tulian time. The Altunino-Shunaksky and Minnibaevsky troughs were slowly growing until the end of the Tulian (Fig. 2, VII), as the difference in the total thickness of terrigenous and carbonate deposits in the center and in marginal parts of the territory varies within 5 m, and the thickness of deposits is 25-30 m (Fig. 3, VI).

The process of alignment of the Altunino-Shunaksky Trough began from the *Aleksinian*, and positive forms present in the relief of the earth's surface at the place of the trough. Carbonate sediments accumulated in *Aleksinian* [6]. The Minnibaevsky Trough continued its development up to the Cenozoic, today there is a depression followed by the Zai River (Fig. 2, VIII).

The time of the formation of the Minnibaevsky Trough, the presence of alternating vertical movements at the Minnibaevsky Trough and negative movements at the Altunino-Shunaksky Trough are thus established. Tectonic processes had almost no effect on the central part of the study area.

Conclusions

The comparison of the structural and thickness maps for each of the considered stratigraphic units combined with seismic and well logging data allowed the location of various structural and tectonic elements in the study area to be accurately determined. It is shown that clarification of the location of buried structural forms can help to optimize reservoir development.

The boundaries of the Altunino-Shunaksky and Minnibaevsky troughs have been corrected based on seismic surveys and well logging data. The Altunino-Shunaksky and Minnibaevsky troughs are linear negative structures. The Altunino-Shunaksky depression is a structure of the second order, the Minnibaevsky depression is, most likely, a local structure of the third order.

The Minnibaevsky depression remains active today, it is expressed in local topography, with a river flowing along it. Our study has shown that the central part of the study area is tectonically relatively stable.

Thus, it can be noted that in the studied area, structural surfaces have an inherited nature and flatten up the section. The structural plans of the Devonian and Carboniferous deposits are similar.

The Altunino-Shunaksky Trough was formed as a depression. The Minnibaevsky Trough is an alternating structure; before the Zavolzhian, it was a positive form, and since the Zavolzhian it became negative.

Compared to terrigenous Devonian, Carboniferous surfaces have more dissected relief, possibly due to biogenic structures, the formation of which began in the Rechitsian time.

Acknowledgements

This work was supported by the Ministry of Science and Higher Education of the Russian Federation (Agreement No. 075-11-2019-032 from 11/26/2019). The work was checked by Faiz Sulaiman, Director of Customer Success, Cognite AS.

REFERENCES

1. Bajdova I. K., Danilova T. E. (1978). O formirovanii devonskih progibov na territorii Tatarii. Tr. TatNIPIneft' 24, pp. 18-24.
2. Mkrtchyan O. M. (1980). Zakonomernosti razmeshcheniya strukturnyh form na vostoke Russkoj plity. M.: Nauka, 133.
3. Klubov V. A. (1973). Paleostrukturnyj analiz vostochnyh rajonov Russkoj platformy. Nedra, Moscow, 176
4. Larochkina I. A. (2007). Altunino-shunakskij progib kak model’ grabenoobraznyh progibov vostochnoj okrainy Russkoj platformy. Geologiya nefti i gaza 5, pp. 24-31.
5. Larochkina I. A. (2013). Koncepciya sistemnogo geologicheskogo analiza pri poiskah i razvedke mestorozhdenij nefti na territorii Tatarstana. Kazan, 232.
6. Geologiya Tatarstana: Stratigrafiya i tektonika. (2003). GEOS, Moskva, 402.
7. Kirmasov A. B. (2011). Osnovy strukturnogo analiza. Nauchnyj mir, Moskva, 368.
8. Hajn V. E., Lomize M. G. (2010). Geotektonika s osnovami geodinamiki. MGU, 559.
9. Danilova T. E. (2008). Atlas porod osnovnyh neftenosnyh gorizontov paleozoya Respubliki Tatarstan. Terrigennye porody devona i nizhnego karbona. Kazan, 440.
10. Hisamov R. S., Gubajdullin A. A., Bazarevskaya V. G., YUdincev E. A. (2010). Geologiya karbonatnyh slozhno postroennyh kollektorov devona i karbona Tatarstana. Kazan, 283.
11. Valeeva I. F., Anisimov G. A., Anisimova L. Z., Novikova S. P. (2016). Geologicheskie predposylki dal’nejshih poiskov nefti v Nizhnekamskom progibe. Georesursy 18 (3), pp. 198-206.
12. Usmanov S. A., SHaripov B. R., Plotnikova I. N., Ahmetov A. N., Delev A. N. (2013). Sovremennaya geodinamika YUzhno-Tatarskogo svoda (na primere Romashkinskogo mestorozhdeniya nefti). Ekaterinburg: Izvestiya vysshih uchebnyh zavedenij. gornyj zhurnal 1, pp.15-21.
13. Morozov V. P., Kozina E. A. (2007). Karbonatnye porody turnejskogo yarusa nizhnego karbona. Kazan, 201.
14. Novikova Svetlana, Delev Alexey, Usmanov Sergey, Sidorov Sergey. (2017). Structural Features, Type and Origin of the Incised Valleys in the Lower Carboniferous of the Volga-Ural Oil and Gas Basin (East European Platform). Kazan Golovkinsky Stratigraphic Meeting, pp. 401-409.

Geochemical Features of The Lower Kazanian Karkali Section, Sheshma River, Russia

NOURGALIEVA Nouria[1], FAKHRUTDINOV Eduard[1]

[1] Kazan Federal University, Kazan (RUSSIA)
Email: nouria.nourgalieva@kpfu.ru

Abstract

This study represents geochemical features of the Lower Kazanian Karkali Section, Sheshma River basin, Russia. The Lower Kazanian deposits unconformably overlie the Ufimian deposits.

These stages, together with the Urzhumian, the Severodvinskian and the Vyatskian stages, compose the Middle Permian (Biarmian) Series. The Lower Kazanian succession in this area is similar to the stratotype Kazanian sections in the Samara region, in the basin of the Sok River (Lower Kazanian Substage, South-Eastern Tatarstan, reference section). The succession is composed of a complex alternation of siliciclastic and carbonate rocks composing three formations up the section (Baitugan, Kamyshla and Krasnyi Yar Beds). The section has been probed by $\delta^{13}C$ and $\delta^{18}O$ with zonation on XRF and ESR data to receive a geochemical framework of the investigated succession. Mean values of $\delta^{13}C$ and $\delta^{18}O$ equal ~0‰ and ~-4‰ V-PDB respectively, and belong to sets of isotopic data of the end of the Paleozoic. The top of the Kamyshla beds have been revealed as a sharp chemostratigraphic boundary caused by paleoclimate change.

Keywords: $\delta^{13}C$ and $\delta^{18}O$ in carbonates, Lower Kazanian section

Introduction

The Basin of the Sheshma river is a part of the Volga and Kama rivers basin. It is known as a unique stratigraphic and paleogeographic object formed in littoral, transitional and continental environments during the Early Kazanian (~ 272-269 million years) [1].

According to zonation proposed in [2] the Kazanian rocks of the Volga-Kama rivers area belong to the zone of marine and lagoon terrigenous-carbonate sediments.

The most interesting Permian sections in the South-Eastern Tatarstan (the Volga-Kama rivers region) are exposed in the upper reaches of the Sheshma River, near the villages of Shugurovo and Karkali.

The Ufimian-Kazanian succession near the villages of Shugurovo and Karkali is well-known to Russian geologists and was studied for over 200 years [2]. Originally, the section attracted attention due to the common occurrences of bitumen on the surface in the basin of the Sheshma River. In the north-eastern vicinity of the village of Shugurovo, outcrops of tar sandstone form a large field of heavy and viscous oil. This field was well-known since the 19th century and was until recently utilized by the Shugurovo Tar Plant. In 2015, the Shugurovo Tar Plant was transformed into the Memorial Park of Geological Heritage [2].

The succession is composed of a complex alternation of siliciclastic and carbonate rocks composing three formations up the section (Baitugan, Kamyshla and Krasnyi Yar Beds).

The present paper shows the geochemical features of the sections near the village of Karkali, that indicates that the Lower Kazanian marine rocks can be represented as specific facial succession.

Methods and results

Geochemical data were obtained by X-ray fluorescence (XRF) [2]; electron spin resonance (ESR) [2] and stable isotope methods [4]. Isotope composition was measured by thermoelectron equipment including mass-spectrometer Delta V Advantage and Gas-Bench-II. Precipitation of probes and standards C-O-1 and NBS-19 was made in H_3PO_4 at temperature 50 °C. $\delta^{13}C$ was determined in (‰) on V-PDB standard. $\delta^{18}O$ was determined in (‰) on V-SMOW standards.

Accuracy of $\delta^{18}O$ and $\delta^{13}C$ detection was ±0.2‰ [4]. The distribution of samples as types of carbonate rocks is shown in Fig.1 (after [3]).

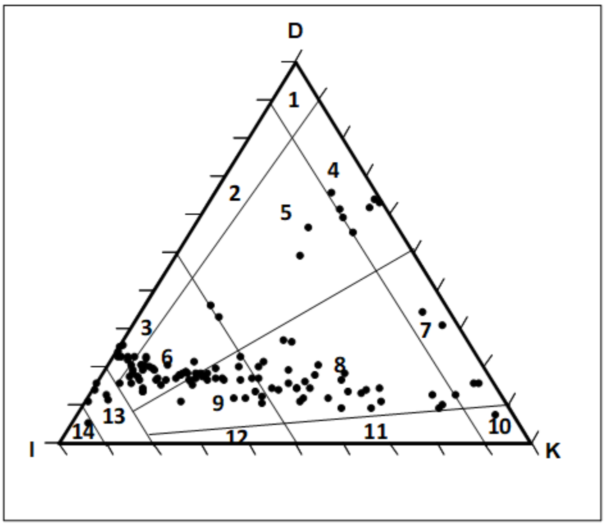

Fig. 1. Regular ternary DKI diagram for classifying carbonate rocks from their weight percentage contents of calcite (%) (K), dolomite (%) (D) and residue (%) (I), after [3]. 1: dolomites; 2: siliceous dolomites; 3: dolomitic cherts; 4: calcareous dolomites; 5: calcareous-siliceous dolomites; 6: dolomitic-calcareous cherts; 7: dolomitic limestones; 8: dolomitic-siliceous limestones; 9: calcareous-dolomitic cherts; 10: more or less magnesian limestones; 11: more or less magnesian siliceous limestones; 12: more or less magnesian calcareous cherts; 13: impure cherts; 14: cherts.

On XRF data, three components are revealed as the most important: silicon (quartz), calcium (carbonate minerals) and aluminum (argillaceous minerals) in the composition of investigated rocks. On the summary section, one can see that the sum of these elements is greater than 70% [4].

Most carbonate rocks samples lay in fields 6, 8, 9 (dolomitic-calcareous cherts; dolomitic-siliceous limestones, calcareous-dolomitic cherts) (Fig. 1). The positions of samples along the section have been built on DKI (dolomite-calcite-insoluble residue) zones with geochemical data.

The dominant calcite mineralization was fixed at the lower part of the section (beds 4-9) on Mn^{2+} labels. The dolomite mineralization (on paramagnetic α label) was observed in the upper part of the section (beds 10-13, 16, 18, 21-24) [2, 4]. The bottom of bed 10 was revealed as the low level of the dolomite mineralization zone. The paramagnetic labels SO^{3-}, PO^{2-}, C_{600} point on unaltered carbonates, especially in beds 10, 12, 16, 18 [2, 4]. The paramagnetic labels of E'-centers and R-centers reflect events of terrestrial flux, especially during Krasnyi Yar time. Beds 23-24 (the Upper Kazanian) are composed of significantly altered carbonates (on the absence of labels SO^{3-}) [2, 4].

The $\delta^{13}C$ values range from -11,8‰ to 3,5‰ with a mean value -0,18‰ and a standard deviation 3,95‰. Most values vary from -4‰ to 4‰. The $\delta^{18}O$ values change from -9,56‰ to 2,08‰ with a mean value -4,41‰ and a standard deviation 4,30‰ [4].

Received values belong to the range of values specific to the Lower Kazanian rocks of the Volga-Kama basin [5].

Discussion

Geochemical variations specifically reflect the lithostratigraphic and facial alternation within the Lower Kazanian succession [2, 4].

The comparison of $\delta^{13}C$ and $\delta^{18}O$ data with isotope curves for the end of the Paleozoic era [7] shows a negative deviation of Karkali mean point at the $\delta^{13}C$ plot and a position of the Karkali mean point nearly $\delta^{18}O$ plot (Fig. 2) but we have to account a specific behavior of isotope systems in terrestrial carbonates and an insufficient background of the standard isotope curves at the end of the Paleozoic era [7].

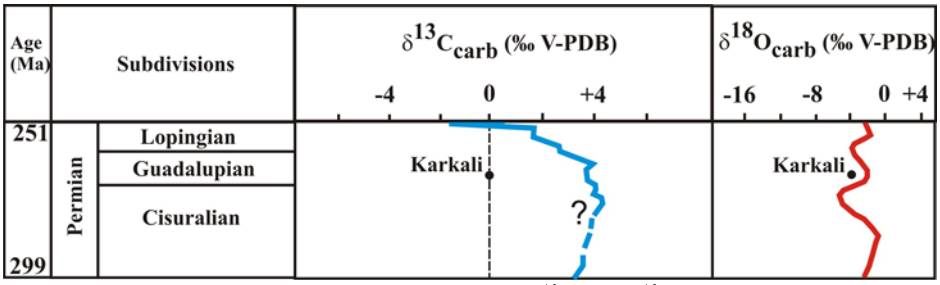

Fig. 2. The plot of the Karkali point (mean values of $\delta^{13}C$ and $\delta^{18}O$) on isotope curves from [7]

Nevertheless, the isotope data supplement essentially the geochemical and facial framework of the Karkali section (Fig. 3).

Two negative shifts of $\delta^{13}C$ in the bottom of the lingula clays (to a value -11,8‰) and in the bed 11 (to a value -4 ‰) have been observed respectively (Fig. 3). These shifts can be interpreted in the terms of decreased biological productivity, increased water mixing or upwelling and increased weathering of organic carbon [7].

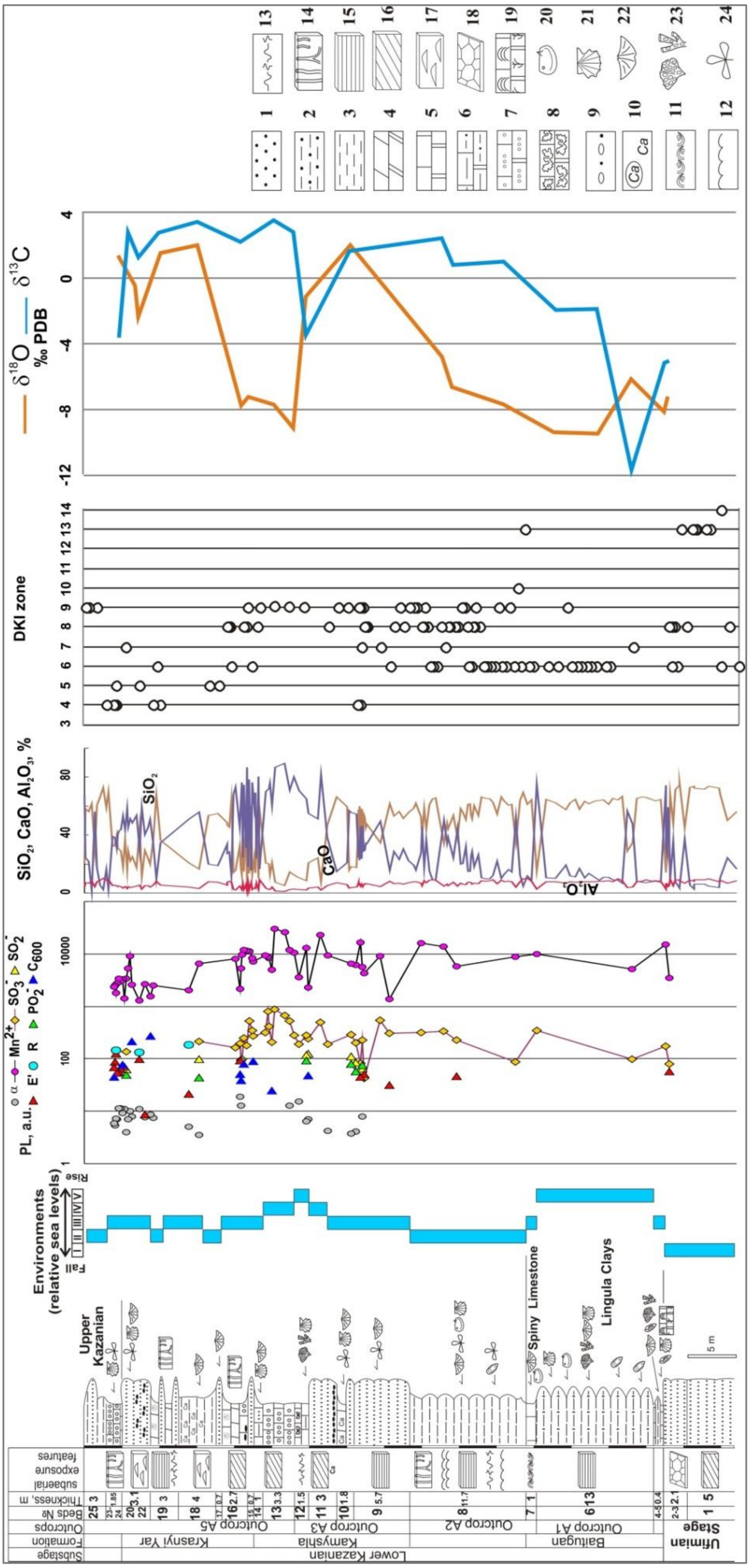

Fig. 3. Summary section of the Lower Kazanian rocks and geochemical variations after [2, 4]. Legends: 1 – sands and sandstones; 2 – silts and siltstones; 3 – shales argillaceous; 4 – marls; 5 – carbonate rocks; 6 – argillaceous and silt carbonate rocks; 7 – oolites; 8 – vuggy carbonate rocks; 9 – gravel, pebbles; 10 – calcareous concretions and calcareous recrystallization; 11 – coquina; 12 – shell pavement; 13 – bioturbated structure; 14 – trace fossils; 15 – horizontal and subhorizontal lamination; 16 – cross lamination; 17 – short lenticular lamination; 18 – fissures of desiccation; 19 – stromatolites and calcareous algae; 20 – marine ostracods; 21 – marine bivalves; 22 – articulated brachiopods; 23- bryozoans; 24 – leaves of higher plants. Depositional environments: I – delta, II – regression, lagoon, III – shallow marine water, IV – littoral, V – transgression, sublittoral

The $\delta^{18}O$ values increase up the section to ~2‰ in bed 10 (increase of $\delta^{18}O$ because of lower water temperature and reducing the energy of the motion of heavy oxygen isotopes during isotopic fractionation). Then the $\delta^{18}O$ values decrease to ~-9‰ at the bottom of bed 13, where $\delta^{13}C$ values increase (Fig.3). Most likely, this pattern can be explained by relative climate warming (increase of light oxygen isotopes, increase of biological productivity) [7].

Thus, a sharp change in the behavior of the isotopic ratios is recorded at the bottom of bed 13 (the top of the Kamyshla beds). The Baitugan and the most of the Kamyshla time can be characterized as relatively cold episodes. Then the climate trend changed to warm and even evaporate conditions (dolomitization) [4-6].

Conclusions

The variations of XRF, ESR and isotope data on the reference surface section in South-Eastern Tatarstan reflect changes in environmental history during the Early Kazanian in the east of the Russian platform and can be used as tool to develop the chemostratigraphic frame of the Biarmian Series.

Acknowledgments

This work was funded by the subsidy allocated to Kazan Federal University for the state assignment #671-2020-0049.

REFERENCES

1. Nurgalieva, N. G., Nurgaliev, D. K. (2015). Cyclical composition of Permian rocks. ARPN JEAS 10 (1), pp. 279-290.
2. Nurgalieva, N. G., Silantiev, V. V., Fakhrutdinov, E. I., Khassanova, N. M., Gareev, B. I., Batalin, G. A., Urazaeva, M. N., Mozzherin, V. V., Egorova, K. A. (2015). Karkali section. Ufimian/Kazanian boundary and the Lower Kazanian in shallow marine facies. Type and reference sections of the Middle and Upper Permian of the Volga and Kama river regions. A field Guidebook of XVIII International Congress on Carboniferous and Permian. Kazan, August, 16-20, 2015 / D.K. Nurgaliev, V.V. Silantiev, S.V. Nikolaeva (Eds.). Kazan: Kazan University Press, pp. 176-192.
3. Mishe, H., Simler, R., Affaton, P., Mickala, O., Boudzoumou, F. (2013). New computerized method for the geochemical classification of Precambrian carbonate rocks: case of a set of African cap carbonates. International Journal of Geosciences 4, pp. 37-49.
4. Nurgalieva, N. G., Silantiev, V. V., Fakhrutdinov, E. I., Gareev, B. I., Batalin, G. A. (2016). The Lower Kazanian rocks as shallow marine facies (South-Eastern Tatarstan) on geochemistry data. ARPN JEAS 11 (23), pp. 13462-13471
5. Nurgalieva, N. G., Silantiev, V. V., Vetoshkina, O. S., Ponomarchuk, V. A., Nurgaliev, D. K., Urazaeva, M. N. (2015). Some new data on isotope stratigraphy of the Permian rocks at the east of the Russian Platform. ARPN JEAS 10 (10), pp. 4436-4442.
6. Nurgalieva, N. G. (2016). Reference section of the Upper Kazanian Substage: cyclic regularities. ARPN JEAS 11 (11), pp. 6928-6934.
7. Chemostratigraphy. Concepts, Techniques and Applications. Ed. By Mu.Ramkumar. (2015). http://dx.doi.org/10.1016/B978-0-12-419968-2.00002-9

X-Ray Fluorescence Spectroscopy of the Domanik Facies

NOURGALIEVA Nouria[1], GAREEV Bulat[1], BATALIN Georgiy[1]

[1] *Kazan Federal University, Kazan (RUSSIA)*
Email: nouria.nourgalieva@kpfu.ru

Abstract

In this paper, the cores from three wells (Eastern Republic of Tatarstan) were studied. The cores were taken from the Domanik succession (Semilukian and Rechitsian Horizons). The study of thin sections revealed the Domanik microfacies types: limestone crystalline, microspar; siliceous-clayey shale with dispersed calcareous and siliceous nodules; nodular bioclastic wackestone; and clayey-siliceous shale with dispersed calcareous nodules. The deposition of the Domanik microfacies began prior to the formation of the Kama-Kinel trough system. During the middle Frasnian, the deposition of the Domanik facies extended across most of the Volga-Ural Province and along the eastern border of the platform. The sediments were deposited in deep water environments. The observed spectrum of pelagic lithofacies shows the increasing clay content ranging from nodular limestones to shales with dispersed calcareous and siliceous nodules of early diagenetic origin. The geochemical characteristics of rocks were obtained using X-ray fluorescence spectroscopy (XRF) with PAAS normalization, as well as by using geochemical classification by Si, Al, K, Ca. Among the rocks studied, the calcareous geochemical type was revealed to be dominant. High concentrations (~700-2600 g/t) of Ni were found, which are an outstanding geochemical indicator of high-carbon Domanik rocks.

Keywords: Domanik formation, XRF, geochemical features

Introduction

During the Late Devonian, warm seas along the eastern coast of Baltica produced abundant marine biota forming the source of most of the region’s oil and gas, the Domanik facies. The distribution of oil and gas fields is controlled by two fundamental factors [1]: (1) the distribution of the Domanik organic rich, fine-grained source rocks that generated most of the basin’s oil (total organic carbon (TOC) exceeds 1%) and (2) the distribution of Devonian sandstones with thickness greater than ~100 m overlying the source rock. The fields confirm the spatial correlation between optimal source and reservoir rocks and the province's largest discoveries, including the super-giant Romashkino field [1, 2].

In the middle Frasnian, the Domanik facies began to form prior to the development of the Kama-Kinel trough system, which includes a group of narrow, interconnected deeper water troughs that persisted into the Early Carboniferous. The Domanik beds are relatively deep-water, dark gray and black bituminous carbonate-clay-cherty facies, rich in organic matter, containing fish remains, tentaculites, ammonoids, thin-walled bivalves and radiolarians [3].

These beds are considered to be the source rocks for the oil accumulated in the Volga-Ural province. The lower Frasnian part of the Domanik sequence is present in the Kazansko-Kirov, Melekess, and Buzuluk depressions, and on the south-eastern slope of the Russian Platform.

During the middle Frasnian, the Domanik facies extended across most of the Volga-Ural province and was thickest in the Melekess and Sernovodsko-Abdulino depressions, the Upper-

Kama depression, and along the eastern border of the platform. These beds were named the Domanik Formation by [4] from outcrops east of Perm.

By the late Frasnian, the Domanik facies was reduced in lateral extent as reef and organic mound limestone deposits began to form along the borders of the Kama-Kinel troughs. As the carbonate deposits accumulated and spread, the deeper water troughs were further narrowed, and the true Kama-Kinel trough system became fully developed and merged northward with the Ural foredeep, north of the Perm-Bashkir arch. By the end of the Frasnian, carbonate deposits had built up to a considerable thickness on several of the high areas of the platform, particularly those of the Tatar and Perm-Bashkir arches, and in several areas along the edges of the Kama-Kinel troughs.

According to [5] tectonic subsidence of several of the main negative paleostructures of the eastern part of the platform formed the foundation for the Kama-Kinel trough system. These include the Buzuluk, Melekess, and Upper-Kama depressions and the Birsk Saddle.

Strong subsidence and deposition of thicker Frasnian series occurred in several other depressed parts of the platform, including the Kazan-Kirov aulacogen (more than 1,000 m), Lower Volga monocline (more than 1,200 m), and the southern Ural foredeep (more than 1,500 m) [3].

Carbonate deposition increased markedly during the Famennian, and except for the deeper Kama-Kinel troughs, reef and organic carbonate mound deposits covered most of the Volga-Ural province at this time. The Kama-Kinel trough system was further narrowed as biohermal carbonate beds accumulated upward and spread to the trough borders, across the flanks of previously deposited reef carbonates. The highly bituminous Domanik facies continued to be deposited in the troughs but in general was thinner and less silty than in the Frasnian. The Famennian and upper Frasnian reef deposits are composed primarily of stromatoporoid and tabulate coral remains, calcareous blue-green, red, and spherical algae, and variable amounts of crinoid, foraminifera, and other skeletal organic material [3]. The reef rocks tend to be very pure carbonate (insoluble residue one percent or less) and are partly dolomitized in places.

Excellent source-rock beds of the Domanik facies are present in the Kama-Kinel trough system that surrounds all of the main carbonate buildup belts. These beds are highly bituminous; organic carbon content is as much as five percent or more. The Domanik beds, however, generally do not intercalate with the carbonate buildup facies and thus may not be as highly effective as source-rock facies for these carbonate reservoirs as they are for the underlying Frasnian and Givetian clastic reservoirs.

Domanik rocks belong to the Semilukian (Domanikian) Horizon of the Frasnian Stage.

Equivalents of the Domanik rocks were also found in the Sargaevian, Rechitsian (Mendymian), Voronezhian, Evlanovian, and Livenian horizons of the Frasnian Stage and in the Eletsian, Lebedyanian, Dankovian horizons of the Famennian Stage. The thickness of Domanik rocks ranges from 10 m to 100 m.

The Domanik sequence (within the Semilukian and Rechitsian horizons) is composed of four microfacies types, observed in the core from the NE well on the western slope of the South-Tatar Arc [6]: limestone crystalline, microspar; siliceous-clayey shale with dispersed calcareous and siliceous nodules; nodular bioclastic wackestone; clayey-siliceous shale with dispersed calcareous nodules. The spectrum of pelagic lithofacies shows the increasing clay content, ranging from nodular limestones to shales with dispersed calcareous and siliceous nodules of early diagenetic origin.

In present paper the core from NE (Novo-Elkhovskaya area) well, VS (Vostochno-Suleevskaya area) well, and Sm (Sarmanovskaya area) well (all wells are at the east of the Republic of Tatarstan) was considered. The core was taken from the Domanik sequence (the Semilukian and Rechitsian horizons). Thin sections were prepared from these samples and the rocks were classified according to [6].

Data on elemental composition were obtained by applying X-ray fluorescence (XRF) analysis and used to identify geochemical indicators of the Domanik formation.

Samples and microfacies position are shown in Fig. 1 in accordance with the principal section of the Domanik Formation of the Volga-Ural province [7].

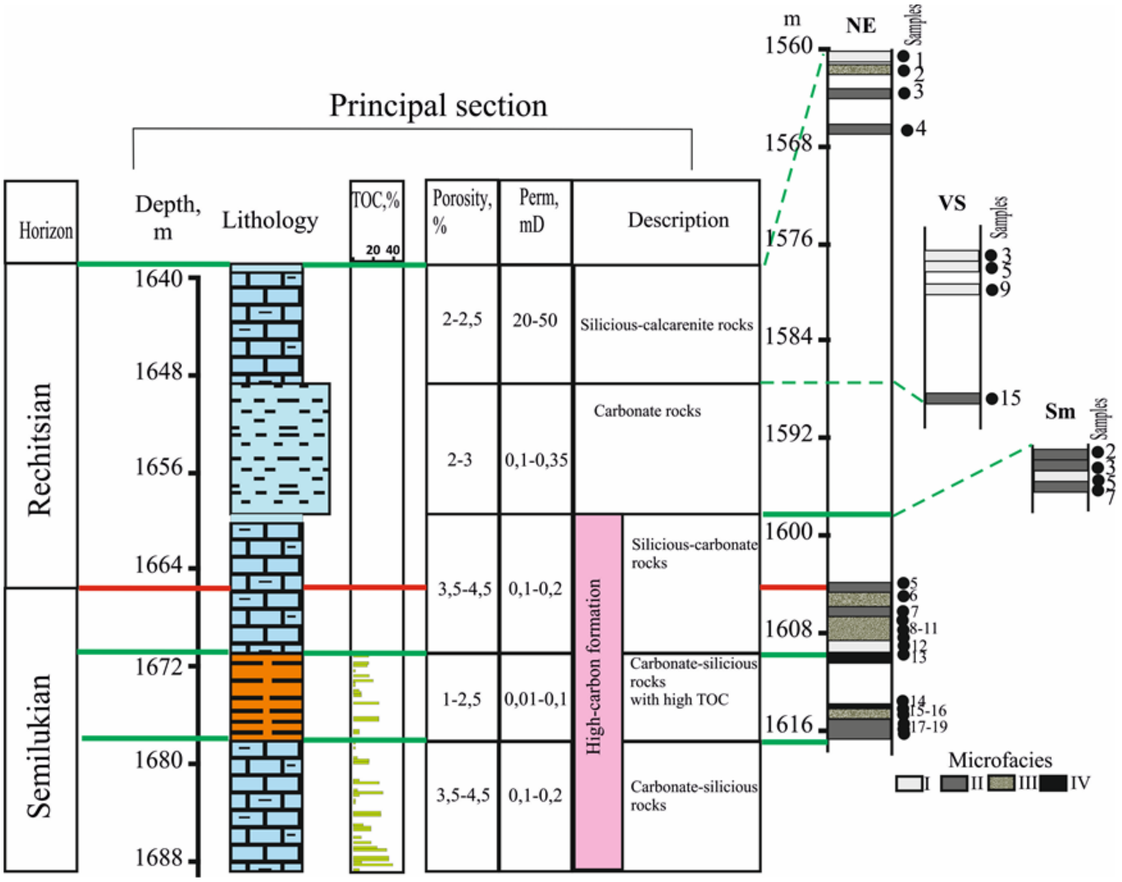

Fig. 1. Sample and microfacies positions in NE, VS and Sm sections in accordance with the principal section of the Domanik formation. Microfacies: I – crystalline limestone, microsparite; II – siliceous-clay shale with scattered calcarenite and siliceous nodules; III – bioclastic wackestone with an abundance of radiolarian remains and sponge spicules of different preservation, some of which are calcified, and some replaced by a micrite substance; IV – clay-siliceous shale with scattered calcarenite nodules

Samples no. 1-4 of the NE-section and the samples no. 3,5,9,15 of the VS-section belong to the Rechitsian Horizon, composed of alternating limestone of crystalline microsparite, bioclastic wackestone and siliceous-clay shale with calcarenite and siliceous nodules.

Samples no. 2, 3, 5, 7 of the Sm-section are from the base of the Rechitsian horizon, simultaneous to the upper part of the high-carbon formation as part of a thin layer of siliceous-carbonate rocks, composed of alternating crystalline microsparite limestone and siliceous-clay shale.

Methods and results

The elemental composition was studied using an S8 Tiger XRF wave dispersion spectrometer (Bruker, Germany), which allows determination of the elemental composition of solid, powdery and liquid samples. The device is equipped with a 4-kW rhodium x-ray tube.

The sample was placed in the grinding set of a planetary ball mill, and the grinding was carried out for 10 minutes to achieve the required particle size of less than 10 microns.

A sample of weight 0.5 g was placed in a ceramic crucible and calcined at 1100 °C for two hours to determine loss on ignition (LOI).

Subsequently, another sample weight of 4 g was weighed on an analytical balance with an accuracy of 100 mg, mixed with organic wax and pressed on a boric acid substrate with a force of 300 kN.

The resulting tablet was placed in a spectrometer, where it was analyzed using the standardized Geoquant method.

The obtained spectrum was processed by the fundamental parameter's method, automatic recognition errors were removed, diffraction phenomena and matrix effects were taken into account, and the value of the LOI was used to account for undetectable elements.

Received data normalized to PAAS (Post Archean Australian Shales) are shown in Fig. 2.

The content of silicon, titanium, aluminum, iron, manganese and potassium oxides are less relative to PAAS. Only in the sample no.15 of the NE-section, the content of silicon oxide is 1.4 times higher than that in PAAS. In sample 5 (VS-section) and sample 7 (Sm-section), there is increased MnO content: 1.2 and 7 times more than in PAAS respectively. The content of phosphorus oxide is approximately 10-12 times higher than that in PAAS (except for sample 15 of the NE-section, where phosphorus is not recorded). The content of magnesium oxide exceeds that in PAAS by about 4.5-10 times (except for the sample of the NE-section – here the content of magnesium oxide is close to PAAS). The content of calcium oxide is 30-60 times higher than that in PAAS. Only in sample no.15 of the NE section, the excess is only twice.

Sr is contained in the range of ~260-1300 ppm (except sample no. 5 from VS-section with a very high value), Cr is in amounts of ~620-760 ppm, Ni is in the range of ~700-2600 ppm, Cu is in the range of 8-120 ppm, Zr is in the range ~50-8582 ppm.

Thus, the studied rocks are significantly enriched with calcium, magnesium, phosphorus, manganese, chromium, strontium and especially nickel.

Discussion

According to the geochemical classification by [8], the samples belong to calcarenite rocks, except for sample no. 15 (siliceous clay rock) of the NE-section.

Studied rocks are significantly enriched with calcium, magnesium, phosphorus, manganese, chromium, strontium and especially nickel (Fig. 2).

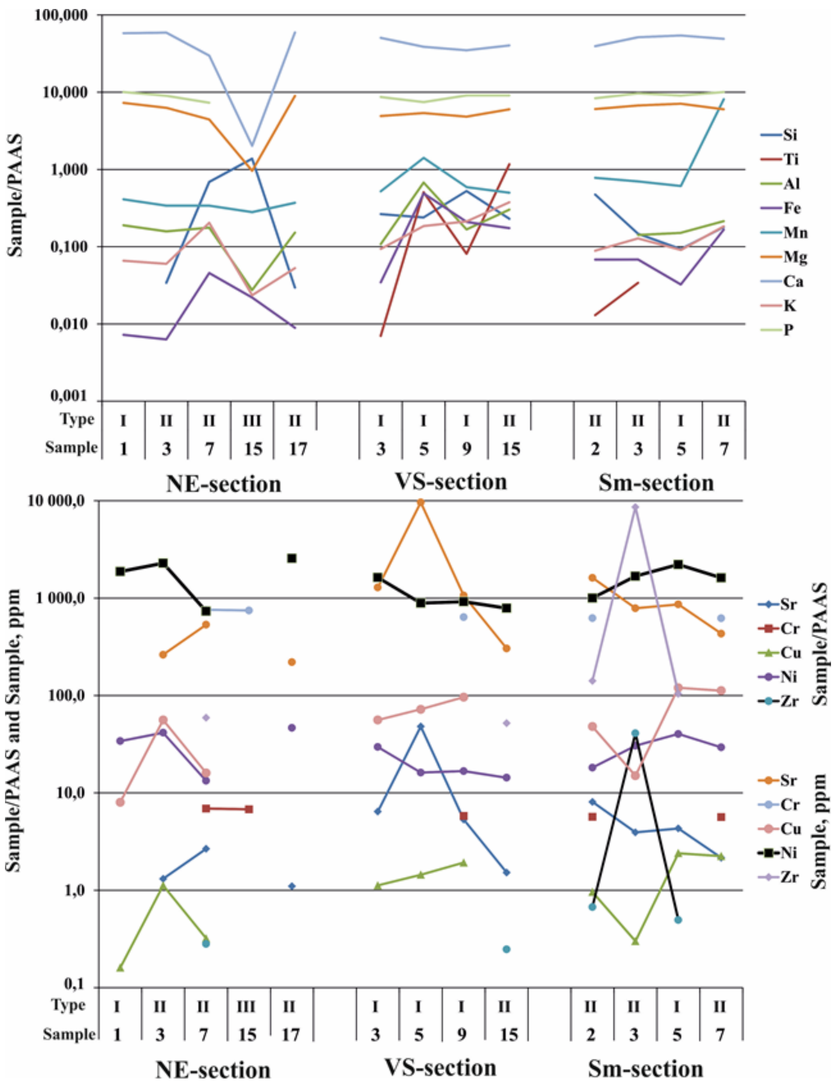

Fig. 2. Elemental composition of the Domanik facies

In sedimentary rocks, Ni can mainly be found in fragments of ferromagnetic silicate minerals, iron and manganese oxides, and clay minerals.

Nickel is mobile in acid and oxide conditions. This element plays an important role in the life of microorganisms. High concentrations of Ni (2000-3000 g/t) are often found in high-carbon black shale formations (for example, black shales of the Ordovician, Silurian and Carboniferous age in the Pyrenees or the Upper Cretaceous oil shales in Safaga – Quseir area in Egypt) [9, 10].

Fig. 2 shows the huge concentrations of Ni in the studied Domanik rocks (~ 700-2600 g/t).

The highest concentration of Ni was found in the rock within the high-carbon formation (sample no. 17 of the NE-section (Fig.1, 2)).

Thus, the established concentrations of Ni can be considered as an outstanding geochemical indicator of the Domanik facies, formed in anoxic environments.

Conclusions

The Domanik formation at the East of the Republic of Tatarstan is composed of geochemical calcareous type of rocks, enriched with Ca, Mg, P, Mn, Cr, Sr, and especially Ni (~700-2600 g/t).

Received geochemical characteristics can be considered as indicator of the high-carbon Domanik formation.

Acknowledgments

The work is performed according to the Russian Government Program of Competitive Growth of Kazan Federal University to receive XRF data.

This work is supported by Russian Foundation for Basic Research (grant 18-55-53051) to make facies and geochemical conclusion.

REFERENCES

1. Grace, J. D. (2005). Russian oil supply: Performance and Prospects – Oxford University Press for the Oxford Institute for Energy Studies, 288.
2. Muslimov, R. Kh. (Editor). (2007). Neftegazonosnost' Respubliki Tatarstan. Geologiya i razrabotka neftyanykh mestorozhdeniy. Fan, Kazan, 316.
3. Peterson, J. A., Clarke, J. W. (1983). Geology of the Volga-Ural Province and detailed description of the Romashkino and Arlan oil fields: U.S. Geological Survey Open-File Report, 90.
4. Murchison, R., Verneuil, E. Keyserling (1845). A. The geology of Russia in Europe and Ural Mountains – London: J. Murray, 1, 700.
5. Maksimov, S. P. (Editor). (1970). Geology of Oil and Gas Fields of the Volga-Urals Hydrocarbon Province. Nedra, Moscow, 807.
6. Nurgalieva N. (2018). Some aspects of Domanik facies – Filodiritto Editore – Proceedings of Kazan Golovkinsky Stratigraphic Meeting, 2017: Advances in Devonian, Carboniferous and Permian Research: Stratigraphy, Environments, Climate and Resources Kazan, Russian Federation, pp. 315-320.
7. Stoupakova A. V., Kalmykov G. A., Korobova N. I., Fadeeva N. P., Gatovskii Yu. A., Suslova A. A., Sautkin R. S., Pronina N. V., Bolshakova M. A., Zavyalova A. P., Chupakhina V. V., Petrakova N. N., Miftakhova A.A. (2017). Oil-Domanik deposits of the Volga-Ural basin – types of section, formation conditions and prospects of oil and gas potential. Georesources. Special Issue. Part 1, pp. 112-124.
8. Baumgardner R. W., Hamlin H. S., Rowe H. D. (2014). High-Resolution Core Studies of Wolfcamp/Leonard Basinal Facies, Southern Midland Basin, Texas – Search and Discovery Article #10607. – Posted June 30, adapted from poster presentation given at AAPG 2014 Southwest Section Annual Convention, Midland, Texas.
9. Geochemical Atlas of Europe. Part 1, 2. W. De Vos & T. Tarvainen (Chief editors) http://weppi.gtk.fi/publ/foregsatlas/
10. Ghanem M. F., El-Fakharany M. A., Temraz M. G., Afife M. M., Shehata A. M. (2018). Upper Cretaceous Duwi Formation shale's oil potentiality Safaga-Quseir, Red Sea, Egypt. Egyptian Journal of Petroleum 27, pp. 1313-1323.

New Carbon Isotope Data in the Pechishchi Section, Russia

NOURGALIEVA Nouria[1], GAREEV Bulat[1], BATALIN Georgiy[1]

[1] Kazan Federal University, Kazan (RUSSIA)
Email: nouria.nourgalieva@kpfu.ru

Abstract

This study represents new carbon isotope data of the Pechishchi Upper Kazanian stratotype section, Volga River basin, Russia. The $\delta^{13}C_{org}$ values are incorporated into previous geochemical framing of the section updated to modification of Noinsky's cyclic scheme. The outline geochemical scheme includes the variations of $\delta^{13}C_{org}$, $\delta^{13}C_{carb}$, $^{87}Sr/^{86}Sr$ in comparing with global data within 273-268 Ma. The $\delta^{13}C_{org}$ values vary from -33,8 ‰ (the transitional component of the Middle Noinsky's cycle) to -24,6 ‰ V-PDB (the terrestrial component of the Upper Noinsky's cycle) with a mean value -27,2 ‰ V-PDB (the marine component of the Lower Noinsky's cycle).

The $\delta^{13}C_{org}$ values correspond to the Permian organic carbon matter properties and can be considered as additional data in the geochemical characteristics of the Upper Kazanian succession in the Volga River basin.

Keywords: carbon isotope data, the Upper Kazanian section, Volga River basin

Introduction

The stratotype of the Upper Kazanian substage is exposed on the south bank of the Volga River opposite Kazan city. The Kazanian stage is correlated with the Roadian (middle Permian) of the International Stratigraphic Chart [1, 2]. The boundary between the Lower and Upper Kazanian and lower part of succession (units 1-7) is exposed in the slope of the bank between villages of Pechishchi and Naberezhnye Morkvashi [1]. M.E. Noinsky was first to describe the section, which consists of eight series or members, and he recognized three depositional cycles [3, 4]. Detailed paleontological analysis of the section was provided by Solodukho and Tikhvinskaya (1977) [1].

This Upper Kazanian succession is well studied, including its elemental and isotopic composition, variations and trends in [5].

The present paper adds the data on $\delta^{13}C_{org}$ to the data on $\delta^{13}C_{carb}$ and $^{87}Sr/^{86}Sr$ along the Pechishchi section, received in [5]. Using the $^{87}Sr/^{86}Sr$ ratio, the Upper Kazanian succession was estimated within 273-268 Ma [5].

The description of the Upper Kazanian section is based on data reviewed in [5]. The section is composed of 31 beds grouping up in the Prikazan beds (nos. 1-13), the Pechishchi beds (nos. 14-21), the Verkhnyi Uslon beds (nos. 22-28) and the Morkvashi beds (no. 29-31). The Prikazan beds include A (Yadrenyi Kamen: beds no.1-8) and B (Sloisty Kamen: beds nos. 9-13) members. The Pechishchi beds consist of C (Podboi: beds no.14-16), D (Seryi Kamen) and E (Shikhany: bed no. 21) members. The Verkhnyi Uslon beds include F (Opoki: beds nos. 22-25) and G (Podluzhnik: beds nos. 26-28) members. The Morkvashi beds comprise H (Perekhodnaya: beds nos. 29-31) member. All member names were taken from [3, 4].

Methods

The isotopic composition of organic carbon in the rock samples has been studied using a Delta V Plus isotope mass spectrometer (ThermoFisher Scientific, Germany) with a Flash HT attachment in constant flow mode. At first, the carbonate component is removed from the sample, for this a 500 mg sample is taken, to which 10 ml of 10% hydrochloric acid solution is added (or until gas discharge is completely stopped). Next, hydrochloric acid is evaporated in an oven at a temperature of 80 °C until a dry residue is obtained. After removal of the carbonate component, a sample of the rock is weighed on XP6 micrometer (Mettler Toledo, Switzerland) and approximately 200 μg is selected. The sample then is placed in a tin crucible that is rolled into a ball. Next, the ball is placed in the autosampler tray. Using an autosampler, each ball with a sample is discharged into a helium-blown quartz reactor at a temperature of 1020°C and filled with chromium oxide and copper wire.

As a result of the reaction of chromium oxide with a ball with a sample, tin is converted to oxide, and the sample completely burns, forming carbon dioxide. Carbon dioxide is transferred to the mass spectrometer using a helium stream, after passing through a desiccant and a special chromatographic column at a temperature of 45 °C. Before the measurements, several portions of standard carbon dioxide with a known carbon isotopic ratio are introduced into the mass spectrometer to calibrate the isotopic ratio of the sample utilizing a software. The IAEA standards are analyzed for the additional control in a series of samples: USGS-40, which is L-glutamic acid with a known carbon isotopic ratio, and IAEA-CH-7, which is a polyethylene film with a known carbon isotopic ratio.

The $\delta^{13}C_{org}$ values of siliciclastic admixtures in carbonate rocks were measured by mass spectrometry in 14 samples up the section from the lower boundary of the section (0,15 mab), bed no. 1 (1,52 mab), bed no. 3 (4,33 mab), bed no. 4 (4,85 mab), bed no. 6 (7,01 mab), bed no. 9 (8,33 mab), bed no. 12 (12,2 mab), bed no. 13 (13,15 mab), bed no. 19 (22,85 mab), bed no. 22 (27,8 mab), bed no. 24 (31,15 mab), bed. no. 26 (34,625 mab), bed no. 30 (50,2 mab) respectively (Fig. 1).

Results and discussion

The geochemical variations specifically reflect the lithostratigraphic and the facies alternation within the Upper Kazanian Noinsky's cyclic scheme (Fig. 1).

The carbonate rocks by [5] are characterized by the mean value of the $\delta^{13}C_{carb}$=6.2 ‰ V-PDB.

The negative excursions of $\delta^{13}C_{carb}$ values (with amplitudes 2-8‰) are ascribed to significant land-derived clastic inputs (Fig. 1). The values of $^{87}Sr/^{86}Sr$ ratio in the data set of justified definitions change from 0.707267 to 0.707417 (mean value is 0.70734). On the Phanerozoic $^{87}Sr/^{86}Sr$ standard curve the observed values are in the interval 273-268 Ma [5].

The comparison of $\delta^{13}C_{carb}$ and $^{87}Sr/^{86}Sr$ data from [5] with isotope curves for the end of the Paleozoic era [6] indicates a position of the Pechishchi mean point nearly $^{87}Sr/^{86}Sr$ plot and its positive deviation at the $\delta^{13}C$ plot (Fig. 2) due to specific fractionation of isotopes in lagoon dolostones and insufficient background of the standard isotope curves in parts of the end of the Paleozoic era [6].

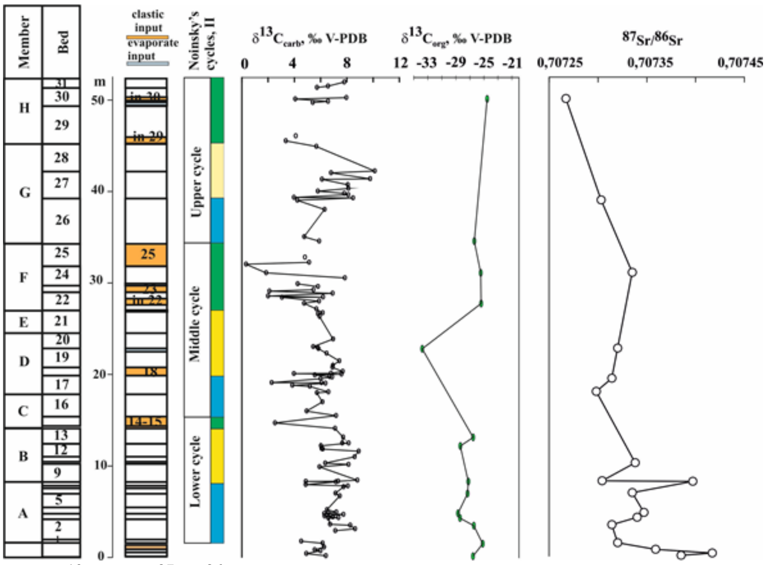

Fig. 1. The variations of $\delta^{13}C$ and $^{87}Sr/^{86}Sr$ along the Pechishchi section. Noinsky's cyclic scheme, II from [5]: each cycle composed of three facies components: marine (blue), transitional (yellow) and terrestrial (green)

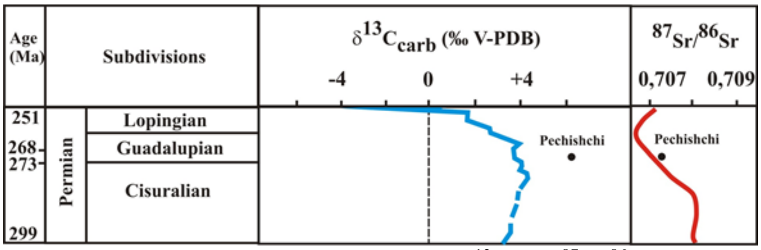

Fig. 2. The plot of the Pechishchi section point (mean values of $\delta^{13}C$ and $^{87}Sr/^{86}Sr$ by [5]) on the isotope curves from [6]

The $\delta^{13}C_{org}$ values vary from –33,8‰ to -24,6 ‰ V-PDB with a mean value -27,2 ‰ V-PDB (Fig.1). The maximum value is in bed 30 (terrestrial cyclic component of section member H). The minimum value corresponds to bed 19 (transitional cyclic component of the section member D).

The marine cyclic component was correctly probed only in the Lower Noinsky's cycle (the section member A) and characterized by a mean $\delta^{13}C_{org}$ value (beds no. 1, 3, 4, 6) (Fig.1).

The new data agree with the known fact that the $\delta^{13}C_{org}$ of Permian organic matter carbon is about 28-32‰ more negative than that of the carbonate carbon [7].

Bulk organic carbon-isotope values of marine sediments (e.g., the investigated section member A) can be influenced by a multitude of factors, such as fractionation for marine phytoplankton with C_3-pathway and heterogeneous biological origin of organic carbon or variable marine – terrigenous – bacterial mixtures [7]. Therefore, the $\delta^{13}C_{org}$ of bulk organics at the sediments may have been, at least temporarily, decoupled from the oceanic surface production of carbonates generating difficulties for utilization of $\delta^{13}C_{org}$ from bulk organics for stratigraphic purposes [7]. Biomarker analyses may be a useful tool for identification of organisms participating in the production of the organic matter (e.g., [8]) and enable better understanding of the organic-matter carbon-isotope values.

The utilization of bulk carbon-isotope values from terrestrial organic matter as a stratigraphic tool is possible, but several factors must be taken into account. Compared with marine deposits, it is more difficult to delineate the secular $\delta^{13}C$ trend from continental sections across the Palaeozoic-Mesozoic transition because, for most levels, the biostratigraphic subdivision and correlation with the marine scale are not very detailed. However, the continental Permian-Triassic boundary (PTB) itself can be stratigraphically identified in several successions (e.g., Dalongkou of Xinjiang, Carlton Heights of South Africa, Nelben section of the Germanic Basin) [7]. The negative $\delta^{13}C$ excursion at the PTB (Fig. 2) is most probably due to a combination of causes and was most likely triggered by a combined effect of the Siberian Trap volcanism and the inflow of anoxic deep waters to very shallow sea levels. Short-term events, such as release of isotopically light methane from the ocean or permafrost soils, or mass extinction itself, are questionable as causes for the carbon-isotope excursions.

Conclusions

The $\delta^{13}C_{org}$ data are considered for the Pechishchi section interpreted in terms of Noinsky's cyclic scheme. The $\delta^{13}C_{org}$ values correspond to the Permian organic carbon matter properties.

The minimum value of the $\delta^{13}C_{org}$ is detected in the transitional component of the Middle Noinsky's cycle. The maximum value of the $\delta^{13}C_{org}$ relates to the terrestrial component of the Upper Noinsky's cycle. The marine component of the Lower Noinsky's cycle is characterized by the mean value of the $\delta^{13}C_{org}$ data set.

Nevertheless, the significance of $\delta^{13}C_{org}$ as a stratigraphic tool is revealed temporarily to be low for the studied section, because of multiple questionable causes of the carbon-isotope changes. The $\delta^{13}C_{org}$ values can be considered as additional data in the geochemical characteristics of the Upper Kazanian succession in the Volga River basin.

Acknowledgments

The work was supported by the Ministry of Science and High Education of the Russian Federation contract no.14.Y26.31.0029 in the framework of the Resolution no. 220 of the Government of the Russian Federation.

REFERENCES

1. Nurgaliev D. K. *et al.*, (eds). (2015). Type and Reference Sections of the Middle and Upper Permian of the Volga and Kama River Regions: A Field Guidebook of XVIII International Congress on Carboniferous and Permian (Kazan: Kazan University Press), 208.
2. Nurgalieva N. G. (2016). Reference section of the Upper Kazanian Substage: cyclic regularities. ARPN JEAS 11(11), pp. 6928-6934.
3. Noinsky M. E. (1899). The Permian sequence on the right slope of the Volga River near the village of Pechishchi opposite the city of Kazan. Trudy Obsh'estva Estestvoispytateley pri Kazanskom Universitete 13(6), pp. 1-34.
4. Noinsky M. E. (1924) Some data on the structure and facies of the Kazanian in the Prikazansky District. Bulletin of the Geological Committee 43 (6), pp. 565-622.
5. Nurgalieva N.G, Gareev B.I., Batalin G.A. (2020). Geochemical variations in the Upper Kazanian (Middle Permian) stratotype section, Russia. IOP Conf. Series: Earth and Environmental Science 516 (2020), 012017. https://doi:10.1088/1755-1315/516/1/012017
6. Chemostratigraphy. Concepts, Techniques and Applications. Ed. By Mu.Ramkumar. (2015). http://dx.doi.org/10.1016/B978-0-12-419968-2.00002-9
7. Korte C., Kozur H. W. (2010). Carbon-isotope stratigraphy across the Permian-Triassic boundary: a review. Journal of Asian Earth Sciences 39, pp. 215-235.
8. Hays L. E., Beatty T., Henderson C. M., Love G. D., Summons R. E. (2007). Evidence for photic zone euxinia through the end-Permian mass extinction in the Panthalassic Ocean (Peace River Basin, Western Canada). Palaeoworld 16, pp. 39-50.

Mineralogy of Layered Silicates Suspended in the Water Column and in the Bottom Sediment of Lake Onega, Russia

OVDINA Ekaterina[1], STRAKHOVENKO Vera[1]

[1] V.S. Sobolev Institute of Geology and Mineralogy of the Siberian Branch of the Russian Academy of Sciences (RAS), Novosibirsk (RUSSIA)
Email: ovdina@igm.nsc.ru

Abstract

Studies of layered silicates in suspension in the water column (on water filters and in sedimentation traps) and bottom sediments collected from various parts of Lake Onega were carried out using a combination of geochemical and mineral-crystal-chemical methods: X-ray diffractometry (XRD), infrared (IR) spectroscopy, and scanning electron microscopy (SEM).

The result shows that layered silicates in suspended material collected from sedimentation traps and bottom sediments in Lake Onega consist of muscovite, biotite, illite, and chlorite.

Sedimentary material from the traps is a colloidal gelatinous silt of pelitic fraction. Scaly aggregates of grains and individual lamellar crystals of layered silicates were divided into two groups according to size.

Large particles (pelitic fraction) ranged in size from 100 µm up to 5 mm in all samples, and the content of iron and magnesium was similar in both chlorites and illites. Fine-scaled aggregates and needle-like grains ($\leq$5 µm) had significantly more iron than magnesium (and in some cases, pure ferruginous varieties) and were found only in traps and bottom sediment. The composition of Mg-Fe chlorites and illites in individual samples of suspended material from sedimentation traps and filters were the same for large grains and fine-scaled aggregates in different parts of Lake Onega.

Keywords: Lake Onega, layered silicate, bottom sediment, water suspended matter

Introduction

Sedimentary material suspended in the water column of lakes and reservoirs provides important lithological information that is usually impossible to obtain from ancient deposits. A detailed study of the chemical and mineral composition of suspended material in Lake Onega relative to the bottom sediments was conducted using a combination of analytical methods relevant to the structural and textural features of the sediment, the contribution of aeolian material, the geochemical role of biota in the formation of authigenic minerals, and the contribution of microparticles of various genesis to the formation of the modern geochemical background in the sediments.

Suspended material in lake water sinks to the bottom, so the bottom sediment represents a fine-dispersed multiphase mixture of individual mineral grains, aggregates, and biogenic detritus.

According to data obtained by A. P. Lisitsyn and colleagues from suspended matter in Arctic seas, the proportion of flake formation in layered silicates from suspended matter was 40% and higher. For example, in the White Sea (Russia), the high content of illite in both pelitic (<0.01 mm) and micropelitic (or subcolloidal <0.001 mm) fractions in the suspension indicate the existence of two forms of illite: coarse-grained and fine-grained, contributing to its widespread distribution; however, there are difficulties in determining fine-grained illite by X-ray diffractometry (XRD) because suspended material is usually enriched with X-ray amorphous material associated with illite, which produces a large halo in the range of 16-30 ºθ on the diffractogram [1].

For many years, ambiguous terms were used to refer to mica minerals (e.g., the term 'illite').

In 1991, Drits and Kossovskaya [2] proposed a new classification for dioctahedral mica minerals. In 1998, the International Mineralogical Association (sub-committee on micas) replaced the definition of 'hydromica' with the definition 'mica with a deficit of interlayer cations' [3].

However, many scientific articles use the term 'illite' to describe the mineralogical composition of modern sea bottom sediments. In this article, the term 'illite' is used for micas with a deficit of interlayer cations.

Lake Onego (61°42′N, 35°25′E, surface area of ca. 9,720 km^2), the second largest inland water-body in Europe after the neighboring Lake Ladoga, is located in the Republic of Karelia, Russia.

The lake is 248 km long and its maximum width is 96 km; the maximum depth is 127 m with an average depth of 30 m [4]. The geological depression occupied by Lake Onego is situated in the contact zone of the Baltic crystalline shield and the Russian plate. Both the geological structure and evolution of the lake as well as its watershed basin have been discussed in many publications (e.g., [5], [6], [7], [8]). A large part of the catchment area consists of abrasion-resistant Precambrian crystalline rocks (Archean granite gneiss and Proterozoic igneous rock with volcanogenic-sedimentary structures). In many areas, crystalline rocks, some of which are covered by Quaternary deposits (interglacial, continental, and marine sediments of Pleistocene age [9]), are severely eroded. According to Kalinenko *et al*., [10], in Quaternary glacial deposits distributed in the catchment area of Lake Onega, the content of illite (Mg-Fe composition, fraction <0.001 mm) ranged from 40 to 90%, and chlorite (Mg-Fe composition) ranged from trace amounts to 35%.

The aim of this work was to study the mineralogical characteristics of layered silicates in sedimentary material in the water column (trapped in suspension on filters and traps) in comparison to the bottom sediments of Lake Onega.

Methodology

The layered silicates in suspension and in bottom sediment were collected over a period of one year. The depth range was 30-100 m. Water samples, samples of suspended material in traps, and samples of bottom sediments were collected in September 2019 at several sites: Big Onego (B1), Small Onego (L11, N1), Central Onego (C4), South Onego (S3), Unitsky Bay (GU-4), Lizhemsky Bay (Gl), Kondopoga Bay (K6), Petrozavodsk Bay (P3), and Povenetsky Bay (W2).

Based on the vertical distribution of water turbidity (measured *in situ* using a multiparameter STD probe), water samples were taken (Rutner bathometer). They were then divided into solid, colloidal, and dissolved parts by sequential filtration (0.8 and 0.45 µm). Bottom sediments were collected with special samplers (Limnos, Alexon), which kept the water-bottom boundary undisturbed, in layers with a step interval of 1 cm. Sedimentary material from traps was extracted by direct vacuum membrane ultrafiltration using nuclear filters with a pore diameter of 0.45 µm.

Eleven samples of material from sedimentation traps, 52 samples from the upper oxidised layer of bottom sediments (from 2 to 35 cm), and 27 samples of a homogeneous aleuropelite layer of bottom sediments (from 5 to 100 cm) were selected and analyzed. Field work was conducted on board the *R/V Ecolog*. After *in situ* visual examination and lithological description of sediment cores, the water parameters (t, pH, Eh, CO_2, and O2) were identified.

Layered silicates in the samples were studied using a combination of geochemical and petrographic-mineralogical methods, including X-ray-fluorescence (XRF) and atomic absorption (AA) analyses. The mineral composition was determined by XRD and infrared (IR) spectroscopy.

A detailed study of the texture and structural features of the sediment, morphological features of minerals, chemical composition and structural data at the level of individual grains and aggregates, and pseudomorphosis was performed using a scanning electron microscope (SEM, (MIRA 3 TESCAN). Analytical work was performed at the at the Analytical Center for multi-elemental and isotope research of the Siberian Branch of the Russian Academy of Sciences, (Novosibirsk).

Results and Discussion

The chemical composition of Lake Onego water is classified as belonging to the calcium hydro carbonate group: $\frac{HCO3-71\ SO4\ 2-18\ Cl-11}{Ca2+49\ Mg2+32\ Na+\ 16\ K+3}$ (numbers in formula are mole percent). Vertical circulation maintains a homogenous composition throughout the water column. The elemental composition of the lowermost layer of water (20 cm above the bottom) showed only minor differences from the total content of the whole water body in terms of O_2, organic N, P, and Si.

In addition to the geochemical and mineral composition of layered silicates in the bottom sediments obtained by XRD and IR spectroscopy, the morphology, phase, and chemical composition of minerals were determined using the SEM as described in Strakhovenko V. D. and co-authors [11] and [12]. These studies showed that Fe-illite and Fe-chlorite are the main iron concentrators in the bottom sediments of Lake Onega. According to the results of XRD and IR spectroscopy, the association of layered silicates is represented by micas (muscovite, illite, biotite) and chlorites, with mixed layers of illite-smectite, chlorite-smectite, and traces of kaolinite as impurities [11].

The SEM examination of samples of Onega sediment in suspension showed the presence of scale formations and aggregates of layered silicates. Large individual grains of minerals (>0.45 µm) of muscovite, illite (Mg, Fe), and chlorite (Mg, Fe) were found on filters and in sedimentation traps and bottom sediments. Smaller formations (<0.45 µm, i.e., size of filter cell) and grains of a more ferruginous composition were only found in sedimentation traps and bottom sediments.

Sedimentary material from sedimentation traps was at the top as the unconsolidated suspension ochre or brownish-red in colour and 1-3 cm thickness with a density close to that of water. An ochre-coloured colloidal gelatinous sludge of a pelitic fraction to 5 cm lies below the unconsolidated suspension. Below the gelatinous sludge, a compacted sludge, sometimes green-grey in colour, was found to a depth of 20-25 cm.

The texture and structural features of the sedimentary material from the sedimentation traps, the morphological features of the minerals found, and the chemical composition and structure of individual grains and aggregates were examined under an optical microscope (Olympus BX50, magnification 20-60x) and the SEM showed that the gross mineral composition from different parts of Lake Onega were uniform. Against a background of fine-dispersed material (quartz, feldspar, illite, muscovite, chlorite, iron hydroxides, biogenic detritus) there are large diatomic shells, and large angular grains of individual crystals of the same minerals, plus dark-coloured and accessory minerals, including actinolite, hornblende, diopside, epidote, titanite, magnetite, ilmenite, zircon, rutile, apatite, and monazite, (Fig. 1).The compositions of the layered silicates (illites and chlorites) were determined from their positions on a Ferre triangle

(Fig. 2). According to previously obtained data, ferruginous varieties of illite and chlorite are a feature of bottom sediments of Lake Onega.

The percentage of iron, magnesium, and potassium in the composition of illites and chlorites in suspended water samples collected on filters and sedimentation traps were the same for large grains and small-scale aggregates in the Mg-Fe chlorites and illites. Only the suspended material from sedimentation traps contained fine flake aggregates of Fe-enriched illite in the presence of significant amounts of magnesium.

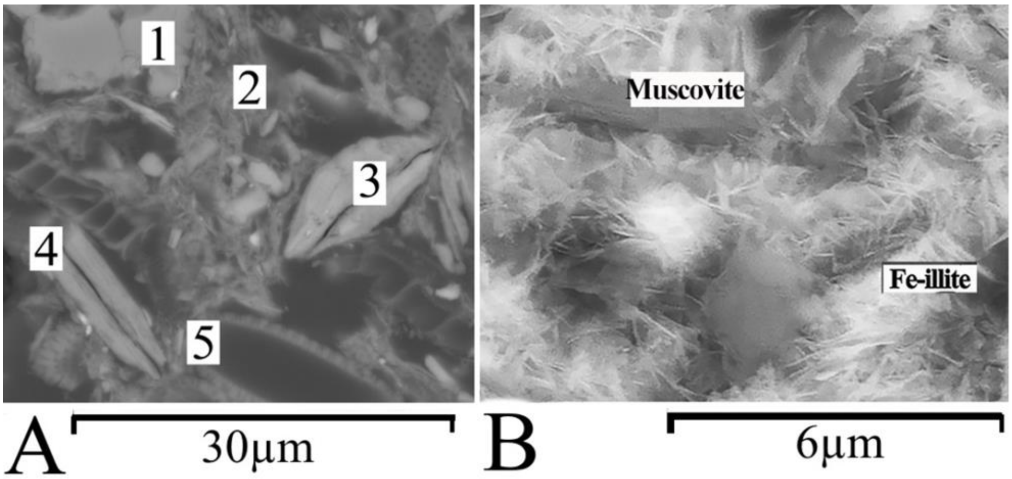

Fig. 1. Microphotographs of suspended material collected from Small Onego (A) from sedimentation trap showing 1 – individual grains of albite, 2 – small cotton-like scaly aggregates of illite (Mg, Fe), 3 – individual crystals of muscovite, 4 – individual grains of chlorite (Mg, Fe), and 5-skeletons and fragments of diatom shells and (B) fibrous microflakes of ferruginous illite and valves of the terrigenous mineral muscovite

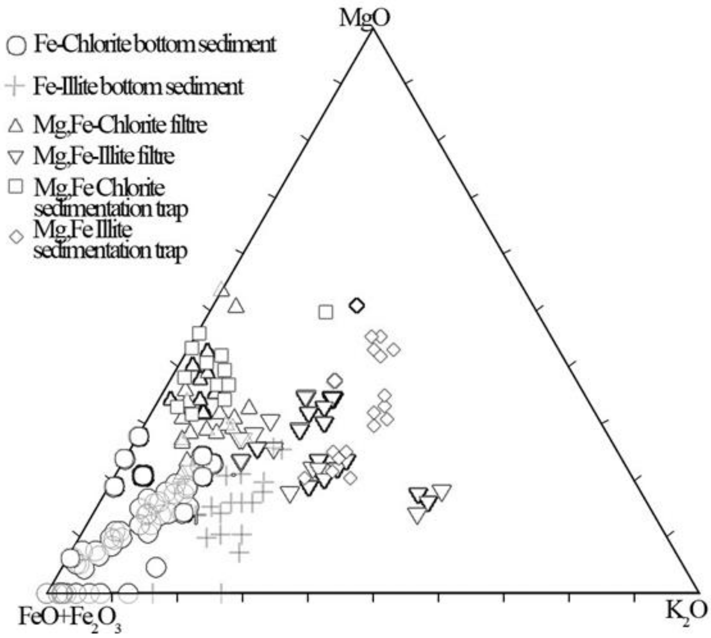

Fig. 2. FeO-MgO-K_2O diagram showing the composition of illites and chlorites on filter, sedimentation trap, and bottom sediment from Lake Onega

Conclusions

The modern analytical study established the presence of layered silicates in the suspended material collected in sedimentation traps and bottom sediments of Lake Onega, consisting of muscovite, biotite, illite, and chlorite. Scaly aggregates of grains and individual lamellar crystals of layered silicates were divided into two groups based on size. Large particles (pelite fraction) ranging in size from 100 μm up to 5 mm were present in all samples, and the content of iron and magnesium in the chlorites and illites was approximately the same. Both fine-grained aggregates and needle-like grains ($\leq$5 μm) had significantly more iron than magnesium in the composition (or pure ferruginous varieties) and were only found in material from sedimentation traps and bottom sediments. In the suspended material from sedimentation traps and on filters, the composition of Mg-Fe chlorites and illites in individual samples were the same for large grains and small-scale aggregates in different parts of Lake Onega.

Under humid conditions in northern latitudes and high concentrations of iron and silicon in the waters of Lake Onega, the unstable components in detrital illites (Fe-Mg) and chlorites (Fe-Mg) are transformed into ferruginous varieties in the bottom sediments. The presence of significant amounts of muscovite in the bottom sediments are attributed to the erosion of older glacial deposits and shungites dominated by sericite with increased resistance to chemical destruction.

Acknowledgments

This work was financially supported by the Russian Foundation for Basic Research project No. 19-05-50014.

REFERENCES

1. Lisitsyn, A. P. (Ed.). (2013). Sistema Belogo Morya. Tom III. Rasseyannyj osadochnyj material gidrosfery, mikrobnye protsessy i zagryazneniya. Nauchnyj Mir, Moscow, 668.
2. Drits, V. A., Kossovskaya, A. G. (1991). Glinistye mineraly: slyudy i khlority. Nauka, Moscow, 175.
3. Rieder, M., Cavazzini, G., D'yakonov, Y. S., Frank-Kamenetskii, V. A., Gottardi, G., Guggenheim, S., Koval, P. V., Muller, G., Neiva, A. M. R., Radoslovich, E. W., Robert, J. L., Sassi, F. P., Takeda, H., Weiss, Z., Wones, D. R. (1998). Nomenclature of the micas. Clays and Clay Minerals 46 (5), pp. 586-595 DOI: 10.1346/CCMN.1998.0460513
4. Filatov, N. N. (Ed.). (2010). Onezhskoe ozero. Atlas. KarNTS RAN, Petrozavodsk, 151.
5. Biske, G. S., Lac, G. Ts., Lukashov, A. D., Goryunova, N. N., Il’in, V. A. (1971). Stroenie i istoriya bassejna Onezhskogo ozera. Trudy IG KarNTS RAN, Petrozavodsk, 73.
6. Kvasov, D. D. (1975). Pozdnechetvertichnaya istoriya krupnykh ozer i vnutrennikh morej Vostochnoj Evropy. Nauka, Leningrad, 278.
7. Demidov, I. (2004). Donnye otlozheniya i izmeneniya urovnya ozera pozdnelednikovogo Onezhskogo ozera. Geologiya i poleznye iskopaemye Karelii 7, pp. 207-218.
8. Subetto, D.A. (2009). Donnye otlozheniya ozer: paleolimnologicheskie rekonstruktsii. Publishing House of the Russian State Pedagogical University A.I. Herzen, St. Petersburg, 348.
9. Glushanin, L. V., Sharov, N. V., Shtiptsov, V. V. (Eds.). (2011). Onezhskoe Paleoproterozojskoe stroenie (geologiya, tektonika, glubinnoe stroenie i mineralogiya). KarNTS RAN, Petrozavodsk, 431.
10. Kalinenko, V. V., Kheirov, M. B., Shevchenko A. Ya. (1974). Glinistye mineraly Belogo morya. Litologiya i poleznye iskopaemye 4, pp. 18-23.
11. Strakhovenko, V., Subetto, D., Ovdina, E., Danilenko, I., Belkina, N., Efremenko, N., Maslov, A. (2020). Mineralogical and Geochemical composition of Late Holocene bottom sediments of Lake Onego. Journal of Great Lakes Research 46 (3), pp. 443-455. DOI: 10.1016/j.jglr.2020.02.007
12. Strakhovenko, V., Subetto, D., Ovdina, E., Belkina, N., Efremenko, N. (2020) Distribution of elements in iron-manganese formations in bottom sediments of Lake Onego (NW Russia) and small lakes (Shotozero and Surgubskoe) of adjacent territories. Minerals 10 (5), 440. DOI: 10.3390/min10050440

Diatoms from Modern Lake Sediments of Lake Lebedinoe (Yamalo-Nenets Autonomous District, West Siberian Arctic, Russia)

PALAGUSHKINA Olga[1], FROLOVA Larisa[1]

[1] *Kazan Federal University, Kazan, (RUSSIAN FEDERATION)*
Email: opalagushkina@mail.ru

Abstract

26 taxa from 2 classes, 14 families and 17 genera of diatoms were identified from modern bottom sediments of Lake Lebedinoe (Yamalo-Nenets Autonomous District – YNAD, West Siberian Arctic, Russia). The diatoms included species with mainly cosmopolitan distributions.

The assemblages were dominated by alkaliphilic benthic diatoms preferring moderate temperature conditions, indifferent to salinity and water flow.

Keywords: diatoms, lake, modern bottom sediments, Yamalo-Nenets Autonomous District, West Siberian Arctic

Introduction

Arctic reservoirs are excellent indicators of the ongoing increase in air temperature on the planet [1]. Diatoms, which inhabit all surface waters of the Earth, can be used as biological indicators of changes in the environment (temperature, hydrochemical) [2], [3], [4], [5], [6].

The West Siberian Arctic, especially its northern part, is poorly studied algologically. The aim of this work was to study the taxonomic composition and ecological characteristics of diatoms in modern sediments of Lake Lebedinoe (YNAD, West Siberian Arctic).

Methodology

In summer 2017, modern bottom sediments were sampled in Lake Lebedinoe (YNAD, West Siberian Arctic) (64°17.135´N, 78°07.449´ E) from a depth of 1.3 m using a UWITEC sampler.

The lake is located in the subarctic climatic zone, where the duration of the frost-free period is 50-70 days. Average January temperatures range from -23 to -27 degrees Celsius, July – from +3 to +9, the amount of precipitation is low: about 400 mm/year [7]. Modern bottom sediments consisted of sandy material with plant detritus. Hydrochemical studies recorded a low value of conductivity – 7.7 ms/cm^{-1}, good oxygen saturation of water 101.7% (9.91 mg/l), pH-6.3, characterized the water medium as weakly acidic. Processing of sediment samples for diatom analysis was performed using the water bath method [8]. Diatom slides were mounted using Naphrax. Diatoms were identified to the lowest possible taxonomic level mainly using Krammer and Lange Bertalot [9], [10], [11], in accordance with modern taxonomy as given in the Algaebase database [12] and classification of diatoms used in Russia [13] with the latest revisions [14], [15].

To detection the species composition, 500 valves were identified and counted in the sample under an Axioplan Zeiss light microscope equipped with an oil immersion objective.

Biogeographical and ecological characteristics of the taxa with respect to habitat preferences, pH, water salinity, temperature, water flow and geographical distribution, were described following Davydova [3], and Barinova [16].

Results

26 diatom taxa were identified from sample from modern bottom sediments of Lake Lebedinoe, belonging to 2 classes, 14 families and 17 genera (Table 1). Diatoms from Centrophyceae were represented by only two species of the genus *Aulacoseira*; the other 24 species belonged to the Pennatophyceae. The species composition is better represented by species belonging to the genera *Eunotia and Pinnularia*.

Table 1. List of diatoms of modern bottom sediments of Lake Lebedinoe

№	Taxon
	Class Centrophyceae
	Family Aulacosiraceae
	Genus *Aulacoseira* Thwaites 1848
1	*Aulacoseira ambigua* (Grunow) Simonsen 1979
2	*Aulacoseira distans var. distan*s (Ehrenberg) Simonsen 1979
	Class Pennatophyceae
	Araphales
	Family Staurosiraceae
	Genus *Staurosira* Ehrenberg 1843
3	*Staurosira construens* Ehrenberg 1843
	Genus *Staurosirella* D.M. Williams & Round 1988
4	*Staurosirella pinnata* (Ehrenberg) D.M. Williams & Round 1988
	Family Fragilariaceae
	Genus *Fragilariforma* D.M. Williams & Round 1988
5	*Fragilariforma constricta* (Ehrenberg) D.M. Williams & Round 1988
6	*Fragilariforma virescens* (Ralfs) D.M. Williams & Round 1988
	Family Tabellariaceae
	Genus *Tabellaria* Ehrenberg 1844
7	*Tabellaria flocculosa* (Roth) Kützing
8	*Tabellaria fenestrata* (Lyngbye) Kützing
	Genus *Tetracyclus* Ralfs, 1843
9	*Tetracyclus glans* (Ehrenberg) F.W. Mills 1935
	Raphales
	Family Amphipleuraceae
	Genus *Frustulia* Rabenhorst 1853
10	*Frustulia rhomboides* (Ehrenberg) De Toni 1891
	Family Neidiaceae
	Genus *Neidium* Pfitzer 1871
11	*Neidium bisulcatum* (Lagerstedt) Cleve 1894
12	*Neidium dubium* (Ehenberg) Cleve 1894
	Family Pinnulariaceae
	Genus *Pinnularia* Ehrenberg 1843
13	*Pinnularia alpine* W. Smith 1853
14	*Pinnularia borealis* Ehrenberg 1843
15	*Pinnularia gibba* (Ehrenberg) Ehrenberg 1843
	Family Stauroneidaceae
	Genus *Stauroneis* Ehrenberg
16	*Stauroneis phoenicenteron* (Nitzsch.) Ehrenberg
	Family Achnanthaceae
	Genus *Achnanthidium* Kützing 1844

17	*Achnanthidium minutissimum* (Kützing) Czarnecki 1994
	Family Eunotiaceae
	Genus *Eunotia* Ehrenberg 1837
18	*Eunotia vanheurckii* R.M. Patrick 1958
19	*Eunotia pectinalis* (Kützing) Rabenhorst 1864
20	*Eunotia serra* Ehrb.
	Family Cymbellaceae
	Genus *Cymbopleura* (Krammer) Krammer 1997
21	*Cymbopleura inaequalis* (Ehrenberg) Krammer 2003
	Family Gomphonemataceae
	Genus *Gomphonema* Ehrenberg 1824
22	*Gomphonema gracile* Ehrenberg 1838
	Genus *Encyonema* Kützing, 1834
23	*Encyonema leibleinii* (C. Agardh) W.J. Silva, R. Jahn, T.A.V. Ludwig, & M. Menezes 2013
24	*Encyonema silesiacum* (Bleisch) D.G. Mann 1990
	Family Sellaphoraceae
	Genus *Sellaphora*
25	*Sellaphora pupula* (Kützing) Mereschkovsky 1902
	Family Mastogloiaceae
	Genus *Aneumastus* D.G. Mann & A.J. Stickle, 1990
26	*Aneumastus tusculus* (Ehrenberg) D.G. Mann & A.J. Stickle 1990

In relation to habitat, benthic species were the most frequent (69.2% of the taxonomic richness), 26.9% of the taxonomic richness were planktonic-benthic and only 3.8% were planktonic species.

In relation to salinity, the species of diatoms found are oligohalobes, the majority of which constituted indifferent species (69%); fewer were halophobes (23.1%) and halophiles (7.7%).

In relation to pH, the majority of species were alkaliphiles (34.6% of the taxonomic richness), with acidophilic species slightly fewer (30.7%), and even fewer indifferent and alkalibiontic species (19.2% and 7.7% respectively). By geographical distribution, most of the species could be attributed to cosmopolitan species (69% of the taxonomic richness), 15.4% have an arctic-alpine distribution and 11.5% are boreal. In relation to water temperature, information is only available for 9 species: 5 of them prefer moderate conditions, 3 are eurythermic and 1 species, *Aulacoseira distans var. distans* (Ehrenberg) Simonsen 1979, is associated with cold water. As for the water flow factor, information is only available about 23 species, of which species of stagnant-flowing waters or indifferent predominated (10). 7 were species of flowing water, and 5 of stagnant water; one aerophilic species, *Pinnularia borealis* Ehrenberg 1843, was also found.

Discussion

The predominance in the species composition of Pennatophyceae benthic cosmopolitan diatoms is characteristic of modern bottom sediments of arctic shallow water bodies [17].

Diversity of species from the genera *Eunotia, Pinnularia* is associated with low values of mineralization for water body of the study area [17]. The main feature of the natural surface waters of the YNAO in hydrochemical terms is their weak mineralization (less than 100 mg/dm3), the lowest values of which were noted during the spring flood. In general, according to the existing classification [18], the surface waters of the West Siberian Arctic belong to the ultrafresh, hydrocarbonate class, sodium, less often calcium group with a low content of sulfates, chlorides and sodium ions. In terms of nutrient content, surface waters are oligotrophic, with a low content of nitrogen compounds, with a low hardness (0.1-0.34 mmol/dm^3), that is, "very soft" [19].

Conclusions

Our studies have shown that diatoms of modern bottom sediments of Lake Lebedinoe (YNAO, West Siberian Arctic) are represented by 26 species, among which cosmopolitan, benthic, alkaliphilic species, indifferent to salinity, temperature and flow factor, prevail. The indicated species of the genera *Eunotia* and *Pinnularia* prefer low values of electrical conductivity and a neutral – weakly acidic environment.

Acknowledgments

We thank all colleagues who helped us during the fieldwork. Our sincere thanks to the anonymous reviewers for their valuable comments. This work was supported by the Russian Science Foundation (project N 20-17-00135). O. P. is supported by the subsidy allocated to Kazan Federal University for the state assignment N 671-2020-0049 in the sphere of scientific activities.

REFERENCES

1. John P. Smol, Alexander P. Wolfe, H. John B. Birks, Marianne S. V. Douglas, Vivienne J. Jones, Atte Korhola, Reinhard Pienitz, Kathleen Rühland, Sanna Sorvari, Dermot Antoniades, Stephen J. Brooks, Marie-Andrée Fallu, Mike Hughes, Bronwyn E. Keatley, Tamsin E. Laing, Neal Michelutti, Larisa Nazarova, Marjut Nyman, Andrew M. Paterson, Bianca Perren, Roberto Quinlan, Milla Rautio, Émilie Saulnier-Talbot, Susanna Siitonen, Nadia Solovieva, and Jan Weckström (2005). Climate-driven regime shifts in the biological communities of arctic lakes. Proceedings of the National Academy of Sciences (PNAS) 102 (12), pp. 4397-4402.
2. Battarbee R. W. (1999). The importance of palaeolimnology to lake restoration. Hydrobiology 395-396, pp. 149-159.
3. Davydova, N. N. (1985). Diatoms as indicators of natural conditions of water bodies in Holocene. Nauka, Leningrad. 244.
4. Palagushkina O., Frolova L., Zinnatova E., Kosareva L., Nurgaliev D. (2018) Diatoms of sediments of Plescheevo Lake (Russia) as indicators of environmental changes in Holocene. 18th International Multidisciplinary Scientific GeoConference, SGEM 2018. Vol. 18, Issue 5.1. Ecology, Economics, Education and Legislation. pp. 283-288.
5. Zinnatova E., Frolova L. (2019). Diatom complexes in the bottom sediments of Big Miassovo lake (South Ural, Russia). 19th International multidisciplinary scientific geoconference SGEM 2019 19(5.1). pp. 181-188.
6. Zinnatova E., Frolova L., Kulikovskiy M., Glushchenko A., Nurgaliev D. (2018). Diatom complexes in the bottom sediments of Rubskoe Lake (the east European Plain, Russia). 18th International Multidisciplinary Scientific GeoConference, SGEM 2018 18 (5.1), pp. 275-281
7. Lazukov G. I. (1975). Geomorphological mapping of the north of the West Siberian Plane. Natural conditions of Western Siberia 5, pp. 20-37.
8. Battarbee R.W. (1986). Diatom analysis. In Handbook of Holocene Palaeoecology and Palaeohydrology. Berglund B.E. (ed). J. Wiley & Sons, pp.527-570.
9. Krammer, K. and Lange-Bertalot, H. (1986). Bacillariophyceae. 1. Teil: Naviculaceae: Suesswasserflora von Mitteleuropa. Gustav Fischer Verlag, Stuttgart, Jena, 976.
10. Krammer, K. and Lange-Bertalot, H. (1988). Bacillariophyceae. 2. Teil: Bacillariaceae, Epitemiaceae, Surirellaceae: Suesswasserflora von Mitteleuropa. Gustav Fischer Verlag, Stuttgart, Jena, 596.
11. Krammer, K. and Lange-Bertalot, H. (1991). Bacillariophyceae. 3. Teil: Centrales, Fragilariaceae, Eunotiaceae: Suesswasserflora von Mitteleuropa. Gustav Fischer Verlag, Stuttgart, Jena, 576.
12. Guiry, M. D. and Guiry, G. M. (2015). AlgaeBase. World-wide electronic publication, National University of Ireland, Galway http://www.algaebase.org
13. Glezer, Z. I., Karaeva, N. I., Makarova, I. V. *et al*., (1988). Classification of diatoms. In Diatoms of the USSR (fossil and modern) Leningrad. 2 (1), pp. 31-35.

14. Genkal, S. I., Kulikovsky, M. S., Mikheeva, T. M., Kuznetsova, I. V., and Lukyanova, E. V. (2013). Diatoms of plankton of Svisloch River and its reservoirs. Scientific World, Moscow, 236.
15. Guiry, M. D. and Guiry, G. M. (2019). AlgaeBase. World-wide electronic publication, National University of Ireland, Galway. https://www.algaebase.org
16. Barinova, S. S., Medvedeva, L. A., and Anisimova, O. V. (2006). Biological diversity of algae-environmental indicators. Pilies Studio, Tel Aviv. 498.
17. Palagushkina, O. V., Nazarova, L. B., Wetterich, S., and Shirrmaister, L. (2012). Diatoms of modern bottom sediments in Siberian Arctic. Contemporary Problems of Ecology 5 (4), pp. 413-422.
18. Alekin O. A. (1970). Fundamentals of hydrochemistry. Leningrad: 444.
19. Genkal S. I., Yarushina M. I. (2017) Interesting finds of diatoms and a new species of *Fragilaria* strelnikovae from reservoirs and streams of the Yamal Peninsula. Novosti sistematiki nizshikh rasteniy 51, pp. 12-22.

Effect of Volcanic Processes on the Lithogenesis of Saprobitumolites from the Onega Structure, Karelia

PERVUNINA Aelita[1], MYASNIKOVA Oksana[1]

[1] *Institute of Geology, Karelian Research Centre, RAS, Petrozavodsk (RUSSIA)*
Email: aelita@krc.karelia.ru

Abstract

The results of the study of the effect of subvolcanic complexes on the formation of a high-carbon pelitomorphic rock (saprobitumolite, C_{org} 35-45%) at the Maksovo Deposit of the Zazhogino Ore Field, Karelia, are reported. The deposit is confined to a sixth productive horizon in the Zaonega Formation of the Ludicovian Superhorizon (2100-1920 Ma) of the volcanotectonic Onega Structure located on the Karelian Craton in the eastern Fennoscandian Shield. Gabbro-dolerite sills were found at the deposit. It was formerly assumed that the technological properties of saprobitumolites at the contact with mafic subsheeted intrusions are not affected by high temperatures.

The results of lithogeochemical studies of the various structural varieties of saprobitumolites, conducted by electron microscopy, as well as silicate and X-ray fluorescence analyses, are reported.

The petrophysical properties of the rocks were analyzed.

The heating of carbon-rich rock horizons was shown to contribute to organic matter transformation and to affect the formation of the body by giving rise to migratory hydrocarbons.

A mechanical effect and thermal conditions, provoked by the intrusion of gabbrodolerites into the variably lithified rocks of the Maksovo Deposit, contributed to changes in the structural-textural properties and petrophysical characteristics of saprobitumolites.

Keywords: shungite, Precambrian, contact metamorphism, natural coke, technological properties

Introduction

During the mining and initial development of Karelia's high-carbon rock deposits in the 1980s the effect of volcanic processes on the technological properties of the raw material was disregarded.

It was assumed that the free carbon content of saprobitumolites was stable within the deposit, and that rock properties at the contact with subsheeted intrusions do not vary significantly.

The Maksovo Deposit of the Zazhogino Ore Field of Proterozoic carbonaceous rocks are confined to a sixth productive horizon of the Zaonega Formation of the Ludicovian Superhorizon (2100-1920 Ma). The deposit is in the volcanotectonic Onega Structure located on the Karelian Craton in the eastern Fennoscandian Shield. The lithostratographic column of the Zaonega Formation was shown to comprise nine productive carbonaceous rock horizons and ten gabbro-dolerite sills [1].

The sills are 20-80 m thick.

The petrochemical composition of carbonaceous rock samples from the Maksovo Deposit was studied by chemical (silicate) analysis and X-ray fluorescent spectrometry. The structural and textural characteristics of rock varieties from the deposit were subjected to electron microscopy using a system of X-ray energy-dispersion microanalysis, Oxford INCA

Energy350, integrated with a VEGA II LSH electron microscope. The petrophysical parameters of the rocks on samples of regular cubic shape were determined. The studies were conducted at the Centre for Collective Use located in the Federal Research Centre of the Karelian Research Centre, Russian Academy of Science.

Geological structure of the Maksovo Deposit

The deposit is a subhorizontally lying saprobitumolite lens (700 m×500 m) which contains 20 to 45% C_{org}. The organic matter (OM) is metasapropel, partly migratory [2], [3]. The central portion of the body is up to 120 m thick. An anticline, produced by the evolution of Maksovo organo-mineral rocks, was revealed there [4]. Saprobitumolites commonly display a pelitomorphic structure and massive, less commonly breccial and layered, texture. The mineral substance of the carbonaceous rocks consists of quartz, albite, chlorite, sericite and pyrite.

Structurally, the Maksovo Deposit comprises three subhorizontally lying gabbro-dolerite bodies that vary in thickness and wedge out along the strike [5]. The cores collected contain gabbro-dolerites underlying the saprobitumolite body. Higher in the sequence, the gabbro-dolerites are exposed onto the day surface and surround the western flanks of the anticline, resting consecutively on the sixth and seventh carbonaceous rock horizons. A feeder channel was observed in one of the sills. A gabbro-dolerite dike with apophyses in its frontal portion, which intruded through the entire deposit, was revealed in the central portion of the deposit.

Petrographic and lithological description of Maksovo rocks

Gabbro-dolerites were highly metasomatized to fine-grained micaite with variable quartz, chlorite and albite concentrations. Dark-gray aphanitic gabbro-dolerites (apodolerites) with amygdales and cavities of oval to irregular shape occur at the endocontact with saprobitumolites (Fig. 1). The amygdales, up to 0.5 cm in diameter, are filled with quartz. The rocks display an amygdaloidal to porphyritic structure with relics of intersertal structure in the matrix.

Silicification, epidotization and carbonization processes are widespread. Plagioclase phenocrysts and microliths are replaced by fine-grained muscovite and albite aggregate.

Observed in the endocontact portion is multiple streaky-disseminated copper-sulfide mineralization composed of pyrite, chalcopyrite, pentlandite, pyrrhotite and sphalerite.

Nickeliferous pyrite, cobalt arsenide and clausthalite were identified.

The central portion of the feeder channel of the sill consists of fine- to medium-grained varieties and its contact is composed of fine-grained varieties. The upper portion of the feeder channel consists entirely of carbonized amygdaloidal-textured apodolerites.

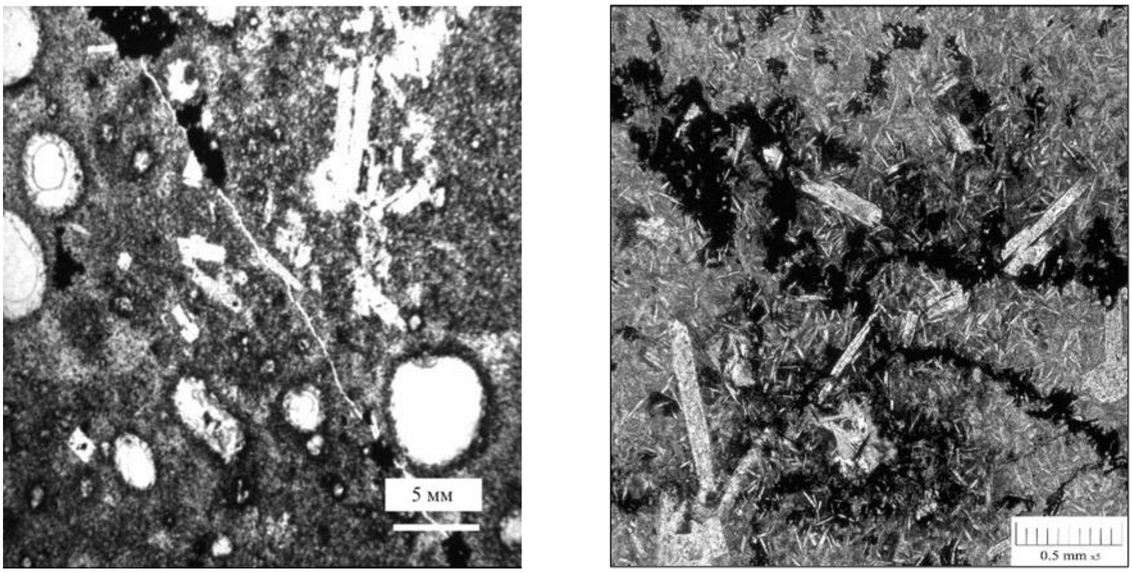

a b

Fig. 1. Carbonized amygdaloidal apodolerite at the endocontact, Maksovo Deposit.
Porphyritic, the matrix displays an intersertal to aphanitic structure. Transparent thin section, without analyzer.
a – anthraxolite (dark-gray) forms rims around silica amygdales; b – anthraxolite (black) fills microfractures

The lower contact of the dolerites is irregular, with a 1-3 cm thick sooty host rock variety.

At the lower endocontact of the sill the carbonized zone is the thinnest. Relics of doleritic structure persist in the centre of the feeder channel and near the base of the sill.

The gabbro-dolerites are broken into numerous fractures, which are filled with saprobitumolites with fine migratory OM (anthraxolite) aggregates. Carbon fills interstices between the grains, fractures, pores and cavities. Anthraxolite is often associated with mica, quartz and pyrite. It seems that the material filled the fractures as a result of a reduction of the saprobitumolite viscosity triggered by heat from intruding magma and local elevated pressure created by rapid OM catagenesis. Saprobitumolite in the fractures consists predominantly of poorly recrystallized silica and OM.

Saprobitumolites have suffered the most profound alterations in fine (20 cm across) xenoliths.

Their OM content decreases to 10%, while their mica (mainly biotite) content increases to 25%.

These are fine-grained fractured and foliated rocks with numerous small cavities, up to 0.5 mm in size, filled with anthraxolite, quartz and biotite. Jarosite and iron hydroxides also occur on the walls of the cavities and open fractures. The rocks display a fluidal microtexture. Biotite, occurring as finely crystalline scales, 1-3 μm in size, is abundant between quartz grains and surrounds the pores. Numerous pyrite grains sometimes form rims around magnetite and biotite grains and contain copper and nickel sulfide inclusions. Pyrite is replaced by jarosite.

A coking zone, up to 1.5 m in thickness, was revealed at the endocontact of saprobitumolites.

The zone consists of two parts (Fig. 2). The structural and textural characteristics, as well as the composition of saprobitumolites vary markedly. A sooty variety with a cavernous texture, 2-8 m in thickness, is observed directly at the contact. Saprobitumolites at the contact generally exhibit a typical prismatic cleavage in the form of elongated prisms measuring 4x10 cm. The prisms are oriented perpendicular to the contact. In cross-section, they look like irregular polygons separated by fractures from each other. Anthraxolite (sometimes pyrite) films evolve on fracture walls. In the upper portion of the feeder channel the prismatic cleavage of saprobitumolites occurs as sheaf-like clusters of curved tetra- and hexahedral prisms up to 1 m in length. The rocks are steel-gray with a dull luster. Coke-like saprobitumolites consist of OM (15-50%), quartz and muscovite (up to 25%); biotite, chlorites, pyrite, rutile, fluorapatite, leucoxene and sometimes K-feldspar are present. The fractures and pores of the cokes are filled with globular anthraxolite, quartz and mica; Mg-Fe and Fe-Mg chlorites are less abundant.

Anthraxolite exhibits a fine-grained mosaic structure. It forms thin undulating streaks around quartz aggregates. The structures of metacolloid quartz aggregates suggest rapid silica crystallization. Large pyrite aggregates with nickel impurities and nickel and copper sulfide inclusions are occasionally encountered.

Fig. 2. Coking zone at the exocontact of saprobitumolites, Maksovo Deposit.
1 – apodolerites, 2 – unconsolidated, cavernous saprobitumolite with relics of prismatic cleavage, 3 – saprobitumolite with a prismatic cleavage, 4 – brecciated saprobitumolite

Slickensides with anthraxolite and chlorite films are observed in the contact zone in saprobitumolites. The coking zone is stable over the entire sill top area. Away from the contact, cokes give way to saprobitumolites, in which signs of the thermal effect of the sill are only detected microscopically at a distance of up to 30 m from the contact.

The characteristics of natural cokes are: prismatic polygonal cleavage, fluidal microtexture and high porosity (Fig. 3, Table 1). The cokes after Maksovo saprobitumolites are similar lithologically to natural cokes evolving in coal strata at the contact with intrusions of varied composition [6].

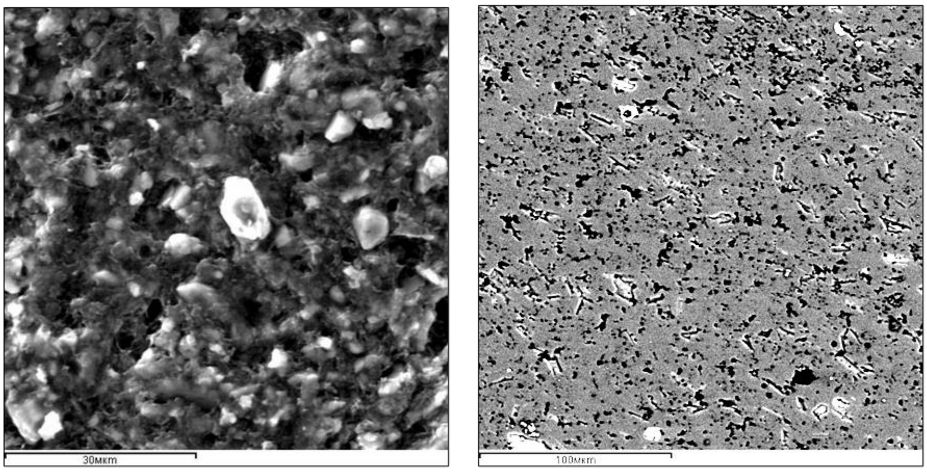

a b

Fig. 3. Fine porosity in natural coke after saprobitumolite, Maksovo Deposit. SED. a. black – pores, b. anthraxolite (black) fills the pores

Table 1. Petrophysical properties of saprobitumolite varieties from the Maksovo deposit

Index	Massive rocks	Brecciated rocks	Exocontact zone
Density, g/cm^3	2.30-2.36 2.32	2.38-2.42 2.40	2.13-2.18 2.15
Water absorption, %	0.54-0.67 0.63	0.24-0.32 0.28	1.05-1.23 1.17
Porosity is effective, %	1.28-1.55 1.46	0.57-0.79 0.67	2.24-2.67 2.52

Discussion

The conformal mode of occurrence of saprobitumolite and gabbro-dolerite strata indicates the simultaneous formation of an injection fold and sill intrusion. Gabbro-dolerite becomes thinner in some portions of the anticline. Originally irregular OM distribution in the rock and structural-textural heterogeneity have affected deformation load distribution within the deposit.

As a result of plastic deformations, an anticline formed and thickness increased in the permeable body zone, which is traced by a gabbro-dolerite dike in the central portion.

The narrow zones of the exocontact show signs of short-term magma-thermal effect of the melt which intruded into the saprobitumolite sequence with the evolution of some secondary hydrocarbon structures. The study of the upper exocontact zone of the dike has shown that the ability of OM to pass into a plastic state and form porous natural coke upon heating is associated with the intrusion of magmatic melt into a poorly lithified organo-mineral complex unaffected by catagenetic transformation. Primary OM has not passed the main phase of oil formation [7].

Poor lithification is indicated by the massive texture of saprobitumolites and the absence of layering characteristic of sedimentary rocks that have passed all sedimentation stages.

Catagenetic OM transformation and the low permeability of pelitomorphic rocks created high pressure, which initiated the saturation of the melt with gaseous hydrocarbons and the decrease of density. The presence of water-bearing minerals in sapropelites, as well as the high thermal capacity and low thermal conductivity of organomineral compounds contributed to the abundance of hydrothermal and metasomatic processes (micatization, chloritization, sulfidization and silicification) in the rocks of the deposit. Hydrothermal processes at the direct contact with the sill are the most vigorous.

Conclusions

Studies have shown that stepwise OM transformation in saprobitumolites results from a thermal effect over a large area of the deposit by the one-act intrusion of gabbro-dolerites and subvolcanic and diatreme facies. A mechanical effect and thermal conditions that resulted from the intrusion of gabbro-dolerites into poorly lithified Maksovo rocks gave rise to mobile hydrocarbons (anthraxolites) which are prone to rapid polymerization. Hydrocarbon migration into the most permeable zones of saprobitumolites was a major factor in the evolution of the anticline and the increase of rock thickness in the central part of the deposit.

The carbon content of an exocontact zone in productive horizon rocks density decreases and porosity increases. Changes in the structural and textural properties of saprobitumolites should be taken into account when mining the deposit.

To answer questions on the formation of the Maksovo Deposit, which is a deformational type of a saprobitumolite deposit associated with intrusive activity, further studies are needed.

Acknowledgments

The study was conducted under a state assignment from the Institute of Geology, Karelian Research Centre, RAS.

REFERENCES

1. Geology of Precambrian shungite-bearing volcanic-sedimentary rocks in Karelia. (1982). (Sokolov V.A., Ed.). Petrozavodsk, Karelia, 204.
2. Filippov M. M. (2002). Shungite-bearing rocks of Karelia. Published by the KarRC RAS, Petrozavodsk, 280.
3. Shvanov V. N., Bazhenova T. K., Frolov V. G. (1998). Organic rocks. Systematics and classification of sedimentary rocks and their counterparts. Nedra, St. Petersburg, pp. 249-269.
4. Filippov M. M., Klabukov B. N., Sukhanov A. V. (2004). Experimental determination of the basic parameters of systems of dome-shaped shungite-bearing structures in the Tolvuja syncline. Roosiyskiy geofizichesky zhurnal 3, pp. 25-30.
5. Filippov M. M., Biske N. S., Pervunina A. V. (2009). Contact metamorphism of shungite-bearing rocks from the Maksovo deposit, Karelia. Proceedings of the 6th All-Russian Fersman Scientific Session, Apatity, pp. 199-203.
6. Ivanov Yu. A., Myasnikova I. P. (2000). Oil and gas potential of the northern Siberian Platform: new prospects. Geologiya nefti i gaza 3, pp. 24-29.
7. Melezhik V. A., Fallick A. E., Filippov M. M., Larsen O. (1999). Karelian shungite – an indication of 2.0-Ga-old metamorphosed oil-shale and generation of petroleum: geology, lithology and geochemistry. Earth-Science Reviews 47, pp. 1-40.

Chemical Composition of Groundwater in Kazan

PETROVA Daria[1]

[1] Kazan Federal University, Kazan (RUSSIA)
Email: DaIPetrova@kpfu.ru

Abstract

Based on the processing of hydrochemical data using of mathematical statistics and GIS-technologies, the consequences of the impact of technogenesis on the underground waters of a large Russian city over the past 60 years are considered. Trends of changes in the chemical composition of the underground hydrosphere are shown.

Keywords: Groundwater, Hydrochemistry, Technogenesis, Monitoring, Mathematical Statistics, GIS, Kazan

Introduction

In connection with the growth of cities and the concentration of the population in a relatively small area, the study and assessment of technogenic factors on changes in the composition of the hydrosphere in industrial-urbanized territories has recently become an urgent direction of hydrogeological research, which studies the transformation of a natural hydroshell into a natural-technogenic and technogenic (e.g., [4], [5]). For example, the study of the chemical composition of water allows the consequences of human activity on the underground hydrosphere to be assessed (e.g., [1], [2], [3], [6], [7], [8]).

The city of Kazan is a large (1.25 million inhabitants) industrial and cultural center of Russia, for which the issues of changing the quality of groundwater are an important element of strategic development. Today, about 20% of the city's drinking water supply is connected with underground water intake facilities, and almost all large enterprises have their own underground water source for industrial water supply (Fig. 1).

Object characteristics and research methods

The territory of Kazan includes the following underground aquifers (from top to bottom): Neogene-Quaternary alluvial complex (aN-Q); Lower Kazanian carbonate-terrigenous complex (P2kz1); Sakmarian sulfate-carbonate complex (P1s). Underground waters are exploited in Kazan by a large number of wells (Fig. 1) and are widely used for industrial water supply of industrial enterprises and household and drinking needs. Regular observations are carried out in the wells. I have collected the results of 2267 chemical analyses of water carried out according to standard methods in certified laboratories. Statistical processing of the initial data was carried out using the STATISTICA software. To build maps-models of spatial variability of components, the “ArcGisMap” software package was used, which provides a wide range of different interpolation methods. Inverse distance weighted and kriging methods were used to analyze chemical parameters.

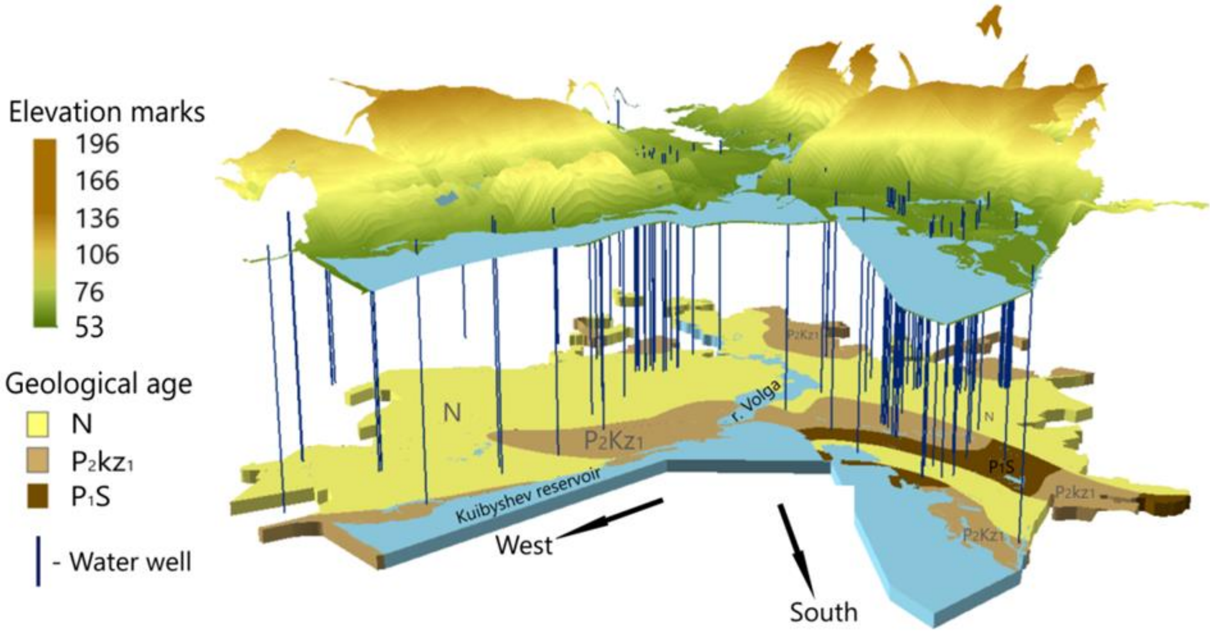

Fig. 1. Modern relief, geological structure and water wells in Kazan

Research results and their discussion

Table 1. Average contens of the main components in the underground hydrosphere of Kazan

Component	Hydrostratigraphic division (observation period)					
	P_1s (1960-2000)	P_1s (2001-2019)	P_2kz_1 (1960-2000)	P_2kz_1 (2001-2019)	N-Q (1960-2000)	N-Q (2001-2019)
Rigidity, ^{O}Ж	15,9	11,2	17,15	17,33	7,55	10,45
pH, unit pH	7.58	7.40	7.16	7.20	7.04	7.27
Oxidizability, mgO/l	1.84	1.35	1.24	1.21	3.34	3.88
Mineralization, mg/l	1048.8	782.3	1266	1227.5	567	653
$Na^{+}+K^{+}$, mg/l	14.1	22.5	23.77	51.6	25.72	16.65
NH^{-}_4, mg/l	0.095	20.76	0.073	0.16	0.14	0.52
Ca, mg/l	176.8	142.6	219.65	274.93	117	108
Mg, mg/l	33.2	39.4	65.84	53.32	32.6	47.7
Fe general, mg/l	0.36	5.58	0.4	0.68	0.78	0.63
Cl, mg/l	7	7.27	16.36	33.23	14.7	25.46
NH^{-}_4mg/l	561.7	231.9	544.94	494.14	131.07	231.12
NO^{-}_3, mg/l	0.94	13.1	1.71	7.61	2.95	8.17
HCO^{-}_3, mg/l	333	364.6	385.5	333.0	347.78	427.16
Number of samples	72	549	970	249	198	205

Data for urban water wells are divided into 2 periods: the first period includes the results from 1960 to 2000, the second period from 2001 to 2019. Some features using the example of the aquiferous Nizhnekazan complex. Most of the components do not exceed the maximum permissible concentrations (MPC) for drinking water according to SanPiN 2.1.4.1074-01. Such components include pH, all cations, chlorides, nitrates, permanganate oxidizability. Excess of MPC relative to drinking standards was noted for mineralization (dry residue), total hardness, sulfates, ammonia, iron. Mineralization is characterized by significant (138-2780 mg/l) fluctuations with average values of 1266 and 1227.5 mg/l, respectively, for the first and second periods (table 1).

Fresh waters with mineralization up to 1000 mg/l are found in the northwestern part of the city on the right bank of the River-Kazanka (Fig. 2).

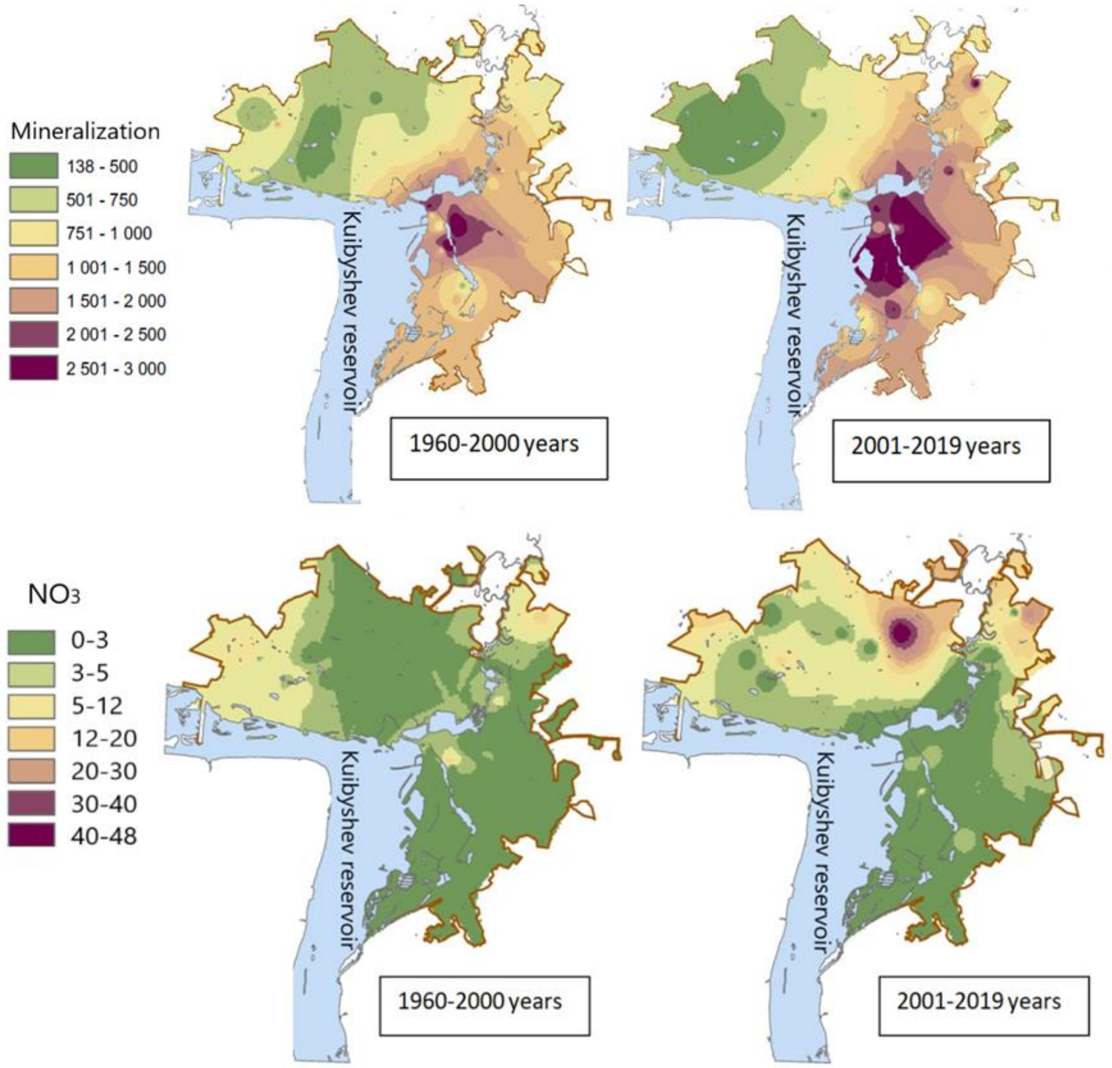

Fig. 2. Models of the contents of the main components (in mg/l) in the underground waters of the Nizhnekazan complex

The central (historical) and southern (industrial) parts of the city are characterized by low-mineralized waters, which may be associated with intensive residential and industrial loads, as well as with a fairly old stock of wells, which has been operating for more than half a century.

For sulfates, approximately the same tendencies are characteristic as for mineralization: significant fluctuations (from the first to 2000 mg/l) with average values of 544.9 and 494.1 mg/l, respectively, for the first (1960-2000) and the second (2001-2019) periods (table 1). There is a noticeable tendency for the expansion of the area of sulfate waters in the central and southern parts of Kazan in the 21st century (Fig. 2) with a simultaneous decrease in the sulfate ions on the right bank of the River-Kazanka. Chlorides are uncharacteristic for the waters of the Lower Kazanian complex (from the first to 270 mg/l), although there is quite a clear tendency toward their increase in recent decades. An increase in nitrate concentrations from 0.43 mg/l in the first period to 9.37 mg/l in the second period may cause relative concern (Fig. 2), although the MPC of nitrates according to SanPiN 2.1.4.1074-01 is 45 mg/l. Presumably, the tendency for an increase in nitrates is due to insufficient treatment of municipal wastewater, which passes through a powerful natural filter of rocks that overlaps the Nizhnekazan complex, and only reaches the aquifers after decades.

The processing of the analysis results of the waters of the Lower Kazanian complex using cluster analysis revealed “natural” and “technogenic” groups of components. The most technogenic components are chlorides and nitrates; less pronounced confinement to this group of mineralization, iron, sulfates and general hardness. The natural components of the water samples of the Nizhnekazan complex are hydrocarbonates, oxidizability, pH, and, possibly, cations. When comparing the data on cluster analysis by observation periods, some differences are revealed, which, in our opinion, may be associated with a different degree of technogenic load on the water of the Lower Kazanian complex of Kazan in the XX and XXI centuries.

Factor analysis showed that technogenic factors for 2 observation periods strongly contrast, while the most significant “natural” factor 1 is rather well distinguished by a set of common components. By the weight of technogenic factors, it is possible to calculate the quantitative contribution of technogenesis to the composition of groundwater. Thus, the technogenic load on the groundwater of the Nizhnekazan complex at the beginning of the 21st century is higher (33%) than in the 20th century (22%), which is confirmed by the contents of the main components (see Fig. 2).

Conclusions

Summarizing the results obtained, the following conclusions can be drawn.

1. For the first time for groundwater in Kazan, a systematic retrospective analysis of hydrochemical data for a long (60 years) observation period was carried out for groundwater in Kazan.
2. The used statistical method of processing hydrochemical information and geoinformation technologies are suitable for monitoring the aquifers of urbanized areas.
3. It is urgent to create, on the basis of modern GIS-technologies, permanent models of groundwater aquifers in Kazan for digital monitoring and development of priority directions of urban environmental policy, taking into account hydrogeological information.

Acknowledgments

This work was funded by a subsidy allocated to Kazan Federal University for the state assignment in the sphere of scientific activities (Project № 0671-2020-0048 of State Assignment № 075-00216-20-05 of 04.06.2020 (Part II Section 1)). The author is deeply grateful to Laboratory Assistant at the “TRIZ Modeling” Research and Education Center Allan Rojas for constructive revision of the English version of the text.

REFERENCES

1. Krainov S. R., Ryzhenko B. N., Shvets V. M. (2004). Geochemistry of underground waters. Theoretical, applied and environmental aspects. Moscow, Nauka, 677.
2. Lisenkov A. B., Fisun N. V., Malkov A. V. *et al*., (2003). Technogenic processes in groundwater. Scientific world, Moscow, 248.
3. Sungatullin R. Kh. (2009) Chemical composition of underground and surface hydrospheres (on the example of Naberezhno-Chelninskaya area). Uchenye zapiski KSU. Natural Sciences 151 (3), pp. 153-166.
4. Sungatullin R. Kh. (2010) Influence of technogenesis on the formation of modern weathering crusts and water-bearing areas. Geoecology. Engineering geology. Hydrogeology. Geocryology 6, pp. 494-502.
5. Sungatullin R. Kh., Khaziev M. I. (2009). A systematic approach to the study of the hydrosphere in industrial-urbanized territories. Geoecology. Engineering geology. Hydrogeology. Geocryology 1, pp. 19-31.

6. Schwartz A. A. (2005) Chemical composition of groundwater in the St. Petersburg region in the light of new requirements for the quality of drinking water. Bulletin of St. Petersburg State University 7 (1), pp. 85-93.
7. Shchukova I. V. (2005). Formation of the chemical composition of groundwater in the zone of active water exchange on the territory of the city of Perm. Avtoref. dis ... cand. geol.-mineral. sciences. Perm, 23.
8. Barrett M. H., Hiscock K. M., Pedley S. *et al*., (1999). Marker species for identifying urban groundwater recharge sources. A review and case study in Nottingham, UK. Water Res 33 (14), pp. 3083-3097.

Features of Zircons from Metamorphic Rocks and Granitoids of the Timano-Ural Region

PYSTINA Yuliya[1], PYSTIN Alexandr[1]

[1] Institute of Geology, RAS Ural Branch, Syktyvkar (RUSSIA)
Email: yuliya_pystina@mail.ru

Abstract

From the example of the polymetamorphic complexes of the Timan-natural Ural region it is shown that rounded zircons (such as “such ball”) crystallize in rocks that have experienced extreme conditions of metamorphism (granulites and eclogites).

For migmatized metamorphic rocks, prismatic zircons are the most characteristic. Zircons and zircon joints of complex shape (such as “cauliflower forms”) are formed mainly in conditions of relatively low levels of amphibolite facies in the absence, or weak manifestation, of the processes of migmatization.

Generation analysis of zircons from granitoids of the Northern part of the Subpolar Urals phase is performed. It is shown that zircons from rocks of different granitoid complexes, occupying different geological positions and having different isotopic ages, differ in the set morphotypes and their ratios.

Keywords: Timan-Ural region, zircons, polymetamorphic complexes, granitoids, typomorphism

Introduction

Zircon is one of the most widely used minerals for reconstructing the formation conditions of the igneous and metamorphic rocks that contain it. Due to its physical and chemical stability, it persists even at sufficiently high temperatures and pressures, while consistently developing geological processes make certain changes in the composition and morphology of existing zircon crystals. That is why a mineral often has a great variety in morphological terms and a complex internal structure. But this is what makes it possible to use zircon as an indicator of geological processes. In addition, due to the presence of U impurity in the mineral at a relatively high closing temperature of the U-Pb isotope system (about 900 °C), zircon is one of the most reliable geochronometers.

This article provides a brief overview of the publications devoted to the theoretical justification of the morphology of zircon and empirical observations of the morphological features of this mineral from rocks of metamorphic and igneous genesis. The results of studying the morphology of zircon from metamorphic and granitoid complexes in some areas of the Timan-Ural region are also presented.

Morphological features of zircons from metamorphic rocks of the Timan-Ural region

Crystal forms of zircon are represented by faces {011}, {100}, {110}, {211}, {031}, {112} etc.

The theoretical form of zircon growth derived from the crystal structure was predicted using the theory of periodic chains of bonds (PCC) [1, 2].

According to the PCR theory [1], the adsorption of cations on the {011} face changes the relative surface energies of possible structures and this, in turn, changes the mechanism and growth rate. If the adsorption makes the surface energies of the two possible structures equal, growth can occur by applying half of the {022} layer, which grows at approximately twice the rate compared to the growth of entire elementary layers {011}.

Theoretical forms are usually not implemented in natural growth conditions, but they serve as a starting point for assessing the influence of external factors.

In natural zircons of magmatic genesis, the crystal shape is mainly manifested by a prism {100} and a dipyramid {011}.

Sometimes, however, there are zircons of prismatic habit with {110} prisms and {011} dipyramids. In very rare cases, natural zircons have a dipyramidal appearance with {011} prisms.

The diversity of metamorphic zircons, according to many researchers [3, 4, 5, 6] reflects the variations in the physical and chemical conditions, and the duration of each metamorphic event and is caused by modifications of previously existing structures and/or the growth of new zircon.

Long-term studies of zircons from gneisses and crystal shales of the polymetamorphic complexes of the Timan-Ural region (Fig. 1) [7, 8, 9, etc.] convince us that in metamorphic rocks, zircons differ, displaying a wide variety of forms and a varying complexity of structure. They contain both allogeneic and authigenic zircons.

Altigen applies only gravel (terrigenous) zircons. They are rounded or ellipsoid in shape and have a rough surface (Fig. 2.1).

The mineral can be colorless or colored in pink tones, ranging up to dark pink.

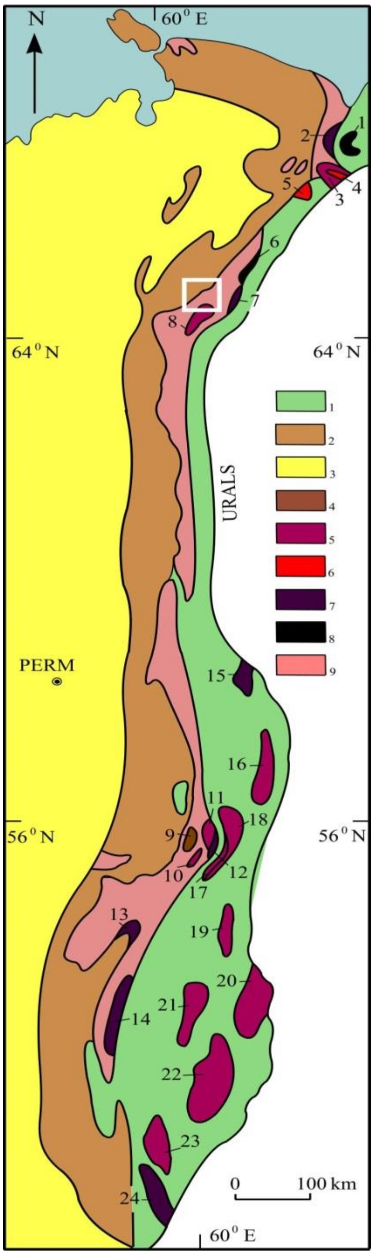

Fig. 1. Location map of polymetamorphic complexes of the Timan-Ural region 1-2 – Paleozoic formations: 1 – paleooceanic; 2 – paleocontinental; 3 – sedimentary cover of the East European Platform; 4-7 – Lower Precocambrian (?) Polymetamorphic complexes: 4 – gneiss-granulitic, 5 – gneiss-migmatite, 6 – crystal-schists, 7 – eclogite-gneiss and eclogite-schists; 8 – granulite-metabasite; 9– Upper Proterozoic formations, mainly undergone green shale metamorphism Polymetamorphic complexes: 1 – Malyk, 2 – Marunkeu, 3 – Hanmeikhoy, 4 – Parikvasshor, 5 – Kharamatalou, 6 – Khordyus, 7 – Nerkayu, 8 – Nyartin, 9 – Taratash, 10 – Alexandrov, 11 – Ufaley, 12 – Eastern Ufaley, 13 – Beloretsk 14 – Maksyut, 15 – Saldin, 16 – Murzin-Aduy, 17 – Selyankin, 18 – Sysert-Ilmenogorsk, 19 – Kochkar, 20 – Mariinsk, 21 – Adamovsk, 22 – Tekeldy-Tau, 23 – Kayrakta, 24 – Taldyk

Among authigenic zircons, the crystallization of which is associated with metamorphic changes in rocks, there are three morphological varieties (three morphotypes) that are most widespread [10]. One of the most common varieties of metamorphogenic zircons in the rocks studied by us is represented by rounded grains (such as “soccer ball”) (Fig. 2. 2-2.7). The surface of the faces is smooth and shiny.

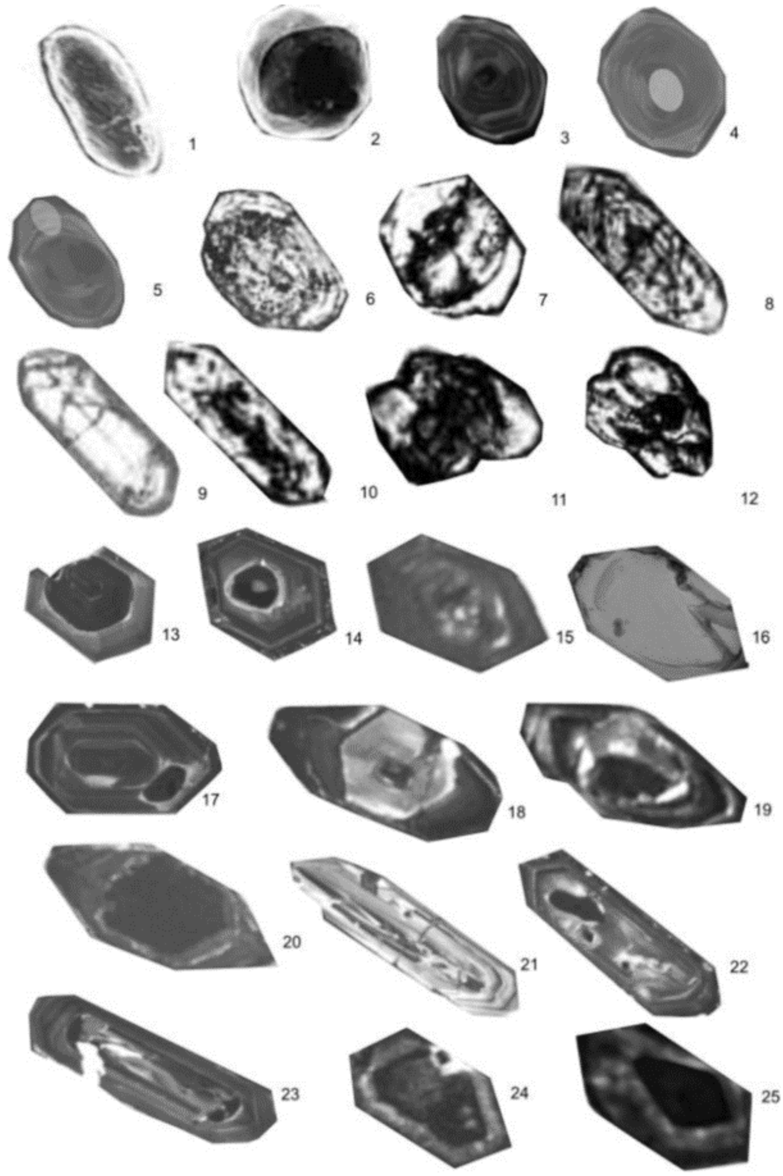

Fig. 2. Morphology of zircons from metamorphic rocks and granitoids of the North of the Urals

The internal structure of such zircons is relatively uniform, but there are crystals with cores of older zircon (Fig. 2.5-2.7). This zircon is typical for granulites, but also for eclogites. Note that in addition to granulite-and eclogite-containing metamorphic complexes, such zircon is found, in small amounts, in metamorphites of the gneiss-migmatite complexes of the Urals (Alexander, selyankinsky, nyartinsky, khanmeykhoy, etc.), composed of rocks of the amphibolite facies. This suggests that the rocks were originally metamorphosed in the granulite facies.

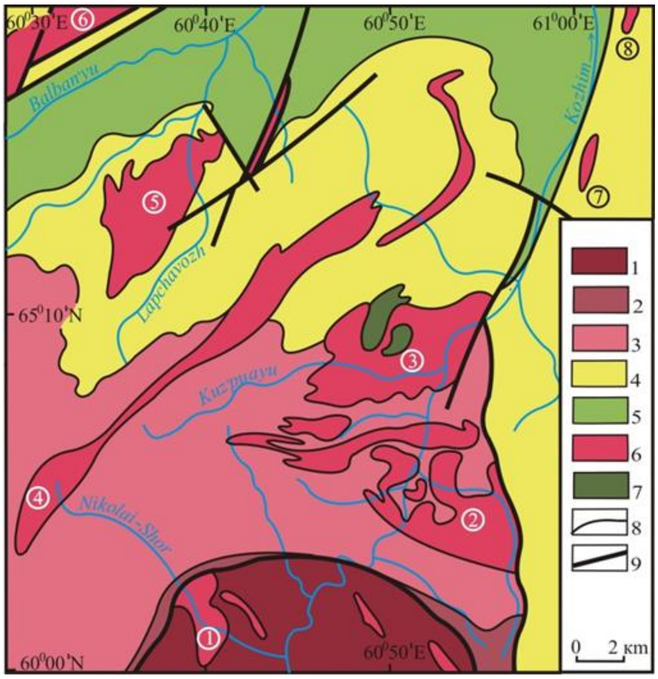

Fig. 3. Scheme of the geological structure of the northern part of the Subpolar Urals.
1 – Nyartin gneiss-migmatite complex (PR1); 2 – schokurya suite (RF_1); 3 – the Puyva suite (RF_2?); 4 – Neoproterozoic deposits (RF3-V), undivided; 5 – Paleozoic deposits ($Є_3$-O), undivided; 6 – granites; 7 – gabbro; 8 – boundaries of stratigraphic and intrusive divisions; 9 – faults.
Massifs (numbers in circles): 1 – Nikolaishor; 2 – Kozhim; 3 – Kuzpuayu; 4 – Khatalambo-Lapchin; 5 – Lapchavozh; 6 – Maldin; 7 – Yarota; 8 – Badiau

Another variety of zircons, which is widely represented in gneiss and crystal shales, has the appearance of transparent and light-colored grains of prismatic habit (Fig. 2.8-2.10). The mineral has developed facets {100}, {110}, {112}, {113}. {331}, or another acute dipyramid is present.

The combination of a small area of acute dipyramid and a well-defined obtuse causes a rounded appearance of the crystal head. In the scale of relation is dominated by the faces of the prisms. The internal structure is multi-zoned. In the Urals, a similar zircon was described by AA. Krasnobaev [11] in biotite, biotite-amphibolite gneisses, and migmatites of the Ilmenogorsky complex of the southern Urals, and assigned to the “migmatite” type.

The third type of zircon is represented by colorless or pale-colored grains of irregular shape (such as “cauliflower”) (Fig. 2. 11-2.12.). When you zoom in, you can see that the crystals are aggregates of two or more individuals. Grain size is 0.10-0.25 mm. The surface of the faces is smooth and shiny. The internal structure of crystals is characterized by the presence of nuclei formed by older zircons. Not by chance, as noted by J. Piyuket and his colleagues [12], such forms are typical for zircons from metamorphic rocks of mafic composition, for which, as is known, the temperature threshold of migmatization is higher. Zircons of this type are found in rocks of the Parikvasshor complex of the Polar Urals and the Mikulka complex of the Kanin Peninsula. Zircons from rocks of different granitoid complexes of the circumpolar Urals (Fig. 3), which occupy different geological positions and differ in isotopic age, differ in the set of morphotypes and their quantitative ratios [13, 14, 15]. In total, they represent all the main morphological types of zircons according to I. V. Nosyrev [4]: zircon, hyacinth, lance – shaped, torpedo-shaped and cirtolite (Fig. 2.13-2.25.). The Zircon morphological type consists of transparent and translucent, pale-colored, and less often, dark brown, zircons of short-prismatic habit. The size of the crystals is 100-250 microns, the elongation coefficient is 1.2-2. Their appearance is due to the development of faces (100), (111), (110), idiomorphic or subidiomorphic. The ratio of the relative areas of the prism and dipyramid shows the clear predominance of the prismatic belt. The surface of the faces is often fractured, and when magnified, uneven terrain is detected. The internal structure of crystals is usually multizonal.

The location of the zones relative to each other is symmetrical. Some crystals have rounded cores, and almost all crystals have regenerative edges (Fig. 2.13-2.14). The Hyacinth morphological type of zircons is represented by semi-transparent, rarely transparent, light-colored crystals of dipyramidal-prismatic or short-prismatic habit.

Grain size is 200-500 microns, elongation coefficient is 1.5-2, and the appearance of crystals is idiomorphic, due to the development of faces (100), (111), (110), (131), (331). The ratio of the face areas of prisms and dipyramids is 1:2. The surface of the faces is smooth and shiny.

The internal structure of the crystals is often multi-zonal, with the zones usually following the contour of the crystal, but often there is a change of faces from a blunt dipyramid to a more acute one and vice versa (Fig. 2.15-2.16). The lance-shaped morphological type of zircon is formed by transparent pale-colored crystals of dipyramidal-prismatic and prismatic-dipyramidal habit. The grain size is 200-450 μm, with an aspect ratio of 2-4. The appearance of the crystals is idiomorphic, due to the development of faces (100), (110), (131), (311). The ratio of the areas of the faces of prisms and dipyramids is 2:3. The surfaces of the faces are smooth and shiny. The internal structure of the crystals is often multi-zonal. The location of the zones relative to each other can be symmetrical or asymmetric, and crystals with rounded cores are noted, as well as cores represented by irregular accretions of relict zircon (Fig. 2.17-2.20).

In some cases, it is possible to observe how the appearance of the crystal changed from zircon to dipyramidal-prismatic – lance-shaped. The torpedo-shaped morphological type is formed by transparent, colorless, or pale yellowish-pinkish colored zircons of prismatic habit.

The crystal size is 100-450 microns, the elongation coefficient is 3-5. The appearance of the crystals, due to the development of faces (100), (110), (113), is idiomorphic. In the scale of relation is clearly dominated by the faces of the prismatic zone. The surface of the faces is often fractured.

The internal structure of crystals is multizonal. The location of zones relative to each other is usually symmetrical. There are rounded and elongated nuclei (Fig. 2.21-2.23). The Cirtolite morphological type is represented by prismatic and long-prismatic crystals of brownish yellow or brown color, opaque, with a slightly flattened shape. The crystal size is 150-650 microns, the elongation coefficient is 3-5. The appearance of the crystals, due to the development of faces (100), (110), (113), (112), is idiomorphic. The surface of the faces is fractured, and the terrain is uneven.

The internal structure of the crystals is characterized by the presence of rounded and elongated nuclei. Occasionally, they have geometric outlines (Fig. 2.24-2.25).

In the granites of the Nikolayshorsky massif, spear-shaped zircons are predominant, which are found only in the rocks of this massif and compose up to 50% of the total amount of the mineral in the sample. The fouling of short – prismatic zircon – crystals (of the zircon morphotype) with dipyramidal-prismatic-lance-shaped ones is noted (Fig. 2.18, 2.20).

The Kozinski, Baclawski and Arotsky granite massifs belong to the shallow formations, under the terms of the formation. This is probably one of the reasons for the absence of lance-shaped zircons in them, which are typical in deep formations. Unlike Badyayu and Yarotsky granites, the Kozhimsky massif contains zircons of the cirtolite morphotype, which is a sign of the metasomatic (or metamorphic) processing of rocks [16].

The badyayu and yarot granites have a similar set of morphotypes of zircon, which, in comparison with the nikolayshor and Kozhim granites, are characterized by the simplest forms of this mineral, which is characteristic of single-phase massifs [17].

Conclusions

With all the morphological diversity, complexity of the internal structure, and composition of zircon in metamorphic rocks, there are certain patterns that allow us to identify the typomorphic features of this mineral associated with the conditions of rock formation. Thus, the empirically established association of rounded zircons with rocks of granulite and eclogite facies allows us to consider rounded zircons (such as "soccer ball") as an indicator of extreme (ultra-high-temperature and ultra-high-pressure) metamorphism conditions. Prismatic zircons of the "migmatite" type, being actually igneous minerals, indicate the manifestation of partial melting processes in rocks.

The presence of complex-shaped zircon aggregates (such as "cauliflower") in metamorphic formations most likely indicates relatively low-temperature conditions of rock change that do not exceed the low stages of the amphibolite facies. Only in metamorphites of the main series, which have a higher temperature threshold of migmatization in comparison with rocks of acidic composition, the "cauliflower" type zircons are preserved under higher temperature conditions.

Zircons from rocks of different granitoid complexes, which occupy different geological positions and differ in isotopic age, differ in the set of morphotypes and their quantitative ratios.

Thus, the presence of lance-shaped zircons in granites indicates the deep conditions of formation of rocks. Zircon of the cirtolite type can be a sign of metasomatic (or metamorphic) processing of granites. The simplest forms of zircons are typical for single-phase granite massifs; more complex forms, for multiphase and polyfacial massifs, as well as granites that have experienced metamorphic and metasomatic transformations.

Acknowledgments

The study was carried out within a framework of State Program no. AAAA-A17-117121270035-0 FITZ Institute of Geology Komi SC UB RAS.

REFERENCES

1. Woensdregt C. F. (1992a). Computation of Surface Energies in an Electrostatic Point Charge Model: I. Theory. Phys. Chem. Minerals 19, pp. 52-58.
2. Woensdregt C. F. (1992b). Computation of Surface Energies in an Electrostatic Point Charge Model: II. Application to Zircon (ZrSi04). Phys. Chem. Minerals 19, pp. 59-69.
3. Nosyrev I. V. (1985). Main features of ontogeny of accessory zircon of metamorphic rocks. Zircon in Precambrian and Phanerozoic rocks. Nauka, Moscow, pp. 15-25.
4. Nosyrev I. V. (1989). Anatomy of accessory zircon crystals and evolution of the mineral-forming medium. Typomorphism, synthesis and use of zircons. Naukova Dumka, Kiev, pp. 37-47.
5. Bibikova E. V., Gracheva T. V., Kirnozova T. I. (1985). Geochronological Dating of metamorphic processes by zircon geological research of the Precambrian based on the study of accessory minerals. Nauka, Moscow, pp. 15-30.
6. Corfu F., Hanchar J. M., Hoskin P. W. O., Kinny P. (2003). Atlas of zircon textures. Reviews in mineralogy and geochemistry 53, pp. 469-500.
7. Pystin A. M., Pystina Yu. I. (2014). Basal deposits of the upper Precambrian in the Timan-North Ural region. Lithosphere 3, pp. 41-50.
8. Pystina Yu. I., Pystin a.m., Potapov I. L. (2008). Morphological features of zircons as a criterion of physical and chemical conditions of metamorphism (on the example of gneiss complexes of the Urals). Proceedings of the fourteenth international conference, pp. 138-139.
9. Pystin A. Pystina J. (2015). The early Precambrian history of rock metamorphism in the Urals segment of crust. International Geology Review 57 (11-12), pp. 1650-1659.
10. Pystin A. M., Pystina Yu. I. Potapov I. L., Panfilov A.V. (2012). Early Precambrian history of metamorphism of rocks of granulite and eclogite complexes of the paleocontinental zone of the Urals. Syktyvkar: Geoprint, 46.
11. Krasnobaev A. A. (1986). Zircon as an indicator of geological processes. Nauka, Moscow, 152.

12. Peucat J. J, Bernard-Griffiths J., Gil Ibarguchi J. I, Dallmeyer R. D., Menot R. P., Cornichet J., Iglesias Ponce de Leon M. (1990). Geohemical and Geochronological cross-section of the deep Variscan crust: The Cabo Ortegal high-pressure nappe (northwestern Spain). Tectonophusics 110, pp. 463-472.
13. Pystin A. M., Pystina Yu. I. (2011). New data on the age of granitoids of the circumpolar Urals in connection with the problem of isolation of the kozhimskaya mid-riolite granite formation. Proceedings of the Komi science center URD RAS, Syktyvkar, 4, pp. 73-78.
14. Pystin A. M., Pystina Yu. I. (2008). Metamorphism and granite formation are the consequence in the Proterozoic-early Paleozoic history of the formation of Propranollo segment of the earth's crust. Lithosphere 8, pp. 25-38.
15. Pystina Yulia I., Denisov V. Yu., (2017). Morphological characteristics of zircons as a criterion for subdivision and correlation of granitoids (on the example of the Northern part of the Subpolar Urals). Bulletin of the Institute of Geology, Komi science center URD RAS, 12, pp. 3-15.
16. Fishman M. V., Yushkin N. P., Goldin B. A., Kalinin E. P. (1968). Mineralogy, typomorphism and Genesis of accessory minerals of igneous rocks of the North of the Urals and Timan. Leningrad. Nauka, 250.
17. Zinchenko O. V., Grinchenko V. F. (1989). On two concepts of evolution of accessory zircon morphology / / Typomorphism, synthesis and use of zircon. Kiev. Naukova Dumka, pp. 20-24.

Mineralogy of the Bazilevo Copper Occurrence in Upper Kazanian Sandstones from the Southwestern Part of the Republic of Bashkortostan

RAKHIMOV Ildar[1]

[1] *Institute of Geology UFRC RAS, Ufa (RUSSIA)*
Email: rigel92@mail.ru

Abstract

A new copper ore occurrence was found in gray coastal-marine sandstones of the Kazanian (Wordian) Stage in the south-west of the Republic of Bashkortostan. Cu-mineralization is confined to fossil tree trunks and is represented by sulfides (chalcocite, bornite, chalcopyrite, covellite), oxides (cuprite), sulfates (brochantite), hydrogen carbonates (azurite, malachite), and native copper. The ores have high concentration of Ag (93 ppm). Ore mineralogy indicates the polygenic origin of the assemblages, replacing each other due to the interaction of Cu-bearing fluids released from the underlying red beds with organic matter and then with early sulfide minerals.

Keywords: Kazanian Stage, copper sandstones, mineralogy, plant fossils

Introduction

Permian sandstones in many regions of the world are copper-bearing [1]. The Kazanian beds in the Cisuralian belt are highly productive in copper mineralization. In Permian sediments in the Bashkir Cisuralia about 770 mines are known, conventionally combined into three groups of deposits: Saraevo-Rudnichnaya, Miyakino-Sterlibashevskaya and Fyodorovsko-Kuz'minovskaya [2]. The Bazilevo ore occurrence accidentally discovered in the last decade belongs to the latter group. The Fyodorovsko-Kuz’minovskaya group of sandstone-hosted ore occurrences is confined to the upper part of the Upper Kazanian (conchiferous) substage.

The Bazilevo copper occurrence was revealed during the excavation of a quarry for sand and gravel material. The quarry (Fig. 1a) is located on small hill 1.3 km north-east of the village of Bazilevo (53°05'20" N, 55°03'04" E) and is 70×40 m in size and the excavation depth is currently up to 9 m. Mineralization is confined to linear zones at the bottom of the open pit (Fig. 1b).

This paper provides the first mineralogical characterization of ore bodies in the Bazilevo occurrence with the aim of reconstructing the genesis of the copper mineralization.

Methodology

Geological and lithological description and sampling was performed by the author.

The chemical composition was determined using X-ray fluorescence analysis (Carl Zeiss VRA-30 spectrometer) at the Institute of Geology UFRC RAS, Ufa.

Fig. 1. View of the Bazilevo sand pit (marked by star on inset map) from the south side (a) and the copper ore body (b). Arrows mark outcrops of copper ore bodies. Photograph by the author

The mineral composition of ores was determined using optical and electron microscopy, as well as X-ray diffraction analysis. Polished sections and thin sections were studied on a Carl Zeiss Axioskop 40 polarizing microscope (Institute of Geology UFRC RAS) and a Jeol JSM-6390LV scanning electron microscope (CCU "Geoanalitik", Zavaritsky Institute of Geology and Geochemistry UB RAS Yekaterinburg). The energy-dispersive spectrometry elemental analyses of minerals obtained using an Oxford Instruments X-Max 80 spectrometer and INCA Energy 450 software.

XRD analysis of powder samples was performed out on a Shimadzu XRD6000 diffractometer using CuKα radiation at the Institute of Geology UFRC RAS. The results were processed in the Match! Crystal Impact software.

Results

The section exposed by the quarry operation is composed of polymictic sandstones with interbeds of sandy gravelstones of the Belebey Formation [3]. The deposits are gray and brownish-gray in color, and are characterized by cross-bedding with an unparallel wedge-shaped lamination and truncation, that is typical of coastal-marine deposits. The sandstone strata are broken into blocks by a system of meridional fractures filled with friable clay-limestone material.

Ore bodies are mineralized trunks of fossil trees. Their diameter reaches 0.6 m, the longest of them has a length of at least 40 m. In total, five ore bodies have been identified, four of which strike WSW ~265°. Below them lies an ore body with a SW strike of 230°. Some of them lie at a slight slope, crossing subhorizontal beds of different granulometric composition. Ore bodies have a zonal structure: the central part is composed of friable wood remains and black coalified matter (~ 10 cm in diameter) surrounded by a crust of massive sulfides (0.n-10 cm), and the marginal part is composed of clastic material with copper bicarbonate cement (5-35 cm). The boundaries of ore bodies are marked by a reddish oxidation zone (1-25 cm). Also, a sulfide shell 1-2 cm thick is sometimes observed closer to the outer part of concentrically zoned ore bodies.

According to X-ray fluorescence analysis, the Cu content in ores varies from 1.4 to 30.4 wt.% (maximum in the central part of the ore body and minimum – in the peripheral). High contents of sulfur (up to 3.6-7.3 wt.%) and phosphorus (1.3-1.4 wt.%) are typical; some samples are characterized by high concentration of Ag (93 ppm), Ba (0.18 wt.%), and Pb (236 ppm).

XRD analysis of ores showed that most of the copper is contained in azurite (~30 wt%), brochantite (~20%), chalcocite (~16%), bornite (~13%) and malachite (~8%). On the diffraction patterns (Fig. 2), there are reliably identified clear base peaks. Also, using this analysis, the presence of the following minerals was diagnosed in the ores: marcasite, pyrite, cuprite, native copper, chalcopyrite, cubanite. Feldspars and quartz are noted among the silicates associated with ore minerals.

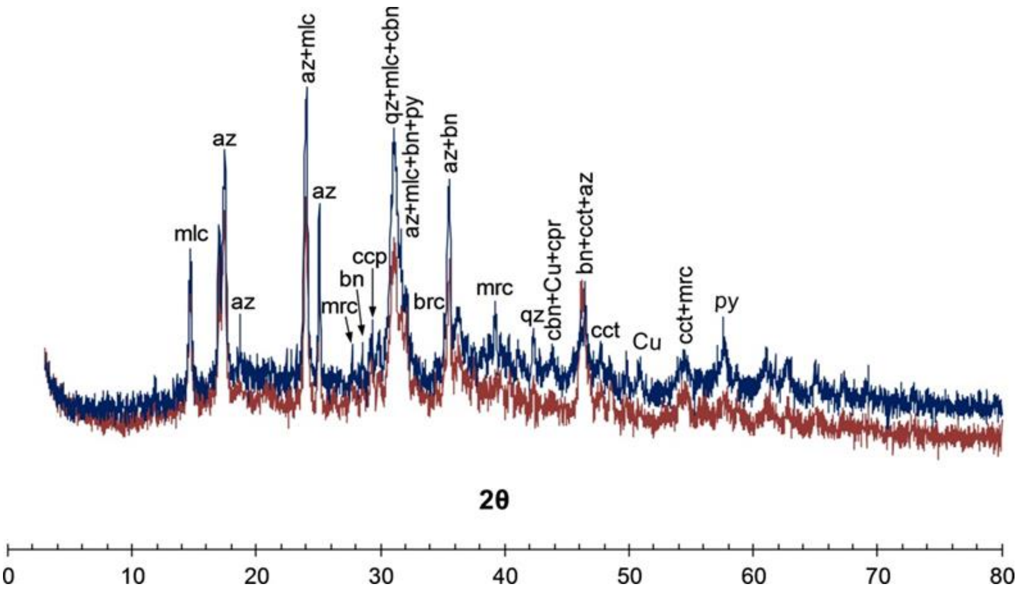

Fig. 2. XRD powder patterns of copper ores from the Bazilevo occurrence.
Note: az – azurite, bn – bornite, brc – brochantite, cbn – cubanite, ccp – chalcopyrite, cct – chalcocite, cpr – cuprite, Cu – native copper, mlc – malachite, mrc – marcasite, qz – quartz, py – pyrite

X-ray spectral analyzes confirm the presence of most of the minerals identified by X-ray diffractometry. Sulfide mineral assemblages are closely related to organic matter, in particular, to wood remains. Texture of plant cell anatomy is well visible in some ore fragments (Fig. 3a).

Sulfide crusts are surrounded by clastic material cemented with calcium carbonates and copper bicarbonates (Fig. 3b). Quartz predominates in the clastic fraction.

Minerals are often difficult to diagnose because they form a finely dispersed mixture of sulfides, sulfates, hydrogen sulfates and hydrocarbonates.

Various mineral phases are presented in cellular texture, and zoning is observed in the structure of individual cells: the nuclei correspond to pyrite (or marcasite), and the outer layers are composed of chalcocite, which form a network of thin veins when it grows together.

However, pyrite (or marcasite) may often be replaced by chalcedony, Fe hydroxides, or Cu bicarbonates; chalcocite is also replaced by them. Bornite forms veinlets 30-80 μm thick, the outer rims of which are chalcocite. Small preserved aggregates of oolitic pyrite were found, in which each spherulite is 10-15 μm in diameter. These aggregates show traces of dissolution and replacement by chalcedony and copper bicarbonates.

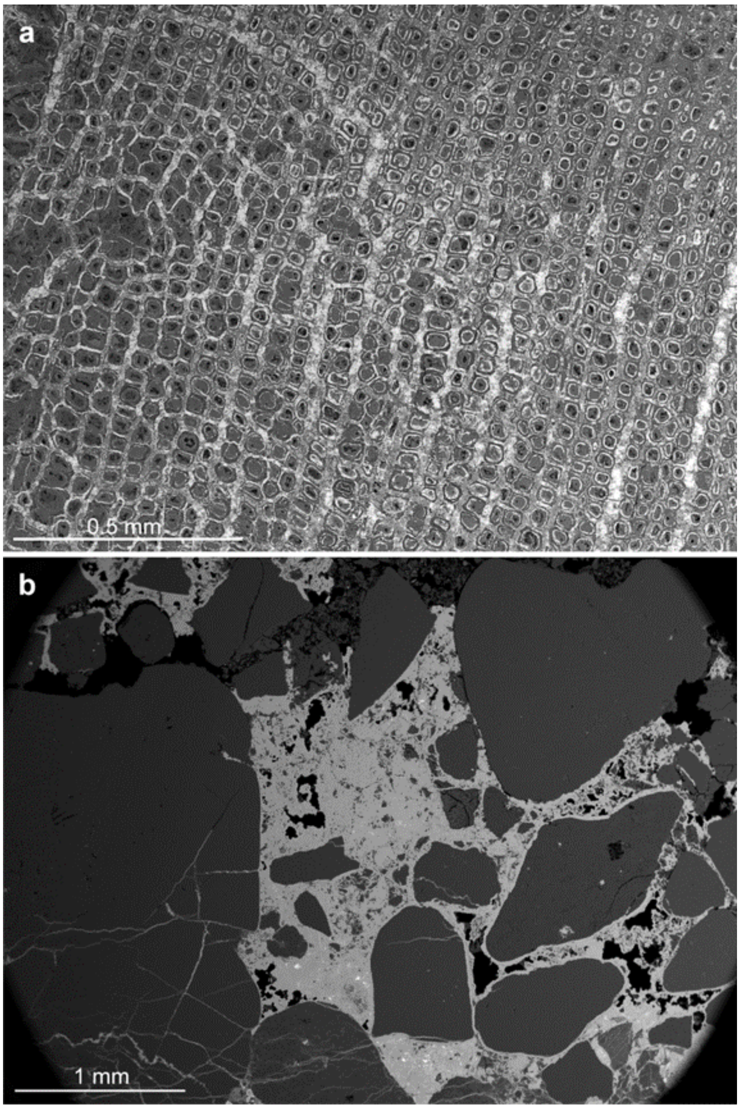

Fig. 3. BSE-images of copper ores from the Bazilevo occurrence: a – sulfide Cu-Fe-mineralization within preserved wood cell-texture, b – hydrogen carbonate Cu- mineralization cementing clastic matter

Cubanite occurs as a vein-like network within pyrite. Covellite was found in clusters consist of lamellar grains surrounded by azurite. Cuprite is represented by vein-like precipitates in fine matrix consisting of a mixture of chalcedony and sulfides, sulfates and hydrocarbonates of Cu and Fe.

This mixture also contains xenomorphic and rarely idiomorphic barite grains up to 0.4 mm in size. Brochantite forms continuous fine inclusions or complex intergrowths in thin veins together with azurite after bornite. The main mass of azurite and malachite is a finely dispersed mixture, as the cement of a detrital mass of ore bodies surrounding the sulfidized parts of wood trunks.

Discussion

The genesis of copper mineralization localized in various sedimentary deposits has been studied in sufficient detail [4]. Therefore, for a newly discovered ore occurrences, it is important to establish the main geological, lithological, mineralogical and geochemical features for comparison with widely known and well-studied occurrences.

The presence of fossils as a biochemical barrier, in particular plant fossils, is an important condition for the deposition of copper minerals. The replacement of organic matter with copper minerals is a widespread phenomenon characteristic of Permian or Neogene ore occurrences [5-7].

Primary precipitation of Fe sulfides (especially pyrite) during syngenetic or diagenetic processes on an organic reductant (plant residues) is common for such ore deposits, as a result of the activity of sulfate-reducing bacteria. Subsequently, iron sulfides are replaced by copper sulfides – chalcocite, bornite, cubanite, chalcopyrite – due to the influence of Cu-bearing fluids that divided from the underlying red layers [8]. Subsequently, the migration of oxidized water in the pore space led to partial dissolution of sulfides and based on that formation of late sulfates and hydrogen carbonates of copper, as well as iron hydroxides [9]. In the ores of the Bazilevo copper occurrence, all of the aforementioned processes are reflected in ore mineralogy, which indicates a similar mechanism of ore formation. Thus, the copper mineralization studied is of polygenic origin.

It was found that many sediment-hosted copper occurrences share close relationship with redbeds, considered as a source of Cu [1]. The ores of the Bazilevo occurrence are hosted by gray coastal-marine sediments, while red rocks are located down the section, i.e., within the lower (spiriferous) substage of the Kazanian Stage.

The visible scale of mineralization at the Bazilevo occurrence is not currently considered significant. However, only a small part of the section has been exposed by the quarry, and the ore bodies are found at different depths in the section, which makes it possible to estimate the growth of ore in both lateral and vertical directions.

Conclusions

A new copper ore occurrence in the gray sediments of the Kazanian Stage in the south-west of the Republic of Bashkortostan was revealed during excavation of a sand quarry. Ore bodies are confined to fossil tree trunks and follow their contours. Ore bodies are located at different levels of the section, and their inner structure is zoned: the central part is composed of friable coalified matter, which is surrounded by a shell of sulfides, and these, in turn, are bordered by clastic material with cement from copper bicarbonates and iron hydroxides. The ores contain high content of Ag (up to 93 ppm). The ore mineralogy indicates the polygenic origin of ores, in which the following sequence of mineral formation was preliminary established: pyrite + marcasite → chalcocite + bornite + cubanite + chalcopyrite → native copper + cuprite → brochantite + azurite + malachite + iron hydroxides.

Acknowledgments

The study is supported by the State Contract of IG UFRC RAS (no. 0252-2017-0012).

REFERENCES

1. Gablina, I. F., Malinovskii, Yu. M. (2008). Periodicity of Copper Accumulation in the Earth's Sedimentary Shell. Lithology and Mineral Resources 43 (2), pp. 136-153.
2. Rakhimov, I. R. (2013). Rudnye poleznye iskopaemye permskoy sistemy Priural'ya Respubliki Bashkortostan. Problems of Geology and Subsurface Development: Proceedings of the 17th International Scientific Symposium of students, Postgraduates and young Scientists devoted to the 150th Anniversary of Academician V.A. Obruchev and 130th Anniversary of Academician M.A. Usov, Founders of Siberian Mining School. Tom I; Tomsk Polytechnic University. Tomsk Polytechnic University Publishing House, Tomsk, pp. 216-218.
3. Knyazev, Yu. G. (2011). Gosudarstvennaya geologicheskaya karta Rossiyskoy Federatsii masshtaba 1:1000000 lista N-40 (tretie pokolenie) (State geological map of Russian Federation in scale 1:1000000, sheet N-40 (third generation)). VSEGEI, St. Petersburg.

4. Lur'e, A. M. (1988). Genesis medistykh peschanikov i slantsev (Genesis of Cupriferous Sandstones and Shales), Nauka, Moscow, 182.
5. Kucha, H. (2014). Geology, mineralogy and geochemistry of the Kupferschiefer, Poland. In Europe's Major Base Metal Deposits; Kelly, J.G., Andrew, C.J., Ashton, J.H., Boland, M.B., Earls, G., Fusciardi, L., Stanley, T.G., Eds.; Irish Association for Economic Geology: Dublin, Ireland, pp. 215-238.
6. Volkov, A. V., Novikov, I. A., Razumovsky, A. A., Murashov, K. Y., Sidorova N. V. (2018). Geochemical features and formation conditions of the cupriferous sandstones of the Orenburg Pre-Urals. Lithosphere 4, pp. 593-606.
7. Pazand, K., Behzadinasab, A., Ghaderi, M. R., Rezvanianzadeh, M. R. (2018). Sedimentary copper mineralization in the upper red formation, Yakhab area, central Iran. Geosystem Engineering 22 (6), pp. 337-346.
8. Azizi, H., Hosseinzadeh, M. R., Moayyed, M., Siahcheshm K. (2018). Geology and geochemistry of the sediment-hosted stratabound red bed-type Cu-Pb (Zn-Ag) mineralization in the Dozkand-Moshampa Area, NW Zanjan, Iran. Neues Jahrbuch für Geologie und Paläontologie 195 (2), pp. 123-143.
9. Khasanov, R. R., Gainov, R. R., Varlamova, E. S., Islamov, A. F. (2009). Substitution of plant residues for copper sulfides in Permian deposits of Vyatka-Kamian copper-bearing zone. Uchenye Zapiski Kazanskogo Universiteta. Seriya Estestvennye Nauki 151 (4), pp. 162-169.

Facies and Cyclicity of the Cap Dolostone of the Kumakh-Ulakh Formation

RUD'KO Sergey[1], RUD'KO Dmitriy[2], SHATSILLO Andrey[2], LATYSHEVA Irina[1], FEDYUKIN Ivan[2], KOZYREV Ivan[3]

[1] Geological institute of RAS, Moscow (RUSSIA)
[2] The Schmidt Institute of Physics of the Earth of the RAS, Moscow (RUSSIA)
[3] Institute of Volcanology and Seismology FEB RAS, Petropavlovsk-Kamchatskiy (RUSSIA)
Email: svrudko@gmail.com

Abstract

The time scales and conditions associated with the formation of Neoproterozoic cap dolostones provide data needed to test the Snowball Earth hypothesis, and reconstruct the Neoproterozoic palaeoclimate. We studied the lithological characteristics and variations in magnetic susceptibility of the cap dolostone of the Kumakh-Ulakh Formation (the Berezovskaya Depression, south of the Siberian Platform). Lithological features similar to those of pelagic evaporites forming under meromictic conditions and different order variations in the magnetic susceptibility are established in the cap dolostone studied. We suggest that long-term variations in magnetic susceptibility may reflect the Milankovitch precession cycles. The sedimentation rate calculated on the basis of this assumption yields 3-4.5 cm/1000 years, which is consistent with the accumulation rates of Holocene sediments from postglacial meromictic basins. The orbital nature of the identified cycles can be further substantiated by studying other cap dolostone sequences worldwide.

Keywords: cap dolomite, Neoproterozoic, Snowball Earth, evaporitic laminites, Milankovitch cycles

Introduction

Paleomagnetic data showed that Neoproterozoic glacial rocks could have formed near the equator. This became the basis for the Snowball Earth hypothesis suggesting that long lasting extensive glaciations took place on Earth in the Neoproterozoic [1]. The unique feature of Neoproterozoic glacial sediments is the cap dolostone horizons, overlying them. Data on the cap dolostone depositional conditions and sedimentation rates are critical for understanding the state of the environment during the end of the glaciations and, in particular, for testing the Snowball Earth hypothesis, which suggests that the glaciations ended almost instantly as a result of a global greenhouse effect [2].

Materials and Methodology

We studied the lithological and cyclostratigraphic characteristics of cap dolostones of the Kumakh-Ulakh Formation (Dal'naya Taiga Group, Berezovskaya Depression, southern Siberia).

The studied horizon is represented by 2 m thick red colored dolomitic marls and dolomites, and crops out on the left bank of the river Sen, 3 km downstream of the mouth of the river Uraga (Fig. 1). These rocks are comparable with the globally distributed cap dolostones [3] due to the following common features: 1) they overlay conformably the Neoproterozoic glacial sediments of Nichatka Formation; 2) they are composed mainly of dolomite; 3) they have tepee-like structures; 4) they have typical carbon isotope composition (δ13C = -2 -3‰ VPDB) [4].

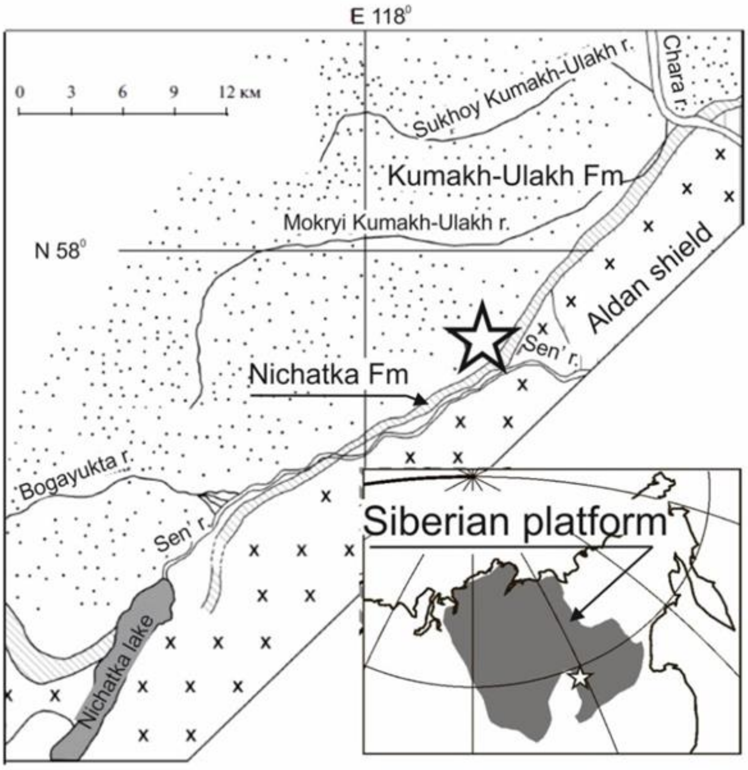

Fig. 1. Geological structure of the study area. The location of the Kumakh-Ulakh cap dolomite sequence is marked with a star

A continuous (145 cm thick) sample of cap dolostone was taken for the study with a handheld portable gasoline cutting machine. The sample was polished and scanned for detailed lithological analysis. The rock composition and the nature of microtextures were studied in thin-sections.

Variations in the magnetic susceptibility along the sample were analyzed for the cyclostratigraphy. The measurements were taken each 5.9 mm. The resulting variation curve was analyzed to identify cycles with period ratios equal to those of the Earth's orbital variations.

Duration of astronomical cycles calculated for 635 million years ago was adopted from [5].

The linear trend was subtracted from the curve prior to cyclostratigraphic analysis. Harmonic analysis was carried out using the multitaper method in Acycle v.2.2 software [6].

Results

Lithological characteristics of cap dolostones of the Kumakh-Ulakh Formation.

The Nichatka Formation diamictites end with a lens of cross-stratified sandstone and a layer of laminated silt-mudstones, 0.5 m thick. They quickly but gradually shift to red-colored dolomite marls with sandy and silty admixture, which in turn are gradually succeeded by laminated clayey dolomite. A closer look at the polished surface of the sample showed that the clayey dolomite is composed of alternating pinkish, sometimes light gray, layers of dolomite (~15 mm) and thinner (~1 mm) cherry-red dark layers of dolomite micrite, with hematite and silty admixture. Very thin lamination is also visible in relatively thick light layers. Silty material is primarily concentrated at the layer interfaces and is represented by quartz, feldspar and mica.

Up the section, the amount of sandy and silty admixtures decreases. The thickness of the layers changes irregularly, although several intervals of rhythmic alternation of light and dark layer pairs can be observed (Fig. 2A).

There are both sharp boundaries and gradual transitions between light and dark layers. In relatively thick light layers, a gradational change in color can be seen from the pinkish bottom to an again pinkish top with the middle part much lighter. Occasionally, coarse-grained dolomite can be found in the middle part of thick light layers (Fig. 2B). The upper boundaries of light layers are often uneven, while the lower boundaries are exceptionally smooth (Fig. 2B, C). Rare thin layers of pure dolomite show pronounced uneven upper and lower boundaries, deforming the host sediment. Finally, there are two creamy-white layers of silicified dolomite, about 0.5 cm thick.

Microscopic studies showed that their internal texture is similar to the rhythmite, described above in the text.

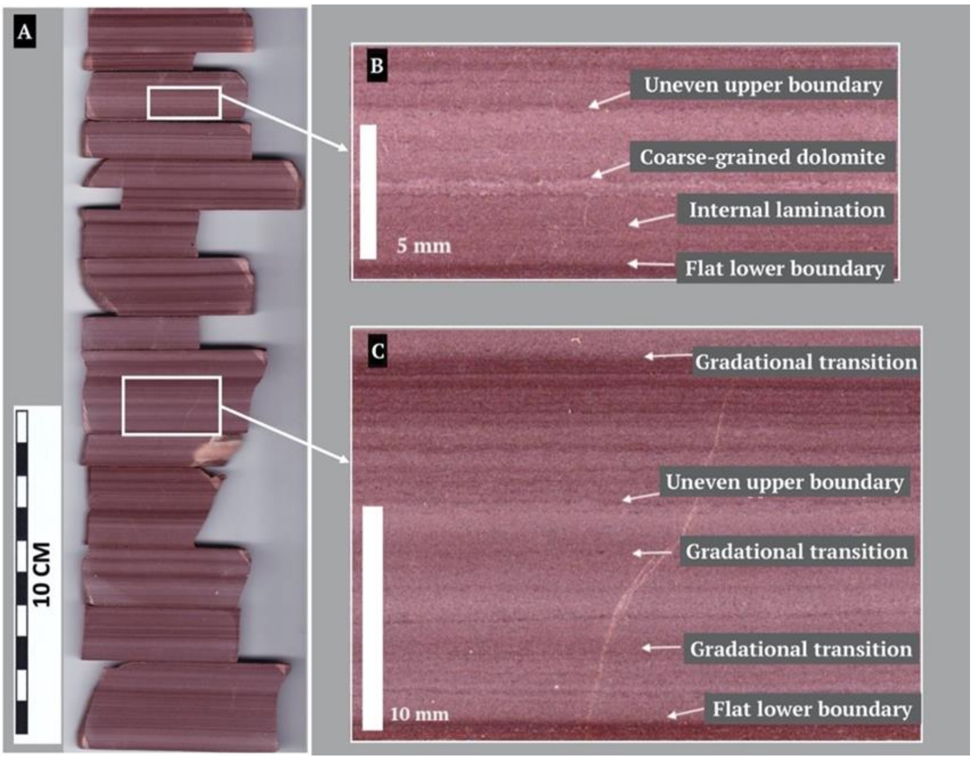

Fig. 2. Fragment of the polished surface of the cap dolostone sample taken from the Kumakh-Ulakh Formation (A) and textural features of the sediments (B, C). See discussion above

Interpretation of sedimentation conditions

The cap dolostone of the Kumakh-Ulakh Formation lacks obvious signs of biogenic origin, such as microbial pelmicrite, peloids, bacterial mats and traces of metabolism products. The studied sequence also had no signs of active shallow-water hydrodynamics and drainage. At the same time, observed laminated marly dolomites are similar to pelagic evaporites formed under meromictic conditions [7], [8], [9]. Signs of evaporite sedimentation are quite numerous: parallel lamination; gradual and sharp transitions in the top and bottom parts of the carbonate layers; traces of dissolution in an undersaturated brine manifested in the form of uneven upper boundaries of the layers. The chemogenic origin of sediments is also indicated by the thickness of dolomite layers, which is sometimes less than 0.1 mm. The stratification of the basin waters is emphasized by the absence of a bottom growth crystal pattern, however, some of the light carbonate layers were formed as a result of crystallization of carbonate or its precursor in unlithified sediments. The gradual change in size of micrite particles and color of the thin layers can be explained by changes in the sedimentation rate and composition against a background of episodic variations in temperature and salinity of the near-surface waters. The red color of the sediments indicates oxidizing conditions which are unusual for meromictic basins. A seasonal mixing of water in this sedimentation basin can therefore be assumed.

Dark cherry-red layers are interpreted as a result of slowing down or complete cessation of evaporite sedimentation followed by slow eolian sedimentation. This is confirmed by the presence of quartz silt impurities at the boundaries of light layers and within dark layers.

Therefore, dark layers correspond to the slowing down of evaporite sedimentation, while light layers reflect the opposite. The transition from terrigenous-carbonate sediments to carbonate ones in the lower part of the cap dolomite sequence reflects a shift to pelagic conditions.

Cyclic variations of magnetic susceptibility

Magnetic susceptibility varies in a wide range ($30\text{-}150 \cdot 10^{-3}$ $m3 \cdot kg^{-1}$) along the sequence.

Different-order variations are clearly visible in Fig. 3A, and this allows us to compare them with the Milankovitch cycles. The periodogram in Fig. 3B shows prominent (with a 95% confidence level) spikes at the ~660 mm and 25-30 mm period lengths. These periods are related to each other as 1:21-25, which is close to the ratio for long-eccentricity/precession.

This interpretation, however, is contradicted by the absence of any pronounced short-eccentricity related cycles and ultra-low sedimentation rate (1.6 mm/thousand years), only known for condensed pelagic clay deposits. The only interpretation that makes sense is that the long-period (~660 mm) variations of magnetic susceptibility are associated with the shortest orbital cycles, the cycles of axial precession. The shorter periods (25-30 mm) are thus sub-Milankovitch ones. The sedimentation rate (without taking account the compaction factor) calculated based on this assumption is slightly less (3-4.5 cm/1000 years) than the sedimentation rate of Holocene carbonate pelagic laminites of postglacial lakes in Canada [7], [8]. Therefore, such an interpretation is consistent with the sedimentation model proposed above.

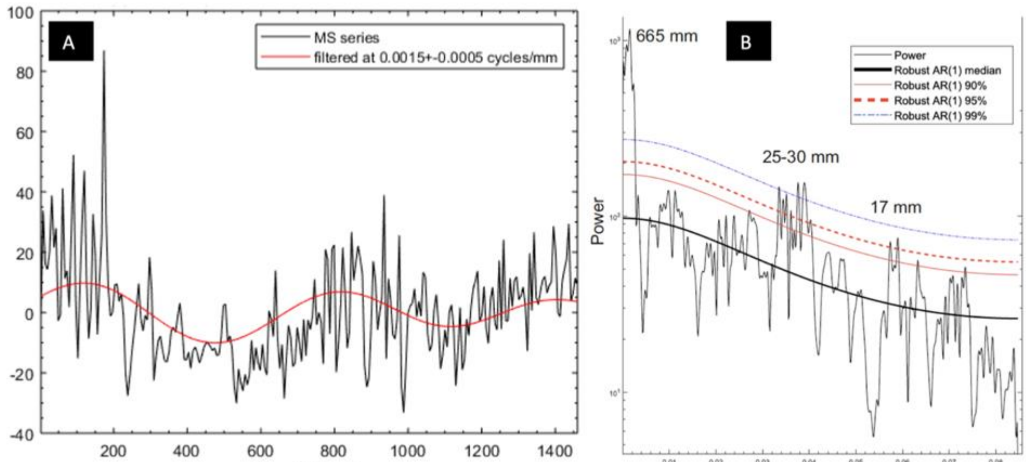

Fig. 3. A. Variations in magnetic susceptibility along the sequence of cap dolomites of the Kumakh-Ulakh Formation. Cycles with a period of about 660 mm, presumably reflecting precession cycles, are represented by a red line; B. Results of spectral analysis of magnetic susceptibility on the cyclogram

Discussion

A distinctive feature of cap dolomites of the Kumakh-Ulakh Formation is that they lack obvious signs of biogenic origin and are similar to evaporite laminites formed under meromictic conditions.

Pelagic evaporites can form in meromictic basins at depths from a few meters to hundreds of meters, depending on the area of the basin and the depth of the halocline [9]. At the same time, carbonate evaporite laminites form under lower salinity conditions compared to salt basins.

Favorable conditions for sedimentation include noticeable changes in the temperature or an increase in the evaporation rate, as well as algal bloom usually caused by seasonal temperature variations.

Thought should also be given to the fact that one of the most recognized global models of cap dolostone formation assumes that the world ocean was stratified during large-scale ice melting [10], [11]. However, if we assume that the Kumaks-Ulakh`s cap dolostones are of lacustrine origin, then their formation can be explained by the processes occurring in modern closed meromictic basins (ignoring the non-actualistic state of the hydrosphere).

The Snowball Earth hypothesis assumes that cap dolomites formed quite fast (during the first thousand or tens of thousands of years) as a reaction to a global greenhouse effect, that removed the planet's ice cover [2]. However, the idea of prolonged formation of cap dolomites is supported by the regional correlation between cap dolostone in Australia with sedimentary sequences, in which transgression-regression cycles are observed [12]. In addition, several zones of magnetic polarity observed throughout the sequence of cap dolostone in Brazil also support slow models of accumulation rates (tens or hundreds of thousands of years) [12].

The accumulation rate of the cap dolostone of the Kumakh-Ulakh Formation estimated based on the interpretation of the precessional nature of sedimentary cyclicity is consistent with the slow model (tens or hundreds of thousands of years) of cap dolostone formation. Although the analysis reported in this paper failed to reliably prove the relationship between magnetic susceptibility variations and precessional cycles, there is reason to believe that this can be achieved in the future by studying other cap dolostone sequences and demonstrating the global manifestations of the identified cycles.

Conclusions

In southern Siberia, in the Neoproterozoic cap dolostones of the Kumakh-Ulakh Formation, facies of pelagic evaporites formed under meromictic conditions were identified. In this regard, the cap dolostone was assumed to be of lacustrine origin. In addition, it was suggested that magnetic susceptibility variations in Kumakh-Ulakh Formation's cap dolostone may reflect orbital-precession cycles. The global manifestations of the cyclicity identified in other cap dolostone sequences may answer the question of how long they were accumulating.

Acknowledgements

This study was funded by Russian Science Foundation (project no. 20-77-10066)

REFERENCES

1. Kirschvink, J. L. (1992). Late Proterozoic Low-Latitude Global Glaciation: The Snowball Earth. In: Schopf, J. and Klein, C. Eds., In the Proterozoic Biosphere: A Multidisciplinary Study, Cambridge University Press, Cambridge, UK, pp. 51-52.
2. Hoffman, P. F., Kaufman, A. J., Halverson, G. P., Schrag, D.P. (1998). A Neoproterozoic snowball earth. Science 281 (5381), pp. 1342-1346.

3. Corsetti, F. A., Lorentz, N. J. (2006). On Neoproterozoic cap carbonates as chronostratigraphic markers. In Neoproterozoic geobiology and paleobiology. Springer, Dordrecht, pp. 273-294.
4. Pokrovsky, B. G., Chumakov, N. M., Melezhik, V. A. and Bujakaite, M. I. (2010). Geochemical properties of Neoproterozoic "cap dolomites" in the Patom paleobasin and problem of their genesis. Lithology and Mineral Resources 45 (6), pp. 577-592.
5. Waltham, D. (2015). Milankovitch period uncertainties and their impact on cyclostratigraphy. Journal of Sedimentary Research 85 (8), pp. 990-998.
6. Mingsong Li, Linda Hinnov, Lee Kump. (2019). Acycle: Time-series analysis software for paleoclimate projects and education, Computers & Geosciences 127, pp. 12-22.
7. Last, W. M., (1993). Geolimnology of Freefight Lake: an unusual hypersaline lake in the northern Great Plains of western Canada. Sedimentology 40 (3), pp. 431-448.
8. Last, W. M., Vance, R.E. (1997). Bedding characteristics of Holocene sediments from salt lakes of the northern Great Plains, Western Canada. Journal of Paleolimnology 17 (3), pp. 297-318.
9. Warren, J. K. (2016). Evaporites: A geological compendium. Springer.
10. Shields, G. A. (2005). Neoproterozoic cap carbonates: a critical appraisal of existing models and the plumeworld hypothesis. Terra Nova 17 (4), pp. 299-310.
11. Liu, C., Wang, Z., Raub, T. D., Macdonald, F. A., & Evans, D. A. (2014). Neoproterozoic cap-dolostone deposition in stratified glacial meltwater plume. Earth and Planetary Science Letters 404, pp. 22-32.
12. Spence, G. H., Le Heron, D. P., Fairchild, I. J., 2016. Sedimentological perspectives on climatic, atmospheric and environmental change in the Neoproterozoic Era. Sedimentology 63 (2), pp. 253-306.

Intercalation of Bentonite Smectite of the 10th Khutor Deposit with Basic Amino Acids

RYAZANOVA Alena[1,2], MOROZOV Vladimir[1], KHAYRULLINA Zulfiya[2]

[1] Kazan Federal University (RUSSIA)
[2] Federal Research Institute of Geology of Nonmetallic Mineral Resources (RUSSIA)
Email: eralien@mail.ru

Abstract

Ready availability, environmental friendliness and unique properties of bentonite clays make them applicable for various industries. Demand for organo-mineral composite materials has made the study of mechanisms of interaction of organic matter with clay minerals increasingly relevant.

he aim of the study was to study the possibility of intercalation of natural smectite of alkaline earth clays with the main amino acids. Intercalation of smectite was carried out in three ways.

The penetration of basic amino acids into the interlayer space of bentonite smectite clay was estimated by X-ray diffraction and thermal analyses. It was found that the intercalation of the basic amino acid (lysine) takes place under conditions of long stirring and subsequent natural sedimentation.

As a result of the study, the clay-amino acid composite was obtained.

Keywords: lysine, organo-mineral interactions, intercalation, clay minerals, composites

Introduction

Bentonites have a large specific surface, high capacity for base exchange, catalytic and sorption activity, as well as increased binding capacity. These properties lead to the high industrial value of bentonites [1].

Bentonite is a relatively inexpensive and environmentally friendly raw material. For this reason, many scientists studying sedimentary rocks, namely smectite, smectite-containing rocks and their modifications, consider clay minerals as the material of the 21st century [2].

The structure and chemical composition allow the use of montmorillonite group minerals in the creation of new materials with predetermined properties by chemical conversion, including the production of organo-mineral composites [3].

The researchers note that the production and use of organo-modified clays has been studied since the 1980s. One of the suitable materials for modifications may be bentonite, which has a content of montmorillonite close to 100% [4-6].

Organo-mineral interactions, as well as their role in mineral formation, is one of the most important problems of 21st century mineralogy [7, 8]. Consequently, the study of the properties of smectite, their interaction with organic matter is an urgent issue in modern minerology.

The aim of this work was to study the ability of smectite components of bentonite to intercalate lysine.

Materials and methods

Bentonitic clay of alkaline earth geological and industrial type of the 10th Khutor deposit was chosen as the research object. The content of smectite in a sample of bentonite clay was 90%. The sample also contained 6% quartz, traces of feldspar, 1% kaolinite and chlorite, 1% mica, 1% plagioclase and 1% siderite. The high content of smectite determined selection of the study object.

Chemical composition of the bentonite sample of the 10th Khutor deposit is given in Table 1.

The results of the main components content were obtained using an atomic emission spectrometer with inductively coupled plasma Optima 4300DV.

Table 1. Chemical composition of bentonite clay of the 10th Khutor deposit

No	Component	Content, %
1	SiO_2	59.8
2	TiO_2	0.69
3	Al_2O	18.12
4	Fe_2O_3	5.12
5	MnO	0.13
6	CaO	1.46
7	MgO	2.86
8	Na_2O	1.35
9	K_2O	1.38
10	P_2O_5	0.22
11	mass loss on ignition	8.20

The intercalation process was performed using three different methods. Lysine was used as the basic amino acid.

The first method was based on the Golubeva's technique [9]. Samples of bentonite clays were treated with an aqueous lysine solution during stirring with thermostat at 45 °C for an hour. The resulting suspension was stood for 24 hours. The supernatant was removed by centrifuging.

The second method of treatment was proposed by Bortnikov and Guska [3, 10]. Samples of bentonite clay in a bucket were wetted to a paste using distilled water. Then, an amino acid was added while stirring, and the bucket was closed and allowed to stand for 24 hours.

The third one was based on the Kollar method [11]. An aqueous bentonite clay suspension was allowed to stand for 24 hours. Then, the pH of the suspension was set to 4, and an amino acid was added while stirring for an hour. The resulting suspension was allowed to stand for 24 hours. The supernatant was removed by centrifuging.

In all methods of saturation, an identical ratio of clay to amino acids was used. Samples after saturation were dried at a temperature of 105 °C and crushed to powder.

The obtained samples were studied by X-ray diffraction on a Bruker D8-Advance powder diffractometer, angle range 2θ=3-60°, CuKα-radiation. Thermal analysis using an STA 409 PC Luxx thermoanalyzer manufactured by Netzsch, was also performed. The amount of organic carbon in the samples before and after lysine treatment was determined using the oxidometric method [12].

Results and discussion

Fig. 1 shows diffractograms of the initial sample of bentonite clay of the 10th Khutor deposit and of the same sample treated with lysine solution by three methods.

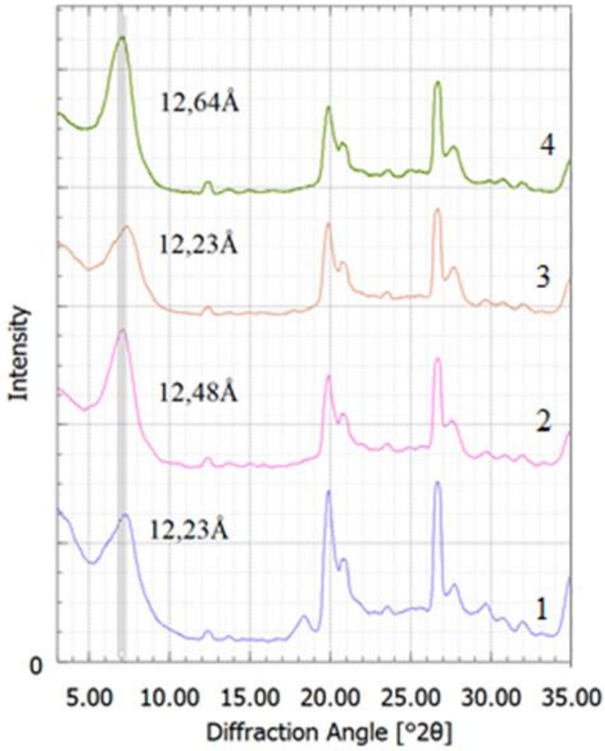

Fig. 1. Diffractrograms of bentonite samples before and after lysine saturation: (1) initial raw clay, (2) after the Golubeva method, (3) after the Bortnikova-Guska method, (4) after the Kollar method

The diffractogram of the raw untreated bentonite sample was characterized by reflex in the 2θ=7.22° (d001=12.23Å) region, which indicates the basal distance between the silicon-oxygen layers of smectite. Treatment using the Bortnikov-Guska method did not result in any significant shift of the reflex, indicating an absence of lysine in the interlayer space of smectite.

The saturation of smectite with lysine solution using the Golubeva method a shift of the diffraction reflex towards the low-angle region 2θ=7.08° (d001=12.48Å) was observed, which indicates successful intercalation of smectite with lysine.

The treatment using the Kollar method also resulted in successful intercalation of smectite with a basic amino acid. The diffractogram reflex of the synthesized clay-lysine composite shows an increase of the interlayer space by 0.41 Å in comparison to the initial sample; the reflex was located in the 2θ=6.99° (d001=12.64Å) region.

Fig. 2 shows the organic matter content in the initial and saturated samples. The results indicate that each treatment method led to an increase in organic matter content in comparison to the original sample. Bentonite samples after saturation using the Golubeva and Kollar methods contained 3.93% and 3.95% of organic matter respectively. Treatment using the Bortnikov-Guska method led to the highest organic matter content of 4.6%.

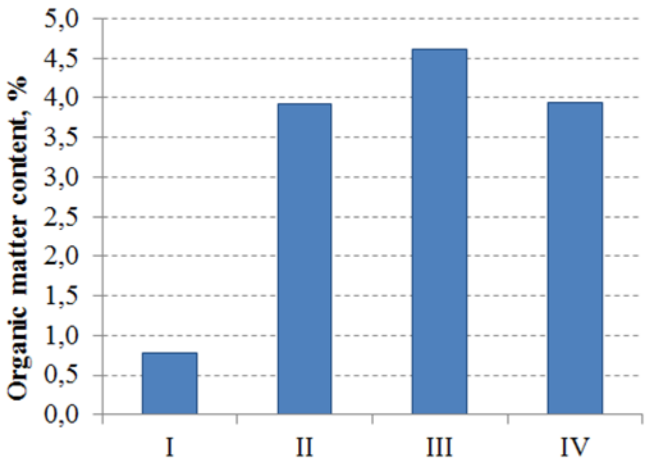

Fig. 2. Organic matter content of the raw and treated bentonite samples: (I) raw bentonite, (II) after the Golubeva method, (III) after the Bortnikova-Gusk method, (IV) after the Kollar method

The presence of organic matter in saturated samples was also confirmed by the complex differential thermal analysis method (Fig. 3). Exothermic effects in the temperature of 240-570 °C, indicating a destruction of organic compounds, were observed in all bentonite samples [13].

The results of thermal analysis showed a weak exothermic effect in the 370-570 °C temperature range, with a maximum at 470 °C (Fig. 3a).

This confirms the presence of natural organic matter in the bentonite under investigation.

The samples treated by the Golubeva method formed a significant exothermic effect in the temperature range of 250-570 °C with a maximum effect at 332 °C (Fig. 3b). The sample saturated by the Bortnikova-Gusk method had an exothermic effect in the temperature range of 250-560 °C with a maximum at 307 °C and 407 °C (Fig. 3c). As a result of saturation with lysine by the Kollar method, the obtained sample had an exothermic effect in the temperature range of 250-570 °C with a maximum effect at 325 °C (Fig. 3d).

The presence of more intensive exothermic effects confirms an increase in the content of organic compounds in the samples after saturation. However, the results of the thermal and X-ray diffraction analyses show that the increase of organic matter content in the sample after the Bortnikova-Guska intercalation method was due to the sorption on the surface of mineral component, rather than in the interlayer space of smectite.

Conclusions

The results of the current study revealed that lysine was capable of penetrating the interlayer space of smectite. The intercalation process depends on saturation conditions. It was found that successful intercalation of natural bentonite with lysine requires long stirring and subsequent natural sedimentation.

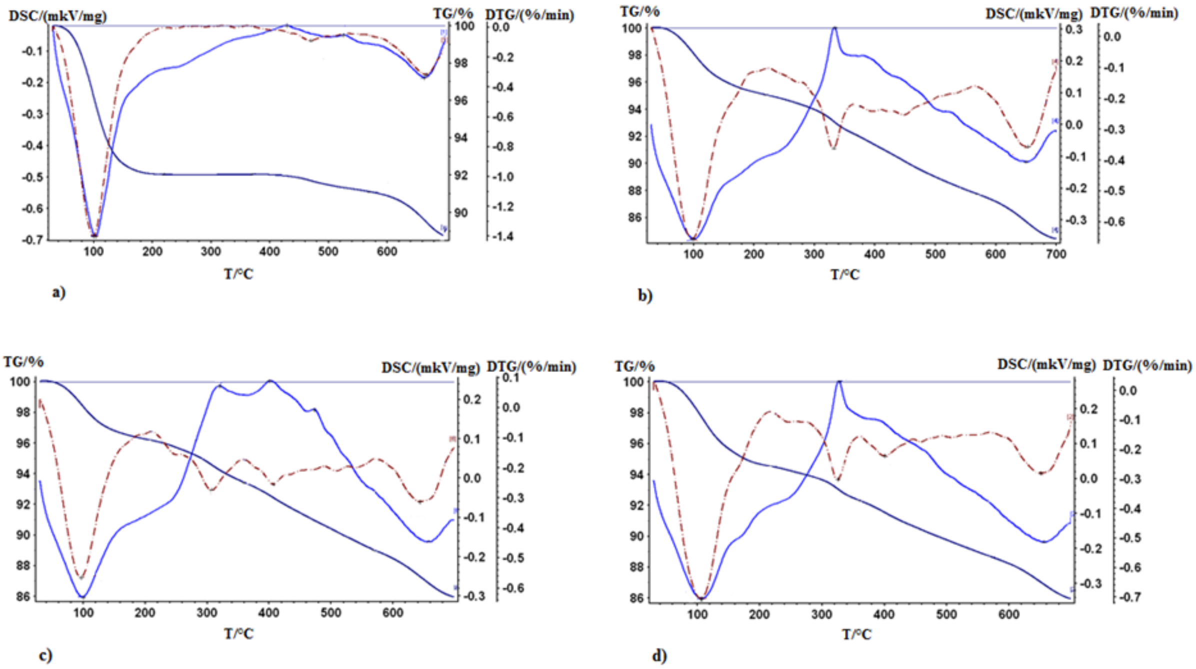

Fig. 3. Thermogravimetry curves (TG), differential thermogravimetry (DTG), differential scanning calorimetry (DSC): a) natural raw sample, b) saturated by the Golubeva method, c) saturated by the Bortnikova-Gusk method, d) saturated by the Kollar method. TG is represented by dark blue line, DTG is light blue line, DSC is red line

Although the treatment of bentonite with lysine solution by the Golubeva and Kollar methods resulted in intercalation of an amino acid molecule into the smectite interlayer space, the bulk of organic matter was sorbed on the surface of the mineral component. Alkaline-earth type of the bentonite samples explained the insignificance of intercalation due to a low degree of replacement of Ca and Mg cations in the interlayer space of bentonite smectite with basic amino acid molecules [3].

A clay-lysine composite with a total organic matter content of 3.93-3.95% depending on the method of saturation was obtained as a result of the study. The synthesized composite was thermally stable up to 250°C.

Acknowledgments

The authors would like to express their gratitude to the Analytical and Technological Service of the Federal State Unitary Enterprise “CNIIgeolnerud” for assistance in the research.

REFERENCES

1. Grim, R. E. (1956). Clay Mineralogy. New York – London – Toronto, Mc Graw-Hill Series in Geology, 454.
2. Bergaya, F. Lagaly, G. (2006). General introduction: clays, clay minerals, and clay science. Handbook of Clay Science. Vol. 1. Developmentsin Clay Science. Elsevier Ltd, Amsterdam, pp. 1-18.
3. Bortnikov, S. V., Gorenkova, G. A. (2018). Poluchenie organomodifitsirovannogo bentonita pri vzaimodeystvii s azotsoderzhashchimi soedineniyami. Uspekhi sovremennogo estestvoznaniya. Khimicheskie nauki 8, pp. 12-17.
4. Vazquez, A., López, M., Kortaberria, G., Martín, L., Mondragon, I. (2008). Modification of montmorillonite with cationic surfactants. Thermal and chemical analysis including CEC determination. Applied Clay Science 41, pp. 24-36.
5. Borisover, M., Davis, J.A. (2015). Adsorption of Inorganic and Organic Solutes by Clay Minerals. Natural and Engineered Clay Barriers. Developments in Clay Science 6c, pp. 33-70.

6. Boeva, N. M., Bocharnikova, U. I., Nasedkin, V. V., Belousov, P. E., Demidenok, K. V. (2013). Termicheskiy analiz ekspress-metod otsenki kachestvennykh i kolichestvennykh kharakteristik prirodnykh i sintezirovannykh organoglin. Rossiyskie nanotekhnologii 8 (3-4), pp. 54-57.
7. Frankel, R. B., Bazylinsky D. A. (2003). Biologically induced mineralization by bacteria. Rev Miner Geochem 54, pp. 95-114
8. Touryan, L. A., Lochhead, M. J., Marquardt, B. J., Vogel, V. (2004). Sequential switch of biomineral crystal morphology using trivalent ion. Nature Materials 3 (3), pp. 239-243.
9. Golubeva, O. U., Pavlova, S. V. (2014). Adsorbtsiya tiamina gidrokhlorida (vitamina V1) sinteticheskimi sloistymi silikatami so strukturoy montmorillonita. Fizika i khimiya stekla 40 (3), pp. 496-502.
10. Guska, R. V., Golubkov, V. A., Vorozhcov E. P. (2020). Obogashchenie prirodnoy bentonitovoy gliny odnozaryadnymi kationami. Mezhdunarodnyy zhurnal gumanitarnykh i estestvennykh nauk 1 (40), pp. 201-204.
11. Kollar, T. Palinko, I., Konya, Z., Kiricsi, I. (2003) Intercalating amino acid guests into montmorillonite host. Journal of Molecular Structure 651-653, pp. 335-340.
12. GOST 21216-2014. (2015). Syr’e glinistoe. Metody ispytaniy. Interstate standard.
13. Gorbunov, I. I., Curyupa, I. G., Shurygina, E. A. (1952). Rentgenogrammy, termogrammy i krivye obezvozhivaniya mineralov, vstrechayushchikhsya v pochvakh i glinakh. Ed. Academy of Sciences of the USSR, Moscow, p. 185.

On the Origin of Brecciated Rocks Extracted from the Jurassic Bazhenov Formation in the Kogalym Region: Significance for the Oil Formation Process

SHAIKHUTDINOVA Gulnara[1]

[1] Kogalymnipineft branch of LUKOIL-Engineering LLC in Tyumen (RUSSIA)
Email: ShayhutdinovaGH@tmn.lukoil.com

Abstract

This paper presents results from the laboratory studies of brecciated rocks extracted from an anomalous section in Bazhenov Formation – from well 431R in the Imilorskoye field. A laboratory experiment was developed to study fracturing caused by fluid entering from the bituminous fragments into the silt matrix. The study was performed using optical-petrographic, geochemical, and pyrolytic methods. The research confirms the role of proto-oil as an agent of hydraulic fracturing and limiting localization of the oil formation process. The output data derived from the laboratory study can be used to justify the parameters of a primary migration in the basin modelling.

Keywords: Bazhenov formation, reservoirs, fracturing, organic material, West Siberia

Introduction

The Bazhenov Formation is distributed throughout almost the entire territory of the West Siberian petroleum basin. Reservoirs of the Bazhenov formation are a thin-bedded alternation of clay-carbonate-siliceous rocks enriched in organic matter (with a variable content of the main rock-forming components). It contains hard-to-recover reserves, and it is a complex object for development in relation to traditional sand reservoirs.

The Bazhenov Formation in the West Siberian basin is a natural reservoir, which is a source rock and has fluid resistance properties [see Kontorovich, Gurari and others]. Reservoir properties are typical of the porous-fractured reservoir type, with a particular emphasis on the natural fracturing of rocks.

According to I.I. Nesterov, F.K. Salmanov and other researchers, a correlation has been established between the processes in the Bazhenov Formation reservoir and the mechanism of a primary migration of hydrocarbons (HC).

It is well known that the reservoir properties of bazhenites are mainly characterized by natural fracturing [1]. Therefore, when constructing a theoretical model of the primary HC migration, it was necessary to correlate it with the observed fracturing. In this work, the author adheres to the hypothesis of primary migration in a water-dissolved state.

The subject and methods of research

The subject of the study is a system of macro- and microcracks in the core material from well 431R, located in the Imilorskoye field, Kogalym region (see Fig. 1).

The study of fractures and HC migration using laboratory data helps to study in more detail the reservoir properties of the rocks of the Bazhenov Formation in the zone of the anomalous section of the Bazhenov Formation (ASB).

Fig. 1. Overall schematic map of well 431R located in the field Imilorskoye

Well 431R contains a unique core material characterized by fracturing, accentuated by the glow of hydrocarbons (HC) under ultraviolet light. Fracturing is clearly traced at the direct contacts of the bituminous rocks of the Bazhenov Formation with sandy-silty rocks (in the ASB zone).

In the macroscopic description, areas of maximum fracturing are identified. From the identified zones, 15 samples were taken for petrographic and geochemical studies. Petrographic studies include the description of microsections (5 samples) in reflected and transmitted light.

Geochemical studies (10 samples) include studies using the pyrolysis (Rock Eval) method and gas chromatography, supplemented by a luminescence-bituminological analysis.

The aim of this work is to study the reservoir properties of the rocks of the Bazhenov Formation in the zone of distribution of ASB at the macro and micro levels for further regional forecasting (well 431R).

The study was performed at the Center for Core and Reservoir Fluids Research of the KogalymNIPIneft Branch of OOO LUKOIL-Engineering in Tyumen.

Results

Based on the study of well 431R core, the mechanism for the formation of ASB was established.

Based on the photographs of the core, it can be assumed that in the Early Valanginian, weakly lithified sediments of bazhenite were eroded off by sandy-silty (Achimov) quicksands during underwater landslides [1, 2]. This process of disrupting the integrity of the sediment can be termed natural hydraulic fracturing.

The landslide body (see Fig. 2) is characterized by alternation of fine-coarse-grained, sandy, calcareous, weakly clayey siltstones (with an olive glow in ultraviolet light) with clay-siliceous bituminous rocks.

Rocks are characterized by textures of plastic flow and swelling, rarely by intrusion textures.

According to geophysical data, the thickness of the landslide body is 40 m; almost all of the interval is represented by a core (interval 3465.0-3502.0 m; thickness 37.0 m).

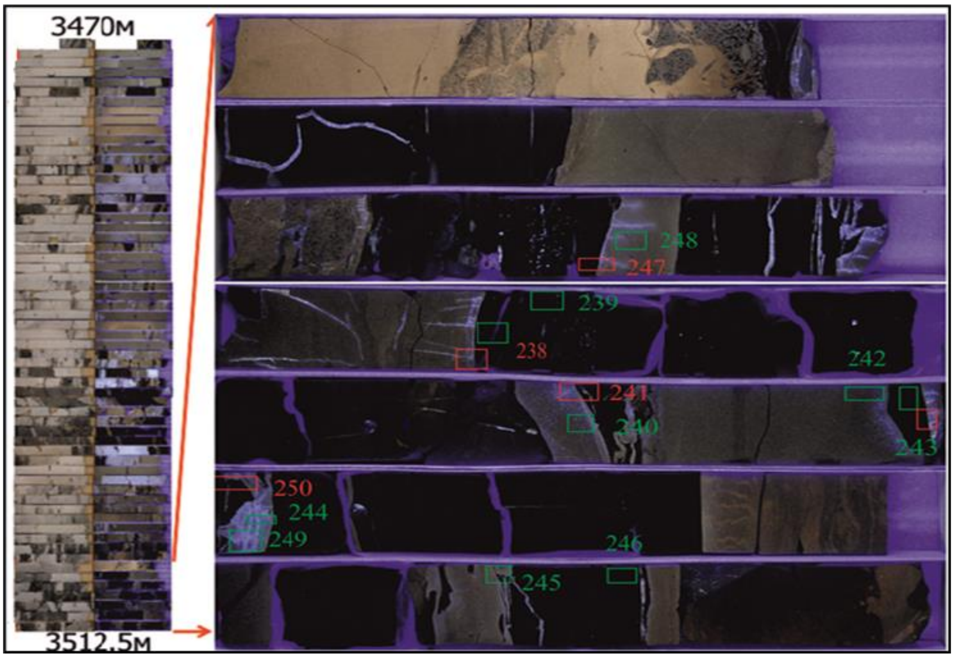

Fig. 2. Sampling points in borehole 431R (photographs of core samples in daylight and UV light)

Samples were taken in the zone of maximum fracturing and studied by optical-petrographic and geochemical methods. The optical-petrographic method made it possible to establish the lithological differences of rocks at the boundary "oil source rock-rock-reservoir" and to study the microfracturing of the rocks (ref. Fig. 2). In microsections, a network of subvertical, rarely subhorizontal microcracks is noted, which are filled in sections with secondary minerals (carbonates), rarely with red-brown organic matter (micro-oil?). These results confirm the hypothesis of natural hydraulic fracturing of rocks. At the same time, the source rock is not only generating oil, but also accumulating it [4, 5].

The preservation of the oil generation potential was assessed using pyrolysis (Rock Eval) and gas chromatography methods. The parameters of the studied samples were compared with similar parameters in the core of the reference wells 401R and 412R of the Imilorskoye Field.

The results of pyrolysis indicate good generation potential of the studied samples and good oil-generating properties of the organic matter contained in them [3]. This suggests that the oil generation potential of the bituminous rocks of the Bazhenov Formation, exposed by well 431R, is not lower than in reference wells 401 R and 412 R.

Fig. 3 shows the petrographic-geochemical characteristics of one of the studied samples from well 431R of the Imilorskoye Field (sample 243). The photographs of the thin section show a system of conjugate microcracks (with organic matter) at the contact of siltstone with signs of oil saturation and hummocky limestone (with signs of oil saturation) in transmitted and reflected light.

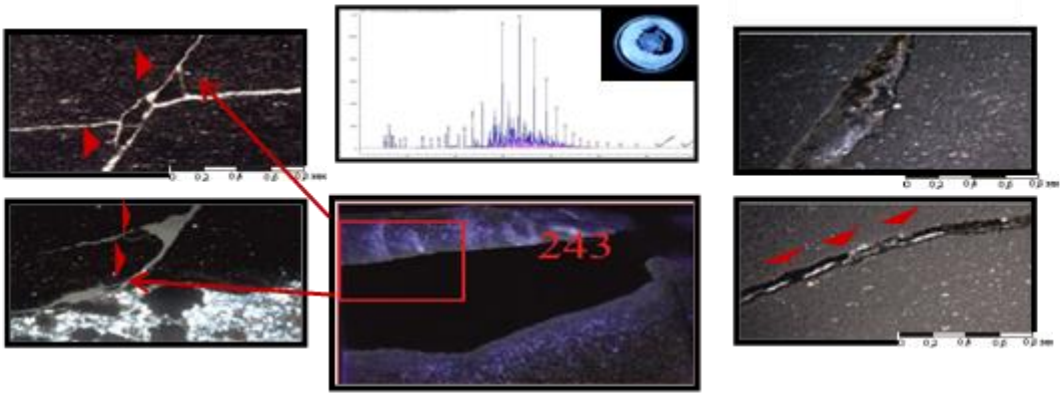

Fig. 3. Petrographic and geochemical characteristics of sample 243

Data from geochemical studies are also presented. According to the results of chromatographic analysis: HC – 0.09703, UVG – 0.01021, TUV – 0.08682 (oil sample).

According to the pyrolysis data: S1 – 2.6, S2 – 6.48. The bitumen content is estimated at 4 points (fluorescent stop test).

The laboratory studies confirm the mechanism of primary oil migration through microcracks.

At the time of intrusion into the Bazhenov Formation of the Achimov sandy-silty rocks in the zone of anomalous sections, the top of the formation was not yet fully lithified [4].

It can be assumed that the main reason for the primary migration of predominantly light hydrocarbons of immature proto-oil from source deposits was their natural hydraulic fracturing.

Conclusions

Laboratory studies of the core material (from well 431R, Imilorskoye Field) showed that the geochemical characteristics of brecciated bazhenites are identical with their lithological analogues from undisturbed sections of the Bazhenov Formation.

The traces of oil recorded in the cracks confirmed the hypothesis of hydraulic fracturing during the primary migration of hydrocarbons [5]. Results serve as evidence not only of general properties of the oil source rock, but also of the ability for the material to act as an intermediate reservoir.

Comprehensive studies and an increase in the volume of the studied core from the ASB can improve the accuracy of predictions of the filtration and reservoir properties of the studied formation at the regional level.

REFERENCES

1. Nezhdanov, A. A. (2017). Anomalous sections of the Bazhenov formation: a view half a century after discovery. Oil and gas 6. pp. 34-42.
2. Grishkevich, V. F., Kasatkin, V. E., Lagutina, S. V., Panina E. V. (2019). Evolution of the fluid-conducting system of deposits of the Bazhenov formation. Ways to realize the oil and gas potential of Western Siberia: Materials of the XXII scientific and practical conference. Khanty-Mansiysk, pp. 105-126.
3. Oleynik, E. V. (2019). Analysis of regularities in the structure of the Bazhenov formation in connection with the oil and gas content of the clinoform part of the Neocomian deposits on the territory of the KHMAO. Dis. kand. GEOL. – min. Sciences. Tyumen: Tyumen industrial University, 153.
4. Grishkevich, V. F. (2019). Petrographic analysis of the mechanism of formation of an anomalous section of the Bazhenov formation in the Imilorskaya area of Western Siberia. Lithosphere 9, pp. 209-227.
5. Simonenko, V. F. (1988). Primary migration of hydrocarbons in water solutions and their initial accumulation. (Geology, methods of search and exploration of oil and gas fields): a review of information from the VIEMS MG SSSR. m.: ONTI VIEMS, pp. 56-60.

Lithological and Petrographic Features and Nomenclature of the Jurassic Productive Horizons of the Sudoch Trough and Adjacent Territories (Ustyurt, Uzbekistan)

SHARAFUTDINOVA Leila[1], DJALILOV Gafur[2]

[1] *University of Geological Sciences (UZBEKISTAN)*
[2] *National University of Uzbekistan named after Mirzo Ulugbek (UZBEKISTAN)*
Email: shleyla1980@gmail.com

Abstract

This article presents the lithological and petrographic features, well as a unified nomenclature of the Jurassic productive horizons of the Sudoch Trough and adjacent territories with a stratigraphic reference. Within the study area, in the section of the Jurassic deposits, up to 20 sandy bodies (layers) have been identified, which are combined into 7 most persistent and laterally traced ones. The reservoir is classified as part of the productive horizon and has the status of an independent production facility, which is indicated by letters and subscripts (for example, J2k-kp1a). The name of the horizon comes from the area where it was first identified (Shakhpakhta horizon), or where its productivity was first established (Kuanysh horizon).

Keywords: Jurassic, Sudochy trough, productive horizons, correlation

Introduction

Stratigraphic methods at regional and prospecting stages require different methodological techniques: identifying and tracing reference horizons, establishing regional breaks, as well as the detailed correlation of these horizons. Subsequently, when the exploration and exploitation of deposits, which are confined to a large extent to the zones of facies replacement and thinning, begins, stratigraphic studies provide a layer-by-layer correlation of productive horizons [1].

Within the limits of Ustyurt (Fig.1), a unified nomenclature of productive horizons has not yet been adopted, which in turn affects the completeness of the assessment of the exposed Jurassic section [2, 3].

Methodology

Existing nomenclature of productive strata does not meet the modern requirements of geological exploration in the area under consideration, productive strata in the section occupy an indefinite position and have a large lithological variability, which excludes the possibility of their correlation in different fields.

The authors of this work [4] carried out studies to clarify the lithological-facies and stratigraphic structure of the Jurassic deposits of the Sudochi Trough, based on the results of which a unified nomenclature and indexation of productive horizons was developed. As a result, new, detailed information was obtained, complex correlative features (structural-textural, mineralogical-petrographic, paleontological) were established in each selected horizon, which made it possible to supplement the results of previous studies and close the existing gaps.

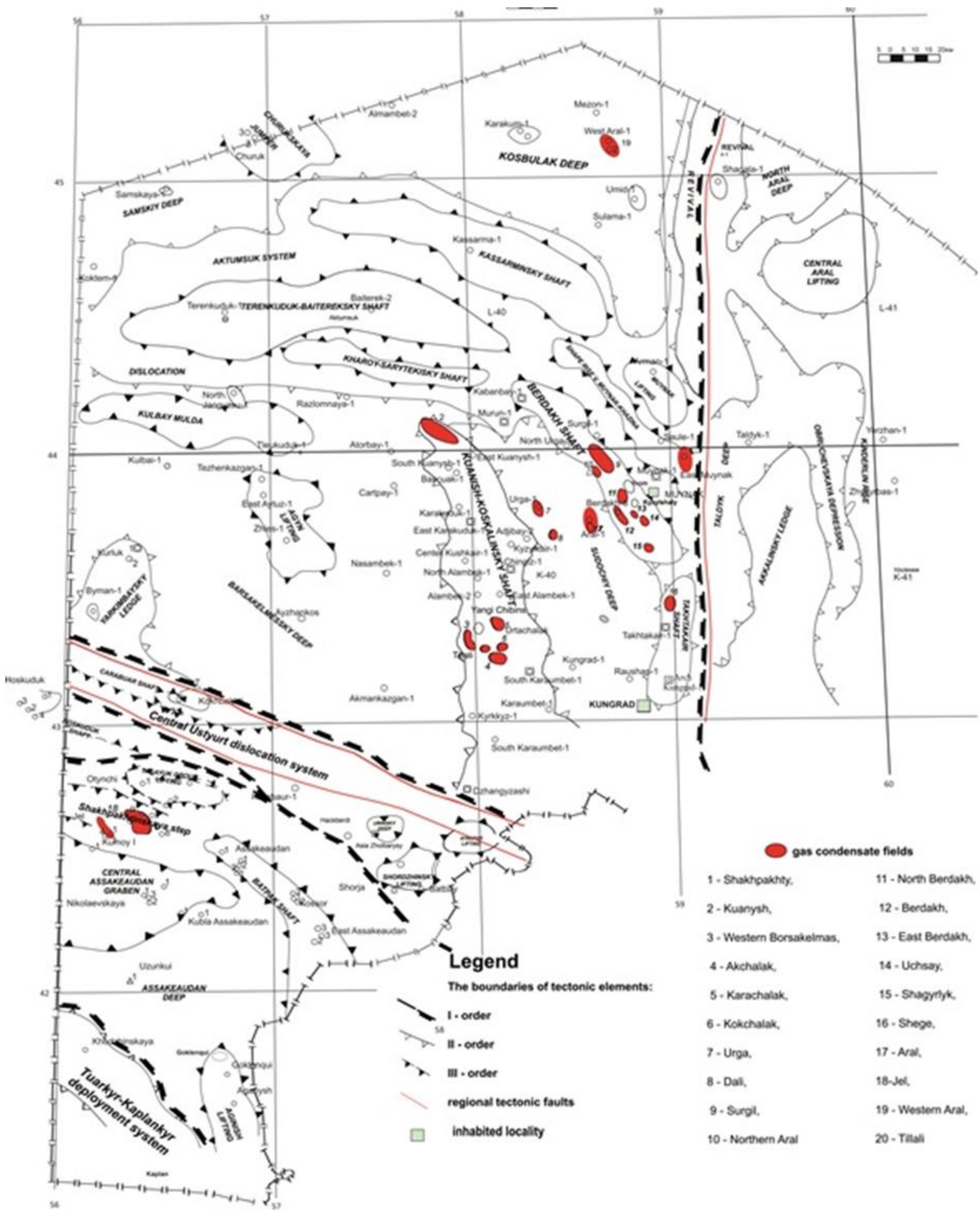

Fig. 1. Map of the actual material of the study area (Ustyurt, Uzbekistan) (based on the tectonic map on the surface of the Jurassic deposits by D.R. Khegai, M.G. Yuldasheva, with additions and changes by the authors)

Results

The generalization of a large amount of factual material based on the lithological and petrographic composition of rocks, taking into account the peculiarities of the geological structure, made it possible to identify up to 20 mature sand bodies in the section of the Jurassic deposits, which are combined into 7 most consistent and well-correlated horizons (Shakhpakhtinsky, Akchalaksky, Karachalak, Aral, Alambek, Muynak and Kuanysh).

At the same time, the reservoir, classified as part of the productive horizon, has acquired the status of an independent production facility, which is indicated by letter and subscripts (for example, J2k-kp1a). The name of the horizon comes from the area where it was first identified (Shakhpakhta horizon), or where its productivity was first established (Kuanysh horizon).

The main correlative features of the productive horizons of the Jurassic system of the Sudoch Trough

Fig. 2. well Samskaya-1P, int. 2520-2526m. J3km + tt-shp. Pelitomorphic limestone with inclusions of bivalve fragments

Shakhpakhti horizon (J3km + tt-shp) in the central part of the Kuanysh-Koskala swell and in the western half of the Sudoch Trough it is represented by carbonates of marine origin (Fig.2), and on the periphery – by sandy, sandy-silty accumulations of bar or delta genesis. The age of this stage is based on the finds of pelecypods, ostracods and a complex of spores and pollen. H.H. Mirkamalov and G.S. Abdullaev found remains of bivalves *Camptonectes cf. grenieri* (Contejean), Astarte sp. (sq. Urga, int. 2220-2225 m). In Samskaya parametric well No. 1, fragments of shells of bivalves *Chlamys sp., Plicatula sp., Ctenostreon sp., Astarte sp.* Were found, at the base of the horizon (well Assake-Audan 1, interval 2437-2441 m) brachiopods *Rhynchonella rollieri eltonica* Makr. *R. haeterhynchia manguichlaci* Pozn. and others that make it possible to date the host rocks as Jurassic (Kimmeridgian-Tithonian stage).

On the logs, these formations are recorded by a sharp change in the configurations of the electric logging curves, with a clear beating of their boundaries in the section of wells located in the southwestern, partly in the northwestern parts of the Sudochy trough (Kyzylkair, Chingiz, Karaumbet, Bashchuak, Kuanysh, South Kuanysh, East Kuanysh, Dali, etc.) (Fig. 1). These horizons in the areas of Urga and Vost. Berdakh are gas-bearing, and in the Western Aral (Kosbulak trough) – oil-bearing.

Akchalak horizon (J_3o-ak). The deposits are represented by rhythmically interbedded variegated calcareous clays (prevailing) and siltstones (sharply subordinate) with interlayers of fine-grained sandstones (Fig. 3). Silty, layered, dense clays. The color is gray, dark gray, greenish gray, rarely dark brown. Down the section, the color changes to brown, brick-red.

From the same deposits I.A. Pechnikova studied foraminifera of the Oxfordian *Trocholina sp.*, *Spirilina ex gr.* Kubl., *Frondiaria glon-dilinoldes*. From the described deposits in well.

Fig. 3. well Balkhan-1, int. 1989-1995m (J3o-ak). Variegated wavy-layered clay-sand rocks

Shakhpakhty-1 (interval 1763-1773 m) G.A. Kholodina identified foraminifera *Spirophaedium* sp., *Lenticulina sp*., *Turrispiridium sp*., *Frondiculia sp*. V.V. Kutuzova from the same breeds identified the pelicipods *Mellogrinella sp*. In the Assakeudan reference well in the upper part of the section (interval 2475-2580 m) A.A. Saveliev identified *Camptonectes cf. Lens* (Sow.), *Trigonia cf. papilata*, testifying, according to experts, to the Oxfordian age of the host rocks.

In the western direction, the thickness of the Akchalak sandy horizon begins to decrease to 4 m (well. Raushan-1, int. 2466-2470 m). Thicker sandy strata are identified in the wells Ajibai-2 (interval 2620-2646 m), North. Urga-1 (int. 1824-1894 m, 1960-2020 m), Surgil-1 (int. 1772-1808 m, 1882-1990 m). The thickness of the wave-breaker sandy strata of the Surgil-North Urga area sharply decreases towards Muynak, Kabanbai and Ajibai, then the lenses pinch out. many areas of the sandy layer are absent (Urga, Ajibay, Karakuduk, etc.). The genesis of the Oxfordian sandy horizons is shallow-marine. It should be noted that within many areas there is no sand layer (Urga, Ajibay, Karakuduk, etc.). The genesis of the Oxfordian sandy horizons is shallow-marine.

Karachalak horizon (J_2k-kr). It stands out in the central, southern and eastern parts of the study area, stretches from north to south, forming deep tongue-like wedges to the west (square Center. Kushkair, Karakuduk).

The age of the deposits of this horizon is established mainly from the found leaf impressions of *Equisetites laterialis* (Phill.) Phill, *Equisetites sp*., *Cladophlebis parvifolia* Genkina., *Phoenicopsis ex.gr. angustifolia* Heer, *Coniopteris hymenophylloides* (*Brongn*.) Sew., C. *furssenkoi* Pryn., *Eboracia lobifolias* (Phyll.) Thomas, *Podozamites lanceolatus* (L. et H.) Schimper, *Hausmannia sp*. (in the well. Berdakh-5, int. 1942-1946 m). They were also identified in the Severnaya Urga-1 well (interval 2310-2316 m), Hoskuduk-2 (interval 1336-1339 m) by V.V. Kutuzova on the pelecypods *Suncyllona sp*., A.A. Savelyev *Astarte aff. pulla* Roem. All these data allow us to determine the age of the sediments containing them as Callovian.

As a result of testing from this horizon in well. Berdakh-5 received product (gas), in well.

Akmankazgan-1 and West.Barsakelmes-1 – water with dissolved gas, in Vost. Karakuduk-1P and North. Karaumbet-1P – water, and on the square. North. Berdakh (Fig. 1) – at different levels in sandy horizons in borehole. 9, 3, 10 – industrial gas flows received.

Aral horizon (J_2bt-ar). At the base of the Bathonian stage, there is a layer of gray, dark gray micaceous sandstones from fine to coarse grained with inclusions of gravel grains and thin lenses of clays and glauconitic greenish gray siltstones (Fig. 4). The deposits of the horizon under consideration were formed in shallow-sea wave-breaking conditions. The genesis of the sandy horizon is submarine deltaic.

In the section of this horizon, the imprints of the following paleoflora species were identified: *Neocalamites hoerensis* Halle, *Neocalamites pinitoides* (Chachl.) Chachl, *Equisetites asiaticus* Pryn., *Equisetites beanii* (Bunb.) Seward, *Marattiopsis munsteri* (Goepp.) Schimp, *Coniopteris hymenophylloides* Brik., *Coniopteris furssenkoi* Pryn. *Coniopteris burejensis* (Za1.) Seward, *Coniopteris simplex* (Lindl. et Hutt) Harris, *Cladophlebis denticulata* (Brongn.) Font., *Cladophlebis haiburnensis* (L. et. H) Seward, *Nilssonia polymorpha* Sch., *Phoenicopsis speciosa* Heer, *Baiera consinna* (Heer) Kawasaki, which allow us to determine the age of this horizon as Jurassic (Bathonian).

Fig. 4. Well Surgil-8. Int. 2407-2415m (J2bt-ar). Sandstone wavy-layered with thin interlayers of clay and vertical carbonaceous remains of the root system of plants, burrows of silt eaters

Fig. 5. Well Surgil-8, int. 2774-2779m (J2b-al). Sandstone is medium-grained, silty, with inclusions of deformed large coalified plant remains

As a result of tests in the sediments of this horizon in well. Surgil-1, Berdakh-5 gas received; in well. Akmankazgan-1, Zap. Barsakelmes-1, Vost. Alambek-1P, Alambek-2, water with dissolved gas was obtained.

Alambek horizon (J_2b-al). The Sudachi Trough during the Bajocian sedimentation period was an almost completely flattened surface dominated by the watershed-eluvial and plain-valley facies belts. On pl.

The Surgil-Alambek horizon (up to 70 m thick) is represented by channel sandstones with the inclusion of gravel and interbeds of siltstones. Sandstones are light gray, gravelitic, coarse-grained, micaceous-quartz, with massive, thin-layered, cross-bedded and randomly bedded texture (Fig. 5). In some places the sandstones are fine-grained, obliquely wavy-layered.

The age of the horizon was determined by the following floristic assemblage: *Equisetites laterialis* (Phill.) Phill., *Coniopteris embensis* Pryn., *Coniopteris cf. maakina* (Heer Pryn), *Coniopteris simplex* (Lindl. et Hutt.) Harris, *Coniopteris spectabilis* Brick, *Coniopteris hymenophylloides* Brongn., *Cladophlebis whitbiensis* Brong., *Cladophlebis lobifolia* (Phillips) Brongn., *Klukia cf. exilis* (Phill.) Racib, *Anomozamites minor* (Brongniart) Nath., *Nilssonia vittaeformis* Pryn., *Podozamites lanceolatus* (L. et H.) Schimp. and others, like the Oxford age.

When testing this formation in the wells of the Surgil field, inflows of water and weak gas were obtained.

On Eastern Karakuduk, Ajibay, Urga, Uchsay, Aral sandy strata are confined to the bottom of the Bajocian. The greatest thickness is found in the Aral – 85 m, Urga – 50 m, Adjibay – 46 m, Eastern Karakuduk – 24 m, in the western direction the horizon wedges out lenticularly.

Muynak horizon (J2a-mk) lies at the bottom of the Aalenian Stage and is represented by a powerful lean sandstone. The age of the horizon is determined by the following paleoflora species: *Sphenobaiera cf. czekanowskiana* (Heer) Florin, *Nilssonia vittaeformis* Pryn, *N. inonyeri* Yok, *Coniopteris cf. spectabilis* Brick., *Cladophlebis sp*., *Cladophlebis cf. lobifolia* (Phill.) Brongn., *Eborasia lobifolia* (Phill.) Thomas., *Phoenicopsis ex. gr. angustifolia* Heer, *Pityophyllum cf. angustifolium.*, *Pterophyllum cf. anarcanum* Schimp., *Czekanowskia cf. rigida* Heer, *Carpolithes heeri* Tur.-Ketova *et al*.

Fig. 6. Well Dali-1, int. 2931-2939m (J2a-m). Medium-grained sandstone with imprints of Anomozamites quadratus

On the Muynak area, the thickness of the horizon is up to 200 m, the rocks are represented by sandstones, gravelstones and small-pebble conglomerates with rare interlayers of siltstones and clays. The thickness of conglomerate strata varies from 20 to 40 m, more often they are interbedded with sandstones. Sandstones light gray, dark gray, massive texture, fine and medium grained, quartz-feldspar-biotite composition, dense (Fig. 6). Sandstones are locally oblique-bedded, interbedded with siltstones and conglomerates. In the eastern part of the region, channel sedimentation covers the Saule, Taldyk, Surgil, Vost. Muynak, Muynak, Uchsay, Shagyrlyk, Kyzylshaly, Aral, Raushan, etc. All wells of the North. Berdakh, the top of the Muynak horizon was opened at a depth of about 2850 m, the average thickness is 25 m. The Takhtakair horizon is composed of thin sandstones (15-20 m) and 40-60 m mudstones. On Raushan, Kungrad, Yuzh. In Karaumbet, the thickness of sandy strata varies from 5 to 20 m. On Zhyltyrbas, the horizon is represented at the bottom of the aalen by 55 m uneven-grained massive sandstones, in the lower part with interlayers of siltstones and silty clays. The reservoir properties of the sandstones are satisfactory, the open porosity reaches 13%. During testing, technical water and oil were obtained.

On Berdakh in well. 4 and 5, when testing the horizon, a gas inflow was obtained with a flow rate of 55 thousand m^3/day.

Kuanysh horizon (J1ksh) named after the area of the same name, where industrial gas flows were first received. The lithological composition is represented by light gray, fine-medium-grained, massive, oblique-wavy-layered, quartz-feldspar-biotite sandstones, with inclusions of well-rounded fine gravel (North Berdakh-9, int. 2645-2648m). The basal layers are composed of different-grained gravelstones with pebble inclusions (Fig. 7). The clastic material is well rounded, the rocks are unsorted, undifferentiated, carbonate-free (Saule-1, int. 3062-3069m).

Coarse clastic rocks are often interbedded with floodplain siltstones and mudstones. Unclear wavy-bedded siltstones (Eastern Muinak-1, int. 3345-3347 m). The rocks are more often characterized by one-sided oblique and diagonal layering. The genesis of the rocks is freshwater-lacustrine (floodplain) – in the upper half and channel – in the lower (Fig. 7).

A rich complex of paleofloras was found in mudstones in sandy horizons, which made it possible to determine the age of these deposits as the Lower Jurassic (Toarcian).

This plant complex is characterized by the constant presence of *Coniopteris*, the appearance of *Todites*, an increase in the diversity of *Cladophlebis*, *Nilssonia*, a relatively wide distribution of *Podozamites* and, to a lesser extent, *Phoenicopsis*.

Discussion

When calculating the hydrocarbon reserves contained in the terrigenous rocks of the Jurassic system of the Ustyurt oil and gas region, experts often face the problem

Fig. 7. Well. Karakum-1, int. 4641-4646m (J1ksh). Medium-grained sandstone, thin-layered

of frequent pinching out and inconsistency of sandy horizons. This, in turn, lowers the reliability of the counting model and distorts inventory volumes. The problem is aggravated by the fragmentation of the nomenclature of the Jurassic sandy horizons of various authors, some of which are "weighted" by excessive granularity, which complicates the dissection and correlation of the already complex, devoid of paleontological remains, terrigenous section.

Based on the study of a large volume of core material (more than 50 wells), characterized by 80-100% removal along the productive part of the Jurassic section, the authors obtained a detailed lithological and petrographic characteristics of sand bodies. The discovered numerous well-preserved floristic imprints and palynological assemblages, together with a regular change in the mineralogical and petrographic composition, structural and textural features, allowed the author to optimize the available countable objects, highlighting the 7 most consistent and well correlated horizons. Each horizon has its own set of lithological, petrographic, porosity-permeability, paleontological and facies features, is quite identical in terms of well logging and is limited by dense mudstones. This system of indices is calculated for areas with the maximum full volume of the Jurassic system. In areas with reduced volumes of Jurassic deposits, the numbering of the horizons is allowed with the omission of individual parts.

Conclusion

Thus, the nomenclature of productive horizons of the Jurassic system has been optimized by obtaining new detailed information, complex correlations have been established (structural-textural, mineralogical-petrographic, paleontological) in each selected horizon. Below is a unified nomenclature and indexation of the Jurassic productive horizons of the Sudoch Trough and adjacent territories optimized by the authors and a brief description of the correlation lithological-petrographic features (Table 1).

Table 1. Unified nomenclature and indexation of the Jurassic productive horizons of the Sudochy Trough and adjacent territories with a brief description of the correlation features

№ пп	Age	Product name, the horizon	Horizon Index	Number of layers	Brief description of correlation features						
					Colour	structure	texture	roundness	relative content of carbonaceous detritus	miner-petrograph. grain composition	facies
1	Kimmeridgian-Tithonian stage	Shakhpakh-tin	J_3km+tt-shp	1	Greenish	Psammitic, lime psammitic with the inclusion of a bat shell	Massive, wavy-layered	weak	low	Carbonates, quartz, feldspars	Shallow sea
2	Oxford tier	Akchalak	J_3o-ak^1 и J_3o-ak^2	2	motley	Pelo-aleuro-psammitic	Unevenly layered	weak	low	Carbonates, quartz, less often feldspars	Shallow-sea, underwater delta
3	Callovian tier	Karachalak	J_2k-кr^1 и J_2k-кr^2	2	green	Psephite-psammitic	Massive	average	low	Quartz, feldspars, rarely glauconite	Shallow sea
4	Batskytier	Aralian	J_2bt-ar^1 и J_2bt-ar^2	up to 2	Gray, dark gray	Fine-medium-grained psammitic	Thin-layered	Average	the average	Quartz, feldspars	submarine delta
5	Bayos tier	Alambek	J_2b-al^1, J_2b-al^2, J_2b-al^3	up to 3	Light gray	Psefo-coarse-grained-psammitic	Layered	Average	Above the average	Fragments, quartz, feldspars	watershed eluvial and plain-valley
6	Aalenian stage	Muynak	J_2a-mk^1 и J_2a-mk^2	up to 2	Light gray	Psepho-psammitic	Cross bedded	above average	Above the average	Fragments, quartz, feldspars	Channel
7	Lower Jurassic	Kuanish	J_1ksh^1 и J_1ksh^2	up to 2	Light gray	Psepho-psammitic	Massive, cross bedded	good	Above the average	Fragments, quartz, feldspars	Channel

REFERENCES

1. Khegai D. R., Yuldasheva M. G. (2008). Application of the method of dismemberment and correlation of the Jurassic section of the Ustyurt region based on geological survey of wells. Uzbek Journal of Oil and Gas 3, pp. 7-9.
2. Alimov K. A. (2006). Stratigraphy of the Jurassic deposits of Ustyurt. Uzbek Journal of Oil and Gas 1, pp. 17-20.
3. Boykobilov I. T., Hayitov N. Sh., Sharafutdinova L. P. Jalilov G. G. (2008). Peculiarities of changes in the material composition of the Jurassic channel deposits of the Sudoch Trough (Ustyurt region). Uzbek. zhurn. oil and gas 3, pp. 12-15.
4. Sharafutdinova L. P., Jalilov G. G., Hayitov N. Sh. (2009). Types of sections of the Jurassic deposits of Ustyurt and the zoning of their distribution. Coll. Theoretical and practical aspects of oil and gas geology in Central Asia and ways of solving modern problems of the industry. Materials of the scientific-practical conference dedicated to the 50th anniversary of IGIRNIGM (October 12, 2009), p. 69.

Evolution of the Superfamily Palaeotextularioidea Galloway, 1933 (Foraminifera) in the Lower Carboniferous

SAKHNENKO Karina[1,2], ZAYTSEVA Elena[1,3]

[1] *Lomonosov Moscow State University, Moscow (RUSSIA)*
[2] *Borissiak Paleontological institute RAS, Moscow (RUSSIA)*
[3] *FBSD VNIGNI, Moscow, (RUSSIA)*
Email: sakh-karina@yandex.ru

Abstract

The evolution of superfamily Palaeotextularioidea (Foraminifera) is considered. Several stages in the development of palaeotextularioids in the Early Carboniferous were recognized: 1. the emergence of biserial forms with a single-layered and double-layered wall and a simple aperture; 2. complication of the aperture structure – there is the conversion from a simple to a cribrate aperture in the last chambers; 3. the appearance of bimorph forms with a complicated cribrate aperture in the uniserial last part of the test.

Keywords: Lower Carboniferous, foraminifers, evolution, palaeotextularioids

Introduction

Foraminifers of the superfamily Palaeotextularioidea occurred in Eurasia, North America and North-West Africa and existed from the late Visean of the early Carboniferous to the Permian inclusive. This group is of interest for its biostratigraphic and correlation potential for lower Carboniferous deposits. Palaeotextularioids is used as zonal taxa for Visean zones (Livian and Warnantian) in Western Europe [1], [2]. The biostratigraphic and correlation potential of this foraminiferal group has been revealed for the upper Visean deposits in the Moscow basin [3].

Results and discussion

The Palaeotextularioidea test is wedge-shaped, completely biserial, sometimes bimorph with a uniserial part in the late stage, less often completely uniserial (Plate 1). The superfamily Palaeotextularioidea includes the family Palaeotextulariidae and the family Koskinobigeneriidae [4]. The main family character is the wall structure. The family Koskinobigeneriidae is characterized by a single-layered microgranular wall, the family Palaeotextulariidae has a double-layered wall with an outer microgranular layer and an inner radial fibrous layer. The radial fibrous layer can be developed to varying degrees. Genus features are the tendency to uniseriality and characters of the aperture (simple or cribrate).

Important morphological features of palaeotextularioids, such as the shape of the test, the structure of the wall, the characteristic of the septa and the aperture, the shape of the chambers, and the tendency to uniseriality, are established in the axial sections. In the lower Carboniferous, the family Palaeotextulariidae is represented by the genera Palaeotextularia, Climacammina, Cribrostomum, and Koskinobigeneriidae includes the genera Consobrinellopsis, Koskinobigenerina and Koskinotextularia.

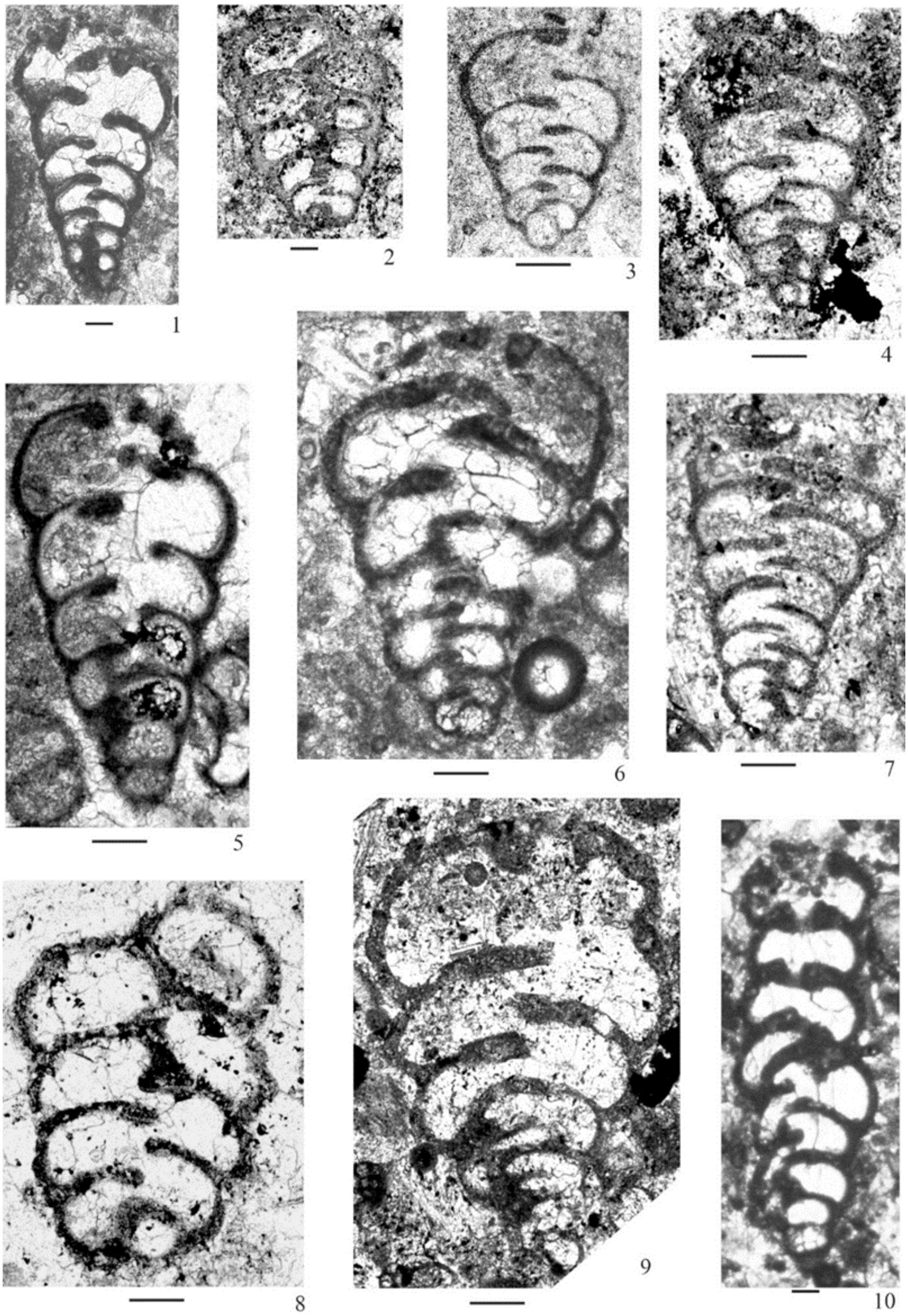

Plate 1. Palaeotextularioidea members. Scale bar 0.1 mm

Fig. 1, 5. *Cribrostomum eximiformis* (Lipina, 1948), axial sections, Ulyanovsk Region, Melekess 1 borehole: (1) ML1300/6 (FBSD VNIGNI, Moscow), upper Visean, Mikhailovian, interval 1432.7-1431.8 m, thin section no. 1300; (5) ML1223/3 (FBSD VNIGNI, Moscow), upper Visean, Venevian, interval 1351.79-1349.74 m, thin section no. 1223;

Fig. 2. *Palaeotextularia crassa* (Lipina, 1948), MSF12-2.3/1 (Moscow State University, Moscow), axial section; Kaluga Region, Mstikhino quarry, upper Visean, Mikhailovian, thin section no. MSF12-2.3;

Fig. 3. *Consobrinellopsis consobrina* (Lipina, 1948), AZ40/1 (FBSD VNIGNI, Moscow), axial section; Republic of Tatarstan, Aznakhaevo 4689 borehole, upper Visean, Mikhailovian, interval 1089-1083 m, thin section no. 40;

Fig. 4. *Consobrinellopsis intermedia* (Lipina, 1948), MSF12-2.3/2 (Moscow State University, Moscow), axial section; Kaluga Region, Mstikhino quarry, upper Visean, Mikhailovian, thin section no. MSF12-2.3;

Fig. 6. *Cribrostomum regularis* (Lipina, 1948), BZ556/4 (FBSD VNIGNI, Moscow), axial section; Orenburg Region, Buzuluk 1 borehole, upper Visean, Mikhailovian, interval 2501-2499.1 m, thin section no. 556;
Fig. 7. *Palaeotextularia bella* Lipina, 1948, MSF4-1-2/1 (Moscow State University, Moscow), axial section; Kaluga Region, Mstikhino quarry, upper Visean, Aleksinian, thin section no. MSF4-1-2;
Fig. 8. *Consobrinellopsis lipinae* (Conil et Lys, 1964), MSF16-IV/1 (Moscow State University, Moscow), axial section; Kaluga Region, Mstikhino quarry, upper Visean, Mikhailovian, thin section no. MSF16-IV;
Fig. 9. *Koskinotextularia bradyi* (Moeller, 1879), MSF10-2/1 (Moscow State University, Moscow), axial section; Kaluga Region, Mstikhino quarry, upper Visean, Mikhailovian, thin section no. MSF10-2;
Fig. 10. *Koskinobigenerina prisca* (Lipina, 1948), BZ594/5 (FBSD VNIGNI, Moscow), subaxial section; Orenburg Region, Buzuluk 1 borehole, upper Visean, Mikhailovian, interval 2463.5-2463.2 m, thin section no. 594.

Palaeotextularioidea originated from members of the family Palaeospiroplectamminidae Loeblich et Tappan, 1984 by reduction of the spiral initial part [5], [6], [7] (Fig. 1). Several stages in palaeotextularioid evolution in the Early Carboniferous can be traced. The earliest representative is *Consobrinellopsis lipinae* (Conil et Lys), which is reliably known from the beginning of the Late Visean (Tulian) time of the East European Platform (EEP) and the Urals, the V2b and V3a zones of Belgium [8] and Cf5 of England [1]. This species has a thick, single-layered, coarse-grained wall and is morphologically similar to *Eotextularia diversa* (Chernysheva) of the Palaeospiroplectamminidae family, differing in the absence of an initial spiral part. *C. lipinae* is probably the descendant of *E. diversa*. The last one is probably also ancestral to the genus Palaeotextularia with similar morphology, but it is described by a reduction of the spiral part and a more complicated double-layered wall structure. It can also be assumed that *Palaeotextularia* originates from *Consobrinellopsis*, secreting a double-layered wall with an inner radial fibrous layer. Thus, this stage is mainly characterized by biserial forms with a simple aperture – genera *Consobrinellopsis* and *Palaeotextularia*.

The second stage of palaeotextularioid development is characterized by the complication of the aperture structure – there is the conversion from a simple to a cribrate aperture in the last chambers.

This occurs simultaneously both in single-layered (the appearance of the genus *Koskinotextularia*) and in double-layered (the appearance of the genus *Cribrostomum*) palaeotextularioids. The first such forms (*Koskinotextularia bradyi* (Moeller), *Cribrostomum eximiformis* (Lipina), *C. stalinogorski* Lipina) are observed from the end of the Tulian of the EEP, the Urals, Tien Shan, and from the Cf5 Zone (Livian) of Western Europe (Fig. 1). The greater distribution and increase in species and quantitative diversity of these genera have been noted since the Aleksinian time.

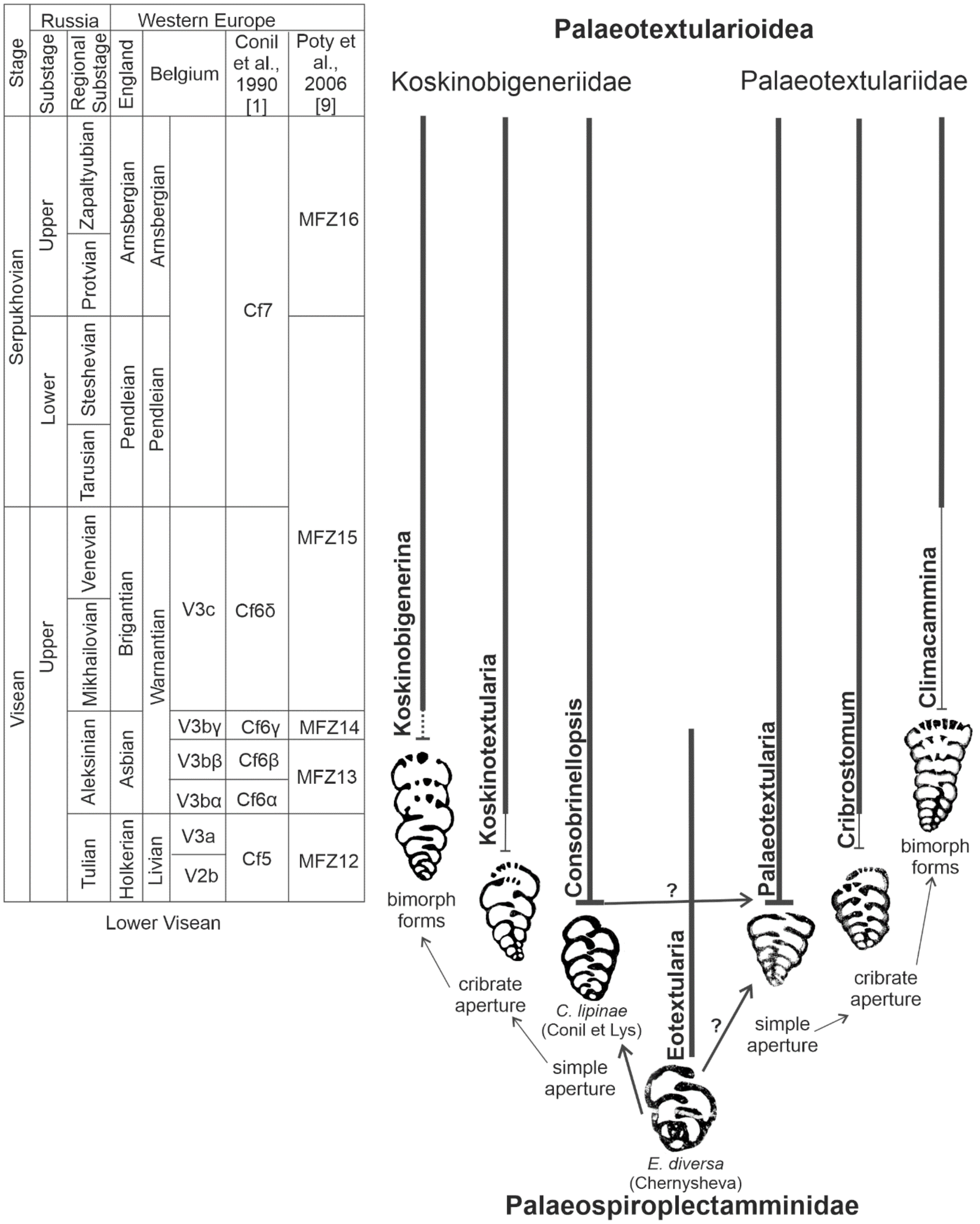

Fig. 1. Evolution of Palaeotextularioidea in Early Carboniferous

The third stage is expressed by a tendency to uniseriality and the appearance of bimorph forms with the complicated cribrate aperture in the last chambers of the uniserial part. Single representatives of palaeotextularioids with a single-layered wall and a uniserial last part (*Koskinobigenerina prisca* (Lipina), *K. breviseptata* (Eickhoff) have been recorded since the end of the Aleksinian in the EEP and the Urals, and from the base of the Cf6γ Zone (Warnantian) in Western European sections (Fig. 1). Bimorph forms with a double-layered wall (*Climacammina antiqua* (Brady)) were found from the Mikhailovian Regional Substage and the Cf6δ Zone of Western Europe (Fig. 1). Consequently, the almost simultaneous appearance of cribrate aperture and uniserial part is noted in single-layered and double-layered palaeotextularioids.

Further significant changes in the morphology of palaeotextularioids are shown in the Middle Carboniferous (the aperture with two parallel oval slits in the last part – genus *Deckerellina*; bimorph test with the same aperture in the uniserial part – genus *Deckerella*; bimorph forms with a terminal single aperture in the uniserial part – genus *Palaeobigenerina*) and in the Permian (uniserial forms with the cribrate aperture – genus *Cribrogenerina*). It is important to note that in the Middle Carboniferous palaeotextularioids with a double-layered wall prevailed. This may indicate that the complicated wall is a more progressive feature.

Thus, at the beginning of the late Visean, there is a rapid diversification of palaeotextularioids, expressed by the appearance of all early Carboniferous genera in the first half of the Late Visean. Further evolution in the Early Carboniferous is shown at the species level.

The complication of the test wall structure and the appearance of a double-layered wall provides the greatest strength of the test. This can probably be an adaptation to more active hydrodynamic environments. The complication of the aperture structure probably increases the strength properties of the test in the part most susceptible to fracture [10]. Examples of gradual complication of the aperture can be found in almost all large taxa [11].

Conclusion

In the early Carboniferous, palaeotextularioids developed towards a more complex aperture, and bimorph forms appeared. In the first half of the Late Visean, palaeotextularioid diversification and the appearance of all early Carboniferous genera: *Palaeotextularia*, *Climacammina*, *Cribrostomum*, *Consobrinellopsis*, *Koskinobigenerina*, and *Koskinotextularia*, are noted. The appearance of new features occurred in parallel among the forms with a single-layered and double-layered wall; however, the bimorph genus *Climacammina* with a double-layered wall is noted slightly later than the bimorph genus *Koskinobigenerina* with a single-layered wall.

The stages of palaeotextularioid development correlate with the following stratigraphic boundaries. The first correlation level is the beginning of the late Visean (Tulian Regional Stage of the EEP and the Urals, Cf5 Zone (Livian) of Western Europe), which fixes the appearance of palaeotextularioids, in particular the species *Consobrinellopsis lipinae*. The next level approximately corresponds to the base of the Aleksinian Regional Substage of the EEP and the Cf6α Zone of Western Europe, characterized by the complication of the aperture structure and increase in palaeotextularioid diversity. The third level corresponds to the Aleksinian-Mikhailovian boundary of the EEP and the Cf6γ Zone (Warnantian) and is described by the development of bimorph forms with the complicated cribrate aperture. The noted correlation levels and wide distribution of palaeotextularioids make this group appropriate for more accurate correlation.

REFERENCES

1. Conil, R., Groessens, E., Laloux, M., Poty E., Tourneur, F. (1990). Carboniferous guide Foraminifera, Corals and Conodonts in the Franco-Belgian and Campine Basins: their potential for widespread correlation. Intercontinental correlation and division of the Carboniferous System. Courier Forschungsinstitut Senckenberg 130 (Frankfurt a. M.), pp. 15-30.
2. Somerville, I. D. (2008). Biostratigraphic zonation and correlation of Mississippian rocks in Western Europe: some case studies in the late Viséan/Serpukhovian. Geological Journal 43, pp. 209-240.

3. Gibshman, N. B., Gutorova, A. V. (2015). Palaeotextulariida Hohenegger et Pillet, 1975 (Foraminifera) pozdnevizeiskogo (nizhniy karbon) Podmoskovnogo basseina. Sovremennaya mikropaleontologiya. Sbornik trudov XVI Vserossijskogo mikropaleontologicheskogo soveschaniya, Kaliningrad, pp. 195-198.
4. Vachard, D. (2016). Macroevolution and Biostratigraphy of Paleozoic Foraminifers. Stratigraphy & Timescales 1, pp. 257-323.
5. Lipina, O. A. (1970). Evolyuciya dvuryadnyh pryamolinejnyh rannekamtyyougol'nyh foraminifer. Akademiya nauk SSSR, Voprosy mikropaleontologii 13, pp. 3-29.
6. Vachard, D.; Pille, L., Gaillot, J. (2010). Palaeozoic Foraminifera: Systematics, palaeoecology and responses to global changes. Revue de Micropaléontologie 53(4), pp. 209-254.
7. BouDagher-Fadel M. K. (2018). Evolution and Geological Significance of Larger Benthic Foraminifera, Second edition. London, UCL Press, 693.
8. Conil, R.; Lys, M. (1964). Matériaux pour l'étude micropaléontologique du Dinantien de la Belgique et de la France (Avesnois): Partie 1, algues et foraminifères, et partie 2, foraminifères. Mémoires de l'Institut géologique de l'Université de Louvain. Ibid, 23, 296.
9. Poty E., Devuyst F., Hance L. (2006) Upper Devonian and Mississippian foraminiferal and rugose coral zonation of Belgium and northern France: a tool for Eurasian correlations. Geological Magazine 146, pp. 829-857.
10. Fursenko A. V. (1978). Vvedenie v izuchenie foraminifer. Akademia nauk SSSR, Sibirskoe otdelenie. Trudy Instituta geologii i geofiziki, Vipusk 391. Novosibirsk, Izdatel'stvo "Nauka", 242.
11. Alimov A. F. (Editor-in-Chief) *et al*., (2000). Protisty, Rukovodstvo po zoologii, chast 1. St. Petersburg, Izdatel`stvo "Nauka", 679.

Non-Ammonoid Cephalopod Assemblages of the Early Permian Shakh-Tau Reef

SHCHEDUKHIN Alexander[1], LEONOVA Tatiana[1]

[1] Borissiak Paleontological Institute, Russian Academy of Sciences, Moscow (RUSSIA)
Email: d_alsch2017@mail.ru

Abstract

This article presents new results of a study of cephalopods from the Early Permian Shakh-Tau Reef. Representatives of three groups – Nautilida, Pseudorthocerida, and Oncocerida – were identified in the Asselian-Sakmarian and Upper Artinskian communities. In total, more than 30 species of coiled and uncoiled nautiloids have been recognized. The new genus, *Barskoceras (B. mirum* Leonova et Shchedukhin), is the latest prospective member of the order Oncocerida. It was previously believed that oncocerids did not continue beyond the Middle Carboniferous. Nautilids of the genera *Temnocheilus* M'Coy and *Megaglossoceras* Miller, Dunbar et Condra, previously known only from the Carboniferous deposits, were found for the first time in the Lower Permian.

The results obtained clearly show a change in the community of endemic cephalopods of a reef environment with an open shelf community, characteristic of other localities of the South Uralian basin.

Keywords: Nautilida, Pseudorthocerida, Oncocerida, Toxeumophorida, Dentoceras, Early Permian, South Urals, Shakh-Tau reef

Introduction

In 2014-2015 a team from the Paleontological Institute of the Russian Academy of Sciences started examination of the localities in the former Shakh-Tau shikhan (mountain). In 2016, the first preliminary definitions of the findings were published. About 15 species from the order Nautilida and three species of uncoiled cephalopods were found [1]. In 2018, I.S. Barskov made a presentation on possible representatives of Discosorida or Oncocerida found in Shakh-Tau [2].

Preliminary results of studying the collected material were published in our previous work in the materials of the Kazan Conference [3]. In a more detailed study, some definitions were revised and refined. This year, papers are published with descriptions of nautiloids of the Asselian-Sakmarian [4] and Late Artinskian assemblages of [5] Shakh-Tau.

Results and Discussion

Two successive assemblages of Lower Permian nautiloids (Asselian-Sakmarian and Upper Artinskian) were discovered in the Shakh-Tau quarry (Russia, Bashkortostan). Representatives of the orders Nautilida and apparently Oncocerida have been identified in the Asselian-Sakmarian assemblage. They include 17 species of 15 genera. In the two orders, 12 species are new (**Nautilida**: *Alexoceras mazaevi* Leonova et Shchedukhin (Fig. 1, I), *Mosquoceras planum* Leonova et Shchedukhin, *Sholakoceras formosum* Leonova et Shchedukhin (Fig. 1, E), *Megaglossoceras barskovi* Leonova et Shchedukhin (Fig. 1, J), *Leniceras ovale* Leonova et

Shchedukhin (Fig. 1, C), *Liroceras shakhtauense* Leonova et Shchedukhin (Fig. 1, H), *Shikhanonautilus siphonoventralis* Leonova et Shchedukhin, *Thyoceras involutum* Leonova et Shchedukhin, *Domatoceras sterlitamakense* Leonova et Shchedukhin, *D. bashkiricum* Leonova et Shchedukhin, *Shatoceras umbilicatum* Leonova et Shchedukhin; **Oncocerida (?)**: *Barskoceras mirum* Leonova et Shchedukhin) [4]. This assemblage contains many unique representatives. Some genera, such as *Temnocheilus* and *Megaglossoceras* (Fig. 1, A, J), are recorded for the first time in the Permian (Asselian-Sakmarian). Representatives of *Temnocheilus* were described in the Carboniferous and Upper Devonian of Western Europe, North America, Moscow Region and Donets Basin (in the Urals, this genus was known from the Lower Carboniferous); the genus *Megaglossoceras* from the suborder Liroceratina was recorded from the Carboniferous of North America, Moscow Region, Donets Basin, the Urals and China [5]. The new genus *Alexoceras* Leonova et Shchedukhin (Fig. 1, I) is a fairly similar to the genus *Valhallites* Shimansky from the Mississippian of North America, the Middle Carboniferous of Verkhoyansk Region and the Lower-Middle Permian of Taimyr [5]. It differs in more smoothed longitudinal striae on the shell and an octagonal cross section [4].

A representative of the genus *Domatoceras*, *D. sterlitamakense*, is recorded for the first time in the Lower Permian (Asselian-Sakmarian) [4]. Other species of this genus were previously described from the Carboniferous and Upper Permian [5]. No species of this genus was reliably known from the interval between the Carboniferous and Upper Permian. Its discovery allows the existing gap in the phylogeny of domoceratids to be filled. A new unique genus and species, *Barskoceras mirum*, assigned to the order Oncocerida, has a curved shell with trochoid coiling and non-contacting whorls [4]. The latest cephalopod, morphologically similar to this species, have been described from the Devonian [1]. *Dentoceras magnum* Ruzhencev et Shimansky (Fig. 1, G), which is, according to V.E. Ruzhencev and V.N. Shimansky is a related nautiloid without a phragmocone [6], is for the first time found in the Asselian-Sakmarian boundary beds [4]. Previously, both species of *Dentoceras* were known only from the Upper Sakmarian and Lower Artinskian of the South Urals [6].

The Asselian-Sakmarian nautiloid assemblage of Shakh-Tau differs from other coeval assemblages of the South Urals both in the presence of taxa previously known only from the Carboniferous deposits and in the significant dominance of benthopelagic coiled taxa over uncoiled. As previously noted by Barskov [1], a similar proportion is characteristic of the Middle Permian cephalopod reef assemblages from of the Volga-Ural region [7]. At the same time, these communities differ significantly taxonomically and morphologically. In contrast to the assemblages from the Roadian localities of Kirov Oblast and the Mari El Republic, quite a few taxa with an ornamented shell were found in Shakh-Tau: with nodes, ribs, spirals and spines [4].

The Artinskian assemblage is significantly different from the Asselian-Sakmarian one. It includes representatives of two orders – Pseudorthocerida and Nautilida. The two orders are shown to include 14 species, of which three are new (Nautilida: *Neodomatoceras delicatum* Shchedukhin et Leonova (Fig. 1, D), *Hemiliroceras artum* Shchedukhin et Leonova (Fig. 1, B), *Condraoceras procerum* Shchedukhin et Leonova) [8]. Compared to the Asselian-Sakmarian assemblage, the Artinskian nautiloid assemblage is more diverse morphologically, as it contains coiled (representatives of the suborders Nautilina, Liroceratina), curved (*Dentoceras latum* Ruzhencev et Shimansky) and straight shells of pseudorthocerids (*Uralorthoceras tzwetaevae Shimansky, U. verneuili* Möller, *Dolorthoceras stiliforme* Shimansky). Nektonic straight cephalopods prevail in number although they are less taxonomically diverse (up to a quarter of all species).

Pseudorthocerids form clusters; shells are located subparallel to each other, occurring together with wood remains. Coiled nautilids constituting the vast majority of assemblage, are identified and described for the first time from the area. The study of the new species

Neodomatoceras delicatum (Fig. 1, D) made it possible to clarify the details of the suture and shell ornamentation for this genus, which was described by Ruzhencev and Shimansky based on a single incomplete shell [6]. The new species, *Hemiliroceras artum* (Fig. 1, B), was assigned to the genus *Hemiliroceras* with some reservations. The studied specimen corresponds to the generic diagnosis but differs in the narrower umbilical perforation (1.5 mm versus 4 mm) [8]. Since the size of the umbilical perforation is an important diagnostic character, a new species has been isolated. It will be possible to solve this question more reasonably when studying additional material. In straight *Uralorthoceras tzwetaevae*, a constriction was present in the upper part of the body chamber. Other researchers indicated the same feature for shells of this species from Shakh-Tau [9]. On the material described by Shimansky from other shikhans, this character was not observed [9]. Perhaps the constriction is a feature of the population that lived in this particular place. Among straight cephalopods, there is shell with a large apical angle (about 20º), without visible partitions (Fig. 1 F). At present, it is tentatively assigned to Toxeumophorida Shimansky, a group of unclear taxonomic affinity described also from finds from the Sakmarian of Shakh-Tau [10]. It is already obvious that the Artinskian nautiloid assemblage of Shakh-Tau is most similar in its taxonomic diversity to the richest Baigendzhinian assemblage of Gil-Tau, containing 16 species of nautilids, four species of ortho- and pseudorthocerids and three species of bactritids [8]. As the study continues, it is likely that the species diversity of the Late Artinskian assemblage of Shakh-Tau could exceed that of the famous Gil-Tau locality. A large number of shared species connect the Artinskian cephalopod assemblage of Shakh-Tau and other South Ural localities. This indicates the equalization of the conditions of existence after the completion of the reef phase in the Sakmarian and the subsequent free exchange of fauna.

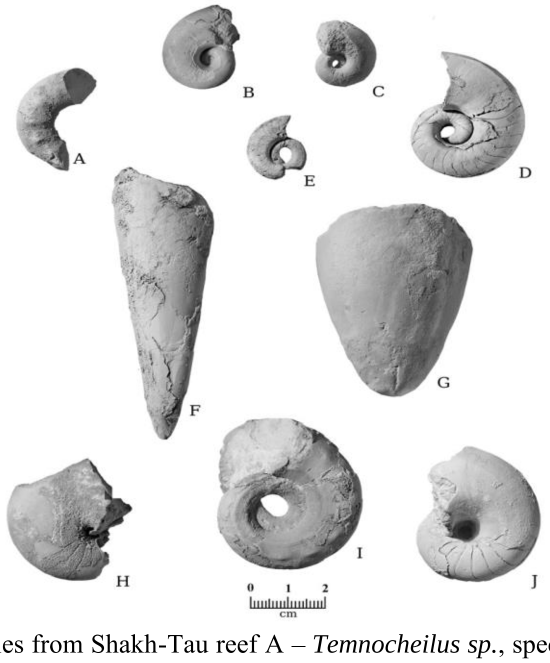

Fig. 1. Some cephalopod species from Shakh-Tau reef A – *Temnocheilus sp.*, specimen PIN no. 5668/38, Upper Asselian-Lower Sakmarian; B – ?*Hemiliroceras artum* Shchedukhin et Leonova, specimen PIN no. 5668/35, Upper Artinskian; C – *Leniceras ovale* Leonova et Shchedukhin, specimen PIN no. 5668/41, Upper Asselian-Lower Sakmarian; D – *Neodomatoceras delicatum* Shchedukhin et Leonova, specimen PIN no. 5668/39, Upper Artinskian; E – *Sholakoceras formosum* Leonova et Shchedukhin, specimen PIN no. 5668/32, Upper Asselian-Lower Sakmarian; F – Toxeumophorida gen. indet., specimen PIN no. 5668/63, Upper Artinskian; G – *Dentoceras magnum* Ruzhencev et Shimansky, specimen PIN no. 5668/47, Upper Asselian-Lower Sakmarian; H – *Liroceras shakhtauense* Leonova et Shchedukhin, specimen PIN no. 5668/76, Upper Asselian-Lower Sakmarian; I – *Alexoceras mazaevi* Leonova et Shchedukhin, specimen PIN no. 5668/24, Upper Asselian-Lower Sakmarian; J – *Megaglossoceras barskovi* Leonova et Shchedukhin, specimen PIN no. 5668/42, Upper Asselian-Lower Sakmarian

Conclusions

Thus, the results of the study show the replacement of a reef community with a predominantly benthopelagic nautiloid community of the open basin with a significant number of nektonic and nektobenthic forms. This conclusion agrees well with the change in facies in the Shakh-Tau section from reef bioherm to terrigenous-coastal. From other previously known assemblages of Perm nautiloid, both communities from Shakh-Tau are distinguished by a large number of ornamented shells, as well as taxonomic "relics" close to the Carboniferous and even Devonian nautiloids. A very large taxonomic and morphological diversity determines the uniqueness of this locality, its highest potential for solving the problems of paleoecology, biogeography and taphonomy of Permian cephalopods.

Acknowledgments

The authors are grateful to the late I.S. Barskov, who stood at the source of these studies, and also to A.V. Mazaev and M.S. Boiko (Paleontological Institute, Russian Academy of Sciences) who collected, gathered and passed to us a unique collection for study.

REFERENCES

1. Barskov, I. S., Boiko, M. S. (2016). Sakmarskie (Nizhnepermskie) nautilidy reefa Shakh-Tau (Bashkortostan). Sbornik Trudov Vserossiiskoi Nauchnoi Konferentsii «Zolotoi vek rossiyskoi malakologii». Moskva-Saratov, pp. 207-211.
2. Barskov I. S., Boiko, M. S., Mazaev, A. V. (2018). "Oni vyzhili!" Pervye nakhodki Discosorida I Oncocerida? (Cephalopoda, Nautiloidea) v permi Shakhtau, Bashkortostan. Sovremennyye problem izucheniya golovonogikh mollyuskov. Morfologiya, sistematika, evolyutsiya, ekologiya I biostratigrafiya, 5, (Leonova, T.B., Barskov, I.S., Mitta, V.V., Eds.), Moscow: Paleontologicheskii Institute, Ross. Akad. Nauk, pp. 70-72.
3. Leonova, T. B., Shchedukhin, A. Yu. (2019). Cephalopods of the Early Permian Shakh-Tau reef. Proceeding of Kazan Golovkinsky Stratigraphic Meeting, Kazan, pp. 155-158.
4. Leonova, T. B., Shchedukhin, A. Yu. (2020). Asselian-Sakmarian Nautiloids of the Shakh-Tau Reef (Bashkortostan). Paleontological Journal 54 (10). pp. 1113-1134.
5. Shchedukhin, A. Yu. Leonova, T. B., (2020). Late Artinskian Nautiloids of the Shakh-Tau Reef (Bashkortostan). Paleontological Journal 54(10). pp. 1135-1151.
6. Shimansky, V. N. (1967). Carboniferous Nautilida. Trudy Paleontol. Inst. Akad. Nauk SSSR 115, pp. 1-258.
7. Ruzhencev, V.E., Shimansky, V. N. (1954). Lower Permian coiled and curved nautiloids of the South Urals. Trudy of Paleontological Institute, Akad. Nauk SSSR 50, pp. 1-150.
8. Barskov, I. S., Leonova, T. B., Shilovsky, O. P. (2014). Middle Permian Cephalopods of the Volga-Ural region. Paleontol. J. 48 (13), pp. 1331-1414.
9. Shimansky, V. N. (1954). Pryamyye nautiloidei i baktritoidei sakmarskogo i artinskogo yarusov Yuzhnogo Urala. Trudy of Paleontological Institute, Akad. Nauk SSSR 44, pp. 1-156.
10. Shimansky, V. N., Barskov, I.S. (1970). New data on the order Toxeumophorida. Paleontological Journal 3, pp. 146-151.

Early Triassic Non-Marine Bivalves *Utschamiella* Ragozin, 1937 from the Kuznetsk Coal Basin: First Microstructural Data

SILANTIEV Vladimir[1], CARTER Joseph[2], URAZAEVA Milyausha[1], NOURGALIEVA Nouriya[1], NIZAMOVA Aigul[1]

[1] *Kazan Federal University, Kazan (RUSSIA)*
[2] *University of North Carolina at Chapel Hill (UNITED STATES OF AMERICA)*
Email: vladimir.silantiev@kpfu.ru

Abstract

The microstructural features of the non-marine bivalve genus *Utschamiella* Ragozin, 1937 [1] from the Lower Triassic deposits of Kuznetsk Coal Basin are described for the first time. The shell consists of two main layers. The outer calcite shell layer is composed of prominent simple vertical irregular prisms (simple prismatic: SP). The inner aragonite shell layer has a crossed lamellar (CL) structure. Primary aragonite is detected by RAMAN spectroscopy.

Geochemical data from fine-grained siltstone with *Utschamiella* indicate a semi-arid climate and anoxic conditions of the depositional environment. The microstructural features of *Utschamiella* distinctly differentiate these forms from externally similar morphotypes of the Permian genus *Palaeomutela* Amalitzky, 1892 [2] with a shell consisting of three layers with a more complicated crossed lamellar structure.

Keywords: non-marine bivalves, Early Triassic, Kuznetsk Coal Basin, Utschamiella

Introduction

In 2015-2020, we collected and studied non-marine bivalves from the Upper Permian and Lower Triassic reference section of the Kuznetsk Basin. This reference section is widely known in the literature as Babiy Kamen. It is one of the few sections in the world where non-marine bivalves occur in both the terminal Permian and the Lower Triassic (Fig. 1).

Early Triassic non-marine bivalves from Siberia were first described by Ragozin [1] as a new genus *Utschamiella* from the basin of the Nizhnyaya Tunguska River. Later Ragozin [3] described several species of *Utschamiella* from the Maltsevo Formation of the Babiy Kamen section. Lebedev [4] re-studied non-marine bivalves from the Babiy Kamen section and refuted Ragozin's identifications. He considered *Utschamiella* a junior synonym of the genus *Palaeanodonta* Amalitzky, 1895 [5] and assigned all Triassic forms of similar outline to this genus. Thus, the question arose about the validity of the genus *Utschamiella* and the possible distribution of the Permian genus *Palaeanodonta* in the Triassic sediments.

This study is an attempt to resolve this issue based on microstructural data.

Geological setting

The geology of the Paleozoic and Mesozoic deposits of the Kuznetsk Coal Basin (often referred to as Kuzbass) is studied in great detail due to intensive coal-field exploration, and therefore this area is often considered as a key region in the study of Angaraland [6].

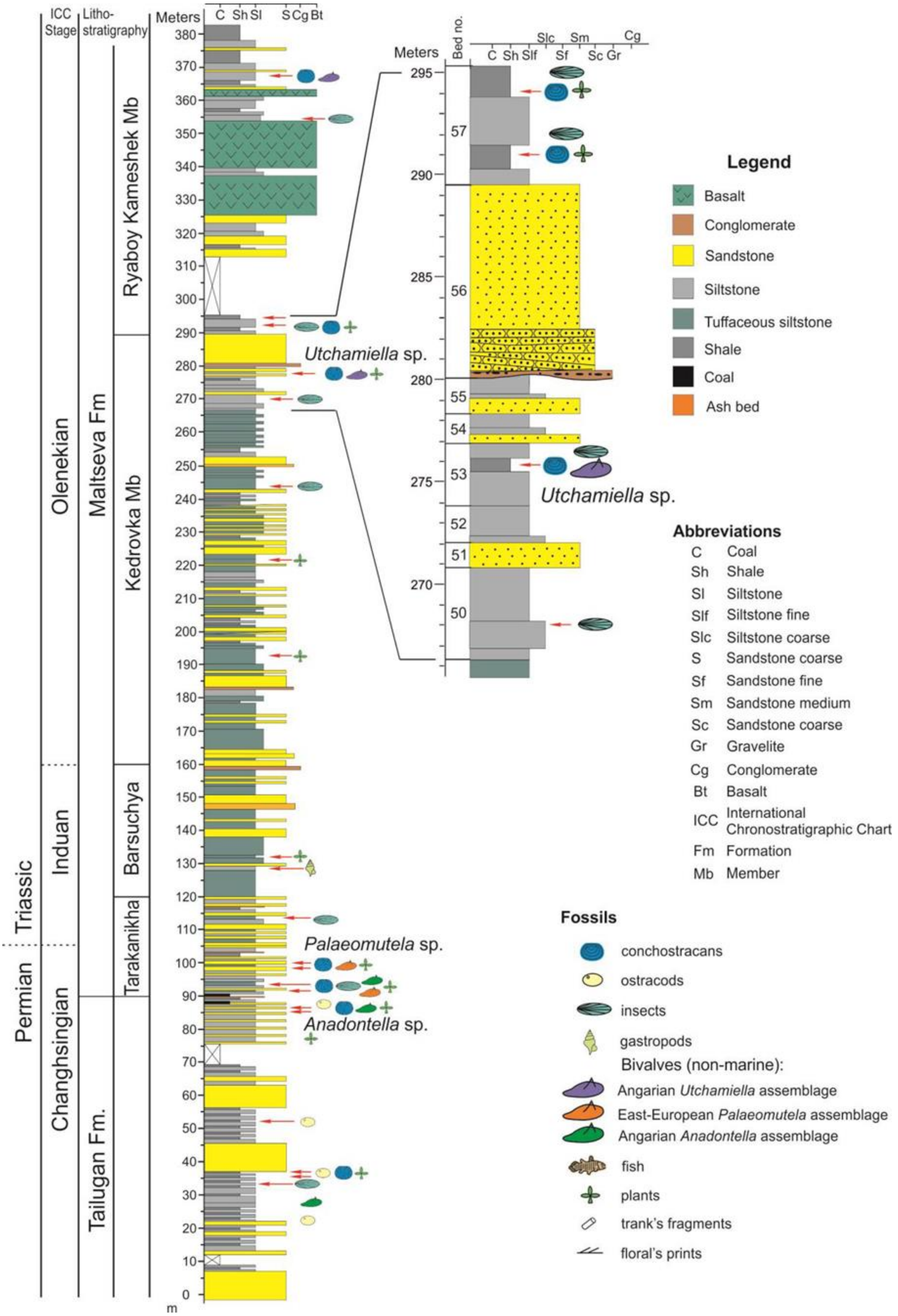

Fig. 1. The Babiy Kamen section showing the locality of the non-marine bivalves *Utschamiella* sp. (the stratigraphic units are shown after Stratigraphy of oil and gas basins of Siberia [7])

Kuzbass is situated in the northwestern part of the Altai–Sayan Folded Area and is bounded from each side by the Paleozoic mountainous systems. It is filled by the Upper Paleozoic coal-bearing siliciclastic molasse of Serpukhovian to Changhsingian age. The uppermost Permian coal-bearing Tailugan Formation is overlain by the Lower Triassic coal-barren volcanogenic-sedimentary succession of Maltsevo Formation (Fig. 1) which overlaps underlying rocks conformably or with stratigraphic unconformity [8].

The Babiy Kamen section is located on the right bank of the Tom River, 15 km downstream of the mouth of the Sredniy Ters River. The section crops out the upper part (upper 100 m) of the Tailugan Formation (Upper Permian) and 250 m of the Maltsevo Formation (Uppermost Permian-Lower Triassic). This section is a stratotype of the Maltsevo Formation and a reference section of the transitional Permian and Triassic deposits of Kuzbass.

The Tailugan Formation consists of a coal-bearing succession including mudstones (shales), siltstones, coal seams and thick sandstone beds.

The Maltsevo Formation overlies the coal-bearing Tailugan Formation without a visual unconformity and consists of alternating sedimentary and tuff-sedimentary packages including several flat-lying basalt bodies. In this paper, we conventionally define the lower boundary of the Maltsevo Formation at the top of the last coal seam. According to Vladimirovich *et al*. [9], the Maltsevo Formation is subdivided into four Members: Tarakanikha, Barsuchya, Kedrovka, Ryaboy Kameshek (Fig. 1).

Biostratigraphic dating of the Tailugan and Maltsevo Formations is possible based on paleobotanical data. According to Dobruskina [10] and Mogucheva and Krugovykh [11] the coal-bearing succession of the Kuznetsk Basin contains the Permian Cordaitalean Flora (about 90% of the fossil plants belong to Cordaitales). The overlying volcano-sedimentary Maltsevo Formation contains coniferous, fern, and lepidophyte assemblages of the Mesophytic Korvunchana Flora which is widespread in the Early Triassic of the Nizhnyaya Tunguska River area [7], [12].

Material and Methodology

The non-marine bivalves *Utschamiella* studied come from the upper part of the Kedrovka Member, Maltsevo Formation (Fig. 1, bed no. 53).

In the paper, we use modern terminology [13], [14], [15], [16] to describe bivalve shell features.

Microstructures were examined using the scanning electron microscopes of the Laboratory of Instrumental Analytics of the Borissiak Paleontological Institute of the Russian Academy of Sciences, Moscow (PIN). We studied vertical splits treated with a weak solution of formic acid.

The mineral composition of shell matter was determined by RAMAN spectroscopic analysis using an inVia Qontor (Renishaw, UK) spectrometer, integrated with a Leica DM2700 M microscope and a Nd: YAG solid-state laser.

The studied collections are deposited in the Geological Museum of Kazan Federal University (KFU) (coll. no. 36BK) and Novokuznetsk Geological Museum, Novokuznetsk, Kemerovo Oblast (NGM) (coll. no. BK3/65-60).

Results

The non-marine bivalves *Utschamiella* are collected from bed no. 53, which is lying in the upper part of Kedrovka Member (about 190 meters above the uppermost (“last”) coal seam) (Fig. 1). The non-marine bivalves occur together with conchostracans and insects in a dark-gray laminated mudstone and are represented by closed and slightly flattened shells with primary aragonite layers.

The *Utschamiella* assemblage contains two dominant morphotypes which differ significantly from one another by shell outline and elongation reflecting H/L ratio: (1) subcircular (Fig. 2 A) and (2) elongate oval-subtriangular (Fig. 2 B-F).

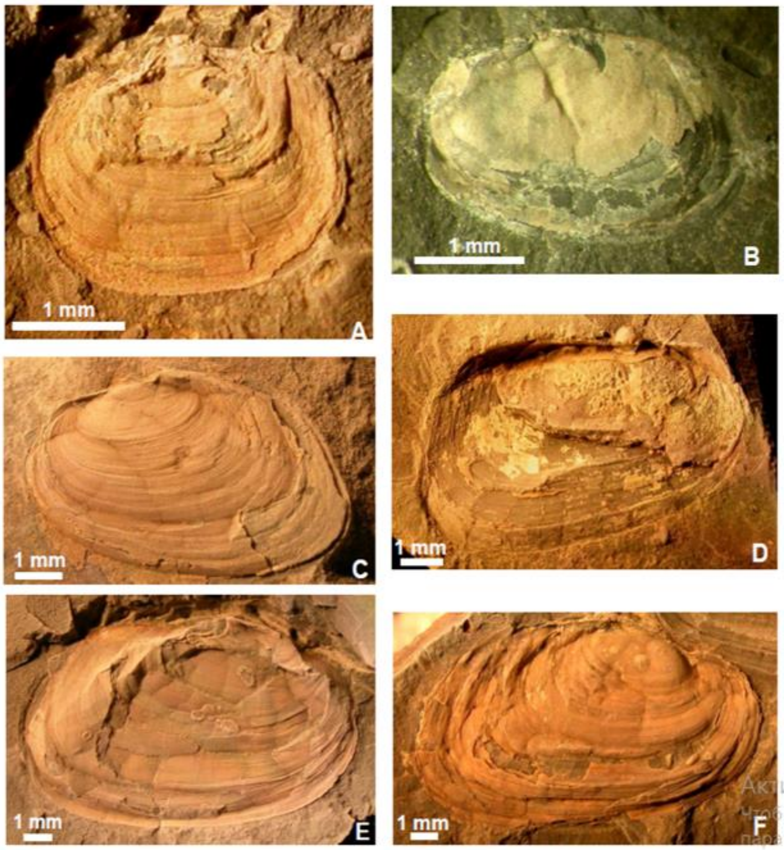

Fig. 2. Non-marine bivalves *Utschamiella* sp., typical Triassic bivalves of Maltsevo Formation, Babiy Kamen section
A – left valve with subcircular outline, NGM BK3/65-60/1-1, B – left valve with oval outline and subcentral umbo, NGM BK3/65-60/40-3, C – left valve of the closed shell, subtriangular outline, NGM BK3/65-60/14, D – internal mould of right valve of the closed shell, thin shell material is preserved near small subcircular umbo, NGM BK3/65-60/40-4, E – right valve with suboval outline, NGM BK3/65-60/10, F – right valve with subrectangular outline, NGM BK3/65-60/13.

(1) The subcircular morphotype is represented by one specimen. The shell is small with a length of 3.6 mm and a height of 2.9 mm. The external outline of the shell is subcircular with straight dorsal and posterior margins. The H/L ratio is about 0.75, tends to increase (up to 20%) with the shell growth (Fig. 2 A). The umbones are small, subcentral, low and do not rise above the line of the dorsal margin. Internal shell features are not preserved.

(2) The elongate oval-subtriangular morphotype dominates in the assemblage. The length of adult shells ranges from 7 to 10 mm, reaching the maximum length of 12 mm. The external outline is oval (Fig. 2, B, E-F) or oval-subtriangular (Fig. 2, C-D), moderately elongated and expanded to the posterior end. The dorsal and posterior margins are straight, forming a roundish angle of about 120-130 degrees. The H/L ratio, ranging from 0.50 to 0.65, tends to increase (up to 20%) with shell growth. The umbones are small, oval, low and slightly rise above the line of the dorsal margin (Fig. 2, D). The ligament is external, opisthodetic. The hinge is edentulous.

Ornamentation consists of fine and regular growth lines.

The microstructure of both morphotypes seems identical (Fig. 3). The shell consists of two main layers. The outer calcite shell layer (30-50 μm thick) is composed of prominent vertical irregular simple prisms (simple prismatic: SP). The inner aragonite shell layer (50-100 μm thick) has a crossed lamellar (CL) structure. Primary aragonite is detected by RAMAN spectroscopy.

Geochemical data from fine-grained (claystone) siliciclastics of the bed no. 53 indicate a semi-arid climate and anoxic conditions (low Eh).

The oval-subtriangular morphotype conditionally referred to *Utschamiella* Ragozin, 1937 whereas the subcircular morphotype appears to represent a new genus of non-marine bivalves.

Discussion

The type material of the genus *Utschamiella* Ragozin, 1937 was collected from the Korvunchana Formation (Triassic) overlying the Late Permian coal-bearing strata in the Nizhnaya Tunguska area [17]. At present, the Korvunchana Formation is distinguished at the rank of a Series that unites two formations: the Uchama Formation and the Bugarikta Formation, the age of which is determined as late Induan – early Olenekian [7]. Ragozin (1937) established a new genus and two species: *U. tungussica* (type species) and *U. opinata*. Both species have shells of elongated suboval outline.

Later, Ragozin [3] described Triassic non-marine bivalves from the Maltsevo Formation of the Babiy Kamen section. According to Ragozin [3], [17], the collection was sampled from a single bed from which Tschernyschev [18] recorded abundant specimens of the conchostracan Estheria minuta Gold. A more precise stratigraphic position of this collection is not given in Ragozin’s works. According to Tschernyschev [18], the conchostracans he studied were collected from the Maltsevo Formation, from beds located “above the basalts” (Fig. 1).

Ragozin (1958) attributed the non-marine bivalves from the Maltsevo Formation of Kuzbass to two genera. Shells elongate suboval in outline were assigned to the genus *Utschamiella*, and shells oval and elliptical in outline were tentatively assigned to the genus *Ferganoconcha* Tschernyshev, 1937 [19] (Jurassic-Cretaceous of North Asia). Ragozin [3] assigned three species to the genus *Utschamiella*: *U. tungussica* Ragozin, known from the Early Triassic of the Lower Tunguska, and two new species, U. babikamensis and *U. obrutschevi*. Probable representatives of *Ferganoconcha* (?) included two species: *F.* (?) *indefinita* Ragozin, 1955 and *F.* (?) *maltseviensis* Ragozin, 1958.

Ragozin attributed *Ferganoconcha* to Chernyshev, 1937, but no type species was designated until Lutkevitch et Nalivkin, 1960 [20], which means that the name was not available at that time [21].

Unfortunately, at present the collections of Ragozin [1], [3] with the type material of *Utschamiella* and *Ferganoconcha* (?) from Nizhnyaya Tunguska and Kuzbass are presumed lost. The attempts of the authors to find these [20] collections have not yet been successful.

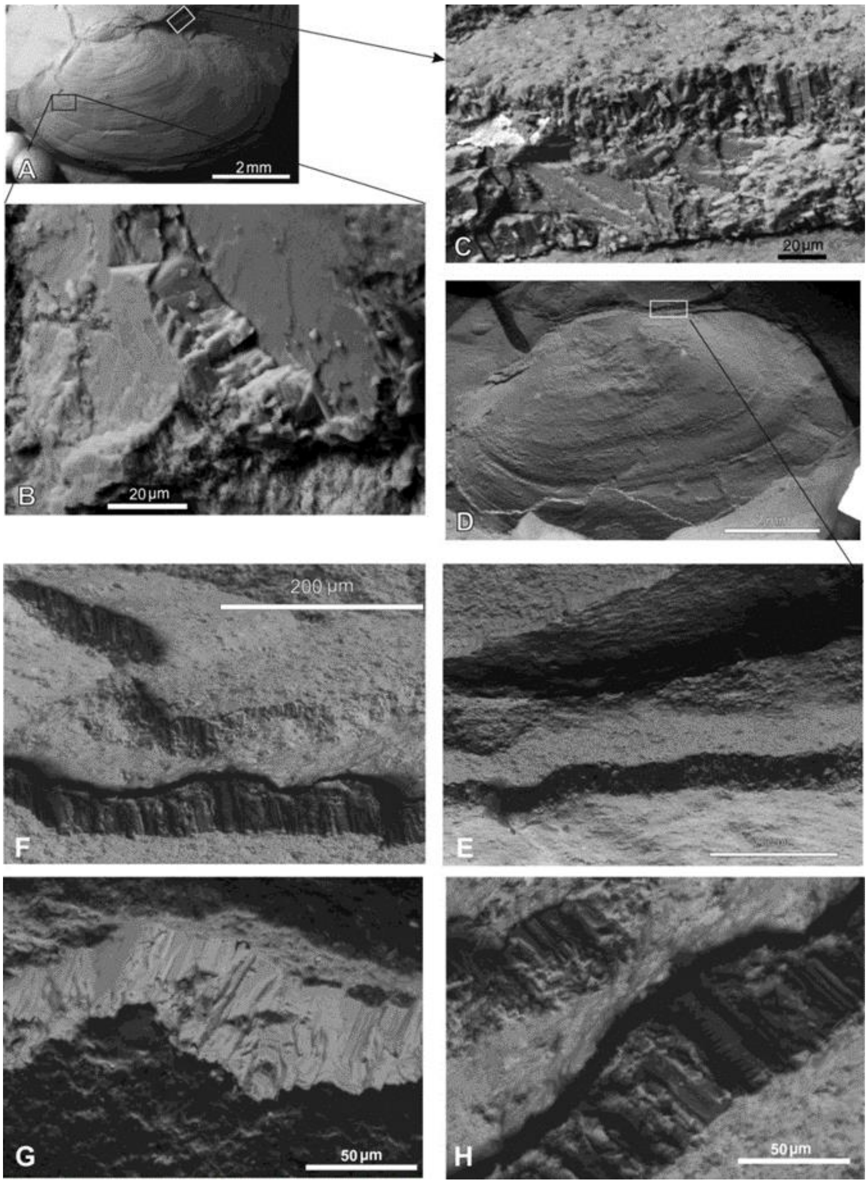

Fig. 3. Microstructure of *Utchamiella* sp.; Kedrovo Member, Maltsevo Formation, Babyi Kamen section, bed no. 53. A-C: specimen NGM, no. NGM BK3/65-60/40-6; A: left valve of the opened shell; B: comarginal split of the middle part of the valve; contact of two main layers of the shell – outer simple prismatic (SP) calcite layer (left) and inner crossed lamellar (CL) aragonite layer (right). C: comarginal split of the dorsal margin of the valve; outer simple prismatic (SP) calcite layer and inner CL aragonite layer. D-H: specimen NGM, no. NGM BK3/65-60/40-2; D: left valve of the opened shell; right valve is broken; E: view to the dorsal margin of the opened shell in the plane of commissure. F, H: outer SP calcite layer consisting of two sublayers; G: irregular dotted surface of outer SP calcite layer (bottom of the photo)

Lebedev [4] used only external characters in the re-examination of non-marine bivalves from the Maltsevo Formation of Kuzbass. Thus, his opinion about the synonymy of the *Utschamiella* and *Palaeanodonta* is uncertain. It should be added that the oval morphotype assigned by Ragozin [3] to *Ferganoconcha* (?), Lebedev attributed to the Permian genus *Microdontella* Lebedev, 1944.

Lebedev [4] considered the nonmarine bivalves from the Maltsevo Formation as Triassic. He assumed that they are descendants of the Late Permian fauna of Kuzbass. Lebedev [4] did not indicate the depositary of the collection he studied, and its location is not known at present.

The elongate oval-subtriangular morphotype is conditionally referred to *Utschamiella* Ragozin, 1937. The two-layered shell with outer simple prismatic layer and the inner crossed lamellar layer distinctly differentiates these forms from externally similar subtrapezoidal shells of *Palaeomutela* which occur in the lower part of the Maltsevo Formation (Fig. 1). The shell of *Palaeomutela* consists of three layers with more complicated crossed lamellar structure.

The subcircular morphotype appears to represent a new genus of non-marine bivalves and requires special taxonomic investigation and description.

Plant remains from the Kedrovka and Ryaboy Kamen Members [22] include *Lobatannularia* sp., *Todites* sp., *Cladophlebis mutnaensis* Vlad., *Katasiopteris polymorpha* Mogutch., *Kchonomakidium srebrodolskae* Schved., *Quadrocladus*? *sibiricus* (Neub.) S. Meyen, *Elatocladus* typ. *pachyphyllus* Pryn. and confidently date this interval to Late Induan-Early Olenekian [7], [12].

This age is supported by data on conchostracans, which include *Pseudestheria novacastrensis* (Mitchell), *Cornia papillaria* Lutkevich, *Megasitum harmonicum* Novojilov, *M. lopokolense* Nov., *Concherisma tomensis* Nov., *Echinolimnadia mattoxi* Nov. (Lutheria (Lutk.) [23], [24].

The data on bivalves do not contradict this dating.

Conclusions

Representatives of the Triassic genus *Utschamiella* are characteristic of the upper beds of the Maltsevo Formation (Kedrovka Member). The microstructural characters of *Utschamiella* confidently distinguish this genus from the externally similar morphotypes of *Palaeomutela*.

The subcircular morphotype occurring with *Utschamiella* appears to represent a new genus of non-marine bivalves and requires proper taxonomic study.

Acknowledgments

The work is performed according to the Russian Government Program of Competitive Growth of Kazan Federal University and by the subsidy allocated to Kazan Federal University for the state assignment # 671-2020-0049 in the sphere of scientific activities.

The collection of non-marine bivalves has been obtained during field work with the support of the Russian Science Foundation grant No. 19-17-00178.

REFERENCES

1. Ragozin, L. A. (1937). O nekotorykh peletsipodakh iz uglenosnoy tolshchi Tungusskogo basseyna. Trudy Tomskogo gosudarstvennogo universiteta 93, pp. 127-146.
2. Amalitzky, V. P. (1892), Über die Anthracosien der Permformation Russlands, Palaeontographica 39 (4-6), pp. 125-214.
3. Ragozin, L. A. (1958). Plastinchatozhabernyye mollyuski iz triasovykh otlozheniya Angaridy. Byulleten' Moskovskogo obschestva ispytatelei prirody. Otdel geologii 33 (1), pp. 79-90.
4. Lebedev I. V. (1962). Fauna peletsipod triasa Sibiri. Biostratirrafiya mezozoyskikh i tretichnykh otlozheniy Zapadnoy Sibiri. Gostoptekhizdat, Leningrad, pp. 15-18.
5. Amalitzky, V. P. (1895). A comparison of the Permian freshwater Lamellibranchiata from Russia with those from the Karroo System of South Africa, Quarterly journal of the Geological Society of London 51 (1-4), pp. 337-351.
6. Budnikov, I. V. (Ed.). (1996). Kuzbass – a key region for the Upper Paleozoic stratigraphy in Angarida. Intergeo, Novosibirsk, 122.
7. Kazakov A. M., Konstantinov A. G., Kurushin N. I. *et al*. (2002). Stratigraphy of oil and gas basins of Siberia. Triassic System. Publ. house SB RAS, Department "GEO", Novosibirsk, 322.
8. Buslov, M. M., Safonova, I. Y., Fedoseev, G. S., Reichow, M. K., Davies, K., Babin, G. A. (2010). Permo-Triassic plume magmatism of the Kuznetsk Basin, Central Asia: Geology, geochronology, and geochemistry. Russian Geology and Geophysics 51 (9), pp. 1021-1036. https://doi.org/10.1016/j.rgg.2010.08.010
9. Vladimirovich, V. P. (1967). Biostratigraphy of Triassic and Jurassic continental deposits of eastern slope of the Urals, northern Kazakhstan and mountain part of western Siberia. Stratigraphy and paleontology

of Mesozoic and Paleogene–Neogene continental deposits of the Asiatic part of the USSR, (G.G. Martinson, ed.). Leningrad. Nauka pp. 46-55.
10. Dobruskina I. A. (1994). Triassic Floras of Eurasia Schriftenreihe der Erdwissenschaftlichen Kommission (H. Zapfe ed.). Band 10. Osterreichische Akademie der Wissenschaften, Springer, Wien, 422.
11. Mogutcheva, N. K., Krugovykh, V. (2009). New data on the stratigraphic chart for Triassic deposits in the Tunguska syneclise and Kuznetsk basin. Stratigraphy and Geological Correlation 17 (5), pp. 510-518.
12. Mogucheva, N. K. (2016). Flora from the Induan stage (Lower Triassic) of Middle Siberia. Stratigraphy and Geological Correlation 24 (3), pp. 252-266. https://doi.org/10.1134/S0869593816020052
13. Silantiev V. V. (2014). Permian nonmarine bivalve zonation of the East European Platform. Stratigraphy and geological correlation 22 (1), pp. 1-27.
14. Silantiev, V. V. Urazaeva, M. N. (2013). Shell microstructure in the Permian nonmarine bivalve Palaeomutela Amalitzky: Revision of the generic diagnosis. Paleontological Journal 47 (2), pp. 139-146.
15. Silantiev, V. V. Carter, J. G. (2011). On changes in taxonomy nonmarine bivalves of the Late Paleozoic in the new edition of the “Treatise on Invertebrate Paleontology”, Byulleten’ Moskovskogo obschestva ispytatelei prirody. Otdel geologii 86 (1), pp. 14-17.
16. Silantiev, V. V. Carter, J. (2015). The Permian nonmarine bivalve Palaeanodonta Amalitzky, 1895: Position in the modern Bivalvia system, Paleontological Journal 49 (10), pp. 1125-1141.
17. Ragozin L. A. (1956). Triasovyye i yurskiye peletsipody iz uglenosnykh otlozheniy Angarskogo materika. Trudy Tomskogo gosudarstvennogo universitet 135, pp. 117-120.
18. Tschernyschev B. I. (1934). O nekotorykh Branchiopoda iz Kuznetskogo basseyna. Trudy Leningradskogo obsxhestva ectectvoispytatelei 63 (2), pp. 115-125.
19. Tschernyschev B. I. (1937). O nekotorykh yurskikh plastinchatozhabernykh iz Fergany. Trudy Sredneaziatskogo geologicheskogo tresta 1, pp. 1-34.
20. Lutkevitch, E. M., Nalivkin, B. V., Pchelintseva, G. T., Saveliev, A. A., Eberzin, A. G. (1960). Otryad Schizodonta. Rasscsheplennozubye. Osnovy paleontologii Tom 3. Mollyuski – pantsirnyye, dvustvorchatyye, lopatonogiye, pp. 93-101.
21. Bieler, R., Carter J. G., Coan E. V. (2010). Classification of Bivalve Families. Nomenclator of Bivalve Families. Malacologia 52 (2), pp. 113-133.
22. Lebedev I. V. (1944). O nekotorykh plastinchatozhabernykh iz kol’chuginskoy svity Kuzbassa. Izvestiya Akademii nauk SSSR. Seriya Biologiya 2, pp. 78-88.
23. Betekhtina O. A., Mogucheva N. K., Batyayeva S. K., Kushnarev M. P. (1986). Granitsa permi i triasa v stratotipe mal’tsevskoy svity Kuzbassa. Biostratigrafiya mezozoya Sibiri i Dal’nego Vostoka. Nauka, Novosibirsk, pp. 31-38.
24. Davydov, V. I., Zharinova, V. V., Silantiev, V. V. (2019). Late Permian and Early Triassic conchostracans from the Babii Kamen section (Kuznetsk coal basin). Uchenye Zapiski Kazanskogo Universiteta 161 (2), pp. 339-347. doi: 10.26907/2542-064X.2019.2.339-347.
25. Sabirova, E. F., Zharinova, V. V., Scholze F., Shneider J. W. (2019). Microsculpture study of Late Permian and Early Triassic conchostracans from the Babii Kamen section (Western Siberia). Uchenye Zapiski Kazanskogo Universiteta 161 (2), pp. 348-357.

Geochemical Types of Archean Banded Iron Formations and the Geodynamic Settings of the Basins, Kostomuksha Greenstone Belt, Karelian Craton, Russia

SLABUNOV Alexander[1], EGOROV Alexander[1], NESTEROVA Natalia[1]

[1] Institute of Geology, Karelian Research Centre, Russian Academy of Sciences, Petrozavodsk (RUSSIA)
Email: slabunov@krc.karelia.ru

Abstract

Two Archean lithostratigraphic associations with BIFs (banded iron formations) in the Kostomuksha Greenstone Belt, Karelian Craton, Russia, are described in the article. These two types of BIFs differ considerably in chemical composition: BIF-I contains higher average SiO_2, MgO, MnO and Sc, while BIF-II is substantially enriched in Al_2O_3, TiO_2, Na_2O, K_2O, Li, Rb, Ba, Sr, V, Zr, Th, U and REE. Also, they differ markedly in normalized REE distribution pattern: BIF-II displays more differentiated pattern. There are HREE-depleted varieties of BIF-I, but both types exhibit a positive Eu anomaly. Such significant differences in the chemical composition of BIFs can be explained by different sedimentation conditions in the basins. It can be assumed that BIF-I was formed in the fore-arc basin of Mesoarchean island-arc system. The basin, in which BIF-II formed seems to have been a back-arc basin of the Neoarchean system.

Keywords: Banded iron formations, Archean, Kostomuksha Greenstone Belt, geochemistry, geodynamic settings

Introduction

The Karelian Archean Craton (Fig. 1a) is a classical structure of this type. It consists predominantly of Archean granitoids, mainly tonalite-trondhjemite-granodiorites (TTG) and greenstone complexes. The latter commonly occur as associations of volcanic and sedimentary (BIFs, etc.) rocks, metamorphosed in greenschist and amphibolite facies.

The Kostomuksha Greenstone Belt (Fig. 1b) is situated in the western part of the Karelian Craton. It is a relatively small (25 km – length; 4.5-7 km – width) structure with the region's biggest iron deposit (1.3 billion tons), associated with banded iron formations.

According to the regional stratigraphic scale [7], Kostomuksha Greenstone Belt (KoGB) falls into two lithostratigraphic associations: Kontokki and Gimoly, consisting of metamorphosed volcanics and sedimentary rocks, respectively.

The Kontokki group consists of:

1) basaltic-komatiitic complex with interbeds of sedimentary and volcanic-sedimentary rocks. The complex is divided into the Niemijarvi and Ruvinvaara Formations. These volcanics are dated Mesoarchean (2.84-2.79 Ga) [2], [3], [4];

2) A tuff, tuffite of the rhyolite – rhyodacite (seldom to andesite) complex with BIF and carbonaceous shale interbeds that belong to the Shurlovaara Formation. The U-Pb isotope age of felsic volcanics is estimated at 2.8-2.79 Ga [2], [3], [10]. In this paper the BIF of this formation is understood to be BIF-I (Table).

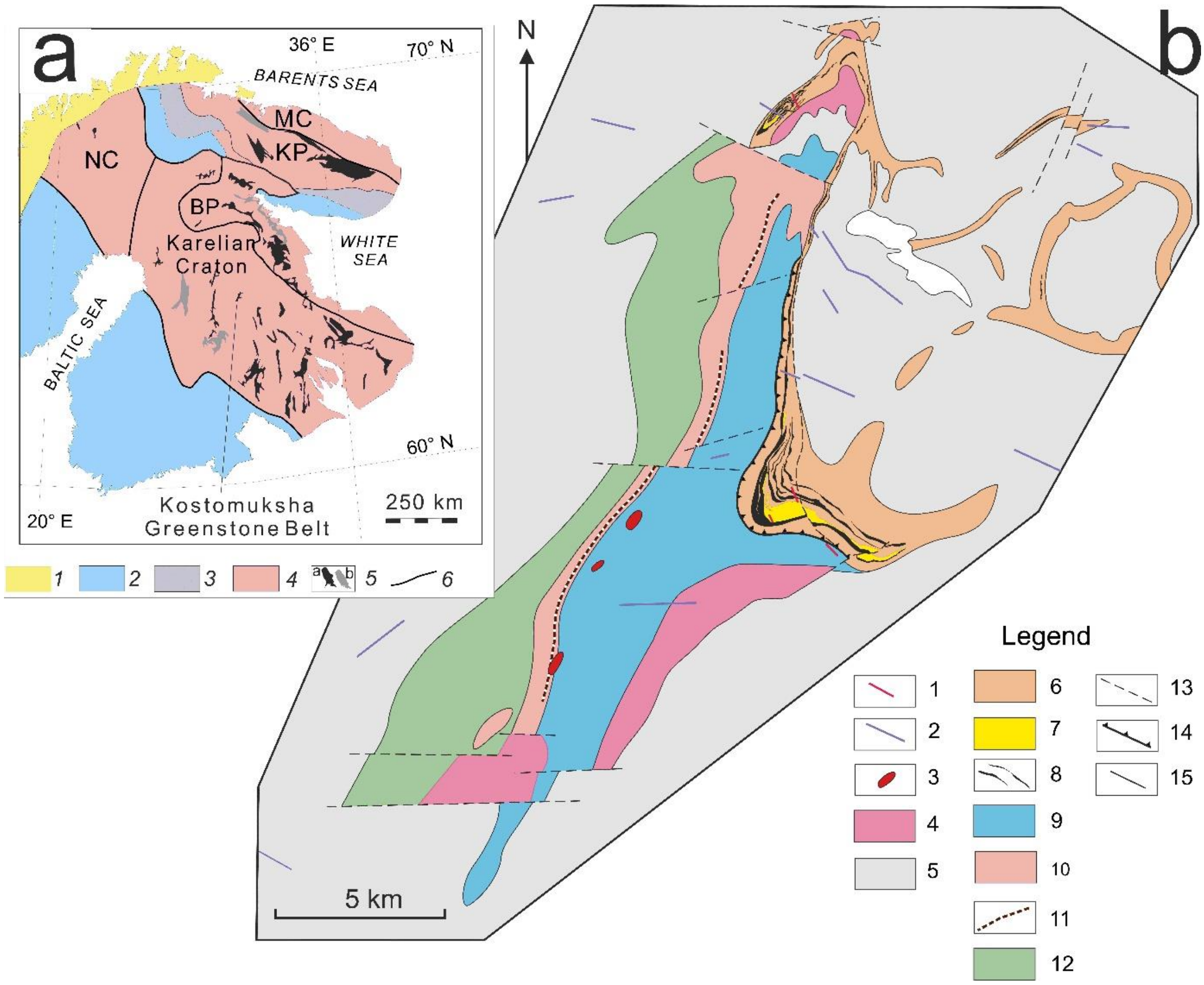

Fig. 1. (a) Location of the Kostomuksha Greenstone Belt in the Fennoscandian Shield [5], [6].
1 – Caledonids, Baikalids and Neoproterozoic rocks; 2, 3 – Paleoproterozoic Earth crust: 2 - juvenile; 3 – with fragments of Archean crust; 4 – Archean Earth crust (NC – Norrbotten Craton; BP – Belomorian Province, KP – Kola Province, MC – Murmansk Craton); 5 – Archean greenstone (a) and paragneiss (b) belts; 6 – Paleoproterozoic boundaries of provinces.
(b) Geological scheme of the Kostomuksha Greenstone Belt. Compiled by the authors using personal observations and [4], [7], [8], [9], [12].
1 – Neoproterozoic (Riphean) lamproites and kimberlites; 2 – Paleoproterozoic (2.4 Ga) dolerites; 3-8 Neoarchean: 3 – 2.7 Ga sanukitoids; 4 – (2.72-2.71 Ga) granites; 5 – 2.78 Ga TTG granitoids; 6-8 – Gimoly Group rocks: 6 – 2.75 Ga metagraywackes; 7 – 2.75 Ga rhyolite sills and dikes (halleflinta); 8 – BIF-II; 9-12 – Mesoarchean (2.84-2.78 Ga) Kontokki Group: 9 – basalts and basalt-komatiites (Ruvinvaara Formation); 10-11 – Shurlovaara Formation: 10 – tuffs, tuffites, rhyolite-rhyodacites; 11 – BIF-I and carbonaceous shales; 12 – basalts and komatiites (Niemijarvi Formation); 13 – faults; 14 – overthrust; 15 – boundaries between formations

Gimoly Group makes up the eastern flank of the greenstone belt and consists of flysch-type metamorphosed psammite-argillitic sediments [11]. The base of the rock sequence contains conglomerates. The lower portion of the sequence carries an abundance of ferruginous quartzites that occurs among schists (metagraywacke) and are identified as BIF-II. The upper portion is dominated by ore-free schists. The replace with BIF unit contains sills and is cut by metarhyolite (halleflinta) dikes that have a U-Pb isotopic age of 2.76-2.74 Ga [12]. The BIF unit is cut by Neoarchean (2707±31, 2675±9 Ma) [3] granite-porphyries and granites (Shurlovaara Massif), respectively.

The aim of the present paper is to discuss the geochemical characteristics of two different-aged types of BIF revealed in the Kostomuksha Greenstone Belt.

Results and Discussion

Table. Average chemical composition BIF-I, II KoGB (Major elements in wt%; trace - in ppm)

	BIF-I	BIF-II
n	*10*	*27*
SiO_2	49.41	47.00
TiO_2	0.09	0.16
Al_2O_3	1.38	2.09
Fe_2O_3	24.73	26.32
FeO	18.83	17.72
MnO	0.12	0.05
MgO	1.87	1.68
CaO	1.43	1.75
Na_2O	0.11	0.41
K_2O	0.06	0.87
P_2O_5	0.23	0.26
H_2O	0.19	0.11
LOI	1.17	1.27
Sc	12.73	5.90
V	9.40	25.03
Cr	25.63	28.98
Co	2.18	2.50
Ni	19.97	20.58
Rb	0.75	54.49
Sr	14.70	58.92
Ba	31.96	118.28
Y	6.69	7.83
Zr	8.50	15.21
Nb	0.52	0.82
La	3.07	5.24
Ce	6.40	10.79
Pr	0.72	1.31
Nd	3.00	5.35
Sm	0.67	1.07
Eu	0.30	0.53
Gd	0.82	1.16
Tb	0.13	0.18
Dy	0.89	1.10
Ho	0.21	0.25
Er	0.64	0.77
Tm	0.10	0.12
Yb	0.67	0.80
Lu	0.11	0.13
Th	0.47	0.89
U	0.13	0.25

The chemical composition of the rocks was determined by gravimetric-photometric (major elements) and ICP-MS (minor elements) methods at the Testing and Matter Analysis Centre, Institute of Geology, KarRC, RAS, Petrozavodsk, Russia.

These two types of BIF differ considerably in chemical composition: BIF-I contains higher average SiO_2, MgO, MnO and Sc, while BIF-II is substantially enriched in Al_2O_3, TiO_2, Na_2O, K_2O, Li, Rb, Ba, Sr, V, Zr, Th, U and REE (Table; Fig. 2, 3). The variation trends of element concentrations on binary FeO_t-SiO_2, MgO diagrams are fairly similar, while in FeO_t-Al_2O_3, TiO_2, MnO, Na_2O, K_2O, Sc, V are differents (Fig. 2). The BIF-II type is substantially enriched in K, Li, Rb, Ba, Sr, V, Zr, Th, U and REE concerning BIF-I (Fig. 3). Also, BIF-I and II differ markedly in normalized REE distribution pattern: BIF-II displays a more differentiated pattern (Fig. 3). There are HREE-depleted varieties of BIF-I and of most part of BIF-II (Fig. 3), both types exhibit a positive Eu anomaly (Eu/Eu^*-1.11-1.89) typical of Archean sedimentary rocks.

Such significant differences in the chemical composition of the two types can be explained by differences in depositional conditions in the basins. The basin in which BIF-I was formed was similar to a fore-arc basin in Mesoarchean island-arc system. Felsic volcanics in this system occur as relics of the volcanic island-arcs, while basaltic-komatiitic rocks are relics of the basement of this system. Fe, Si and other elements, including Sc, seem to have been supplied into the basin mainly by hydrothermal processes associated with island-arc magmatism.

The basin in which BIF-II was formed, differed from BIF-I not only in age but also in a sedimentation setting: it was supplied with clasts that made up an ore-hosting psammite-argillitic greywacke sequence.

Sedimentation was also accompanied by felsic magmatism of an island-arc type. BIFs were formed only in periods when lesser quantities of clasts were supplied but hydrothermal activity remained. The basin discussed seems to have been a back-arc basin in a Neoarchean island-arc system.

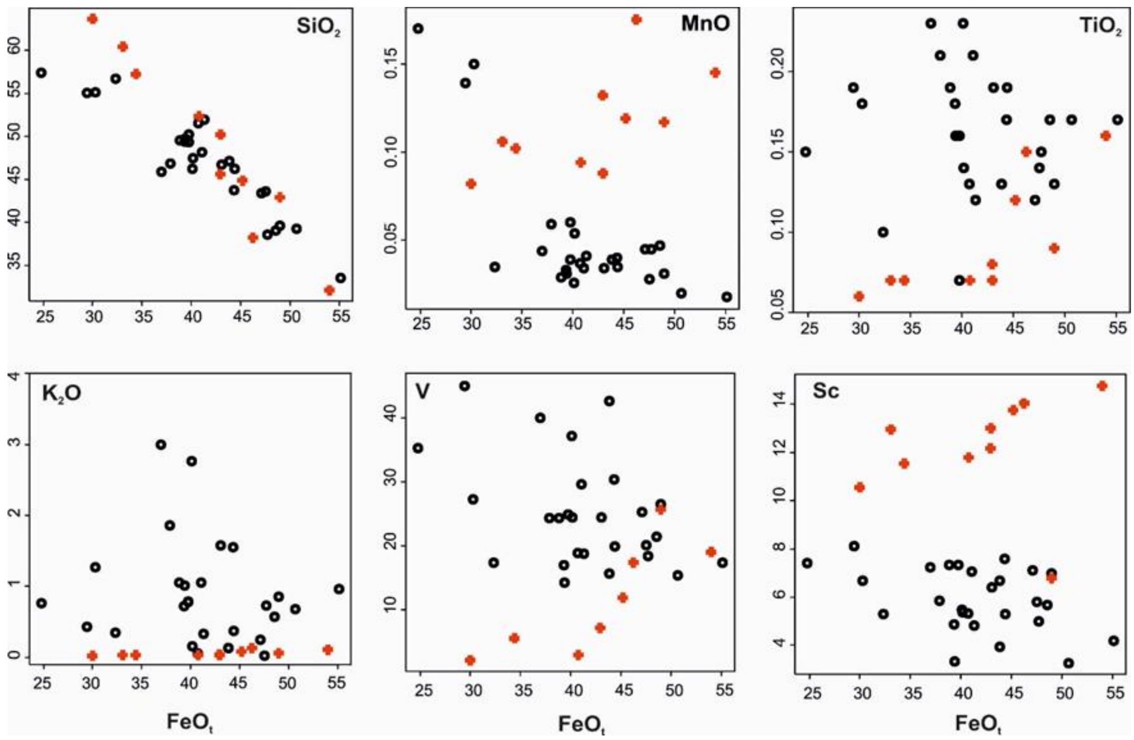

Fig. 2. Variations in the composition of BIF-I (red crosses), BIF-II (black circles) from KoGB on the FeO_t-oxides, V and Sc diagrams

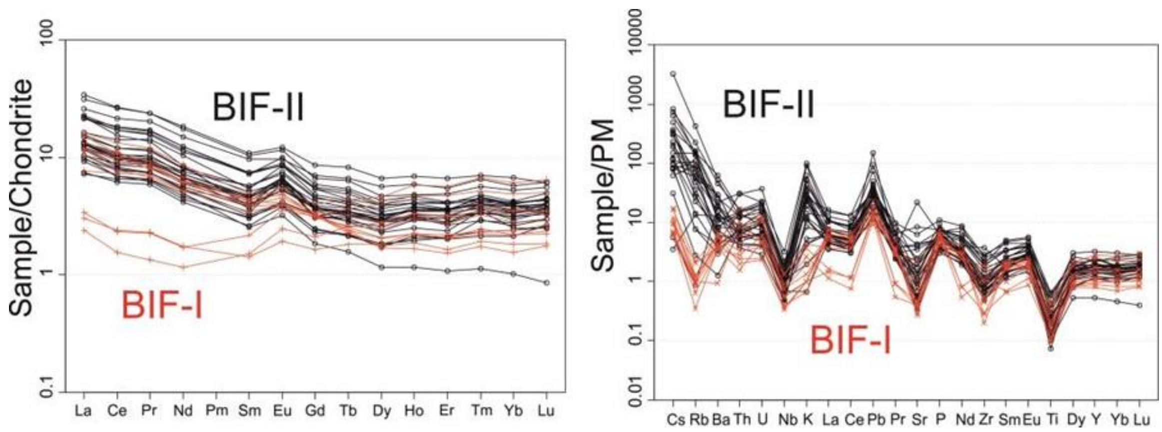

Fig 3. Chondrite-normalized (Nakamura, 1974) and Primitive Mantle-normalized (Sun & McDonough 1989) patterns elements in BIF-I (red crosses) and BIF-II (black circles) from KoGB

Conclusions

1. 2.8 Ga BIF-I (Shurlovaara Formation, Kontokki Group) is associated with felsic volcanics and occurs among basalt-komatiites, and 2.75 Ga BIF-II (Kostomuksha Formation, Gimoly Group) is closely related to metagraywackes and associated metarhyolite sills.
2. BIF-I and BIF-II display essential geochemical differences: BIF-I contains higher average SiO_2, MgO, MnO and Sc, while the BIF-II is substantially enriched in Al_2O_3, TiO_2, Na_2O, K_2O, Li, Rb, Ba, Sr, V, Zr, Th, U and REE. The formations differ because two types of BIFs formed in island-arc systems but in basins of various types: BIF-II – in a fore-arc basin, and BIF-I in a back-arc basin.

Acknowledgments

This work is a contribution to research projects of the Karelian Research Center, RAS A18-118020290085.

REFERENCES

1. Bekker, A., Slack, J. F. Planavsky, N., Krapez, B., Hofmann, A., Konhauser, K. O., Rouxel, O. J. (2010). Iron Formation: The sedimentary product of a complex interplay among mantle, tectonic, oceanic, and biospheric. Economic Geology 105, pp. 467-508.
2. Puchtel, I. S., Hofmann, A. W., Mezger, K., Jochuma, K. P., Shchipansky, A. A., Samsonov, A. V. (1998) Oceanic plateau model for continental crustal growth in the Archaean: a case study from the Kostomuksha greenstone belt, NW Baltic Shield. Earth Planet. Sci. Lett. 155, pp. 57-74.
3. Lobach-Zhuchenko, S. B., Arestova, N. A., Mil'kevich, R. I., Levchenkov, O. A., Sergeev, S. A. (2000). Stratigraphy of the Kostomuksha Belt in Karelia (Upper Archean) as Inferred from Geochronological, Geochemical and Isotopic Data. Stratigraphy and Geol. Correlation 8 (4), pp. 319-326.
4. Kozhevnikov, V. N., Berezhnaya, N. G., Presnyakov, S. L., Lepekhina, E. N., Antonov, A. V., Sergeev, S. A. (2006). Geochronology (SHRIMP II) of Zircons from Archean Stratotectonic Associations of Karelian Greenstone Belts: Significance for Stratigraphic and Geodynamic Reconstructions. Stratigraphy and Geol. Correlation 14 (3), pp. 240-259.
5. Kulikov, V. S., Svetov, S. A., Slabunov, A. I., Kulikova, V. V., Polin, A. K., Golubev, A. I., Gorkovets, V. Ya., Ivashchenko, V. I., Gogolev, M. A. (2017). Geological map of South-eastern Fennoscandia (scale 1:750 000): a new approach to map compilation. Transactions of the Karelian Research Centre of the RAS 2, pp. 3-41.
6. Slabunov, A. I., Lobach-Zhuchenko, S. B., Bibikova, E. V., Balagansky V. V., Sorjonen-Ward P., Volodichev O. I., Shchipansky A. A., Svetov S. A., Chekulaev V. P., Arestova N. A., Stepanov V. S. (2006). The Archean of the Baltic Shield: Geology, Geochronology, and Geodynamic settings. Geotectonics 40 (6), pp. 409-433
7. Gor'kovets, V. Ya., Raevskaya, M. B., Belousov, E. F., Inina, K. A. (1981). Geologiia i metallogeniia raiona Kostomukshskogo zhelezorudnogo mestorozhdeniia Petrozavodsk, Karelia. 143.

8. Kozhevnikov, V. N. (1982). Usloviia formirovaniia strukturno-metamorficheskikh paragenezisov v dokembriiskikh kompleksakh. Nauka, Leningrad, 184.
9. Kuleshevich, L. V., Furman, V. N. (2009). Zolotorudnoe mestorozhdenie Taloveis v Kostomukshskoi dokembriiskoi zelenokamennoi strukture Karelia. Geologiya rudnykh mestorozhdeniy 51(1), pp. 58-76.
10. Bibikova, E. V., Samsonov, A. V., Petrova, A. Yu., Kirnozova, T. I. (2005). The Archean Geochronology of Western Karelia. Stratigraphy and Geol. Correlation 13 (5), pp. 459-475.
11. Mil’kevich, R. I., Myskova, T. A. (1998). Late Archean Metaterrigenous rocks of the Western Karelia: Lithology, Geochemistry and Provenances). Lithology and Mineral Res. 33 (2), pp. 155-171.
12. Slabunov A.I., Nesterova N.S., Egorov A.V., Kuleshevich L.V., Kevlich V.I. (2021). Formation age of an Archean Iron Ore-hosted sequence in the Kostomuksha Greenstone Belt, Karelian Craton, Fennoscandian Shield: constraints on the geochemistry and geochronology of zircons. Geochemistry Int. (4)

Stratigraphy and Paleogeographic Formation Conditions of Black Shale Deposits in the Aramil-Sukhtelya Zone (South Urals)

SNACHEV Alexander[1], SNACHEV Vladimir[1]

[1] *Institute of Geology-Subdivision of the Ufa Federal Research Centre of the Russian Academy of Sciences (RUSSIA)*
Email: SAVant@rambler.ru

Abstract

This paper briefly describes the stratigraphy, mineralogy and petrography of black shale deposits in the Bulatovo Series (S_1-D_1bl) well developed in the central and northern parts of the Aramil-Sukhtelya zone of the South Urals. It is shown that the rocks of which it is formed relate to low-carbonaceous and carbonaceous types and belong to the siliceous-carbonaceous formation. Maximum C_{org} concentrations (3.0-7.8%) in the deposits are confined to the north-western flank of the structure-formational zone under investigation, and carbon they contain is of a biogenic nature. The paleogeographic depositional environment of the rocks in the Bulatovo Series was generally in conformity with the actively-bent distal part of the water basin. The western portions of the central and northern areas were the deepest within its limits, where there were reducing conditions with a minimum amount of terrigenous admixture. It is precisely this part of the Aramil-Sukhtelya zone composed of black shale rocks with high C_{org} concentrations that evokes the greatest interest for shale-gas and oil production.

Keywords: Southern Urals Aramil-Sukhtelya zone, black shales, Bulatovo Series

Introduction

In recent decades, carbonaceous deposits have been attracting growing interest all over the world. This is associated with the significant fact that they provide highly informative material for reconstructing paleogeographic physicochemical conditions of sedimentary deposition, represent a favourable geochemical environment where noble and rare metals might accumulate [1], [2], [3] and also serve as source rocks for shale-gas and oil production [4], [5], [6]. In this case the estimation of the carbon potential on one or another site is based on C_{org} analysis in black shale units. In this respect, the Bulatovo Series (S_1-D_1bl) is an ideal object for study within the fold area of the South Urals as they are well developed in the central and northern parts of the Aramil-Sukhtelya zone and possess considerable thickness and maximum C_{org} concentrations.

The authors have obtained the materials used in the paper in collaboration with staff members of the "Chelyabinskgeolsyemka" Open Joint-Stock Company during the 1:200,000 scale geological mapping works (sheets: N-41-I, Kyshtym; N-41-VII, Miass and N-41-XIII, Plast).

Geological Setting

The Bulatovo Series was named after the village of Bulatovo where it was thoroughly described and paleontologically characterized [7]. It is mapped as submeridionally oriented stripes bordered by faults that lie in parallel with major tectonic dislocations. In some places the boundaries are traced by serpentinite bodies (Fig. 1). The series is uniform in composition and consists of carbonaceous-siliceous, carbonaceous-clayey-siliceous, and siliceous shales.

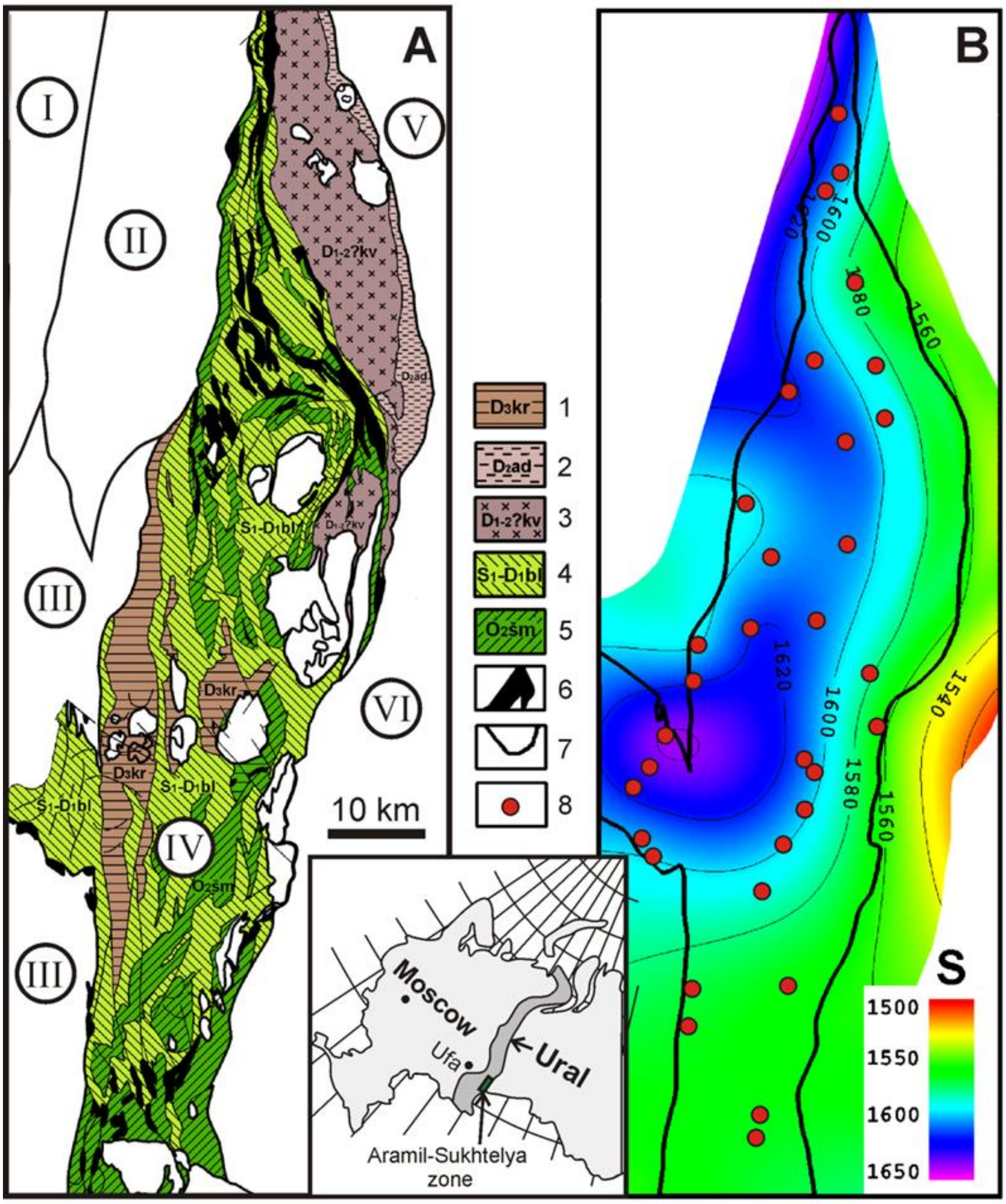

Fig. 1. Geological map of the Aramil-Sukhtelya zone. Compiled by the authors based on materials: V.I. Petrov, A.V. Moiseev A.V. Tevelev *et al*. (**A**). The distribution of the parameter S [11] within it (**B**).
Legend: 1 – Krasnokamensk Series (trachybasalts and their tuffs); 2 – Ajatar Series (basalts, andesibasalts); 3 – Kuluyev Series (basalts, andesibasalts); 4 – Bulatov Series (carbonaceous shales); 5 – Shemetov Series (basalts); 6 – hyperbasite massifs; 7 – contours of intrusive massifs; 8 – analysis points to build. The zones are shown in Roman numerals on the diagram: I – Voznesensko-Prisakmar, II – Sysert-Ilmenogorsk, III – Uysko-Novoorenburg, IV – Aramil-Sukhtelya, V – Kasargino-Reftinsk; VI – Kochkar-Adamovsk

The shales are predominantly composed of quartz (90-95%). Carbonaceous (graphite-like) substance makes up 1 to 8%. Sericite and biotite are present in insignificant amounts. The size of the quartz grains varies between 0.001 and 0.08 mm. They are usually isometric and have irregular-shaped edges. Carbonaceous material is dispersed uniformly and is often so abundant that it makes the rock absolutely non-transparent. Sericite (biotite) is either evenly distributed over the rock or located in the form of thin layers. Its flakes are oriented along cleavage planes.

Very often the shales contain oval-shaped relics of radiolarian fossils. They are replaced by coarser grained quartz as compared to the primary tissue. In the event that carbonaceous substance is preserved, it follows the contours of radiolarian shells. The rocks usually contain dispersed pyrite, pyrrotine and magnetite. Accessory minerals are represented by rutile, sphene, apatite, zircon and rarely turmaline. Areas near the villages of Novokumlyak, Polovinki and Nikolskoe are known for phosphorite fragments and lenses.

The lower boundary of the Bulatovo Series has been studied in detail. In conformity with interbedding, black shale deposits overlie the volcano-sedimentary succession of the Shemetovo Series (O_2sm). According to the data of recent geological mapping works its upper boundary is tectonic, and the thickness reaches 800-900 m.

The age of the strata is determined on the basis of numerous radiolaria found by B.M. Sadrislamov and graptolites found by Plyusnin [7] near the village of Bulatovo. They include *Stomatograptus grandis* (Suess.), *Pristiograptus sp. indet., Monograptus ex gr. priodon* (Bronn.), *Monoclimacis linnarsoni* (Tullberg), *M.* aff. *vomerina* (Nicholson), *M. crenulata* (Torqv.), *Spirograptus spiralis* (Gienits), *Oktavites spiralis* (Gienits). According to T.N. Koren who identified the graptolite species, they date the beds as the Late Llandovery-Wenlock boundary beds. In the black shale deposits westward of the village of Mirnyi, V.N. Puckov and K.S. Ivanov [8] found Late Silurian conodonts *Ozarkodina* aff. *ziegleri* Wall. and others, and Lower Devonian graptolites and conodonts within the other block. Thus, judging from the available fossils the age of the studied deposits covers the interval from Early Silurian to the Early Devonian.

Results and Discussion

Below the reconstructed paleogeographic conditions of the carbonaceous shale sedimentation in the Bulatovo Series and its C_{org} concentrations are considered. For this purpose, silicate analysis of 113 samples that evenly covered the central and northern parts of the Aramil-Sukhtelya zone (Fig. 1) was performed in the Institute of Geology, Ufa Federal Research Centre, Russian Academy of Sciences (Ufa, analyst S.A. Yagudina) and also chemical analysis of 34 samples for C_{org} was done in the Analytical Certificate Testing Centre, N.M. Fedorovsky All-Russian Institute of Mineral Raw Materials (Moscow, head of the Institute S.V. Kordyukov).

The composition of black shale deposits is homogenous: rock-forming minerals are silica (85 to 98%, the average of 113 samples is 93.5%) and C_{org} (1.1 to 7.8%), the sum of other oxides is within the range of 2-10%. According to the classification put forward by Yudovich and Ketris [9], rocks of the Bulatovo Series are of either low-carbonaceous (1-3%) or carbonaceous (3-10%) types. It is notable that, first, maximum C_{org} concentrations are confined to the north-western flank of the Aramil-Sukhtelya zone (the deepest one as will be shown below) and, second, C_{org} makes up almost 100% of carbon in the rock, while CO_2 accounts for 0.3-0.9% (5 samples) at best and the rest (29 samples) have less than 0.1%.

Investigations of the carbon isotopic composition appeared to be useful as well. The analyses were carried out in the Institute of Geology, Komi Scientific Centre, Ural Branch, Russian Academy of Sciences, at the “Geonauka” Centre for Collective Use (Syktyvkar, analyst I.V. Smoleva) using a Delta V Advantage mass-spectrometer in combination with an elemental analyzer Flash EA. It was found out that in black shales of the Bulatovo Strata the isotopic carbon composition $\delta^{13}C_{PDB}$ (‰) falls into the range of (–22.6) – (–28.7) (the average of 20 determinations is –25.9), which indicates its biogenic nature [10].

The ***diagram A-S-C*** was used to determine the formation affiliation of the black shales under consideration [11] (Fig. 2). More than 95% of the results fall into the field of the siliceous-carbonaceous formation, suggesting homogeneity of their chemical composition over the whole area in question. The inverse correlation between the parameters A and S and also between C and S is indicative first of the bio-chemogenic and volcanogenic source of silica, but not its terrigenous supply and, second, of independent sources of silica and carbonate. The situation with the clear-cut shortage of CaO and excess of SiO_2 is typical of all subsiding distal regions of basins.

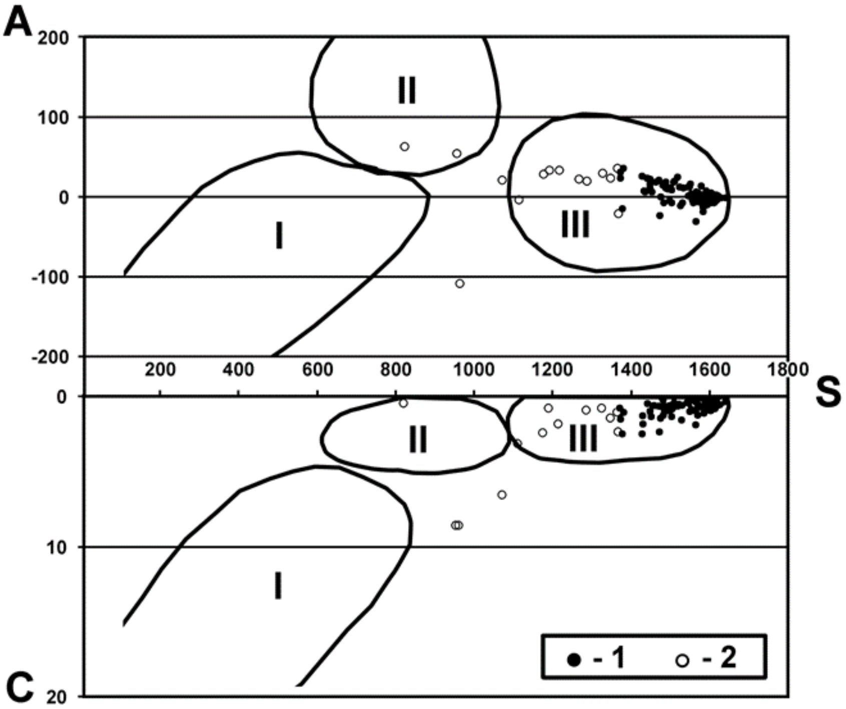

Fig. 2. Typification of carbonaceous schists of the Aramil-Sukhtelya zone using Gorbachev and Sozinova's diagram [11].
Formation Fields: I – carbonate-carbonaceous, II – terrigenous carbonaceous, III –silicon-carbonaceous. A = (Al_2O_3 – (CaO + K_2O + Na_2O)) × 1000, S = (SiO_2 – (Al_2O_3 + Fe_2O_3 + FeO + CaO + MgO)) ×1000 (expressed in molecular quantities); C = (CaO + MgO) – in mass fractions of oxides. 1 – carbonaceous-siliceous schists, 2 – carbonaceous-clay and carbonaceous-sericite schists

The most informative among these three parameters is parameter S related inversely to the fraction of the terrigenous admixture in the deposits, which, in turn, serves as a main indicator for the distance of the depositional region from the coastline [11]. Fig. 2 demonstrates that most points are located on the right-hand side of field III indicating the minimum concentration of the terrigenous admixture. However, the greatest interest lies not in the change of the parameter S westwards and southwards, but primarily in its absolute values, this enabling us to assess the fraction of the terrigenous admixture in the deposits of the Bulatovo Series over the whole area in question. Analysis of the material shows that the deposits on the eastern flank of the Aramil-Sukhtelya zone have minimum values of the parameter S (1499-1527 units) (Fig. 1B). In its axial and western parts, this parameter comprises, 1542-1588 and 1590-1650 units, respectively. This indicates the relative shallowness of the deposits along the eastern flank, their intermediate depth in the axial part of this structure and maximum depth values along the western flank.

The ***protoxide modulus*** (PM=FeO/Fe_2O_3) makes it possible to solve the issue regarding the conditions of deposition in the water basin (PM>1.0 for reduction and PM<0.1 for oxidation) [9]. About 91% of carbonaceous rocks in the Bulatovo Series have PM>1.0 (7.1 on the average).

This indicates sharply reducing conditions of their formation. Its highest values are observed in the central and northern parts of the western flank of the Aramil-Sukhtelya zone. Similar conclusions have also been drawn on the value of the ***titanium modulus*** (TM=TiO_2/Al_2O_3) [12], with minimal values typical for coastal deposits and the maximum ones for deep-water deposits. The ***Fe/Mn indicator*** is related inversely to the depth of the sedimentary basinRozen *et al*., [13] proposed the following gradation of sedimentary rocks depending on a decrease of this parameter: >160 – shallow-water and coastal, 40-160 – shallow-water, <40 – deep-water.

Within the Aramil-Sukhtelya zone, the value of this indicator gradually decreases northwards from 53 to 37 units and westwards from 46 to 32 units, correlating to increasing depth of the water basin.

Conclusions

The black shale of the Bulatovo Series (S_1-D_1bl) is well developed in the central and northern parts of the Aramil-Sukhtelya zone, has considerable thickness and is reliably dated by conodonts, radiolarians and graptolites. The rocks of which it is formed are of low-carbonaceous and carbonaceous types and belong to the siliceous-carbonaceous formation.

Maximum C_{org} concentrations (3.0-7.8%) in the deposits are recorded in the north-western flank of the structure-formational zone under study, and carbon they contain is of a biogenic nature. The paleogeographic depositional environment of the rocks in the Bulatovo Series was generally in conformity with the actively subsiding distal regions of the basin. The western portions of the central and northern areas were the deepest within its limits, where there were reducing conditions with a minimum amount of the terrigenous admixture. It is precisely this part of the Aramil-Suchtelya zone composed of black shale rocks with high C_{org} concentrations that evokes the greatest interest for shale-gas and oil production.

Acknowledgements

The authors express gratitude to analysts S.A. Yagudina, S.V. Kordyukov and I.V. Smoleva for investigations they carried out, and M.P. Maslova for helping to translate the manuscript.

The research has been performed under Government Contract no. 0246-2019-0078.

REFERENCES

1. Demin Yu. I., Snachev V. I. (1981). Thermal fields of the Akhunov massif and the regularities of the mineralization distribution in them. Doklady Akademii Nauk SSSR 261 (1), pp. 152-156.
2. Rykus M. V., Snachev V. I., Kuznetsov N. S., Savel'yev D. Ye., Bazhin Ye. A., Snachev A.V. (2009). Rudonosnost' dunit-gartsburgitovoy i chernoslantsevoy formytsiy pogranichnoy zony mezhdu Yuzhnym i Srednim Uralom. Neftegazovoye delo 7 (2), pp. 17-27.
3. Snachyov A. V., Kuznetsov N. S., Snachyov V. I. (2011). The Chernoe Ozero gold occurrence in carbonaceous deposits of the ophiolite association: The first object of such a type in the southern Urals. Doklady Earth Sciences 439 (1), pp. 906-908. DOI: 10.1134/S1028334X11060249
4. Kotarba M. J., Clayton J. L., Rice D. D., Wagner M. (2002) Assessment of hydrocarbon source rock potential of Polish bituminous coals and carbonaceous shales. Chemical Geology 184 (1), pp. 11-35 DOI: 10.1016/S0009-2541(01)00350-3
5. Lukin A. E. (2013) Chernoslantsevyye formatsii evksinskogo tipa – megalovushki prirodnogo gaza. Geologiya i poleznyye iskopayemyye Mirovogo okeana 4, pp. 5-28.
6. Pandey B., Pathak D. B., Mathur N., Jaitly A. K., Singh A. K., Singh P. K. (2018). A preliminary evaluation on the prospects of hydrocarbon potential in the carbonaceous shales of Spiti and Chikkim formations, Tethys Himalaya, India. Journal of Geological Society of India 92, pp. 427-434.
7. Plyusnin K. P., Plyusnina A. A., Zenkov I. I. (1965). Novyye dannyye o graptolitovykh slantsakh vostochnogo sklona Yuzhnogo Urala. Izvestiya AN SSSR. Seriya Geologiya 11, pp. 121-123.
8. Puchkov V. N., Ivanov K. S. (1989). K stratigrafii chernoslantsevykh tolshch na vostoke Urala. Yezhegodnik-1988 IGiG UFAN SSSR, Sverdlovsk, pp. 4-7.
9. Yudovich Ya. E., Ketris M. P. (2015) Geokhimiya chernykh slantsev. Moscow-Berlin, Direkt-Media, 272.
10. Van Kaam-Peters H. M. E., Schouten S., Koster J., Sinninghe Damste J. S. (1998). Controls on the molecular and carbon isotopic composition of organic matter deposited in a Kimmeridgian euxinic shelf sea: Evidence for preservation of carbohydrates through sulfurisation. Geochimica et Cosmochimica Acta 62, pp. 3259-3284. DOI: 10.1016/S0016-7037(98)00231-2

11. Gorbachov O. V., Sozinov N. A. (1985). Nekotoryye petrokhimicheskiye i geokhimicheskiye aspekty tipizatsii uglerodistykh otlozheniy dokembriya. Problemy osadochnoy geologii dokembriya. Nauka, Moscow, pp. 46-57.
12. Yefremova S. V., Stafeyev K. G. (1985) Petrokhimicheskiye metody issledovaniya gornykh porod. Moscow, Nedra, p. 512.
13. Rozen O. M., Zhuravlev D. Z., Lyapunov S. M. (1994). Geokhimicheskiye issledovaniya osadochnykh otlozheniy Timano-Pecherskoy provintsii. Razvedka i okhrana nedr 1, pp. 18-21.

Geochemical Data for the Upper Carboniferous Interval of the Usolka Section, Southern Urals, Russia

SUNGATULLIN Rafael[1], SUNGATULLINA Guzal[1], BUSLAEV Roman[1], GAREEV Bulat[1], BATALIN Georgii[1]

[1] *Kazan Federal University, Kazan (RUSSIA)*
Email: Rafael.Sungatullin@kpfu.ru

Abstract

The geochemical features of rocks from the Usolka section, which has been proposed as an international standard for global correlation of the lower boundaries of the Kasimovian and Gzhelian Stages, has been considered. The tectonic setting of the drift sources was corresponded to the passive continental margin. Based on the analysis of chemical weathering indices, it was shown that the climate in the Late Carboniferous was transitioning from humid to arid, with rocks being characterized by a low degree of chemical weathering.

Anomalously low values of stable isotopes that are not associated with diagenetic changes in the rocks were confirmed.

Keywords: Carboniferous, geochemistry, lithology, Usolka, Pre-Uralian Foredeep

Introduction

The Usolka section is located in the southern part of the Pre-Uralian Foredeep (Fig. 1) and is represented by continuous, thick, marine, mixed carbonate-siliciclastic deposits with a diverse conodont fauna. [1, 2, 3, 4, 5]. In the Usolka section, the absolute age of sediments has been determined [6], and it has been proposed to be the Global Stratotype Section and Point (GSSP) for the lower boundary of the Gzhelian Stage. [1, 7, 8]. The presented work is devoted to the geochemical characterization of the Upper Carboniferous sediments of the Usolka section, cleared in autumn 2019 to create the Toratau Geopark (Fig. 2). This allowed sampling for isotope studies, and for the determination of the chemical composition of the rocks. We conducted similar geochemical studies for the Lower Permian sections Dalniy Tulkas and Mechetlino [9, 10] – GSSP candidates, respectively, of the Artinskian and Kungurian Stages.

Methodology

To determine the macro- and microchemical composition of the rocks, an S8 Tiger X-ray fluorescence spectrometer (Bruker, Germany) and an inductively coupled plasma mass spectrometer iCAP Qc (Thermo Fisher Scientific, Germany) were used. The isotopic composition of carbon and oxygen was determined using a Delta V Plus isotope mass spectrometer (Thermo Fisher Scientific, Germany) with a Flash HT attachment in constant flow mode. All analyzes were performed in KFU laboratories. For the geochemical characterization of the Upper Carboniferous rocks of the Usolka section, the results of 75 X-ray fluorescence analyses, 22 ICP-MS analyses, and 46 isotope analyses, were used.

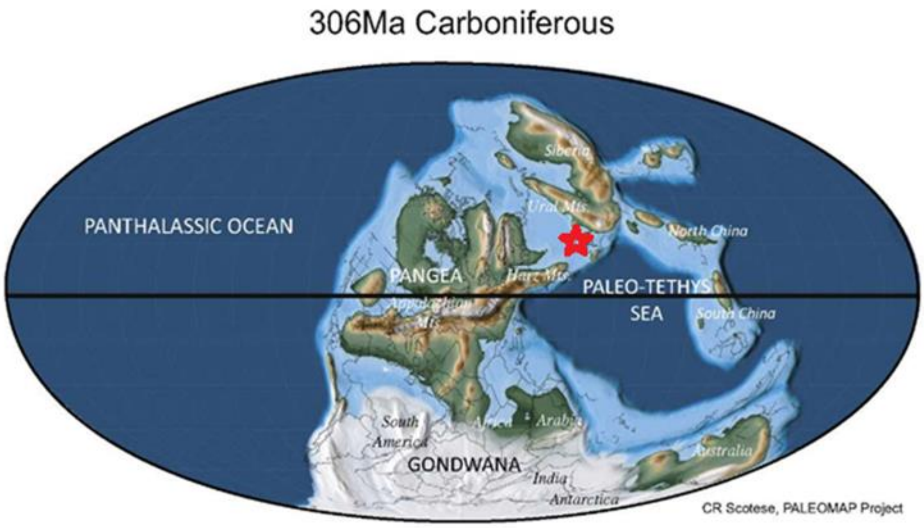

Fig. 1. Kasimovian paleogeographic reconstruction [6]. An asterisk indicates the location of the Usolka section

Results and Discussions

The section is represented by terrigenous-carbonate rocks of the flysch formation (Fig. 2): calcareous mudstones, limestones, dolomites, sandstones. There are thin (up to the first centimeters) layers of volcanic tuffs. Organogenic limestones contain crinoids, brachiopods, corals, foraminifera, gastropods, ammonoids, radiolarians (Fig. 3). At the boundary of the Kasimovian and Gzhelian Stages, phosphorite nodules occur.

Fig. 2. Upper Carboniferous deposits of the Usolka section

According to geochemical data, the tectonic position of the section in the Pennsylvanian is defined as a passive continental margin (Fig. 4). The climate during the formation of the Upper Carboniferous deposits was transitional from humid to arid (Fig. 5). Previously obtained geochemical data on sections of the Lower Permian [10] indicate at an aridification of the climate in the Pre-Uralian Foredeep, and are confirmed by the paleogeographic position of the Usolka section (Fig. 1). The paleo-environment in the Urals is characterized by indices of chemical weathering of rocks. Thus, an analysis of the coefficient $CIA=Al_2O_3/(Al_2O_3+CaO+Na_2O+K_2O) \times 100$ [11] indicates weak weathering of the rocks (Fig. 6). For most of the Kasimovian and Gzhelian mudstones, the CIA is 40-70 (average value ~ 63), while for volcanic ash it is 70-80 (average value 72.5).

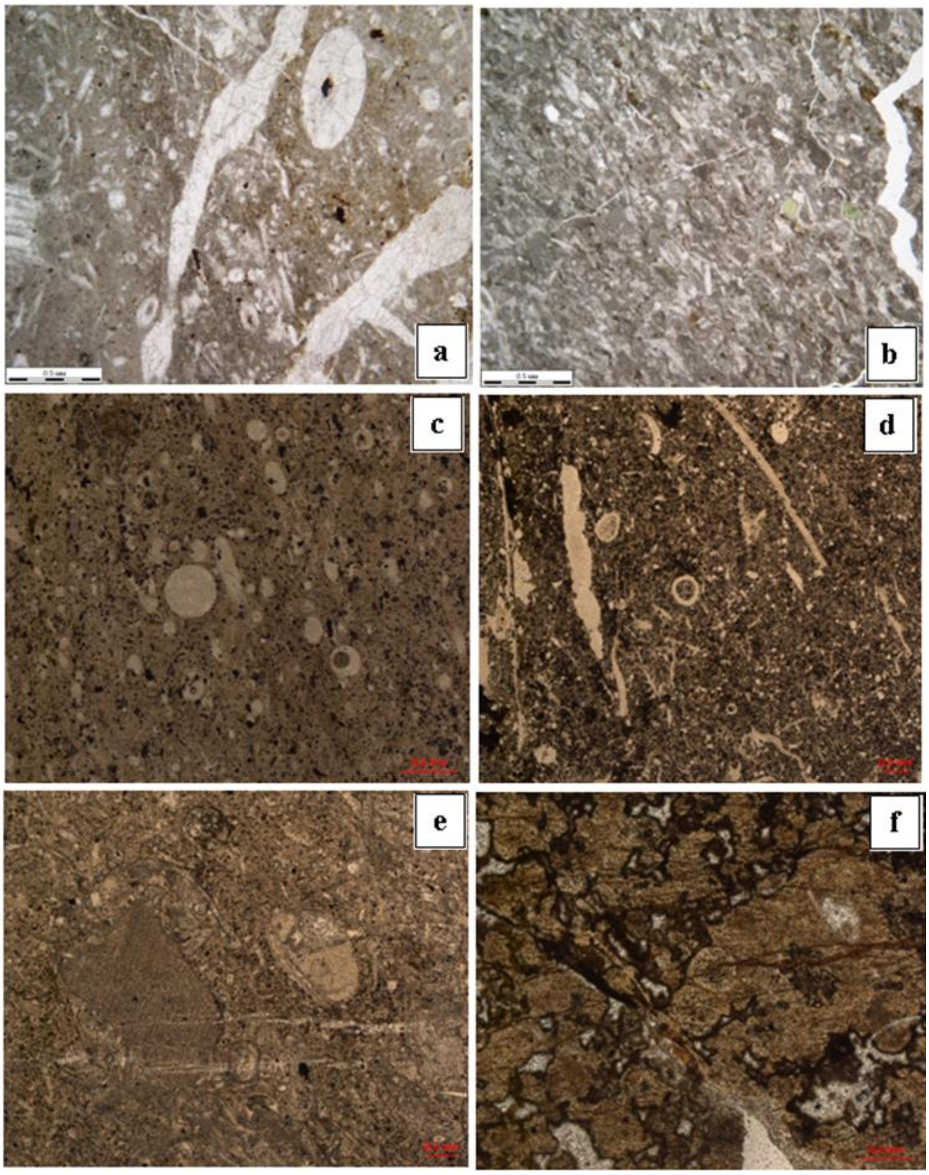

Fig. 3. Upper Carboniferous carbonates of the Usolka Section. a – limestone, Moscovian Stage; b, c – limestone, Kasimovian Stage.

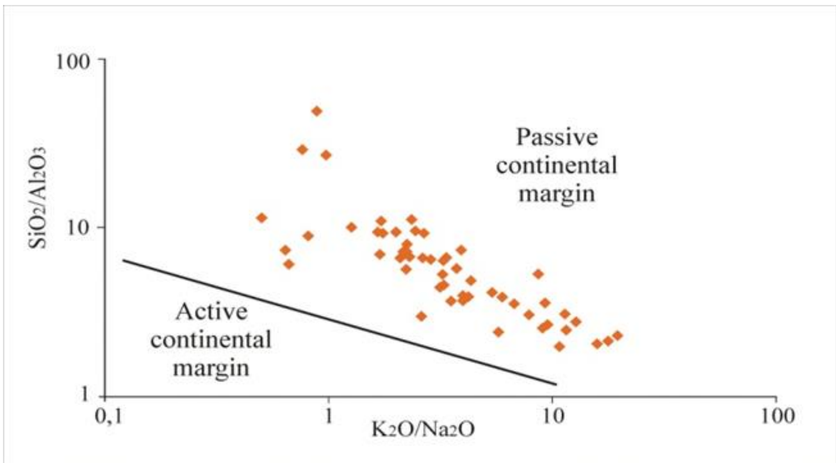

Fig. 4. The position of the figurative points of the composition of the rocks of the Usolka section on the diagram SiO_2/Al_2O_3 – K_2O/Na_2O [13].

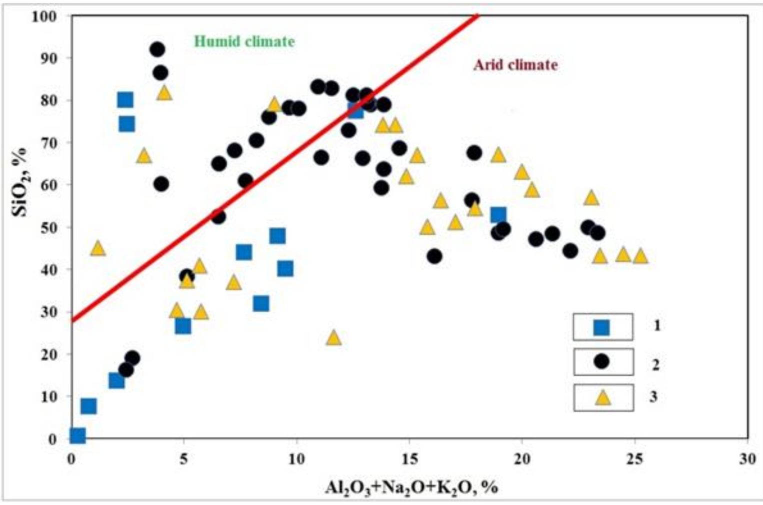

Fig. 5. The climate in the Late Carboniferous Age by lithochemical parameters. The position of the figurative points of the rocks of the Usolka section. on the diagram ($Al_2O_3 + Na_2O + K_2O$)-SiO_2 [14].
1 – Moscovian Stage, 2 – Kasimovian Stage, 3 – Gzhelian Stage

In general, this indicates the difference between sedimentary and sedimentary-volcanogenic rocks. A sharp decrease in CIA values is observed at the Moscovian/Kasimovian and Kasimovian/Gzhelian boundaries (Fig. 6), which may indicate the weak weathering of rocks in the Urals and continuous sedimentation at these boundaries.

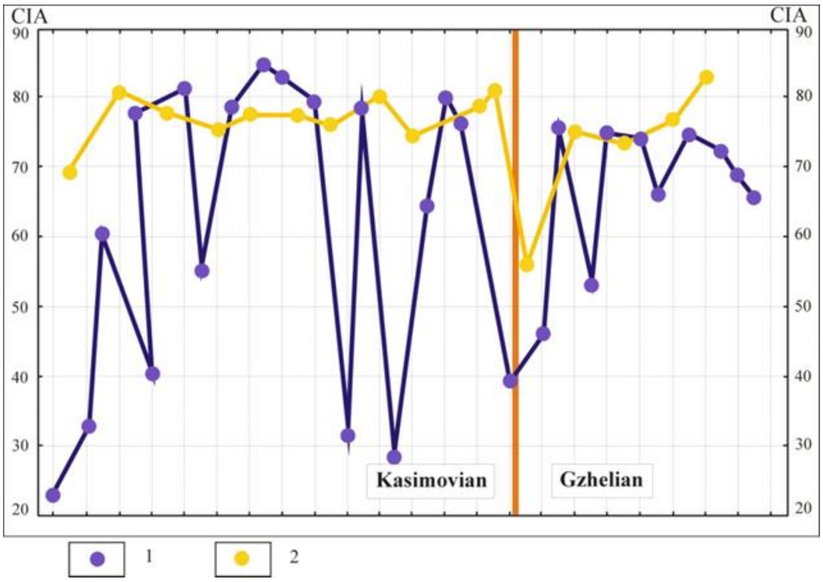

Fig. 6. The average CIA value of mudstones (1) and volcanic ash (2) of the Usolka section.

Cluster analysis of the main elements showed the presence of two main genetic groups of elements: marine (Ca, Mg, Mn, Sr and S) and terrigenous (Si, Al, Fe, Ti, V, etc.). The V/Cr ratio [12] indicates the oxide conditions of sedimentation in the Late Carboniferous Age of the deposits of the Usolka section (V/Cr less than 2).

The results of isotope analysis of carbonates show (Fig. 7) that the $\delta^{13}C$ (PDB) values range from 2.45 ‰ to -11.27 ‰, and the $\delta^{18}O$ (PDB) values range from 1.98 ‰ to -21.5 ‰ (average -3.8 ‰). In general, from the Moscovian Stage to the Gzhelian Stage, there is an increase in $\delta^{18}O$ and a relief in $\delta^{13}C$. According to the original data, the relationship between $\delta^{13}C$ and $\delta^{18}O$ is positive with a pair correlation coefficient of 0.56 (Fig. 8). The average value of $\delta^{13}C$ for the upper part of the Moscovian Stage is 0.2 ‰, for the Kasimovian Stage it is -3.02 ‰, and the Gzhelian Stage is -8.05 ‰. Thus, in the Gzhelian Stage, the lightest carbon values are noted

(Fig. 7). The negative $\delta^{13}C$ anomalies could be caused by deep-sea sedimentation conditions and the presence of methane emissions at the bottom of the marine paleobasin [16], by Gondwana glaciation with a decrease in sea water salinity, by tectonic features, space events and meteorite bombardments [17], or by the combined effect of all these reasons. Large fluctuations in $\delta^{18}O$ can also indicate a fairly frequent change in climatic conditions in the Late Carboniferous Age. In a joint analysis of the distributions of $\delta^{13}C$ and $\delta^{18}O$, 2 regions can be distinguished. The first region ($\delta^{13}C$ from -4.54 to -8.25 ‰, $\delta^{18}O$ from 1.87 to -5.67 ‰) includes carbonates with a low clay content, the second region ($\delta^{13}C$ from -7.73 to -10.18 ‰, $\delta^{18}O$ from 0.72 to -15.54 ‰) is limestones and calcareous dolomites.

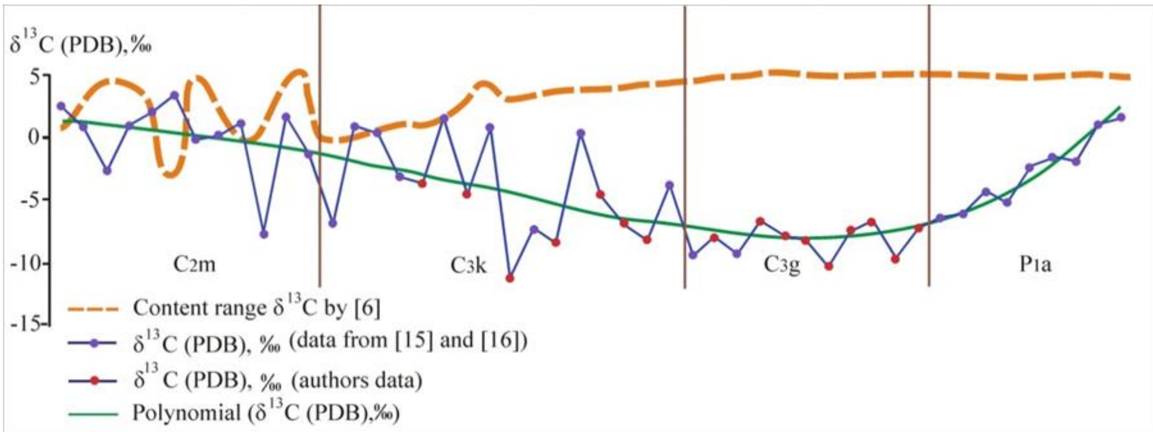

Fig. 7. Graph showing the change in $\delta^{13}C$ values in Upper Carboniferous carbonates

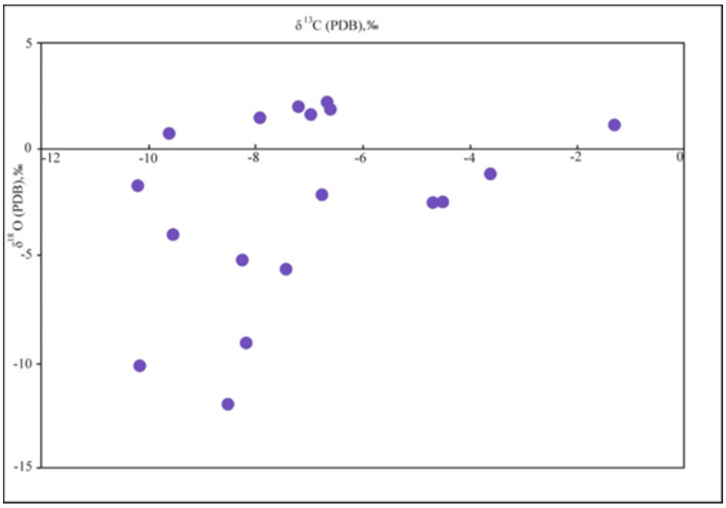

Fig. 8. Stable isotopes values in Upper Carboniferous carbonates

Thus, the Upper Carboniferous deposits of the Usolka section are characterized by abnormally low values of stable isotopes, which confirms the results obtained in laboratories in the USA, China, and Russia, for the Urals [15, 16, 18, 19]. All this may indicate the correctness of isotopic data that are not associated with diagenetic changes in rocks [3, 18].

Conclusions

The studies carried out allowed us to obtain the following results:

1. New geochemical data for the Upper Carboniferous rocks of the Usolka section made it possible to carry out paleotectonic and paleoclimatic reconstructions.
2. Chemical indices showed a low degree of weathering of rocks in the Urals.

3. Anomalously low values of stable isotopes that are not associated with diagenetic changes in the rocks are confirmed.
4. Geochemical parameters are an additional tool for the correlation of sections and for determining the genesis of flysch deposits.

Acknowledgements

The work is performed according to the Russian Government Program of Competitive Growth of Kazan Federal University.

REFERENCES

1. Chernykh V. V., Chuvashov B. I., Davydov V. I., Snyder W. S. (2006). Potential candidate for GSSP to define base of Gzhelian Stage in global chronostratigraphic scale: Usolka section, Southern Urals, Russia. Newsletter on Carboniferous Stratigraphy 24, pp. 23-29.
2. Chernykh V. V., Chuvashov B. I., Davydov V. I., Schmitz M., Snyder W. S. (2006). Usolka section (southern Urals, Russia): a potential candidate for GSSP to define the base of the Gzhelian Stage in the global chronostratigraphic scale. Geologija 49, pp. 205-217.
3. Chuvashov B. I., Djupina G. V., Mizens G. A., Chernykh V. V. (1990). Opornie razrezi verkhnego karbona i nizhnei permi zentralnoi zasti Belskoi bpadini. Sverdlovsk: Uralian Branch, USSR Academy of Sciences. 368.
4. Sungatullina G. M. and Davydov V. I. (2015). New data on conodonts from the Kasimovian Stage of the Usolka section, southern Ural Mountains. Paleontological Journal 49 (10). pp. 1142-1149.
5. Sungatullina G.M., Davydov V.I., Barrick J.E., Sungatullin R.Kh. (2016). Conodonts of Kasimovian-Gzhelian transition, Usolka section, Southern Urals, Russia: New data. Newsletter on Carboniferous Stratigraphy 32, pp. 54-57.
6. Ogg J. G., Ogg G. M., Gradstein F. M. (2016). A Concise Geologic Time Scale. Elsevier B.V. Res. 234.
7. International Chronostratigraphic Chart 2020/01.
URL: http://www.stratigraphy.org/ICSchart/ChronostratChart2020-01.pdf.
8. Southern Urals. Deep water successions of the Carboniferous and Permian. (2015). A Field Guidebook of XVIII International Congress on Carboniferous and Permian. Pre-Congress A3 Trip, August, 6-10, 2015. V. V. Chernykh, B. I. Chuvashov, V. I. Davydov, C. M. Henderson, S. Shen, M. D. Schmitz, G. M. Sungatullina, R. Kh. Sungatullin, J. E. Barrick, O. P. Shilovsky.Kazan: Academy of Sciences of the Republic of Tatarstan Press. 88.
9. Chernykh V. V., Kotlyar G. V., Chuvashov B. I., Kutygin R. V., Filimonova T. V., Sungatullina G. M., Mizens G. A., Sungatullin R. Kh., Isakova T. N., Boiko M. S., Ivanov A. O., Nurgalieva N. G., Balabanov Y. P., Mychko E. V., Gareev B. I., Batalin G. A. (2020). Multidisciplinary study of the Mechetlino Quarry section (Southern Urals, Russia) – The GSSP candidate for the base of the Kungurian Stage (Lower Permian). Palaeoworld 29 (2), pp. 325-352.
10. Mizens G. A., Sungatullin R. Kh., Sungatullina G. M., Gareev B. I., Batalin G. A., Sadriev F. F. (2018). Geohimicheskaya kharakterichnika etalonnikh razrezov priuralskogo otdela permskoi sistemi. Litosfera 18 (6), pp. 819-838.
11. Nesbitt H. W., Young G. M. (1982). Early Proterozoic climates and plate motions inferred from major element chemistry of lutites. Nature 299, pp. 715-717.
12. Bond D., Wignall P. B., Racki G. (2014). Extent and duration of marine anoxia during the Frasnian-Famennian (Late Devonian) mass extinction in Poland, Germany, Austria and France. Geological Magazine 141(2), pp. 173-193.
13. Maynard J. B., Valloni R., Yu H. S. (1982). Composition of Modern Deepsea Sands from Arc-Related Basins. In: Leggett, J. K., Ed., Sedimentation and Tectonics on Modern and Ancient Active Plate Margins. Geological Society of London, Special Publication 10, pp. 551-561.
14. Suttner L. J., Dutta P. K. (1986). Alluvial Sandstone Composition and Palaeoclimate Framework Mineralogy. Journal of Sedimentary Petrology 56, pp. 329-345.
15. Sungatullina G. M., Sungatullin R. Kh., Zakirov M. I., Gareev B. I., Batalin G. A. (2014). Izotopnii sostav ugleroda kamennougolnikh otlozhenii razreza Usolka, Yuzhnii Ural. Proceedings of Voronezh State University. Series: Geology 4, pp. 13-16.
16. Zeng Jun, Cao Chang-qun, Davydov V. I., Shen Shu-zhong (2012). Carbon isotope chemostratigraphy and implications of palaeoclimatic changes during the Cisuralian (Early Permian) in the southern Urals, Russia. Gondwana Research 21, pp. 601-610.

17. Sungatullin R.Kh., Sungatullina G.M., Zakirov M.I., Tsel'movich V.A., Glukhov M.S., Bakhtin A.I., Osin Yu.N., Vorob'ev V.V. (2017). Cosmic microspheres in the Carboniferous deposits of the Usolka section (*Urals foredeep).* Russian Geology and Geophysics 58, pp. 59-69.
18. Nelson S. T., Ritter S. M. (1999). A large carbon isotope anomaly at the Carboniferous-Permian boundary: the Usolka River section of Russia. Permophiles 33, pp. 19-21.
19. Zakirov M. I., Sungatullin R. Kh. (2015). Anomalnie soderzhania $\delta^{13}C$ в v verkhnekamennougolnikh onlozheniyakh Preduralskogo progiba. Proceedings of Voronezh State University. Series: Geology 2, pp. 26-30.

Conodonts and Radiolarians across the Kasimovian/Gzhelian Boundary of the Usolka Section (South Urals, Russia)

SUNGATULLINA Guzal[1], AFANASIEVA Marina[2], SUNGATULLIN Rafael[1]

[1] *Kazan Federal University, Kazan (RUSSIA)*
[2] *Borissiak Paleontological Institute, Russian Academy of Sciences, Moscow (RUSSIA)*
Email: Rafael.Sungatullin@kpfu.ru

Abstract

The Usolka geological section, located in the South Urals, is the Global Stratotype Section and Point (GSSP) for the base of the Sakmarian Stage of the Permian System of the International Stratigraphic Scale. Recently, work on the study of the lower boundary of the Gzhelian Stage of the Carboniferous System has been resumed at the section. In the boundary interval, the data on conodonts are supplemented by the results of the study of radiolarians. For the first time, on the border of the Kasimovian and Gzhelian stages, ecozones were identified based on radiolarians (*Haplodiacantus circinatus – Albaillella protractosegmentata, Astroentactinia luxuria – Triactofenestrella nicolica*, and *Entactinia austrouralica – Polyentactinia multifora*).

Keywords: Usolka section, conodonts, radiolarians, Carboniferous, Gzhelian Stage, GSSP

Introduction

The Usolka geological section, located in the South Urals (Fig. 1), is the Global Stratotype Section and Point (GSSP) for the base-Sakmarian Stage [1], [2]. This section is composed of terrigenous-carbonate rocks in the stratigraphic range from the Moscovian Stage of the Carboniferous to the Sakmarian Stage of the Permian [3], [4]; the section contains tuff interlayers with zircons, according to which the absolute age of the deposits is established [5].

The Usolka section has several stage boundaries characterized by conodonts [6], [7], [8]. For example, the GSSP of the Sakmarian Stage (Lower Permian) is established by the first appearance of the conodont *Mesogondolella monstra* Chernykh [1], the boundary of the Gzhelian Stage is determined by the appearance of *Streptognathodus simulator* Ellison [9], [10], the conodont *Swadelina subexcelsa* (Alekseev et Goreva) marks the Kasimovian boundary [11], [12]. The species *Swadelina subexcelsa* (Alekseev et Goreva) does not yet have the status of an international marker of the Kasimovian boundary for a number of reasons, one of which is the endemicity of conodonts at the beginning of the Kasimovian Age in many regions [13].

Methodology

To study conodonts in the Usolka section, bed-by-bed sampling of samples weighing up to 15-20 kg was performed. Limestones and dolomites are processed according to the standard method of extracting conodonts by dissolving carbonates in 10% acetic acid. Clay rocks were soaked in water, washed from clay particles, dried, sieved, viewed under a binocular microscope. Together with conodonts, other groups of fossils found in the insoluble residue (radiolarians, ammonoids, teeth and fish scales) were selected. The section description is presented in the geological excursion guide [14].

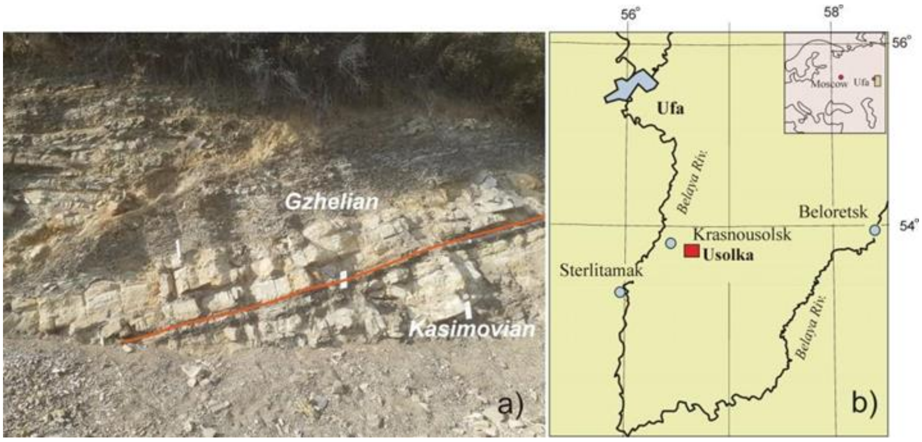

Fig. 1. Usolka Section. a) – Kasimovian/Gzhelian boundary of the Usolka section, b) – location

Results and Discussions

In recent years, the boundaries of the Stages of the Carboniferous have been intensely studied in the Usolka section. The fact that the Carboniferous deposits of the Usolka section contain a large number of conodonts makes it possible to consider it as a GSSP candidate for the base of the Gzhelian [9] and, possibly, Kasimovian Stages [11] (Fig. 2). For the paleontological characterization of the Kasimovian/Gzhelian boundary, radiolarians were used for the first time along with conodonts.

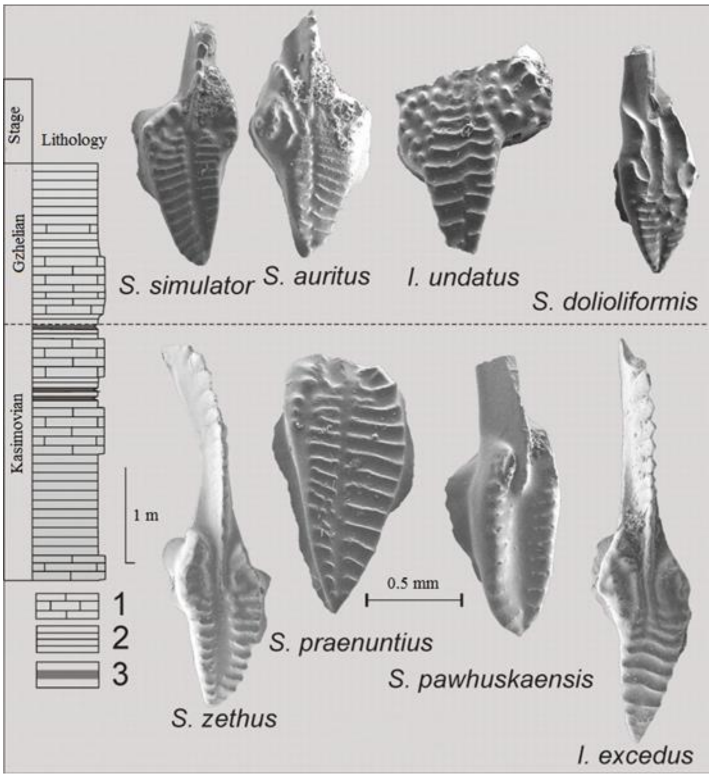

Fig. 2. Conodonts on the Kasimovian/Gzhelian boundary. 1 – limestone, 2 – mudstone, 3 - volcanic ash

The upper part of the Kasimovian Stage of the Carboniferous is dominated by conodonts of the genus *Streptognathodus* represented by *S. crassus* Chernykh, *S. firmus* Kozitskaya, *S. gracilis* Stauffer and Plummer, *S. pawhuskaensis* Harris and Hollingsworth, *S. praenuntius* Chernykh, *S. zethus* Chernykh and Reshetkova. *Idiognathodus excedus* Chernykh, *I. magnificus* Stauffer and Plummer, *I. toretzianus* Kozitskaya, *I. undatus* Chernykh are also present.

For the first time, radiolarians corresponding to two ecozones were found in the upper part of the Kasimovian.

Ecozone *Haplodiacantus circinatus – Albaillella protractosegmentata*, which includes, along with the zonal taxa, the species *Parafollicucullus fusiformis* Holdsworth et Jones, 1980 (Fig. 3, Fig. 1-3) [15].

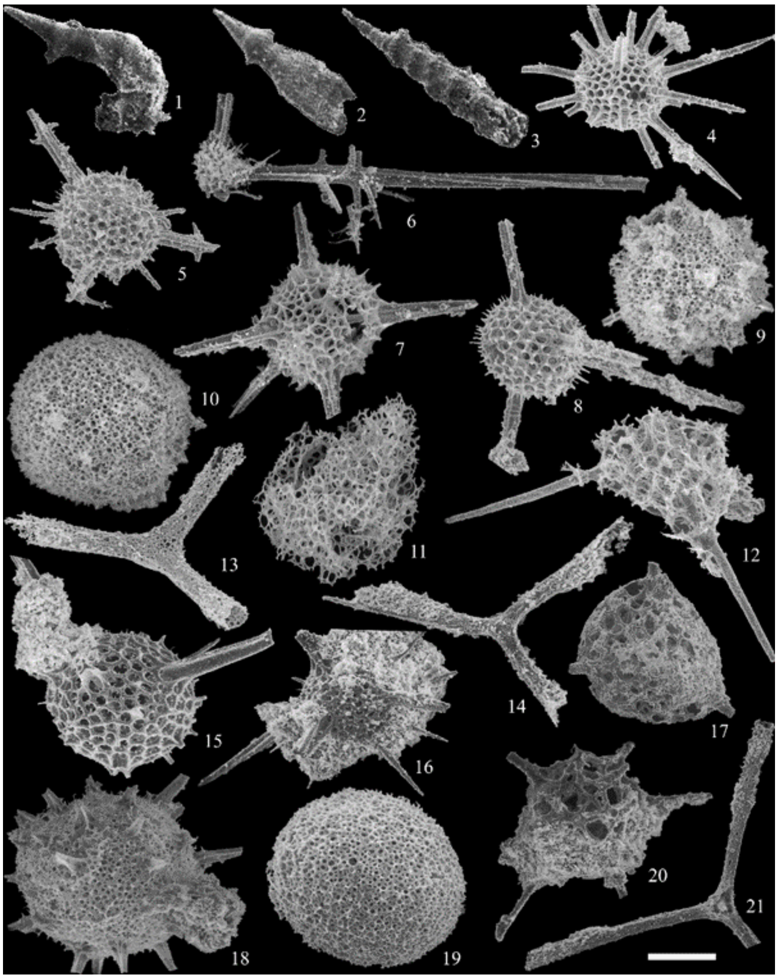

Fig. 3. Radiolarians of the Usolka section.

Fig. 1. *Haplodiacanthus circinatus* Nazarov et Ormiston, 1985, no. 5508/361, line = 120 μm. Fig. 2. *Parafollicucullus fusiformis* Holdsworth et Jones, no. 5508/364, line = 120 μm. Fig. 3. *Albaillella protractosegmentata* Nazarov in Isakova et Nazarov, 1986, no. 5508/363, line = 120 μm. Fig. 4. *Astroentactinia luxuria* Nazarov et Ormiston, 1985, no. 359-158-1, line = 114 μm. Fig. 5. *Apophysiacus sakmaraensis* (Kozur et Mostler, 1989), no. 256-158-6, line = 95 μm. Fig. 6. *Apophysiacus pycnoclada* (Nazarov et Ormiston, 1985), no. 176-158-14, line = 90 μm. Fig. 7. *Bientactinosphaera inusitata* (Foreman, 1963), no. 020-158-15, line = 130 μm. Fig. 8. *Entactinis* sp. 353, no. 353-158-5, line = 79 μm. Fig. 9. *Copicyntra acilaxa* Nazarov in Isakova et Nazarov, 1986, no. 201-158-17, line = 142 μm. Fig. 10. *Copicyntra fragilispinosa* Kozur et Mostler, 1989, no. 256-158-12, line = 129 μm. Fig. 11. *Somphoentactinia saecularis* Afanasieva et Amon, 2016, no. 278-158-13, line = 93 μm. Fig. 12. *Tetragregnon piramidatum* Nazarov in Isakova et Nazarov, 1986, no. 244-158-4, line = 129 μm. Fig. 13. *Triactofenestrella nicolica* Nazarov et Ormiston, 1984, no. 309-158-11, line = 131 μm. Fig. 14. *Latentifistula neotenica* Nazarov et Ormiston, 1985, no. 247-158-16, line = 84 μm. Fig. 15. *Entactinia spinifera* Amon, Braun et Chuvashov, 1990, no. 271-171-1, line = 74 μm. Fig. 16. *Entactinia austrouralica* Nazarov in Isakova et Nazarov, 1986, no. 273-171-9, line = 84 μm. Fig. 17. *Tetragregnon piramidatum* Nazarov in Isakova et Nazarov, 1986, no. 244-171-5, line = 128 μm. Fig. 18. *Copicyntra robustodentata* Kozur et Mostler, 1989, no. 255-171-2, line = 67 μm. Fig. 19. *Copicyntra fragilispinosa* Kozur et Mostler, 1989, no. 256-171-7, line = 66 μm. Fig. 20. *Polyentactinia multifora* Nazarov in Isakova et Nazarov, 1986, no. 360-171-4, line = 76 μm. Fig. 21. *Quadriremis* sp., no. 250-171-6, line = 186 μm

The *Astroentactinia luxuria – Triactofenestrella nicolica* ecozone located higher in the section is characterized by a more diverse composition of radiolarians: *Astroentactinia luxuria* Nazarov et Ormiston, 1985, *Apophysiacus sakmaraensis* (Kozur et Mostler, 1989), *A. pycnoclada* (Nazarov et Ormiston, 1985), *Entactinis* sp., *Bientactinosphaera inusitata* (Foreman, 1963), *Copicyntra acilaxa* Nazarov in Isakova et Nazarov, 1986, *C. fragilispinosa* Kozur et Mostler, 1989, *Latentifistula neotenica* Nazarov et Ormiston, 1985, *Somphoentactinia saecularis* Afanasieva et Amon, 2016, *Tetragregnon piramidatum* Nazarov in Isakova et Nazarov, 1986, *Triactofenestrella nicolica* Nazarov et Ormiston, 1984 (Fig. 3, Fig. 4-14).

In the Gzhelian stage, a group of conodonts appears that have an asymmetrically located median groove on the platform: *Streptognathodus auritus* Chernykh, *S. gravis* Chernykh, *S. simulator* Ellison, *S. sinistrum* Chernykh. *Idiognathodus toretzianus* Kozitskaya, *I. verus* Chernykh, *I. undatus* Chernykh, *Streptognathodus crassus* Chernykh, *S. dolioliformis* Chernykh, *S. gracilis* Stauffer et Plummer are also present. The lower boundary of the Gzhelian Stage is marked by *Streptognathodus simulator* Ellison [9].

The lower boundary of the Gzhelian Stage is marked by the entry of *Copicyntra fragilispinosa* Kozur et Mostler, 1989, *Tetragregnon piramidatum* Nazarov in Isakova et Nazarov, 1986, *Entactinia spinifera* Amon, Braun et Chuvashov, 1990, *Entactinia austrouralica* Nazarov in Isakova et Nazarov, 1986, *Copicyntra robustodentata* Kozur et Mostler, 1989, *Polyentactinia multifora* Nazarov in Isakova et Nazarov, 1986, *Quadriremis* sp. (Fig. 3, Figs. 15-21), allowing a new ecozone *Entactinia austrouralica – Polyentactinia multifora* to be recognized

Conclusions

The study showed that the Kasimovian/Gzhelian boundary of the Usolka section is characterized by abundant and diverse conodonts. The first finds of radiolarians at the Kasimovian/Gzhelian boundary increase the correlation potential of the section. The rich and diverse composition of fossils, the possibility of establishing an absolute age, and continuous marine deposition, allow the Usolka section to be proposed as the GSSP for the base of the Gzhelian Stage (Upper Carboniferous).

Acknowledgements

The work is performed according to the Russian Government Program of Competitive Growth of Kazan Federal University.

REFERENCES

1. Chernykh V. V., Chuvashov B. I., Shen S. Z. and Henderson C. M. (2016). Proposal for the Global Stratotype Section and Point (GSSP) for the base-Sakmarian Stage (Lower Permian). Permophiles 63, pp. 4-18.
2. Kotlyar G. V. (2019). Globalnyi stratotipicheskii razrez i tochka (GSSP) nizhnei granitsy sakmarskogo yarusa priural’skogo otdela permskoi sistemy (Yuzhnyi Ural, Rossia) [Global Stratotype Section and Point (GSSP) for the lower boundary of the Sakmarian Stage of the Cisuralian, the Permian (South Urals, Russia)]. Regionalnaya geologiya i metallogeniya 77, pp. 6-10.
3. Chuvashov B. I., Mizens G. A., Dyupina G. V., Chernykh V. V. (1983). Opornye razrezy verkhnego karbona i nizhnei permi tsentral’noi chasti Bel’skoi vpadiny. USC AS USSR, Sverdlovsk, 56.
4. Chuvashov B. I., Chernykh V. V. Razrez «Krasnousolskii» 2002. Putevoditel’ geologicheskih ekskursii po karbonu Urala. Part 1. South Ural tour. IGG UB RAS, Yekaterinburg, pp. 18-33.
5. Schmitz M. D., Davydov V. I. (2012). Quantitative radiometric and biostratigraphic calibration of the Pennsylvanian – Early Permian (Cisuralian) time scale and pan-Euramerican chronostratigraphic correlation. Geological Society of America Bulletin 124, pp. 549-577.
6. Chernykh V. V. (2008). Opredelenie yarusnykh granits Mezhdunarodnoi stratigraficheskoi shkaly po conodontam. Lithosphere 1, pp. 3-17.

7. Davydov V. I., Leven E. Y., Chuvashov B. I. (1999). Fusulinid Biostratigraphy in Asselian – Sakmarian transition in stratotype area Southern Urals, Russia. Permophiles 35, pp. 30-31.
8. Davydov V. I., Wardlaw B. R. (2005). Progress on the Cisuralian (Lower Permian) timescale, Southern Urals, Russia. Permophiles 45, pp. 9-11.
9. Chernykh V. V., Chuvashov B. I., Davydov V. I., Schmitz M., Snyder W. S. (2006). Usolka section (Southern Urals, Russia): a potential candidate for GSSP to define the base of the Gzhelian Stage in the global chronostratigraphic scale. Geologija 49, pp. 205-217.
10. Sungatullina G. M., Davydov V. I., Barrick J. E., Sungatullin R. Kh. (2016). Conodonts of Kasimovian-Gzhelian transition, Usolka section, Southern Urals, Russia: New data. Newsletter on Carboniferous Stratigraphy 32, pp. 54-57.
11. Sungatullina G. M., Davydov V. I. (2015). New data on conodonts from the Kasimovian Stage of the Usolka section, southern Ural Mountains. Paleontological Journal 49 (10), pp. 1142-1149.
12. Sungatullina G., Sungatullin R., Shilovsky O., Statsenco E., Aysina R., Karimullina I. (2018). Kasimovian Conodonts and Ammonoids of the Usolka Section (Southern Urals). Proceedings Kazan Golovkinsky Stratigraphic Meeting «Advances in Devonian, Carboniferous and Permian Research: Stratigraphy, Environments, Climate and Resources». Bologna: Filodiritto Publisher, pp. 230-238.
13. Aleksees A.S., Goreva N.V. (2012). Conodonty pogranichnogo intervala moskovskogo i kasimovskogo yarusov (carbon) na Yuzhnom Urale. Trudy XV Vserossiiskogo mikropaleontologicheskogo soveshchaniya «Sovremennaya micropaleontologiya». Gelendzhik, pp. 189-193.
14. Chernykh V. V., Chuvashov B. I., Davydov V. I., Henderson C. M., Shen S., Schmitz M. D., Sungatullina G. M., Sungatullin R. Kh., Barrick J. E., Shilovsky O. P. (2015). Southern Urals. Deep water successions of the Carboniferous and Permian. A Field Guidebook of XVIII International Congress on Carboniferous and Permian. Pre-Congress A3 Trip. Academy of Sciences of the Republic of Tatarstan Press, Kazan, 88.
15. Afanasieva M. S., Amon E. O., Chuvashov B. I. (2002). Radiolarii v biosratigraphii i paleogeographii carbona Prikaspia i Juzhnogo Preduralia. Lithosphere 4, pp. 22-62.

Biostratigraphy and Lithology of the Makarovo Horizon Deposits (Famennian Stage) in the Stratotype Section (Western Slope of the Southern Urals)

TAGARIEVA Rezeda[1]

[1] *Institute of Geology, Subdivision of the Ufa Federal Research Centre of the Russian Academy of Sciences, Ufa, (RUSSIA)*
Email: trezeda88@mail.ru

Abstract

This paper presents a new detailed lithological and paleontological description of the Famennian Makarovo Horizon deposits in the Kuk-Karauk stratotype section (Sikasya River, western slope of the Southern Urals). The Horizon consists of six lithogenetic types (microfacies) of light-gray organogenic-polydetrital limestones: (1) medium- to coarse, bioclastic grainstone; (2) fine, bioclastic wackestone; (3) medium- to coarse, bioclastic grainstone-packstone; (4) intraclast (clot) wackestone-packstone; (5) medium- to coarse, bioclastic, intraclast (clot) packstone; (6) fine, bioclastic, intraclast (clot) wackestone. The Makarovo Horizon stratigraphic interval is defined more accurately. It is equal to the Upper *triangularis,* Lower *crepida, rhomboidea,* Lower and Upper *marginifera* conodont zones.

Conodont assemblages are represented by rich taxonomic and quantitative diversity (7 genera and 49 species). Taxa of the genus *Palmatolepis* (up to 92 percent), representatives of deep-water palmatolepid biofacies, predominate.

Keywords: Southern Urals, Famennian stage, Makarovo Horizon, stratotype, microfacies, conodonts, biofacies

Introduction

The Makarovo Horizon is the largest regional subdivision of the Famennian (D_3fm) in the western slope of the Southern Urals. Since the 1930s it has been known as the beds with *Cheiloceras, Zilimia polonica* and *Cyrtospirifer archiaci* [9], [10]. Based on conodonts, it corresponds to the interval of the Upper *triangularis*, *crepida*, *rhomboidea* and Lower *marginifera* conodont zones [1], [4], [6], [7], [15]. The Horizon deposits consist of light-gray, pinkish-gray fine and medium-bedded organogenic-polydetrital limestones of marine origin, containing numerous remains of rugoses, crinoid segments, algae, brachiopod shells, ostracods, conodonts and fish. They have a cyclic structure and are represented by alternated grainstones-packstones and wackestones. The Makarovo Horizon deposits rest on the brachiopod shellstones of the Famennian Barma Horizon and are overlain by limestones of the Murzakai Horizon (D_3fm). The Makarovo Horizon is not represented in its complete succession everywhere, even in the stratotype locality. The stratigraphic gaps are fixed at the base and inside this unit. The duration of the gaps ranges from one to several conodont zones [1], [2], [3], [17], [18], [19]. The Kuk-Karauk section is a stratotype of the Makarovo Horizon [16]. It is located in the West Uralian Folded Zone on the right bank of the Sikasya River opposite the mouth of Kuk-Karauk Creek (N53°43'40.41" and E56°39'11.67", Fig. 1).

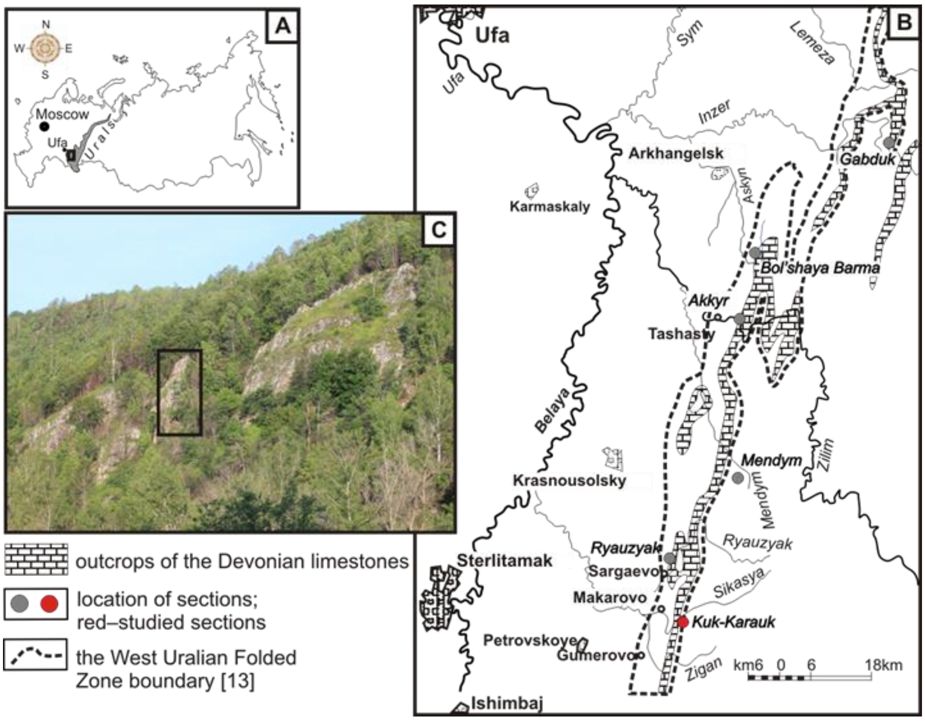

Fig. 1. A – sketch map showing the location of the studied area in Russia; B – the location of the Kuk-Karauk section (from V.A. Maslov [11] with additions); C – photograph of a general view of the studied section

Material and Methods

Material from the Kuk-Karauk sections was collected during fieldwork in 2008-2013.

Investigations of the section were carried out in the most detailed way with centimeter-by-centimeter simultaneous sampling. The weight of each of the 30 samples was about 2 kg.

Polished slabs and the thin section micrographs of limestones were made for all samples.

Disintegration of rocks followed the traditional method in a 3-5 percent solution of formic acid. The microfauna selection from the insoluble sediment and its further study were carried out under a stereo microscope. The collection includes more than 1400 specimens of platform elements belonging to 49 species of seven genera. It is kept in the Laboratory of Paleozoic stratigraphy, IG UFRC RAS (Ufa).

The Rock Succession and Lithology

The Makarovo Horizon stratotype is located in the upper part of the steep slope of the Sikasya River. Middle – Upper Devonian and Lower Carboniferous carbonate deposits are exposed in the exotic rocks (see Fig. 1B, C) [1], [2], [3], [5], [6], [7], [8], [9], [10], [11], [14], [19], [20].

Markovsky [9] was the first to study deposits with *Leiorhynchus polonicus* Gür. (= *Zilimia polonica* or "Makarovo beds") on the right bank of the Sikasya River opposite the mouth of Kuk-Karauk Creek. He described six limestone beds of 2.70 m in thickness.

A.N. Abramova, V.I. Baryshev and V.N. Pazukhin investigated this section in detail using conodonts, to produce a new Devonian stratigraphic chart in 1993 [15]. The Makarovo beds with *Zilimia polonica* correspond to Upper *triangularis* and Lower *marginifera* standard conodont zones [14].

The stratotype section was re-studied in 2008-2013 by the present author. The sampling in Makarovo deposits was carried out up the top of the Barma Horizon represented by brachiopod shellstones. The boundary between these units is indicated by sharp lithological and paleontological changes (see Fig. 2 III).

Bed 1; 0.30 m thick (corresponding to Bed I of Markovsky [9]). – Limestone brownish-light-gray colored, coarse-grained, organogenic-polydetrital and slightly dolomitized (Fig. 2 I, II, III, A). In thin section, the rock is represented by medium- to coarse-grained, bioclastic grainstone (microfacies 1, see Fig. 2a) containing abundant crinoid segments and fragments of echinoderms and rare brachiopod shells, ostracods, gastropods, conodonts and fish fauna (*Phoebodus* sp.) in micrite. They range in size from 0.05 to 2.10 mm. There are recrystallization bioclasts, hematite aggregates and microfractures.

Bed 2; 0.05-0.10 m (similar limestone was fixed by Markovsky [9] within Bed I). – Dark-gray limestone, thin-bedded, fine-grained, bioclastic-stromatolite, hard and compact, slightly dolomitized and ferruginous (see Fig. 2 I, II, B). Petrographically it is represented by a stromatolite bioherm fragment and consists of fine-bioclastic wackestone (microfacies 2, see Fig. 2 b). This microfacies is characterized by smooth and crinkled millimeter thick laminae, and alternating micrite and microsparite laminae, containing fine bioclasts (up to 0.50 mm) of ostracods, green algae and conodonts. There are numerous microfractures filled with collomorphic aggregates of hematite.

Bed 3; 0.30 m (Bed II of Markovsky [9]). – Limestone pinkish-light-gray colored, medium-grained and enriched with fine-crushing organogenic-clastic material (Fig. 2 I, II, C). In thin section the rock represented by medium- to coarse bioclastic grainstone-packstone (microfacies 3, see Fig. 2 c) with abundant large fossils. The larger fossils are usually dominated by rugoses, brachiopod shells and crinoid segments. Smaller fossils include ostracods, green algae fragments and conodonts. They range in size from 0.50 to 2.50 mm. Iron coating on bioclasts is common.

Bed 4; 0.40 m (corresponding to bed III by Markovsky [9]). – Light-gray limestone, fine-grained, organogenic-polydetrital, hard and compact, slightly dolomitized (see Fig. 2 I, D).

Petrographically it is represented by intraclast (clot) wackestone-packstone (microfacies 4, see Fig. 2 d), containing abundant fragments of crinoid segments, ostracods and green algae in micrite. Size of the bioclasts ranges from 0.05 to 1.50 mm. Most of the bioclasts have been micritized, reducing them to carbonate clots. There are stylolitic surfaces in the rock filled with iron hydroxide.

Bed 5; 0.50 m (compared to bed IV by Markovsky [9]). – Limestone brownish-light-gray colored, coarse-grained, organogenic-polydetrital, recrystallizated and containing various fossils (Fig. 2 I, E). In thin section, the rock represented by medium- to coarse-sized, bioclastic, intraclast (clot) packstone (see Fig. 2 I, e). Brachiopods shells and ostracods are dominant within these facies. Minor amount of bioclasts such as crinoid segments, green algae fragments and conodonts in micrite cement. They range in size from 0.05 to 0.50 mm. The binding material is generally micrite with patches of intergranular sparite.

Bed 6; 0.70 m (corresponding to bed V by Markovsky [9]). – Light-gray limestone, fine-grained, hard and compact, slightly dolomitized (see Fig. 2 I, F). Petrographically it is represented by fine-sized, bioclastic, intraclast (clot) wackestone (see Fig. 2 f) having scattered fine bioclasts (up to 1.50 mm) of crinoid segments and ostracods. The clots are composed of dark-gray micrite – of diverse form – oval, isometric, elongated and triangular.

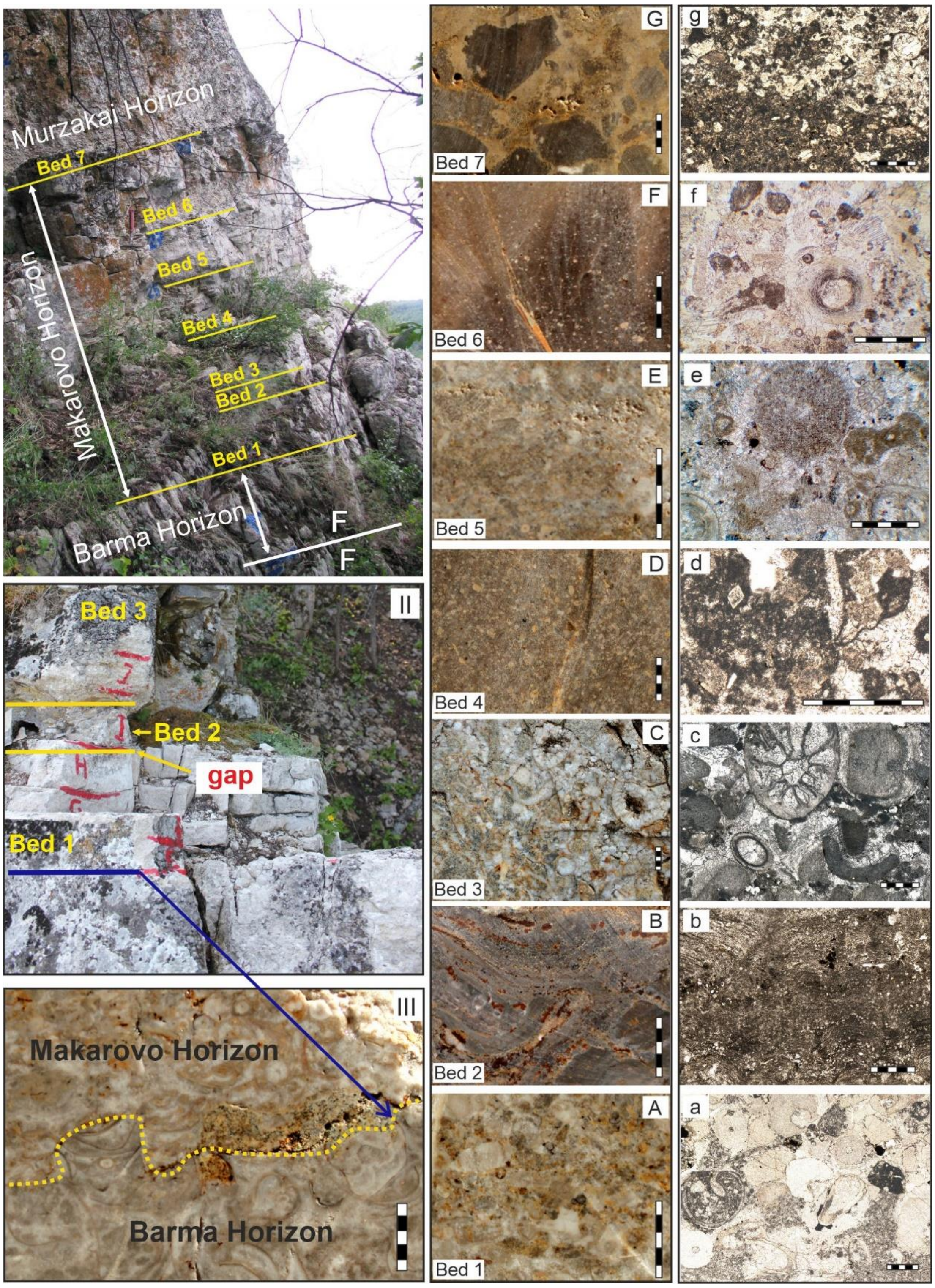

Fig. 2. The Makarovo Horizon (Famennian) deposits in the stratotype section of Kuk-Karauk. I – photograph of the general view of the studied section; II – photograph of the lower part of the Makarovo Horizons deposits; III, A-G – polished slab of shellstones (scale 1 cm); III – photograph of Barma and Makarovo boundary; a-g – thin section micrograph of limestones (normal light, scale 1 mm): A, a – medium- to coarse bioclastic grainstone, Lower *crepida* Zone, sample T12-20; B, b – fine-sized, bioclastic wackestone, *rhomboidea* Zone, sample K-I-I; C, c – medium- to coarse bioclastic grainstone-packstone, Lower *marginifera* Zone, sample T12-22; D, d – intraclast (clot) wackestone-packstone, Lower *marginifera* Zone, sample T12-24; E, e – medium- to coarse, bioclastic, intraclast (clot) packstone, Upper *marginifera* Zone, sample T12-26; F, f – fine, bioclastic, intraclast (clot) wackestone, Upper *marginifera* Zone, sample T12-28; G, g – fine- to medium, bioclastic, wackestone-packstone, Upper *marginifera* Zone, sample T12-30

Bed 7; lower 0.15 m (Bed VII of Markovsky [9], beds with *Leiorhynchus ursus* Nal. or "Murzakai beds" of Famennian Stage D_3). Limestone light-gray colored, hard and compact, polydetrital-clots, slightly dolomitized (see Fig. 2 I, G). Petrographically it is represented by fine- to medium, bioclastic, wackestone-packstone (see Fig. 2g) containing abundant clots and lumps of calcite (microsparite) and fine bioclasts (crinoid segments, green algae fragments, brachiopod shells, foraminifers and conodonts). The beds contain dispersed fine coaly material.

The thickness of the Makarovo Horizon deposits in the Kuk-Karauk sections (Beds 1-6) is 2.30 m.

Conodont Biodiversity, Biostratigraphy and Biofacies

The Makarovo Horizon deposits in the studied sections are subdivided into the Upper *triangularis*, Lower *crepida*, *rhomboidea*, Lower and Upper *marginifera* zones of the standard conodont scale [1], [2], [3], [4], [17], [18], [19], [22]. The conodont complex biodiversity is characterized by a rich taxonomic composition. Taxa of the genera *Palmatolepis*, *Polygnathus* and *Icriodus* form the basis for conodont assemblages in all samples.

The **Upper *triangularis* Zone**. The zone corresponds to the base of the Makarovo Horizon [1], [2], [4], [15]. The lower boundary of the Upper *triangularis* Zone is drawn at the bottom of Bed 1 by the first appearance of the zonal species *Palmatolepis minuta minuta* Br. & M. (Fig. 3A). The conodont association is taxonomically diverse and consists of five genera and 23 species (see Fig. 3A). Species of the genus *Palmatolepis* outnumber all other conodonts (70-88 percent, see Fig. 3B). This conodont assemblage is characteristic of the palmatolepid (deep-water) biofacies [12]. *Pa. triangularis* Sann., *Pa. subperlobata* Br. & M. and *Pa. d. postdelicatula* Schul. are predominant. Thickness of the Upper *triangularis* Zone is 0.10 m.

The ***crepida* Zone**. It is represented by the **Lower *crepida* Zone** only. The lower boundary is recognized by the first appearance of the marker species *Palmatolepis crepida* Sann. (see Fig. 3A). Along with transit taxa, the assemblage contains *Pa. m. wolskae* Szulc. and *Ic. cornutus* Sann. (Fig. 3A). The genus *Palmatolepis* is clearly dominant (up to 80 percent of all taxa) (see Fig. 3B). Thickness of the Lower *crepida* Zone is 0.20 m.

The interval of **Middle, Upper** and **Uppermost *crepida* zones** corresponds to a gap in the succession (see Fig. 3).

The ***rhomboidea* Zone**. The lower boundary of the zone is established at the base of Bed 2 by the appearance of the marker species *Palmatolepis rhomboidea* Sann. and *Pa. poolei* Sand. & Ziegl. (see Fig. 3A). Its entire thickness is only 0.05-0.10 m. The greatest part of the conodont assemblage consists of taxa of the genus *Palmatolepis* (12 species, up to 92 percent, see Fig. 3B) and characterizes the palmatolepid (deep-water) biofacies. Species of the genera *Polygnathus*, *Icriodus* and *Nothognathella* are represented by single specimens.

The ***marginifera* Zone**. The base of this zone is determined at the base of Bed 3 by the first appearance of the zonal species *Palmatolepis marginifera marginifera* Helms (see Fig. 3A).

The conodont association from the lower part of the **Lower *marginifera* Zone** (Bed 3) is characterized by high taxonomic diversity, and includes five genera and 17 species (see Fig. 1A). A single *Polylophodonta confluens* Ul. & Bas. specimen was found in this zone for the first time. Representatives of the genus *Palmatolepis* dominate over the other taxa (82 percent, see Fig. 3B). *Palmatolepis m. marginifera* Helms and *Pa. g. pectinata* Ziegl. are prevalent species.

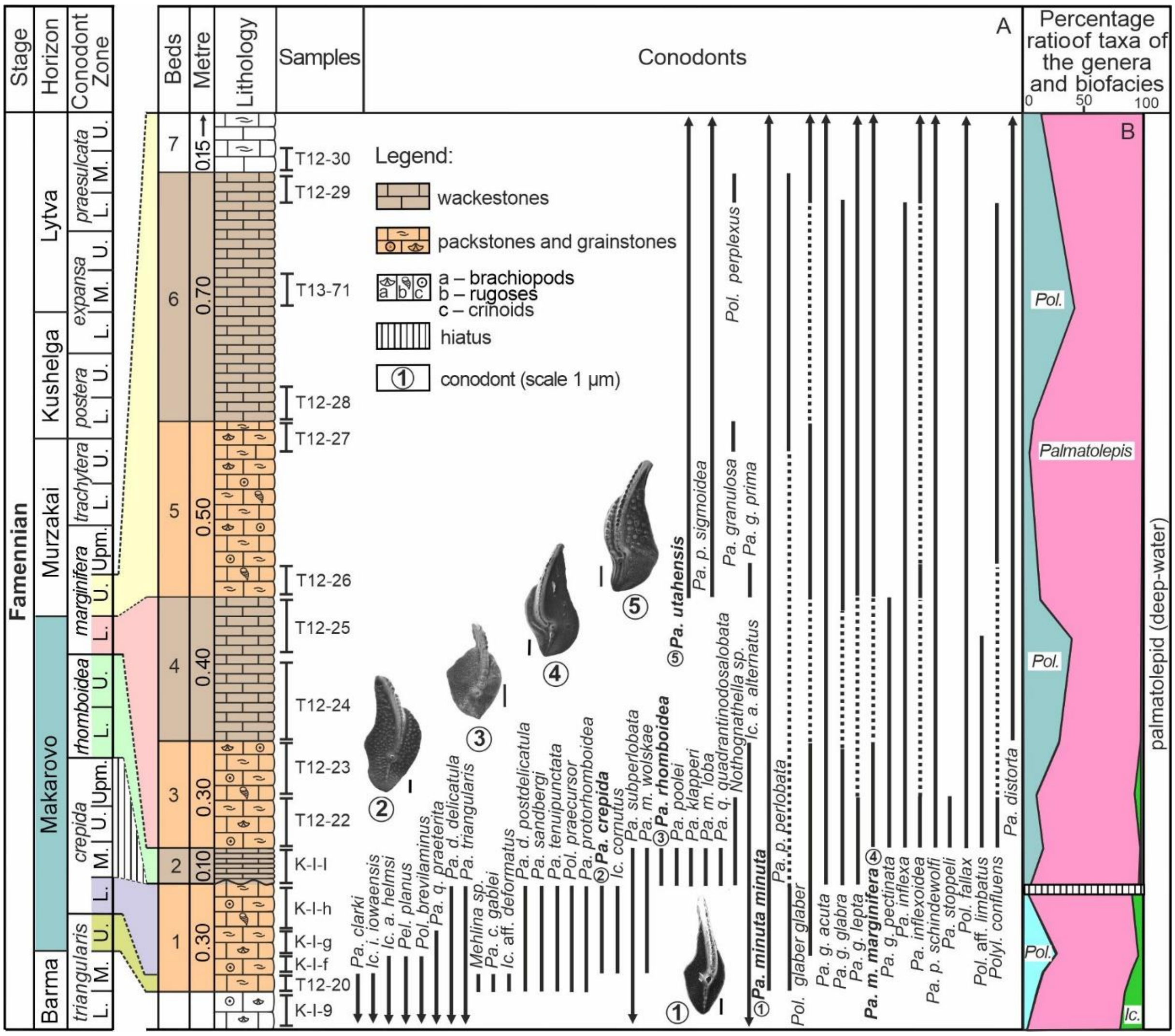

Fig. 3. Distribution of conodonts in the Makarovo Horizon deposits in the Kuk-Karauk section (A) and interpretation of paleoecological and paleogeographic settings (B).
Abbreviations for conodont genera and species throughout the figure and the text paper: *Ic. – Icriodus; Pa. – Palmatolepis; Pel. – Pelekysgnathus; Pol. – Polygnathus; Polyl. – Polylophodonta; a – alternatus; d – delicatula; i – iowaensis; m – marginifera; q – quadrantinodosalobata; p – perlobata; g – glabra*

At the base of Bed 4, conodont occurrence is extremely low. There is only rare transit taxa *Palmatolepis distorta* Br. & M., *Pa. inflexa* Mull., *Pa. g. acuta* Helms, *Pa. g. pectinata* Ziegl., *Pa. m. minuta* Br. & M., *Pa. p. schindewolfi* Mull. and *Polygnathus fallax* Helms & Wolsk. in the conodont association (see Fig. 3A). Thickness of the Lower *marginifera* Zone (Beds 3-4) is 0.70 m.

The bottom of the **Upper *marginifera* Zone** is established at the base of Bed 5 by the first appearance *Palmatolepis utahensis* Ziegl. & Sand. (see Fig. 3A). The conodont biodiversity tends to increase and includes three genera and 18 species. The *Palmatolepis* taxa, representatives of deep-water palmatolepid biofacies, outnumber the other conodonts (up to 95 percent, see Fig. 3B). The abundance of *Pa. utahensis* Ziegl. & Sand. and *Pa. m. marginifera* Helms. is noted in almost every sample. Thickness of the Upper *marginifera* Zone (Beds 5-6) is 1.20 m.

Conodonts characteristic of the Upper *marginifera* Zone are accumulated in the limestones of the Murzakai Horizon (Bed 7 and Bed VII of Markovsky [9], see Fig. 3A).

In the Kuk-Karauk section, the conodont zonation of Makarovo horizons of the Famennian Stage is incomplete. The Middle-Uppermost *crepida* zones are absent (see Fig. 3).

Conclusions

New detailed lithological and paleontological description, zonal conodont-based subdivision and establishment of microfacies and biofacies have been performed on the Famennian Makarovo Horizon deposits in the stratotype section (Kuk-Karauk, Sikasya River) of the western slope of the Southern Urals. The studied rocks comprise light-gray, pinkish-gray fine and medium-bedded, slightly dolomitized, bioclastic-polydetrital limestones 2.30 m in thickness. Fossils show a diverse, open-marine assemblage comprising rugoses, crinoid segments, brachiopods shells, ostracods, green algae, conodonts and fish. Six lithogenetic types (microfacies) of limestones are established: (1) medium- to coarse, bioclastic grainstone; (2) fine bioclastic wackestone; (3) medium- to coarse, bioclastic grainstone-packstone; (4) intraclast (clot) wackestone-packstone; (5) medium- to coarse, bioclastic, intraclast (clot) packstone and (6) fine, bioclastic, intraclast (clot) wackestone (see Fig. 2 a-g). Supposedly, these limestones were formed on the shoals in the open sea, in the high-energy environment [11]. According to Wilson’s classification [21], such formations are characteristic of shoals on the outskirts of carbonate platforms (facies zone 6).

The new Makarovo Horizon stratigraphic content on conodonts corresponds to the interval of the Upper *triangularis*, Lower *crepida, rhomboidea,* Lower and Upper *marginifera* zones.

The Lower *crepida* and *rhomboidea* zones are revealed for the first time in the studied section [18]. The Makarovo Horizon’s conodont zonation is incomplete. The Middle, Upper and Uppermost *crepida* zones are absent in stratigraphic sequence (see Fig. 3).

The Makarovo Horizon deposits in the Kuk-Karauk section include richest taxonomic composition of conodonts with 49 species belonging to seven genera: *Icriodus*, *Mehlina, Nothognathella*, *Palmatolepis*, *Pelekysgnathus*, *Polygnathus*, *Polylophodonta* (see Fig. 3A).

The selected conodont assemblages consist mainly of taxa of the genus *Palmatolepis* (up to 92 percent). They are representatives of deep-water palmatolepid biofacies (see Fig. 3B).

In the Makarovo Horizon, the stratotype section of the Kuk-Karauk zonal conodont sequence is not complete. The absence of intervals equivalent to the Middle – Uppermost *crepida* zones is an example of the hiatus phenomenon (see Fig. 3B). However, in this locality there are well studied sections (Akkyr, Ryauzyak, Mendym etc., see Fig. 1B) [1] with fuller paleontological content. They may be considered for filling the gaps in the stratotype, in order to maximize the value of this subdivision.

Acknowledgements

The author would like to express deep gratitude to her research supervisor Prof. Dr. Olga V. Artyushkova (IG UFRC RAS) for the most valuable recommendations and critical comments during the preparation and translation of this paper. The author is also grateful to Dr. Lyudmila I. Kononova (Faculty of Geology at Moscow State University, Moscow) for consultations on conodonts, and to Valentina F. Kondratenko (RPB “Orenburggazgeofizika”), Dr. Elena N. Gorozhanina and Prof. Elena I. Kulagina (IG UFRC RAS) for advice on the description of thin sections. The work was a realization of the state task subject “The Phanerozoic Stratigraphic subdivisions boundaries as a repercussion of regional and global biotic and abiotic events”, no. AAAA-A19-119011790053-5.

REFERENCES

1. Abramova, A. N. (1999). Franskii yarus zapadnogo sklona Yuzhnogo Urala. Preprint. IG UfNC RAN. Ufa, 55.
2. Abramova, A. N., Artyushkova, O. V. (2004). The Frasnian-Famennian Boundary in the South Urals. Geological Quarterly 48 (3), pp. 217-232.

3. Artyushkova, O. V., Maslov, V. A., Pazukhin, V. N., Kulagina, E. I., Tagarieva, R. Ch., Mizens, L. I., Mizens, A. G. (2011). Devonian and Lower Carboniferous type sections of the western South Urals: Pre-Conference Field Excursion Guidebook. International Conference "Biostratigraphy, Paleogeography and Events in Devonian and Lower Carboniferous", Ufa, Sterlitamak, Russia, July 20-25, 2011. Ufa, 92.
4. Baryshev, V. N., Abramova, A. N. (1996). Zonal'noe raschlenenie verkhnedevonskikh otlozhenii zapadnogo sklona Yuzhnogo Urala po konodontam. Yezhegodnik – 1995. IG UfNC RAN. Ufa, pp. 26-30.
5. Domrachev, S. M. **(**1952). Devon khrebta Kara-Tau i prilegayushchikh raionov Yuzhnogo Urala. Devon zapadnogo Priural'a. Trudy VNIGRI. Novaya seriya. Vypusk 61. Gostoptekhizdat, Leningrad, Moskva, pp. 5-21.
6. Kononova, L. I. (1969). Kompleksy konodontov iz verkhnedevonskikh i nizhnekamennougol'nykh otlozhenii razreza r. Sikazy (Yuzhnyi Ural). Bull. MOIP. Otdel geol. XLIV (1), pp. 121-138.
7. Kononova, L. I., Lipina, O. A. (1971). Sootnosheniye zonal'nykh skhem verkhnego Famena i nizhnego Turne po foraminiferam i konodontam na zapadnom sklone Yuzhnogo Urala. Voprosy mikropaleontologii 14. Nauka, Moskva, pp. 39-69.
8. Kochetkova, N. M., Pazukhin, V. N., Reitlinger, Ye. A., Sinitsyna, Z. A. (1985). Opornye razrezy pogranichnykh otlozhenij devona i karbona zapadnogo sklona Yuzhnogo Urala. Biostratigrafiya pogranichnykh otlozhenij devona i karbona. Akademiya nauk SSSR. Dal'nevost. nauch. centr, Sev. – Vostoch. kompleks. nauch-issled. in-t. 6. SVKNII. Magadan, 66.
9. Markovsky, B. P. (1937). Materialy k izucheniyu devonskikh otlozhenii zapadnogo sklona Yuzhnogo Urala. Chast' 3. CNIGRI, Leningrad (Unpublished), 59.
10. Markovsky, B. P. (1948). Ocherk stratigrafii devonskikh otlozhenii zapadnogo sklona Srednego i Yuzhnogo Urala. Mat-ly Vses. nauchno-issled. Geol. in-ta. Obshch. Ser. 8. Gosgeolizdat, Leningrad, pp. 22-28.
11. Maslov, V. A. (1959). Litologiya i fatsial'nye osobennosti verkhnedevonskikh karbonatnykh otlozhenii zapadnogo sklona Yuzhnogo Urala. Diss. … kand. geol.-min. nauk. Ufa, 304.
12. Seddon, G., Sweet, W. C. (1971). An ecological model for conodonts. Journal of Paleontology 45, pp. 896-880.
13. Seravkin, I. B., Znamensky, S. E., Kosarev, A. M. (2001). Razryvnaja tektonika i rudonosnost' Bashkirskogo Zaural'ja. Poligrafkombinat, Ufa, 318.
14. Sinitsyna, Z. A., Pazukhin, V. N., Kulagina, E. I., Kochetkova, N. M. Klimenko, T. V. Abramova A. N., Kozlov V. I. (1995). The Sikaza Section. In: Guidebook of geological excursion for the Paleozoic and Upper Precambrian sections on the western slope of the Southern Urals and Pre-Ural region (V.N. Puchkov, Ed). IG USC RAS. Ufa, pp. 57-93.
15. Stratigraficheskie skhemy Urala. Dokembrii, paleozoi. (1993). Ekaterinburg.
16. Stratigraficheskii slovar' SSSR. Kembrii, ordovik, silur, devon. (1975). Nedra, Leningrad, 622.
17. Tagarieva, R. Ch. (2013a). Conodont biodiversity of the Frasnian-Famennian boundary interval (Upper Devonian) in the Southern Urals. Bulletin of Geosciences 88 (2), pp. 297-314.
18. Tagarieva, R. Ch. (2013b). Famennian conodont zonation in the Barma and Makarovo deposits at the Kuk-Karauk-I section (South Urals). International Field Symposium "The Devonian and Lower Carboniferous of northern Gondwana" in memory of Dr. Volker Ebbighausen, 22nd – 29th March 2013. Abstracts book, pp. 120-122.
19. Tagarieva, R. Ch., Mizens, A. G. (2015). Sections in the western slope of South Urals perspective for the choice of the Famennian regional boundary stratotype point. Lithoshera, 2015 (3), pp. 33-56.
20. Tyazheva, A. P. (1961). Stratigrafiya devonskikh otlozhenii zapadnogo sklona Yuzhnogo Urala. In Devonskie otlozheniya Bashkirii. Chast' 1. Stratigraphiya (A. I. Olli, Ed). Akademiya nauk SSSR, Moskva, pp. 5-130.
21. Wilson, J. L. (1980). Karbonatnye fatsii v geologicheskoj istorii. Perevod s angliiskogo. Nedra, Moskva, 463.
22. Ziegler W., Sandberg C. A. (1990). The Late Devonian Standart Conodont Zonation. Cour. Forsch. Inst.Senckenberg 121. pp. 1-115.

Gneisses of the Kharbei Metamorphic Complex in the North of the Urals

ULYASHEVA Nataliya[1]

[1] N.P. Yushkin Institute of Geology, Komi Science Centre, Ural Branch, RAS Syktyvkar (RUSSIA)
Email: nataliaulyashewa@yandex.ru

Abstract

Gneisses within the Precambrian uplift of the Kharbei metamorphic complex in the north of the Urals are represented by para- and orthorocks. The protoliths of metamorphosed sedimentary formations, represented by sandstones, are most likely of the same age as the substratum of interbedded amphibolites and may have different provenance area of terrigenous material. Orthogneisses, apparently represented by metamorphosed granodiorites, were formed simultaneously or later than paragneisses during collisional processes.

Keywords: north of the Urals, gneisses, Precambrian, protolith, provenance area

Introduction

In the north of the Urals, basements of ancient platforms are exposed and available for study.

One of them is represented by metamorphosed formations – (amphibolites and gneisses) of the Early Proterozoic Harbei complex (Fig. 1) [1]. The age of the metamorphic changes in the rocks, reaching the conditions of a high-temperature amphibolite facies of metamorphism, is also considered Precambrian [2]. There are different ideas about the geodynamic setting of the formation of the substratum of the metamorphic rocks of the Kharbei complex. According to the concepts based primarily on the study of the geochemical functions of amphibolites, metamorphic protoliths were formed in a trappean province, in the continental riftogenic setting or in the island arc system [1], [2]. The study of the petrogeochemical composition of gneisses interbedded with amphibolites will make it possible to clarify the geodynamic setting of the formation of the substratum of metamorphic rocks of the Kharbei complex and an idea of the tectonic and sedimentation processes that took place on ancient platforms.

Methods

Attention is paid to the gneisses of the Kharbei complex, interbedded with amphibolites and forming strata up to 2-3 m thick. The mineral composition of the gneisses of the Kharbei complex was studied under a polarizing microscope. The contents of rock-forming oxides in these rocks were obtained using wet chemical analysis combined with X-ray fluorescence analysis at the Institute of Geology, Komi Science Center, Ural Branch of the Russian Academy of Sciences (Syktyvkar). The concentration of trace elements in these rocks was determined by acid decomposition of the initial samples and further analysis using a sector mass spectrometer with ionization in inductively coupled plasma using a high-precision ICP-MS method at the Zavaritsky Institute of Geology and Geochemistry (Yekaterinburg). Velikoslavinsky's discriminant function [3], as well as Predovsky's [4] and Neelov's [5] identification diagrams, were used to identify the composition of the gneiss protolith.

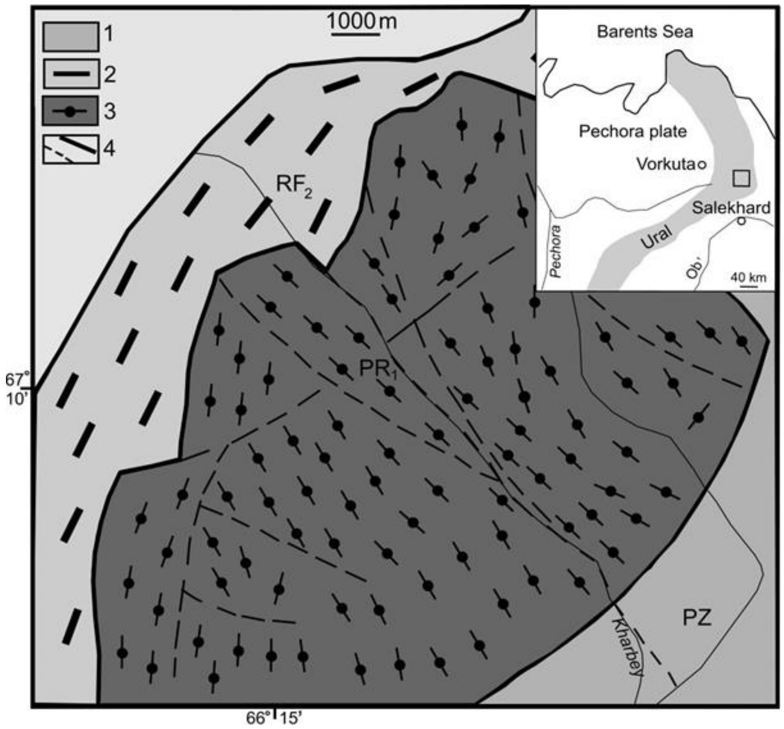

Fig. 1. Schematic geological map of the Kharbei metamorphic complex [1]: 1 – Paleozoic deposits; 2 – Upper Proterozoic deposits; 3 – Kharbei metamorphic complex: 4 – tectonic disturbances

Results and Discussion

Petrographic studies of the gneisses of the Kharbei complex have shown abundant presence of garnet-epidote-two-mica, biotite-epidote-amphibole, garnet-biotite-amphibole, garnet-muscovite-amphibole, biotite-amphibole and amphibole-epidote-muscovite rocks (Fig. 2).

They have granoblastic structures and shale texture. Most of them do not contain potassium feldspar, so they can be classified as plagiogneisses. Only in garnet-epidote-two-mica and biotite-epidote-amphibole formations is up to 1-2% of this mineral observed. Plagioclase in all rocks is represented by albite. The garnet-amphibole-muscovite rock contains an increased proportion of quartz (up to 70%).

According to the discriminant function and identification diagrams, the rocks were divided into para- and orthogneisses. Garnet-muscovite-amphibole plagiogneisses with a high quartz content were most likely formed from sedimentary formations – sandstones. They have high contents of rare earth elements (∑ REE – 195 ppm) and low values of europium anomaly (Eu/Eu* – 0.59) and were probably products of erosion of post-Archean felsic rocks.

Amphibole-epidote-muscovite plagiogneisses occupy an area of uncertainty in terms of discriminant functions, and according to identification diagrams they are located in the area of graywacke sandstones. These rocks have low contents of rare earth elements (∑ REE – 45 ppm) and a positive europium anomaly (Eu/Eu* – 1.17). In the case of the sedimentary nature of these plagiogneisses, they may have formed from Archean rocks of intermediate composition (Fig. 3).

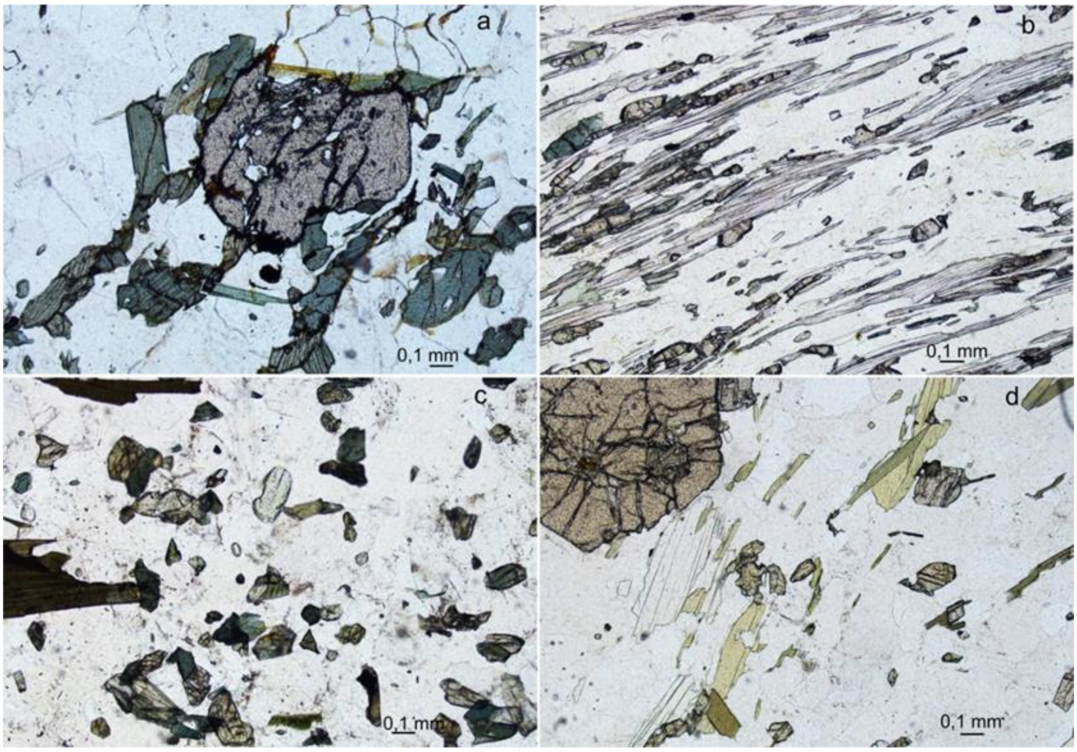

Fig. 2. Photographs of thin sections in transmitted light of garnet-amphibole (a), amphibole-epidote-muscovite (b), biotite-amphibole (c) and garnet-two-mica (d) gneisses of the Kharbei metamorphic complex

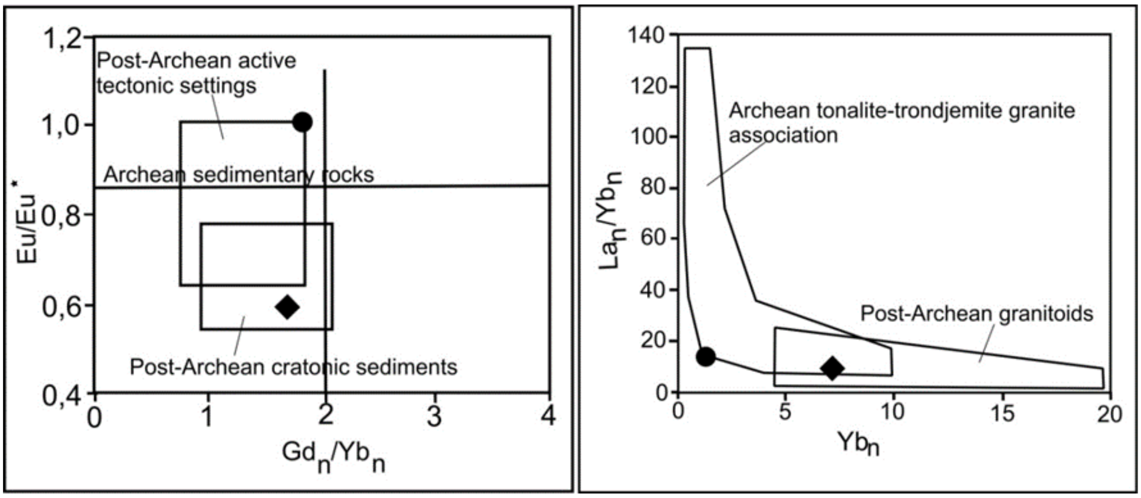

Fig. 3. Provenance area for garnet-muscovite-amphibole (rhombus) and amphibole-epidote-muscovite (circle) paragneisses of the Kharbei metamorphic complex, a – [6], b – [7]

Garnet-biotite-amphibole and biotite-amphibole gneisses occupy an area of uncertainty between para- and orthogneisses and could have formed due to tuffites or they are granitized amphibolites.

Garnet-epidote-two-mica and biotite-epidote-amphibole gneisses, according to discriminant functions, are orthogneisses, metamorphosed analogs of igneous rocks – granodiorites. They are close in geochemical features to granitoids of I and S types of island arc and collisional environments. Garnet-two-mica gneiss is characterized by zircons with resorbed forms and moderately smoothed edges, which may be a sign of high-temperature metamorphic transformations of the rock and, possibly, of its Precambrian age.

Conclusions

The gneisses of the Kharbei metamorphic complex are represented by para orthogneisses, and possibly also formations of mixed composition. Paragneisses, metamorphosed sandstones, are of the same age as amphibolites and may have different provenance area. Orthogneisses – metagranodiorites, most likely also have a Precambrian age and were formed either simultaneously with protoliths of amphibolites, or later – during collisional processes.

REFERENCES

1. Pystina, Yu. I., Pystin, A. M. (2002). Cirkonovaya letopis' ural'skogo dokembriya, UrO RAN, Ekaterinburg, 168.
2. Ulyasheva, N. S. (2012). Metabazity kharbejskogo kompleksa (Polyarnyj Ural). Geoprint, Syktyvkar, 98.
3. Velikoslavinskii, S. D., Glebovitskii, V. A., Krylov, D. P. (2013). Separation between sedimentary and magmatic silicate rocks by discriminant analysis of major element contents. Doklady Earth Sciences 453 (1). pp. 1150-1153.
4. Predovskiy, A. A. (1970). Geohimicheskaya rekonstrukciya pervichnogo sostava metamorfizovannyh vulkanogenno-osadochnyh obrazovanij dokembriya. Apatity, 115.
5. Neelov, A. N. (1980) Petrohimicheskaya klassifikaciya metamorfizovannyh osadochnyh i vulkanicheskih porod. Nauka, Leningrad, 100.
6. Taylor, S. R., McLennan, S. M. (1985) The Continental Crust: Its Composition and Evolution. Blackwell, Oxford, pp. 1-312.
7. Martin H. (1986) Effect of steeper Archean geothermal gradients on geochemistry of subduction-zone magmas. Geology 14 (9), pp. 753-756. DOI: https://doi.org/10.1130/0091-7613

First Geochemical Data on Lacustrine Sediments, Lake Bannoe (Bannoe), Southern Urals

YUSUPOVA Anastasia[1], KUZINA Dilyara[1], BATALIN Georgii[1], GAREEV Bulat[1], NOURGALIEVA Nouria[1]

[1] *Kazan Federal University, Kazan (RUSSIA)*
Email: yusupovaanast095@gmail.com

Abstract

This study is focused on the geochemical analysis of the bottom sediments sampled from Lake Bannoe. High sensitivity to climate change, a wide variety of facies in the sedimentary sections, and high sedimentation rate make lakes one of the best archives of paleoecological data. This study was driven by the fact that lake sediments are of great significance for understanding of climate changes. The main goal of this work was to obtain the most complete high-quality record of climate changes through geochemical analysis of lacustrine sediments.

Keywords: lake sediments, geochemical investigating, humidification of climate

Introduction

Lake sediments are formed from terrigenous and chemically dissolved material, as well as due to activity of biota. Lake sediments accumulate in dissected topography under humid conditions with intensive surface runoff. Soils and rocks in the catchment area are the main sources of terrigenous material [1]. Elemental analysis of lake sediments along with chemical weathering indices of the soils from distributive province and catchment area can help to decipher paleoclimatic changes recorded in the sediment [2, 3].

This work is devoted to the study of the bottom sediments sampled from Lake Bannoe, Southern Urals. The main goal is to identify the geochemical zones in the study area and related climatic periods in the Holocene.

Lake Bannoe (55º35’48” N 58º37’47” E) is located in the Abzelilovo District, Republic of Bashkortostan. The lake basin is of tectonic origin. The lake area is 7.7 km², the catchment area is 36.3 km², the length is 4.17 km, and the average width is 1.88 km. The maximum depth of the lake is 28 m; the average depth is 10.6 m. The water is fresh, bicarbonate-magnesium.

The climate in the Abzelilovo District is continental.

The selection of the study object was based on a priori and acoustic data to ensure the optimal conditions for core sampling [4].

Four core columns, 3.8-5.14 m long, were obtained based on the acoustic data. About 1000 samples were taken in total. All core samples were cut into smaller pieces (2 cm thick) for laboratory studies. Core column #3 was chosen as the object of this study.

Materials and methods

Nine conventional ^{14}C ages were obtained during the analysis of the samples taken from Lake Bannoe. The samples were sent to the Department of Geosciences of the National Taiwan University (NTUAMS ^{14}C-dating Lab), where the measurements were carried out using the

1.0 MV HVE accelerator mass spectrometer. Then, the radiocarbon ages were calibrated to the OxCal v4.2.4 Bronk Ramsey (2013) ages using and the IntCal 13 calibration curve.

The mineralogical composition of 26 samples (Column #3) was determined using the Bruker D2 Phaser diffractometer with 20 cm step.

The samples used for the determination of major and trace element composition were collected at 10 cm intervals using the Bruker S8 Tiger X-ray Fluorescence spectrometer. The output values were corrected with loss on ignition, which was determined through combustion for 1.5-2 h at 1100 °C.

Chemical analysis data were used to calculate the chemical weathering indices (such as [5]). One of the basic indicators of weathering, usually calculated from the major element geochemistry of clay sediments, is the CIA index:

$$CIA= ([Al_2O_3/(Al_2O_3+CaO^*+Na_2O+K_2O)] \times 100,$$

where CaO* is the amount of CaO in silicate minerals only) [6].

In this work, the indicators of weathering variability, such the mobile/immobile ratio, were used. A number of studies have demonstrated that Ca, Mg, K and Y are more soluble and mobile. Al and Si, however, are considered insoluble and stable [5]. All the elements were normalized by Al to evaluate chemical solution, hydrolysis and migration with respect to Al, which is the most common and insoluble element (under both oxic and anoxic conditions).

(Ca+Mg+K)/Al, K/Al, Fe/Al and Ca/Al [5] were used to reflect chemical weathering in the drainage basin. The higher ratios indicate predominance of soluble and mobile elements as a result or stronger chemical weathering (rainfall increasing), and vice versa [5].

The higher amount of Sr in the sediment suggests stronger chemical weathering because Sr is more mobile and, consequently, is more easily removed from parent rocks [5]. The CaO/MgO (Ca/Mg) ratio can be used as an indicator of water budget. Higher CaO/MgO (Ca/Mg) ratio generally suggests larger amounts of authigenic carbonate formed under warm and dry climate conditions [5, 7]. Since Fe and Mn are sensitive to redox conditions, the higher Fe/Al and Mn/Al ratios usually reflect oxic conditions at the time of deposition, and vice versa [8].

Results

The radiocarbon dates obtained during the analysis are given in Table 1. The values of LOI (loss on ignition), SiO_2, P_2O_5, Na_2O, K_2O, Al_2O_3, TiO_2, Fe_2O_3, CaO, MgO, MnO, Rb, Sr and their variations are presented in Fig. 1. To sum up, six geochemical zones were revealed. The ratios of the major elements are used to quantify the intensity of chemical weathering and evaluate weathering indices such as (Ca+Mg+K)/Al, Ca/Al, K/Al, Ca/Mg, Na/Al, Si/Al, Fe/Al.

The variations of (Ca+Mg+K)/Al, Ca/Al, K/Al, Ca/Mg, Na/Al, Si/Al, Fe/Al and CIA are shown in Fig. 2. The CIA at 506-468 cm have lower values. The ratios of mobile elements to immobile Al, such us (Ca+Mg+K)/Al, Ca/Al, K/Al, Ca/Mg, Na/Al are high. The values of Si/Al and Fe/Al are low.

Table 1. ^{14}C dating results for core column DH-99B

Sample	Depth (cm)	Age (calendrical), years	Error (±)	Age, years (^{14}C)	Error (±)
516	32	1580	170	1693,727	84
545	90	2910	160	2762,015	82
575	150	4270	180	3873,758	76
608	214	5260	225	4594,664	85
651	300	6805	200	5957,942	84
669	336	7880	185	7090,745	109
703	404	8865	265	8021,161	93
732	462	9690	235	8634,794	100
753	504	12555	175	10627,02	101

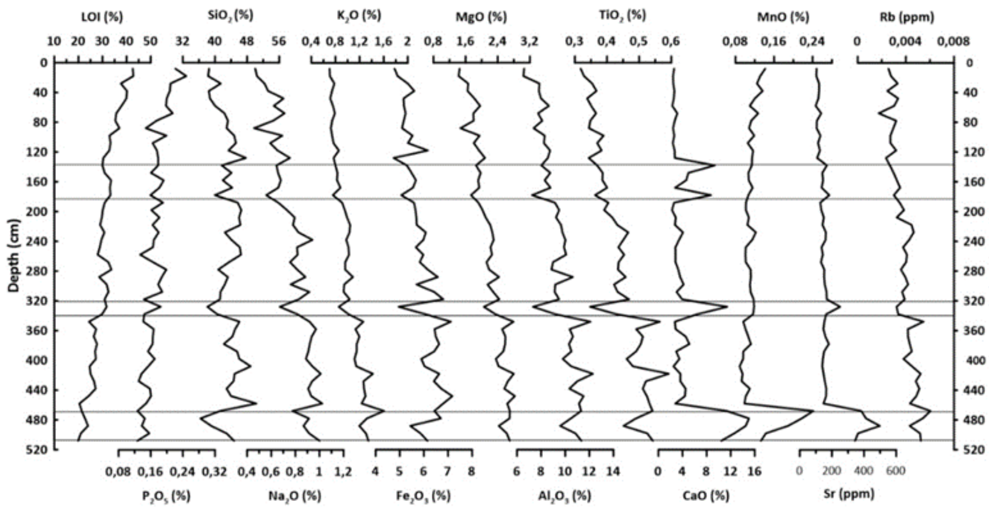

Fig. 1. Vertical distribution of major oxides (%), trace elements and LOI values

Between 468 and 340 cm, the values of (Ca+Mg+K)/Al, Ca/Al, K/Al Ca/Mg, Na/Al decrease sharply. Si/Al increases from 3.21 to 4.14, Fe/Al varies from 0.71 to 0.85. The values of CIA are low and vary from 67.3 to 70.85.

The interval between 340 and 320 cm is characterized by a sharp increase in the values of the weathering indicators: (Ca + Mg + K)/Al, Ca/Al, K/Al, Ca/Mg, Si/Al, Fe/Al. The values of Na/Al vary from 0.124 to 0.128. The CIA values decrease and change from 67.3 to 68.08.

Up the section, between 320 and 182 cm, the values of the main indicators, such as (Ca + Mg + K)/Al, Ca/Al, K/Al, Ca/Mg, Na/Al, Si/Al, decrease as well. The values of Fe/Al. on the other hand, increase. The CIA varies from 67.6 to 71.9.

A sharp increase of (Ca + Mg + K)/Al, Ca/Al, Ca/Mg, Na/Al, Si/Al can be seen between 182 and 138 cm. The values of CIA vary between 69.96 and 71.57. Values of K/Al vary from 0.07 to 0.08; Fe/Al varies from 0.82 to 0.92.

In the last section (138-0 cm), the CIA values increase from 67.97 to 74.1. The values of (Ca + Mg + K)/Al, Ca/Al, Ca/Mg, Na/Al decrease, and values of K/Al change between 0.068 and 0.084. The values of Si/Al and Fe/Al also increase.

X-ray diffraction analysis was used to determine the mineralogical composition of the sediment (Fig. 3). Quartz (5-30%), chlorite (5-10%), albite (10-30%), mica (5-20%), pyrite (1-5%), dolomite (1-5%), gypsum and microcline were found. Talc (1-5%) and hornblende (5-10%) were noted at a depth of 486 cm. Cristobalite (1-5%) and tridymite (1-5%) were found between 6 and 446 cm, dolomite (1-5%) and microcline (5-10%) were noted at a depth of 346 cm. Aragonite (1-10%) was found at a depth of 466-506 cm. Hornblende (5-10%) was found at a depths of 246 and 486 cm. Gypsum (1-5%) was found at a depth of 26-46 cm.

Depth (cm)	Quarts	Pyrite	Chlorite	Albite	Mica	Cristobailite	Tridymite	Microclaine	Calcite	Aragonite	Hornblende	Dolomite	Gypsum
6	++++		++	++++	++	+	++	++					
26	++++		++	++++	++	+	++	++					+
46	+++		++	++++	+++	+	++	++					+
66	++++		++	++++	++	+	+	++					
86	++	+	++	++++	++	+	++	++					
106	++	+	++	++++	+++	+	++	++					
126	++++		++	++++	+++	+	+	++					
146	++++	+	++	++++	++	+	+		+++			+	
166	++++		++	++++	+++	+	+	++	+				
186	++++	+	++	++++	+++	+	+	++				+	
206	++++	+	++	++++	+++	+	+						
226	++++	+	++	++++	+++	+	+		+				
246	++++	+	++	++++	++	+	+		+		++	+	
266	++++	+	++	++++	+++	+	+					+	
286	++++	+	++	++++	+++	+	+		+++			+	
306	++++	+	++	++++	+++	+	+		+			+	
326	++++	+	++	+++	++	+	+	++	+++			+	
346	++++	+	++	++++	+++	+	+	++	+				
366	++++	+	++	++++		+	+		+++			+	
386	++++	+	++	++++	+++	+	+		++			+	
406	++++	+	+++	++++	+++	+	+					+	
426	++++	+	++	++++	+++	+	+		+			+	
446	++++	+	++	++++	+++	+	+		++			+	
466	++++	+	++	+++					++	++		+	
486	++++	+	++	+++	++				+++	++	++	+	
506	++++	+	++	+++	+++				+++	+		+	

(+, 1-5%; ++, 5-10%; +++, 10-20%; ++++, 20-30%)

Fig. 3. Mineralogy of Lake Bannoe

Discussion

The variations in the values of CIA, Ca/Al, CaO/MgO, Mn/Al, K/Al, Mg/Al, Fe/Al and Si/Al are shown in Fig. 4 derived from Fig. 1 and Fig. 2. It shows the variation of indicators with depth taking into account the radiocarbon data.

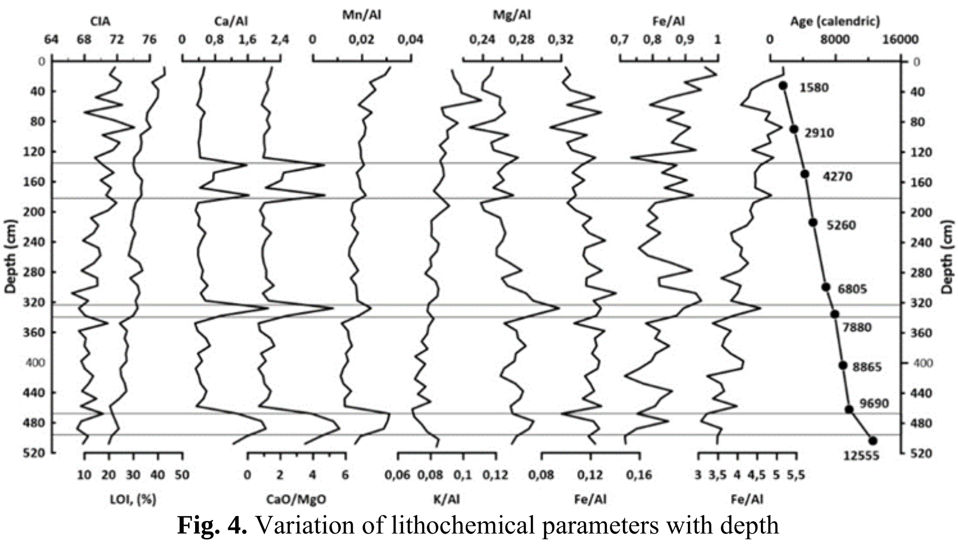

Fig. 4. Variation of lithochemical parameters with depth

The interval between 506 and 468 cm (12691-9963 years) is marked by increased values of CaO/MgO, Ca/Al, Fe/Al, Mn/Al, Mg/Al and Na/Al indicating increased rainfall. The next zone (9963-7908 years, 468-340 cm) is characterized by decreased values of Ca/Al, CaO/MgO, Mn/Al, Fe/Al and CIA. Probably, at that time the climate was, likely, drier. The values of CaO/MgO, Ca/Al, Mg/Al, Na/Al, Fe/Al, Mg/Al and Si/Al increase again between 340 and 320 cm (7908-7343 years): the rainfall increased. Low values of Fe/Al, Ca/Al, Mn/Al, Mg/Al and high values of CIA between 320 and 182 cm (7343-4750 years) indicate a decrease in rainfall. The values of Ca/Al, CaO/MgO, Si/Al, Fe/Al, Mg/Al, K/Al increase between 182 and138 cm (4750-3998 years) due to an increase in the intensity of weathering. The rainfall, probably, increased at that time as well. The values of Ca/Al, CaO/MgO, Mg/Al and Na/Al between 138 and 0 cm (3998 - 892 years) are low and point likely on rainfall decreasing [5].

The revealed intervals have been linked with stratigraphic and climate schemes (Table 2) [9, 10].

Table 2. The column #3, lake Bannoe by stratigraphic and climate terms. [9, 10]

Series/ Epoch	Stage/ Age	Age, years	Climatic staging (Europe)	Column No.3, Lake Bannoe		
			Stage (interval, years)	Interval, years	Depth, cm	Rainfall increase by geochemical data (+)
Holocene	Meghalayan	4250-0	SA (~2500-0)	3998-892	138-0	
			SB (~5000-2500)	4750-3998	182-138	+
	Northgrippian	8236-4250	AT (~8000-5000)	7343-4750	320-182	
				7908-7343	340-320	+
	Greenlandian	11700-8236	BO (~9000-8000)	9963-7908	468-340	
			PB (>~9000)			
Pleistocene	Tarantian	12900-11700		12691-9963	506-468	+

The interval between 506 and 468 cm refers mainly to the Tarantian stage of the Pleistocene. The interval between 468 and 340 cm (9963-7908 years) belongs to the Grendlandian stage and the Preboreal (PB) and Boreal (BO) climatic stages. The intervals between 340 and 320 cm (7908-7343 years) and 320 and 182 cm (7343-4750 years) belong to the Northgrippian stage and to the Atlantic (AT) climatic stage. The sediments in the intervals between 182 and 138 cm (4750-3998 years) and 138 and 0 cm (3998 - 892 years) were formed during the Meghalayan stage and the Subboreal (SB) and Subatlantic (SA) climatic stages.

Conclusions

The radiocarbon data showed that the sediments of Lake Bannoe are about 12,700 years old. Six geochemical zones were identified. These zones were compared with the stratigraphic scale of the Holocene and Pleistocene and the corresponding climatic stages. The lithochemical analysis showed that chemical weathering increased between 12691 and 9963 years (Late Pleistocene), 7908 and 7343 years (Atlantic), 4750 and 3998 years (Subboreal), and decreased between 9963 and 7908 years (Boreal), 7343 and 4750 years (Atlantic), 3998 and 892 years (Subboreal and Subatlantic).

Acknowledgments

This work was funded by the subsidy allocated to Kazan Federal University for the state assignment # 671-2020-0049 in the sphere of scientific activities. Sediment sampling and radiocarbon dating was funded by the Russian Science Foundation under the grant #18-17-00251.

REFERENCES

1. Bertrand, S., Xavier, B., Julie, C., Charlet, F., Urrutia, R., Espinoza, C., Lepoint, G., Charlier, B. & Fagel, N. (2005). Temporal evolution of sediment supply in Lago Puyehue (Southern Chile) during the last 600 yr and its climatic significance. Quaternary Research 64, pp. 163-175.

2. Nurgaliev, D., Kuzina, D., Krylov, P., Gareev, B., Kosareva, L. Climate changes over the last 13500 years based on lake sediments studies (Lake Bolshoe Miassovo, South Ural, Russia). International Multidisciplinary Scientific GeoConference Surveying Geology and Mining Ecology Management, SGEM 19 (4.1), 2019, pp. 925-930.
3. The magnetic properties of sediments of lake Bolshoe Yarovoe and reconstruction of the paleoclimate at the interval from 500 to 8000 years ago/V. p. Shcherbakov, L. R. Kosareva, D. K. Nurgaliev *et al.*, Proceedings of the 12th international school-conference Problems of Geocosmos (October 8-12, 2018, Saint Petersburg, Russia), pp. 258-263.
4. Krylov P. S, Nurgaliev D. K, Yasonov P. G. (2020). Seismoacoustic research of Lake Bannoe bottom sediments (South Ural, Russia). ARPN Journal of Engineering and Applied Sciences 15 (1), pp. 133-135.
5. Zhong, W., Zhangdong, P., Xue, J., Ouyang, T., Tang, X., Cao, J. (2012). Geochemistry of sediments from Barkol Lake in westerly influenced northeast Xinjiang: Implications for catchment weathering intensity during the Holocene. Journal of Asian Earth Sciences 50, pp. 7-13.
6. Nesbitt H.W., Young G. M. (1982). Early Proterozoic climates and plate motions inferred from major element chemistry of lutites. Nature 299, pp. 715-717.
7. Lasaga A. C., Soler J. M., Ganor J., Burch T. E., Nagy K. L. (1994). Chemical weathering rate laws and global geochemical cycles. Geochim Cosmochim Acta 58, pp. 2361-2386. doi: 10.1016/0016-7037(94)90016-7
8. Wang S. M., Yu Y. S., Wu R. J., Feng M. (1990b) The Daihai Lake: environment evolution and climate change. University of Science and Technology of China Press, Hefei, pp. 1-191 (in Chinese)
9. Mangerud, Jan, Anderson, Svend T., Berglund, Bjorn E., Donner, Joakim J. (1974). Quaternary stratigraphy of Norden: a proposal for terminology and classification (PDF). Boreas 3 (3), pp. 109-128. doi:10.1111/j.1502-3885. 1974.tb00669. x.
10. The official website for the Quaternary system stratigraphy is http://quaternary.stratigraphy.org/major-divisions/

Lithological and Mineralogical Features of the Volga Oil Shale Sections Near Gorodishche Village (Undory)

ZAKHAROVA Nadezhda[1], ESKIN Aleksey[1], KOROLEV Albert[1], KHAYUZKIN Aleksey[1]

[1] *Kazan Federal University, Kazan (RUSSIA)*
Email: zaharova.nadyuch@mail.ru

Abstract

This paper considers the lithological and mineralogical features of the Volga oil shale sections near Gorodishche village. Optical-microscopy, SEM, X-ray and thermal studies of high-carbon rocks have shown their complex polymineral composition. Based on the data obtained, the main sources of mineral and organic matter input into the Central Russian paleobasin during the oil shale formation have been established. The conditions of the formation of high-carbon deposits in shale strata of the Tithonian Stage were modelled using sedimentation analysis and ratio of main components.

Keywords: Central Russian paleobasin, Tithonian stage, oil shale, shale composition and conditions of formation

Introduction

Geological sections of the Ulyanovsk region, exposed in outcrops on the right bank of the Kuibyshev Reservoir, have long attracted the attention of geologists studying Upper Jurassic deposits ([1], [6], [7]). In recent years, interest in them has been aroused by the discovery of increased concentrations of rare earth elements in the Tithonian stage terrigenous complex ([2]) and also new technological possibilities for development of oil shale ([3], [8], [9]). Considering the relevance of this topic, a lithological and mineralogical study was carried out of the high-carbon deposits located near Gorodishche village in the north of the Ulyanovsk region.

Objects and Methodology

Based on morphological features of oil shale and carbonaceous clays, the main methods for studying rocks were X-ray, optical-microscopy, thermal and electron-microscopic (SEM) analyses. X-ray analysis, to examine composition of samples, was carried out on a D2 Phaser diffractometer (Bruker, Germany). Research modes: X-ray tube voltage – 30 kV, current – 30 mA, scanning step – 0.02; speed – 1 deg/min; scanning angles in the Bragg-Brentano geometry – 3 to 40°; using a standard powder sample. Thermal analysis was carried out on an STA 449 Jupiter F3 device to determine the heat of combustion and phase transitions of oil shale structural components. The firing interval was from 30 to 1000 °C; heating step – 10 deg/min; with continuous air purging. Optical-microscopic studies were carried out on a Zeiss AXIO Imager A2 polarizing microscope equipped with an AxioCam ICc 5 digital camera.

In the Gorodishche village sections, high-carbon rocks are found in upper parts of outcrops, just below the cliff edges. Below and above, they are limited by greenish-gray calcareous clays with a horizontally layered texture. Due to their brownish, dark gray and black color, they stand out well against the background of lighter colored rocks. The apparent thickness of oil shale layer on the Volga River right bank is about 4.0 m. The rocks are characterized by a hiddengrained structure, a horizontal thin-layered texture, and clearly visible schistosity along the depositional bedding. Oil shales contain large inclusions of calcareous organic remains: bivalve mollusks, ammonites and belemnites. Along with marine fauna fragments, there are relatively large (up to 1.5 cm) pyrite aggregates scattered in the rocks. Due to oxidative processes, finely dispersed pyrite inclusions partially transform into earthy aggregates of gothite-hydrogoethite, which mark oil shale by a brownish color. Within the production zone, high-carbon rocks are broken up by systems of vertical and horizontal fractures and form platy units of various sizes.

Yellow earthy jarosite aggregates are noted along cracks on water infiltration paths ([5]).

Results

According to X-ray data, oil shale has a complex polymineral composition. It contains clay and clastic minerals. The total clay component is 15-24%, dominated by mixed-layer phases of illite-montmorillonite composition, muscovite in smaller quantities (9-13%), and chlorite (3-6%) and kaolinite (4-6%) are also noted. The next most important rock-forming minerals are calcite (23-38%), quartz (17-32%), albite (3-6%), pyrite (2-3%) and gypsum (1-2%).

According to optical-microscopic studies data, oil shales have a pelitic structure and a horizontally layered texture, which is caused by an uneven layered distribution of organic matter (Fig. 1). The rocks are composed of finely dispersed clay particles with axially oriented texture. Due to the well-developed contacts along the basal planes, clay minerals form a dense aggregate with general optical extinction. In the intergranular space of clay particles, there are numerous inclusions of organic matter, which cause the black color of the rock. Organic matter forms scattered colloidal clots, films, and wavy microlayers. In some samples, it fills the cavities of sedimentation-diagenetic cracks which formed as a result of organo-mineral ooze sediment stratification during its lithification. Oil shales contain numerous inclusions (up to 25%) of silt size clastic grains. Among them, semi-rounded quartz grains predominate; angular fragments of feldspars and muscovite flakes are present in smaller quantities. Some mineral fragments are scattered in rock, some are concentrated in lenticular segregations. Also, rocks contain unevenly distributed inclusions of calcareous organic remains (up to 15%). Large shells of mollusks have a predominant orientation according to rock bedding; small detritus is located chaotically. Aggregates of pyrite and chalcedony are authigenic minerals. Pyrite, in the form of framboidal segregations, and chalcedony in the form of small lenses composed of fine-grained silica. Microscopic studies indicate that the rocks are weakly porous (first %). The pores are of subcapillary dimension, oriented along the basal planes of clay particles.

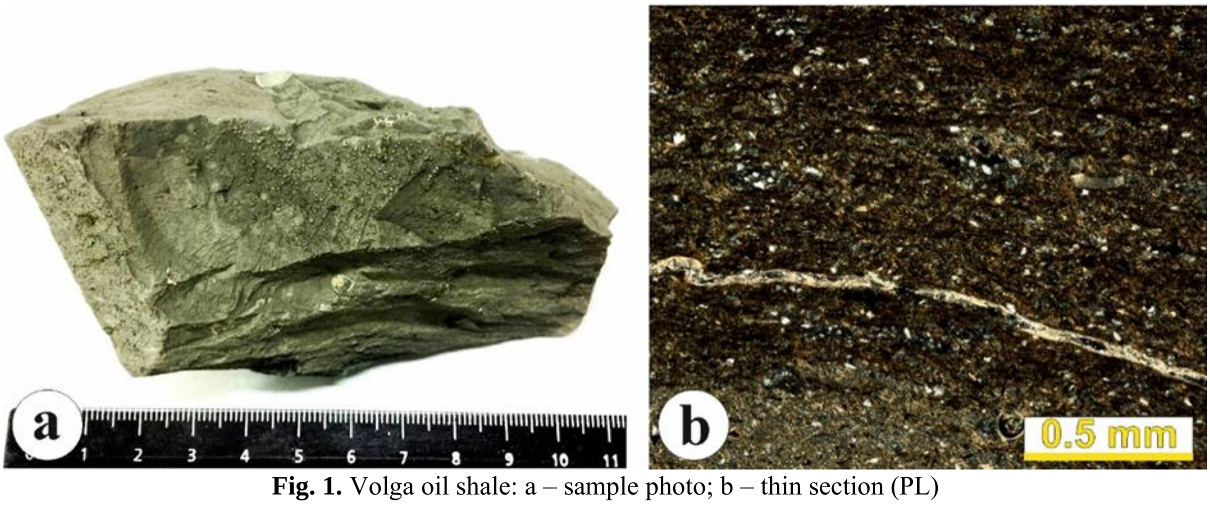

Fig. 1. Volga oil shale: a – sample photo; b – thin section (PL)

SEM data enabled more detailed studies of the relationships between mineral components in rocks. Analysis of the sheared surface of oil shale showed the predominance of laminar, matrix and fine-celled microstructures (Fig. 2). Laminar types of microstructures prevail in places where clay particles accumulate. They form separate thin layers without inclusions of large mineral fragments. Clay minerals create extended wavy microaggregates due to the subparallel arrangement of lamellar structural elements. These aggregates are oriented according to the sedimentation bedding of the rock. The clay component is evenly distributed; there are no visible boundaries between them. Clay particles are well sorted and have a high degree of bedding orientation. All this gives the elongated microaggregates the appearance of a laminar (plane-parallel) flow. In localization places of relatively large mineral fragments and organic remains, clay aggregates form matrix or cellular microstructures. The matrix structure is expressed in the enveloping of large, isolated fragments with clay aggregates, like a “shirt”.

In this case, clay particles are oriented by their basal planes parallel to the solid substrate surface. The lamellar structural elements in the enveloping microaggregates are located somewhat more randomly compared to clay minerals of laminar microstructures. Fine-cellular structure prevails in places where planktonic remains of coccolithophorids have accumulated.

In this case, clay particles fill the spaces between organic residues. Analysis of oil shale structure shows that dispersed-coagulated microstructures predominate in the rock, the formation of which occurred during slow lithification of bottom silty sediment under conditions of gradual increase in pressure of overlying strata ([10]).

Along with mineral component analysis, the organic matter of the oil shale was studied to determine the industrial importance of shales as high-carbon rocks. It is known that natural organic matter is mostly multicomponent. It combines various molecular compounds with specific boiling points. The composition of studied organic components can be determined from the DSC, differential thermal analysis curve, using reference thermograms ([11]). The combination of DSC with the TG weight loss curve makes it possible to determine the quantitative content of organic component in rock.

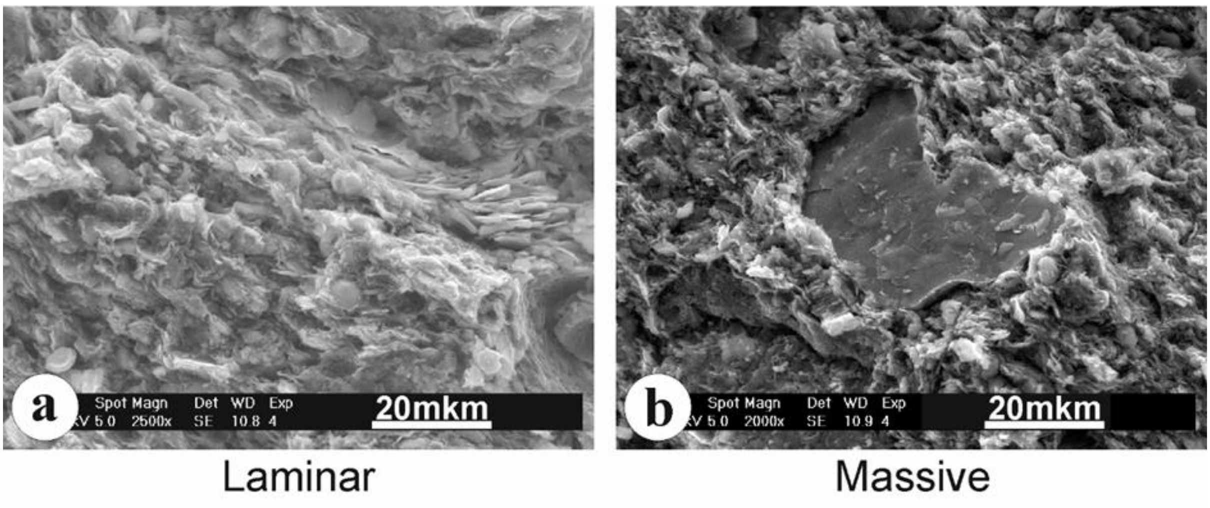

Fig. 2. SEM photo of oil shale sheared surfaces with different microstructures

The study of organic matter pyrolysis in oil shale showed that with a sequential increase in heating temperature of high-carbon rocks samples, several exothermic effects appear on the DSC curve in the temperature range 200-600 °C (Fig. 3). According to previous studies ([4]), similar exo-effects in the interval analyzed are associated with depolymerizing of kerogen macromolecules. In this case, the resulting decomposition products (hydrogen, carbon dioxide, water, light and heavy resins, etc.) are successively released in the form of gases, leading to the exo-effects on the DSC curve. By analogy with hydrocarbon (HC) of the oil series: the observed exo-effect at a temperature of 220-300 °C can be interpreted as boiling of light HC fractions; the appearance of an exo-effect at a temperature of 300-420 °C – as boiling of middle HC fractions; the appearance of an exo-effect at a temperature of 420-550 °C – as boiling of heavy HC fractions. The total weight loss of oil shale during release of organic matter on the TG curve is from 5 to 20%.

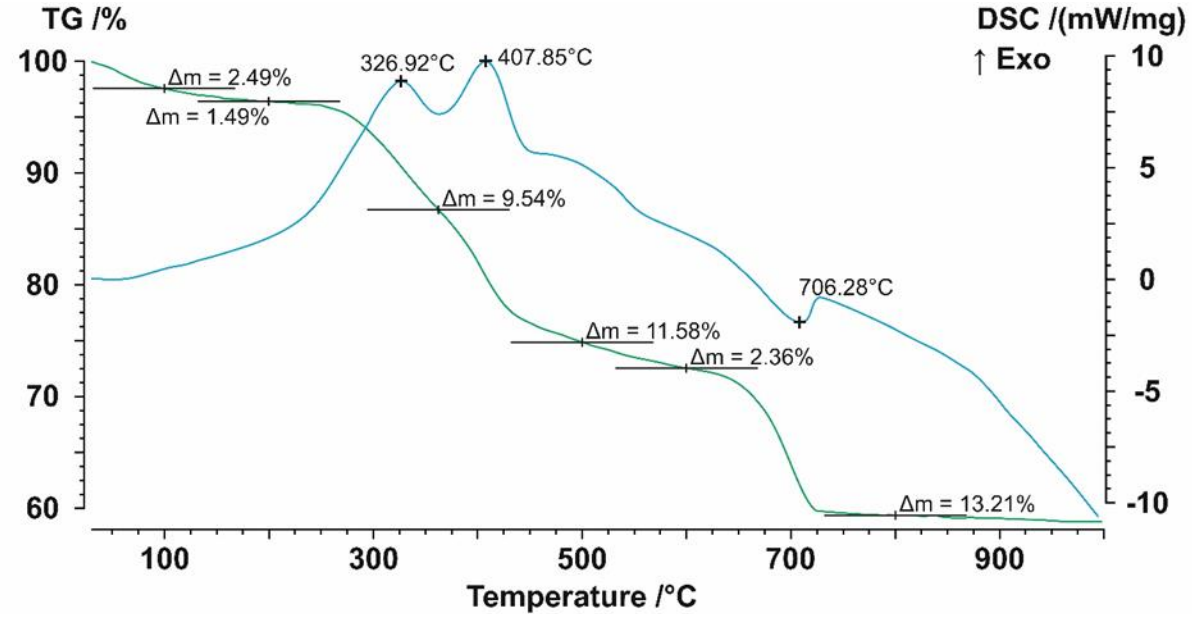

Fig. 3. Synchronous thermal analysis data of oil shale. The blue line is the differential scanning calorimetry (DSC) curve, the green line is the mass loss curve (TG)

Discussion

Studies have shown that oil shales were formed under the influence of many factors. Their mineral component is determined by features the lithological composition and geomorphological structure of coastal part of the Central Russian Paleosea. The gently sloping plain that existed in the Tithonian in the Ulyanovsk region, adjacent to the marine paleobasin edge provided a constant influx of clastic material. The source of incoming material was the Middle Permian carbonate-terrigenous deposits, which compose the Ural land. This explains why the composition of the Volga oil shales clay minerals is similar to the composition of Urzhumian clays.

The mild warm humid climate favored the development of abundant vegetation along the coastal strip. The root layer of soil and marshiness of territory prevented intensive erosion of the Urzhumian rocks. Therefore, mainly finely dispersed material and plant detritus entered the sea basin with surface rainfall. Introduced minerals and rock fragments in the basin were supplemented with biogenic components. A shallow warm sea of normal salinity, with the usual oxygen and gas regime, was favorable for development of marine fauna and flora. The massive distribution of planktonic algae (Coccolithophorida), belemnites, ammonites, bivalves, and graptolites resulted in a high carbonate content of the shale series. The high productivity of phytoplankton and stagnant conditions in depressions of the Central Russian Paleosea contributed to the establishment of anoxic conditions in the deep parts of the basin. The low oxygen content inhibited subsequent decomposition of organic matter, and the development of benthic communities of cyanobionts enriched the forming rocks with pyrite aggregates. The thin parallel lamination in strata indicates calm depositional conditions, which created preconditions for slow clay mineral aggregation. During the stage of watered silty sediment, the centers of aggregation were fragments of mineral grains and organic remains. They were a solid substrate in a colloidal solution and collected clay particles on their surface, which, enveloping them, formed microaggregates like a "shirt". With subsequent compaction and dehydration of the silty sediment, the clay microaggregates formed laminar microstructures.

During this period, the face to face type aggregation of clay plates and scales was dominant.

In the process of clay mineral coagulation and mud compaction, organic matter was simultaneously adsorbed onto finely dispersed aggregates. These processes contributed to the gradual accumulation of oil shales with polymineral composition.

Acknowledgements

The study was supported by the Russian Science Foundation, project № 19-77-00019.

REFERENCES

1. Linovsky, E. (1930). Undrovskiy shale (their value and prospects). Pub. h. of Ulyanovsk, Ulyanovsk, p. 50.
2. Samoilov, A. G., Engalychev, S. Yu., Zozyrev, N. Yu., Shelepov, D. A., Ilyasov, V. N. (2018). Renewability of the Upper Jurassic oil shale in the central part of the Volga shale basin. Metallogenia 75, pp. 67-78.
3. Korolev, E., Barieva, R., Eskin A. (2018). Perspective usage estimation of Volga region combustible shale as a power generating fuel alternative. IOP Conference Series: Earth and Environmental Science 155, pp. 1-7.
4. Korolev, E., Eskin, A., Korolev, A., Barieva, E. (2019). Stages of thermal transformation of oil shales organic-mineral substance of the Middle Volga region during combustion. IOP Conference Series: Earth and Environmental Science 282 (1), art. 012035.
5. Korolev, E. A., Kolchugin, A. N., Eskin A. A., Bakhtin, A. I., Barieva, E. R. (2019). Geochemical conditions of exogenous minerals formation of the weathering zone in the upper Jurassic deposits of the middle Volga region. SGEM 19 (3), pp. 835-840.
6. Mitta, V. V., Kostyleva, V. V., Glinskikh, L. A., Shurygin, B. N., Starodubtseva, I. A. (2014). Middle Jurassic stratigraphy in the southwestern part of the Republic Tatarstan. Stratigraphy and Geological Correlation 22 (1), pp. 28-43.
7. Zorina, S. O. (2007). Stratigraphy of middle upper Jurassic deposits in the East Russian plate. Stratigraphy and Geological Correlation 15 (3), pp. 32-41.
8. Zozyrev, N. Yu., Ilyasov, V. N. (2011). The multifunctional potential of the oil shales of the Volga Basin. Inovations in the anti-crisis economy. Oil and gas Geology 1, pp. 110-116.
9. Strizhakova, Yu. A. (2011). Modern directions of pyrolysis of oil shale. Chemistry of Solid Fuel 4, pp. 8-13.
10. Osipov, V. I., Sokolov, V. N., Rumyantseva, N. A. (1989). Microstructure of clay rocks. Pub. h. Nedra, 211.
11. Ivanova, V. P., Kasatov, B. K., Krasavina, T. N., Rozinova, E. L. (1974). Thermal analysis of minerals and rocks. Pub. h. Nedra, 399.

The *Phycosiphon*-Like and *Diplocraterion* Trace Fossils from the Permian and Triassic of the Southern Verkhoyanie (Republic of Sakha – Yakutia, Russian Federation)

MIFTAKHUTDINOVA Dinara[1], SILANTIEV Vladimir[1], KUTYGIN Ruslan[1,2], DAVYDOV Vladimir[1,3], KILYASOV Afanasiy[2]

[1] *Kazan Federal University, Kazan (RUSSIA)*
[2] *Diamond and Precious Metal Geology Institute, Siberian Branch of the Russian Academy of Sciences, Yakutsk (RUSSIA)*
[3] *Department of Geosciences, Boise State University, Boise (USA)*
Email: DNMiftakhutdinova@kpfu.ru

Abstract

Trace fossils are described from the marine Upper Permian and Lower Triassic siliciclastics of Southern Verkhoyanie Mountain System for the first time. The ichnogenera *Phycosiphon*, *Zoophycos* and *Diplocraterion* are dominant in the recognized ichnofossil assemblages. The Middle to Late Permian *Phycosiphon* and *Zoophycos* assemblages correspond to *Zoophycos* ichnofacies and are specific to deep-water environments. The Early Triassic *Diplocraterion* traces refer to the *Skolithos* ichnofacies.

Keywords: Ichnotaxonomy, paleoenvironment, Southern Verkhoyanie, Russia

Introduction

The marine siliciclastics Upper Paleozoic and Triassic of the South Verkhoyanie Mountain System were studied during the mapping of the territory in the second half of the last century, but numerous traces of ichnofossils did not attract the attention of researchers and remained unstudied until now. The results of the preliminary study of the Permian and Lower Triassic ichnofossils from the Tiryakh-Kobyume reference section are published in this paper for the first time. We discuss their stratigraphic distribution and environmental significance of the recognized in this investigation ichnofossils and their assemblages.

Geological background

The collection of trace fossils has been obtained from the Tiryakh-Kobyume section (N 63.374284, E 140.945873) during fieldwork in 2019.

The Tiryakh-Kobyume section is located in the mouth of the Tiryakh-Yuryakh River, right tributary of the Kobyume River and in the downstream of the Kobyume on a distance about 4 km (Fig. 1B, C). The succession consists of the Permian (Kungurian-Changhsingian; about 4000 m thick) and Triassic (Induan, about 500 m thick) marine sediments [1], [2]. The succession has a transgressive-regressive architecture [3] and comprised of intercalating of sandstones, siltstones, and shales (Fig. 2) with subordinate interbeds of siderite and carbonate concretions, diamictites and rare bentonites. Numerous trace fossils are randomly distributed in the highly bioturbated rocks. The studied succession is a reference for the middle-late Permian Kobyume, Tiryakh, Lugovaya, and Privol'nyj Formations in the Kobyume subbasin of Verkhoyanie Basin that stretched along the eastern passive margin of Siberian Platform [4]. This thick siliciclastic succession is cyclic in nature filled the subbasin.

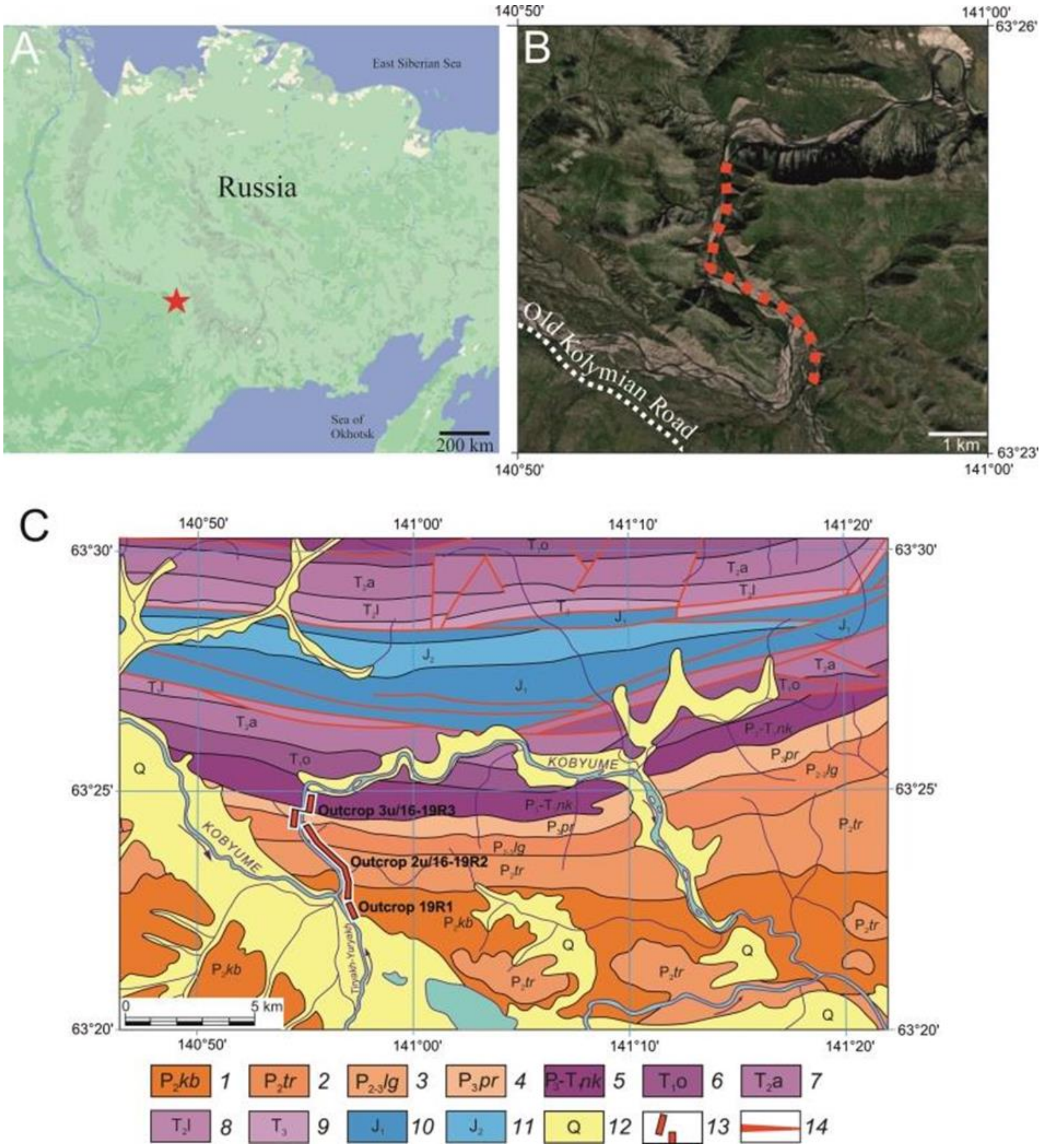

Fig. 1. Field locality (A, B) and geological map (C) (compiled from [5]) of the Tiryakh-Kobyume section. Formations: 1 – Kobyume, 2 – Tiryakh, 3 – Lugovaya, 4 – Privol'nyj, 5 – Nekuchan; Stages: 6 – Olenekian, 7 – Anisian, 8 – Ladinian; Series: 9 – Upper Triassic, 10 – Lower Jurassics, 11 – Middle Jurassic, 12 – Quaternary deposits, 13 – Tiryakh-Kobyume section, 14 – tectonic faults

The chronostratigraphic age of the Permian Formations was determined by bivalve and brachiopod assemblages [2].

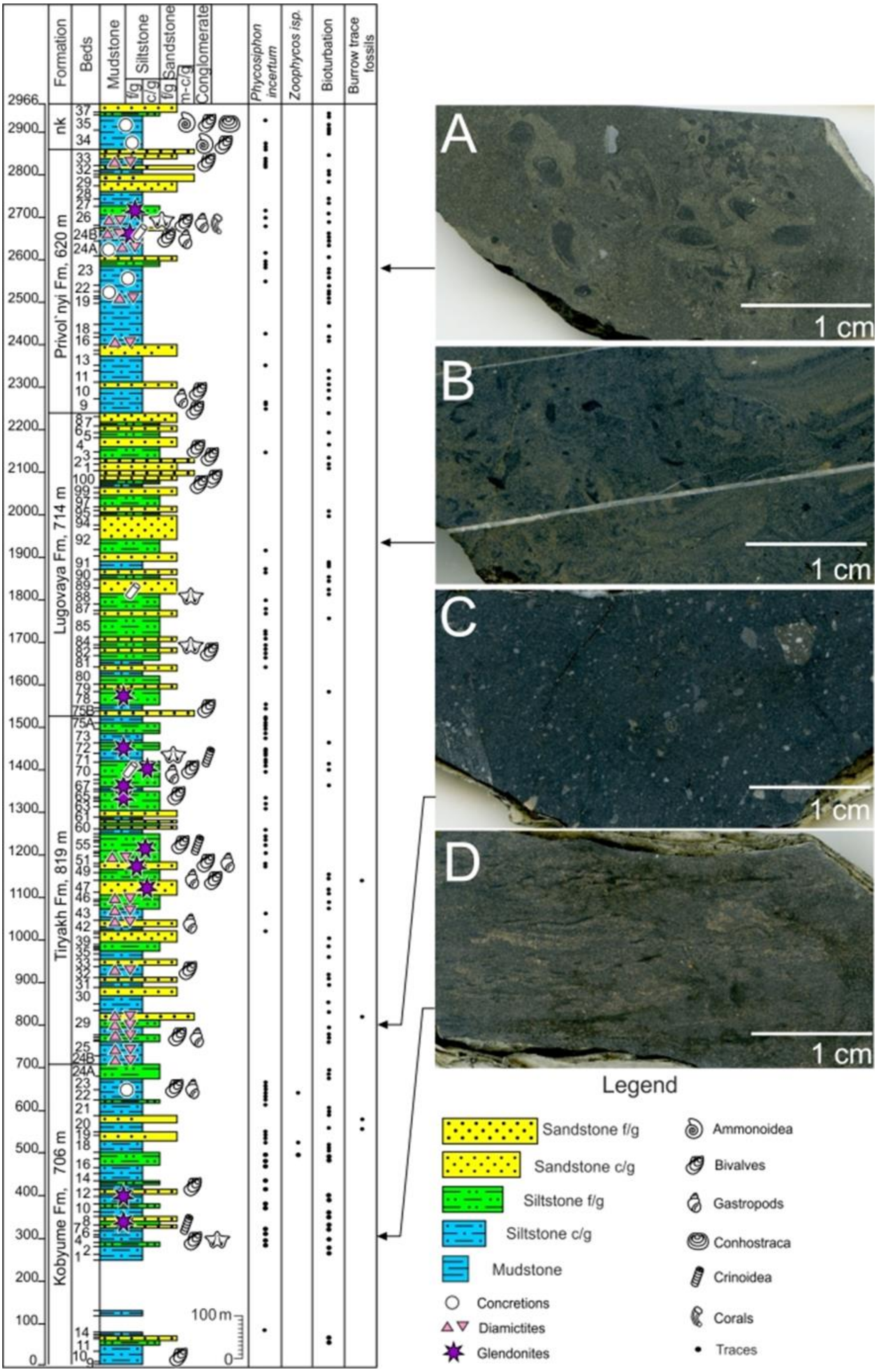

Fig. 2. Stratigraphic log of the section with the trace distribution and bioturbation: (A) siltstone with trace fossils (bed 23, Privol'nyj Fm); (B) bioturbated siltstone (bed 92, Lugovaya Fm); (C) diamictite (bed 29 Tiryakh Fm); (D) bioturbated siltstone (bed 5, Kobyume Fm)

Kobyume Fm composed mainly of siltstones with interbeds (1-4 m, rarely up to 10 m) various-grained sandstones and was formed in relatively calm conditions of the deep-water outer shelf. The Tiryakh Fm is characterized by the widespread distribution of diamictites. The sediments of the Tiryakh Fm accumulated in the marginal part of the shelf and were accompanied by the sedimentation of the mud flows. The glacial nature of diamictites is not excluded [6]. The Lugovaya Fm composed by a coarse alternation of thick (up to 10-40 m) beds of fine- to medium-grained sandstones with the units of a frequent interbedding of variably grained siltstones and sandstones. Rare horizons of gravel conglomerate and conglomerate are observed as well. The arrival of coarse psammitic material, closely related to the activity of large river deltas, indicates a significant sea level drop during the Lugovaya time.

The Privol'nyj Fm is characterized by alternating of mostly fine-grained siltstones (10-40 m, sometimes up to 70 m) with thick sandstone interbeds (from 1-2 m, up to 10-20 m in the upper part of formation). The lower part of the formation was formed in the conditions of the outer shelf. Sedimentation of the upper part of the formation occurred during a period of large regression that is documented in the entire Verkhoyansk basin.

The Triassic succession is composed of predominantly siltstones and rare sandstone units of the Nekuchan Fm, which is mostly referred to the Induan Stage. The boundary between the Permian and Triassic is conventionally drawn at 2.5 m above the base of the Nekuchan Formation based (Fig. 2) where the first occurrence of ceratite *Otoceras boreale* Spath is found [2].

The structure of the lower part of Nekuchan Fm is dominated by fine-grained siltstones (beds 34-36) with numerous carbonate-siliceous nodules containing ammonoids, bivalves, and conchostracans. These sediments accumulated in calm conditions of a relatively deep shelf without the influx of coarse terrigenous material. The upper part of Nekuchan deposits (bed 37 and above) is composed of various-grained sandstones, and probably associated with turbidite flows.

Material and methods

The collection contains 50 rock slabs with large (up to 10 cm) and medium-sized (1-5 cm) ichnofossils. Polished surfaces of the rock samples, which have been sampled for palaeomagnetic (195 samples), and geochemical (347 samples) studies were utilized in this investigation. More than 500 samples were totally studied. The hand samples were photographed during fieldwork and the polished slabs were scanned with EPSON scanner.

Results

Generally, fine-grained sediments, such as shales and siltstones, contain numerous trace fossils, although sometimes they were found in sandstone as well. Several trace fossils: *Phycosiphon incertum* (Fig. 3A-B), *Zoophycos* isp. (Fig. 3C), *Diplocraterion* isp. (Fig. 3D) were identified with certainty in our taxonomic interpretation.

Elongated blades, *Phycosiphon* Fischer-Ooster, 1858 are most common trace fossil in the siltstones of the entire section. They are flat or slightly inclined to the bedding plane. In polished samples, *Phycosiphon* traces form "Frogspawn" ichnofabric (Fig. 4A-D) [7]. In the Permian part of the section, these traces are characterized by relatively large size (2-4 mm) and are often found together with the *Zoophycos* Massalongo, 1855 – a helical or tongue-shaped multi-level system of spreite burrows (Fig. 3C).

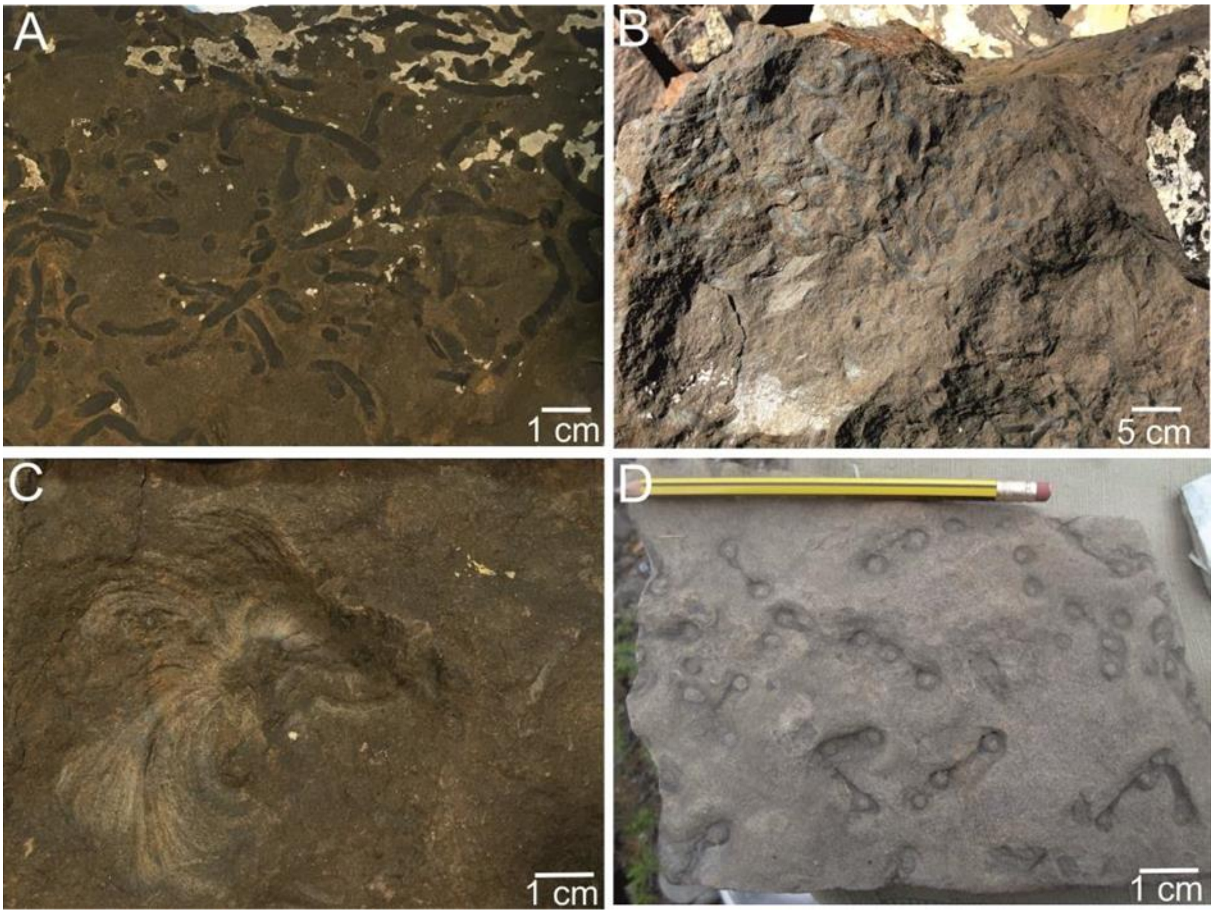

Fig. 3. Trace fossils of the Tiryakh-Kobyume section. (A), (B), Phycosiphon incertum of Permian siltstone beds. (A – bed 24B, Privol'nyj Fm; B – bed 90, Lugovaya Fm); (C) Zoophycos isp. (bed 86, Lugovaya Fm); (D) Diplocraterion parallelum of Triassic sandstones (bed 37, Nekuchan Fm)

No trace fossils were observed within the diamictite horizons and/or with glendonites (a calcite pseudomorphes after ikaite, formed in marine conditions in near-freezing waters).

Nevertheless, the bioturbation index (BI 4-5) of the intervals lacking of trace fossils indicates a high degree of the sediment processing (Fig.4E).

In the transitional Permian-Triassic interval, only *Phycosiphon*-like forms occur. The size of these forms decreases from 2-4 mm in Privol'nyj Fm to 0.5-1.5 millimeters in Nekuchan Fm, but the bioturbation index of rocks still remains quite high (BI 3-4) (Fig. 4F).

In the Triassic part of the section, the diversity of ichnofossils sharply decreases, although the bioturbation index remains high. In the sandstones of the Nekuchan Fm, we identify only vertical U-shaped spreite traces belonging to the ichnogenus *Diplocraterion* Torell, 1870.

Discussion

Phycosiphon and *Zoophycos* traces are among the most abundant ichnofossils of the marine sediments. Detailed interpretations of these remains depend on the taxonomy and co-occurrence of different taxa of trace fossils in ichnofossil assemblages, the nature of the ground and the age of the deposits [8]. *Phycosiphon* can be found at a wide range of depths: from the shelf to deep-water plains and indicates a large amount of organic matter in matrix, which is required for feeding animals [9].

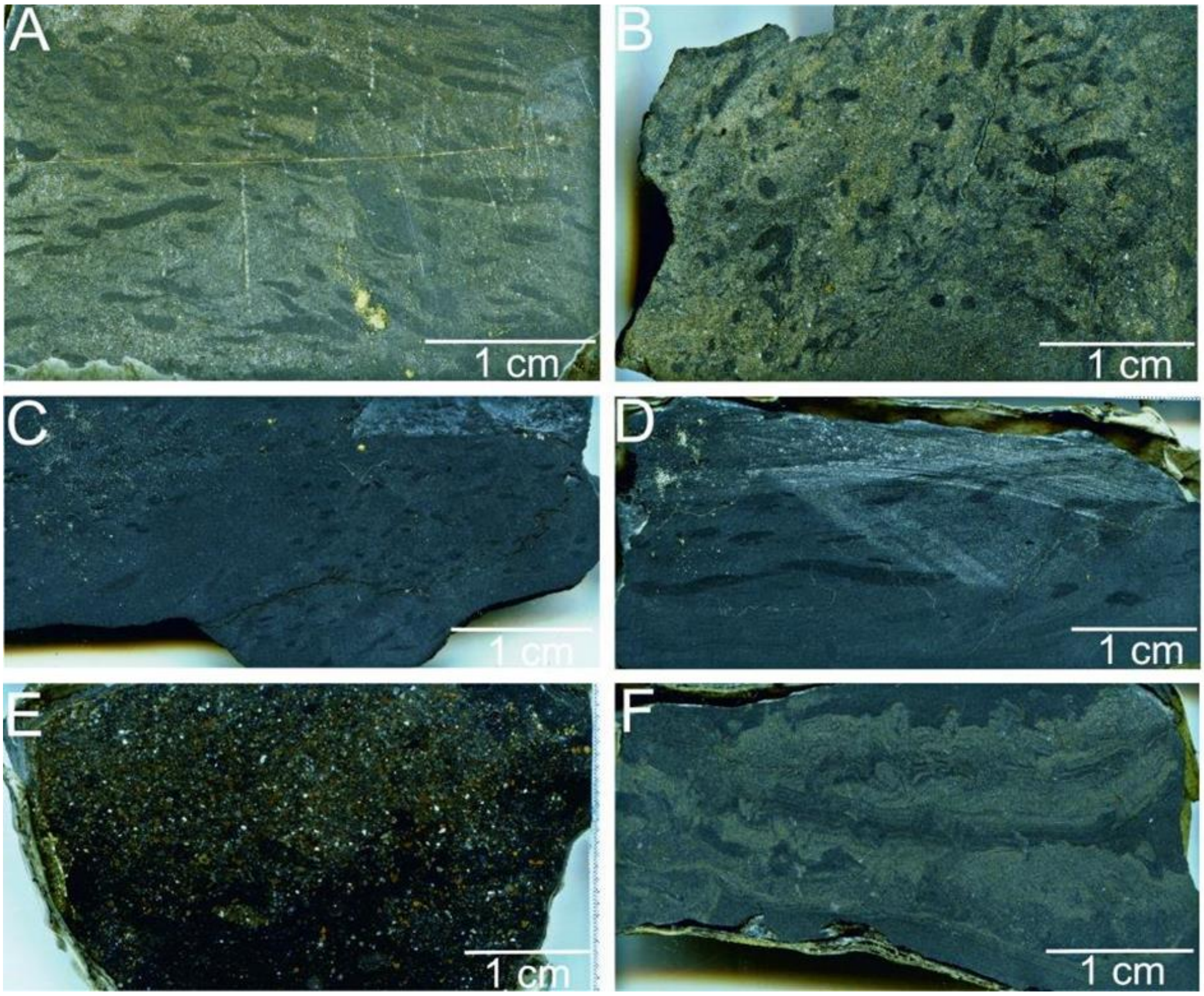

Fig. 4. Polished slabs with trace fossils. (A), (B), (C), (D) “Frogspawn” ichnofabric of Phycosiphon incertum traces (A – bed 34, Nekuchan Fm; B – bed 33, Privol’nyj Fm; C – bed 25 Privol’nyj Fm; D – bed 70 Tiryakh Fm); (E) bioturbated diamictite, bed 33, Privol’nyj Fm; (F) bioturbated siltstone (bed 27, Tiryakh Fm)

The horizontal and subhorizontal orientation of the *Phycosiphon* to the bedding plane indicates calm and lower energy conditions of sedimentation in the moderate-deep-sea shelf below the base of storm waves with low oxygen content [10], [11]. It can also indicate an uneven sedimentation pattern with alternating episodes of slow sedimentation and enrichment of sediment with organic matter and episodes of rapid sedimentation poor in organic matter. This is also typical for relatively deep-water conditions [12].

The depth of habitats of *Zoophycos* increases throughout the Phanerozoic. In the Upper Paleozoic-Lower Mesozoic deposits, the *Zoophycos* traces are confined to relatively deep-sea deposits (offshore) [13].

The *Diplocraterion* traces from the Nekuchan Formation sandstones (bed 37) are characteristic for a highly dynamic intertidal coastal-marine environment with repeated erosion and deposition [8], but, possibly, may occur in turbidite facies, as in the case of Kobyume section.

The bioturbation index of the rocks of all formations of the Tiryakh-Kobyume section varies: in some interbeds primary bedding is observed (predominantly, in siltstones); other beds are completely reworked and homogenized after repeated bioturbation (diamictites, sandstones). Such diffuse bioturbate textures can be formed when the sediment is densely populated by animals during a low sedimentation rate, or can be a result of multiple superpositions of traces of life activity within one bed [14].

Results of our study are consistent with the bathymetric constructions of Seilacher [15]. According to Seilacher, there is a gradual transition from complex horizontal traces in deep-water deposits to vertical traces in shallow water. The shape of the traces also confirms this: animals excavate complex horizontal traces for maximum exploration of the ground; burrows in shallow water should be simple and stable.

Conclusions

Numerous trace fossils *Phycosiphon* and *Zoophycos* are in the Permian interval of the Tiryakh-Kobyume section, can be attributed to the *Zoophycos* Ichnofacies, characterized by low energy environments, oxygen-depleted settings, and located below a storm wave's base [16]. The Early Triassic *Diplocraterion* ichnofabrics (bed 37) are typical for highly dynamic water environments [17] with increased oxygenation [18].

The *Diplocraterion* ichnocenosis can be attributed to the *Skolithos* Ichnofacies.

Acknowledgments

The work is performed according to the Russian Government Program of Competitive Growth of Kazan Federal University and by the subsidy allocated to Kazan Federal University for the state assignment # 671-2020-0049 in the sphere of scientific activities. The collection of trace fossils has been obtained during fieldwork with the support of the Russian Science Foundation grant No. 19-17-00178.

REFERENCES

1. Budnikov, I. V., Kutygin, R. V., Shi, G. R., Sivtchikov, V. E., Krivenko, O. V. (2020). Permian stratigraphy and paleogeography of Central Siberia (Angaraland) – A review. Journal of Asian Earth Sciences 196 (104365), pp. 1-21.
2. Kutygin, R. V., Budnikov, I. V., Biakov, A. S., Davydov, V. I., Kilyasov, A. N., Silantiev, V. V. (2019). First findings of *Otoceras* (Ceratitida) in the Kobyuma zone of the Southern Verkhoyansk region, Northeastern Russia. Uchenye Zapiski Kazanskogo Universiteta. Seriya Estestvennye Nauki. 161 (4), pp. 550-570.
3. Budnikov, I. V., Grinenko, V. S., Klets, A. G., Kutygin, R. V., Sivtchikov, V. E. (2003). Model' formirovaniya verhnepaleozoyskich otlozhenyi vostoka Sibirskoy platform i ee skladchatogo obramleniya. Otechestvennaya geologiya 6, pp. 86-92.
4. Abramov, B. S. (1974). Stratigraphiya verhnepaleozoyskich otlozhenyi Yuzhnogo Verchoyania. Nauka, Novosibirsk, 96.
5. Gosudarstvennaya geologicheskaya karta SSSR. Mas'shtab 1:200000. Seriya Verchoyanskaya, list P-54-III. (1987). VSEGEI, Sankt-Peterburg.
6. Kutygin, R. V. (2018). Main stratigraphic and paleogeographic features of Lower Dulgalakhian regional substage of Permian system of Yakutia. Arctic and Subarctic Natural Resources 25 (3), pp. 5-21.
7. Bromley, R. G. (1996). Trace Fossils: Biology, Taphonomy and Applications, 2nd edition. Chapman & Hall, London, 361.
8. Knaust, D. (2017). Atlas of Trace Fossils in Well Core: Appearance, Taxonomy and Interpretation. Springer, Switzerland. 209.
9. Wetzel, A, Bromley, R. G. (1994). *Phycosiphon incertum* revisited: *Anconichnus horizontalis* is its junior subjective synonym. J Paleontol 68, pp. 1396-1402.
10. Ekdale, A. A., Mason, T. R. (1988). Characteristic trace-fossil associations in oxygen-poor sedimentary environments. Geology 16, pp. 720-723.
11. Uchman, A. (1995). Taxonomy and palaeoecology of flysch trace fossils: the Marnoso-arenacea Formation and associated facies (Miocene, Northern Apennines, Italy). Beringeria 15, pp. 3-115.
12. Dronov, A. V., Raimbekov, Y., Kushlina, V. B. (2014). O nakhodke iskopaemych sledov *Phycosiphon* v triasovykh otlozheniyakh Yugo-Vostochnogo Pamira. Vestnik RUDN. Seriya Inzhenernye issledovaniya 3, pp. 87-92.
13. Seilacher, A. (2007). Trace fossil analysis. Springer, Berlin, 226.

14. Yan, P. A., Vakulenko, L. G. (2011). Smena sostava ichnofossilyi v kellovey-oksfordskich otlozheniyach Zapadno-Sibirskogo basseina kak otrazhenie ciklichnosti sedimentogeneza. Geologiya i geofizika 52 (10), pp. 1517-1537.
15. Seilacher, A. (1967). Bathymetry of trace fossils. Marine Geology 5, pp. 413-428.
16. Mikuláš, R., Dronov, A. (2006). Palaeoichnology – Introduction to the study of trace fossils. Institute of geology, Academy of Sciences of Czech Republic, 122.
17. Fürsich, F. T. (1974). On *Diplocraterion* Torell 1870 and the significance of morphological features in vertical, spreiten-bearing, U-shaped trace fossils. Journal of Paleontology 48, pp. 952-954.
18. Buatois, L., Mangano, M. G. (2011). Ichnology. Organism-Substrate Interaction in Space and Time. Cambridge University Press, Cambridge, 358.

Kazan Golovkinsky Stratigraphic Meeting

2020

Kazan Federal University
Institute of Geology and Petroleum Technologies

Kazan Golovkinsky Young Scientists' Stratigraphic Meeting 2020

Sedimentary Earth Systems: Stratigraphy, Geochronology, Petroleum Resources

October 26-30, 2020, Kazan, Russia

PROCEEDINGS

€ 20,00

ISBN 979-12-80225-03-0